Design and Synthesis of 3-D Fragments and 3-D Building Blocks for Fragment Elaboration

Hanna Klein

Doctor of Philosophy

University of York

Chemistry

November 9, 2020

Abstract

This thesis describes the design and synthesis of 3-D fragments and 3-D building blocks for fragment elaboration. Chapter 1 provides an overview of fragment based drug discovery with an emphasis on the importance of 3-D fragments in drug development and recent approaches in 3-D fragment synthesis and/or generation. Chapter 2 covers the design and synthesis of 41 3-D fragments **A-D**. Fragments were designed to exhibit favorable physicochemical properties (based on industry guidelines) and occupy under-explored areas of chemical space as demonstrated by principal moments of inertia (PMI) analysis.

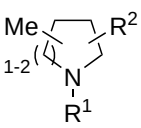

A
20 fragments

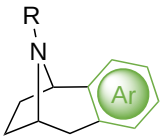

B
2 fragments

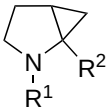

C
6 fragments

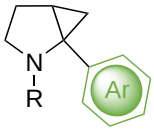

D
13 fragments

Chapter 3 describes the physicochemical properties and molecular shape of 42 3-D fragments (of which 41 were synthesised in Chapter 2) as well as the York 3-D compound collection as a whole (115 compounds). Physicochemical properties and 3-D shape are compared to six commercial fragment libraries. The solubility and stability of the York 3-D fragment library is also discussed. Finally, preliminary screening results of the York 3-D fragment library (four screening campaigns against six protein targets) are disclosed. Chapter 4 presents efforts in the design and synthesis of five 3-D building blocks **E-I** with distinct 3-D synthetic vectors for elaboration. Suzuki-Miyaura cross-coupling to the cyclopropyl-B(MIDA) group is demonstrated in all cases. A strategy for the elaboration of 2-D fragment hits to 3-D lead compounds using 3-D building blocks such as **E-I** is also described.

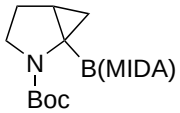

E

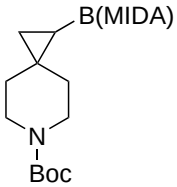

F

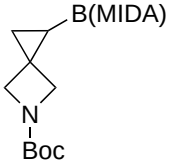

G

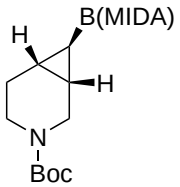

H

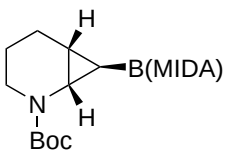

I

Acknowledgements

I would first like to thank Professor Peter O'Brien for guiding me through the ups, downs, obstacles and detours of the last four years. It certainly has been an education, which is no doubt ongoing, and I am so grateful to be (almost) safely on the other side. I would also like to thank Professor Richard Taylor for his encouragement and input as my TAP member.

Numerous people have contributed to and collaborated on this project along the way. In particular, thank you to FragNet for the opportunity to travel, collaborate and learn about the field and a big thank you to Professor Iwan de Esch and Professor Rod Hubbard for coordinating and organising everything behind the scenes. I would also like to thank my industrial supervisor Dr Ben Davis, together with Dr Lisa Baker and Dr Pawel Dokurno at Vernalis for giving me a crash course in fragment screening.

Next, I would like to thank the POB group and YSBL for the steady and seemingly endless supply of cake and other baked goods. In particular, thank you to Eleni and Sophie for making me laugh and letting me cry, respectively. And (not forgetting this time) thank you to James Firth for knowing everything (all the things!) and for buying me beer. This research would not have been possible without the technical support of the staff within the Department of Chemistry. My sincere thanks goes to Steve and Mike from stores, Chris from the electronics workshop, Heather for running the NMR service, Adrian for X-ray crystallography, Karl for mass spectrometry and Graeme for providing dry solvents.

Finally a special thank you to my family and friends (both near and far). Much love and thanks to my mother, brother and sister for supporting me wherever I go and in whatever I do. I could not do anything without you. Thank you.

Declaration of Authorship

I declare that this thesis is a presentation of original work and I am the sole author. This work has not previously been presented for an award at this, or any other, University. All sources are acknowledged as References.

Contents

List of Tables

1 Introduction

1.1 Overview of Fragment Based Drug Discovery (FBDD)

Over the last 20 years, fragment based drug discovery (FBDD) has become a well-established method for generating hits and leads in drug development.[1–7] This has led to the approval of four FBDD-derived drugs: Vemurafenib (Zelborag) in 2011,[8] Venetoclax (Venclexta) in 2016,[9] Erdafitinib (Balversa) in 2018[10] and Pexidartinib (Turalio) in 2019.[11] Furthermore, eleven FBDD-derived drugs have entered advanced clinical Phase II-III trials.[12]

There are many approaches to drug discovery but FBDD and high-throughput screening (HTS) remain the two most prominent methods in the field (Figure 1.1). The key to FBDD rests on the identification of low molecular weight (MW) compounds or fragments (typically < 300 Da) which bind to a protein target (Figure 1.1 A). The small size of fragments allows for the efficient exploration of chemical space which in turn facilitates the use of small libraries consisting of a few thousand compounds. However, due to their small size, fragment binding affinity is low (mM to μM range) when compared to larger lead-like compounds which bind in the nM range. Sensitive biophysical techniques (Surface Plasmon Resonance (SPR), NMR spectroscopy, Isothermal Titration Calorimetry (ITC), Thermal Shift Assay (TSA), Weak Affinity Chromatography (WAC) and X-ray crystallography) and high fragment solubility are therefore required to detect weak protein-fragment interactions. Fragment hits can then be linked, merged or grown into lead-like compounds which in turn can be used to probe protein binding pockets for drug development.

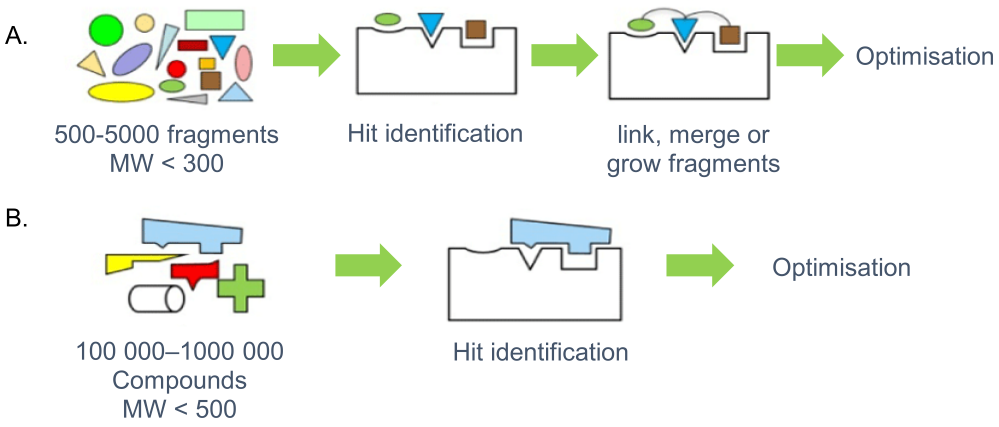

Figure 1.1: FBDD (Fragment Based Drug Discovery) versus HTS (High Throughput Screening)

In contrast, HTS involves the screening of hundreds of thousands of lead-like (MW > 350) compounds (Figure 1.1 B). During the 1990s and early 2000s, HTS screening was primarily used by the pharmaceutical industry and at the time it was the mainstay for drug discovery. Although this strategy resulted in the discovery of many drug-like compounds it was costly and failed to generate leads against lesser known and more difficult targets.[13] Moreover, the overall success rate of pharmaceutical companies decades after the implementation of HTS remains low as illustrated in Figure 1.2 which depicts a typical drug discovery cascade.[14] 40% of HTS hits were found to be false positives and only one in every 2-5 leads were identified as drug candidates.

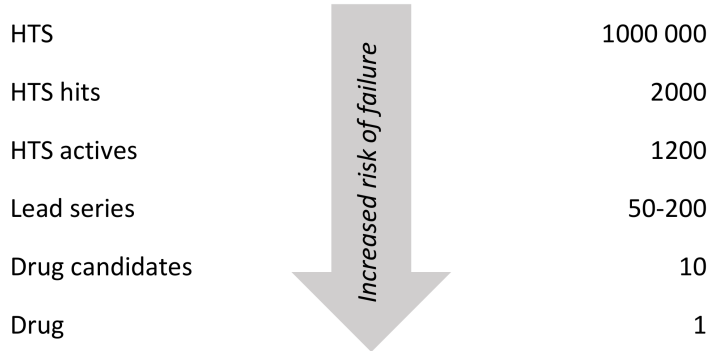

Figure 1.2: A Typical Drug Discovery Cascade

In the face of high attrition rates in drug development, it has been proposed that fragments may provide a better starting point for drug discovery. The idea of a small

molecule or fragment was first introduced by Jencks in 1981,[15] where the benefits of merging or linking small molecules in terms of Gibbs free energy were detailed. Jencks noted that although protein binding of an individual part or fragment may result in an entropic penalty, this can be overcome by the interaction energy gained on merging or linking to another binding part. The first practical example of a FBDD-based approach to drug design was reported in 1996 by Fesik and co-workers at the pharmaceutical company Abbot in their groundbreaking paper on 'structure-activity relationships (SAR) by NMR'.[16] Fragment hits binding in different protein sites were identified by protein-observed NMR and subsequently linked together to form a potent inhibitor. As such, this paper also marked the first practical demonstration of how a fragment might be optimised to a lead compound. Since then, the field has greatly advanced across both industry and academia alike. During the late 1990s and early 2000s, companies such as Abbot, Astex, Sunesis and Vernalis helped to develop the field. The use of small fragment libraries (1000-5000 compounds) which could be rapidly established and easily maintained together with advances in high-throughput crystallographic screening methods made an FBDD-based approach to drug discovery both attractive and accessible. Indeed, by the mid-2000s both academia and the pharmaceutical industry were making use of fragments in research and drug development.

Two key ideas which have significantly shaped the field of FBDD are based around molecular complexity and ligand efficiency (LE). In the first instance, Hann introduced the concept of molecular complexity which suggested that compounds should have limited points for intermolecular interactions in order to both reduce binding mismatch and increase the probability of finding a hit.[17,18] To this end, smaller compounds (less complex) with limited (one to two) pharmacophores for binding are attractive starting points in fragment design. The second idea, ligand effiency, is useful in describing protein-ligand interactions which are often challenging in FBDD due to the low protein binding affinity exhibited by small fragments.[19,20] In particular, LE is useful in the design of screening assays required for the dectection of ligand-protein binding. It can

be defined as a measure of the binding energy (ΔG_{bind}) per heavy atom (HA) of a given fragment in kcal mol^{-1} HA^{-1} according to the equation:

$$LE = \frac{(-2.303RT)}{HAC} \times logK_d$$

where HAC is the heavy atom count or number of non-hydrogen atoms, R is the ideal gas constant, T is the temperature in Kelvin and K_d is the binding affinity. LE is a useful parameter for fragments as it normalises the binding affinity or free energy of binding to the size of the molecule so that compounds of different sizes and affinities can be compared. During the hit-to-lead optimisation process, LE is often used as a metric to track fragment growing, linking or merging. It is also particularly useful in designing a suitable screening assay as it can be used to predict the binding affinity (K_d) of a fragment which in turn determines the concentration at which a fragment must be screened in order to be detected.

1.2 Molecular and Structural Properties of Fragments

There are a number of considerations in fragment design which are often based on guidelines for the molecular and structural properties of fragments. Although these are not thought of as strict rules and can be adjusted, considering these parameters at the outset of a fragment-based design project is paramount for increasing the overall success rate of future lead-to-drug development.

The pharmaceutical company, Astex, suggest the following structural design strategies based on their collection of fragments.[21] These include: (i) the incorporation of a single pharmacophore of high polarity for protein binding, (ii) avoiding reactive and/or aggregating functional groups along with those that give false positives, (iii) synthetic tractability such that designed compounds can be accessed in ≤ 4 steps from commercially available compounds in yields high enough to give 50-100 mg of the target compound, (iv) the inclusion of synthetic vectors to allow for fragment growth in order to explore different binding modes as well as allowing efficient hit-to-lead elaboration and (v) limiting the number of freely rotatable bonds (NROT) (0-3) and stereogenic centres (0-2) required to access a variety of 3-dimensional shapes. In addition to these ideas, fragments need to be sufficiently soluble (≥ 5 mM in 5% DMSO, or other screening co-solvents in buffer) and stable (> 24 h in solution) for screening purposes. The inclusion of an aromatic substituent or ^{19}F atom can also be helpful in NMR screening.

Suggested ranges for key physicochemical properties of fragments and lead compounds have also been reported and can be used as a guideline in fragment design. Lipinski initially proposed 'the rule of five' for orally bioavailable drugs. This suggested that adequate absorption and permeation is more likely for compounds that meet the following criteria: MW ≤ 500 Da, ClogP ≤ 5, hydrogen bond donors (HBD) ≤ 5 and hydrogen bond acceptors (HBA) ≤ 10.[22] More recently, Astex set out a 'rule of three' (Ro3) for fragments based on their analysis of a set of structurally diverse fragments

used in X-ray crystallographic screening studies.[23] Compounds with MW $<$ 300 Da and ClogP $<$ 3 with three or less hydrogen bond donors and acceptors were found to generate hits against a series of protein targets. These parameters have since been modified to MW 140-230 Da, ClogP 0-2 and the number of rotatable bonds 0-3.[21]

The MW of a fragment is of particular importance in terms of limiting the size of a fragment library required to cover or explore a given area of chemical space. In 2015, Reymond and co-workers quantified the size of chemical space by determining the number of organic molecules (of up to 17 atoms of C, N, O, S, and halogens) possible.[24] Using computational tools, a database of 166.4 billion molecules was generated and this suggested that the size of chemical space increases by approximately 8-fold for each heavy atom in a molecule. This means that a library of 1000 fragments with MW of 190 Da would cover an equivalent percentage of chemical space to 10^8 molecules with MW 280 Da or 10^{18} molecules with MW 440 Da.[5] Practically speaking, this means that a fragment library of a few thousand compounds with MW $<$ 300 Da can be used to efficiently sample the available chemical space.

In 2012, Churcher and co-workers at GlaxoSmithKline defined fragment and lead-like space as a function of physicochemical properties, ClogP and MW (Figure 1.3).[25] Lipophilicity (ClogP) and complexity (approximated by MW) tend to increase during hit-to-drug optimisation (purple arrow) such that the control of key molecular properties (MW, ClogP and the fraction of sp^3 carbon atoms, Fsp^3) early on in the drug discovery process remains crucial for successful drug development. Ideally, starting points for drug discovery should fall within fragment and lead-like space (blue circles). In this respect, fragments are advantageous as they allow for a greater drift in molecular properties compared to lead- and drug-like compounds.

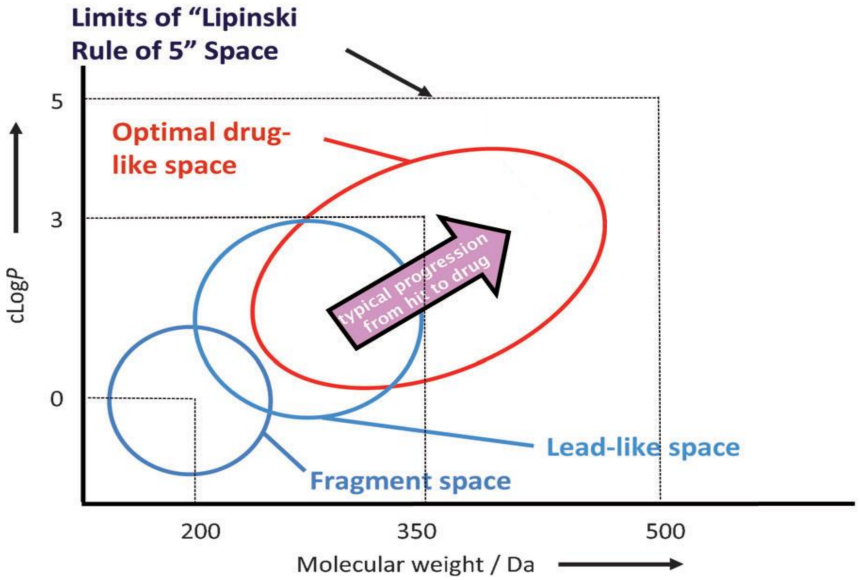

Figure 1.3: Fragment and Lead-like Space as a Function of ClogP and MW

1.3 FBDD-based Approach to Drug Development: a Case Study

The most recent example of an approved drug developed using a FBDD-based approach is the highly specific kinase inhibitor, Pexidartinib (Turalio). It is prescribed for the treatment of symptomatic tenosynovial giant cell tumour (TGCT) and giant cell tumour of the tendon sheath (GC-TS), a rare cancer of the tendon sheath which is unresponsive to surgery. The drug was developed in 2013 by Zhang and co-workers at Plexxikon.[11,26] It was found that Plexidartinib exhibited dual activity against two enzymes, McDonough feline sarcoma viral (v-fms) oncogene homologue (FMS or CSF1R) and v-kit Hardy-Zuckerman 4 feline sarcoma viral oncogene homologue (KIT), which are involved in the regulation of macrophage and mast cell development and have been implicated in cancer and inflammation.

Key steps towards the development process of Pexidartinib are shown in Figure 1.4. The team started with fragment hit, 7-azaindole **1**, which had been previously identified by the same group in their discovery of the first FBDD-derived drug, Vemurafenib in 2011. A key hydrogen bond interaction between the methoxy group of an early derivative PLX070 and a conserved amide group of the protein was used to develop clinical candidate PLX647 which exhibited good activity against both CSF1R and KIT. Pharmacokinetic and pharmacodynamic studies in animals were also positive. Further optimisation of PLX647 by adding a pyridine pharmacophore led to Pexidartinib. Protein binding modes between derivative PLX647 and Pexidartinib differed slightly with the additional pyridine group of Pexidartinib proving crucial in stabilising a unique conformation of the enzyme.

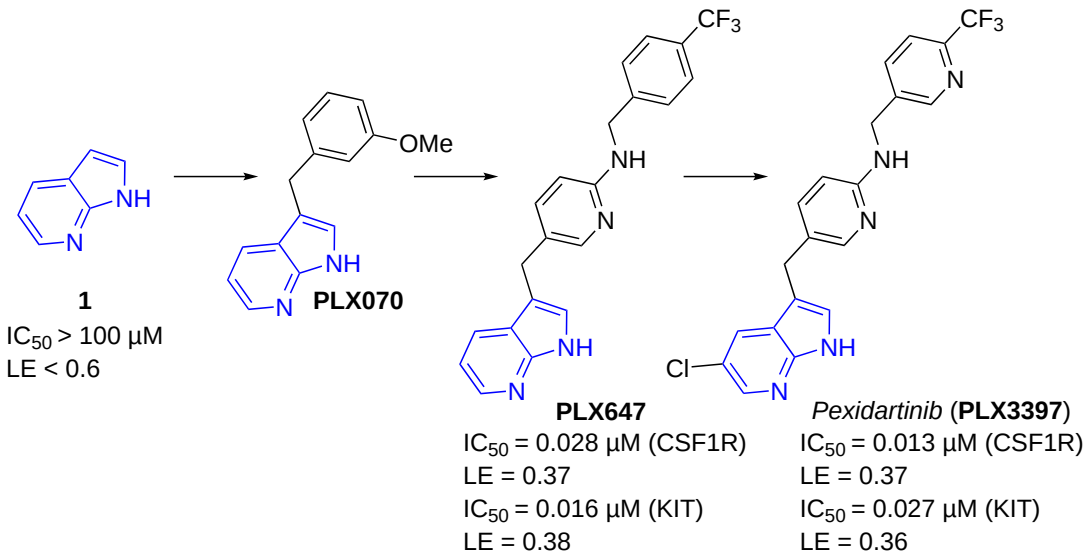

Figure 1.4: A FBDD-based Approach to the Development of Pexidartinib. The original fragment hit is highlighted in blue

1.4 3-D Shape in Medicinal Chemistry

Historically, fragments have been largely based around the Ro3 with far less consideration given to compound shape. Although the control of physicochemical properties remains crucial for successful hit-to-lead progression, there has been a growing interest in shape diversity and in 3-D shape in particular in drug molecules. Fragment screening collections are dominated by an abundance of planar, heterocyclic 2-D compounds which reside in limited areas of chemical space.[27–29] In this sense, the inclusion of 3-D shaped compounds in fragment libraries offers an opportunity to both diversify and balance current compound collections while exploring new areas of chemical space. On the other hand, structural complexity as a consequence of 3-D shape could, according to Hann's concept of molecular complexity, reduce hit rates due to protein binding mismatch.[17,18,30] However, 3-D fragments also offer advantages in terms of increased solubility and providing distinct vectors for fragment elaboration.[21] Furthermore, it has been suggested that the high pharmacophore coverage exhibited by 3-D fragments could allow for the development of drugs against challenging biological targets.[31]

There are a number of tools and descriptors for assessing 3-D molecular shape. Principal moment of intertia (PMI) plots[32] and plane of best fit (PBF)[33] remain the most popular methods as they are highly effective for visualising the shape of a compound collection. Both analyses generate the minimum energy conformers of molecules computationally using simple molecular mechanics. PMI assesses molecular shape according to how rod-, disc- or spherical- shaped compounds are. Normalised ratios of principal moments of inertia (NPR1/NPR2) are calculated and used to generate triangular 2-D plots with the top-left, bottom and top-right vertices representing rod-, disc- and spherical-shaped compounds such as polyalkyne, benzene and adamantane respectively (Figure 1.5).

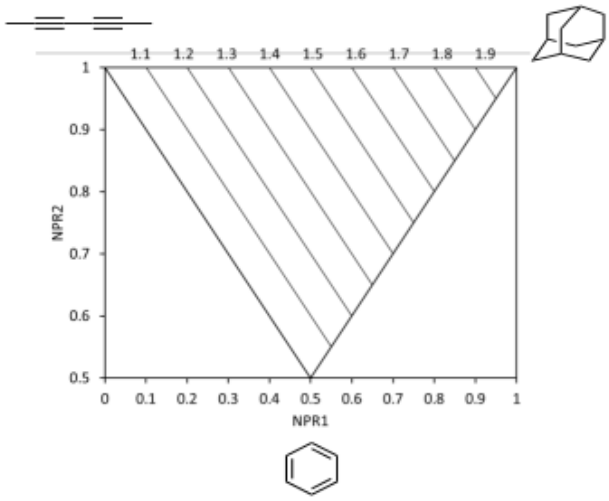

Figure 1.5: Example of a PMI Plot (NPR1 *versus* NPR2) with polyalkyne, benzene and adamantane represented

PMI plots were first described by Sauer and Schwarz in 2003[32] and can be computationally generated using software packages such as Pipeline Pilot which uses simple molecular mechanics to determine the ground-state conformation of a compound. The values for NPR1 and NPR2 are derived from the principal moment of inertia of a given compound in the x, y and z axes. These values are arranged in ascending order to give values for I_1, I_2 and I_3. NPR1 and NPR2 can then be calculated using these two equations:

$$NPR1 = \frac{I_1}{I_3}$$

$$NPR2 = \frac{I_2}{I_3}$$

Plotting NPR1 *versus* NPR2 generates a PMI plot with co-ordinates of (0,1), (0.5, 0.5) and (1,1) representing the top-left, bottom and top-right vertices respectively. The sum of NPR values (ΣNPR = NPR1 + NPR2) then corresponds to a data point on the plot with a value between 1-2. The value for ΣNPR gives an idea of molecular shape as values closer to 2 (disc-sphere axis) will be more 3-D in shape when compared to compounds which exhibit a ΣNPR closer to 1 (rod-disc axis).

Shape analysis by PBF correlates well with PMI and was first designed and used by

Firth *et al.*[33] The PBF descriptor differentiates between 2-D and 3-D molecules in terms of deviation from a plane across which all the heavy atoms of a given compound have been mapped (Figure 1.6). The central point of mass of the heavy atoms contained within 2-D compounds lie within this plane whereas the heavy atoms of more 3-D compounds tend to lie a distance from it. A quantitative value for how far removed a given compound is from being 2-D in shape is generated by measuring the average distance of all heavy atoms from the PBF. Importantly, unlike PMI, PBF varies with size and should be used to assess shape between compounds of similar mass or HAC.

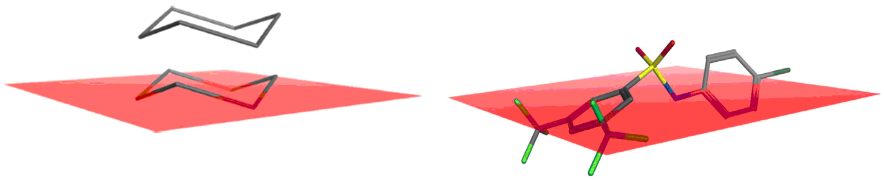

Figure 1.6: Example of the PBF for Two Compounds and their Deviations from Planarity

The fraction of sp^3 hybridised carbon atoms (Fsp^3) is also frequently cited as a 3-D shape descriptor. Although it has been shown that compounds with a higher Fsp^3 and fewer aromatic rings have an increased success rate in drug development,[27,34] our group along with others,[30,33,35,36] have verified that Fsp^3 is a poor predictor of 3-D shape. For example, Bloomberg and co-workers found that substituted amide fragments (with $Fsp^3 < 1$) exhibited a higher ΣNPR than their amine intermediates ($Fsp^3 = 1$) (Figure 1.7).

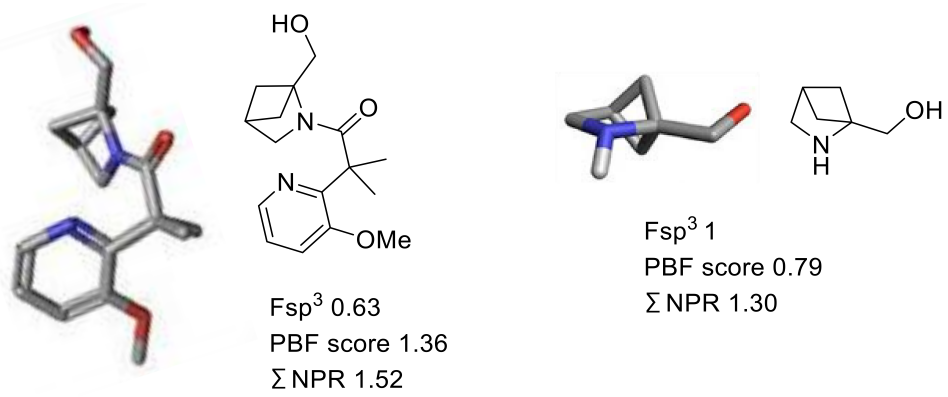

Figure 1.7: Comparison of 3-D Shape Descriptors (Fsp^3, PBF and ΣNPR) for a Substituted Amide Fragment and an Amine Intermediate

This observation was supported by work done by Firth *et al.* which showed poor correlation between Fsp^3 and PBF for 2465 fragment-like molecules.[33] More recently, a member of our group analysed Fsp^3 and PMI for six commercially available 2-D and 3-D focused fragment libraries.[35] Analysis was carried out on groups of fragments (with 1000 compounds per group) and showed no correlation between Fsp^3 and PMI. Interestingly, PMI analysis of both the 2-D and 3-D commercial collections inidicated similar 3-D shape with the 3-D libraries designed using Fsp^3 as a descriptor or guide for 3-D shape. Thus, when assessing 3-D molecular shape, Fsp^3 can be used as a rough guide for comparative purposes but it should be used alongside other 3-D descriptors such as PMI and PBF.

1.5 Overview of Recent Approaches in 3-D Fragment Synthesis and/or Generation

The advantages of and need for more 3-D shaped compounds in fragment library collections has been highlighted by the 3-D Fragment Consortium[28] and others.[27,37] Interestingly, a survey of recent literature shows that both academic groups and industry have indeed begun to address this challenge by focusing their research on developing synthetic methodology for 3-D fragment generation. To this end, various approaches for accessing 3-D fragments have been reported, with an emphasis on generating structurally diverse compounds using an efficient synthetic route (typically ≤ 5 steps). In this section, the different approaches used to synthesise 3-D fragments are reviewed, together with other approaches for generating 3-D fragments.

1.5.1 Diversity Oriented Synthesis (DOS)

Diversity Oriented Synthesis (DOS) aims to generate structurally diverse compounds which cover a broad area of chemical space by applying a variety of reaction conditions to a common synthetic scheme and was a concept first introduced by Shreiber *et al.*[38] In 2011, Young and co-workers combined DOS with fragment oriented synthesis to synthesise 35 Ro3 compliant fragments using a build-couple-pair (b/c/p) strategy (Scheme 1.1).[31] During the 'build' phase, proline-based, chiral building blocks **2**-**4** were selected as starting materials. Proline serves as an attractive starting point for synthesis as both enantiomers are commercially available allowing stereochemical diversity to be introduced at the outset.

Functional complexity was introduced using amide and sulfonamide forming reactions during the 'couple' phase. Intermolecular reactions with **2** were used to functionalise the secondary amine and introduce the second alkene into amide **5** and sulfonamide **6**. Finally, the alkenes were intramolecularly 'paired' using Ru-catalysed, ring-closing metathesis (RCM) to afford a series of 5-6, 5-7, 5-8 and 5-9 fused bicyclic and spiro-

cyclic compounds such as **7** and **8**. Applying this strategy to the enantiomers of **2** and **3** gave rise to all possible stereoisomers. Functional group interconversion of the generated scaffolds by methyl ester hydrolysis and alkene reduction, termed the 'postpairing phase', further increased functional diversity and saturation of the library. In this way, the synthesis of a set of 35 structurally and stereochemically diverse fragments was achieved in 3-5 steps from chiral building blocks **2**-**4**.

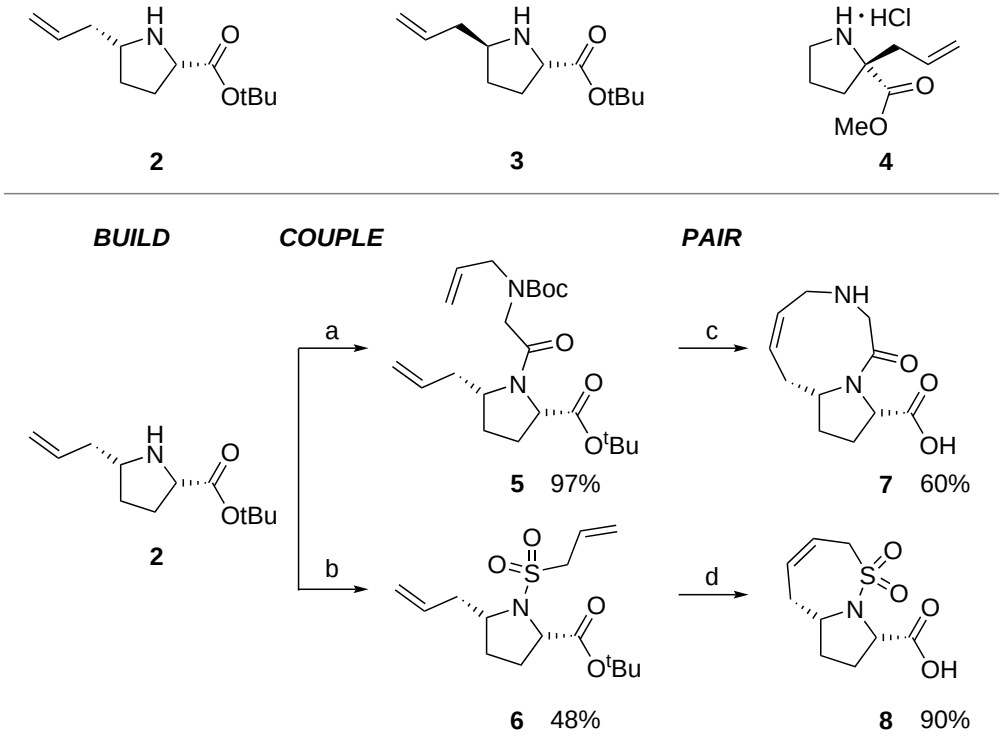

(a) RCO_2H, EDCI, Oxyma, Et_3N (b) RSO_2Cl, Et_3N (c) (i) Grubbs I, reflux (ii) TFA (d) (i) Grubbs II, reflux (ii) TFA

Scheme 1.1

The molecular shape and physicochemical properties of the fragment collection were compared to 18,534 fragments contained within the ZINC database. PMI analysis showed greater uniform coverage or variance of the 35 fragments, which was confirmed by a Kolmogorov-Smirnov (KS) test. Furthemore, all synthesised fragments were found to have a ΣNPR value ≥ 1.2 indicating that they had 3-D shape whereas 75% of compounds within the ZINC database were found to occupy the ΣNPR 0-1.2 section of

the plot. Comparison to a smaller sub-set of compounds with similar molecular and physicochemical properties gave comparable results. Physicochemical properties were found to be similar to the commercially available compounds with MW < 300 Da and AlogP < 3 for all synthesised fragments.

Subsequently, in 2016, the Young group used the DOS-based, b/c/p synthetic approach to generate 86 fragments which were screened against glycogen synthase kinase 3β (GSK3β). Using this strategy, hit analogues were elaborated efficiently into more potent compounds in the absence of X-ray structural binding data.[39]

Similarly, Nelson and Marsden's group reported a divergent approach in their synthesis of 22 diverse molecular scaffolds from four α,α-disubstituted amino acids.[40] Although the target scaffolds were designed as part of a lead-oriented synthetic approach, the physicochemical properties (HAC, AlogP) of the deprotected scaffolds fall within the boundaries of Ro3, 3-D fragment space. Their synthetic strategy is shown in Scheme 1.2. Functionalised amino acid derivatives **9** were *N*-alkylated (blue) to form a trifunctional intermediate **10**. Cyclisation between either the alkene (red) and the *N*-group (blue) or ester (green) and *N*-group (blue) generated scaffolds **11** and **12** respectively. Application of this methodology with α,α-disubstituted amino acids **9a-d** generated 22 structurally diverse scaffolds. A representative example is also shown in Scheme 1.2. *N*-alkylation and RCM with α,α-disubstituted amino acids **9a-d** generated structurally diverse scaffolds **13-16**. An additional four sets of scaffolds were systematically synthesised in 49 transformations by varying the amino acid (acycylic/cyclic), *N*-group or cyclisation conditions.

Analysis of the 22 scaffolds was carried out by creating a virtual library of 1110 compounds derived from deprotection and/or *N*-functionalisation of each scaffold with typical groups used in medicinal chemistry. Of these lead-like compounds, 66% were found to have favourable molecular properties (HAC, AlogP, Fsp^3) and PMI analysis

indicated good 3-D shape. Furthermore, a substructure search of the compound collection against ZINC and CAS databases showed a high degree of novelty and structural diversity.

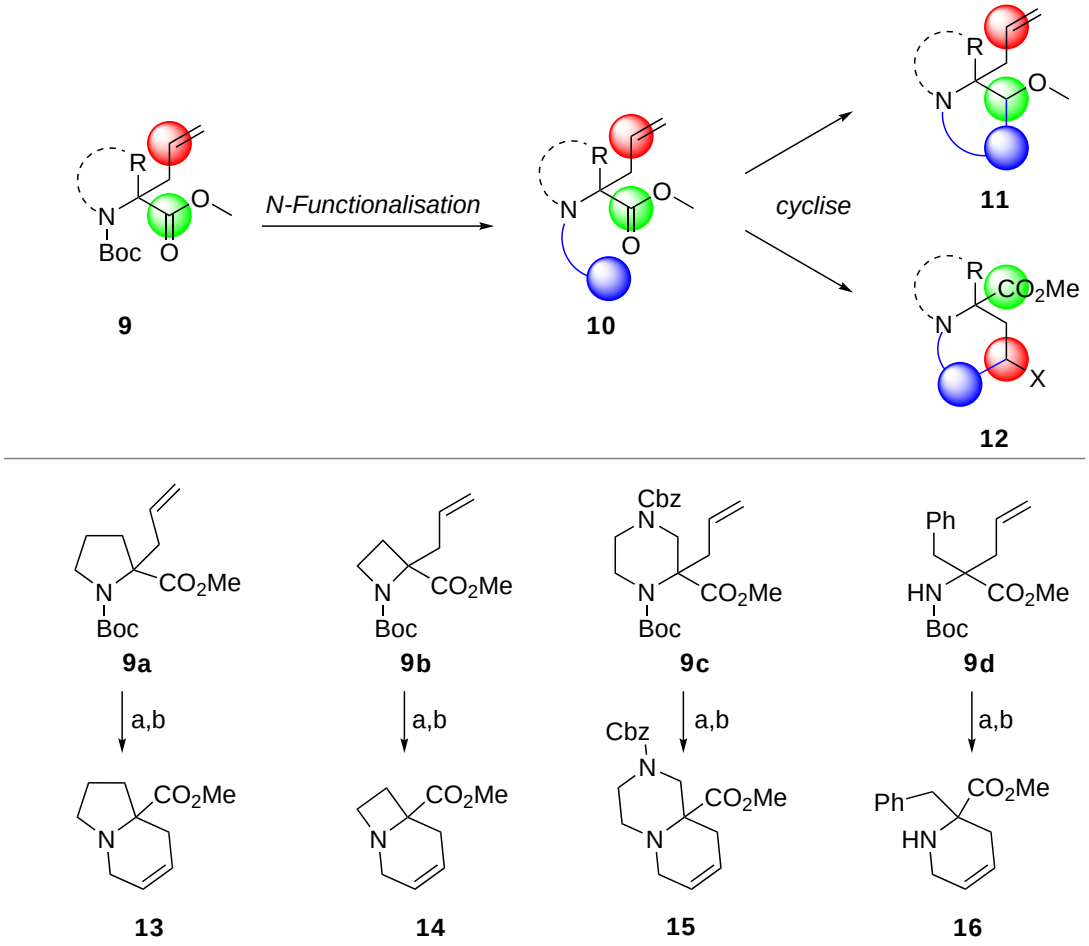

(a) (i) TFA (ii) allyl bromide, K_2CO_3 (b) 2.5 mol% Grubbs II, TsOH, PhMe, reflux

Scheme 1.2

Another example of a DOS-based approach for 3-D fragment synthesis was demonstrated by Spring's group with the synthesis of 30 structurally diverse, *N*-substituted quaternary carbon containing scaffolds from α,α-disubstituted amino ester **17** (Scheme 1.3). Initially, amine (green), ester (blue) and alkyne (red) groups of building block **17** were used as synthetic handles to install the necessary functionality for subsequent steps. Then, various transformations were used to generate their DOS-derived library. For example, metal-catalysed cyclisation between installed alkyne and/or pyr-

role groups afforded bicyclic scaffolds **18** and **19**. Alternatively, modification of the alkyne group to form a vinyl iodide followed by Buchwald-Hartwig coupling furnished scaffold **20**. Finally, scaffold **21** was generated following lactamisation between the ester group and the quaternary amine. Subsequent derivatisation of 27 scaffolds gave 40 structurally diverse, 3-D fragments in less than five synthetic steps.

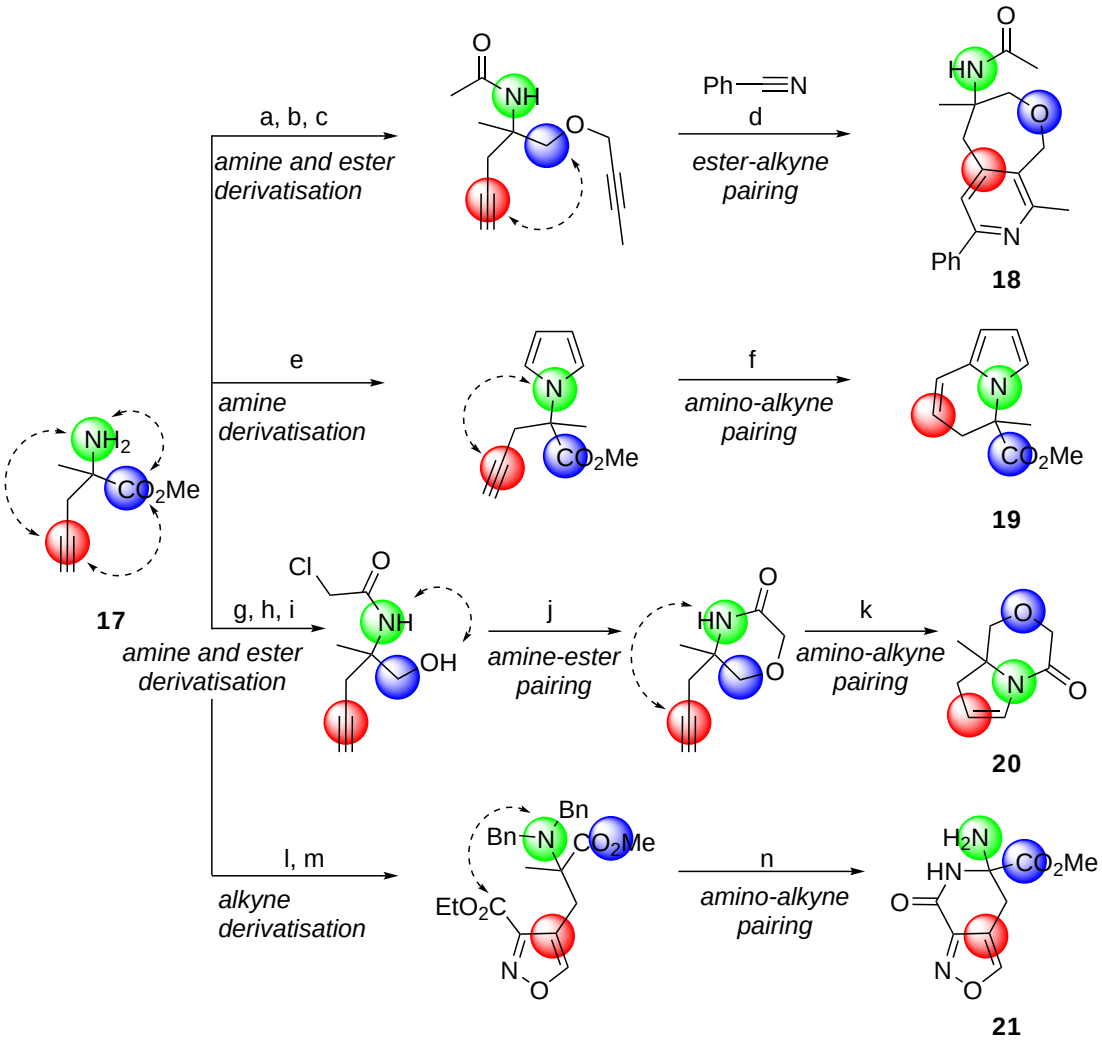

(a) acetyl chloride, Et_3N (b) $LiBH_4$ (c) propargyl bromide, NaH (d) $CpCo(CO)_2$, 110 °C (e) NaOAc, 2,5-dimethoxytetrahydrofuran, DCE: H_2O: AcOH, 90 °C (f) $AuSPhos(MeCN)SbF_6$, 40 °C (g) Boc_2O, 70 °C (h) $LiBH_4$ (i) HCl (ii) chloroacetyl chloride, Et_3N (j) *t*-BuOK, 30 °C (k) (i) $InCl_3$, DIBAL-H, –78 °C (ii) Et_3B (iii) I_2 (l) BnBr, DIPEA, 80 °C, (m) ethyl 2-chloro-2-(hydroxyimino)acetate, Cp*RuCl(COD), 80 °C (n) $Pd(OH)_2$, H_2

Scheme 1.3

The molecular shape and distribution of the compound collection was assessed by PMI analysis. In this case, 93% of the library was found to have a ΣNPR $\geq$ 1.1. This compared favourably to the Maybridge core 1000-member Ro3 fragment library in which only 28% of compounds were found to have a ΣNPR $\geq$ 1.1. Comparison of the PMI data against a DOS Ph virtual library (40 structurally similar molecules with a Ph substituent at the quaternary stereocentre) showed that substitution of the *N*-Me group at the quaternary centre could be used to adjust molecular shape. Calculated physicochemical properties SlogP, MW, HBA and HBD fell well within the Ro3. The number of stereogenic centres and fraction of aromatic atoms per molecule were also calculated and compared favourably to the Maybridge Ro3 core collection and Chembridge libraries. Finally, the coverage of the DOS generated library across biologically relevant chemical space was assessed by comparison to bioactive molecules and two target focused synthetic libraries. In this respect, the compound collection was also found to be biologically diverse and thus useful for screening against different targets.

Spring recently followed up this work by screening the 40 fragment collection against three distinct protein targets (P. aeruginosa Penicillin Binding Protein 3 (PBP3), CFI_{25} and Activan A) using X-ray crystallography.[41] Notably, protein targets CFI_{25} and Activan A have no known small molecule binders. Rapid elaboration of the DOS-derived library in multi-directions was possible using previously established (modular, DOS) chemistry from amino ester **17**. Furthermore, asymmetric synthesis of substrate **17** was demonstrated over 4 steps such that analogues could also be isolated as single enantiomers. This proved crucial for determining the precise binding mode of hit analogues in follow-up screening experiments. Overall, a minimum of four synthetic vectors was used to access 10-14 analogues of each hit in 3-6 synthetic steps. The identification of four fragment hits provided proof-of-concept and demonstrated the importance of fragment library diversity in screening.

1.5.2 Computational 3-D Fragment Generation

A 3-D fragment library can be created from commercially available collections using computational analysis, in which compound selection could be based on shape diversity and physicochemical properties. The 3-D Fragment Consortium, which is a network of UK-based research institutes and groups, adopted this approach in their aim to build and collate a shape-diverse, fragment collection with a particular focus on incorporating 3-D structure to better explore new areas of chemical space.[28] Initially, 13.4 million compounds were selected from two commercial collections, eMolecules and the ZINC database. Filtering based on favourable physicochemical properties (HAC 9-18, XlogP < 3, total polar surface area < 100 and rotatable bond number (RBN) < 4) together with the removal of compounds with reactive groups and pan-assay interference compounds (PAINS) gave 180,000 compounds. PMI analysis was then used to select 5000 compounds based on shape diversity. Finally, visual inspection and compound selection by medicinal chemists narrowed the fragment library down to 200 compounds. 30 of these compounds were commercially unavailable or failed QC studies leaving a library of 170 compounds. Compound shape and diversity were assessed by PMI analysis, maximum similarity and mean complexity. In terms of 3-D shape, the 170 fragment set compared favourably to a 1000 compound commercial collection but $\geq 70\%$ of the library were still found to have ΣNPR < 1.1 highlighting the 2-D shape of commercially sourced compounds.

In 2019, Nelson's group described the design and collation of a library of 80 shape-diverse, sp^3-rich fragments.[42] The collection included both commercially sourced compounds and a synthesised fragment set. Initially, scaffolds, primarily designed on the basis of synthetic tractability, were used to generate a virtual library of 66814 compounds. The virtual library together with the ZINC database were then filtered according to molecular size ($18 \leq$ HAC ≤ 22), lipophilicity ($-1 <$ AlogP < 3), shape coverage and diversity to give 20 virtual and 60 commercially available compounds.

The 20 virtual compounds were synthesised from four scaffolds as shown in Scheme 1.4. Simple building blocks were used to construct precursors **22** and **23a-c** in 1-2 steps. Cyclisation of α-allyl α-amino ester **22** gave hydantoin-based scaffold **24**. Alternatively, Ugi reactions between tetrahydropyrazines **23a-c** and substituted isocyanides gave piperazines **25a-c**. Notably, scaffolds **25b** and **25c** were formed with high diastereoselectivity. Scaffold elaboration was possible following deprotection and/or oxidative cleavage of the alkenes. Then, reductive amination, sulfonylation, acylation and urea formation gave the 20 3-D fragments. Four representative examples of these relatively complex 3-D fragments are shown.

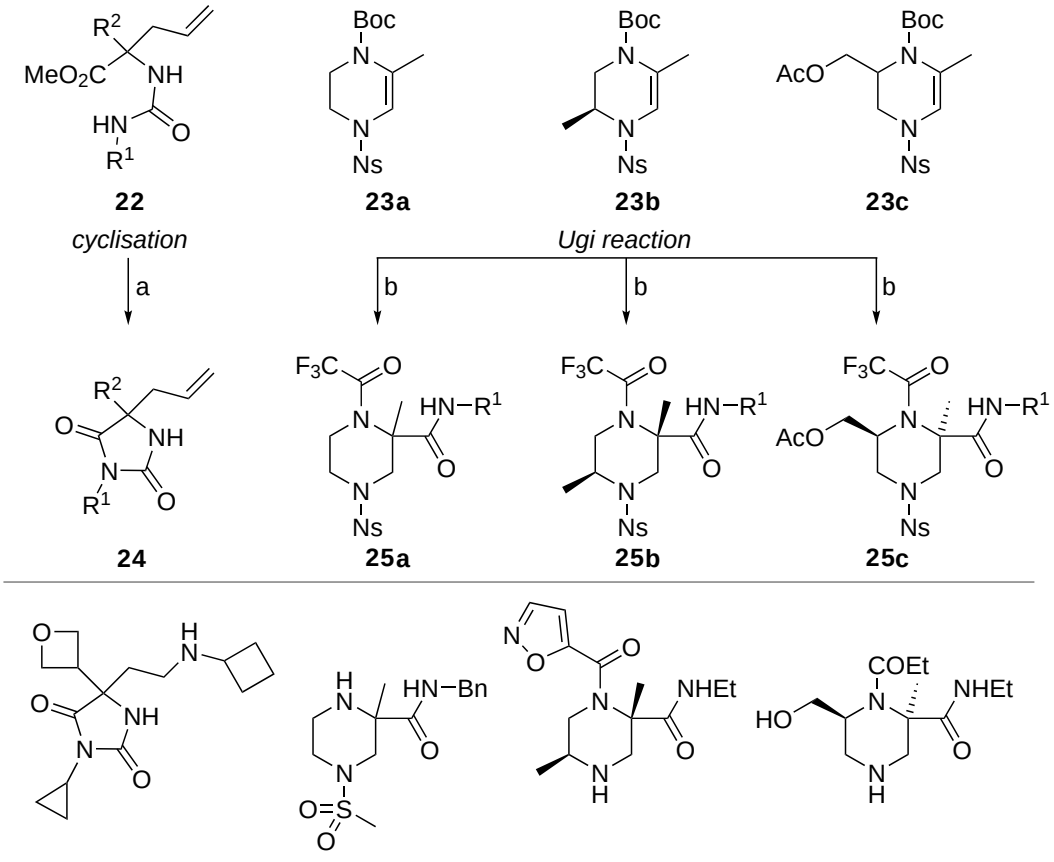

Scheme 1.4

PMI analysis of the 80 compound collection showed that they were 3-D with only two of 80 ground-state conformations falling close to the rod-disc axis. The synthesised

compounds were found to exhibit better 3-D shape with fewer aromatic rings when compared to the commercial compounds. The number of stereogenic centres and cyclic substituents also compared favourably for the synthesised set highlighting its value in complementing commercial compound collections. Screening of the library by high-throughput, X-ray crystallography against Aurora-A kinase revealed four allosteric binders, demonstrating the value of the compound set.

1.5.3 Natural Product-Derived 3-D Fragments

The high number of stereogenic centres and sp^3 hybridised carbon atoms inherent in natural products makes them attractive synthetic targets for generating small molecules with both diverse and 3-D shape. In contrast, the synthetic tractability of such complex scaffolds is often limited. In this respect, a top-down synthetic approach to natural product-derived 3-D fragments can be useful.

In 2013, Waldmann and co-workers developed a computational protocol for generating fragments from natural products. An algorithm governed by rules around ring disconnection and side-chain shortening was used to disconnect over 180,000 natural products into fragment sets as illustrated in the fragmentation of the natural product, Renieramycin P, which can be deconstructed into six compounds (Scheme 1.5). Following this process, 750,000 natural product-derived fragments were generated. Three successive rounds of filtering based on favourable physicochemical properties and structural constraints gave 110,000 fragments.

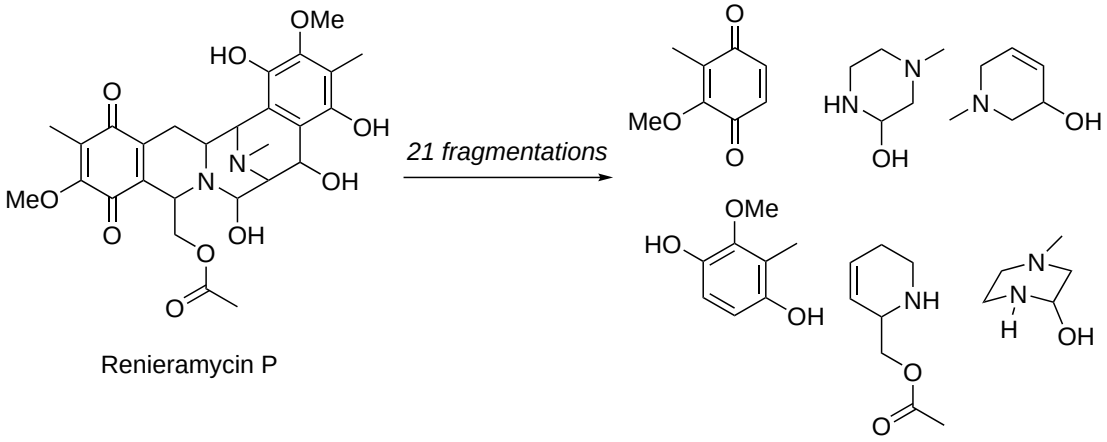

Scheme 1.5

Iterative pharmacophore clustering identified 2000 clusters of fragments which were used as a representative set for further analysis. Principal component analysis (PCA) against a fragment subset from the commercially available ZINC database showed minimal overlap, highlighting the differences in structural properties and coverage of chemical space exhibited by the natural product-derived fragments. Analysis by PCA of fragments generated by an analogous study using commercially available compounds against the natural product derived fragment set gave similar results.

In order to show the usefulness of the natural product-derived fragment collection for drug discovery, a screening campaign against p38α MAP kinase and several phosphatases was carried out. To this end, 193 fragments or structurally similar compounds were synthesised or selected from commerical sources. X-ray crystallographic screening identified nine hits against p38α MAP kinase with two compounds adopting novel binding modes. In addition, several potential phosphatase inhibitors were identified. The results of this screening campaign provide proof-of-principle that the structural diversity inherent within sp^3-rich natural product-derived scaffolds are advantageous in exploring new areas of chemical space and discovering novel small molecule inhibitors.

Novartis used an alternative strategy in the construction of a 150 compound, natu-

ral product-like 3-D fragment library.[43] Fragments were derived using *in silico* guided degradation of larger natural products or by chemical modification of smaller natural products. Commercially available and in-house 3-D shaped natural product-like fragments were also selected to complement the collection. Using the first deconstructive approach, 17,000 in-house compounds were computationally subjected to different cleavage reactions (ozonolysis, ester hydrolysis, Baeyer-Villiger oxidation,) to give 66,000 products. A further 9,000 fragments were selected based on favourable physicochemical properties (150<MW<300 and ClogP<3). Molecular shape and novelty were then assessed by PMI analysis and compared to 25,000 in-house fragments. PMI analysis showed a wide distribution of conformations across the plot. Literature precedence and synthetic tractability were also considered before selecting fragments to purchase or synthesise. An example of this natural product degradation for 3-D fragment generation is shown in Scheme 1.6. Dihydroxylation and periodate cleavage of Sanglifehrin A generated intermediate **26** which was converted into 3-D fragment **27**.

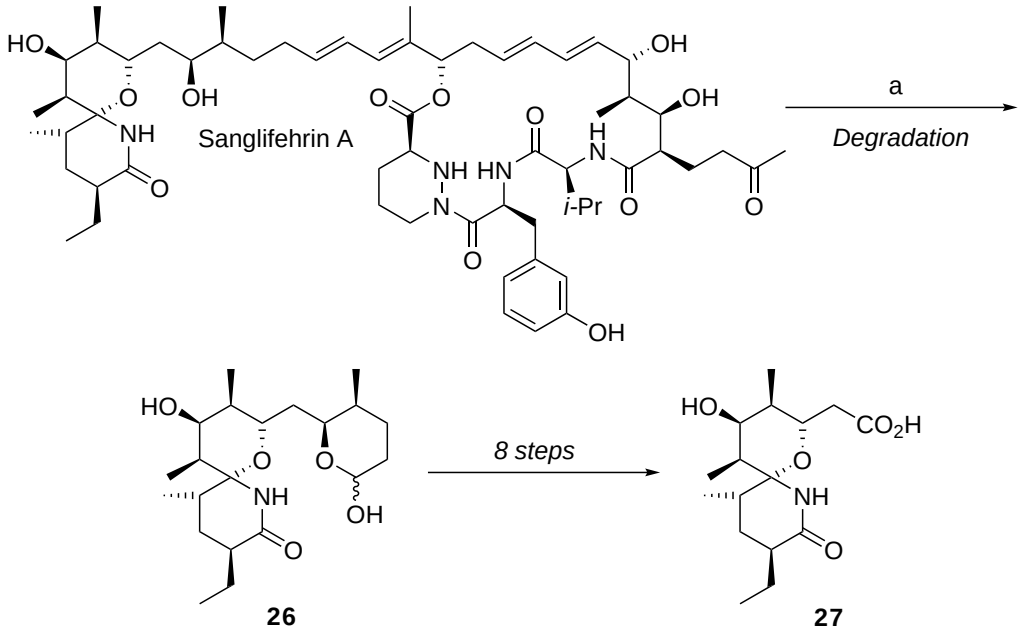

(a) (i) OsO_4, $(DHQ)_2PHAL$, $K_3Fe(CN)_6$, K_2CO_3, $CH_3SO_2NH_2$ (ii) $NaIO_4$

Scheme 1.6

In a second approach to 3-D natural product fragment generation, smaller natural

products were chemically modified to form 3-D fragments of interest. For example, stereoselective reduction of Massarigenin C gave fragments **28** and **29** (Scheme 1.7). Compound **30** formed by a rearrangement of unknown mechanism was also isolated as a side product and used to synthesise fragments **31** and **32** by functional group conversion. Using the three described approaches, the team at Novartis were able to collate a sp^3 rich, natural product-derived 3-D fragment library of 150 compounds which, when combined with their in-house compound collection, allows for greater exploration of chemical space.

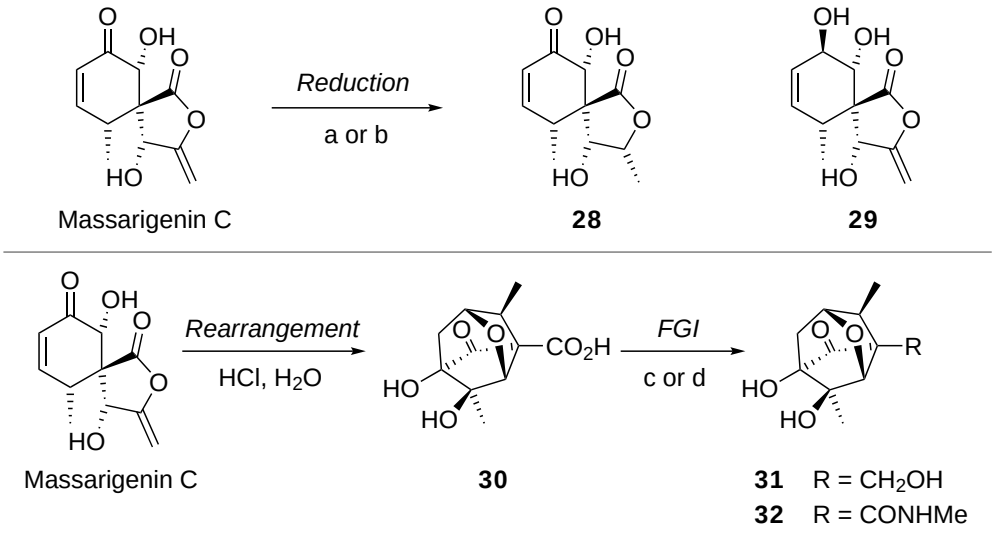

Scheme 1.7

1.5.4 Scaffold Diversity Synthesis

Scaffold diversity synthesis provides an efficient synthetic route to 3-D fragments as only a limited number of common intermediates or scaffolds are synthesised which then can be diversified using a range of different transformations. In this way, a large number of structurally different compounds can be constructed in relatively few steps. Bull's group used this approach in the synthesis of 2-sulfonyl-oxetane 3-D fragments.[44,45] The oxetane motif was formed in 3 steps from sulfides **33** (Scheme 1.8). Alkylation with ethylene glycol gave alcohols **34**. Tosylation and oxidation with *m*CPBA gave sulfones

35. Then, the key 4-exo-*tet* cyclisation step using optimised conditions (LHMDS in THF at 0 °C for 1 h) afforded the oxetane motif in good yield and the reaction proved scalable ($\geq$ 6.5 mmol). Selected examples of the synthesised oxetanes are shown.

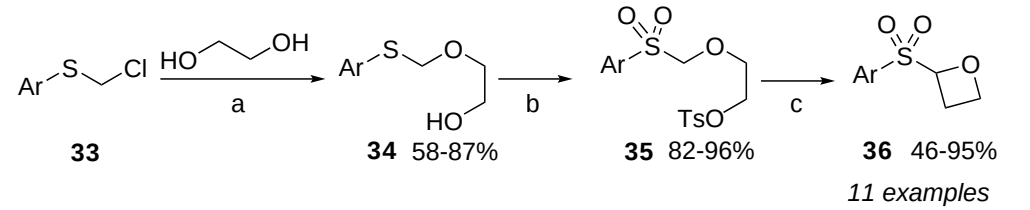

(a) NaH, NaI, 0 °C-rt; (b) (i) TsCl, Et_3N, $Me_3N{\cdot}HCl$, 0 °C-rt (ii) *m*CPBA, 0 °C (c) LHMDS, 0 °C

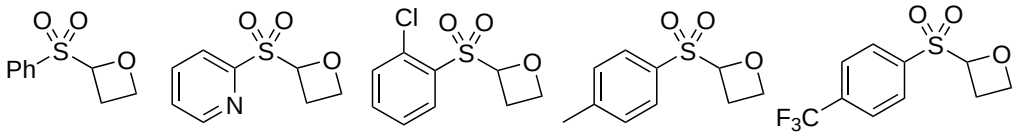

Scheme 1.8

Fragment elaboration was then implemented using three strategies (Scheme 1.9). First, lithiation-trapping chemistry with various electrophiles was used to functionalise the oxetane motif and gave fragments **38a-c**. Diversification by cross-coupling of aryl halide containing compounds such as **39** using either Suzuki-Miyaura or Fe-catalysed cross-coupling conditions gave fragments **40** and **41** respectively. Finally, sulfone directed *ortho*-metallation was used to install a methyl group in the *ortho* position of **42**.

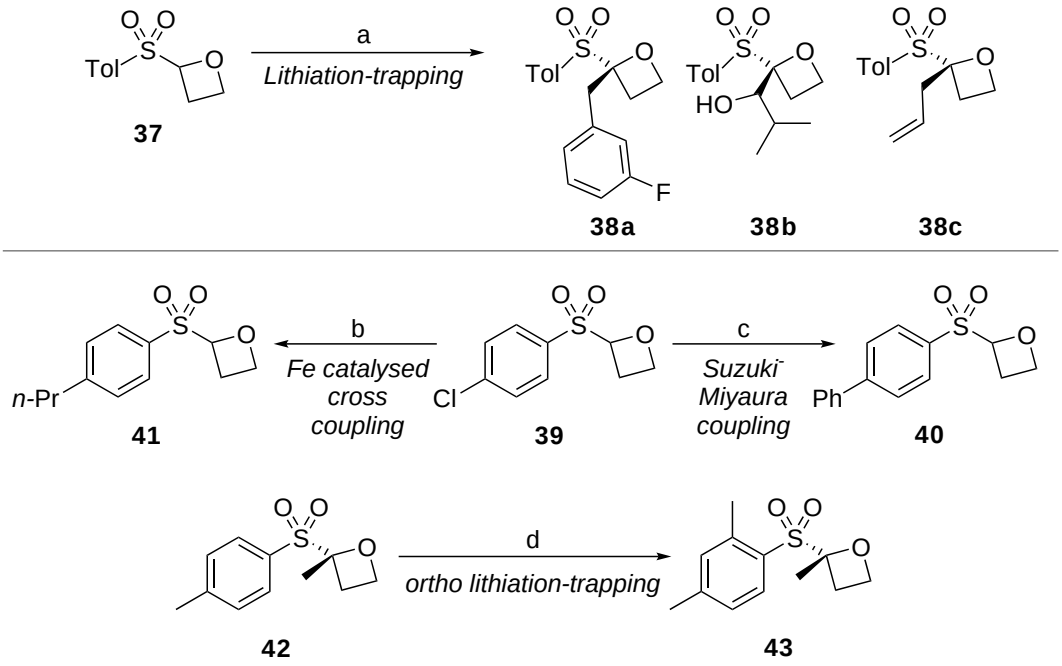

(a) (i) LiHMDS or *n*-BuLi, –78 °C (ii) E^+ (b) $Fe(acac)_3$, *n*-PrMgBr 0 °C-rt (c) $ArB(OH)_2$, $Pd(OAc)_2$, SPhos, K_2CO_3, 65 °C (d) (i) *n*-BuLi, –78 °C (ii) MeI

Scheme 1.9

Calculated physicochemical properties (MW, ClogP, HAC, HBD, HBA) for the 16 fragment collection were found to be favourable. The stability of all synthesised compounds was also assessed. α-Alkylated oxetanes such as **38a-c** (Scheme 1.9) were ultimately excluded from the library due to instability on prolonged storage even under low temperature conditions (-20 °C). pH Stability studies of mono-substituted sulfonyl oxetanes showed that the fragments had good half-lives across a broad pH range (1-10). Solubility studies were limited to three compounds and it was found that solubility was low in aqueous phosphate buffer (pH 7.4).

In 2017, Bull's group used a similar strategy in the divergent synthesis of 50 bifunctional cyclopropane-based fragments from a single precursor.[46] Co-catalysed cyclopropanation was used to access key building blocks, *trans*- and *cis*-ethyl 2-(phenylsulfanyl)-cyclopropane-1-carboxylates **44**, on gram-scale in high yield. Notably, either enantiomer of each diastereomer could be accessed in $\geq$97% ee using chiral staionary phase

(CSP) chromatography. Orthogonal elaboration in two directions was demonstrated using sulfide and ester motifs as synthetic handles. Ester to acid hydrolysis followed by coupling chemistry gave amides **45**. Further functionalisation on the sulfide by oxidation with excess *m*-CPBA gave sulfones **46**. Some examples of fragments synthesised in this manner are shown.

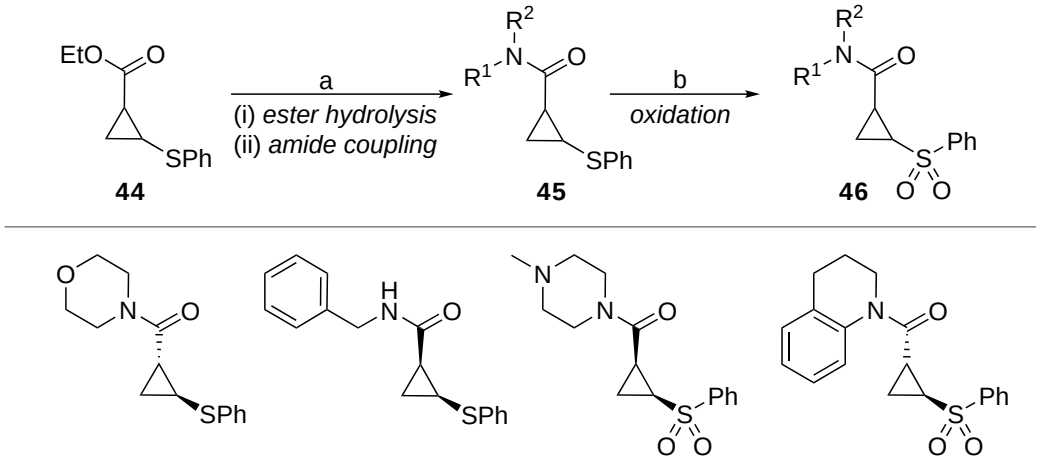

Scheme 1.10

Direct diversification of the cyclopropyl ring was achieved by sulfoxide-magnesium exchange followed by reaction with various electrophiles (Scheme 1.11). To this end, sulfides **44** were oxidised to sulfoxides **47** with *m*CPBA and reacted with *i*-PrMgCl. Reaction of the so-generated cyclopropyl Grignard reagent with various electrophiles gave fragments such as **49** and **50**. Fragment **51** was formed following intramolecular lactonisation with the ester. (Hetero)aryl cyclopropanes could also be synthesised by Negishi coupling of the cyclopropyl organozinc species with different aryl bromides to form fragments such as **52** and **53**.

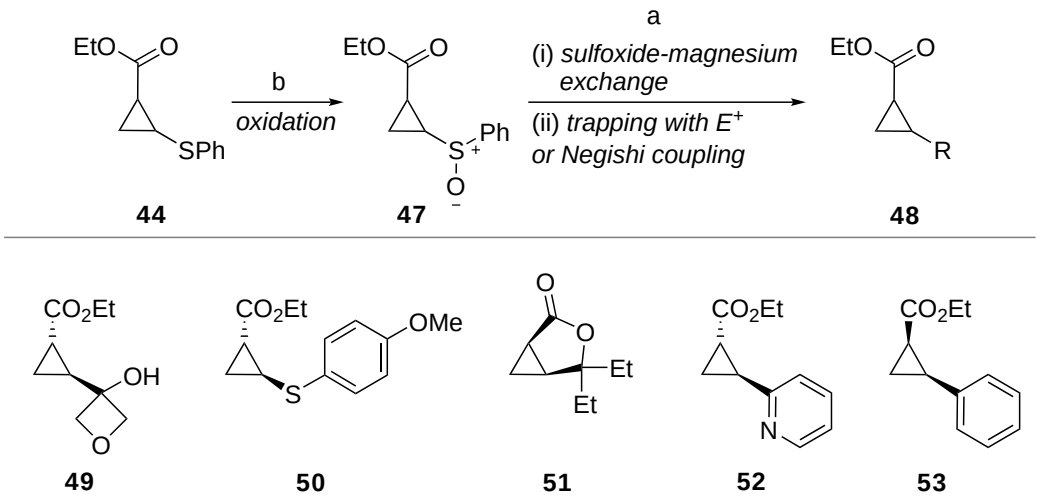

(a) *m*CPBA (b) (i) *i*-PrMgCl, –78 °C (ii) E^+ or ArBr, $ZnCl_2$, $Pd_2(dba)_3$, (*t*-Bu)$_3$P, 0-25 °C

Scheme 1.11

Correlation between AlogP and MW showed that the 50-fragment library occupied new areas of chemical space. PMI shape analysis using LLAMA (Lead-Likeness and Molecular Analysis) software indicated that the collection had good 3-D shape and that there was significant shape diversity between the different diastereomers.

Young's group used a scaffold diversity approach in the synthesise of a family of *N*-protected 2,3-, 2,5- and 2,6-disubstituted-piperazine scaffolds.[47–49] Three distinct synthetic routes were developed to access each substitution pattern starting from amino acid **54** and amino alcohol **55** (Scheme 1.12). In each case, cyclisation reactions of intermediates **56**-**59** were used to access the piperazine scaffold. 2,3- and 2,6-disubstituted piperazines were isolated as single diastereomers following chromatographic separation of *cis*- and *trans*-**60** and *cis*- and *trans*-**61** respectively. In contrast, the synthesis of the 2,6-disubstituted scaffold was highly diastereoselective and could be tuned to favour the formation of either *cis*- or *trans*-**62**. Furthermore, each scaffold could be isolated as both (*R*)- and (*S*)-**54** and **55** are commercially available. Overall, 68 regio- and stereochemically-diverse scaffolds were synthesised in 4-6 steps and in most cases synthetic routes were shown to be scalable (multi-gram quantities). Scaffold elaboration is

currently underway with the aim to generate a library of sp^3-rich saturated compounds.

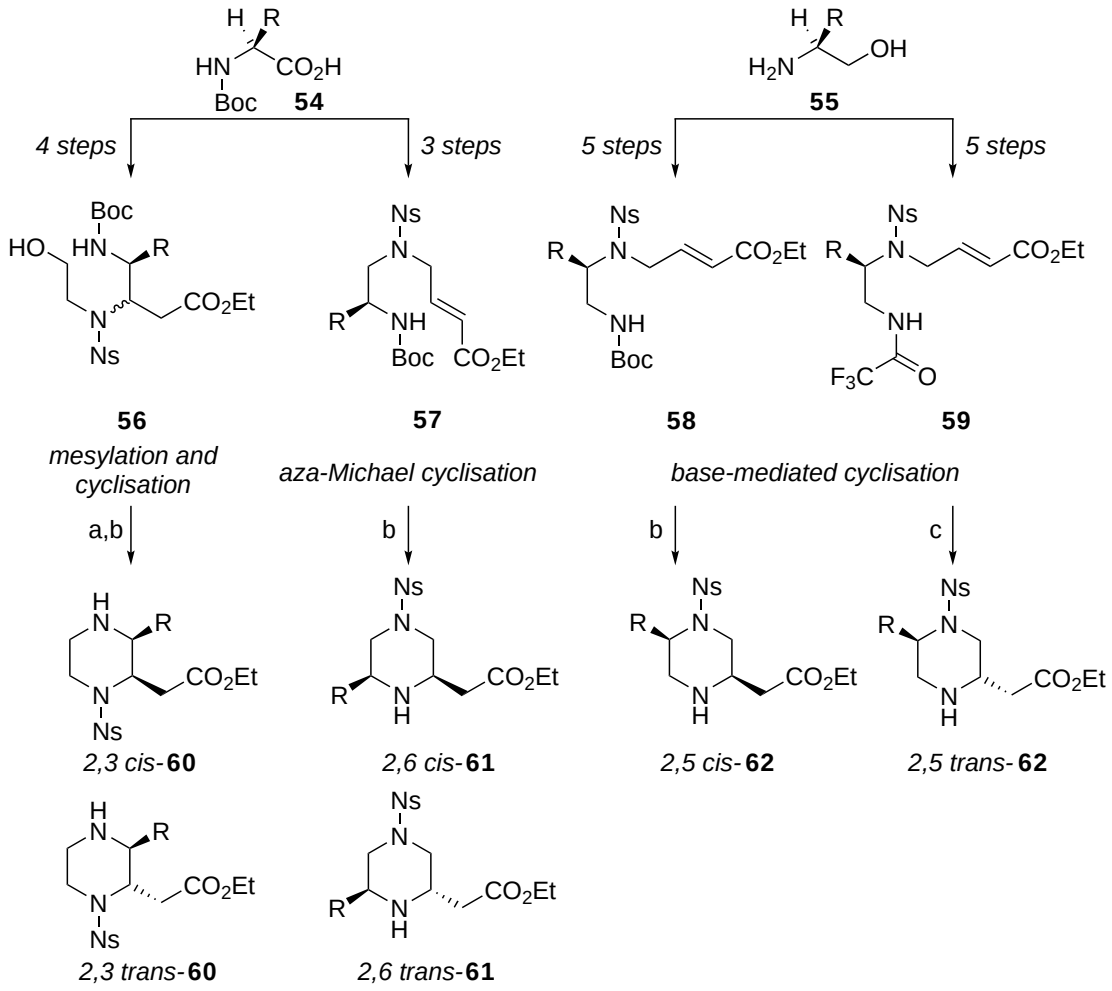

(a) Et_3N, MsCl (b) (i) TFA (ii) $NaHCO_3$ (c) (i) Cs_2CO_3 (ii) $NaBH_4$

Scheme 1.12

The efficiency of using a scaffold diversity synthetic approach to 3-D fragment generation was demonstrated by Spring and co-workers with the synthesis of 42 partially saturated bicyclic heteroaromatic fragments.[50] Pyrazole and pyridine-based building blocks **63** and **64** were synthesised in a similar manner (Scheme 1.13). Terminal alkene groups were attached to the heterocyclic core using Pd-catalysed, Suzuki-Miyaura cross-coupling and alkylation respectively. RCM of the alkenes then furnished carbocycles, **63** and **64**. Changing the carbon chain length of the installed alkene groups allowed for control over both ring size and alkene position. Diversification of the endo-

cyclic alkene using simple one-, two- or three- step modifications allowed for elaboration of the saturated ring system and the generation of new stereocentres. Overall, a library of 50 fragments was synthesised and a representative set of the collection is shown.

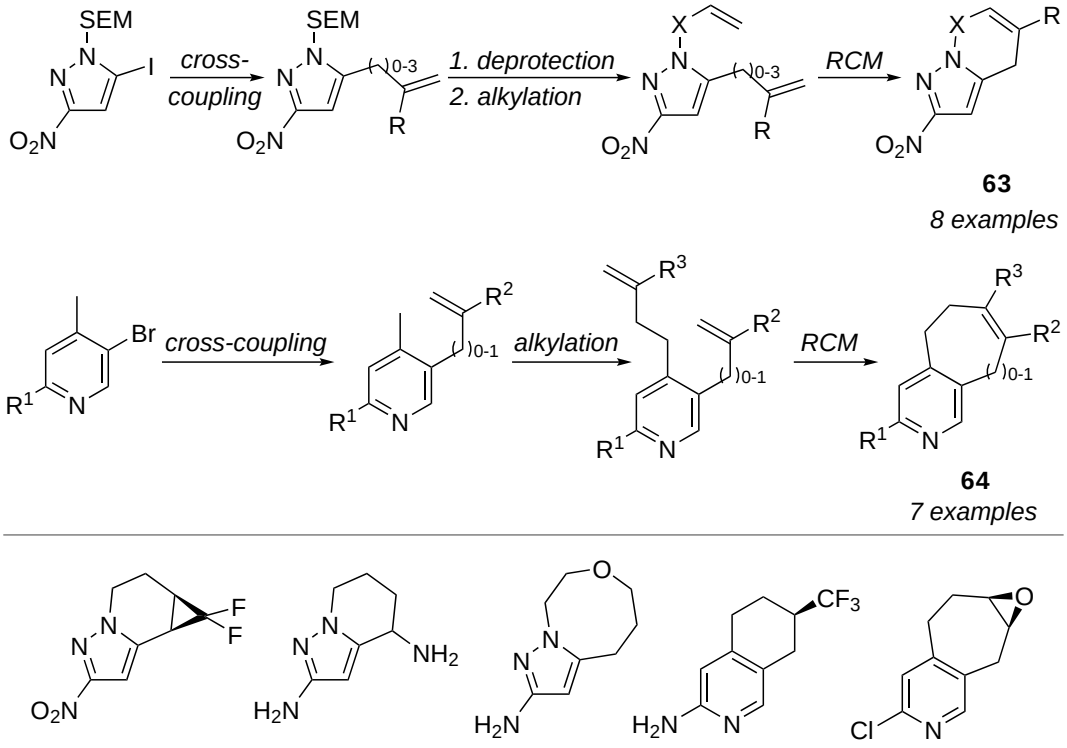

Scheme 1.13

Calculated physicochemical properties for the library fell well within the boundaries defined by the Ro3. Physicochemical properties, MW, SlogP, fraction aromatic and the number of stereogenic centres, compared particularly favourably with ChemBridge and Maybridge commercial collections. Furthermore, these fragments contain 3-D growth vectors allowing for future elaboration.

In 2019, Spring's group used a similar approach in the synthesis of sp^3-rich, spirocyclic 3-D fragments.[51] Eight carbocycle/heterocycle containing, spirocyclic-based scaffolds were synthesised in < 5 steps from α,α-disubstituted amino acid building blocks **65** (Scheme 1.14). The terminal alkene groups of starting materials **65** were used to synthesise carbocycle **66** *via* RCM. An intramolecular, base-mediated reaction between

the alcohol and *N*-Boc group of intermediate **66** formed oxazolidinone **68a**.

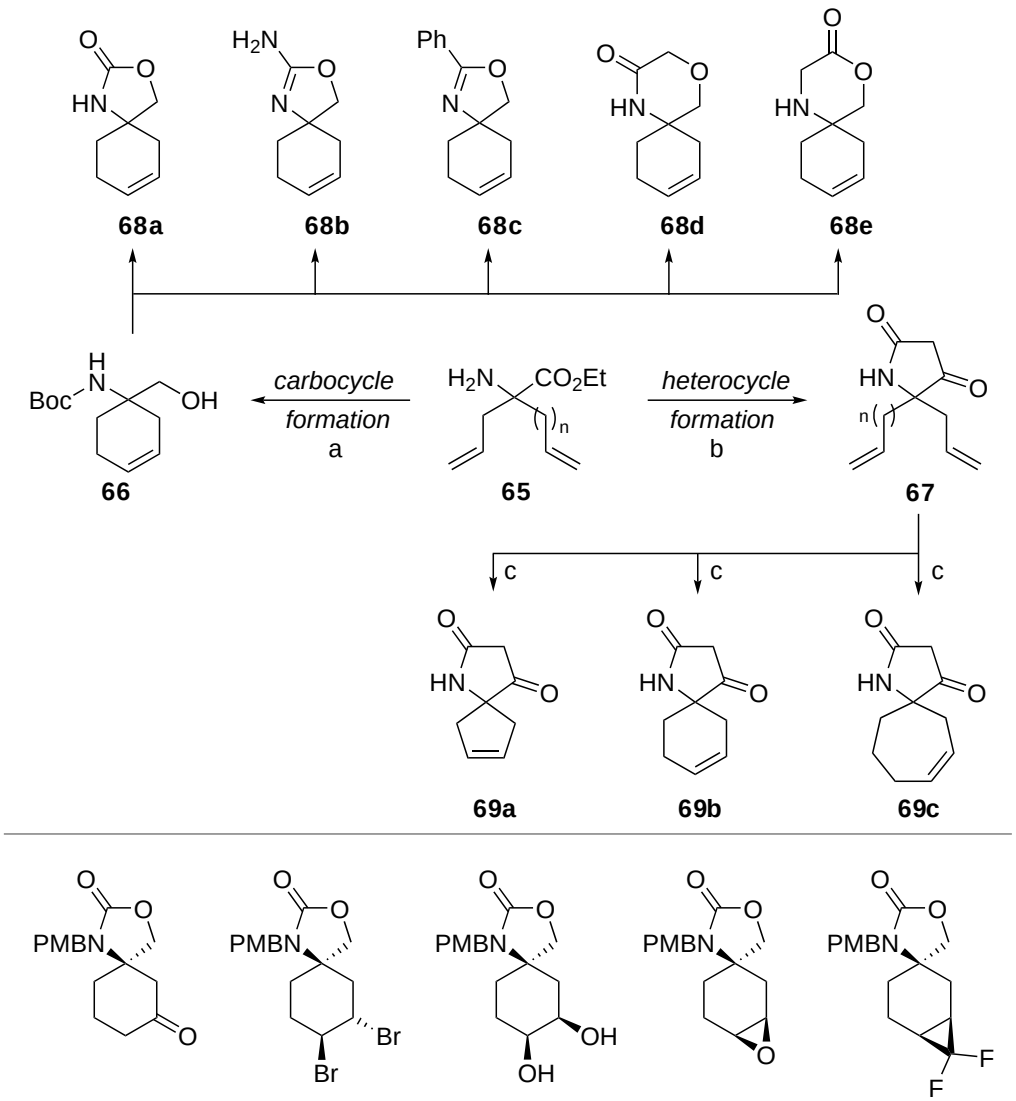

(a) (i) Boc_2O (ii) Grubbs II, reflux (iii) $LiBH_4$, (b) (i) ethyl malonyl chloride, Et_3N (ii) *t*-BuOK then aq. HCl (c) Grubbs II, 70 °C

Scheme 1.14

Similarly, amino oxazoline **68b**, phenyl-substituted oxazoline **68c** and morpholines **68d** and **68e** were synthesised by *N*-Boc removal followed by reaction of the alcohol and amine with different pairing reagents. Alternatively, the ester and amino synthetic handles in **65** could be used to generate the heterocyclic motif of **67**. RCM of intermediate **67** was used to synthesise 5-, 6- and 7- membered ring scaffolds **69a-c**.

Crucially, it was also shown that asymmetric synthesis of scaffolds **69a-c** was possible by synthesising enantiomerically pure (*R*)-**69b**. Derivatisation of the alkene in scaffolds **68a-e** and **69a-c** by Wacker oxidation, dihydroxylation, difluorocyclopropanation, aziridination, epoxidation and dibromination gave 28 3-D, spirocyclic fragments, five of which derived from compound **69b** are shown in Scheme 1.14.

Analysis of physicochemical properties (MW, HBD, HBA and total polar surface area (TPSA)) showed that the library was Ro3 compliant. Overall, the spirocyclic scaffold was found to impose rigidity to the library. The synthesised compounds also had a low lipophilicity especially when compared against the commercially available Maybridge core fragment collection. Fsp^3 centres (0.52), fraction of aromatic rings and number of stereogenic centres were also found to be higher than commercial compounds suggesting that these spirocyclic fragments had greater stereochemical diversity. PMI analysis against both the 1000-member Maybridge library and a 147 fragment sub-set (with similar heavy atom count) showed that none of the synthesised spirocyclic fragments exhibited ΣNPR 0-1.1 whereas 70% of the Maybridge collection and 75% of the sub-set were found to lie within this area of the plot.

Clausen recently reported the synthesis of 115 fluorinated, Fsp^3-rich fragments, which were primarily designed to both increase structural diversity and facilitate rapid ^{19}F based NMR screening.[52] Initially, cycloaddition and Michael addition initiated cyclisations were used to construct nine shape-diverse scaffolds **74-82** from trifluoromethylated α,β-unsaturated compounds **70-73** (Scheme 1.15).

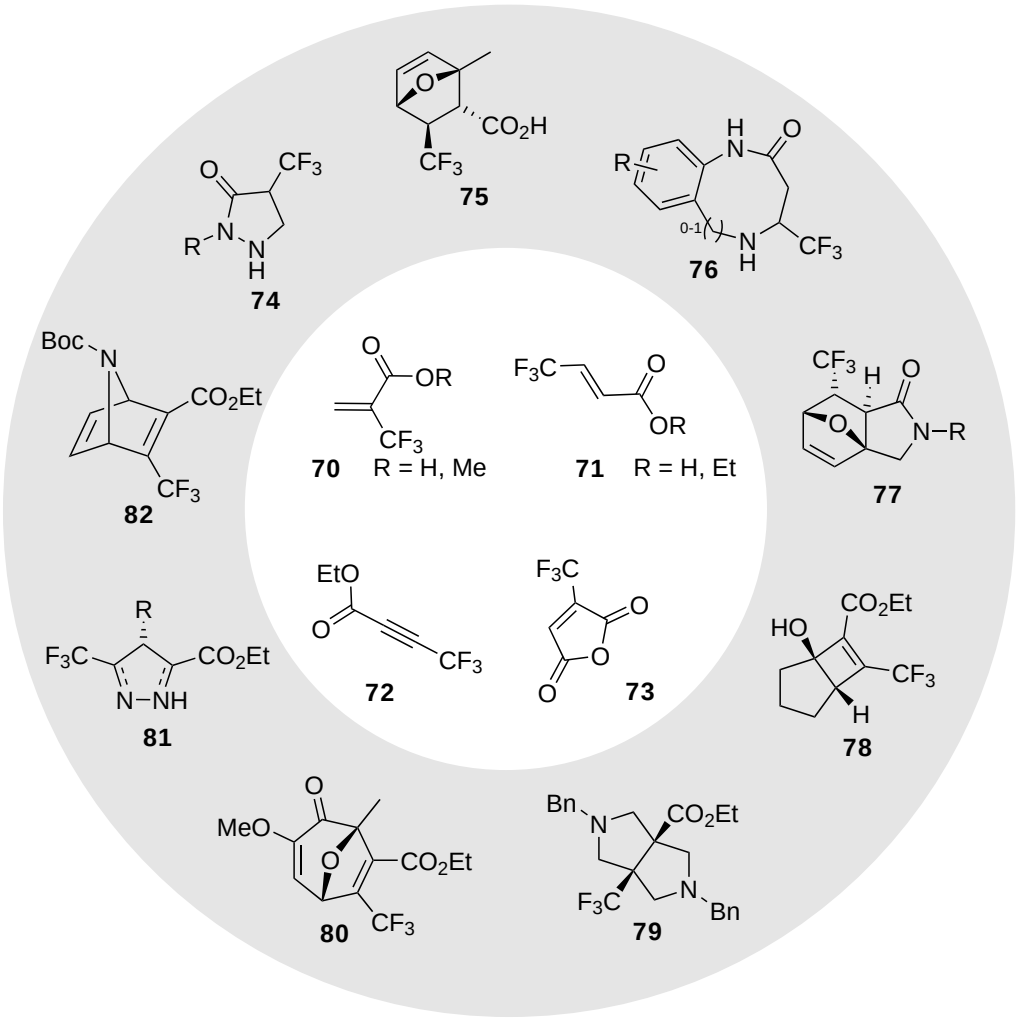

Scheme 1.15

Scaffold elaboration of modules **74**-**82** was carried out using 3-5 synthetic handles in < 5 steps. For example, hydrogenation, cycloaddition or oxidation of the alkene in scaffolds **78**, **82** and **77** gave fragments **83**, **84** and, after another two transformations, **85** respectively (Scheme 1.16). Alternatively, reduction of the ester and *N*-functionalisation of scaffold **79** gave fragment **86**.

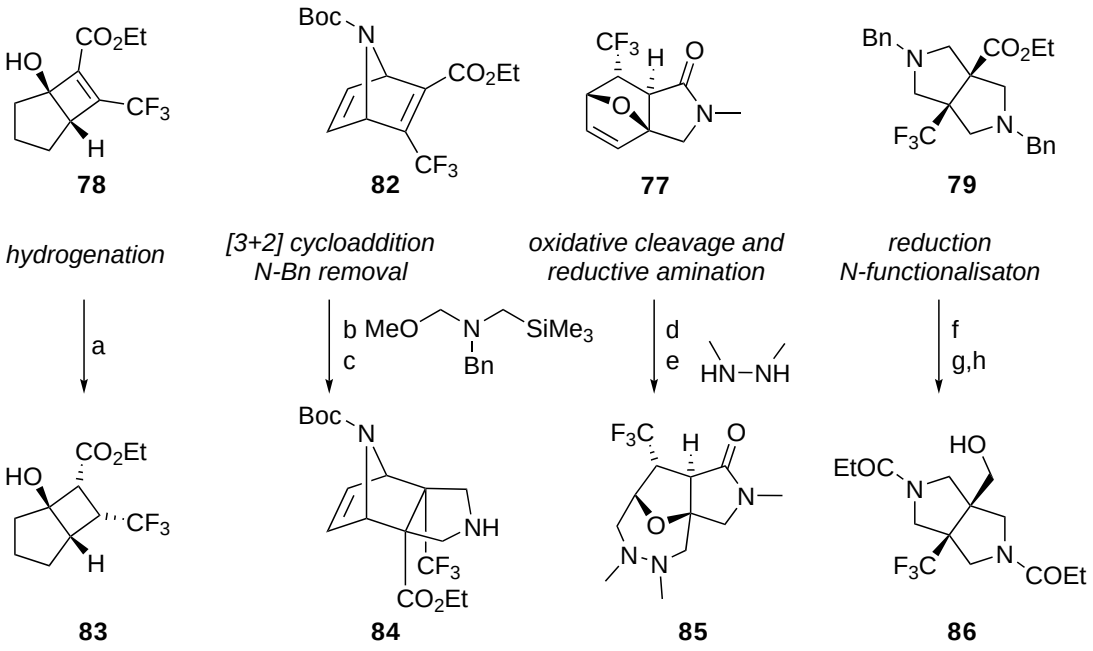

(a) Pd/C, H_2 (b) TFA (c) Pd/C, H_2 (d) *N*-methylmorpholine oxide, $K_2OsO_4 \cdot 2H_2O$ (e) (i) $NaIO_4$ then DMS (ii) Amine then $NaBH_3CN$ (f) $LiAlH_4$ (g) Pd/C, H_2 (h) Et_3N, propionyl chloride

Scheme 1.16

The calculated physicochemical properties (MW, AlogP, HBA, HBD, Fsp^3) of the 115 compound collection fit well within the Ro3 defined boundaries. In particular, ALogP (0.8) was found to be significantly lower when compared to two commercially available fluorinated fragment collections. In addition, the synthesised compounds were found to have high Fsp^3 (0.7) and natural product-likeness, the latter determined against a collection of 2712 natural products. The molecular shape of the synthesised library was evaluated by PMI analysis and compared to both a commercial fluorinated fragment library (Key Organics) and a collection of 1356 natural products. Only 5% of synthesised compounds were found in the ΣNPR value < 1.1 section of the plot indicating good 3-D shape. Interestingly, the distribution of conformations between the library and the natural product collection were similar confirming a high degree of natural product-likeness. Screening of 102 compounds against four protein targets (p70S6K1, p38γ, BACE1 and DC-SIGN) by ^{19}F NMR spectroscopy gave 30 hits with an impressive hit rate of 3–11%. Hits were found for eight of the nine scaffold classes emphasising

the importance of structural diversity in screening collections.

1.5.5 Fragment Synthesis Using Common Methodology

Fragment synthesis based on or around a single piece of common methodology can offer an efficient route for library generation. Using this approach, structural diversity can be introduced directly by simply changing the starting material. In this way, long multi-step and bespoke synthetic routes can be avoided.

The versatility of this synthetic approach was illustrated by Fagnou and co-workers in the synthesis of substituted isoquinolines and 3,4-dihydroisoquinolines using a mild, Rh(III)-catalysed reaction (Scheme 1.17).[53] However, it should be noted the reaction was developed as a general strategy to access the isoquinoline group and was not originally intended for fragment synthesis.

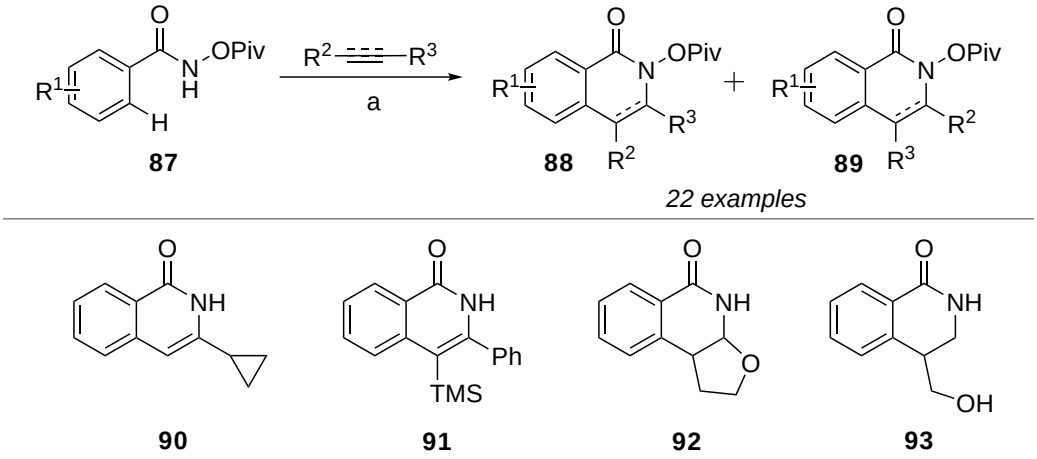

Scheme 1.17

The nitrogen motif of **87** acts as both an internal oxidant (for Rh catalyst turnover) and directing group (to effect cyclometalation at the C-H bond). Alkyne or alkene insertion and reductive elimination of the C-N bond gave heterocycles **88** and **89**. Where applicable, regiosomers **88** and **89** could be separated by chromatography. Alkynes, terminal alkynes and alkenes were all tolerated yielding both monosubstituted iso-

quinolones such as **90** and **91** together with saturated heterocycles including **92** and **93**. In this way, 22 isoquinolones with various substitution patterns were generated.

Rees and Murray have highlighted the importance of Fagnou's work in the field of FBDD by applying Rh(III) chemistry in the elaboration of dihydroisoquinolone **94** (Figure 1.8). Fragment **94** was initially identified as an attractive starting point for fragment elaboration due to its favourable physicochemical properties (MW 147, ClogP 1.0 and aqueous solubility > 5 mM) and structural simplicity (one polar binding group). Fagnou's synthetic methodology[53] was used to incorporate synthetic handles, heteroatoms and binding groups at multiple positions on the dihydroisoquinolone scaffold, as indicated in Figure 1.8.

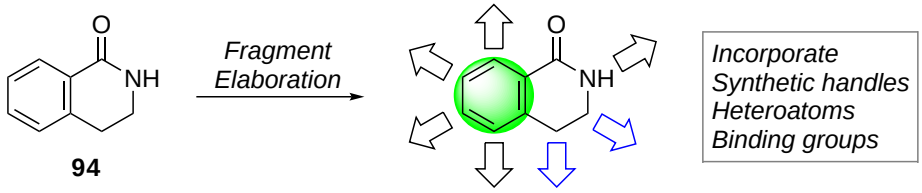

Figure 1.8: Proposed Strategy for Fragment Elaboration of Dihydroisoquinolone

Dihydroisoquinolones, **97** and **98** were accessed from hydroxamates **95** using Rh(III)-catalysed C-H activation chemistry (Scheme 1.18). Modifications at different positions of the dihydroisoquinolone core were made possible by simply changing the aryl group (green) of hydroxamates **95** and/or R group (blue) of alkenes **96**. For example, reaction of hydroxamate **95** (with Ar = Ph) with *N*,*N*-dimethyl allylamine gave fragment **99** as a single regioisomer with favourable physicochemical properties (HAC 15, MW 204, ClogP 1.3, aqueous solubility ≥5 mM). Alternatively, reaction of hydroxamates **95** in which the Ar group is an aryl aromide with *N*,*N*-dimethyl allylamine gave aromatic bromides (fragments **100** and **101**), providing opportunity for future fragment growth. Regioisomers of thiophene and thiazole groups were also successfully synthesised (compounds **102**-**105**), enabling the incorporation of heteroatoms for fragment growth and/or modulation of physicochemical properties. In this way, the use of

Rh(III) chemistry as FBDD-enabling methodology in the synthesis and elaboration of substituted dihydroisoquinolones was demonstrated.

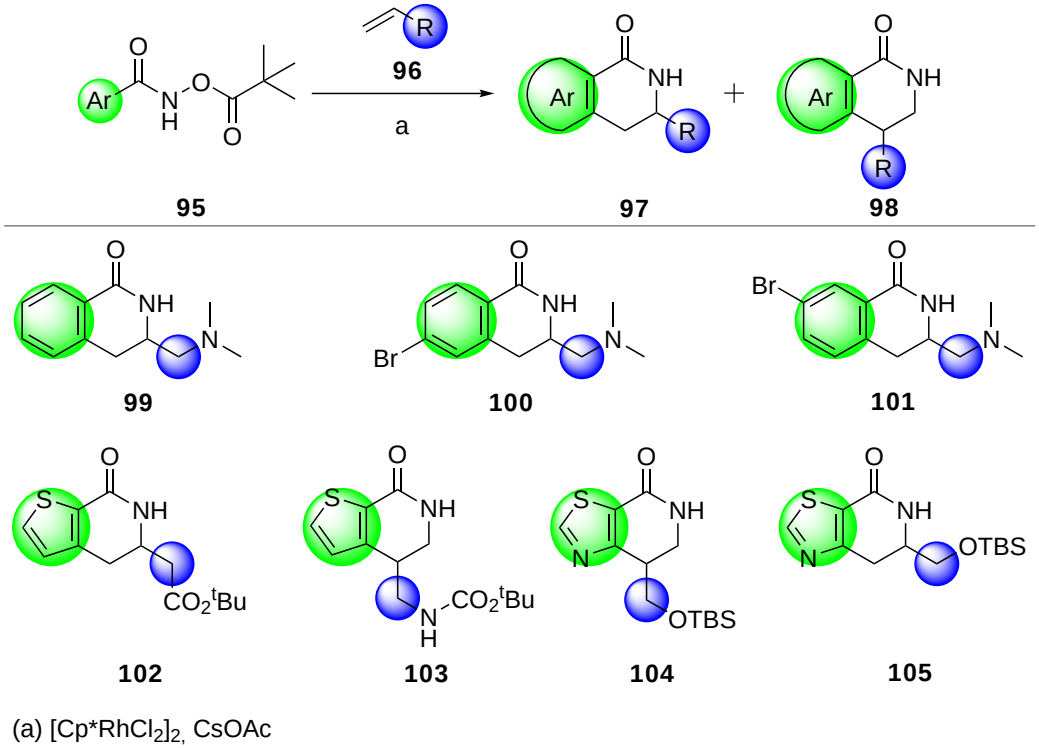

Scheme 1.18

In 2015, Willand reported the synthesis of 21 functionalised 2-isoxazoline 3-D fragments using a one-pot 1,3-dipolar cycloaddition between an alkene and a chloro-oxime (Scheme 1.19).[54] *In situ* chlorination of aldoximes **106** with NCS gave the hydroxyiminoyl chloride intermediates **107**. Reaction with Et_3N formed the nitrile oxide dipole which, when reacted with alkenes **108**, gave the desired spiro-isoxazolines **109**. Structural variation of oximes **107** and gem-disubstituted alkenes **108** led to the synthesis of 21 structurally diverse fragments, four of which are shown. Eight fragments were isolated as hydrochloride salts following removal of the Boc group. Notably, the lactone could be elaborated further by reaction with different amines.

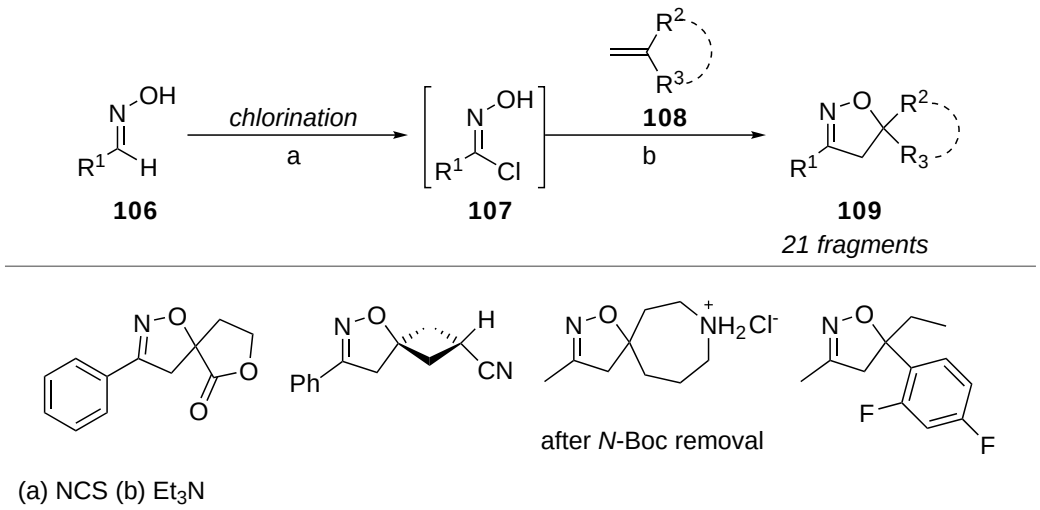

Scheme 1.19

The molecular shape of the compound collection was assessed by PMI analysis against 471 commercially available fragments. A mean ΣNPR of 1.19±0.08 indicated good 3-D shape compared to the commercial set (ΣNPR of 1.09±0.07) with most compounds adopting rod/spherical conformations. The MW, Fsp^3 and solubility were also determined. The Fsp^3 value ranged from 0.25-0.92 and the fragments had a suitable MW range of 140.2–291.3 Da. Importantly, 15 out of 18 fragments were $\geq$ 1 mM soluble in aqueous phosphate pH 7.4 buffered saline solution suggesting that the fragments would be suitable for screening.

Willand's group also reported the synthesis of 27 functionalised spirohydantoin 3-D fragments using a microwave assisted approach.[55] Classical conditions for spirohydantoin formation were optimised to reduce the reaction time, temperature and number of equivalents of cyanide. To this end, cyclic ketones **110** were reacted with ammonium carbonate and potassium cyanide under microwave conditions at 90 °C to give spirocyclic, spirohydantoin scaffolds **111** (Scheme 1.20). Structural diversity was introduced by changing the ring size and substitutents of ketones **110** to give 27 compounds. Selective *N*-alkylation of the hydantoin ring was also demonstrated providing a synthetic route to more elaborated compounds. A representative sample is shown. PMI analysis

of the fragment set indicated good 3-D shape and a high degree of shape diversity with conformations falling close to all three axes of the 2-D PMI plot. Physicochemical properties were in line with the Ro3. Importantly, the fragment set also showed good aqueous solubility with 24 out of 27 fragments being $\geq$ 0.8 mM soluble in aqueous phosphate pH 7.4 buffered saline solution.

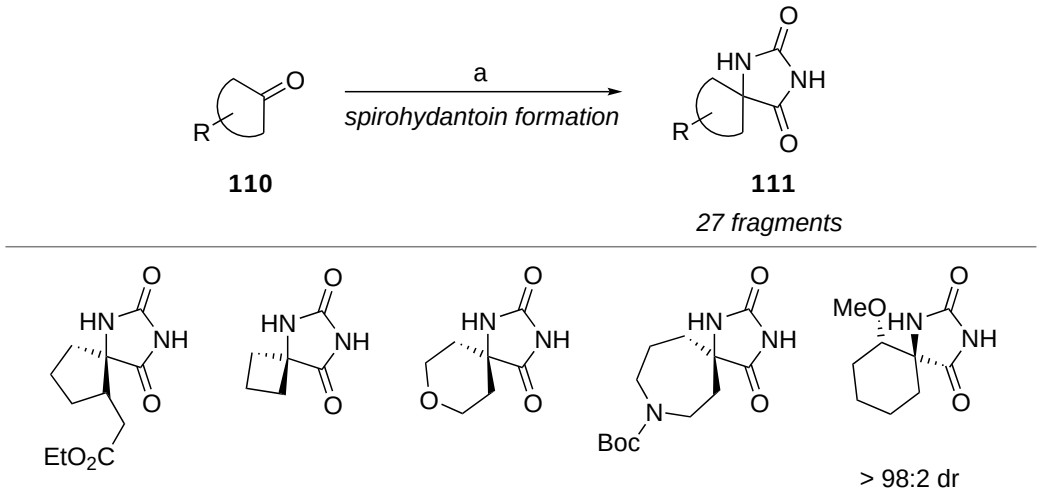

Scheme 1.20

Dömling and co-workers used a simple approach in the generation of 40 tetrazole compounds.[56] Both 5-substituted 1*H*- and 1-substituted 5*H*-tetrazoles were synthesised in order to assess differences in protein binding between the two isomers. Reaction between amines and cyano- and isocyanoacetyl methyl esters **112** and **113** gave the corresponding amides **114** and **115** (Scheme 1.21). Then, a 1,3-dipolar cycloaddition between nitriles **114** with sodium azide furnished the desired 1*H*-tetrazole motif **116**. Similarly, reaction between isocyanates **115** and TMS azide gave the isomeric 5*H*-tetrazoles **117**. In most cases, products would precipitate during aqueous work-up and could be easily isolated by filtration. Using this approach, 40 tetrazole-based fragments were synthesised in a highly efficient manner (< 3 steps). A representative set is shown. Physicochemical properties, MW and ClogP, were calculated and compared to a virtual library of 500 1*H*- and 5*H*-tetrazoles. The fragment library together with the virtual compounds was found to occupy fragment Ro3 space with most compounds

having MW < 300 Da and ClogP < 3.

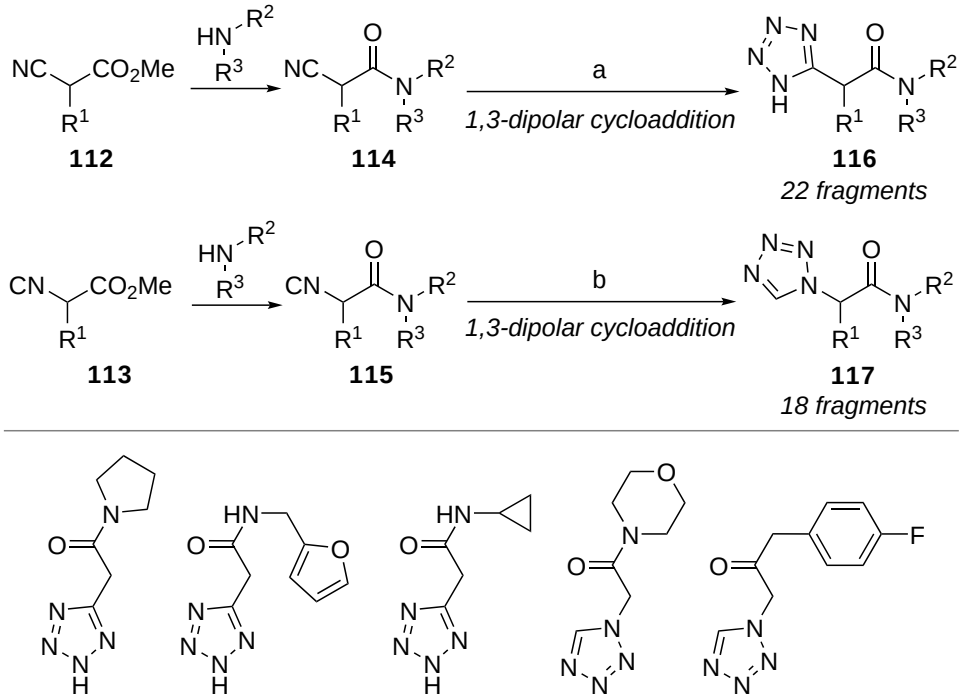

Scheme 1.21

In 2017, Mykhailiuk reported the use of a [3+2] cycloaddition approach to generate a library of spirocyclic pyrrolidine fragments.[57] An azomethine ylide was generated *in situ* from compound **119** using either catalytic TFA or LiF. Then, a [3+2] cycloaddition furnished the desired spirocyclic scaffold **120** (Scheme 1.22). Changing the electron withdrawing group (EWG), R group or X group furnished 20 structurally diverse compounds. The value of the library was demonstrated by modification of the deprotected amine, EWG or X group to give 13 building blocks. Importantly, it was shown that the compounds could be synthesised in high er using enzymatic resolution, chiral HPLC or a chiral auxillary. Overall, the synthesis was highly efficient (2 steps) and generated useful structures with two to three points for further diversification.

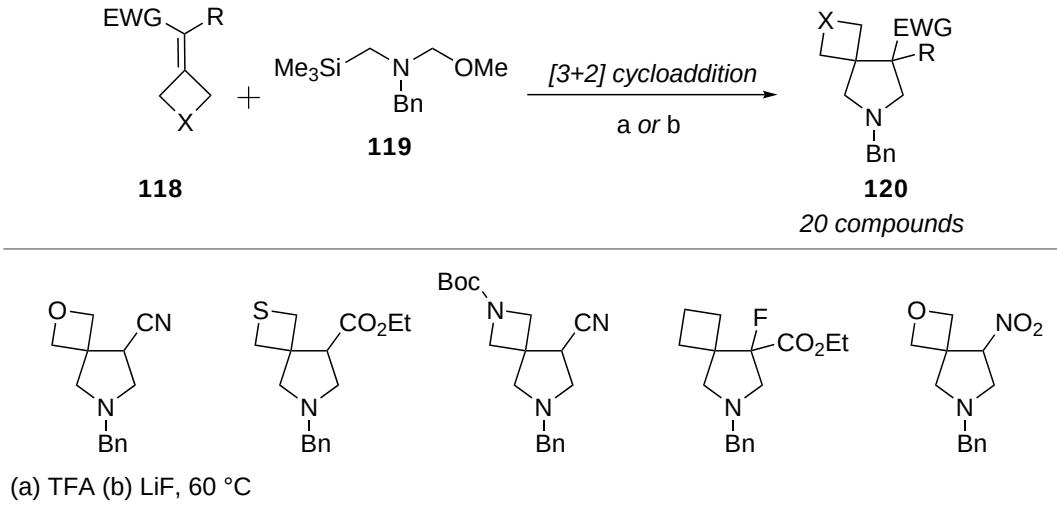

Scheme 1.22

Nelson and co-workers reported the synthesis of 22 bridged fragments based on a twisted bicyclic lactam scaffold.[58] To this end, bicyclo[3.3.1]nonane and bicyclo[4.3.1]decane ring systems, **123** and **124**, were accessed in moderate yield using *n*-Bu_2SnO-mediated cyclisation (Scheme 1.23). Using this approach, fragments **128** and **129** were accessed directly from building block **122**. The ketone group in keto-lactams **123** could be further functionalised using a range of transformations. Ring annulation gave tricyclic fused fragments such as **125**. Ketone reduction to the alcohol followed by base-mediated reaction with aryl halides furnished ethers including **126**. Chloroenamine formation with $POCl_3$ followed by Suzuki-Miyaura cross-coupling gave arylated compounds such as **127**. PMI analysis of the 22 fragment library, within the LLAMA software, showed that the bicyclic bridged scaffold was highly three-dimensional. The fragment collection also had favourable physicochemical properties, having controlled HAC < 17 and ClogP < 2.5 from the outset. Furthermore, the fragments were found to be structurally unique when compared against a subset of commercially available compounds sourced from the ZINC database.

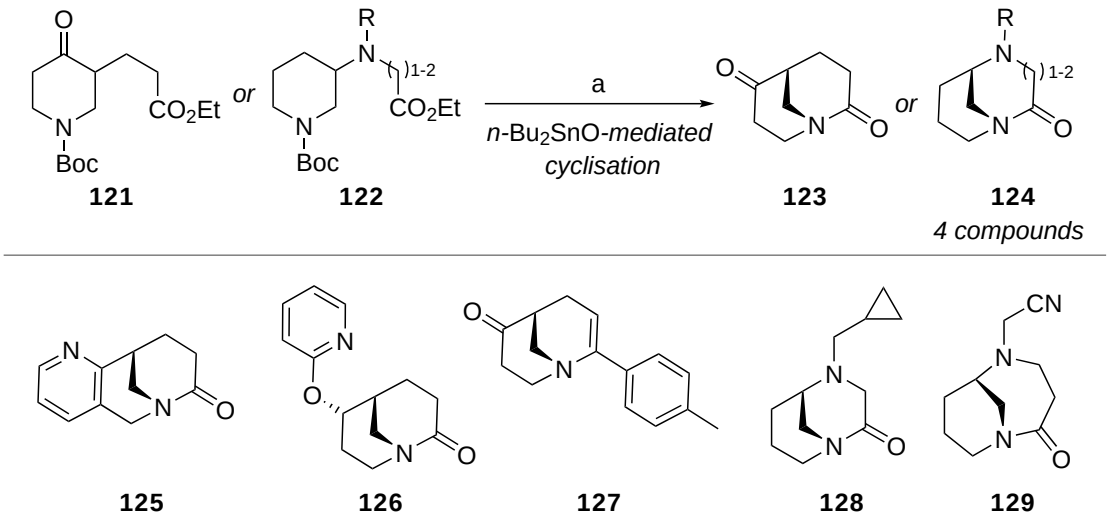

(a) (i) NaOH, 70 °C (ii) 6 N HCl (iii) *n*-Bu_2SnO, 120 °C

Scheme 1.23

Spring's group used [3+2] or [2+2] cycloaddition reactions in the synthesis of nine heterocyclic spirocyclic fragments.[59] Alkenes **130** and **132** as well as imine **131** were synthesised in 1-2 steps from commercially available starting materials (Scheme 1.24). Then, a regioselective [3+2] or [2+2] cycloaddition furnished spirocyclic heterocycles **133a-c** and **134** in one step, directly. The spirocyclic motif of **136** was constructed following cycloaddition using the amine and ester groups as synthetic handles. Ester reduction followed by base-mediated intramolecular ring closure generated carbamate **136**. Removal of Bn, Ac and PMP protecting groups led to a structurally diverse set of [4,5]-, [4,6]-, [5,5]-, [5,6]- and [5,7]- spirocyclic fragments incorporating a variety heterocycles in < 3 steps. Furthermore, the fragments contain ester and amine groups allowing for further elaboration. Physicochemical properties (MW, ClogP, PSA, HAC, HBA, HBD, RBN) for the deprotected scaffolds were calculated and showed that all synthesised fragments were Ro3 compliant. Values for the Fsp^3 hybridised centres (0.54), mean number of stereogenic centres (1.20), molecular shape index and molecular complexity indicated good 3-D shape.

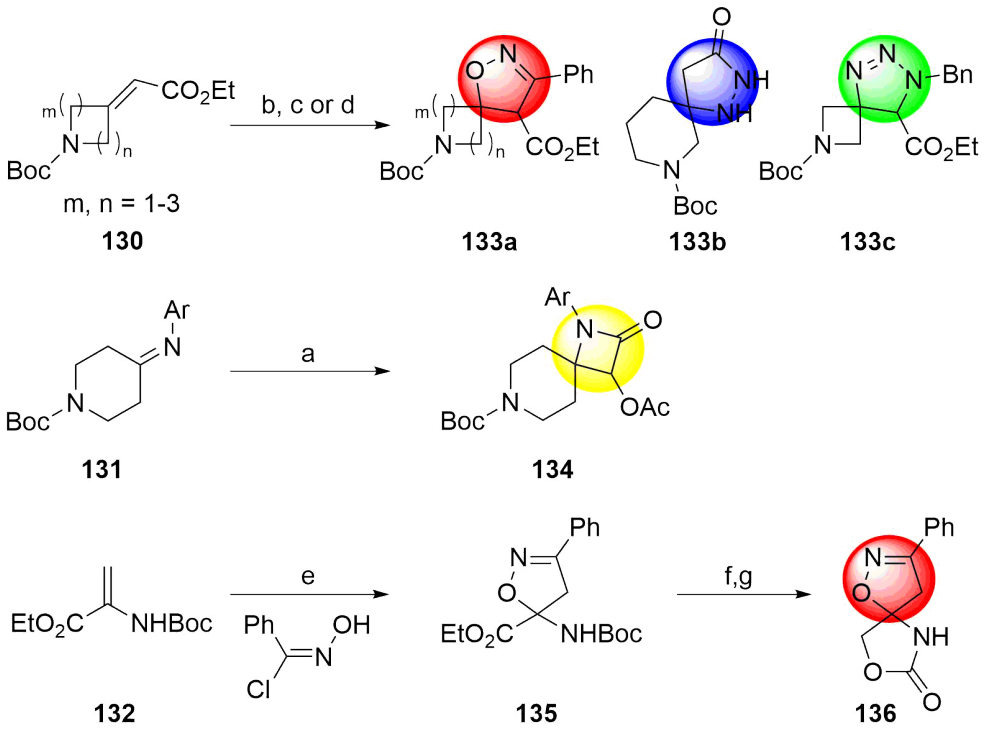

(a) acetoxyacetyl chloride, Et_3N, –78 °C-rt (b) ONCPh, 100 °C (MW) (c) $NH_2NH_2{\cdot}H_2O$, 70 °C (d) BnN_3, 100 °C (e) Et_3N (f) $NaBH_4$, 0 °C-rt (g) KO*t*Bu, 0 °C

Scheme 1.24

Recently, Erdman's group reported using a chiral auxillary controlled 1,3-dipolar cycloaddition reaction in the design and synthesis of 48 pyrrolidine-based fragments, which were isolated as single enantiomers (Scheme 1.25).[60] Initially, the imine was formed by condensation between heterocyclic aldehydes **137** and chiral amine **138**. Coordination to either a Ag(I) or Cu(I) catalyst followed by reaction with acrylonitrile gave cycloadducts *endo*-**139** or *endo*-**140** and *exo*-**141** or *exo*-**142** respectively. The use of the Oppolzer camphorsultam chiral auxiliary (COX) allowed access to both enantiomers. Derivatisation of the chiral auxillary gave rise to methyl ester and alcohol containing fragments *endo*-**143** and *endo*-**144**. Structural diversity could also be introduced by simply changing the heteroaromatic group in aldehydes **137**. A representative sample of the saturated, shape-diverse 48 fragment collection is shown. The physicochemical properties and molecular shape of these 3-D pyrrolidine fragments were assessed using AbbVie's internal design platform. Calculated physicochemical

properties (MW, AlogP and Fsp^3) fit well within the Ro3 guideline. 3-D Shape was assessed by both PMI analysis and PBF. A total of 47 out of 48 fragments were found to have a ΣNPR $\geq$ 1.07 and PBF score $\geq$ 0.6 suggesting good 3-D shape.

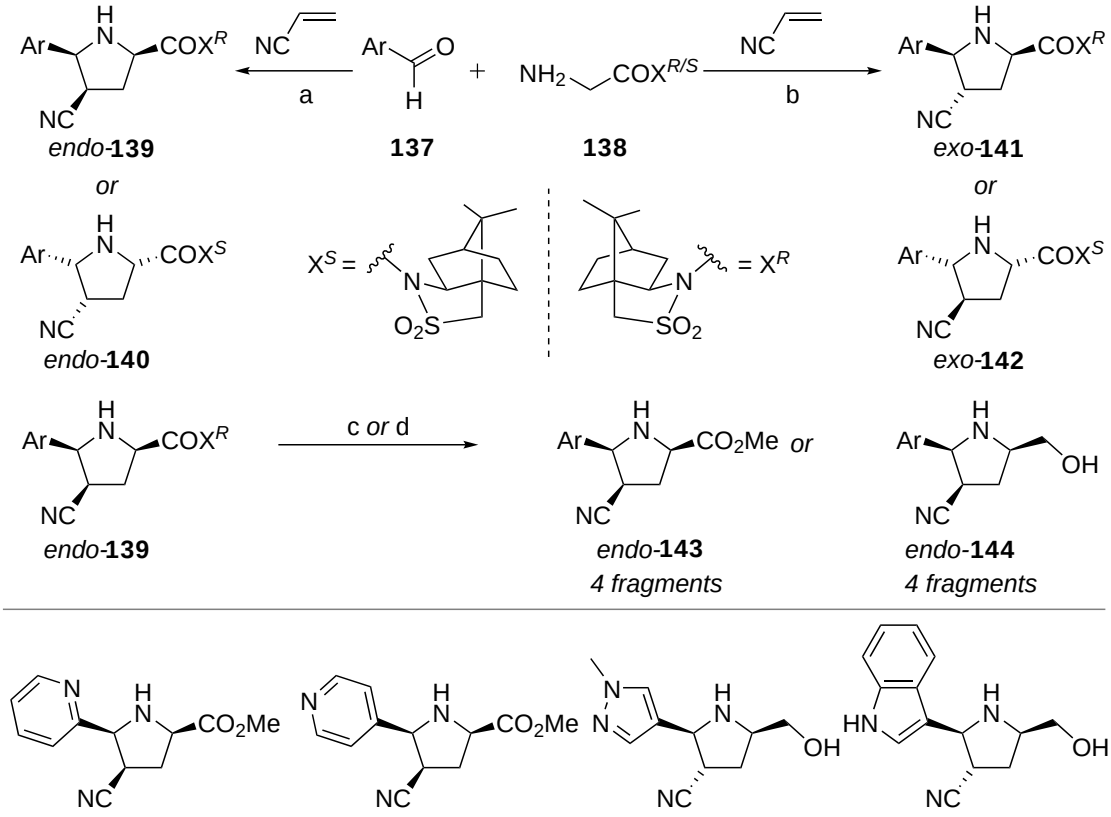

(a) 10 mol % AgOAc (b) 5.0 mol % $Cu(MeCN)_4PF_6$, 5.5 mol % dppb (c) $Sm(OTf)_3$ (d) $NaBH_4$

Scheme 1.25

In 2019, Grainger and co-workers developed a photocatalytic route to α-aryl heterocyclic fragments using photocatalysis.[61] Reaction conditions were established using a nanoscale high-throughput experimentation platform which allowed for the screening of 768 reactions on a nanomolar scale. The optimised conditions were then used to carry out cross-dehydrogenative coupling between heterocycles **145** and heteroarenes **146** to give 112 α-arylated heterocycles **147** (Scheme 1.26). Notably, by changing the cyclic amine and/or heteroamine starting substrate, 4-, 5- and 6-membered rings with different heteroatoms (N, O, and S) could be synthesised. Spirocyclic, bridged and fused bicyclic scaffolds were also generated. Scale-up using continuous flow chemistry

was also demonstrated with **149** being synthesised on a multi-gram scale (1.3 g) in moderate yield (58%).

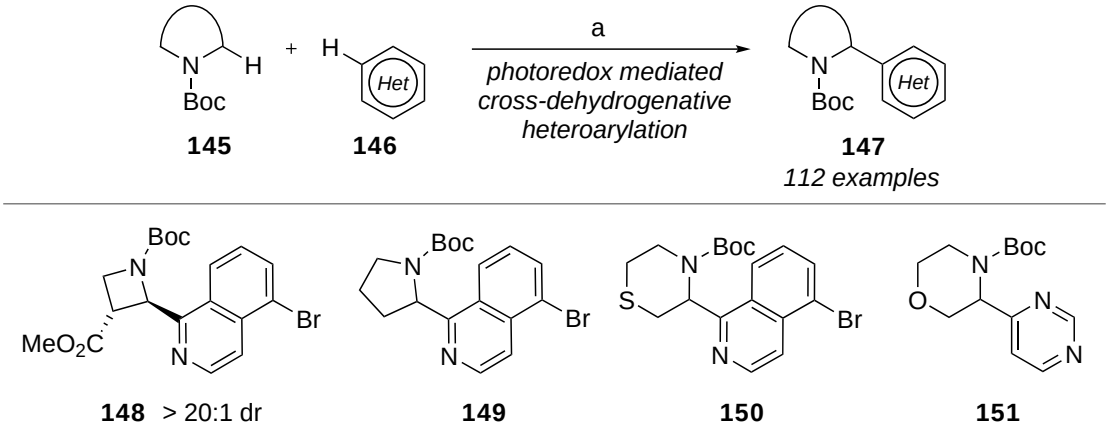

(a) Ir photocatalyst, $(NH_4)_2S_2O_8$, $TsOH{\cdot}H_2O$, blue light

Scheme 1.26

Importantly, Grainger's synthetic approach addresses challenges in fragment elaboration by providing a strategy for late stage C-H functionalisation of medicinally-relevant heterocycles during fragment hit-to-lead optimisation. Furthermore, the authors noted that synthetic handles present in the target compounds (nitriles, esters, ketones, amides and halogens) could also aid in future elaboration.

Recently, Bloomfield and co-workers used a [2+2] photocycloaddition to generate 54 3-D bridged pyrrolidine fragments.[36] Photo-induced [2+2] cycloaddition of dienes **152** or **153** afforded the bridged pyrrolidine scaffold (Scheme 1.27).

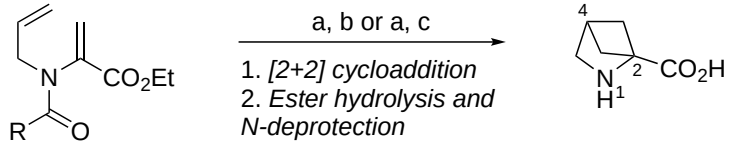

(a) *hv* (b) 6 N HCl (c) aq KOH

Scheme 1.27

Analogues of 2,4-methanoproline **154** (compounds **155** and **162**) were then used to

synthesise two sets of 1,2- and 1,2,4-substituted fragments (Scheme 1.28). To this end, functional group interconversion of the carboxylic ester and *N*-group of bridged pyrrolidine **155** gave amines **156**-**158**. Subsequent *N*-functionalisation with different acids or isocyanates generated fragments **159**-**161**. A similar approach was used to synthesise 1,2,4-substituted fragments **166** and **167**. In this case, the 4-carboxylic ethyl ester of bridged pyrrolidine **162** could be selectively modified over 3 steps before functional group interconversion of the 2-carboxylic methyl ester. Using this approach, two parallel libraries of novel 1,2-substituted and 1,2,4-substituted bridged pyrrolidine 3-D fragments were synthesised.

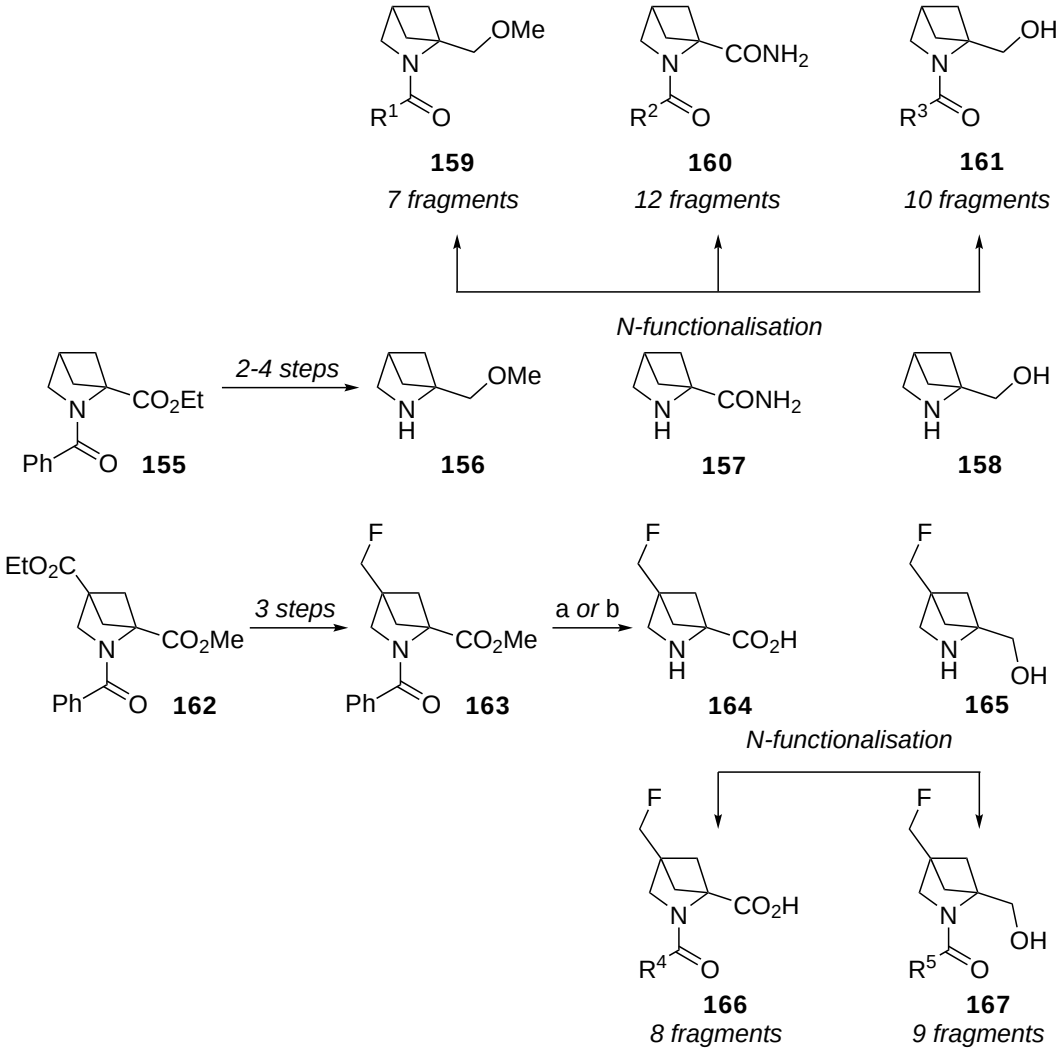

(a) TFA, H_2O (b) $LiAlH_4$, then ammonium formate, Pd/C

Scheme 1.28

Computational analysis by both PMI and PBF showed that the compound collection was significantly more 3-D than the commercially available AbbVie Ro3 compliant library with 91% of synthesised fragments occupying regions of 3-D space (ΣNPR $\geq$ 1.07 and PBF score $\geq$ 0.6). The calculated physicochemical properties were also found to fit within fragment Ro3 guidelines.

Recently, Shipman and co-workers reported the synthesis of an sp^3-rich, shape-diverse hydrazine-based fragment library.[62] The hydrazine scaffold was accessed using a two-step approach (Scheme 1.29). Firstly, a Ru-catalysed asymmetric transfer hydrogenation of protected hydrazine ketones **168** gave the corresponding alcohols **169** with high enantioselectivity. Structural diversity could be easily incorporated by varying the length of the linker and the R^1 group in protected hydrazine ketones **168**. Then, ring closure and stereochemical inversion using Mitsunobu conditions furnished substituted hydrazines **170** in high % ee.

Iterative functionalisation (acylation, reductive amination or Pd-catalysed Buchwald-Hartwig arylation) of each nitrogen atom following orthogonal *N*-Ts or *N*-Boc removal of hydrazine **171** gave the 22 compound library based on scaffold **172**. Importantly, % ee was maintained following *N*-functionalisation, to give enantioenriched products. Notably, three points of diversification furnished structurally diverse, 4- to 7- membered ring hydrazines with varied *C*- and *N*- substituents. A representative set is shown. PMI analysis using LLAMA software showed that the hydrazine-based compounds were shape-diverse and three-dimensional. Interestingly, the wide distribution of PMI data suggested that substituents R^1, R^2 and R^3 had a greater influence on 3-D shape than the central hydrazine scaffold.

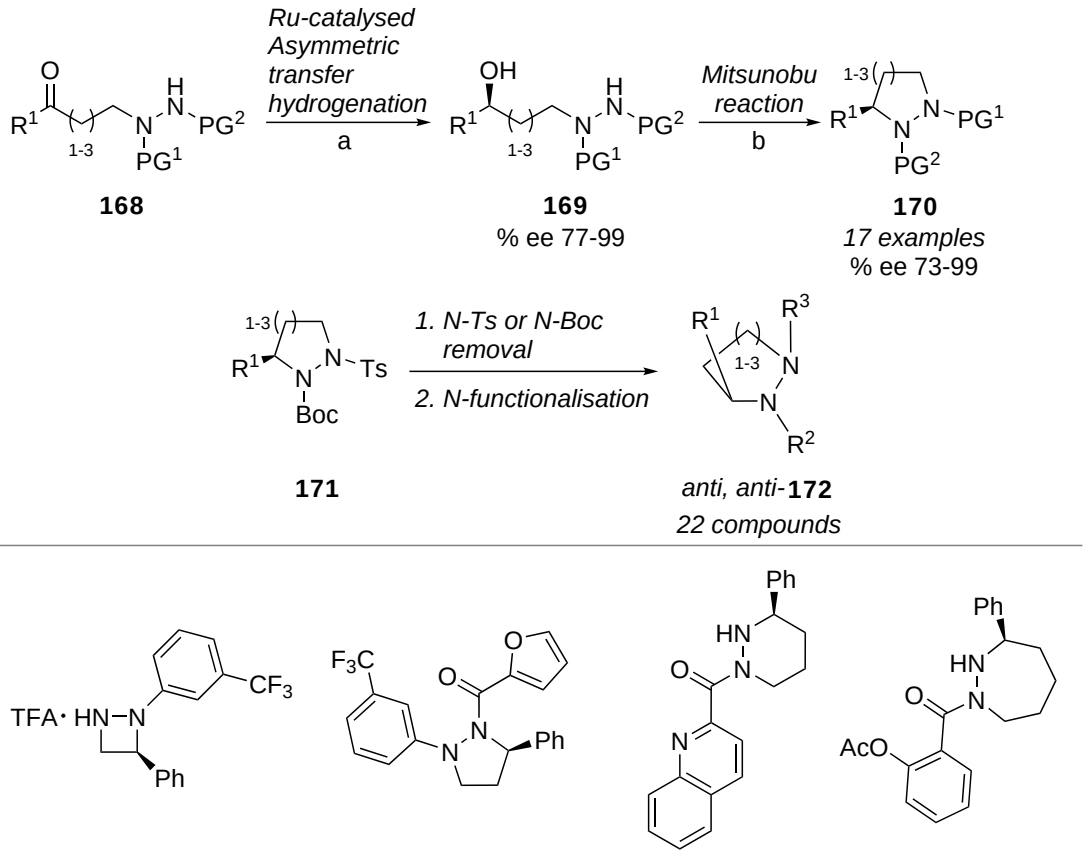

(a) *S,S*-[Ru] catalyst (1 mol%), HCO_2H:Et_3N (b) PPh_3, DEAD

Scheme 1.29

Since the 3-D Fragment Consortium and others first highlighted both the advantages and need for more 3-D shaped compounds in current collections, numerous synthetic strategies, methodology and other approaches for accessing 3-D fragments have been developed. Notably, the best examples have been reported in the last three to four years, the timescale that the work described in this thesis was carried out. DOS, scaffold diversity synthesis and use of common methodology have proved to be the most effective strategies for 3-D fragment synthesis. Indeed, Young, Nelson and Spring's groups have all demonstrated the use of a DOS approach in the construction of 3-D fragment libraries (< 100 compounds) in an efficient manner (typically < 5 steps).[31,39,40,63] Arguably, the most impressive work has been carried out using scaffold diversity synthesis demonstrated by Clausen's 115 fluorinated, Fsp^3-rich fragments library which was gen-

erated using this approach.[52] Spring's group have also demonstrated the effective use of this strategy in the synthesis of 42 structurally diverse bicyclic heteroaromatic fragments[50] and 28 3-D spirocyclic fragments.[51] Overall, fragment collections are highly shape-diverse and were accessed using a limited number of synthetic transformations. There are several examples of using common methodology in 3-D fragment synthesis. Although synthesis is highly efficient (typically 1-2 steps) and the chemistry reliable, structural diversity is often limited due to constraints inherent in the common methodology used.

1.6 Design and Synthesis of 3-D Fragments at York

Initial ideas on fragment design at York focused on synthesising fragments in under-represented areas of chemical space. In particular, 3-D fragments were of interest as most library collections contain an abundance of flat, heterocyclic compounds. The plan was to address this deficiency by designing and synthesising a library of 3-D fragments, which could be used to supplement commercial screening collections.

1.6.1 3-D Fragment Design, Shape Analysis and Selection

Disubstituted pyrrolidine and piperidines were chosen as 3-D scaffolds as they are the most common five- and six- membered nitrogen heterocycles in FDA-approved drugs (Figure 1.9).[64] Furthermore, the O'Brien group has expertise in this area of research, having worked on the chemistry of nitrogen heterocycles for several years.[65–68] Scaffolds were decorated with methyl and methyl ester or methyl and hydroxymethyl substitutents. The methyl group provides a hydrophobic substituent and could aid in future NMR screening campaigns (since its resonance would come in a region separate from resonances due to amino acids in the protein) whereas the carboxylic methyl ester and hydroxymethyl substituents were selected based on their ability to form hydrogen bonding interactions and act as synthetic handles for future elaboration. Variation at the nitrogen (H, Me, Ac and SO_2Me) introduced structural diversity and a second potential protein binding group. Furthermore, functionalisation of the secondary amine could provide a synthetic handle for future elaboration.

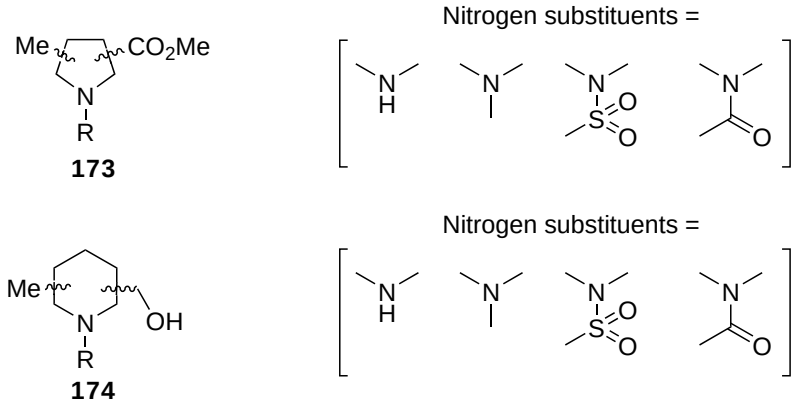

Figure 1.9: 3-D Fragment Scaffold Design with R = H, Me, Ac, SO_2Me

Initially, all possible regio- and diastereomers were virtually enumerated to give 56 and 92 racemic or achiral isomers for disubstituted pyrrolidines **173** and piperidines **174** respectively. Two sets of criteria were then used to select appropriate target 3-D fragments from the 148 compound set. Firstly, key physicochemical properties were controlled (HAC < 18, MW < 300 Da, AlogP < 3, HBA and HBD ≤ 3) to broadly fall within Ro3 fragment space. Secondly, PMI analysis was used to assess the degree of fragment 3-D shape and, uniquely, as a selection tool for synthesis in order to target compounds in under-explored areas of chemical space.

PMI plots were constructed using a Pipeline Pilot protocol, based on simple molecular mechanics, for all conformations with a relative energy of 1.5 kcal mol^{-1} above the energy of the global minimum energy conformer (582 conformations for scaffold **173** and 373 conformations for scaffold **174**). The value of ≤ 1.5 kcal mol^{-1} corresponds to all accessible conformers at physiological pH and temperature - for example, at 37 °C, a conformer that was 1.5 kcal mol^{-1} above the energy of the global minimum energy conformer would be present in $\sim$8%. Using this approach, conformational diversity of 3-D fragments (and thus 3-D shape diversity) could also be assessed. In addition, Pipeline Pilot generates physicochemical data such as AlogP, HAC, RBN and TPSA which, were used to satisfy the first set of criterion for compound selection. Following PMI analysis, fragments furthest from the rod-disc axis were selected for synthesis

from section ≥ 1.36 for pyrrolidines **173** and section ≥ 1.39 for piperidines **174** of the PMI plot. These values correspond to fragments with the most 3-D shape for example 25% of pyrrolidines have ΣNPR ≥ 1.36. The Pipeline Pilot protocol and workflow for 3-D fragment selection was developed by Paul Bond in the York Structural Biology Laboratory (YSBL) and a previous group member, Mary Wheldon.[69,70] Notably, the workflow is distinct from previous approaches to 3-D fragment synthesis (see sections 1.5.1, 1.5.4 and 1.5.5) where PMI plots were used retroactively to analyse 3-D fragment shape as opposed to using it as a selection tool to aid fragment design.

Using our group's established workflow, the first generation of 3-D pyrrolidine and piperidine fragments were generated as follows. PMI analysis of the 148 compound set indicated wide-ranging 3-D molecular shape (Figures 1.10a and 1.10b) with no conformations occupying the rod-disc axis. This is particularly apparent when compared to PMI analysis of the commercially available Maybridge library (1000 compounds) (Figure 1.10c) in which the majority of compounds adopt a global minimum energy conformation on or close to the rod-disc axis. The number of different regio- and diasteromers generated (148 compounds from two scaffolds) together with the degree of conformational diversity (955 conformations $\leq$ 1.5 kcal mol^{-1}) was striking given the structural simplicity of scaffolds **173** and **174**.

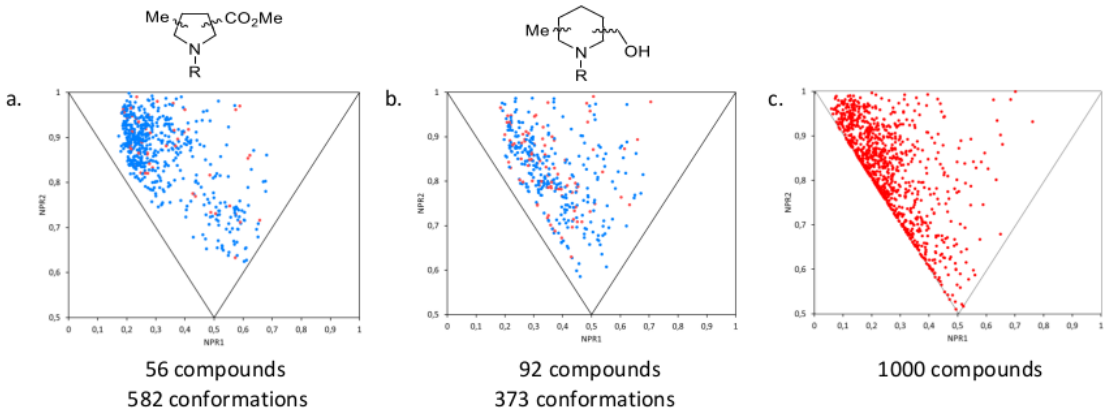

Figure 1.10: (a) Conformers of Pyrrolidine Scaffold (b) Conformers of Piperidine Scaffold (c) Conformers of 1000 Compound Maybridge Library. Red dots indicate global minimum energy conformers and blue dots indicate higher energy conformers

In order to select compounds in under-represented areas of 3-D chemical space, away from the rod-disc axis, the PMI plot was divided into 10 sections with lines parallel to the rod-disc axis representing the sum of NPR values (ΣNPR = NPR1 + NPR2) (Figures 1.11b and 1.12b). Conformations with 3-D shape would fall into sections that lie furthest from the rod-disc axis (ΣNPR = 1.00). With this in mind, 14 pyrrolidine (117 conformations) and 19 piperidine (58 conformations) fragments were selected for synthesis from sections ΣNPR $\geq$ 1.36 and ΣNPR $\geq$ 1.39 (Figures 1.11c and 1.12c) resulting in 33 fragments for synthesis. The structures of the 33 selected 3-D fragments are shown in Figure 1.13.

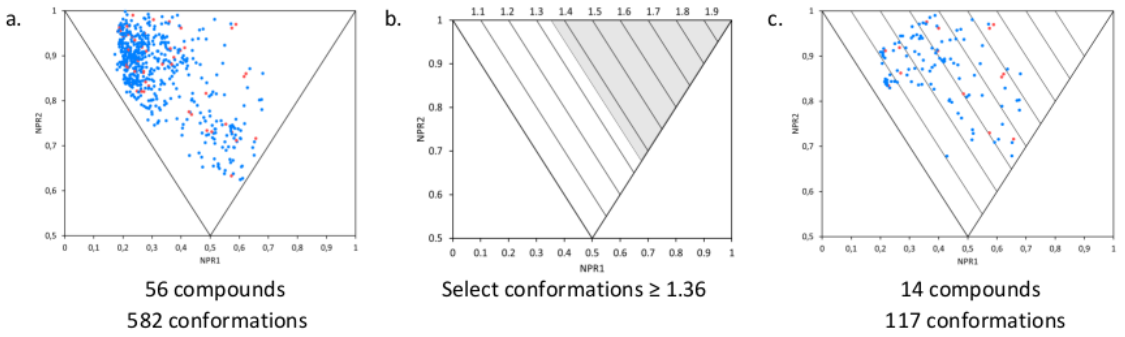

Figure 1.11: Selection of Pyrrolidine Fragments

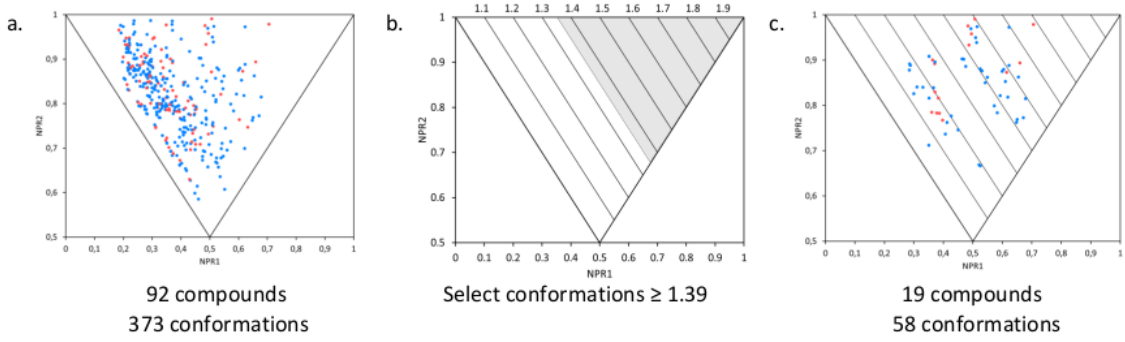

Figure 1.12: Selection of Piperidine Fragments

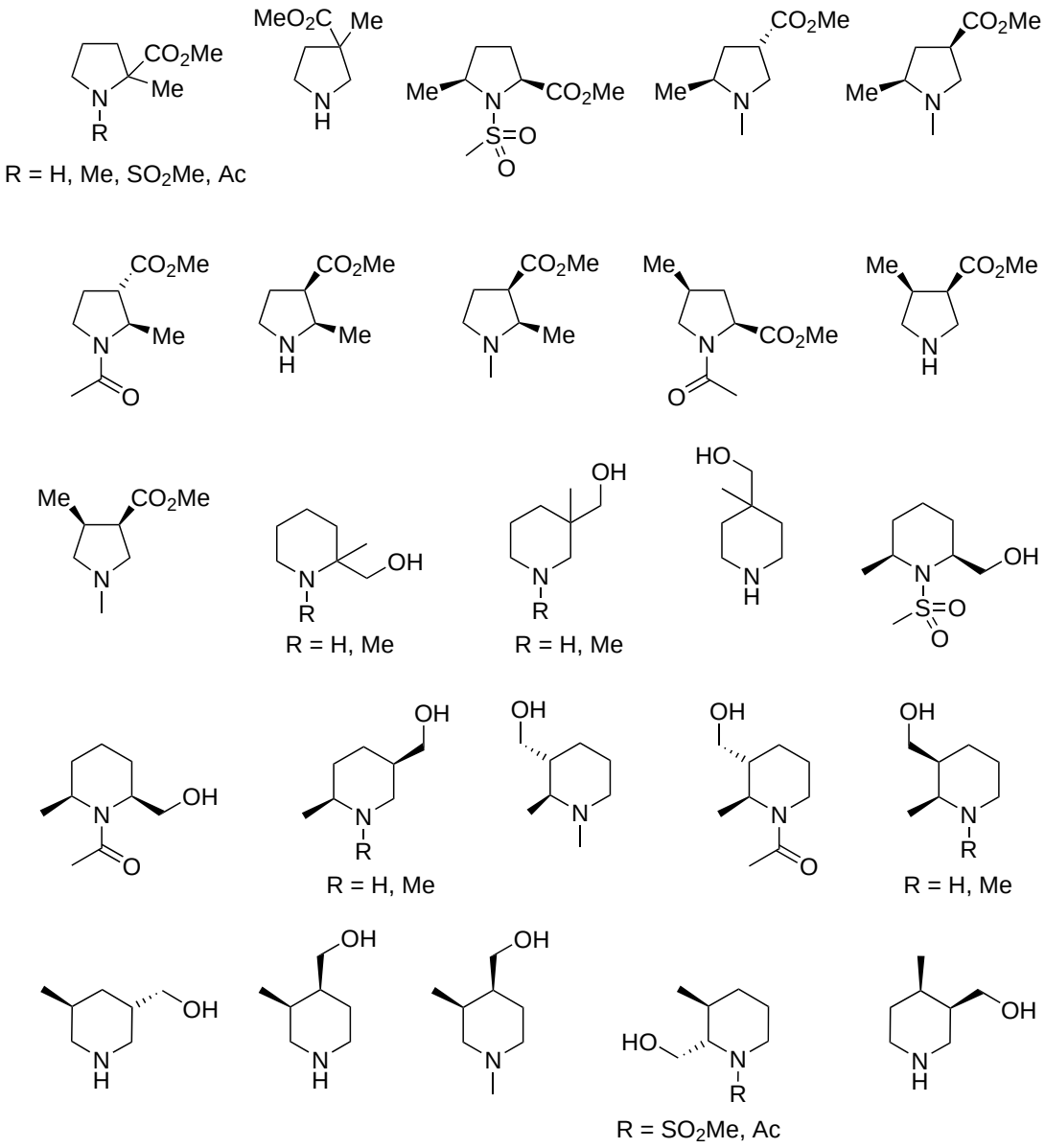

Figure 1.13: Structures of the 33 3-D Fragments Selected for Synthesis

1.6.2 3-D Fragment Synthesis

Target fragments were synthesised using a combination of known literature routes and new reactions (Scheme 1.30). Geminal disubstituted pyrrolidines and piperidines **176** were accessed in <4 steps from *N*-Boc esters **175** by generating an enolate intermediate and trapping with MeI. Functional group interconversion and *N*-functionalisation gave ten fragments. Stereoselective hydrogenation with hydrogen and 10-30 mol% PtO_2 was

used to synthesise 3,4-, 2,3-, 2,6-, 3,5- and 2,5-disubstituted piperidines **180**. With the exception of the 3,5-disubstituted piperidine scaffold, all piperidines were isolated as their *cis*-diastereomer in 70:30 to >95:5 dr. The corresponding *trans*-diastereoisomers of four fragments were accessed by alkoxide-mediated epimerisation of the *cis*-esters **180**. Functional group interconversion and *N*-functionalisation then gave 14 fragments.

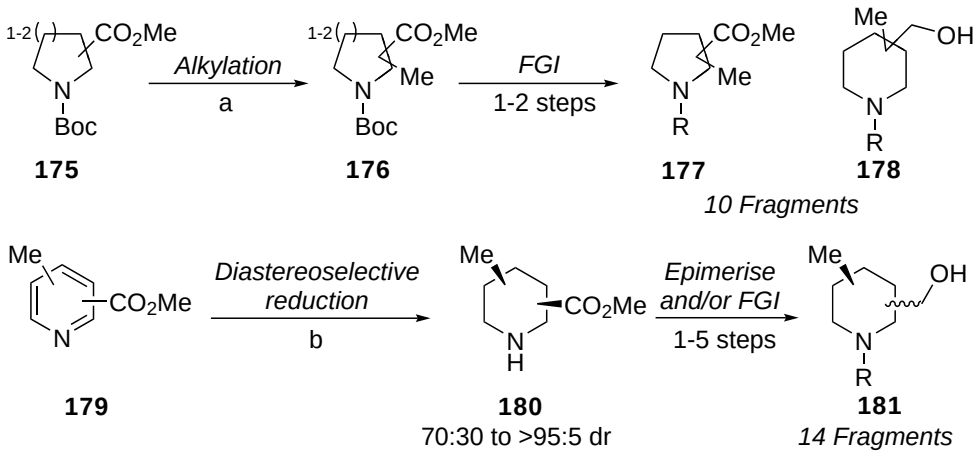

(a) (i) NaHMDS or LHMDS (ii) MeI (b) H_2, PtO_2, AcOH

Scheme 1.30

Seven out of the nine targeted pyrrolidines were accessed by bespoke synthesis using different diastereoselective reduction processes outlined in Scheme 1.31. Intermediates **183** and **186** were formed in high dr (>95:5) *via* reduction of iminium ions (formed following *N*-Boc removal and reduction of the nitrile group respectively). Then, *N*-functionalisation (by acylation or reductive amination) gave fragment **184** and *t*-Bu-protected fragment **187**. Stereoselective reduction of enamine **188** followed by *N*-functionalisation (acylation) furnished fragment **190**. An intramolecular Pd-catalysed enolate cross-coupling reaction of **191** gave the α,β-unsaturated ester which, following *N*-Bn removal, gave fragment **192**. Subsequent *N*-methylation gave fragment **193**. Finally, fragments **198**, **199** and **200** were accessed in 4 steps from β-ketoester **194**. Reaction of ester **194** with 1,2-dibromo ethane gave activated cyclopropane **195** which, on reaction with α-methyl benzylamine, gave dihydropyrrole **196**. Reduction of **196** gave pyrrolidine *cis*-**197** in 75:25 dr which, following *N*-functionalisation, gave frag-

ments **198**, **199** and **200**.

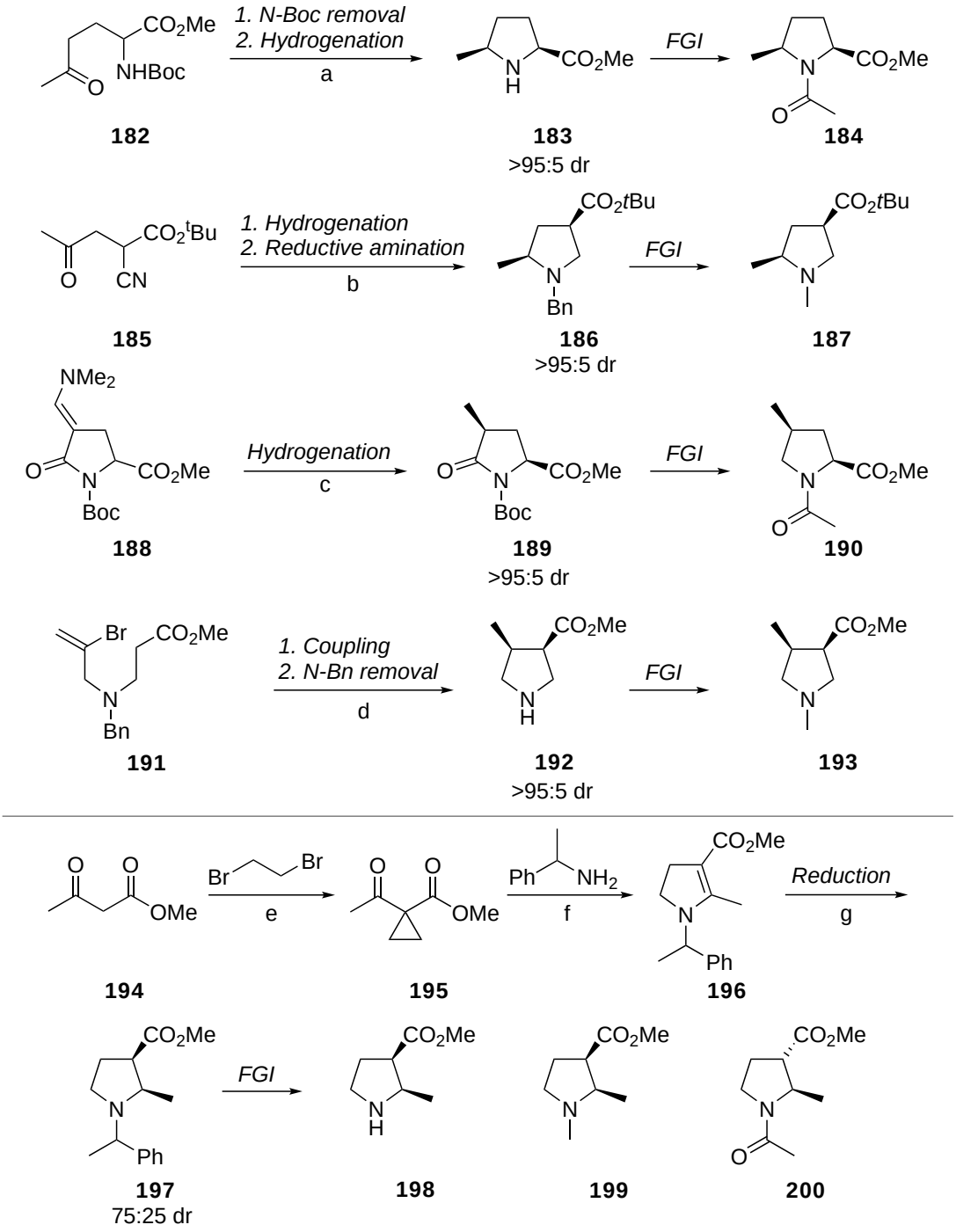

(a) (i) TFA (ii) H_2, Pd/C (b) (i) H_2, PtO_2 (ii) PhCHO, $NaBH(OAc)_3$ (c) H_2, Pd/C (d) (i) $Pd(PPh_3)_4$, NaO*t*Bu, PhOH (ii) H_2, Pd/C (e) K_2CO_3, 82 °C (f) PhMe, 110 °C (g) $NaBH(OAc)_3$, AcOH

Scheme 1.31

Using this approach, 31 conformation- and shape-diverse 3-D fragments (out of 33 targeted 3-D fragments) were successfully synthesised. The majority of fragments were Ro3 compliant and (by design) exhibited 3-D shape in under-explored areas of chemical space. Despite our successes, limitations relating to synthetic tractability and fragment elaboration remained. Synthesis had proved challenging with several fragments requiring bespoke synthetic routes. Overall, seven synthetic multi-step (2-7 steps) routes were required. Furthermore, the fragment set contained a limited number of synthetic handles for fragment elaboration, failing to address the ultimate goal of being able to grow or elaborate a potential fragment hit in 3-dimensions.

1.7 Project Outline

The two aims of this project are to design a library of conformation- and shape-diverse 3-D fragments and 3-D building blocks to enable fragment elaboration in 3-dimensions. The pyrrolidine and piperidine 3-D fragments (31 compounds) previously synthesised in the group are regioisomerically related with an abundance of primary alcohol and carboxylic ester groups. Therefore, the design and synthesis of a second set of 3-D fragments was carried out with the primary intention of introducing more structural diversity into the collection. Synthetic tractability was also considered at the outset in order to address challenges with previous multi-step bespoke fragment synthesis. To this end, it was hoped that functional group interconversion of key intermediates and existing compounds in the York 3-D fragment library would provide an efficient synthetic route (3-4 steps) to 2,2-disubstituted pyrrolidines **201** and 2,3-disubsituted piperidines **202** and **203** with alternative binding groups (Figure 1.14). The results of this study are presented in Chapter 2.

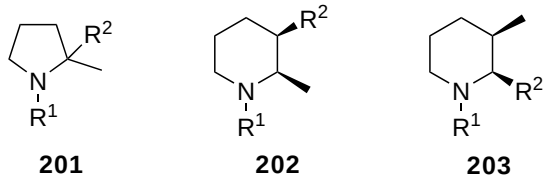

Figure 1.14: Structures of 2,2-Disubstituted Pyrrolidine and 2,3-Disubsituted Piperidine Scaffolds

In addition, it was also planned to explore alternative methodology to increase scaffold diversity and incorporate aromatic groups (for protein binding and screening by ^{1}H NMR spectroscopy). To this end, synthetic efforts towards tropanes **204** and **205** would be investigated (Figure 1.15). Furthermore, it was envisioned that lithiation-trapping chemistry and Suzuki-Miyaura cross-coupling of a cyclopropyl-B(MIDA) building block could be used to synthesise 2,3-fused cyclopropyl pyrrolidine fragments **206** and **207** respectively. This work is also detailed in Chapter 2.

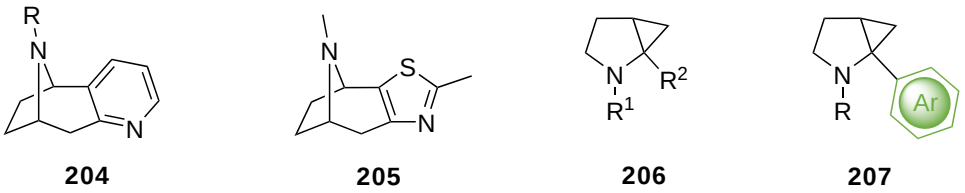

204 **205** **206** **207**

Figure 1.15: Structures of Tropane and 2,3-Fused Cyclopropyl Pyrrolidine Scaffolds

Chapter 3 covers the physicochemical properties and molecular shape of York 3-D fragments using literature guidelines (the Ro3 and updated Ro3) and PMI analysis respectively. Analysis of both a subset of 42 3-D fragments (of which 41 were synthesised in Chapter 2) as well as the York 3-D compound collection as a whole is described and compared against six commercial fragment libraries. In addition, quality control (QC), stability and solubility studies for the York 3-D fragment library together with preliminary screening results of four screens against six protein targets are presented. Finally, Chapter 4 describes progress made in the development of a modular synthetic platform that would enable elaboration of 2-D fragment hits *via* multiple growth points into 3-D lead compounds. In particular, the design and synthetic efforts towards ten chemically-enabled, cyclopropyl-B(MIDA) bifunctional 3-D building blocks **209-214** (Figure 1.16) with unique 3-vectors is presented (synthesis of **208** is in Chapter 2). Elaboration of the cyclopropyl-B(MIDA) group by Suzuki-Miyaura cross-coupling is also demonstrated.

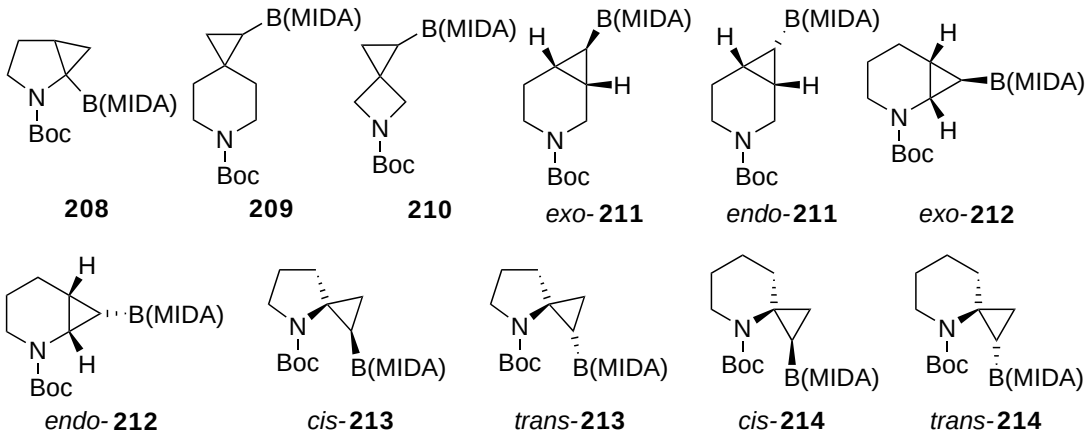

208 **209** **210** *exo*-**211** *endo*-**211** *exo*-**212**

endo-**212** *cis*-**213** *trans*-**213** *cis*-**214** *trans*-**214**

Figure 1.16: Structures of Targeted Cyclopropyl-B(MIDA) 3-D Building Blocks

2 Design and Synthesis of 3-D Fragments

In this Chapter, the development of synthetic routes towards 2,2-disubstituted pyrrolidine and *cis*-2,3-disubstituted piperidine fragments **215**, tropane fragments **204** and **205** and 2,3-fused cyclopropyl pyrrolidine fragments **206** and **207** (Figure 2.1) is discussed. An overview of previous approaches towards each scaffold is outlined before the synthetic efforts are described.

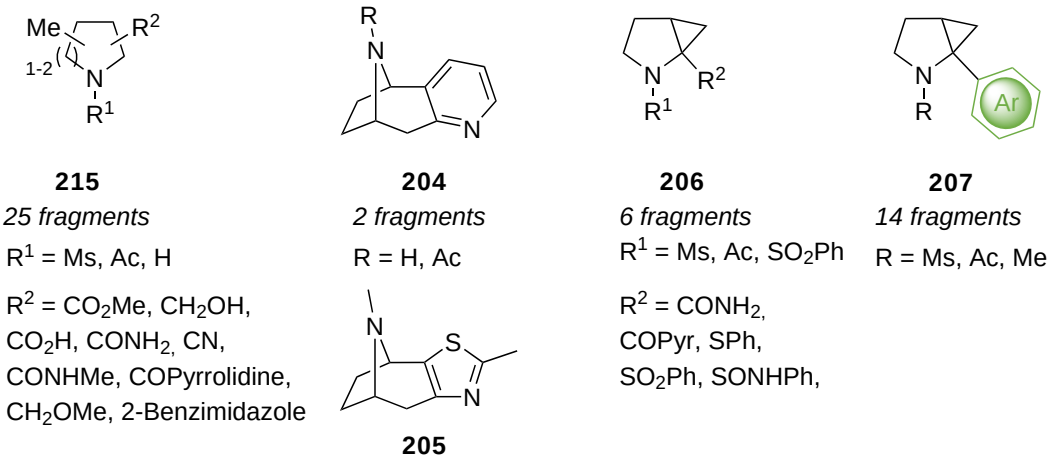

Figure 2.1: Structures of 2,2-Disubstituted Pyrrolidine, *cis*-2,3-Disubstituted Piperidine, Tropane and 2,3-Fused Cyclopropyl Pyrrolidine Scaffolds

Specifically, sections 2.1 and 2.2 cover efforts in the synthesis of 2,2-disubstituted pyrrolidine and *cis*-2,3-disubstituted piperidine fragments **215**. Here, the strategy was to use methodology previously established in the group to access a common ester intermediate from which 3-D fragments (with acid, amide, nitrile and primary alcohol groups) could be accessed *via* 1-3 step modifications of the ester group. In section 2.3, attempts to increase scaffold diversity and incorporate aromatic groups with the synthesis of tropane fragments **204** and **205**, using a single piece of methodology, is described. Finally, in section 2.4, the use of lithiation-trapping chemistry and Suzuki-Miyaura coupling of a cyclopropyl-B(MIDA) building block to synthesise 2,3-fused cyclopropyl pyrrolidine fragments **206** and **207** respectively are presented.

2.1 Synthesis of 2,2-Disubstituted Pyrrolidine Fragments

2.1.1 Design and PMI Analysis of 2,2-Disubstituted Pyrrolidine Fragments

The 2,2-disubstituted pyrrolidine scaffold served as an attractive starting point for the synthesis of our first iteration of 3-D fragments in terms of both synthetic tractability and 3-D shape. It was envisioned that the desired scaffold could be constructed using methodology previously established in the group from *rac*-proline (Scheme 2.1).[70] To this end, enolate trapping chemistry would be used to synthesise key intermediate **216** in 3 steps. Then, *N*-Boc removal and functionalisation (mesylation or acylation) followed by transformation of the ester group in pyrrolidine **216** using well-established reactions should furnish acid, amide and nitrile groups. Alternatively, transformation prior to Boc group removal would provide access to NH fragments (R^1 = H). Using this approach, we intended to synthesise a structurally diverse set of 3-D fragments **203** with variation of both the R^1 group (H, Me, Ac or SO_2Me) and R^2 group (CO_2H, $CONH_2$, CN, CH_2OH and CH_2OMe). Notably, target fragments were designed to have two sites for protein binding and/or future elaboration. In addition, a methyl group was incorporated as a third substituent to aid in NMR screening. The polarity and size of the methyl group should have minimal impact on key physicochemical properties (NROT, ClogP and molecular weight) and structural complexity. In addition, the methyl group provides a hydrophobic substituent for potential interaction with the protein.

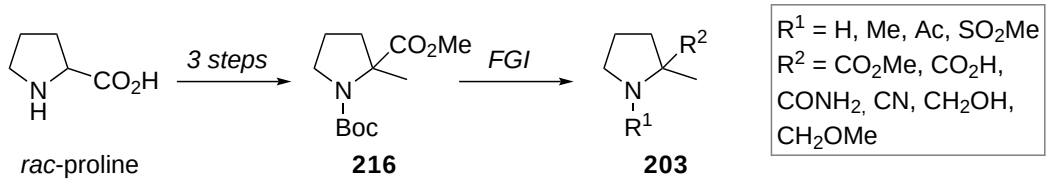

Scheme 2.1

In addition to synthetic tractability *via* the route shown in Scheme 2.1, 3-D shape was key to the selection of the 2,2-disubstituted scaffold in these fragments. The previously synthesised 3-D fragments based on the 2,2-disubstituted pyrrolidine scaffold

(with R^1 = H, Me, SO_2Me, Ac and R^2 = CO_2Me) were found (by PMI analysis) to exhibit appropriate 3-D shape. Therefore, it was anticipated that structural variants of such 3-D fragments should also show conformations in the more attractive area of the PMI plot, away from the rod-disc axis. The effect of ester modification to acid, amide, nitrile, primary alcohol and methyl ether groups on 3-D shape for the 2,2-disubsituted pyrrolidine scaffold (with R^1 = H) was assessed. PMI analysis of the previously synthesised fragment **217** together with derivatives **218**-**222** is shown in Figure 2.2. The 3-D shape of fragments **218**-**222** was maintained on modifying the ester with all conformations up to 1.5 kcal mol^{-1} above the energy of the global minimum energy conformer for each fragment having ΣNPR values > 1.20. Clearly, the 2,2-disubsituted pyrrolidine scaffold plays a greater role in imparting 3-D shape than the ring substituents.

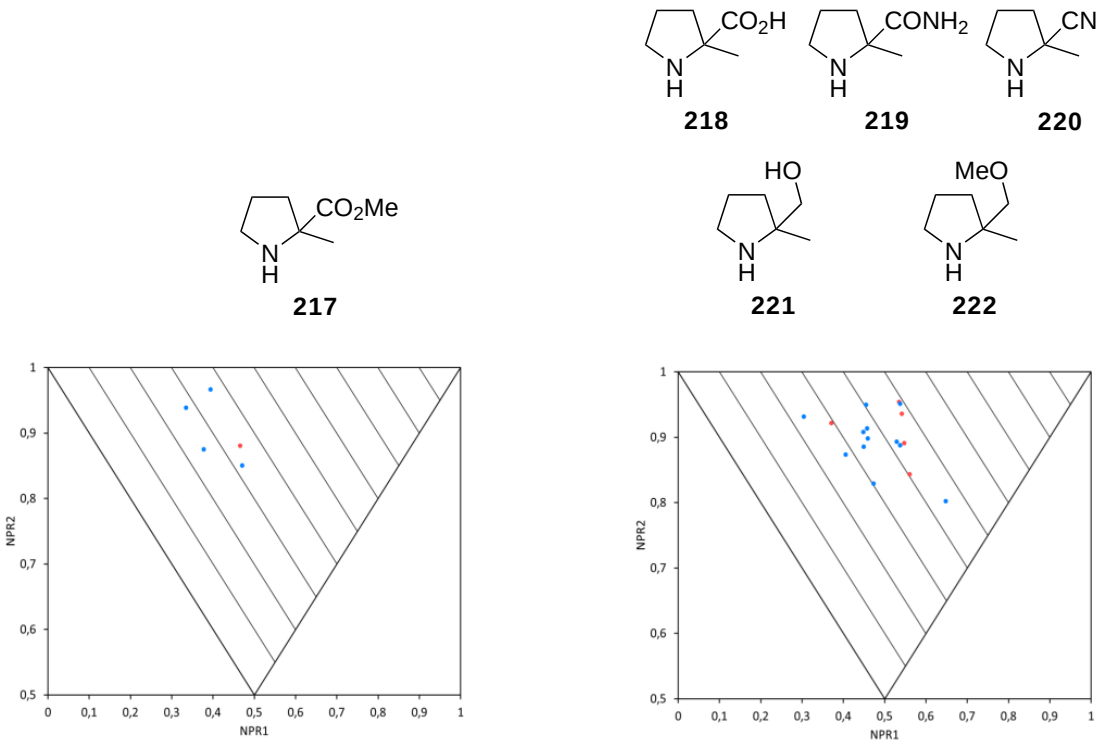

Figure 2.2: PMI Analysis of Potential Fragments. Red dots indicate global minimum energy conformers and blue dots indicate higher energy conformers

The effect of the nitrogen substitutent (R^1 = H, Me, SO_2Me and Ac) on 3-D shape was

also considered. To this end, 2,2-disubstituted pyrrolidines (with $R^2 = CO_2H$, $CONH_2$, CN, CH_2OH and CH_2OMe) were divided into five sub-groups and PMI analysis with R^1 = H, Me, SO_2Me and Ac was carried out. Overall, five PMI plots of these 20 compounds were generated (not shown). For example, the 3-D shape of amides **219**, **223**, **224** and **225** (Figure 2.3) exhibited ΣNPR values > 1.3 and, ultimately, fragments **219**, **224** and **225** were selected for synthesis.

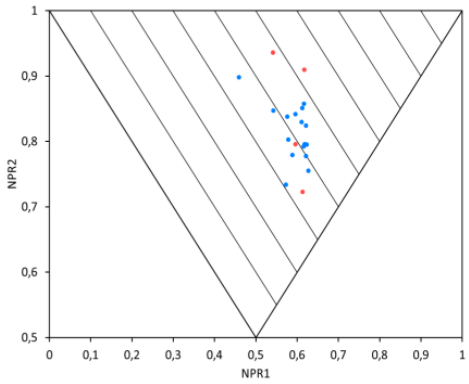

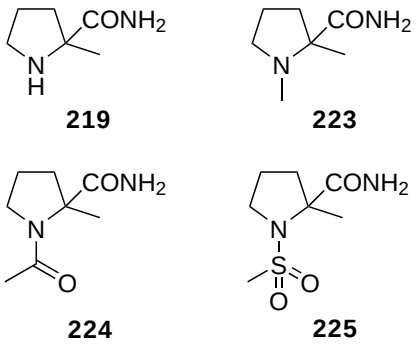

Figure 2.3: PMI Analysis of Potential Fragments. Red dots indicate global minimum energy conformers and blue dots indicate higher energy conformers

Following PMI analysis of all synthetically accessible 2,2-disubstituted pyrrolidines (20 compounds), the eight fragments shown in Figure 2.4 were selected for synthesis. By design, targeted fragments are conformationally diverse with ΣNPR values > 1.20 for all conformations. Moreover, incorporation of various functional groups on the nitrogen and pyrroldine ring scaffold (*via* modification of the ester group) would deliver a set of structurally diverse, 3-D fragments to complement the 33 3-D fragment collection described in section 2.1.3.

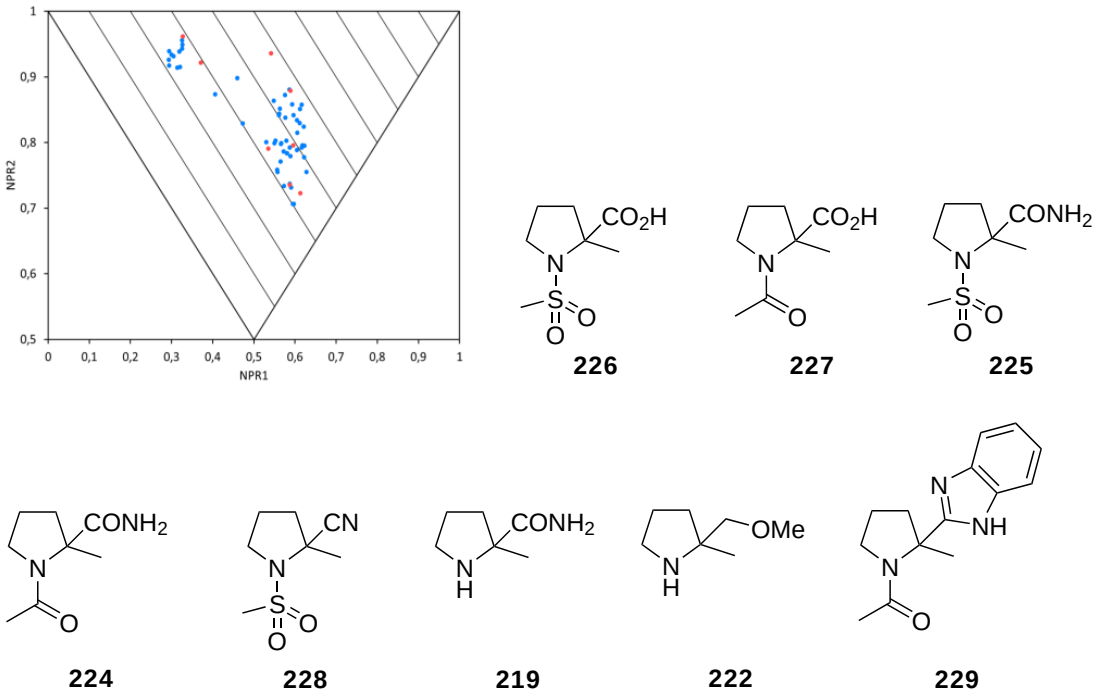

Figure 2.4: PMI Analysis of Targeted Fragments. Red dots indicate global minimum energy conformers and blue dots indicate higher energy conformers

2.1.2 Overview of Previous Synthetic Routes towards 2,2-Disubstituted Pyrrolidines

The literature is replete with examples of the synthesis of 2,2-disubstituted pyrrolidines.[71–79] For example, Confalone and co-workers used (*S*)-proline as a starting point in their synthesis of anthramycin derivative **232**, a potential DNA cross-linking reagent (Scheme 2.2).[73] (*S*)-Proline derived ester **231** was deprotonated with LHMDS in THF at −78 °C to generate a planar enolate intermediate which, following trapping with allyl bromide, formed racemic α-methyl ester **9a**. A further 10 steps gave imino epoxide **232**.

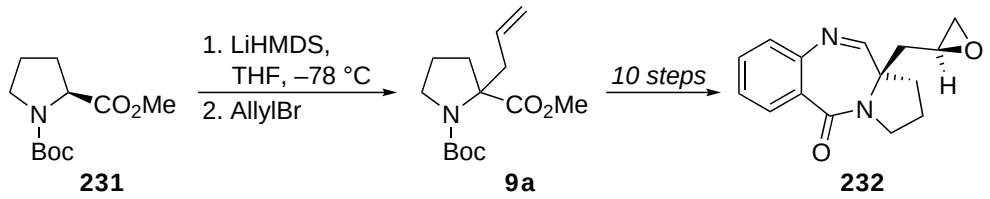

Scheme 2.2

Kelleher and co-workers made use of the experimental conditions established by Confalone (for enolate alkylation) in their synthesis of enantiomerically pure and racemic proline-derived [4.4]-spirolactams (Scheme 2.3).[71] To this end, LHMDS and allyl bromide[73] were used to synthesise racemic α-methyl ester **9a** in 80% yield. Oxidative cleavage of alkene **9a** (with $OsO_4/NaIO_4$) to the aldehyde and subsequent reductive amination with (*R*)- or (*S*)-α-methylbenzylamine and $NaBH_4$ gave amines **233**. Then, cyclisation of the amine onto the ester (with sodium amide in toluene at reflux) gave four *N*-Boc protected spirolactams as pairs of diastereoisomers which, following chromatography, could be separated. Deprotection (and subsequent reduction with $LiAlH_4$ for (*R,R*)-**235** and (*R,S*)-**237**) gave a series of spirolactams and sprirodiamines including compounds **234**-**237**. Overall, eight compounds were synthesised and used in subsequent studies as organocatalysts for asymmetric Michael addition reactions.[72]

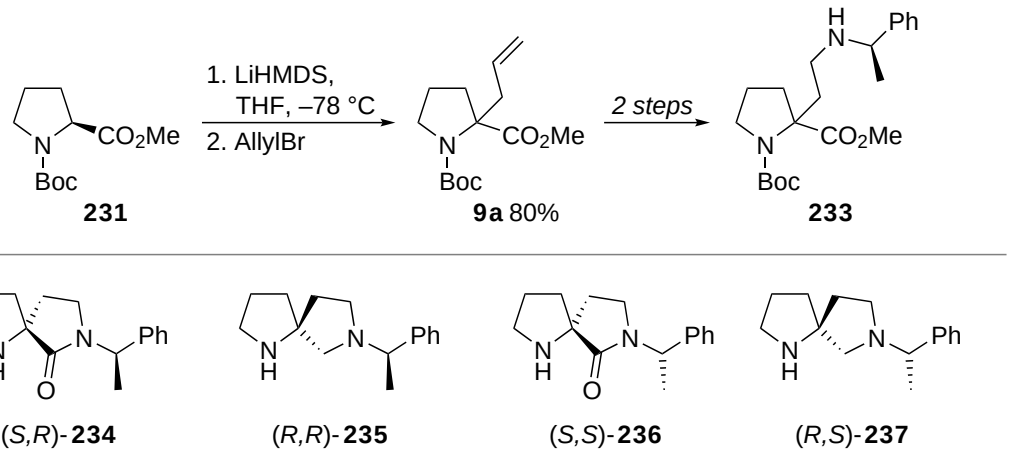

Scheme 2.3

Similarly, in 2010, the Kelleher group used enolate trapping chemistry to generate α-methyl prolinamides for use in organocatalysis (Scheme 2.4).[72] Eight stereoisomers were synthesised in 4 steps from *N*-Boc methyl ester **231**. Enolate alkylation of ester **231** with LHMDS and methyl iodide gave racemic α-methyl ester **216** in 72% yield, which was converted into acid **238**. Coupling of racemic **238** with (*R*)- or (*S*)-*N*,α-dimethylbenzylamine or (*R*)- or (*S*)-α-methylbenzylamine generated two sets of four diastereomers. Deprotection under acidic conditions gave the corresponding *N*-Me or *N*-H α-methyl prolinamides shown in Scheme 2.4.

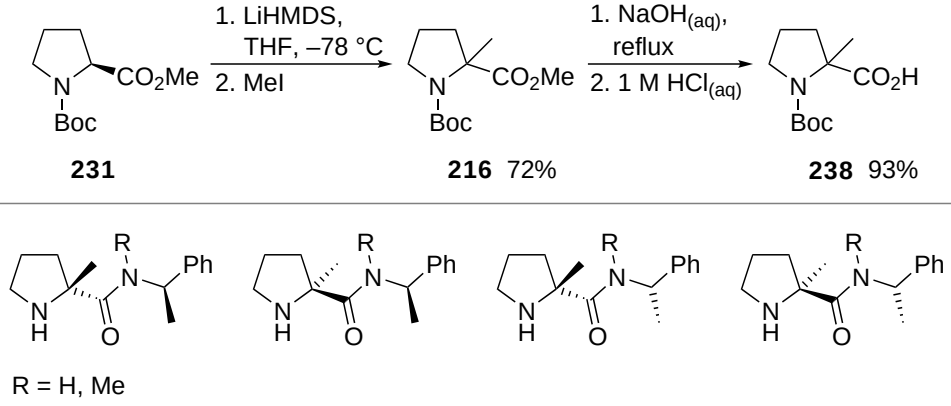

Scheme 2.4

The enantioselective synthesis of 2,2-disubstituted pyrrolidines using an enolate trapping approach has also been reported. For example, Seebach and co-workers developed

an asymmetric synthesis of α-substituted proline derivatives.[74] The synthetic sequence is shown in Scheme 2.5. (*S*)-Proline was condensed with pivaldehyde to form *N,O*-acetal **239**. Deprotonation with LDA formed chiral enolate **240** which could be trapped with different electrophiles to produce alkylated products **241** as single diastereomers. In this way, the chirality of (*S*)-proline could be effectively relayed to compound **241** as the incoming electrophile selectively added from one face of enolate **240**. Cleavage of bicyclic scaffold **241** with HBr gave 2,2-disubstituted pyrrolidines **242** and **243**. Alternatively, nucleophillic reagents could be used for ring cleavage. To this end, compounds **244**, **245** and **246** were formed after treatment with methyllithium, *N*-methyl lithium amide and $LiAlH_4$ respectively. Overall, the synthetic strategy allowed for alkylation of (*S*)-proline with retention of configuration in the absence of a chiral auxiliary.

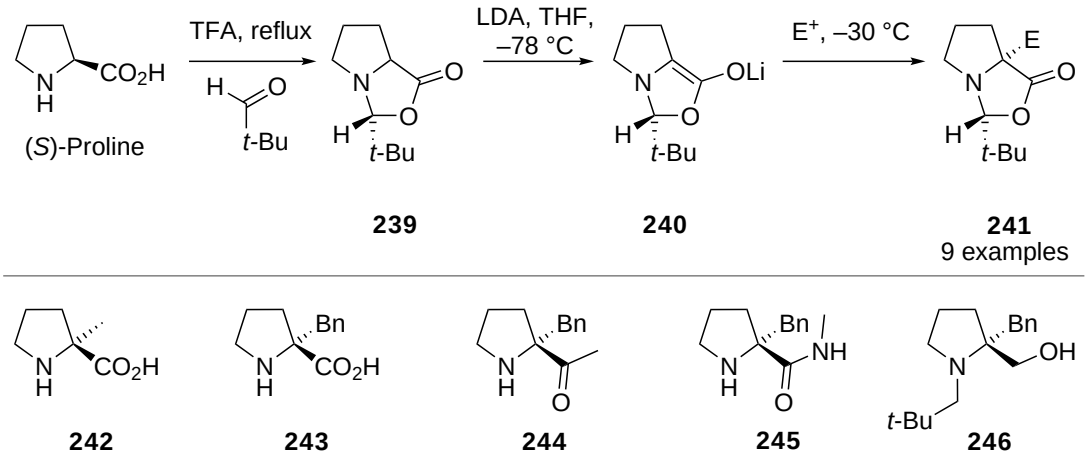

Scheme 2.5

Since then, several groups have applied Seebach's methodology in the total synthesis of natural products.[75–77] For example, Wang and co-workers featured Seebach's enantioselective alkylation as a key step in the synthesis of the alkaloid hypoestestatin 2.[75] The key reactions are summarised in Scheme 2.6. Enolate formation and alkylation of *N,O*-acetal **247** gave oxazolidinone **248**. Ring cleavage with thionyl chloride and methanol furnished the 2,2-disubstituted pyrrolidine scaffold **249** which, on further reaction (3 steps), gave the natural product.

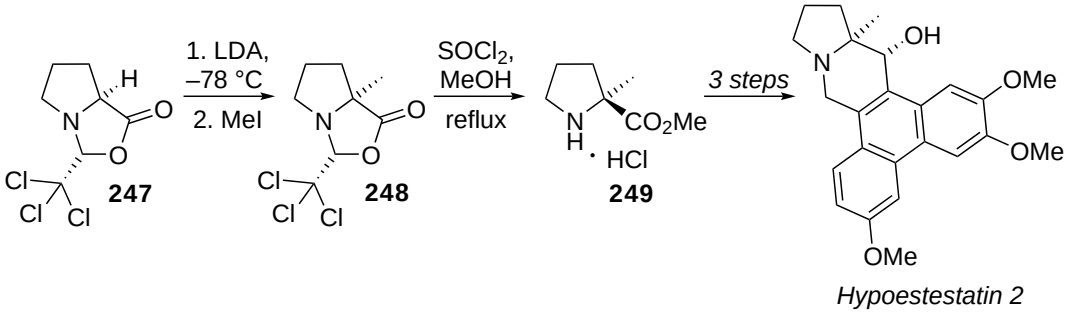

Scheme 2.6

Kawabata and co-workers also used enolate chemistry in their asymmetric synthesis of 2,2-disubstituted pyrrolidines.[78] As in Seebach's work, no chiral auxiliaries or chiral catalysts were required. In this case, reaction of (*S*)-amino acid **250** with powdered KOH in DMSO at 20 °C generated an axially chiral enolate intermediate which underwent an enantioselective intramolecular cyclisation (*via* memory of chirality) to form 2,2-disubstituted pyrrolidines in high er (Scheme 2.7). Interestingly, racemisation of the axially chiral enolate intermediate was not observed. The authors attributed this result to the kinetics of cyclisation (approximately 10^{-3} sec at 20 °C) which in this case allowed intramolecular cyclisation to occur before racemisation (energy barrier of approximately 15.5 kcal mol^{-1}).

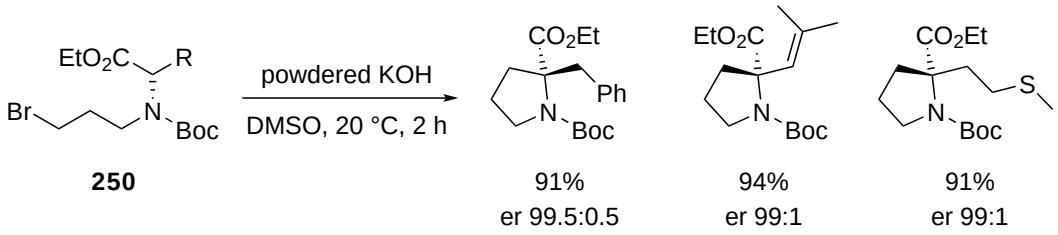

Scheme 2.7

An alternative synthesis for the construction of the 2,2-disubstituted pyrrolidine scaffold was reported in 2012 by Coldham and O'Brien.[79] Lithiation-substitution was used to synthesise *N*-Boc-2-phenyl-2-substituted pyrrolidines **253** (Scheme 2.8). Earlier work established conditions for the lithiation-transmetallation-Negishi coupling of *N*-Boc pyrrolidine **251** to form arylated pyrrolidine **252**.[80] Lithiation of **252** with *n*-BuLi at 0 °C and subsequent trapping with different electrophiles gave a range of 2,2-

disubstituted pyrrolidines **253**. An asymmetric synthetic route to enantioenriched 2,2-disubstituted pyrrolidines **253** was later established delivering the target compounds (≥92:8 er) in high yield.[81]

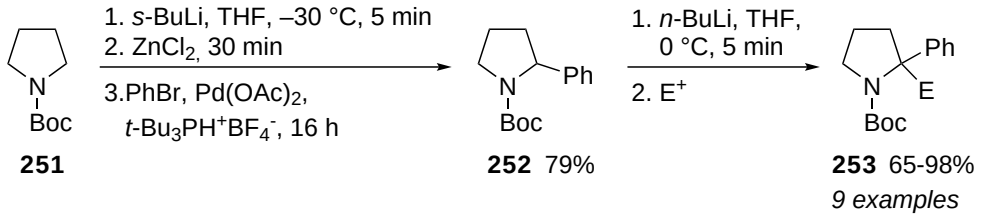

Scheme 2.8

More recently, Bull's group reported the use of a one-pot, Rh catalysed N–H insertion and cyclisation sequence for the construction of saturated nitrogen heterocycles including the 2,2-disubstituted pyrrolidine scaffold.[82] Reaction of *N*-Boc-2-chloroethylamine **254** with diazoesters **255** under optimised conditions gave 2,2-disubstituted pyrrolidines **256**. Various aryl groups were tolerated delivering 2,2-disubstiuted pyrrolidines including nicotine derivatives. Notably, further functionalisation of the products (*via* amine, ester and aryl derivatisation) was demonstrated to afford both α,α-disubstituted amino acids as well as potential 3-D fragments.

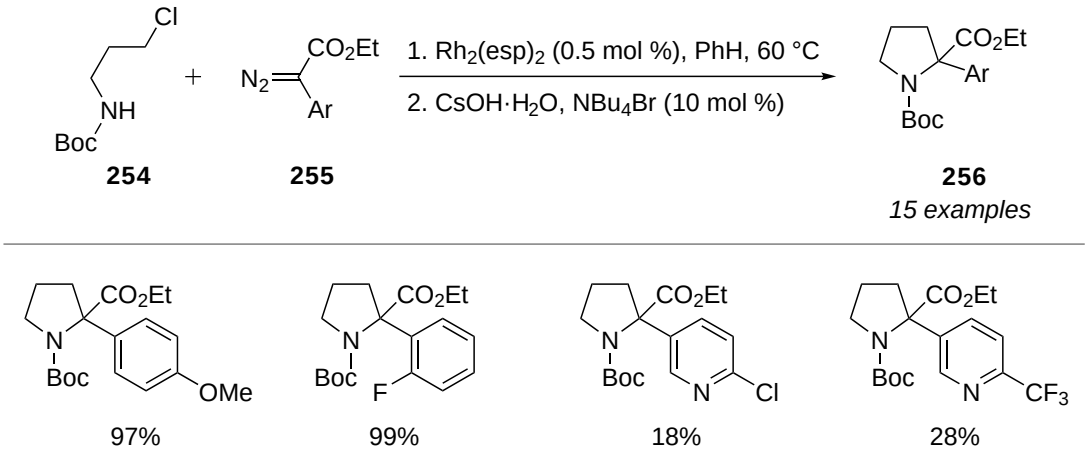

Scheme 2.9

Given the literature precedence of enolate trapping chemistry for the construction of the 2,2-disubstituted pyrrolidine scaffold[71,72,74–77] we decided to use this approach

as a strategy for the synthesis of 2,2-disubstituted pyrrolidine based 3-D fragments. Moreover, Seebach's work demonstrates that such 3-D fragments could be synthesised as single enantiomers if necessary. Although, for practical reasons, all targeted 3-D fragments would be synthesised and screened as racemates, synthetic access to single enantiomers remains crucial in FBDD in order to identify the active compound during subsequent screening, SAR studies and hit-to-lead optimisation.

2.1.3 Synthesis of 2,2-Disubstituted Pyrrolidine 3-D Fragments

The plan was to synthesise 2,2-disubsituted pyrrolidine-based fragments **226**-**228** from common intermediate **216** (Scheme 2.10). Deprotection and functionalisation (mesylation or acylation) followed by FGI of the ester group would furnish acid, amide and nitrile groups. Alternatively, amine fragments **219** and **222** could be accessed by rearranging the steps. To this end, FGI of the ester group would give *N*-Boc protected amide and methyl ether intermediates which, following deprotection, could furnish fragments **219** and **222**. Fragment **229** could be synthesised in a similar manner.

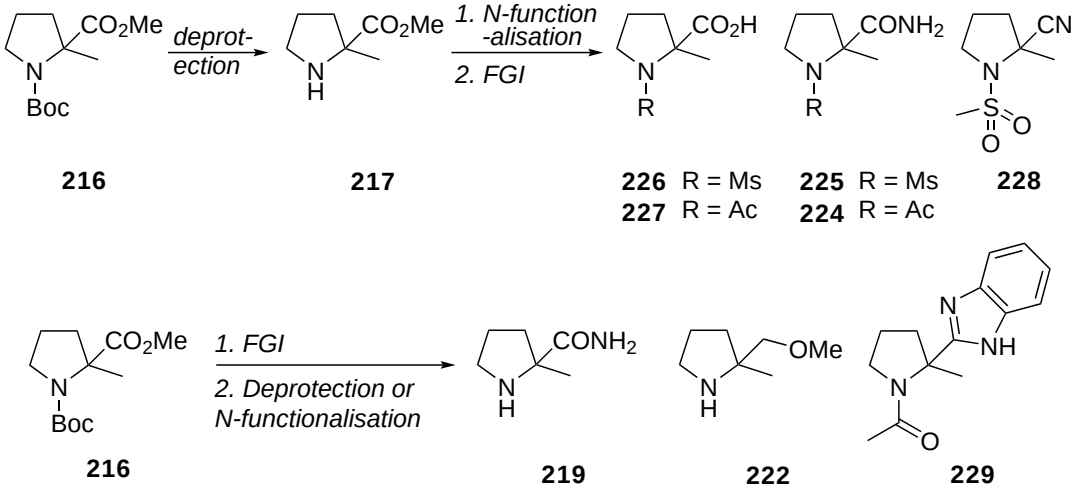

Scheme 2.10

The synthesis of key intermediate **216** has previously been established in the group following methodology developed by Confalone *et al.*[73] and Kelleher *et al.*.[72] Thus, commercially available *rac*-proline was reacted with thionyl chloride and MeOH. Crude methyl ester **257** was formed after refluxing for 1 h and, following evaporation, isolated as its hydrochloride salt **257**·HCl. Treatment of **257**·HCl with Et_3N and protection with Boc_2O in CH_2Cl_2 gave, following chromatography, *N*-Boc methyl ester **231** in 74% yield over 2 steps (Scheme 2.11). Importantly, the two-step procedure proved scalable (7.40 g of **216** prepared), ultimately allowing for the synthesis of large amounts of key intermediate **216**. Enolate formation on **231** with LHMDS in THF at −20 °C followed by treatment with MeI gave methylated ester **216** in 93% yield. On a large

scale, methylated ester **216** was isolated in 73% yield (5.76 g of **216** prepared). Facile scalability and high yields made this an attractive starting point towards the target fragments.

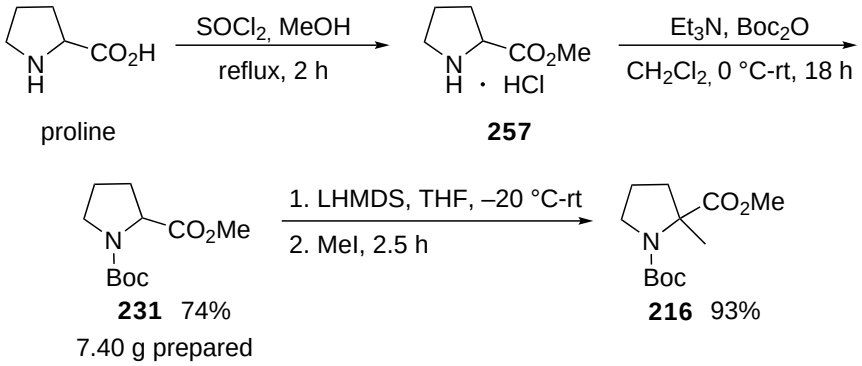

Scheme 2.11

With *N*-Boc methyl ester **216** in hand, efforts were focused on synthesising mesylated and acylated fragments **226**-**228**. Using standard conditions previously established in the group[70] for the synthesis of acetamide and methanesulfonamide fragments, deprotection of ester **216** with TFA or HCl followed by mesylation (with MsCl and Et_3N) or acylation (with Ac_2O in pyridine) of the secondary amine gave esters **258** and **259** in 70% and 96% yield respectively over 2 steps (Scheme 2.12). Ester hydrolysis of intermediates **258** and **259** with LiOH in a MeOH/H_2O solution at 40 °C furnished acids **226** and **227** in 85% and 80% yield respectively.

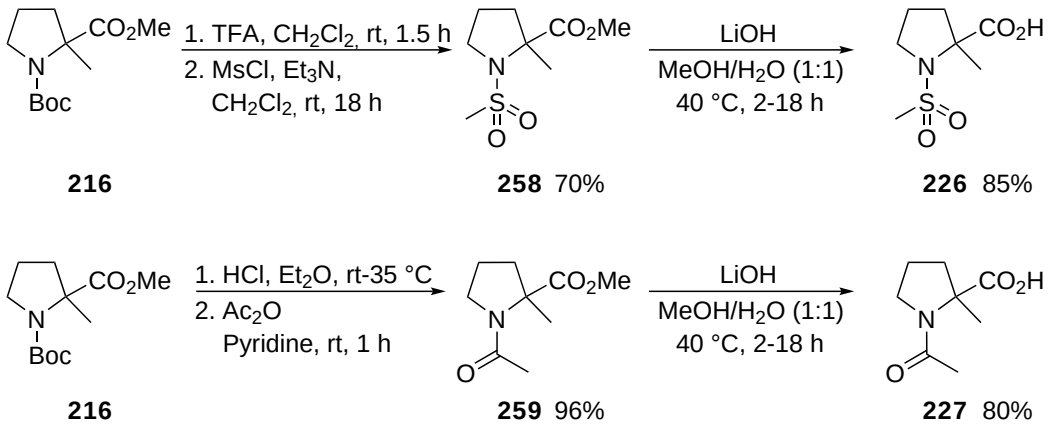

Scheme 2.12

With acid **226** in hand, acid to amide conversion was carried out following a literature procedure for the coupling of racemisation-prone acids and amines.[83] To this end, reaction of acid **226** with T3P, 35% $NH_{3(aq)}$ and DIPEA in EtOAc-CH_2Cl_2 at 60 °C for 18 h gave amide **225** in only 25% yield (Scheme 2.13). The low yield is likely due to the steric hindrance caused by the adjacent quaternary centre. Then, following methodology for the mono-substituted *N*-Boc pyrrolidine scaffold,[84,85] dehydration of amide **225** to nitrile **228** with trifluoroacetic anhydride and Et_3N in THF at 0 °C to rt for 1 h proceeded smoothly affording nitrile **228** in 85% yield. The ^{13}C NMR spectrum of **228** showed a signal at 120.3 ppm, which is characterisitic of the nitrile group.

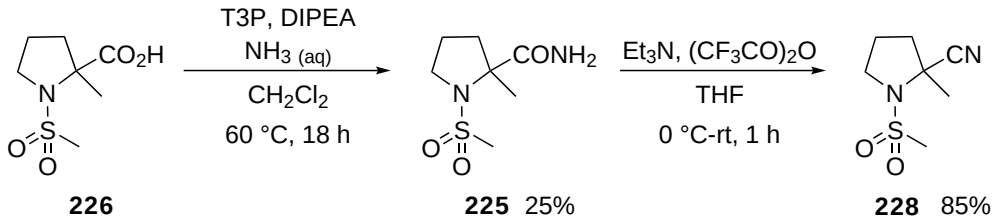

Scheme 2.13

Attention then turned to the synthesis of fragment **224**. We anticipated that the amide group could be furnished in a similar manner to the synthesis of fragment **225** (*via* amidation of acid **227**). Unfortunately, acid to amide conversion using established experimental conditions (T3P, DIPEA and 35% $NH_{3(aq)}$) was unsuccessful resulting in only traces of the desired product **224**. Alternative coupling conditions[86] for the mono-substituted *N*-Boc pyrrolidine (with isobutylchloroformate and Et_3N) gave the intermediate isobutyl carbamate only. Literature conditions[87] used on the mono-substituted *N*-Ac pyrrolidine, namely DCC and $(NH_4)_2CO_3$ in CH_2Cl_2 or MeCN, also failed to give desired fragment **224**.

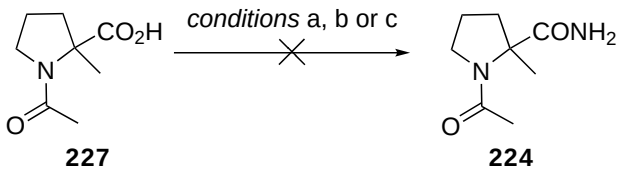

conditions
a T3P, 35% NH_3 (aq), EtOAc-CH_2Cl_2, DIPEA, rt, 1 h
b (i) Et_3N, Isobutyl chloroformate, THF, 20 °C-rt, 0.5 h (ii) 35% NH_3 (aq), 0.5 h
c DCC, $(NH_4)_2CO_3$, CH_2Cl_2 or CH_3CN, rt, 18 h

Scheme 2.14

The synthetic route towards fragment **224** was therefore revised. In particular, it was decided to explore the reaction of acid **227** with allyl amine to give the allyl amide. *N*-Deallylation would then furnish target fragment **224**. Although amide formation using allyl amine under the standard T3P conditions afforded the protected amide **260** in 38% yield, literature conditions[88] for allyl deprotection (*N*,*N*'-dimethylbarbituric acid, $Pd(PPh_3)_4$, CH_2Cl_2, rt, 24 h) failed to give desired product **224** with only starting material recovered following work-up. An alternative protection-deprotection strategy in the synthesis of fragment **224** was therefore considered using dimethoxybenzyl-protected amide **261** as an intermediate (Scheme 2.15). Amide formation from acid **227** using the T3P conditions gave amide **261** in 83% yield. Then, two procedures for *N*-dimethoxybenzyl removal were trialled.[89,90] Firstly, hydrogenolysis with Pd/C (10 mol%) in $AcOH/H_2O$ under a H_2 atmosphere at rt for 18 h was carried out. Only starting material was isolated after work-up, confirmed by ^1H NMR spectroscopy. In a second attempt, deprotection under acidic conditions with TFA at 70 °C for 4 h gave fragment **224** following chromatography in a low yield of 9%.

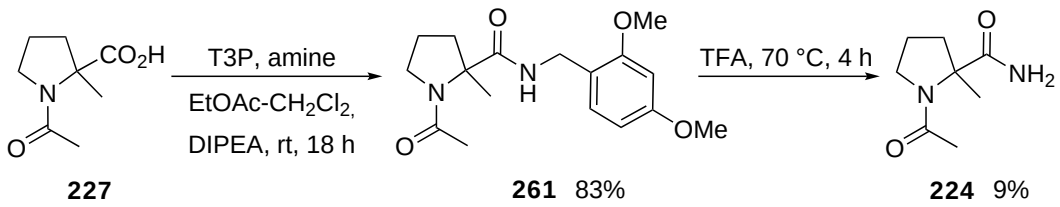

Scheme 2.15

Next, amine fragments **222** and **219** were targeted. Reduction of the ester in **216** to the primary alcohol using conditions previously established in the group[91] ($LiBH_4$ in THF) afforded alcohol **263** in 89% yield after chromatography (Scheme 2.16). Methylation of alcohol **263** using literature conditions for the mono-substituted *N*-Boc pyrrolidine[92] (with NaH and methyl iodide in THF at −78 °C-rt over 18 h) gave methyl ether **264** in 37% yield after chromatography. Finally, deprotection under acidic conditions gave fragment **222** in high yield, isolated as the HCl salt.

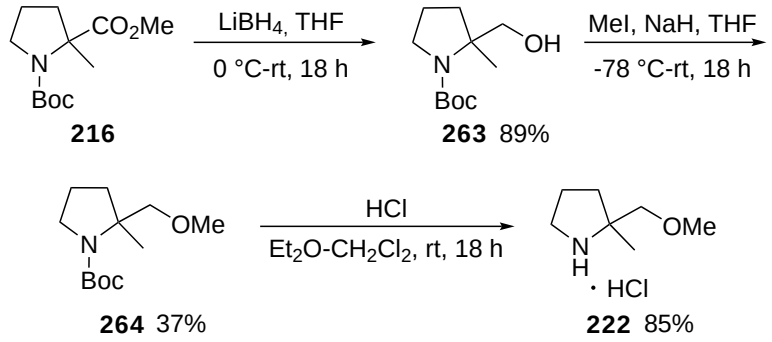

Scheme 2.16

Similarly, intermediate **216** was used to synthesise fragment **219**. Hydrolysis of ester **216** with NaOH in a $MeOH/H_2O$ solution at 80 °C for 2 h furnished acid **238** in 93% yield (Scheme 2.17). Coupling of acid **238** with Et_3N and isobutyl chloroformate in THF at −20 °C followed by the addition of $NH_{3(aq)}$ gave amide **262** in 36% yield after chromatography. Deprotection under acidic conditions then generated amine **219**·HCl.

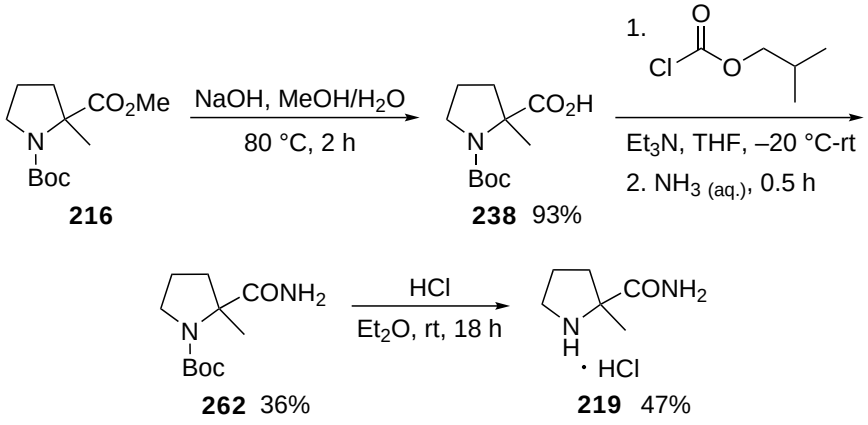

Scheme 2.17

Finally, the synthesis of benzimidazole fragment **229** was attempted. Initial concern over steric hindrance at the 2-position of the 2,2-disubstituted pyrrolidine for installing the benzimidazole group necessitated a model study to be carried out in which the key cyclocondensation step was tested on mono-substituted proline derivative (*S*)-**265** (Scheme 2.18). Following literature conditions for the same substrate,[93] acid (*S*)-**265** was reacted with Et_3N and isobutyl chloroformate in THF at −20 °C to yield the mixed anhydride intermediate which, following reaction with diaminobenzene, gave the amide. Cyclisation (by refluxing with acetic acid for 18 h) furnished the desired benzimidazole heterocycle (*S*)-**266** in 60% yield after chromatography.

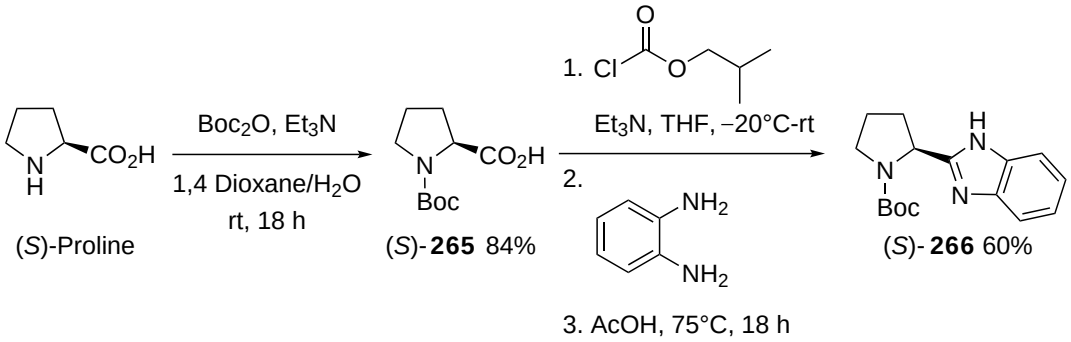

Scheme 2.18

Cyclisation and benzimidazole formation on the 2,2-disubstituted pyrrolidine scaffold was then tested (Scheme 2.19). Starting from acid **238**, benzimidazole formation was attempted using the previously established experimental conditions. Unfortunately, cyclisation was unsuccessful and dicarbamate **268** was isolated in quantitative yield. Starting material was also recovered in 16% yield. Presumably, the formation of dicarbamate **268** results from the mechanism proposed in Scheme 2.19 in which diaminobenzene reacts twice at the less sterically hindered site of mixed anhydride intermediate **267** to form dicarbamate **268**.

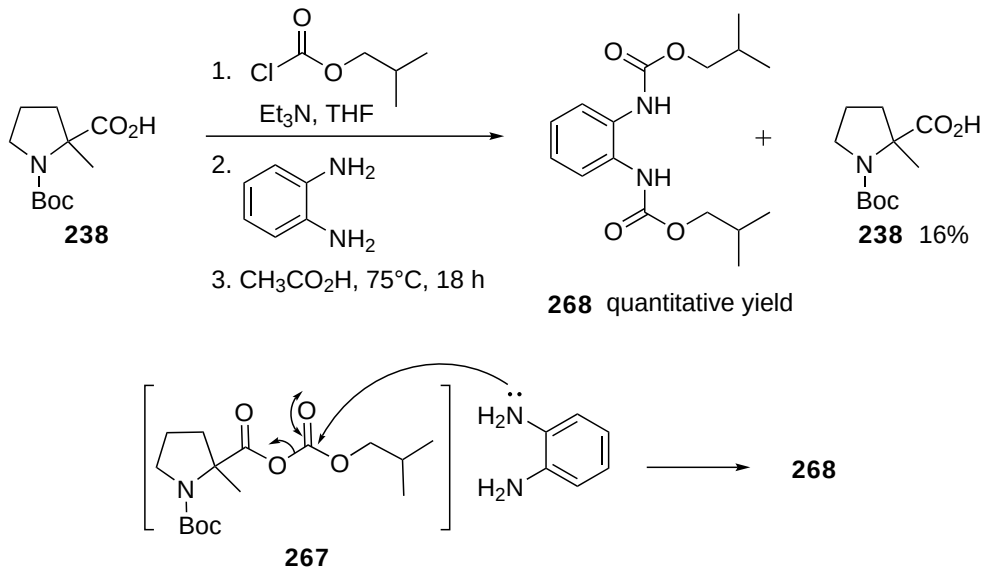

Scheme 2.19

In summary, FGI and *N*-functionalisation of a key ester intermediate **216** were used to access fragments with acid, amide, nitrile and methyl ether functionality in an expedient manner. To this end, six 2,2-disubstituted pyrrolidine fragments were synthesised in 3-5 steps. The synthesis of fragments **224** and **229** proved more challenging. Three coupling reagents and two different protection-deprotection strategies were investigated for the synthesis of fragment **224** but none were successful. The steric hindrance created by the 2,2-disubstituted scaffold also proved problematic in the synthesis of fragment **229**. In this case, it was not possible to convert the acid in **238** into the desired benzimidazole group.

2.2 Synthesis of 2,3-Disubstituted Piperidine Fragments

2.2.1 Design and PMI Analysis of *cis*-2,3-Disubstituted Piperidine Fragments

In a similar way to the 2,2-disubstituted pyrrolidine fragments, the design and synthesis of 3-D fragments based on the *cis*-2,3-disubstituted piperidine scaffold hinged primarily on synthetic tractability and 3-D shape. It was envisioned that the desired scaffold could be synthesised starting from pyridine **269** using methodology previously developed in the group[91] (Scheme 2.20). To this end, esterfication and hydrogenation of pyridine acid **269** would give key intermediate *cis*-**270** in 2 steps. Then, *N*-functionalisation (mesylation or acylation) followed by transformation of the ester group in piperidine *cis*-**270** using previously established reactions should give fragments containing primary alcohol, acid, amide and nitrile groups. Alternatively, transformation of *N*-Boc protected piperidine ester *cis*-**271** followed by Boc group removal would provide access to NH fragments (R^1 = H).

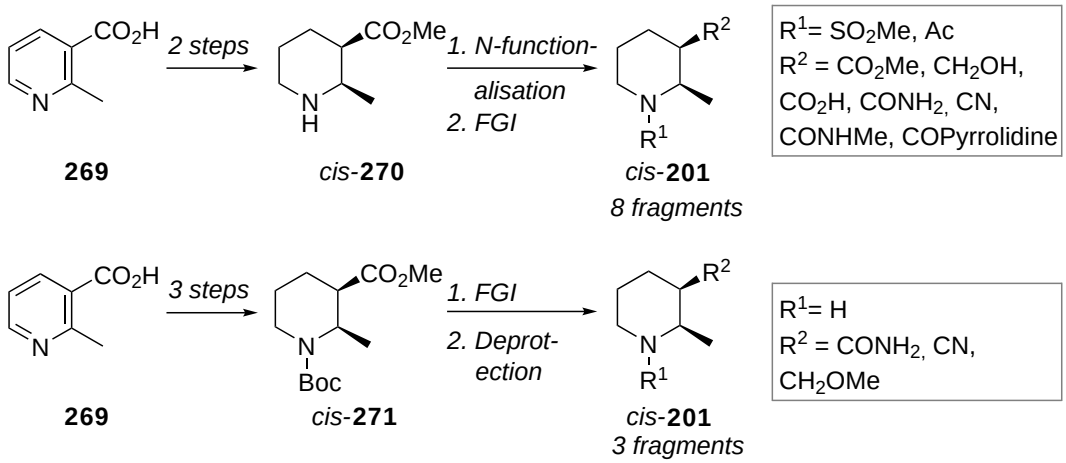

Scheme 2.20

Fragments based on the *cis*-2,3-disubstituted piperidines with functionality in the 2-position could also be accessed using a hydrogenation strategy from pyridine ester **272** (Scheme 2.21). Previous work in the group[91] showed that, in this case, *cis*- and *trans*-diastereoisomers were not separable by chromatography. Therefore, *N*-Boc protection

would be investigated for the separation of *cis*- and *trans*- diastereomers. Then, *N*-Boc removal of piperidine *cis*-**274** followed by *N*-functionalisation (mesylation or acylation) and ester reduction (for one fragment) would give 3-D fragments *cis*-**202**. In this way, the use of established synthetic methodology followed by modification of the ester group, would provide an efficient synthetic route to structurally diverse piperidine fragments. Importantly, design ideas established for the first iteration of pyrrolidines (two binding pharmacophores R^1 and R^2 and, a methyl group) were incorporated in the structural design of the *cis*-2,3-disubstituted piperidine fragments.

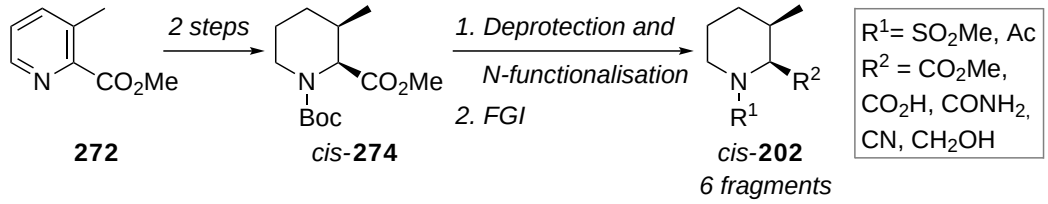

Scheme 2.21

Analysis of 3-D shape was carried out in the same way as for the 2,2-disubstituted pyrrolidines. Ester modification of key intermediates *cis*-**270** and *cis*-**273** to acid, amide, nitrile, primary alcohol and methyl ether groups (with $R^1 = H$) had little effect on 3-D shape (Figures 2.5 and 2.6). Indeed, all conformations up to 1.5 kcal mol^{-1} above the energy of the global minimum energy conformer for each fragment (with $R^2 = CO_2Et$, CO_2H, $CONH_2$, CONHMe, COPyrrolidine, CN, CH_2OH, CH_2OMe) fell within a similar range of ΣNPR values 1.10-1.50 for scaffold *cis*-**201** and ΣNPR values 1.10-1.20 for scaffold *cis*-**202**. As with the 2,2-disubstituted pyrrolidines, 3-D shape of the *cis*-2,3-disubstituted piperidines appears to depend more on the scaffold structure itself and less on the ring substituents.

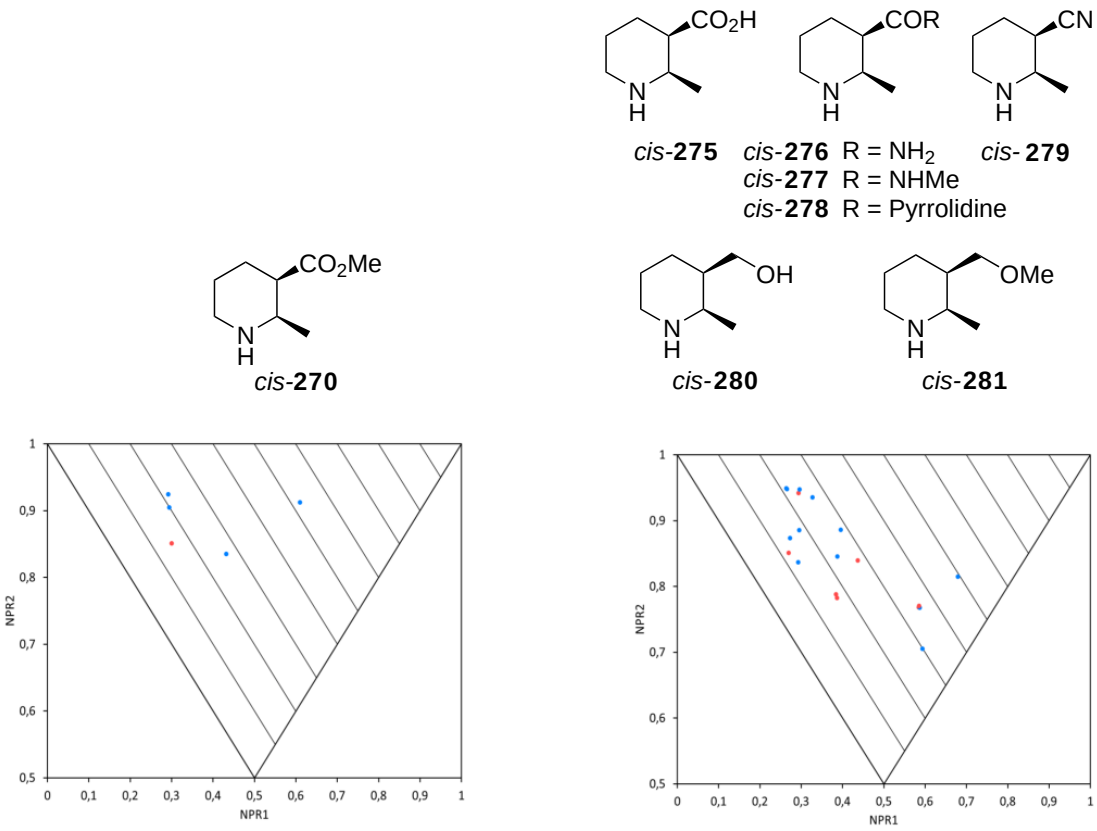

Figure 2.5: PMI Analysis of Potential Fragments. Red dots indicate global minimum energy conformers and blue dots indicate higher energy conformers

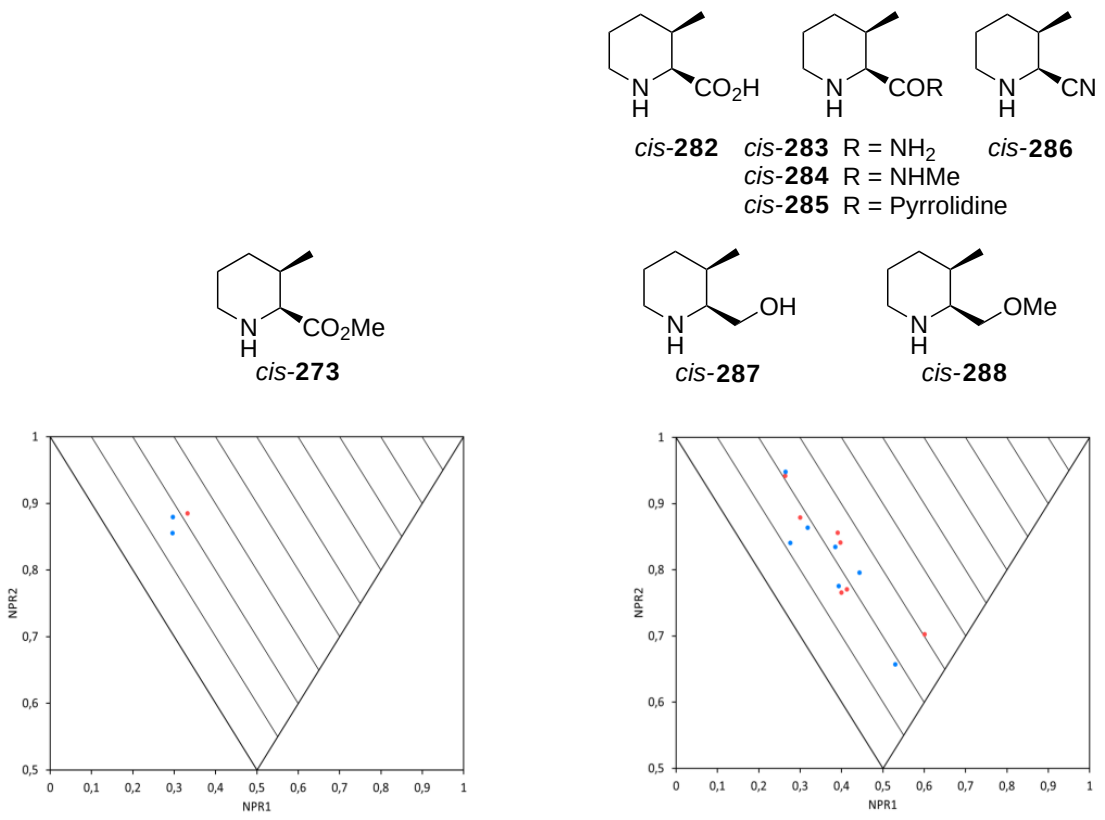

Figure 2.6: PMI Analysis of Potential Fragments. Red dots indicate global minimum energy conformers and blue dots indicate higher energy conformers

The effect of the nitrogen substitutent (R^1 = H, Me, SO_2Me and Ac) on 3-D shape was also explored. PMI analysis of modified fragments *cis*-**275** to *cis*-**288** (with R^1 = H, Me, SO_2Me and Ac) was carried out resulting in 14 PMI plots of 56 compounds (not shown). Ultimately, the 17 fragments shown in Figures 2.7 and 2.8 were selected for synthesis. Although piperidines *cis*-**276**, *cis*-**279**, *cis*-**281** and *cis*-**289**-*cis*-**296** (Figure 2.7) were found to be structurally similar (conformations fall within the same area of the PMI plot), all target compounds were synthetically tractable as many targeted fragments act as intermediates for further fragment generation. Moreover, we reasoned that as a whole, structural diversity would be maintained by combining all synthesised 3-D fragments. Importantly, all targeted fragments have at least one conformation with a ΣNPR value of $\geq$ 1.1 and display a diverse range of functional groups on both the nitrogen and piperidine scaffold.

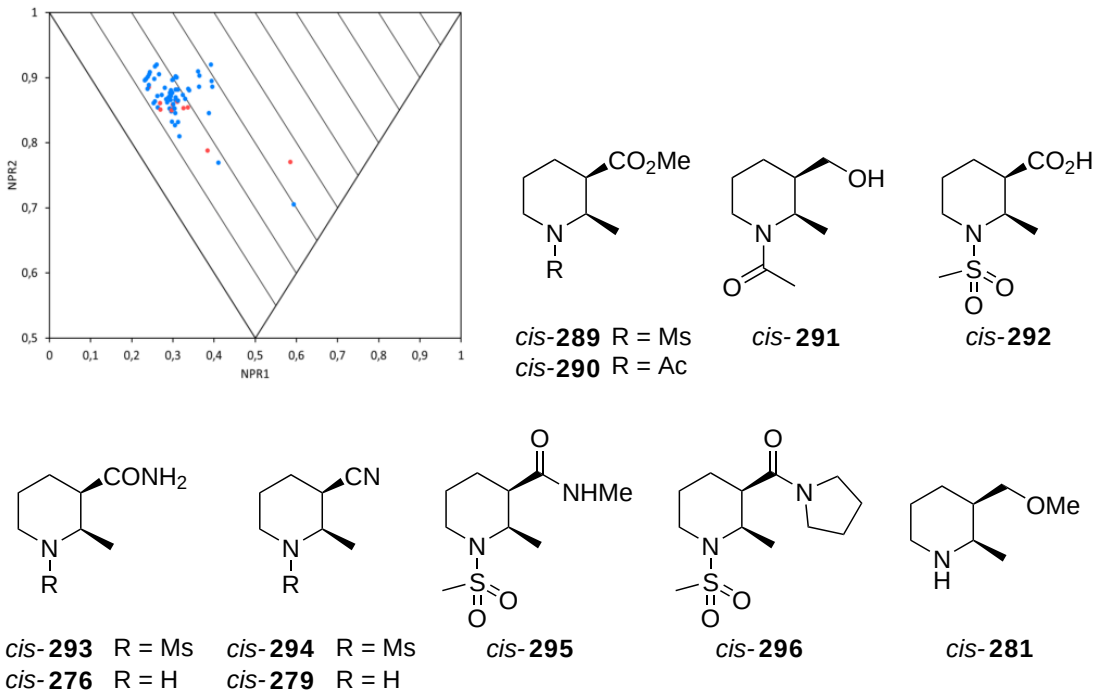

Figure 2.7: PMI Analysis of Targeted Fragments. Red dots indicate global minimum energy conformers and blue dots indicate higher energy conformers

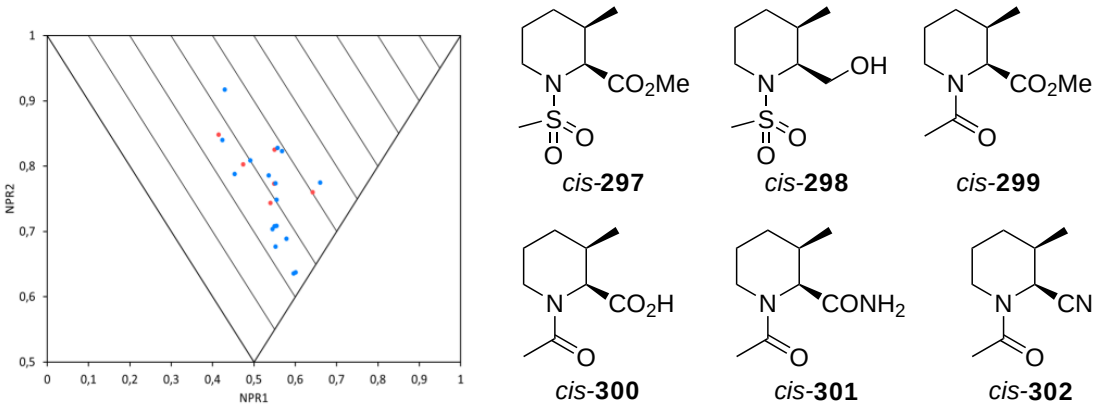

Figure 2.8: PMI Analysis of Targeted Fragments. Red dots indicate global minimum energy conformers and blue dots indicate higher energy conformers

2.2.2 Overview of Previous Synthetic Routes towards *cis*-2,3-Disubstituted Piperidines

Hydrogenation of disubstituted pyridines is the mostly widely used approach for the synthesis of the disubstituted piperidine scaffold.[94–96] Coordination of the Pd or Pt catalyst to the pyridine facilitates preferential *cis*-addition of hydrogen such that hydrogenation typically proceeds with high *cis*-diastereselectivity. Depending on the substitution pattern, access to the corresponding *trans*-diastereoisomer with an ester substituent is sometimes possible using base-mediated epimerisation.

Selected examples which use hydrogenation as a synthetic approach to access the 2,3-disubstituted scaffold are shown in Scheme 2.22. Typical conditions involve the use of a PtO_2 or $Pd(OH)_2$ catalyst with H_2 in MeOH or EtOH. In all cases, 2,3-disubsituted piperidines *cis*-**282** and *cis*-**305** were accessed as single diastereoisomers in high yield.[94–96]

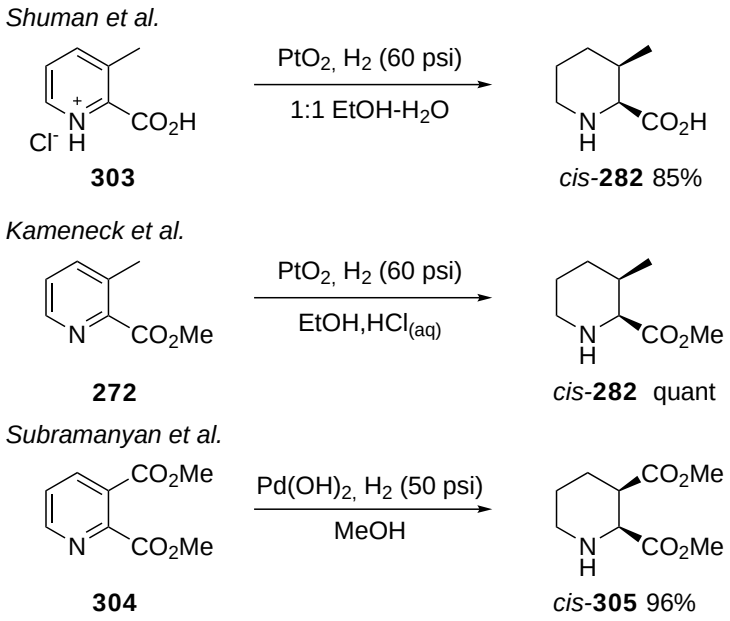

Scheme 2.22

An alternative approach for the synthesis of the 2,3-disubstituted piperidine scaffold was reported by Whitten and co-workers.[97] Cyclisation of the enolate intermediate

formed on deprotonation of iodo ester **306** with LDA at −78 °C gave a mixture of *trans*-**307** and *cis*-**307** (Scheme 2.23). However, adjustment of the temperature (from −75 °C to −35 °C) and the proton source (from acetic acid to 2,6-diisopropylphenol) resulted in *cis*-selectivity and *cis*-**307** was isolated in 65% yield.

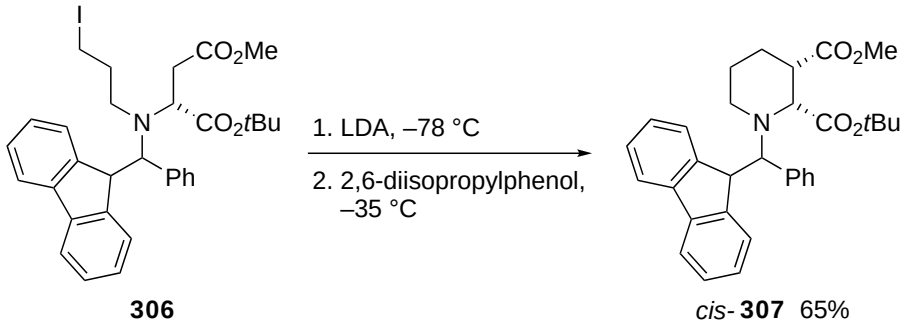

306 *cis*-**307** 65%

Scheme 2.23

Normant *et al.* also used an alternative approach in the synthesis of di-, tri-, tetra-, and penta-substituted piperidines.[98] In this case, carbocyclisation of an amino zinc enolate **309** furnished *cis*-**310** as a single diastereomer. Enolate formation from ester **308** with LDA in Et_2O at −78 °C followed by transmetallation with zinc bromide gave the *Z*-α-amino zinc enolate **309**. Coordination of the alkene and enolate by zinc bromide allowed for stereochemical control to give only the *cis*-diastereomer. On warming, cyclisation gave zincate *cis*-**310** as a single diastereomer. Subsequent hydrolysis, iodinolysis or reaction with allyl bromide gave piperidines *cis*-**311**, *cis*-**312** and *cis*-**313**. Epimerisation with LDA provided access to the corresponding *trans*-diastereomers including piperidine *trans*-**311**.

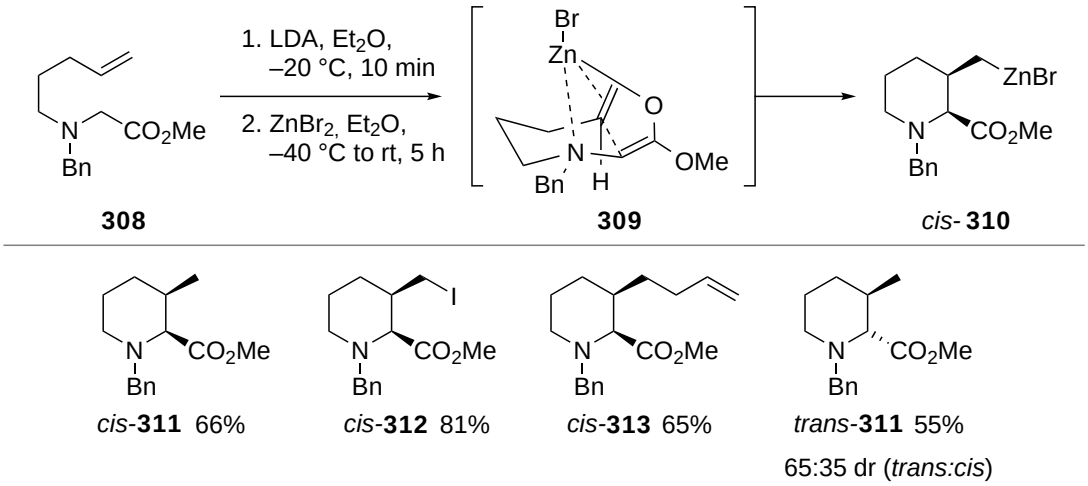

Scheme 2.24

The literature precedence for, and convenience of, the hydrogenation strategy (from pyridine) in the synthesis of the 2,3-disubstituted piperidine scaffold led us to use this approach in the synthesis of the targeted *cis*-2,3-disubstituted piperidine 3-D fragments.

2.2.3 Synthesis of *cis*-2,3-Disubstituted Piperidines

The plan was to synthesise 2,3-disubstituted fragments *cis*-**289**-**296** from common intermediate, piperidine *cis*-**270** (Scheme 2.25). *N*-Functionalisation (mesylation or acylation) followed by modification of the ester group (for fragments *cis*-**291**-**296**) using well known functional group conversion chemistry would give a structurally diverse set of piperidines *cis*-**289**-*cis*-**296**. Alternatively, amine fragments *cis*-**276**-**281** could be synthesised from *N*-Boc protected piperidine *cis*-**271**. Modification of the ester group to amide, nitrile and methyl ether groups followed by *N*-Boc removal would give piperidines *cis*-**276**, *cis*-**279** and *cis*-**281**.

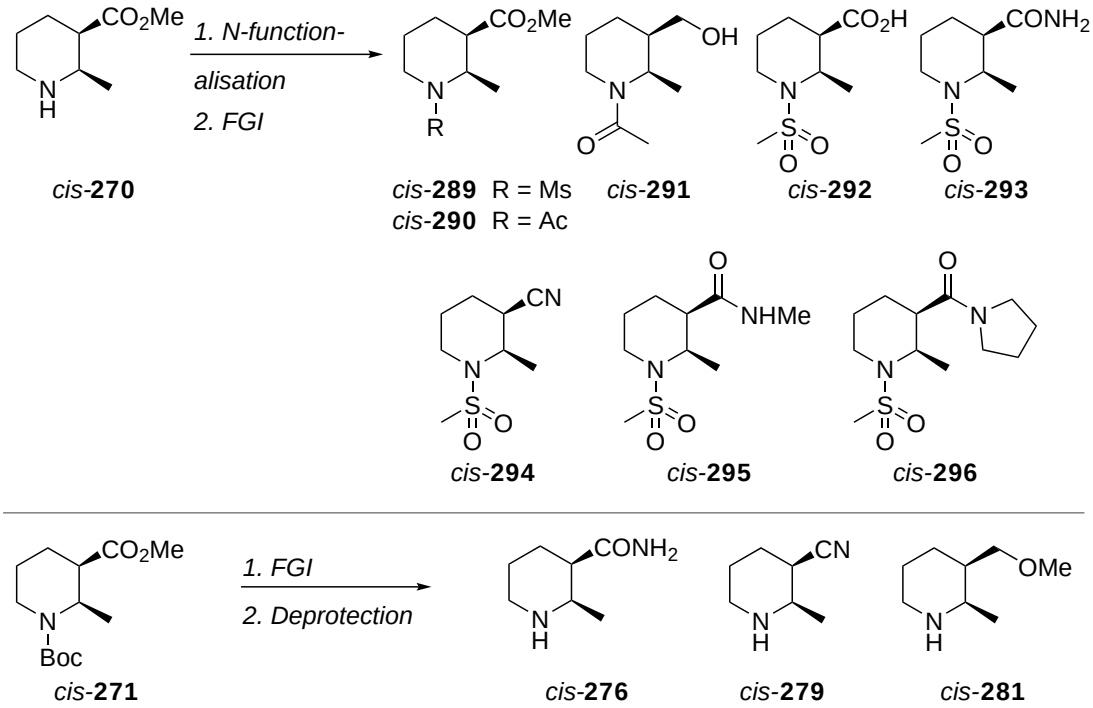

Scheme 2.25

The synthesis of piperidine *cis*-**270** is outlined in Scheme 2.26. Pyridine ester **314** was synthesised from the corresponding acid **269** using previously established methodology in the group[91] (with $SOCl_2$ and MeOH at reflux) to give, following evaporation, ester **314**·HCl as its hydrochloride salt which was used without further purification. The synthesis of piperidines *cis*- and *trans*-**270** has previously been reported by Cox *et al.*

in their synthesis of 2,3-disubstituted piperidine amide compounds as antagonists for orexin receptors.[99] Following their procedure, ester **314**·HCl was hydrogenated with 10 mol% PtO_2 in acetic acid under a H_2 atmosphere for 18 h. ^{1}H NMR spectroscopic analysis of the crude product obtained after a basic work-up showed a 90:10 mixture of piperidines *cis*- and *trans*-**270**, which following chromatography gave piperidine *cis*-**270** in 67% yield and a 90:10 mixture of piperidines *cis*- and *trans*-**270** in 22% yield. Although diagnostic ^{1}H NMR spectroscopic signals differ slightly from those in the literature (doublets at 1.25 and 1.07 ppm were reported for piperidines *cis*- and *trans*-**270** respectively[99] whereas our values were 1.04 and 0.98 ppm) we are confident in our assignment of relative stereochemistry as *cis*-**270** was subsequently converted into fragments *cis*-**292** and *cis*-**294** and their stereochemistry was established by X-ray crystallography (see Figure 2.10).

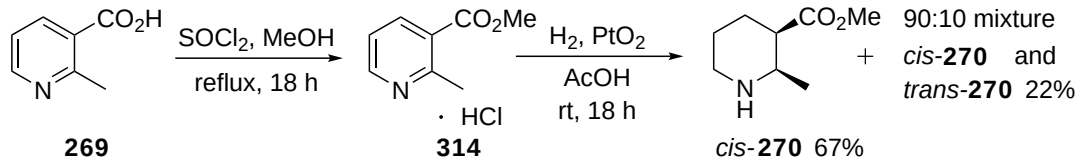

Scheme 2.26

The *cis*-2,3-disubstituted piperidine scaffold of **270** can adopt one of two possible chair conformations (Figure 2.9). The *cis*-arrangement leads to an equatorial-axial relationship such that if the carboxylic ester is in the equatorial position, the methyl group must be placed in an axial position (conformation A). The opposite holds true for conformation B. In this case, ^{1}H NMR spectroscopy was used to distinguish between the two conformations. In the ^{1}H NMR spectrum of *cis*-**270**, the C*H*CO_2Me proton appears as a ddd with J values of 13.5, 4.0 and 4.0 Hz due to $^3J_{ax-ax}$ coupling and two instances of $^3J_{ax-eq}$ coupling consistent with conformation A. This is a surprising result as the methyl group has a larger A-value (1.7 kcal mol^{-1}) than the ester group (1.27 kcal mol^{-1}).[100]

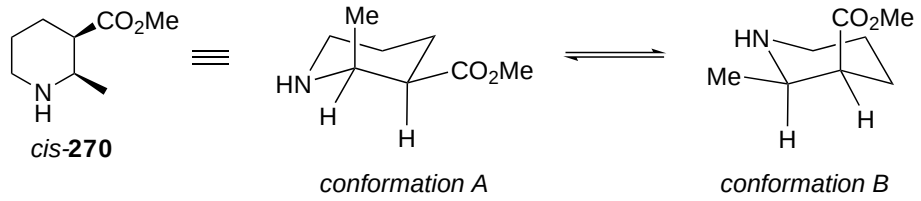

Figure 2.9: Conformations of the *cis*-2,3-disubstituted Piperidine Scaffold

With piperidine *cis*-**270** in hand, fragments *cis*-**289** and *cis*-**292**-**294** were synthesised in a successive manner using previously established conditions for functional group conversion (Scheme 2.27). Mesylation of amine *cis*-**270** gave ester *cis*-**289** in 88% yield. Then, modification of the ester group *via* ester hydrolysis, amide formation and dehydration gave fragments *cis*-**292**, *cis*-**293** and *cis*-**294** respectively in moderate to high yield. Using this approach, four targeted fragments were accessed in 1-4 steps from piperidine *cis*-**270**.

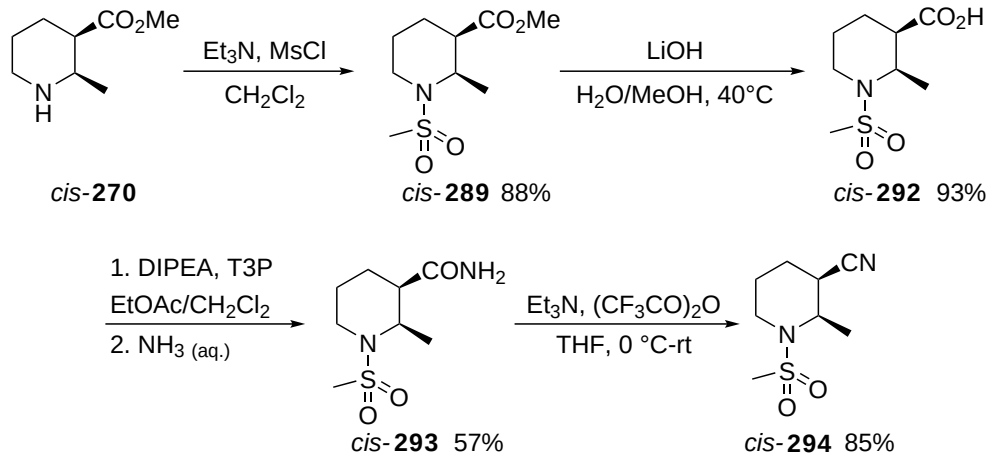

Scheme 2.27

Amide fragments *cis*-**295** and *cis*-**296** in turn were synthesised from acid *cis*-**292** using the standard T3P conditions for amide formation (Scheme 2.28). The relative *cis*-configuration of all fragments in Schemes 2.27 and 2.28 was confirmed by ^{1}H NMR spectroscopy with characteristic $^3J_{ax-ax}$, $^3J_{ax-eq}$ and $^3J_{ax-eq}$ coupling constants consistent with a conformation in which the methyl group was axial and the other substituent was equatorial.

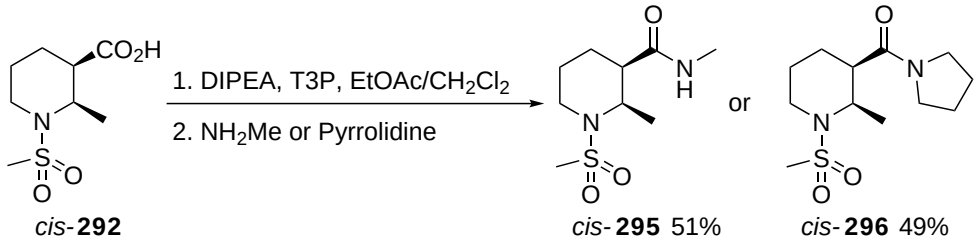

Scheme 2.28

Further evidence for the proposed *cis*-configuration of fragments *cis*-**289** and *cis*-**292**-**296** was provided by X-ray crystal structures of fragments *cis*-**292** and *cis*-**294** (Figure 2.10). X-ray crystallography confirmed the *cis*-arrangement of the acid (or nitrile) and methyl groups with the acid (or nitrile) group lying in the equatorial position. Furthermore, the X-ray crystallographic data showed that the nitrogen was sp^2 hybridised. Presumably, if the methyl group adopted an equatorial position, there would be a significant steric clash with the *N*-mesyl group.

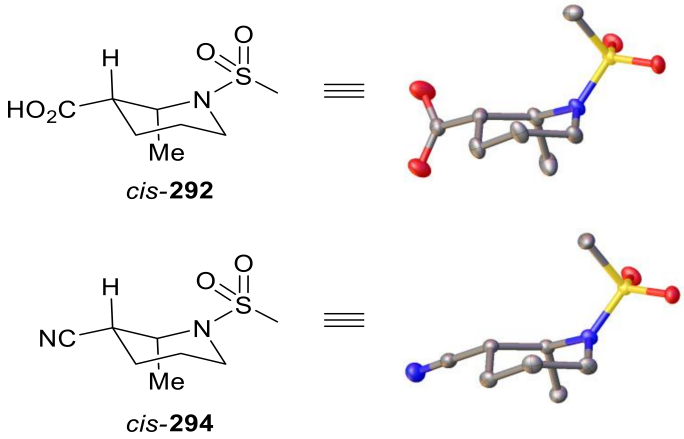

Figure 2.10: X-ray Crystal Structures of Fragments *cis*-**292** and *cis*-**294**

Fragments *cis*-**290** and *cis*-**291** were synthesised directly from a mixture of piperidines *cis*- and *trans*-**270** (Scheme 2.29). Acylation of the 90:10 piperidine mixture (*cis*-**270** and *trans*-**270**) gave ester *cis*-**290** in 83% yield following chromatography; *trans*-**290** was not isolated. The ^{1}H NMR spectrum for *cis*-**290** showed a duplicate set of signals which were confirmed to be rotamers after high temperature ^{1}H NMR spectroscopy (100 °C in DMSO) resulted in coalescence of signals into a single set. Next, reduction

of ester *cis*-**290** with $LiBH_4$ in THF afforded alcohol *cis*-**291** in 64% yield.

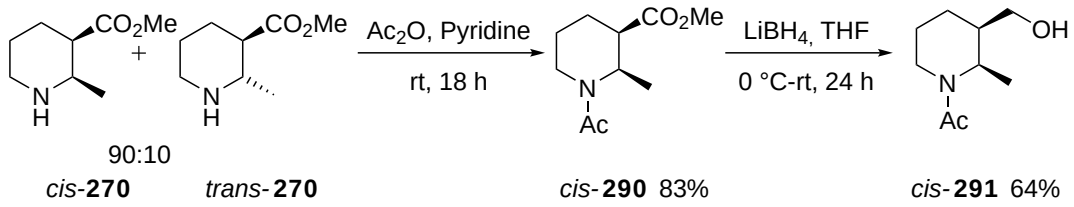

Scheme 2.29

Attention then focused on the synthesis of amine fragments *cis*-**276**, *cis*-**279**, *cis*-**281**. *N*-Boc protection of the 90:10 mixture of piperidines *cis*- and *trans*-**270** gave the *N*-Boc methyl esters which were separable by chromatography. This gave *N*-Boc methyl esters *cis*-**271** and *trans*-**271** in 78% and 4% yield respectively over 3 steps from pyridine acid **269** (Scheme 2.30). ^{1}H and ^{13}C NMR spectroscopic data for compound *cis*-**271** was consistent with those reported in the literature.[101] In the ^{1}H NMR spectrum of *cis*-**271**, the C*H*CO_2Me proton appears as a ddd with J values of 13.0, 4.0 and 4.0 Hz due to $^3J_{ax-ax}$ coupling and $^3J_{ax-eq}$ couplings. This indicates that *N*-Boc methyl ester *cis*-**271** has a conformation with an axial methyl group and an equatorial ester group, similar to the mesyl compounds discussed above. Presumably, if the methyl group adopted an equatorial position, there would be a significant steric clash with the *N*-Boc group.

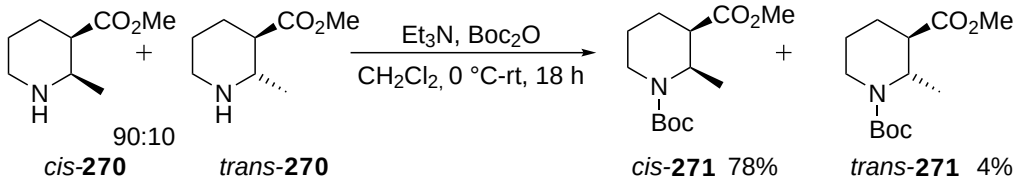

Scheme 2.30

With *N*-Boc methyl ester *cis*-**271** in hand, modification of the ester group delivered targeted fragment *cis*-**276**·HCl over 3 steps (Scheme 2.31). Established conditions for ester hydrolysis, amidation and *N*-Boc removal were used to access acid, amide and amine groups. In all cases, ^{1}H NMR spectroscopy supported the assignment of a conformation with an axial methyl group and the other substituent in an equatorial position, with coupling constants as expected for intermediates *cis*-**315**, *cis*-**316** and fragment

cis-**276**·HCl. Fragment **279**·HCl was in turn synthesised from *N*-Boc amide *cis*-**316** detailed as follows (Scheme 2.31). Dehydration of amide *cis*-**316** to nitrile *cis*-**317** proceeded smoothly affording nitrile *cis*-**317** in 80% yield. Fragment *cis*-**279**·HCl was obtained following *N*-Boc removal with HCl in Et_2O in quantitative yield.

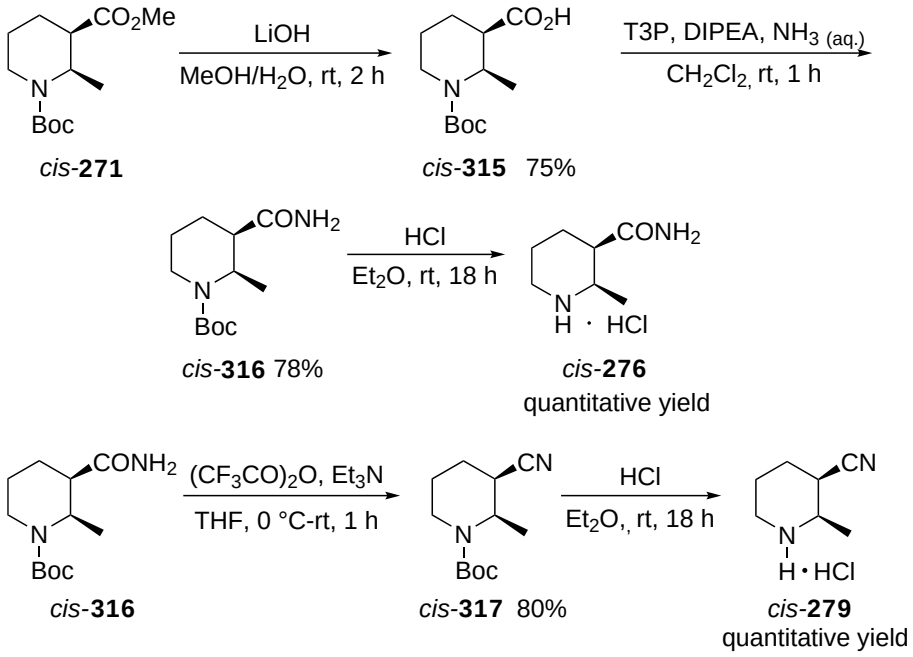

Scheme 2.31

Finally, reduction of *N*-Boc ester *cis*-**316** to the corresponding alcohol was carried out with $LiAlH_4$ to afford alcohol *cis*-**318** in 73% yield (Scheme 2.32). Methylation of alcohol *cis*-**318** with NaH and methyl iodide gave methyl ether *cis*-**319** in 96% yield. *N*-Boc removal under acidic conditions then gave targeted fragment *cis*-**281**·HCl in quantitative yield.

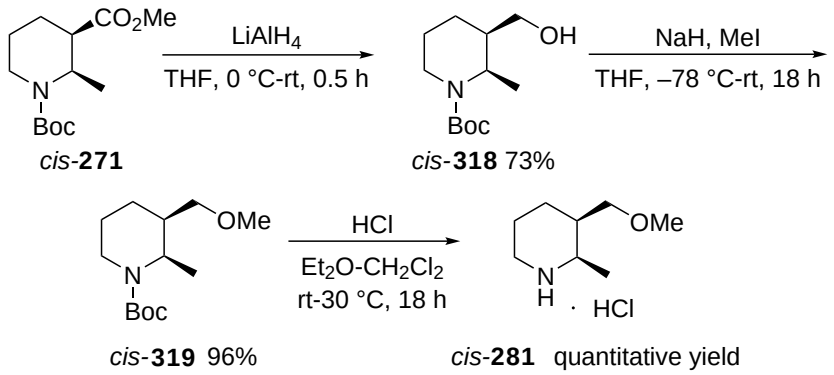

Scheme 2.32

For the analogous *cis*-2,3-disubstituted piperidine fragments with functionality in the 2- position, it was envisioned that they could be synthesised using a similar approach. Therefore, *N*-Boc removal and amine functionalisation (mesylation or acylation) of ester *cis*-**230** would give fragments *cis*-**297** and *cis*-**299** (Scheme 2.33). Further modification of the ester group would then deliver functionalised fragments *cis*-**298** and *cis*-**300**-**302**.

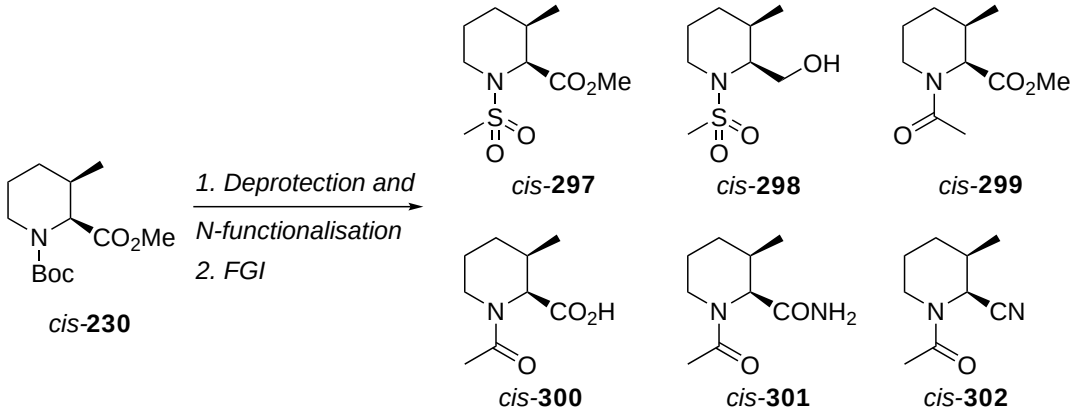

Scheme 2.33

N-Boc methyl ester *cis*-**230** was synthesised by hydrogenation and *N*-Boc protection from commercially available pyridine ester **272** (Scheme 2.34). Hydrogenation using 10 mol% PtO_2 gave an 80:20 mixture of piperidines *cis*-**273** and *trans*-**273** by ^{1}H NMR spectroscopic analysis of the crude product. Piperidines *cis*- and *trans*-**273** were distinguished by signals for the methyl group at 0.89 ppm and 0.83 ppm respectively. Spectroscopic data was consistent with those reported in the literature for for piperi-

dine ester *cis*-**273**.[102] Then, *N*-Boc protection of piperidines *cis*-**273** and *trans*-**273** allowed for separation and isolation of *N*-Boc methyl ester *cis*-**230** in 70% yield over 2 steps from pyridine ester **272**. An 85:15 mixture of *trans*-**273** and *cis*-**273** was also isolated in 19% yield. The ^{1}H NMR spectroscopic data for compound *cis*-**230** was consistent with those reported in the literature[102] and enabled assignment of the relative stereochemistry in this series of compounds.

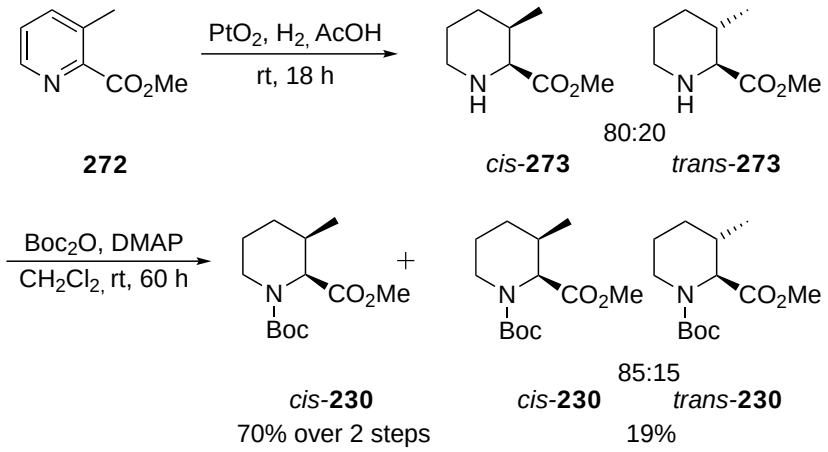

Scheme 2.34

The synthesis of fragments *cis*-**297** and *cis*-**298** is outlined in Scheme 2.35. *N*-Boc group removal from *N*-Boc methyl ester *cis*-**230** under acidic conditions followed by mesylation of the TFA salt *cis*-**273**·TFA generated fragment *cis*-**297** in 73% yield after chromatography. The relative stereochemistry of *cis*-**297** was confirmed by ^{1}H NMR spectroscopy. The C*H*CO$_2$Me proton of *cis*-**297** appears as a doublet with a J value of 6.0 Hz due to $^3J_{eq-eq}$ coupling, confirming the *cis*-arrangement of the methyl and carboxylic ester groups. Then, reduction of ester *cis*-**297** using $LiAlH_4$ gave fragment *cis*-**298** in 19% yield.

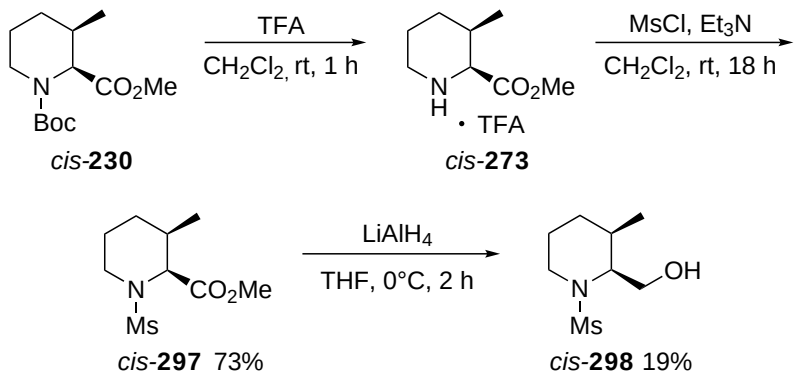

Scheme 2.35

Acylated ester *cis*-**299** was synthesised using the a similar approach. Thus, starting from *N*-Boc methyl ester *cis*-**230**, *N*-Boc removal under acidic conditions followed by acylation of the secondary amine gave fragment *cis*-**299** in 94% yield (Scheme 2.36). ^{1}H NMR spectroscopic data showed two sets of doublets (rotamers) for NC*H*CO_2Me at 5.16 and 4.32 ppm with $^3J_{eq-eq}$ coupling constants as expected for the *cis*-diastereoisomer. Then, hydrolysis of ester *cis*-**299** (with LiOH in MeOH/H_2O) *en route* to fragment *cis*-**300** was attempted. This gave a 75:25 mixture of acid *cis*- and *trans*-**300**, which could not be distinguished. In the ^{1}H NMR spectrum, the NC*H*CO_2Me proton appeared as two doublets at 5.08 ppm and 4.51 ppm with J values of 6.0 and 5.5 Hz respectively. The magnitudes of these two J values are consistent with $^3J_{eq-ax}$ coupling in acid *cis*-**300** and with $^3J_{eq-eq}$ in acid *trans*-**300** although it was not possible to assign each set of signals to a particular diasteroemeric acid. In order to rule out the possibility of the two sets of signals being due to rotamers, high temperature ^{1}H NMR spectroscopy (80 °C in DMSO) was carried out but the two sets of signals did not coalesce into one set. Alternative milder conditions with KOTMS in THF resulted in a 75:25 mixture of *cis*- and *trans*-**300**. Refluxing fragment *cis*-**299** with aqueous HCl for 2 h also failed to form the desired compound *cis*-**300** and no product was isolated in this case. Attempts to access amide and nitrile fragments *cis*-**301** and *cis*-**302** from reaction of the mixture of piperidines *cis*- and *trans*-**300** were not carried out. At this point, synthesis of amide and nitrile fragments *cis*-**301** and *cis*-**302** was halted.

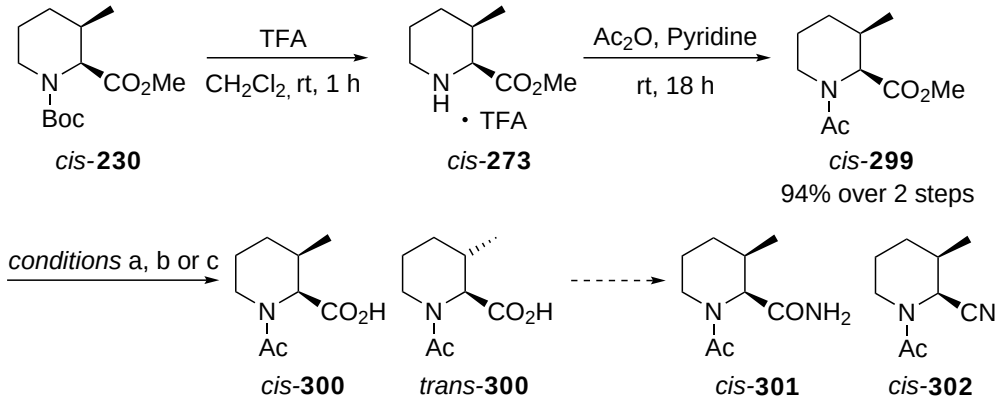

conditions

(a) LiOH, MeOH/H_2O (1:1), rt, 18 h (b) KOTMS, THF, rt, 2 h (c) $HCl_{(aq)}$, reflux (100 °C), 2 h

Scheme 2.36

In summary, 14 *cis*-2,3-disubstituted piperidine fragments were synthesised from key intermediates *cis*-**270**, *cis*-**271** and *cis*-**230**. A combination of *N*-Boc removal, *N*-functionalisation and, in some cases, modification of the ester group furnished the targeted piperidine 3-D fragments. Notably, these fragments are structurally diverse with ester, acid, amide, nitrile, primary alcohol and methyl ether groups represented. Moreover, successive functional group interconversion between fragments allowed for a highly expedient route (1-4 steps from the key intermediate) to the desired products. In most cases, the relative stereochemistry of intermediates and fragments could be conveniently assigned by ^{1}H NMR spectroscopy. In two cases, confirmation of stereochemistry was provided by X-ray crystal structures (fragments *cis*-**292** and *cis*-**294**). Synthesis of fragments *cis*-**300**, *cis*-**301** and *cis*-**302** proved more challenging due to epimerisation of acid *cis*-**300** during the ester hydrolysis of fragment *cis*-**299**. As a result, synthesis of 3-D fragments *cis*-**301** and *cis*-**302** was not possible.

2.3 Synthesis of Tropane Fragments

2.3.1 Design and PMI Analysis of Tropane Fragments

The 3-D fragments targeted thus far in the group had focused on the disubstituted pyrrolidine and piperidine scaffolds. In order to increase scaffold diversity, the search was widened to consider other scaffolds. In this context, the tropane scaffold attracted our interest due to its rigidity, with the potential to lower the entropic binding penalty, as well as its presence in naturally occurring tropane-based alkaloids and biologically active compounds.[103] The design and synthesis of fragments based on the tropane scaffold focused primarily on synthetic tractability, by using a single piece of methodology, and included the incorporation of aromatic groups. The latter consideration stemmed from limitations identified in the design of the pyrrolidine and piperidine fragments which were saturated heterocycles decorated with a methyl group and 1-2 points of functionality. The absence of aromatic groups resulted in a lower than average HAC across the 3-D fragment collection, and it was postulated that this could potentially lead to a lower hit rate. Furthermore, the lack of aromatic protons made fragment screening by NMR challenging, despite the incorporation of a methyl group for this purpose.

For the tropane fragments, the approach would start with the commercially available *N*-methyl tropinone **320** and two approaches for annulating a heteroaromatic ring would be explored (Scheme 2.37). Thus, starting from tropinone, bicyclic scaffold **204** could be accessed in 3 steps (Scheme 2.37). Initially, *N*-Me exchange with a Cbz group would be used to protect the primary amine of tropinone **320**. Then, Au-catalysed amination-cyclisation-aromatisation should deliver the pyridine group of **204**. *N*-Cbz removal and amine functionalisation would then give tropane-based, bicyclic fragments **204**. Notably, Au-catalysed cyclisation of tropinone with propargylamine to generate tricycle **204** (with R = H) is known[104] and the application of this methodology to 3-D fragment synthesis has also been reported.[58] Alternatively, the *N*-Cbz intermediate

321 could be used to access the methyl-thiazole group of **323**. Synthesis of the thiazole group from α-bromo ketones is well known with various methods reported.[105–107] Using a similar approach, bromination to form the α-bromo ketone *exo*-**322** followed by cyclocondensation with thioacetamide should give (following *N*-functionalisation) tropane-based fragments **323**.

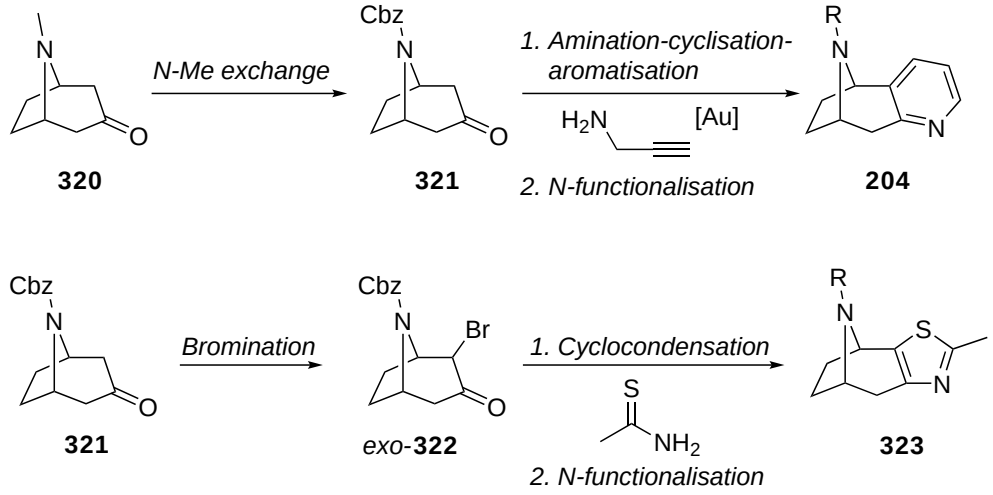

320 **321** **204**

321 *exo*-**322** **323**

Scheme 2.37

Prior to synthesis, the 3-D shape of potential tropane fragments was assessed by PMI analysis. The generated PMI plots for tropane scaffolds **204** and **323** (with R = H, Ac, SO_2Me, Me) are shown in Figure 2.11. Conformational diversity was limited (with three conformations up to 1.5 kcal mol^{-1} above the energy of the global minimum energy conformer for scaffolds **204** and **323**), presumably due to the rigidity imposed by the bridged bicycle. On the other hand, compounds exhibited 3-D shape in the less populated areas of 3-D chemical space, with six out of eight designed fragments (with R = Ac, SO_2Me, Me) having conformations with ΣNPR value > 1.30. Pyridine and methyl-thiazole fragments **324** and **328** (with R = H) had a comparably lower ΣNPR value but, being an intermediate *en route* to other targeted fragments and with ΣNPR value ≥ 1.1, were also considered for synthesis. Ultimately, fragments **324**, **326** and **205** were selected for synthesis.

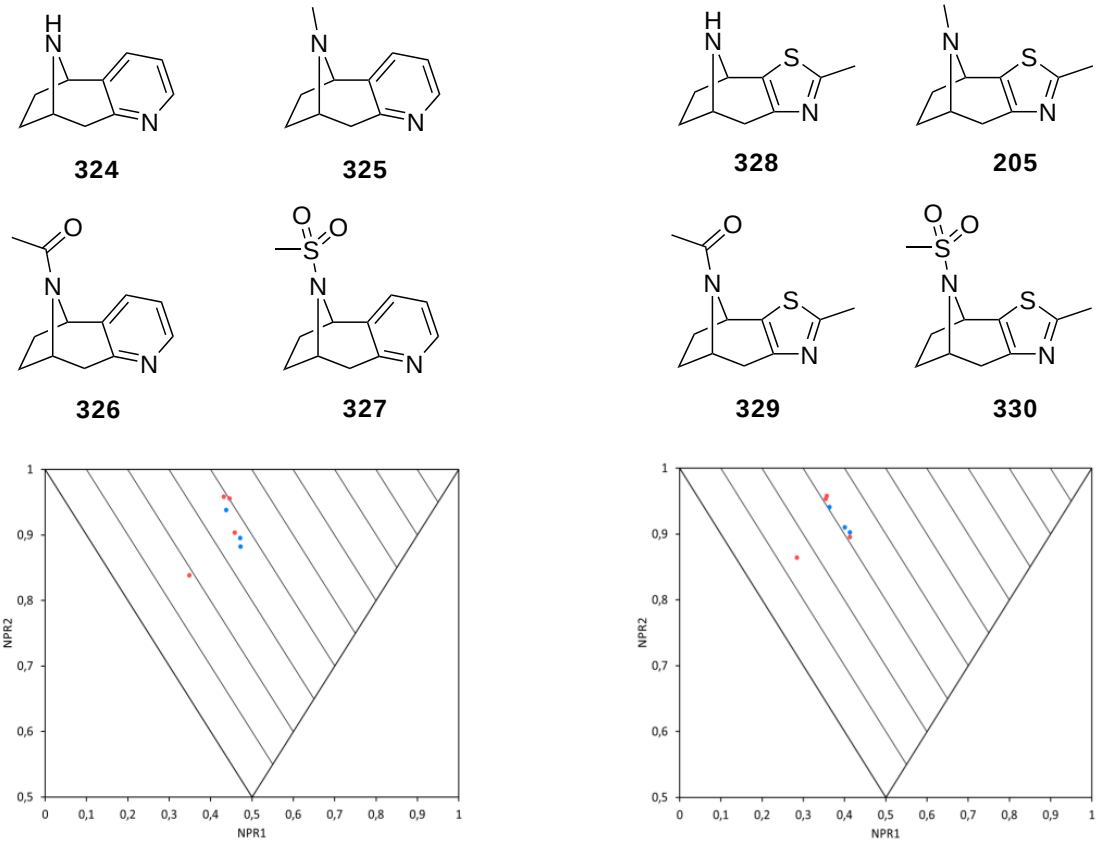

Figure 2.11: PMI Analysis of Potential Fragments. Red dots indicate global minimum energy conformers and blue dots indicate higher energy conformers

2.3.2 Synthesis of 3-D Fragments based on the Tropane Scaffold

In 2003, Abbiati *et al.* reported a Au/Cu salt-catalysed 6-*endo*-dig cyclisation reaction which was used to generate twenty functionalised pyridines (Scheme 2.38). Amination of commercially available ketones (or aldehydes) with propargylamine gave *N*-propargylenamine derivatives. Then, sequential 6-*endo*-dig cyclisation and aromatization furnished the pyridines. Notably, pyridine **325** is the *N*-Me derivative of target fragments **324** and **326**.

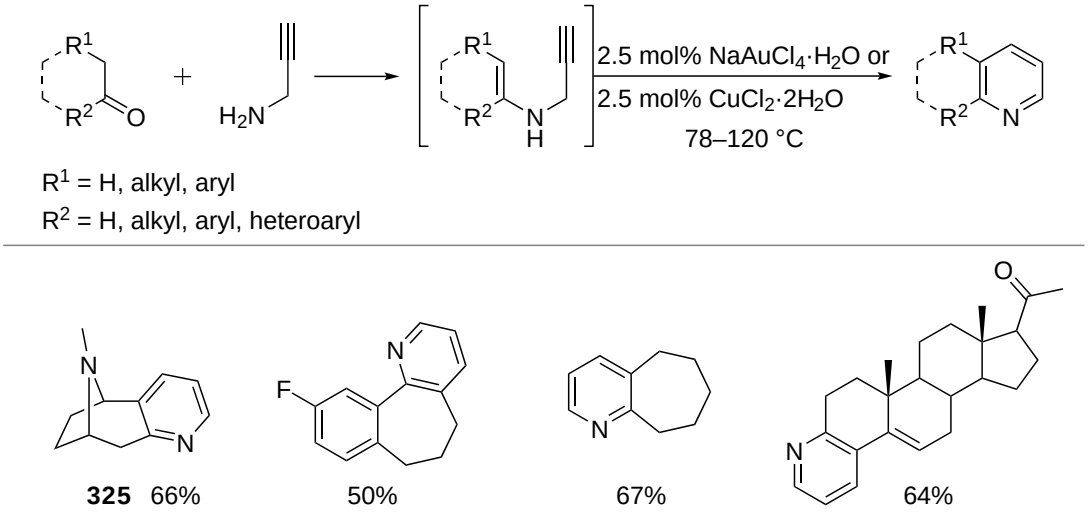

Scheme 2.38

Therefore, the plan was to explore whether this pyridine annulation methodology could be used to prepare a set of tropane-pyridine 3-D fragments. For our purposes, the *N*-Cbz analogue **321** would be used in place of *N*-Me tropinone. The use of a common protecting group instead of an *N*-Me group should provide a versatile strategy for generating various *N*-substituted tropanes. Starting from commercially available tropinone **320**, reaction of **320** with CbzCl following a literature procedure[108,109] gave the *N*-Cbz protected tropinone **321** (Scheme 2.39). Here, acylation occurs and then the chloride removes the *N*-methyl group in a S_N2 reaction on the ammonium salt intermediate. Then, following literature conditions,[104] ketone **321** was reacted with propargylamine in EtOH at 100 °C for 7 h. Au-catalysed cyclisation and aromatisation (with 2.5 mol% $NaAuCl_4{\cdot}2H_2O$) of the enamine intermediate furnished pyridine

331 in low yield (13%). Carrying out the reaction for a longer time (20 h) led to a moderate improvement in yield (24%). Notably, this result is lower yielding than that reported for the tropane *N*-Me derivative (66%, see Scheme 2.38).[104] Attempts to replicate Abbiati's work (starting from tropinone **320**) failed to give *N*-Me derivative **325**.

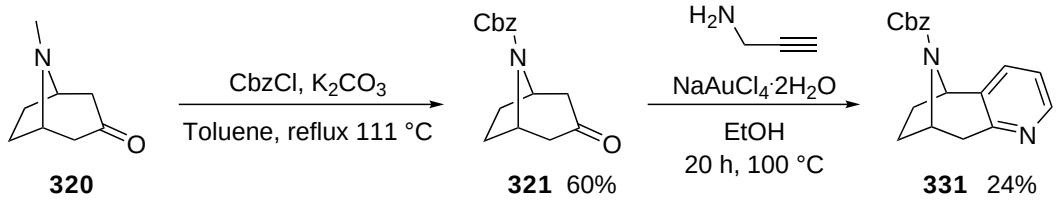

320 **321** 60% **331** 24%

Scheme 2.39

With pyridine **331** in hand, *N*-Cbz removal proved straightforward (Scheme 2.40). Hydrogenolysis of pyridine **331** using Pd/C and H_2 gave fragment **324** in excellent yield (96%). Subsequent acylation furnished *N*-acyl fragment **326** in 68% yield.

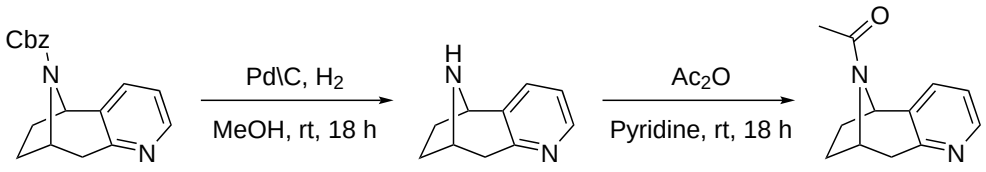

331 **324** 96% **326** 68%

Scheme 2.40

Next, attention turned to the synthesis of tropane-based fragment **205**. It was envisioned that the 2-methyl thiazole group of fragment **205** could be constructed in 2 steps (Scheme 2.41) *via* an α-bromoketone using a well-established general approach.[110] Firstly, following previously reported chemistry in the group for the α-bromination of enones,[111] enolate formation from intermediate **321** (with LHMDS in THF at −78 °C) and subsequent trapping with Me_3SiCl gave the silyl enol ether intermediate which, on reaction with NBS at 0 °C, furnished α-bromo ketone *exo*-**322** in 83% yield. The *exo*-stereochemistry is assumed but is likely due to *exo*-face attack of the enolate by NBS. Lithium enolate formation from tropinone using similar conditions (with *n*-BuLi/bis(1-

phenylethyl)amine in THF at 0 to −78 °C) followed by reaction with different electrophiles is known to be selective for the *exo*-diastereomer,[112] supporting the assumed stereochemistry of *exo*-**322**. Then, 2-methyl thiazole formation by reaction of α-bromo ketone *exo*-**322** with thioacetamide was trialled using several conditions[107,110,113,114] (Scheme 2.41). However, 2-methyl thiazole **332** was not isolated and in many cases starting materials, α-bromo ketone *exo*-**322** and thioacetamide, were recovered.

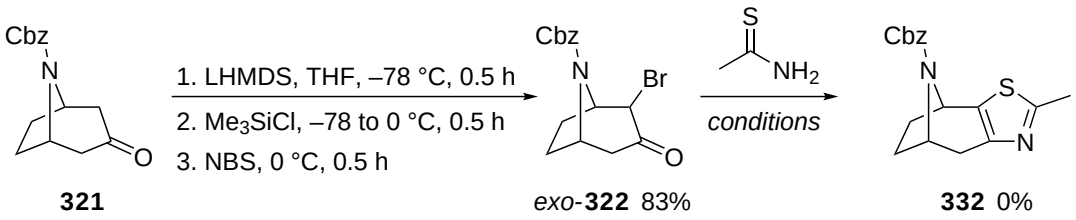

321 *exo*-**322** 83% **332** 0%

Conditions

1. EtOH, 100 °C, 4 h
2. DMF, 120 °C, 18 h
3. Toluene, Pyridine, 114 °C, 36 h
4. Pyridine, microwave, 110 °C 0.5 h

Scheme 2.41

In summary, tropane-based fragments **324** and **326** were successfully synthesised in 3 or 4 steps respectively from commercially available tropinone **320**. Use of a common synthetic scheme using a Au-catalysed amination-cyclisation-aromatisation reaction proved useful in generating the desired fragments in an expedient manner. In contrast, synthesis of fragment **332** proved more challenging. In particular, cyclocondensation of α-bromo ketone *exo*-**322** with thioacetamide failed to give fragment **332** using four sets of experimental conditions.

2.4 Synthesis of 2,3-Fused Cyclopropyl Pyrrolidine Fragments

2.4.1 Design and PMI Analysis of 2,3-Fused Cyclopropyl Pyrrolidine Fragments

The O'Brien group has experience in developing organolithium methodology for the synthesis of nitrogen heterocycles, having worked in this area of research for several years.[65–68] In particular, methodology for the asymmetric synthesis of the azabicyclo[3.1.0]hexane scaffold has been previously developed in the group.[115] Therefore, fragment design around this 2,3-fused cyclopropyl pyrrolidine was of interest since targeted fragments based on this scaffold would be, using previously established work, synthetically tractable. Moreover, the cyclopropyl group is present in eighteen FDA-approved drugs and, due to its structural rigidity and metabolic stability, is considered to be a privileged scaffold in medicinal chemistry.[116]

In terms of synthesis, two pieces of related methodology were identified for the construction of the 2,3-fused cyclopropyl pyrrolidine scaffold. In the first instance, lithiation-trapping chemistry developed by Beak and co-workers[117] could be used to construct bicycle **206** in 2-4 steps from *N*-Boc 4-chloropiperidine **333** (Scheme 2.42). Trapping with various electrophiles would allow for the introduction of functionality at the α-position (R^2 = CO_2H, SPh, C(O)3-pyridinyl) in an expedient manner. Functional group modification of the acid group (R^2 = CO_2H) would give an amide (R^2 = $CONH_2$) whereas modification of the thioether (R^2 = SPh) would give a sulfone and sulfoximines (R^2 = SO_2Ph, S(O)NHPh). The introduction of aromatic groups was also of interest to aid ^{1}H NMR screening and potentially improve protein binding. To this end, Negishi cross-coupling (of an organozinc reagent formed after transmetallation from lithium to zinc) which has previously been reported in the group[115] would enable access to α-arylated fragments **207**. Then, *N*-Boc removal and functionalisation (sulfonamide formation, acylation, mesylation, reductive amination and Buchwald-Hartwig coupling) would deliver targeted fragments **207** with R^1 = SO_2Ph, Ac, SO_2Me, Me and

3-pyridinyl groups.

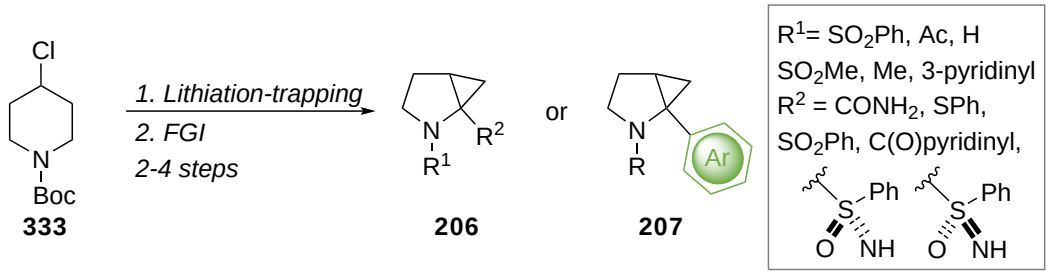

Scheme 2.42

Using this approach, structural diversity could be introduced by simply changing the electrophile (in lithiation-trapping chemistry) or aryl bromide (in Negishi cross-coupling) thereby increasing the structural diversity of our 3-D fragment collection. In addition, targeted 3-D fragments were designed to have two sites for protein binding and/or future elaboration (R^1 and R^2/Ar). The introduction of SO_2Ph (by sulfonamide formation) and 3-pyridinyl groups (by Buchwald-Harwig coupling) on the nitrogen would be used as a second strategy for incorporating aromatic groups into targeted 3-D fragments.

With a proposed synthetic strategy to access the 2,3-fused cyclopropyl pyrrolidine scaffold in place, the molecular shape of potential 3-D fragments based on bicycles **206** and **207** was assessed by PMI analysis. The azabicyclo[3.1.0]hexane scaffold was found to be inherently 3-D in shape with all conformations for 3-D fragments based on scaffold **206** having ΣNPR values > 1.20 (Figure 2.12). Interestingly, both conformational and structural diversity were apparent with a high number of conformations up to 1.5 kcal mol^{-1} above the energy of the global minimum energy conformer represented (blue dots) and a significant spread across the PMI plot for targeted fragments **334-338**.

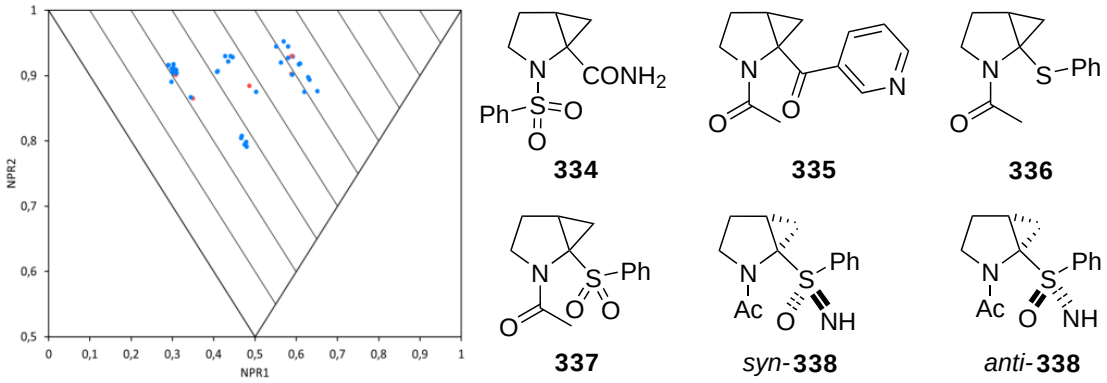

Figure 2.12: PMI Analysis of Targeted Fragments. Red dots indicate global minimum energy conformers and blue dots indicate higher energy conformers

In assessing the molecular shape of 3-D fragments based on scaffold **207**, a number of possible α-aryl and heteroaryl groups were considered (based on commercial availability of the aryl bromide). Then, the effect of changing the nitrogen substituent (R^1 = H, SO_2Me, Ac, Me) on 3-D shape for each aryl or heteroaryl group in turn was assessed. For example, PMI analysis of 2-subsituted pyridine fragments **339-342** (with R^1 = H, SO_2Me, Ac, Me) is shown in Figure 2.13. All conformations up to 1.5 kcal mol^{-1} above the energy of the global minimum energy conformer for compounds with R^1 = SO_2Me, Ac, Me were found to have $\Sigma NPR > 1.20$ such that 3-D fragments **340-342** were targeted for synthesis. Overall, eight PMI plots of 32 compounds were generated (not shown). Molecular shape of compounds with R^1 = 3-pyridinyl, SO_2Ph were also considered on an individual basis (not shown).

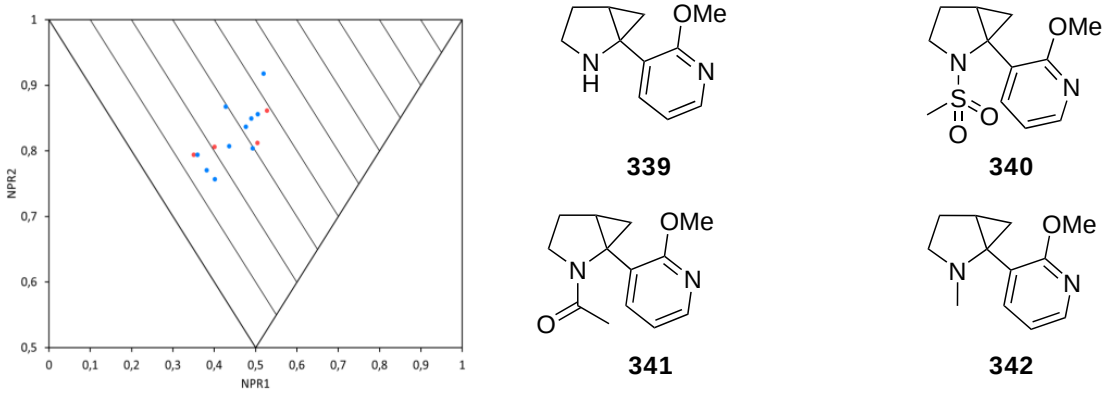

Figure 2.13: PMI Analysis of Potential Fragments. Red dots indicate global minimum energy conformers and blue dots indicate higher energy conformers

PMI analysis of all targeted 3-D fragments based on bicycle **207** (14 compounds) is shown in Figure 2.14. All conformations (by design) have ΣNPR values > 1.10.

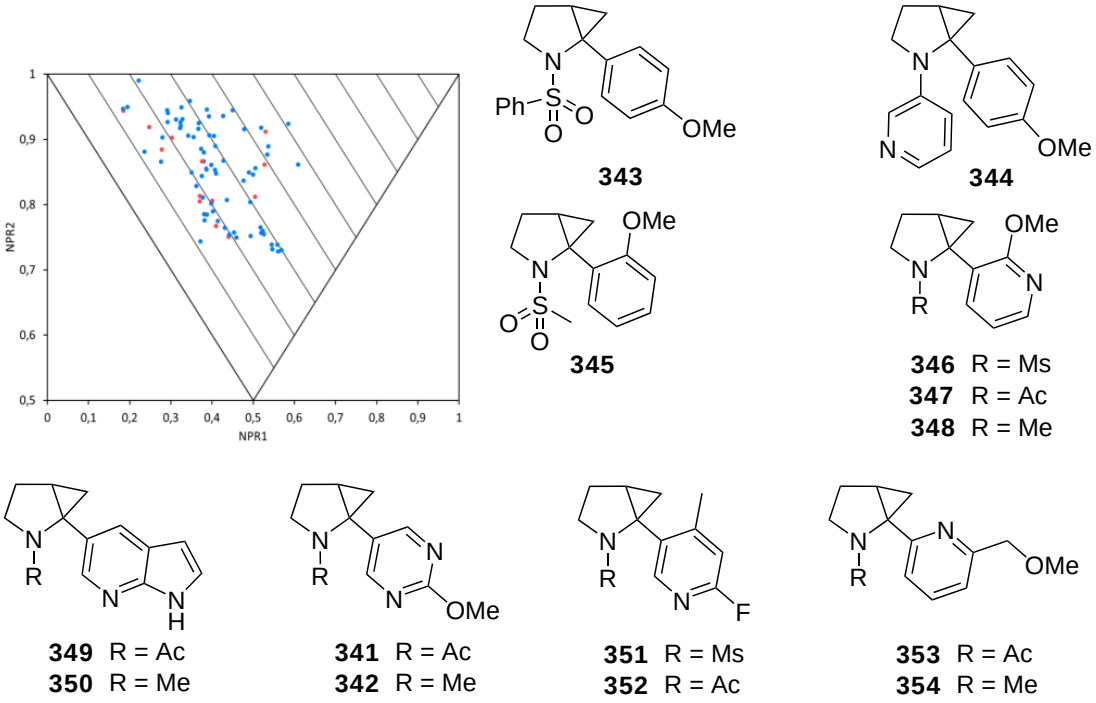

Figure 2.14: PMI Analysis of Targeted Fragments. Red dots indicate global minimum energy conformers and blue dots indicate higher energy conformers

2.4.2 Overview of a Lithiation Approach to 2,3-Fused Cyclopropyl Pyrrolidines

The synthesis of the 2,3-fused cyclopropyl pyrrolidine scaffold (an azabicyclo[3.1.0]hexane) was reported by Beak and co-workers in 1994.[117] Lithiation-cyclisation of *N*-Boc 4-chloropiperidine **333** furnished α-substituted cyclopropyl pyrrolidines (Scheme 2.43). Treatment of *N*-Boc 4-chloropiperidine **333** with 2.2 eq. of *s*-BuLi/TMEDA gave α-lithiated piperidine **355** which cyclises to give bicycle **356**. Notably, cyclisation of intermediate **355** occurs with inversion of configuration at the α-carbon. Deprotonation of 2,3-fused cyclopropyl pyrrolidine **356** with a second equivalent of *s*-BuLi (occuring as a result of the increased acidity of the cyclopropyl proton in **356**) gave lithiated intermediate **357** which, on trapping with various electrophiles, furnished 2,3-fused cyclopropyl pyrrolidines **358**.

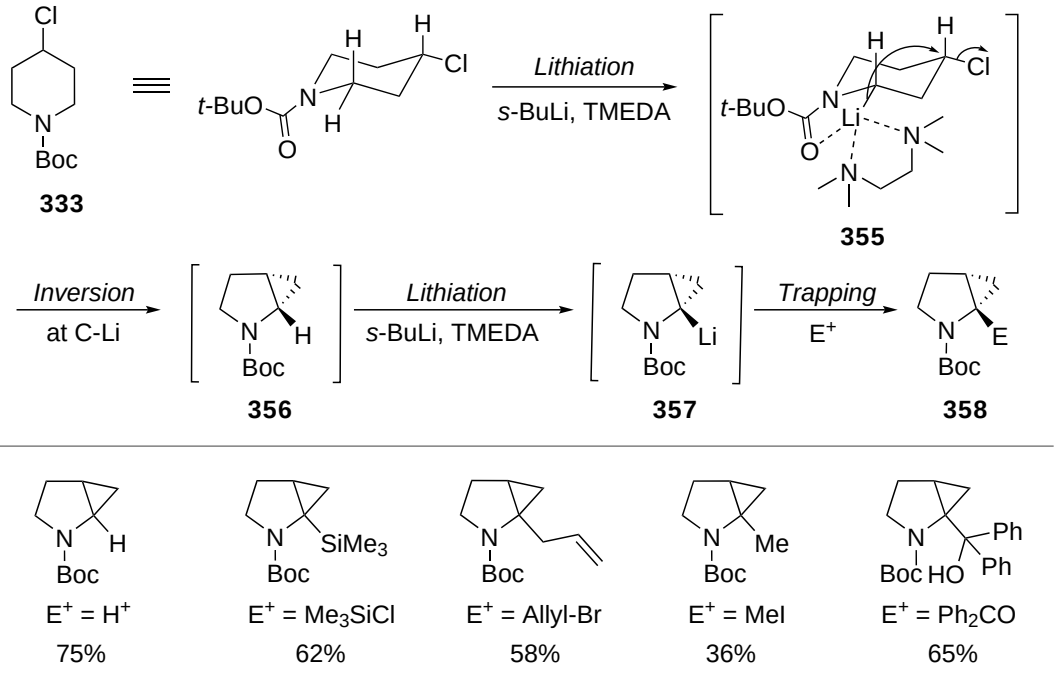

Scheme 2.43

In 1996, Beak and co-workers investigated the asymmetric lithiation-trapping of substrate **333** using a chiral ligand, (−)-sparteine.[118] Lithiation of *N*-Boc 4-chloropiperidine **333** using similar conditions to those used for the asymmetric lithiation of *N*-Boc

piperidine (2.2 eq. *s*-BuLi/(−)-sparteine in Et_2O at −78 °C)[119] and subsequent trapping with trimethylsilyl chloride gave bicycle **360** in 71% yield and 50:50 er. Attempts to improve the enantioselectivity of the reaction using different leaving groups (such as OTs in compound **359**) gave bicycle **360** in 78:22 er (Scheme 2.44). Further optimisation (using different solvents, chiral ligands and lower temperatures) did not improve the enantioselectivity.

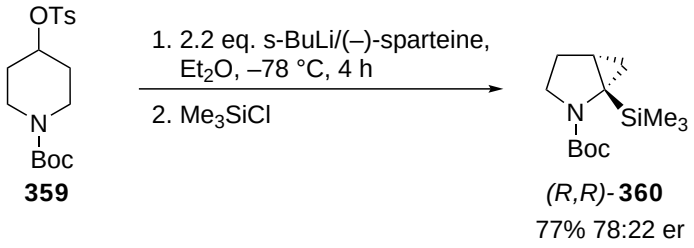

Scheme 2.44

In 2013, the O'Brien group reported an improved asymmetric route to the 2,3-fused pyrrolidine scaffold (with products isolated in 99:1 er) using a chiral diamine and enantiopure electrophile (Andersen's sulfinate).[115] Asymmetric deprotonation of **333** with *s*-BuLi/chiral diamine (*R,R*)-**362** and subsequent trapping with Andersen's sulfinate (S_S)-**363** gave α-amino sulfoxide *syn*-**361** in 99:1 er (Scheme 2.45). Under these conditions, sulfoxide *anti*-**361** was accessed in comparably lower er (87:13). However, sulfoxide *anti*-**361** could be formed in 99:1 er by using the corresponding chiral amine (*S,S*)-**362** and sulfoxide (R_S)-**363**.

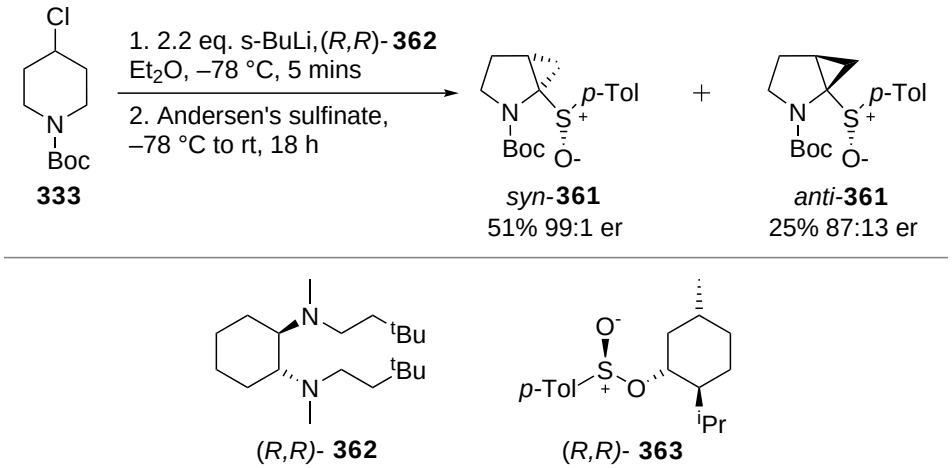

Scheme 2.45

Having established a viable synthetic route to access sulfoxide *syn*-**361** in high enantioselectivity (99:1 er), two approaches were used to access α-substituted 2,3-fused cyclopropyl pyrrolidines (*R,R*)-**358** and (*R,R*)-**382** in an enantiospecific manner from sulfoxide *syn*-**361** (Scheme 2.46). First, sulfoxide-Mg exchange (rt, 1 min) of sulfoxide *syn*-**361** with *i*-PrMgCl furnished enantiomerically pure α-functionalised chiral Grignard reagent (*R,R*)-**364** which was found to be configurationally stable at rt for 30 min. Subsequent electrophilic trapping with different electrophiles furnished a range of α-amino substituted products (*R,R*)-**358** such as (*S,R*)-**365** and (*R,R*)-**366** in 99:1 er. Alternatively, transmetallation of Grignard reagent (*R,R*)-**364** with zinc(II) chloride and subsequent Pd-mediated Negishi cross-coupling with a range of aryl bromides delivered arylated heterocycles (*R,R*)-**382** including (*S,R*)-**367** and (*S,R*)-**368** in 99:1 er. Notably, the methodology enabled the synthesis of both enantiomers of α-substituted 2,3-fused cyclopropyl pyrrolidines in 99:1 er by making use of commercially available chiral ligands and Andersen's sulfinate.

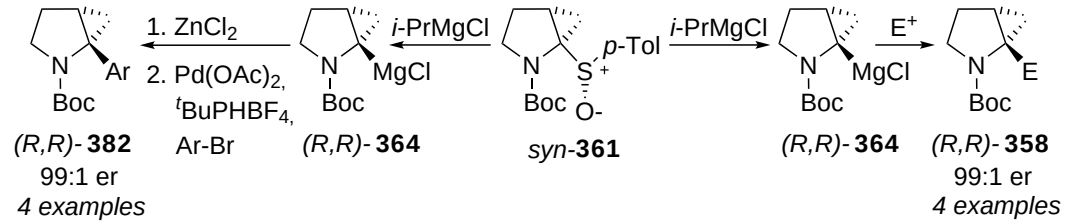

(R,R)-**382**
99:1 er
4 examples

(R,R)-**364**

syn-**361**

(R,R)-**364**

(R,R)-**358**
99:1 er
4 examples

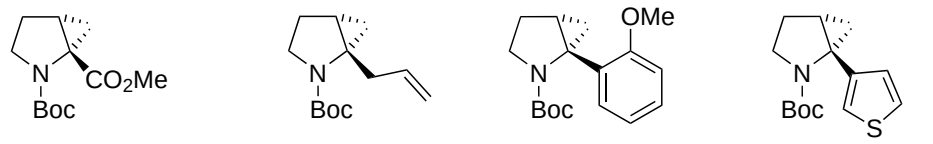

(S,R)-**365** 89%
$E^+ = MeO_2CCl$

(S,R)-**366** 69%
$E^+ = CuBrMe_2S$
then allyl-Br

(S,R)-**367** 68%

(S,R)-**368** 72%

Scheme 2.46

2.4.3 Synthesis of 2,3-Fused Cyclopropyl Pyrrolidines

It was envisioned that 2,3-fused cyclopropyl pyrrolidines **334**-**336** could be generated from *N*-Boc 4-chloropiperidine **333** using direct lithiation-trapping chemistry[117] and subsequent *N*-functionalisation (sulfonation or acylation) (Scheme 2.47). Fragment **336** in turn would be used as an intermediate *en route* to sulfoxide and sulfoximine fragments **337**, *syn*- and *anti*-**338**, which could be generated in 1-2 steps from thioether **336**.

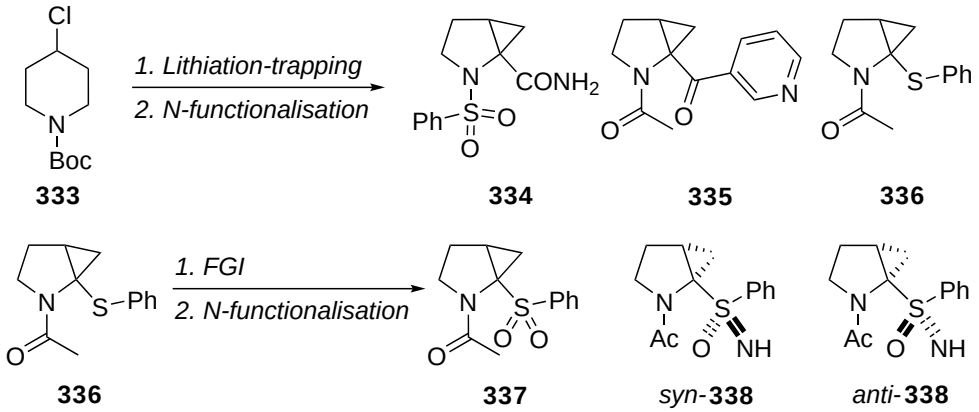

333 **334** **335** **336**

336 **337** *syn*-**338** *anti*-**338**

Scheme 2.47

The synthesis of *N*-Boc 4-chloropiperidine **333** is known[120] and it has been reproduced previously in the group.[115] Following the reported conditions, an Appel reaction of *N*-Boc 4-hydroxyl piperidine with triphenylphosphine and *N*-chlorosuccinimide in CH_2Cl_2 afforded *N*-Boc 4-chloropiperidine **333** in a moderate yield of 40% (Scheme 2.48). However, the reaction was scalable (15 mmol) such that piperidine **333** could be isolated in similar yields of 40% and 52% on small (2.5 mmol) and large scale (15 mmol) respectively. Higher yields were not attainable due to the formation of alkene **370** (formed *via* elimination of compound **333**) which was also isolated as an 80:20 mixture with piperidine **333** and made chromatography challenging.

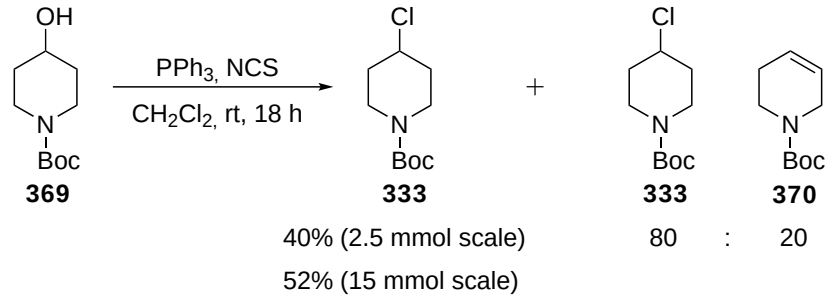

Scheme 2.48

Then, applying methodology developed by Beak *et al.*,[117] lithiation of piperidine **333** with 2.6 eq. *s*-BuLi/TMEDA in Et_2O at −78 °C followed by trapping with various electrophiles gave *N*-Boc 2,3-fused cyclopropyl pyrrolidines **371**-**373** in varying yields (Scheme 2.49). Acid **371** was then used as an intermediate to synthesise fragment **334** *via* a 2-step sequence. To this end, standard T3P conditions gave amide **374** in 64% yield. Subsequent *N*-Boc removal and functionalisation with $PhSO_2Cl$ gave targeted fragment **334** in 80% yield.

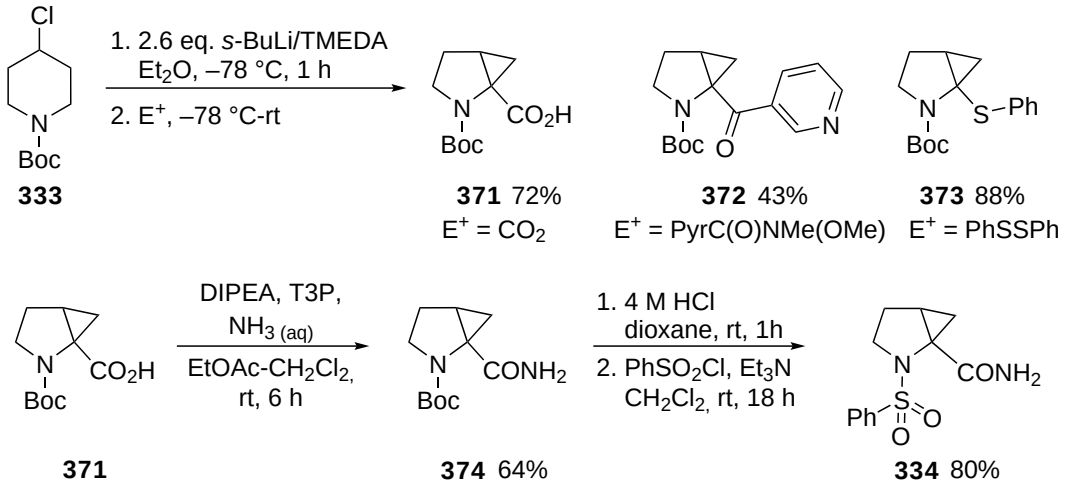

Scheme 2.49

N-Acyl fragments **335** and **336** in turn were synthesised following *N*-Boc removal and acylation of the secondary amine (with Ac_2O in pyridine). This gave targeted fragments **335** and **336** in good yields of 77% and 91% respectively (Scheme 2.50).

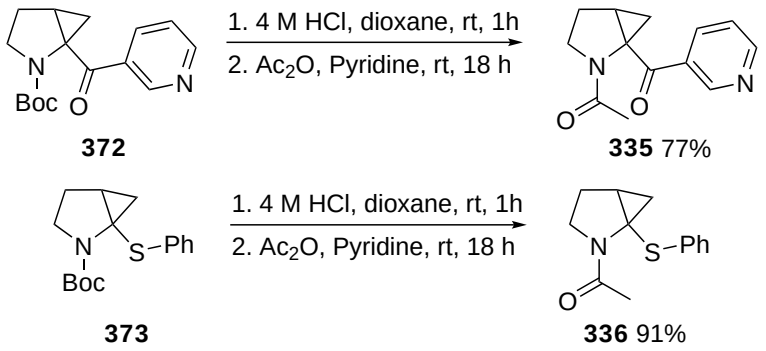

Scheme 2.50

Then, *N*-Boc protected thioether **373** was used as a common intermediate to synthesise sulfone and sulfoximine containing fragments **337**, *syn*-**338** and *anti*-**338**. Following a literature procedure for oxidation of substituted sulfides directly to their corresponding sulfones,[121] thioether **373** was oxidised (with UHP and phthalic anhydride) to *N*-Boc protected sulfone **375** in 93% yield (Scheme 2.51). Then, *N*-functionalisation using the standard procedure for acylation gave targeted fragment **337** in 82% yield.

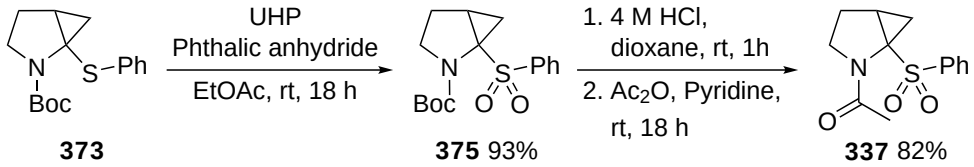

Scheme 2.51

The sulfoximine group of targeted fragments *syn*- and *anti*-**338** was generated using a 2-step sequence from the corresponding thioether **373** (Scheme 2.52). Firstly, literature conditions for thioether to sulfoxide conversion[122] (with *m*-CPBA and sodium carbonate in CH_2Cl_2 for 18 h) were carried out with thioether **373** to give separable sulfoxides *syn*- and *anti*-**376** after chromatography. The relative stereochemistry was assigned based on a comparison with the ^{1}H NMR spectroscopic data of the tolyl-derivatives of *syn*- and *anti*-**376** which had previously been synthesised in the group (and whose stereochemistry had been assigned).[115] Then, following a procedure for sulfoxide to sulfoximine conversion,[123] reaction of sulfoxide *syn*-**376** with $PhI(OAc)_2$ and ammonium carbamate delivered sulfoximine *syn*-**377** in 66% yield. Initial attempts to synthesise

fragment *syn*-**338** *via* *N*-Boc functionalisation led to the formation of doubly acylated product *syn*-**378** in 74% yield.

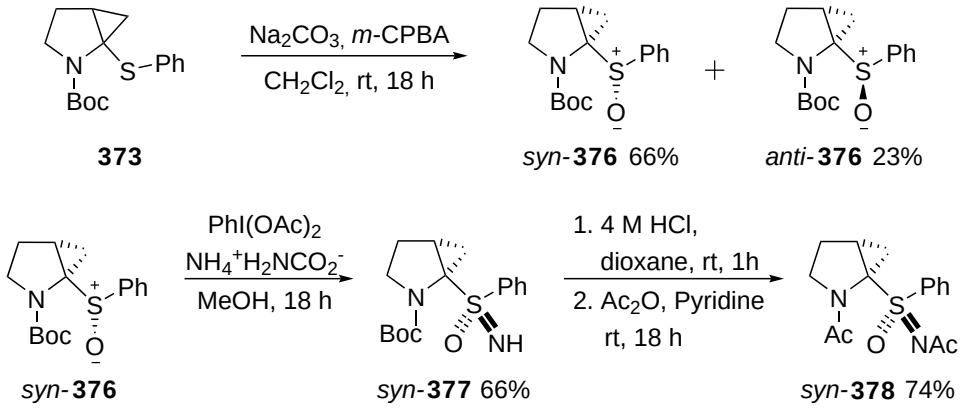

Scheme 2.52

The synthetic route to sulfoximines *syn*- and *anti*-**338** was therefore revised and the steps re-ordered according to Scheme 2.53. Firstly, *N*-Boc removal (with 4 M HCl in dioxane) followed by acetylation gave acylated sulfoxides *syn*- and *anti*-**379** in 65% and 82% yield respectively. Then, sulfoximine formation using the established conditions delivered targeted fragments *syn*- and *anti*-**338**.

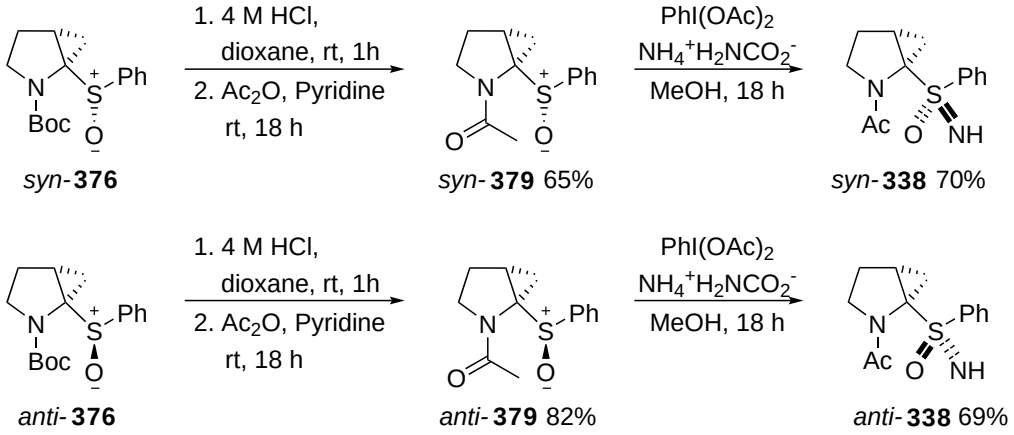

Scheme 2.53

Having succesfully synthesised six 2,3-fused cyclopropyl pyrrolidines **334**-*anti*-**338**, attention turned to the synthesis of α-arylated 3-D fragments **207**. Initially, the plan was to use Negishi cross-coupling to install functionality at the α-position of the azabicyclo[3.1.0]hexane scaffold as previously reported.[115] However, using this approach would

require an organometallic reaction for the installation of each aryl group. Instead, it was decided to explore a new approach focusing on the Suzuki-Miyaura cross-coupling of a cyclopropyl-B(MIDA) building block. For this approach, the key B(MIDA) building block **208** would first be synthesised by lithiation-trapping of **333** with a boronate electrophile (Scheme 2.54). Then, Suzuki-Miyaura cross-coupling of B(MIDA) **208** with various aryl bromides should enable functionalisation of the α-position of scaffold **208** with different aromatic groups. Fragments **207** (R^1 = SO_2Ph, SO_2Me, 3-pyridinyl, Me) could be delivered following *N*-Boc removal and functionalisation. The use of B(MIDA) building blocks for iterative cross-coupling in small molecule synthesis has been popularised by Burke *et al.*[124–127] Essentially, the B(MIDA) group acts as a 'masked' boronic acid, enabling facile purification and long-term storage of key building blocks. Indeed, as presented in Chapter 4, this design feature has been successfully used in the generation of five cyclopropyl-B(MIDA) 3-D building blocks. Overall, in terms of fragment generation, it was anticipated that the use of a common intermediate such as B(MIDA) building block **208** would provide an expedient synthetic route to targeted fragments **207**.

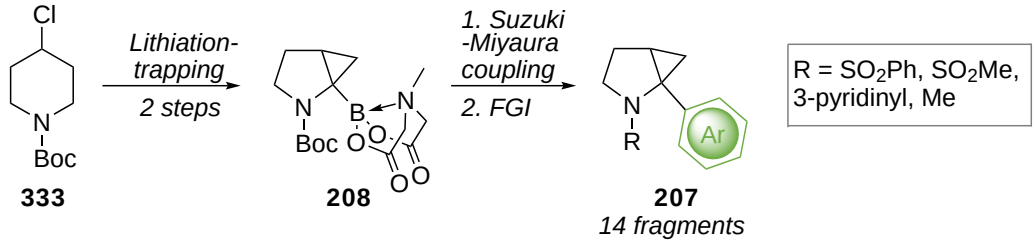

Scheme 2.54

Cyclopropyl-B(MIDA) building block **208** was synthesised in 2 steps as outlined in Scheme 2.55. First, lithiation of *N*-Boc 4-chloropiperidine **333** using the previously established lithiation conditions followed by trapping with $(i\text{–PrO})_3B$ gave, after hydrolysis of the boronate during work-up, boronic acid **380** in 83% yield after chromatography. Then, following a literature procedure for aryl $B(OH)_2$ to B(MIDA) conversion,[124] reaction with MIDA (in toluene/DMSO at 120 °C for 18 h) gave cyclopropyl-B(MIDA)

208 in 59% yield after chromatography. Notably, previous synthetic attempts to access the pinacol boronate (*via* lithiation-trapping with *i*-PrOB(pin) or HB(pin)) were unsuccesful due to the instability of the cyclopropyl-B(pin) compound which behaved strangely on silica. Recently, the synthetic route towards cyclopropyl-B(MIDA) **208** has been optimised in the group by James Donald. Changing chromatographic conditions for facile separation of *N*-Boc 4-chloropiperidine **333** from alkene **370** allowed for the isolation of *N*-Boc 4-chloropiperidine **333** on a multi-gram scale. This in turn enabled the synthesis of $>$ 5 g of cyclopropyl-B(MIDA) **208** which was isolated by recrystallisation.

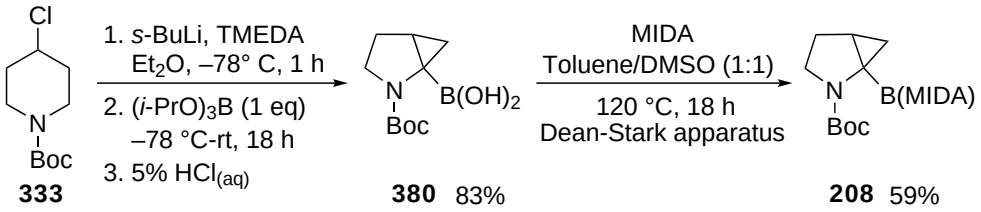

Scheme 2.55

Having established a viable synthetic route to cyclopropyl-B(MIDA) building block **208**, α-arylation using Suzuki-Miyaura cross-coupling of the cyclopropyl-B(MIDA) group was explored. A short overview of cross-coupling reactions of cyclopropylboronates is provided in section 4.3.1 as a prelude to a wider study of such cross-coupling reactions. For pyrrolidine cyclopropyl-B(MIDA) **208**, a range of Suzuki-Miyaura cross-coupling reaction conditions from the literature (including patents) was selected.[125,128–131] In most cases, α-arylated pyrrolidine **381** was formed together with protodeborylated pyrrolidine **356** in varying ratios (Table 2.1, entries 1-5). The conditions from the literature mostly focused on $Pd(OAc)_2$ in combination with electron-rich and sterically hindered monodentate phosphine ligands such as the Buchwald ligands SPhos and Ruphos or PCy_3.[132,133] Coupling of cyclopropyl-B(MIDA) **208** with 4-bromoanisole using conditions reported by Burke *et al.*[125] (5 mol% $Pd(OAc)_2$, 10 mol% SPhos and K_3PO_4 in dioxane/H_2O at 60 °C in a sealed tube for 18 h) afforded a 35:65 mixture of α-arylated and protodeborylated pyrrolidines **381** and **356** (entry 1).

Increasing the temperature to 100 °C improved the amount of desired **381** generated (entry 2). After chromatography, α-aryl pyrrolidine **381** was isolated in 18% yield.

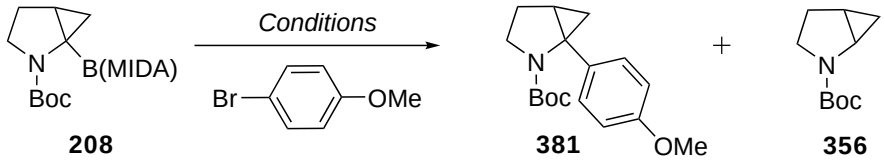

208 **381** **356**

Table 2.1: Optimisation of Suzuki-Miyaura Cross-Coupling Conditions

Entry	Conditions	**381**:**356**[a]	Yield %[b]
1	5 mol% $Pd(OAc)_2$, 10 mol% SPhos, K_3PO_4, dioxane/H_2O, 60 °C, 18 h, [sealed tube]	35:65	-
2	5 mol% $Pd(OAc)_2$, 10 mol% SPhos, K_3PO_4, dioxane/H_2O, 100 °C, 18 h, [sealed tube]	50:50	18
3	7 mol% $Pd(OAc)_2$, 13 mol% RuPhos, K_2CO_3, toluene/H_2O, 100 °C, 18 h, [sealed tube]	50:50	48
4	6 mol% RuPhos Pd G2, K_2CO_3, dioxane/H_2O, 110 °C, 18 h, [sealed tube]	50:50	-
5	3 mol% $Pd(OAc)_2$, 20 mol% PCy_3, K_3PO_4, toluene/H_2O, 120 °C, 18 h, [sealed tube]	20:80	-
6	15 mol% $Pd(OAc)_2$, 30 mol% PCy_3, Cs_2CO_3, toluene/H_2O, 100 °C, 20 h, [sealed tube]	100:0	77

[a] Determined by ^{1}H NMR spectroscopy of the crude product
[b] % Yield of **381** after chromatography

Then, using similar coupling conditions to those reported by Duncton *et al.*,[128] cyclopropyl-B(MIDA) **208** and 4-bromoanisole were reacted with 7 mol% $Pd(OAc)_2$, 13 mol% RuPhos and K_2CO_3 in toluene/H_2O at 100 °C in a sealed tube over 18 h. Although the ratio of products **381** and **356** was only 50:50, the yield of isolated **381** increased to 48% (entry 3). The use a second generation Buchwald precatalyst, Ru PhosPd G2 (6 mol%), with K_2CO_3 in dioxane/H_2O at 110 °C in a sealed tube over 18 h as reported by Gilead and co-workers[129] also gave a 50:50 mixture of products **381** and **356** (entry 4). Alternative patent conditions[130] using 3 mol% $Pd(OAc)_2$, 20 mol% PCy_3 and K_3PO_4 in toluene/H_2O at 120 °C in a sealed tube over 18 h resulted predominantly in

protodeborylation with a 20:80 mixture of cyclopropyl-B(MIDA) **208** and **356** being formed (entry 5). However, increasing the catalyst loading to 15 mol% $Pd(OAc)_2$ and 30 mol% PCy_3 and changing the base (from K_3PO_4 to Cs_2CO_3) according to conditions from a different patent[131] gave pyrrolidine **381** in 77% isolated yield, with no evidence of any protodeborylation product **356** in the ^1H NMR spectrum of the crude product (entry 6).

Having optimised conditions for Suzuki-Miyaura cross-coupling of cyclopropyl-B(MIDA) **208** with 4-bromoanisole, the synthesis of α-arylated fragments was undertaken. Suzuki-Miyaura cross-coupling of cyclopropyl-B(MIDA) **208** with 2-bromoanisole proceeded smoothly (73% yield of **367**) whereas coupling to *N*-TIPS protected 3-bromoazaindole proved to be more problematic with cyclopropyl pyrrolidine **383** isolated in low yield (25%) (Scheme 2.56). It is possible that *N*-TIPS removal occured under the reaction conditions to give a polar product that did not elute during chromatography. This could provide an explanation for the low yield observed in this case. Then, *N*-Boc removal under acidic conditions and *N*-functionalisation (by mesylation) gave targeted 3-D fragments **343** and **345** in good yield (Scheme 2.57).

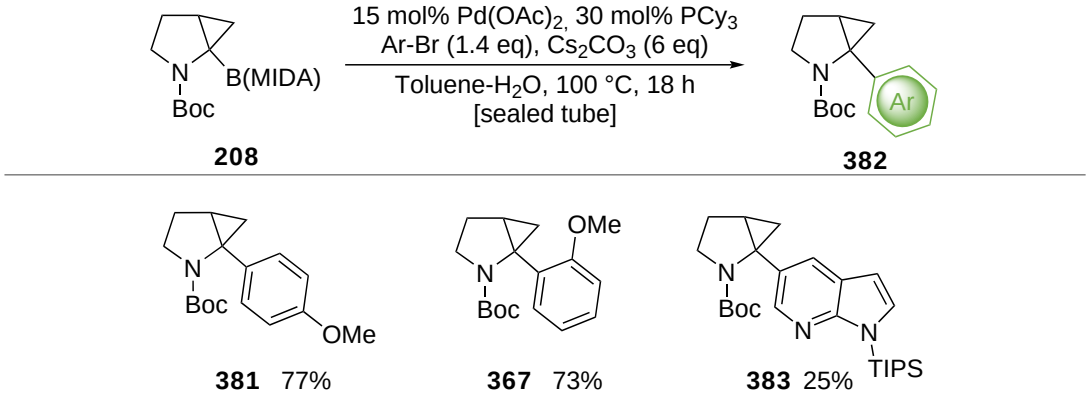

Scheme 2.56

N-Functionalisation of cyclopropyl pyrrolidine **383** (*via* *N*-Boc removal and acylation) initially gave a 45:55 mixture of azaindole **349** and doubly acylated azaindole **384**, following chromatography (Scheme 2.58). Presumably, *N*-TIPS removal of azaindole

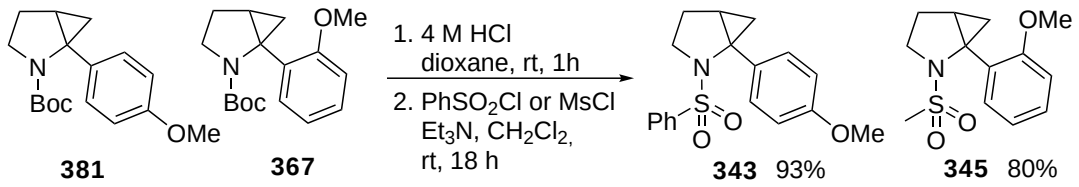

Scheme 2.57

383 occured as well as *N*-Boc removal (in the first step) allowing for subseqent acylation (in the second step) of both secondary amines. Selective *N*-Ac hydrolysis of the more labile azaindole *N*-Ac group by treatment of the 45:55 mixture of cyclopropyl pyrrolidines **349** and **384** with $NaOH_{(aq)}$ in $MeOH/H_2O$ over 2 h gave 3-D fragment **349** in 19% yield over 2 steps.

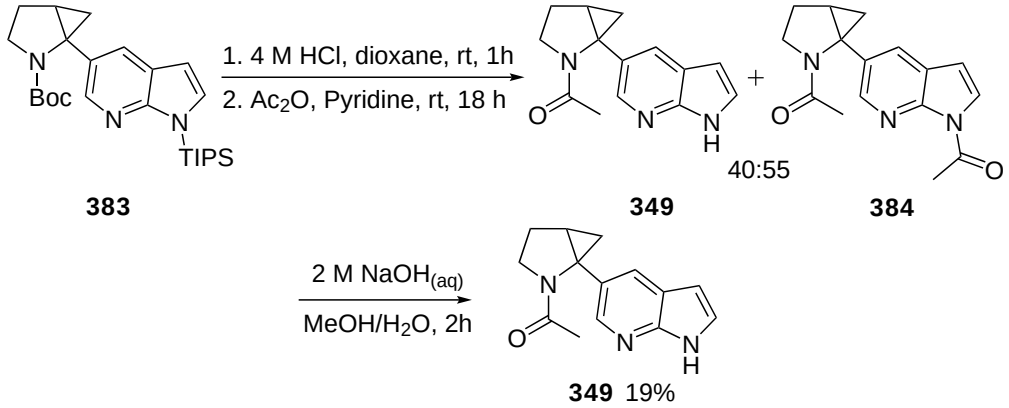

Scheme 2.58

Attempts to synthesise 3-D fragment **344** by *N*-Boc removal and Buchwald-Hartwig coupling were unsuccessful. Literature conditions for coupling of pyrrolidine and 3-bromopyridine[134] gave aryl imine **385** in 32% yield with no aryl pyrrolidine **344** isolated (Scheme 2.59). A mechanism for the formation of aryl imine **385** is outlined in Scheme 2.59. Cyclopropyl ring opening with the adjacent nitrogen lone pair of amine **386** in the presence of palladium would give intermediate alkyl palladium species **387** which on reductive elimination would form aryl imine **385**. Metal-catalyzed ring opening of aminocyclopropanes under similar conditions is known,[135–137] supporting the proposed mechanism.

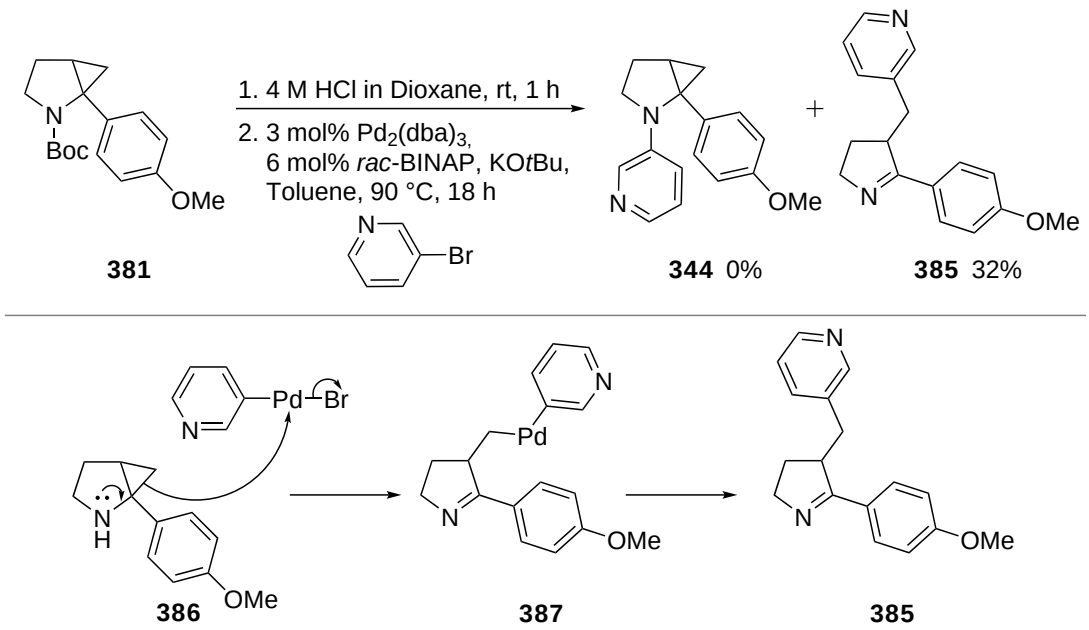

Scheme 2.59

Having established the principle for functionalisation of both the B(MIDA) (using Suzuki-Miyaura cross-coupling) and *N*-Boc group (by acylation, mesylation), another member of the group, Rebecca Appiani, carried out the synthesis of the other targeted α-aryl pyrrolidine 3-D fragments. Using the standard Suzuki-Miyaura cross-coupling conditions, coupling of cyclopropyl-B(MIDA) **208** with various subsituted pyridine, pyrimidine and azaindole bromides proceeded smoothly with most cyclopropyl pyrrolidines isolated in good yields (Scheme 2.60). Notably, coupling of cyclopropyl-B(MIDA) **208** with *N*-Ts protected bromoazaindole furnished α-aryl pyrrolidine **392** in higher yield (78%) than cross-coupling with the *N*-TIPS derivative (25% yield, see Scheme 2.56), indicating that the *N*-Ts group is stable under the Suzuki-Miyaura cross-coupling conditions used.

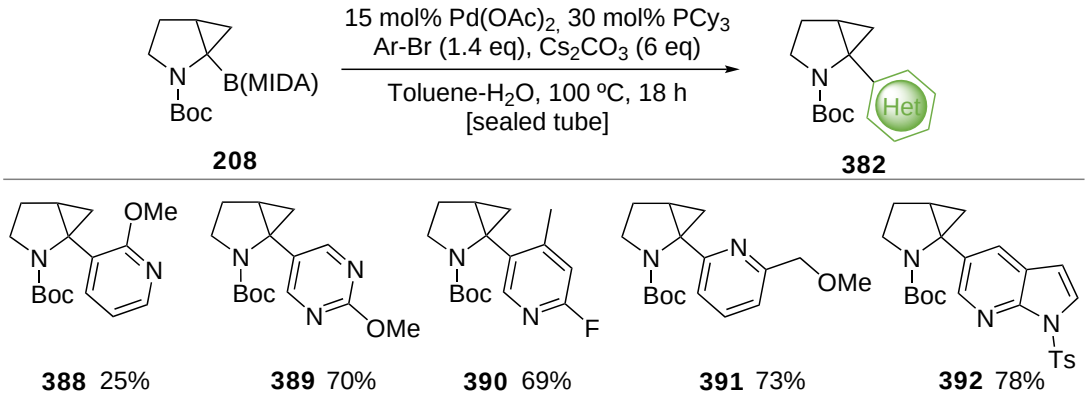

Scheme 2.60

Mesylated fragments **346** and **351** were accessed in one step from α-arylated compounds **388** and **390** respectively after *N*-Boc removal and mesylation (Scheme 2.61). *N*-Functionalisation *via* *N*-Boc removal and acylation gave four α-arylated 3-D fragments **341**, **347**, **352** and **353** in one step (Scheme 2.62).

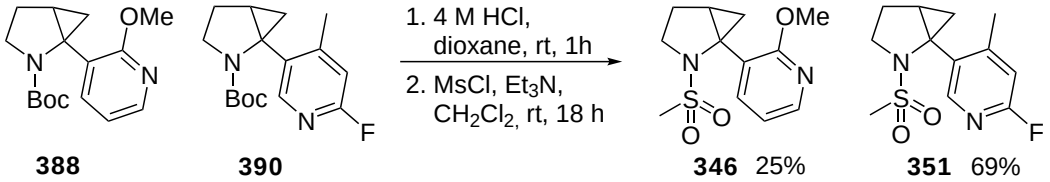

Scheme 2.61

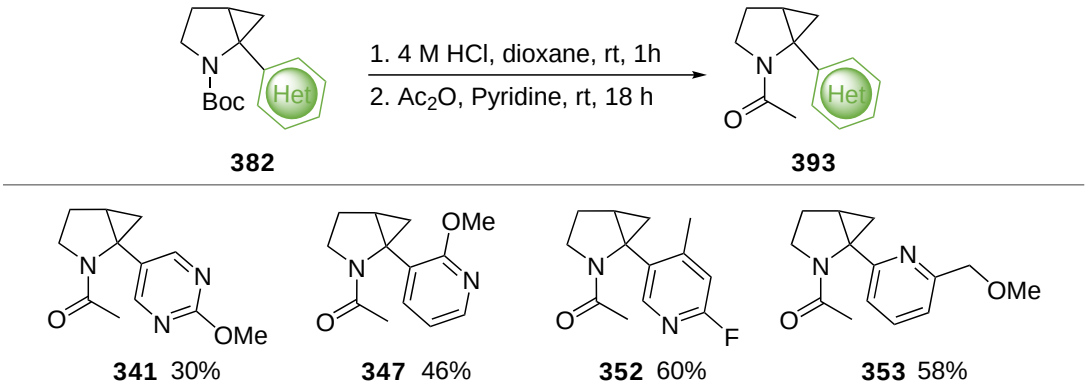

Scheme 2.62

The remaining set of *N*-functionalised α-arylated, 2,3-fused cyclopropyl pyrrolidines **342**, **348** and **354** were accessed by *N*-Boc removal and reductive amination. Reductive amination conditions for the methylation of pyrrolidine-based fragments has previously been established in the group.[91,138] Following that procedure (using aqueous formaldehyde, sodium triacetoxyborohydride and $MgSO_4$ in 3:1 CH_2Cl_2–AcOH) gave methylated fragments **342**, **348** and **354** in 39-45% yields (Scheme 2.63).

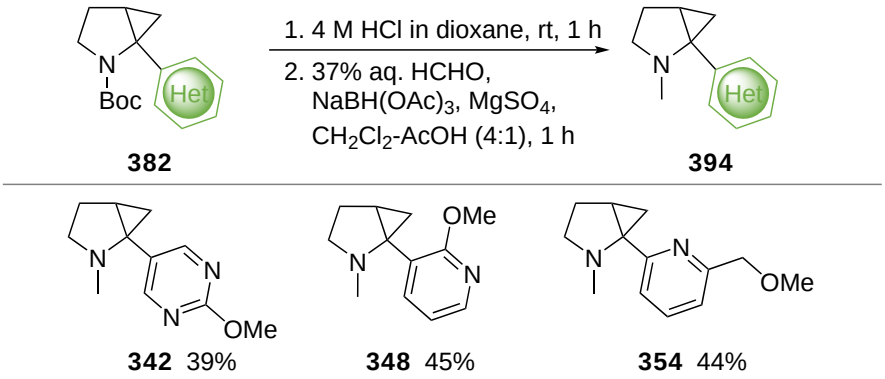

Scheme 2.63

Azaindole **350** was synthesised over 2 steps from *N*-Ts protected azaindole **392** as outlined in Scheme 2.64. *N*-Boc removal and reductive amination of *N*-Ts azaindole **392** using established conditions gave methylated pyrrolidine **395** in 79% yield after chromatography. Unlike the *N*-TIPS group, the *N*-Ts group was stable to both the mildly basic conditions used in Suzuki-Miyaura cross-coupling and the acidic conditions used in *N*-Boc removal and reductive amination. Then, *N*-Ts removal with $Cs_2CO_{3(aq)}$ in THF-MeOH at rt for 18 h furnished azaindole fragment **350** in 60% yield.

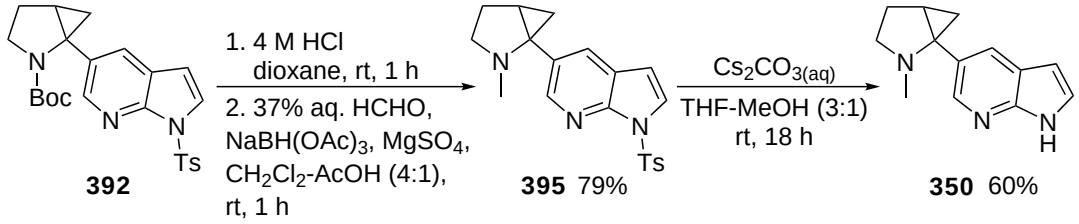

Scheme 2.64

With 19 3-D fragments in hand, a route to access enantiopure arylated compounds was briefly explored. The plan was to use resolution. In 2019, Burke and co-workers

reported the use of a chiral IDA ligand to access all possible Csp^3 stereoisomers of xylarinic acid B *via* resolution.[127] Using a similar strategy, boronic acid **380** was reacted with pinene-derived **396**, previously used as a chiral auxiliary in stereoselective epoxidations of vinyl boronates,[139] to generate diastereomeric cyclopropyl-B(IDA)s **397**. Although the reaction went to completion (based on ^{1}H NMR spectroscopy of the crude reaction mixture), yields were low. After chromatography, cyclopropyl-B(IDA)s **397a** and **397b** were isolated in 12% and 10% yield respectively although it was clear (by ^{1}H and ^{13}C NMR spectroscopy) that they were not completely pure (Scheme 2.65). Nevertheless, Suzuki-Miyaura cross-coupling with each of **397a** and **397b** with 4-bromoanisole were successful. Thus, cross-coupling with cyclopropyl-B(IDA)s **397a** and **397b** gave single enantiomers of α-arylated, 2,3-fused cyclopropyl pyrrolidines **381** and *ent*-**381** in 78% and 62% yield respectively after chromatography with >99:1 er by CSP-HPLC (in each case) (Scheme 2.65).

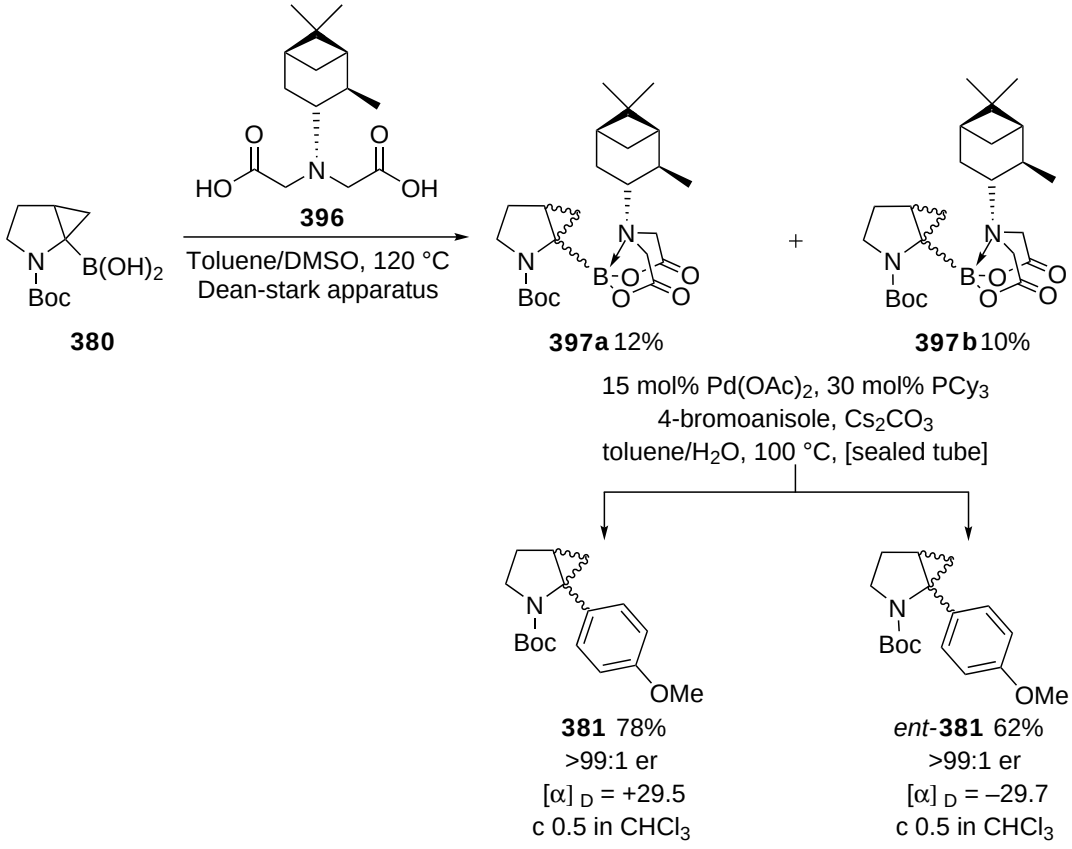

Scheme 2.65

Overall, the use of pinene-derived iminodiacid **396** enabled separation of diastereomeric B(IDA)s **397a** and **397b** which ultimately allowed access, following Suzuki-Miyaura cross-coupling, to enantiomeric α-arylated pyrrolidines **381** and *ent*-**381**. However, the low yields resulting from attachment of chiral ligand **396** to boronic acid **380** ultimately make this 2-step synthetic route to access single enantiomers unfeasible. To this end, investigation of alternative chiral iminodiacetic acids such as cyclohexylethyl-iminodiacetic acid or 2-(benzyloxy)cyclopentyl-iminodiacetic acid (which was used by Burke for resolution[127]) could provide a more efficient route.

In summary, 19 3-D fragments based on the 2,3-fused disubstituted pyrrolidine scaffold were successfuly synthesised using two synthetic strategies. In the first instance, lithiation-trapping chemistry of *N*-Boc 4-chloropiperidine **333** with various electrophiles allowed for direct functionalisation of the α-position to give α-functionalised 3-D fragments **334**, **335**, **336** and **337** in 3-4 steps. The synthesis of targeted sulfoximines *syn*-**338** and *anti*-**338** was less straightforward. In this case, reversal of synthetic steps (*N*-Boc functionalisation and sulfoximine formation) was necessary to avoid acylation of both the NH group and pyrrolidine. Overall, the six targeted 3-D fragments were structurally diverse with acid, amide, 3-pyridinyl ketone, thioether, sulfoxide and sulfoximine groups represented. A second set of 2,3-fused disubstituted pyrrolidines were synthesised from cylopropyl-B(MIDA) building block **208**. Suzuki-Miyaura cross-coupling of the cyclopropyl-B(MIDA) group allowed for the generation of 13 α-arylated pyrrolidine 3-D fragments in 5 steps from *N*-Boc 4-chloropiperidine **333**.

In addition, a synthetic route to access single enantiomers of α-arylated 3-D fragments **343-354** was established using resolution with the aid of a pinene-derived ligand. Although attachment and separation of diastereomeric chiral B(IDA)s was possible, yields were low. In this respect, previous work carried out in the group[115] which established an asymmetric route to the 2,3-fused cyclopropyl pyrrolidine scaffold could provide an alternative more viable route to access single enantiomers of this scaffold. To this end,

syn- or *anti*- α-amino sulfoxides of the 2,3-fused cyclopropyl pyrrolidine scaffold could, using a chiral diamine and Andersen's sulfinate, be accessed in 99:1 er (see Scheme 2.45). Then, sulfoxide-Mg exchange and subseqent electrophilic trapping with a boron electrophile could, following reaction with MIDA, give cyclopropyl-B(MIDA) **208** in 99:1 er. Finally, Suzuki-Miyaura coupling of the cyclopropyl-B(MIDA) with various aryl bromides could give α-arylated 3-D fragments in 99:1 er.

3 Analysis of Physicochemical Properties, 3-D Shape, Solubility and Stability of York 3-D Fragments and Preliminary Fragment Screening Results

The York 3-D fragment library was designed and synthesised by several members of the O'Brien group. In total, 155 3-D fragments were synthesised in the group and this collection covers two generations of 3-D fragments including disubstituted pyrrolidines, piperidines and spirocycles in addition to other second generation heterocycles. A representative set is shown in Figure 3.1. This chapter describes the physicochemical properties (MW, HAC, ClogP, RBN, HBD and HBA) and molecular shape of 42 3-D fragments (of which 41 were synthesised in Chapter 2) as well as the York 3-D compound collection which totalled 115 compounds after several compounds were omitted from the final library due to purity, stability or solubility issues (*vide infra*).

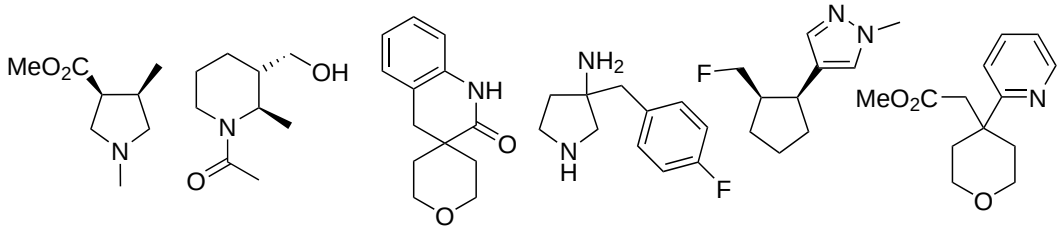

Figure 3.1: A Representative Set of York 3-D Fragments

In sections 3.1 and 3.3, physicochemical properties and 3-D shape are assessed using literature guidelines (Ro3 and updated Ro3) and PMI analysis respectively. Section 3.3 also presents comparative results of the physicochemical properties (MW, HAC, Fsp^3 and ClogP) and molecular shape (by PMI analysis and PBF) of the York 3-D fragment library against six commercial libraries (Maybridge, Chembridge, Enamine Ro3, Life Chemicals 3D, ChemDiv 3D and Enamine 3D). Section 3.2 covers the purity, solubility and stability studies of the compounds in the York 3-D fragment library in both DMSO stock solutions and aqueous buffer. Finally, section 3.4 presents the results of four screening campaigns against six protein targets. Overall, the usefulness of the

compound collection to FBDD in terms of being suitable for fragment screening and generating fragment hits is determined.

3.1 Physicochemical Properties and Shape Analysis of 42 3-D Fragments

Literature descriptors and suggested guidelines for favourable physicochemical properties in fragment design vary widely (see section 1.2). Lipinski initially proposed 'the rule of five' for orally bioavailable drugs which follow the criteria of MW $\leq$ 500 Da, ClogP $\leq$ 5, HBD $\leq$ 5 and HBA $\leq$ 10.[22] More recently, Astex defined the Ro3 for fragments with MW $<$ 300 Da, ClogP $<$ 3, HBD $\leq$ 3 and HBA $\leq$ 3.[23] The MW descriptor is of particular importance as fragments are typically defined as compounds with MW $<$ 300 Da. Moreover, MW is critical in terms of limiting the size of a fragment library required to cover or explore a given area of chemical space. In 2016, Astex, based on experience from their own FBDD screening campaigns, modified Ro3 to more narrowly defined parameters of MW 140-230 Da, ClogP 0-2 and the RBN 0-3.[21] For our purposes, physicochemical properties (MW, HAC, ClogP, RBN, HBD and HBA) of York 3-D fragments were compared against both the Ro3 and its updated version. Importantly, both sets of parameters are used as rough guidelines in fragment design such that only fragments which do not fit within the more broadly defined Ro3 were omitted from the compound collection.

The structures of 42 3-D fragments that are analysed in this section are shown in Figure 3.2. The synthesis of 41 of these fragments was successfully achieved (see Chapter 2). There was one fragment (compound **344**) which we initially believed we had synthesised and so it was included in the analysis. However, it was subsequently shown that we had not synthesised **344** and instead had obtained imine **385** (see Scheme 2.59).

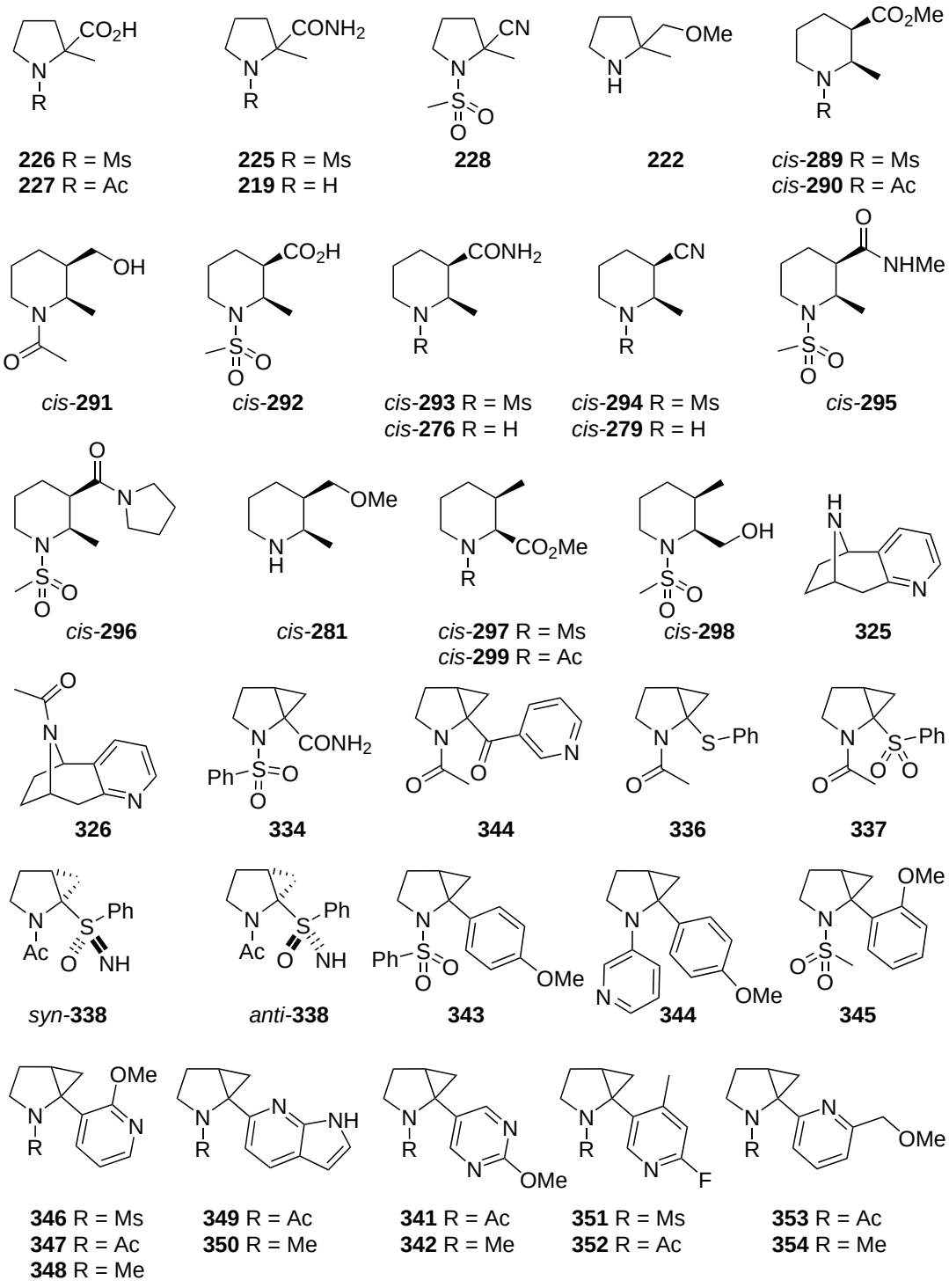

Figure 3.2: Structures of the 42 3-D Fragments from Chapter 2

The physicochemical properties (MW, HAC, ClogP, RBN, HBD, HBA) and 3-D shape (by PMI analysis) of the 42-compound collection were analysed. CLogP values were

calculated at AstraZeneca whereas physichochemical properties (MW, HAC, RBN, HBD, HBA) together with PMI plots were generated using Pipeline Pilot software. The physicochemical properties of the 42 3-D fragments are shown in Table 3.1. They were designed to fit within the Ro3 guidelines and this subset also adhered to the stricter criteria stipulated by the updated Ro3 guidelines. Overall, compounds were quite polar with an average ClogP of 0.38.

Table 3.1: Physicochemical Properties of the 42 3-D Fragments from Chapter 2

Property	Ro3	Updated Ro3	42 3-D Fragments[a]
MW (Da)	≤ 300	140-230	218
HAC	-	10-16	15.1
ClogP	≤ 3	0-2	0.38
RBN	≤ 3	-	1.88
HBD	≤ 3	-	0.81
HBA	≤ 3	-	2.40

[a] Parameters are reported as mean values

Throughout the project, assessment of molecular shape (by PMI analysis) was key to fragment design and selection. To this end, PMI plots were generated in order to assess both the 3-D shape of targeted fragments as well as their conformational and shape diversity. Conformational diversity is determined by the number of high energy conformers (represented by blue dots in all of the PMI plots presented in this thesis) which are up to 1.5 kcal mol^{-1} above the energy of the global minimum energy conformer for each fragment. Shape diversity, on the other hand, can be visualised by the overall spread of data points across the PMI plot with a larger spread representing a higher number of rod-, disc- and spherical-shaped compounds in the collection. PMI analysis for the 42 3-D fragments of all conformations up to 1.5 kcal mol^{-1} above the energy of the global minimum energy conformer for each fragment indicated that there were no fragments with ΣNPR value < 1.1 (Figure 3.3). The 42 3-D fragments were also found to be structurally diverse with all conformations falling within a wide area of the plot having ΣNPR values from 1.1-1.6.

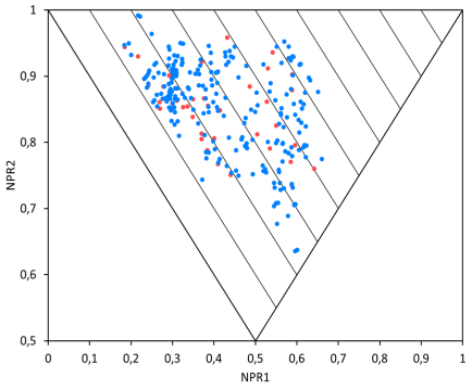

Figure 3.3: PMI Analysis of the 42 3-D Fragments. Red dots indicate global minimum energy conformers and blue dots indicate higher energy conformers

Overall, the 42 3-D fragments met design criteria for favourable physicochemical properties and 3-D shape with all fragments adhering to the updated Ro3 guidelines in addition to occupying different and under-represented areas of chemical space.

3.2 Analysis of Purity, Stability and Solubility of York 3-D Fragments

The work described in this thesis has been part of a larger programme in the design, synthesis and collation of the York 3-D fragment library. The project has, as highlighted elsewhere in this thesis, involved many group members over a five-year period and collectively has resulted in the synthesis of 155 3-D fragments. Important considerations for fragment screening are purity, stability (in aqueous buffer and on storage in DMSO) and solubility (in aqueous buffer). Indeed, prior to screening, several of the synthesised fragments were removed from the library due to issues with one or more of these considerations. This section describes the results of quality control (QC) as well as stability and solubility studies for the York 3-D fragment library (155 fragments) which was necessary for the design of robust screening assays to detect fragment binding and to avoid false positives.

Initially, compound purity was determined by ^{1}H NMR spectroscopy at a concentration of 2 mM in d_6-DMSO solutions. Compound verification or QC is important because fragment screening is carried out at concentrations in the low mM to high μM range such that a 1% impurity at 1 mM will be present at 10 μM which is high enough to bind and result in false positives. Following analysis of the ^{1}H NMR spectroscopic data, nine fragments (Figure 3.4) were removed due to additional signals in their ^{1}H NMR spectra arising from impurities and/or decomposition.

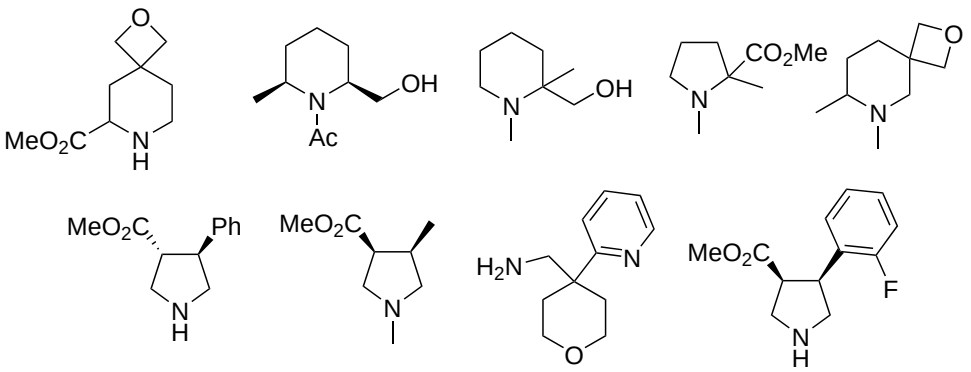

Figure 3.4: Structures of the Nine 3-D Fragments Removed Following QC

For screening purposes, fragments need to be sufficiently soluble (> 5mM in aqueous buffer) in order to be detected by biophysical techniques (SPR, TSA/Differential Scanning Fluorimetry (DSF)), NMR spectroscopy and X-ray crystallography) which measure weak fragment-protein interactions in the low mM to high μM range. Indeed, precipitation or the formation of aggregates as a result of poor solubility is known to interfere with fragment screening. It is also important to determine fragment stability (> 6 weeks in DMSO and > 24 h in aqueous buffer) in order to accurately identify hits during screening. Fragments are stored in a 200 mM DMSO stock solution which is used throughout the screening process which can take several weeks. DMSO is a mild oxidant which in some cases can lead to fragment decomposition. Furthermore, DMSO is hygroscopic and the presence of water can similarly result in compound decomposition and/or precipitation.

Fragment solubility and stability were assessed in a 20 mM sodium phosphate pH 7.48 buffer (1 mM of fragment) and DMSO (2 mM of fragment). Following analysis of the ^{1}H NMR spectroscopic data for 146 fragments in a 20 mM sodium phosphate pH 7.48 buffer, 14 fragments (Figure 3.5) were removed as it appeared that hydrolysis of the carboxylic ester to the corresponding acid was occurring. Given that several library fragments contain methyl ester substituents, it is suprising that only 14 fragments were susceptible to hydrolysis. A further four fragments were excluded due to decomposition.

Fragment stability was assessed in d_6-DMSO by running a second set of ^{1}H NMR spectra after a 24 h period and after 6 weeks. Comparison of the two sets of ^{1}H NMR spectroscopic data suggested that the 128 fragments were stable in d_6-DMSO.

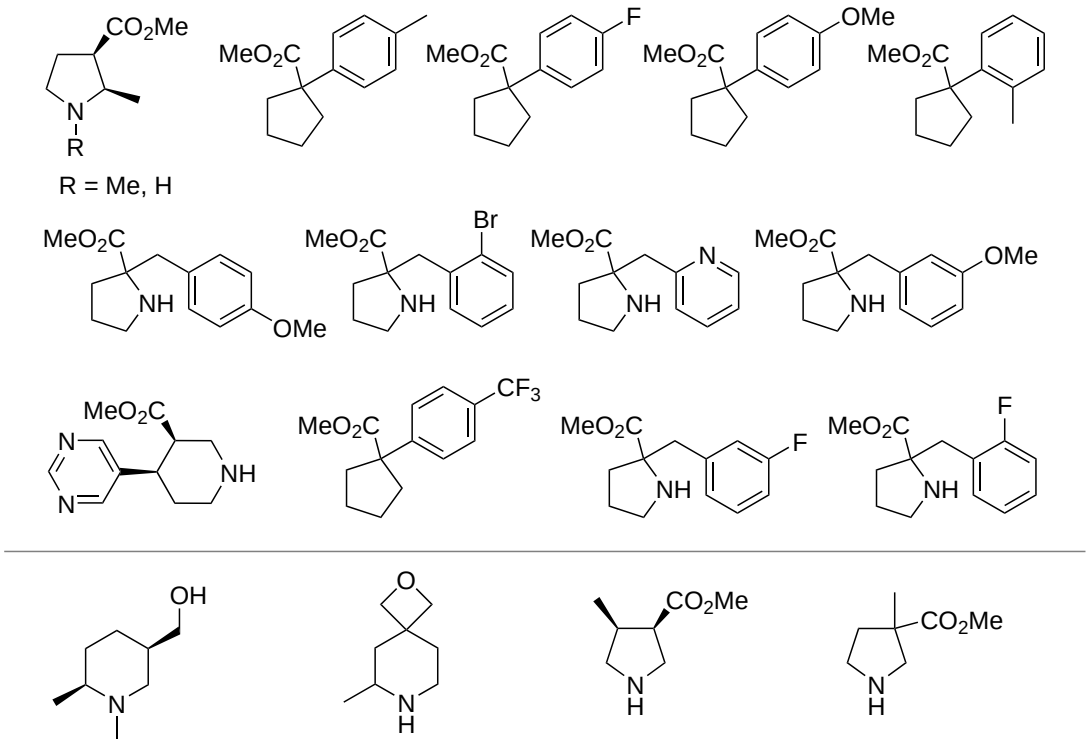

Figure 3.5: Structures of the 14 3-D Fragments Removed due to Buffer Instability and/or Decomposition

Secondly, the solubility of the 128 3-D fragments in a 20 mM sodium phosphate pH 7.48 buffer (1 mM fragment) was determined quantitatively by ^{1}H NMR spectroscopy in the presence of 4,4-dimethyl-4-silapentane-1-sulfonic acid (DSS), a calibration compound. In the ^{1}H NMR spectra, integrals of key signals due to the fragment were compared with those of DSS and the fragment concentration was calculated using the following formula:

$$Cx = \frac{I_x}{I_{cal}} \times \frac{N_{cal}}{N_x} \times C_{cal}$$

where I and N, and C are the integral area and number of nuclei, of the fragment (x) and C is the concentration of the calibrant (cal). Following analysis, 13 fragments

(Figure 3.6) were removed from the collection due to poor solubility (< 5mM in aqueous buffer).

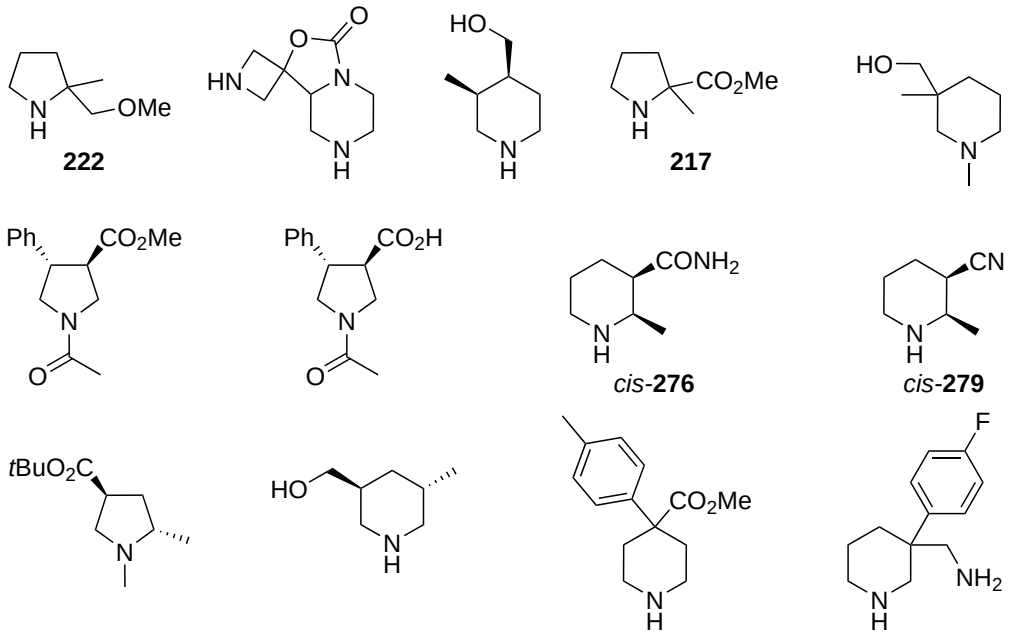

Figure 3.6: Structures of the 13 3-D Fragments Removed due to Poor Buffer Solubility

Overall, the stability and solubility of 146 fragments showed that all 146 compounds were stable to prolonged storage in DMSO stock solutions (> 6 weeks). Of these, 128 fragments were stable in aqueous buffer for > 24 h. Crucially, 115 fragments were soluble at a concentration of > 0.5 mM in aqueous buffer and are therefore suitable for biophysical screening.

3.3 Physicochemical Properties and Shape Analysis of York 3-D Fragments

The physicochemical properties (MW, HAC, ClogP, RBN, HBD, HBA) and molecular shape of the York 3-D fragment library (115 compounds) was assessed and compared with six commercially available fragment libraries. Table 3.2 summarises the mean values of MW, HAC, ClogP, RBN, HBD and HBA for the 115 fragment set. Unsurprisingly, as they had been designed with the Ro3 parameters in mind, the mean values fitted well within the Ro3 guidelines. They were also well within the Astex updated Ro3 ranges for MW, HAC and ClogP.

Table 3.2: Physicochemical Properties of 115 York 3-D Fragments

Property	Ro3	Updated Ro3	115 3-D Fragments[a]
MW (Da.)	≤ 300	140-230	210
HAC	-	10-16	14.7
ClogP	≤ 3	0-2	0.89
RBN	≤ 3	-	2.14
HBD	≤ 3	-	2.66
HBA	≤ 3	-	0.66

[a] Parameters are reported as mean values

PMI analysis of the York 3-D library is shown in Figure 3.7. Global minimum energy conformers (red dots) and higher energy conformers (blue dots) were far from the rod-disc axis with very few conformations having ΣNPR values < 1.1. Furthermore, the collection was found to be conformationally diverse with fragments adopting a total of 772 conformations. The spread of conformations was also wide-ranging indicating a high degree of structural diversity with all conformations up to 1.5 kcal mol^{-1} above the energy of the global minimum energy conformer for each fragment having ΣNPR values 1.1-1.7.

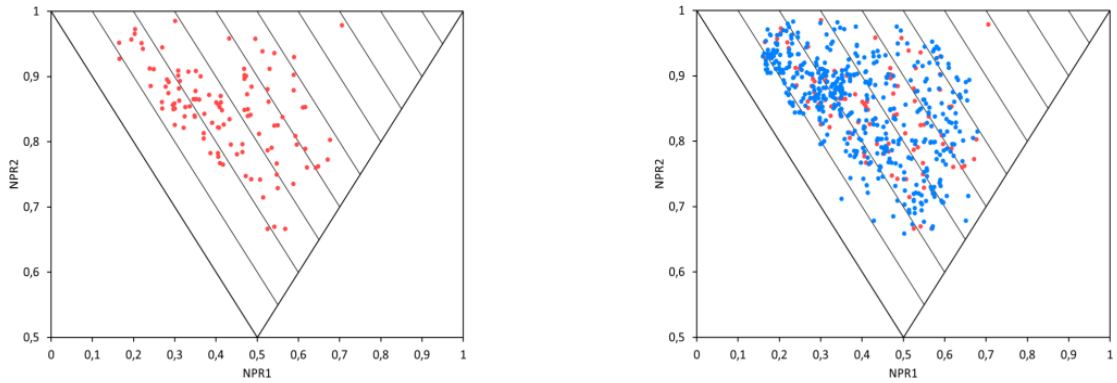

Figure 3.7: PMI Analysis of 115 York 3-D Fragments. Red dots indicate global minimum energy conformers and blue dots indicate higher energy conformers

In order to determine whether the York 3-D fragment library could be used to effectively complement commercial collections, both physicochemical properties (MW, HAC, Fsp^3, ClogP) and 3-D shape (*via* PMI analysis) of the 115 compound collection were compared against six commercially available fragment collections (Maybridge, Chembridge, Enamine Ro3, Life Chemicals 3D, ChemDiv 3D and Enamine 3D). The distribution of properties of the York 3-D library and six commercial fragment libraries is shown in Figures 3.8-3.11.

In terms of MW, York 3-D, Maybridge and Chembridge fragment collections showed a similar profile (Figure 3.8). Enamine Ro3 and Enamine 3D collections were comparable in distribution but on average exhibited a higher MW compared to York 3-D and the Maybridge libraries. Life Chemicals 3D and ChemDiv 3D libraries were also comparable in distribution with significantly higher MW ($>$ 40% of fragments with MW 275-300) than other commercial collections. Since MW and HAC are broadly the same parameter, a similar set of trends was observed for the HAC distribution (Figure 3.9). Overall, the York 3-D fragment collection was found to have a comparably lower HAC with 58% of the library having a HAC $<$ 16. By contrast, 39% and 42% of fragments within Enamine Ro3 and Enamine 3D collections have HAC $>$ 16. Life Chemicals 3D and Chem Div 3D libraries showed significantly higher HAC with 72% and 79% of fragments with HAC $>$ 16.

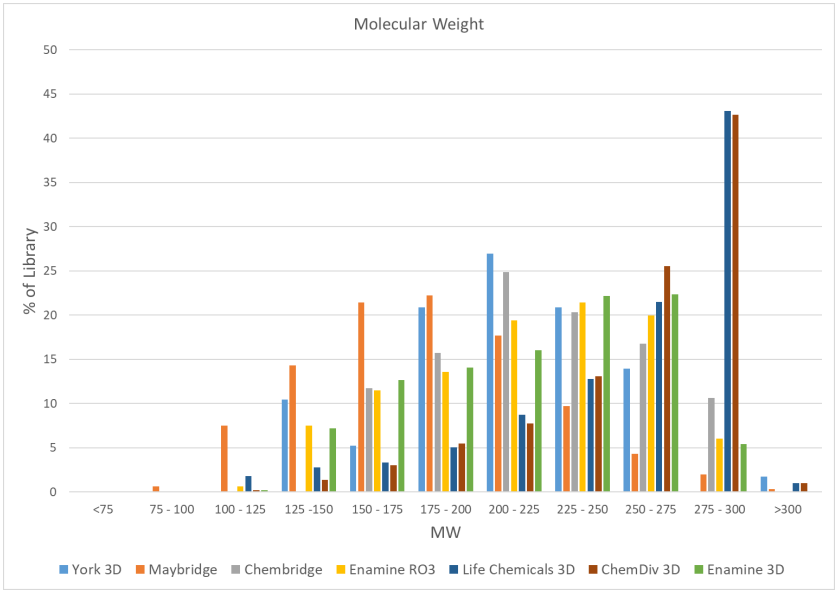

Figure 3.8: MW Distribution Comparing York 3D (light blue), Maybridge (orange), Chembridge (grey), Enamine Ro3 (yellow), Life Chemicals 3D (dark blue), ChemDiv 3D (maroon) and Enamine 3-D (green) Fragment Libraries

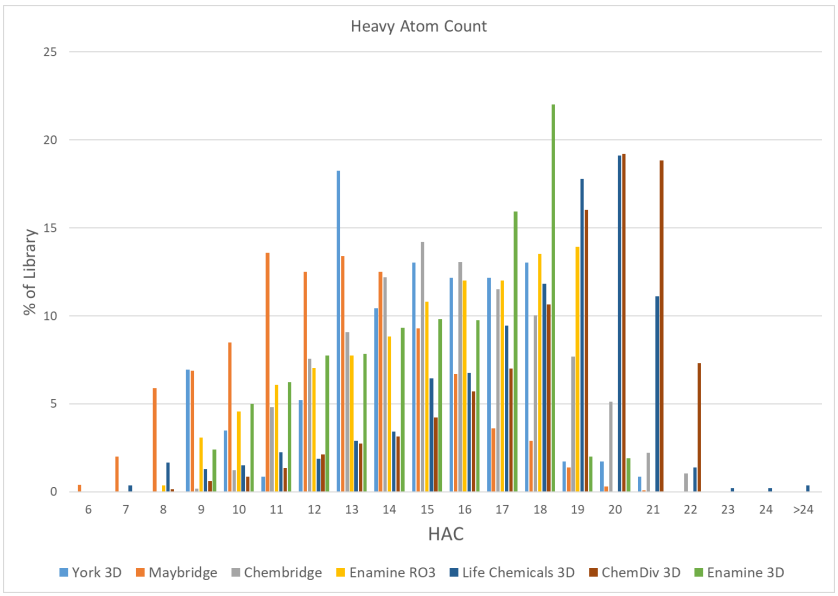

Figure 3.9: HAC Distribution Comparing York 3D (light blue), Maybridge (orange), Chembridge (grey), Enamine Ro3 (yellow), Life Chemicals 3D (dark blue), ChemDiv 3D (maroon) and Enamine 3-D (green) Fragment Libraries

Although Fsp^3 is widely used as a 3-D-shape descriptor for fragment libraries it is a poor predictor of 3-D shape with no correlation between Fsp^3 and PMI (see section 1.4). On the other hand, Fsp^3 can be useful for providing different growth vectors[31,37] and as an indicator of complexity and saturation, the latter being an important factor for buffer solubility. For our purposes, it served as a useful comparison in general terms. To this end, the distribution of Fsp^3 for the York 3-D fragment library compared favourably against five of the six libraries with 42% of fragments with $Fsp^3 < 0.5$ (Figure 3.10). By contrast, the Maybridge, Chembridge and Enamine Ro3 collections showed a Fsp^3 distribution of 68-85% of fragments with $Fsp^3 < 0.5$.

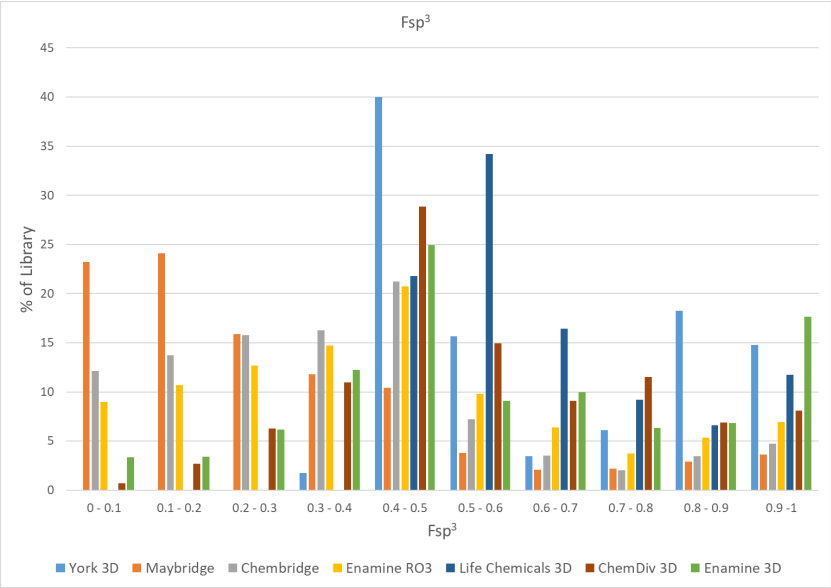

Figure 3.10: Fsp^3 Distribution Comparing York 3D (light blue), Maybridge (orange), Chembridge (grey), Enamine Ro3 (yellow), Life Chemicals 3D (dark blue), ChemDiv 3D (maroon) and Enamine 3-D (green) Fragment Libraries

ClogP is a measure of compound lipophilicity such that compounds with lower ClogP tend to exhibit higher buffer solubility, a crucial factor for ensuring high enough compound concentration (> 0.5 mM in aqueous buffer) for fragment screening. The ClogP distribution of the York 3-D fragment library was compared against two libraries (Maybridge and Chembridge) for which ClogP data was available. Overall, the ClogP distribution showed the York 3-D fragment library to have a comparably lower than average ClogP with 60% of compounds having ClogP ≤ 1 (Figure 3.11). By contrast, May-

bridge and Chembridge libraries had 24% and 35% of compounds with ClogP ≤ 1.

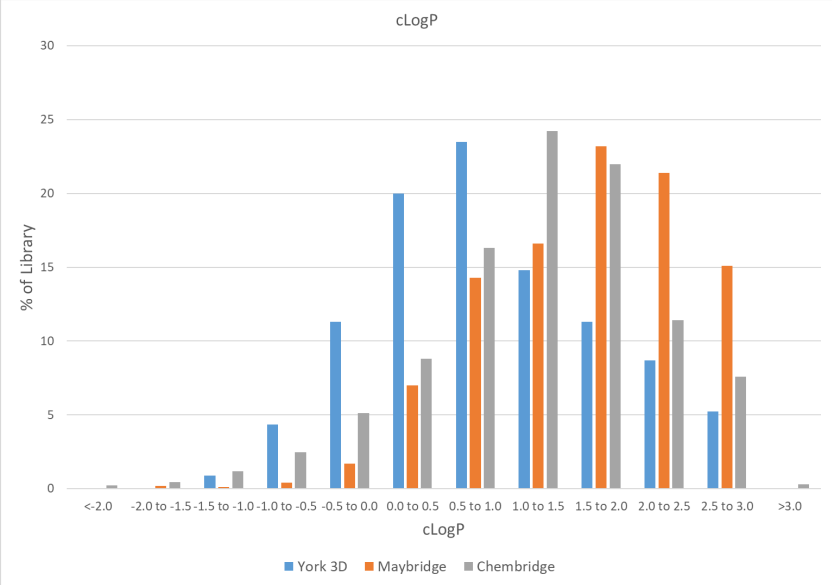

Figure 3.11: ClogP Distribution Comparing York 3D (light blue), Maybridge (orange) and Chembridge (grey) Fragment Libraries

Finally, a cumulative PMI analysis of the York 3-D fragment library was carried out and used to compare the 3-D shape and area of fragment space targeted against six commercially available fragment libraries (Maybridge, Chembridge, Enamine Ro3 and 3-D focused libraries: Life Chemicals 3D, ChemDiv 3D, Enamine 3D). Unlike standard PMI plots, cumulative PMI plots indicate the percentage of fragments which fall within a defined mean distance from the rod-disc axis (ΣNPR = 1). Initially, all conformers of the York 3-D fragment library (up to 1.5 kcal mol^{-1} above the energy of the global minimum energy conformer) were generated. The ΣNPR for each fragment was then averaged to account for the number of conformations. Therefore, a single value of ΣNPR was calculated for all low energy conformations of each given fragment in order to prevent more flexible compounds (with a higher number of conformations) from biasing the dataset. PMI analysis of the six commercial fragment libraries was based on a random selection of 1000 compounds from each library. In this case, only ground state conformers were analysed. A plot of the cumulative percentage of fragments against ΣNPR is shown in Figure 3.12. Strikingly, data for the York 3-D collection

lies furthest to the right of the plot with 50% of the library having ΣNPR > 1.5. Furthermore, data for the York 3-D library compared favourably against 3-D focused libraries, Life Chemicals 3D, ChemDiv 3D and Enamine 3D. Clearly, when compared to commerical fragment collections, the York 3-D fragment library targets different areas of chemical space (with greater ΣNPR values) with the potential for providing fragment hits against difficult and/or diverse protein targets.

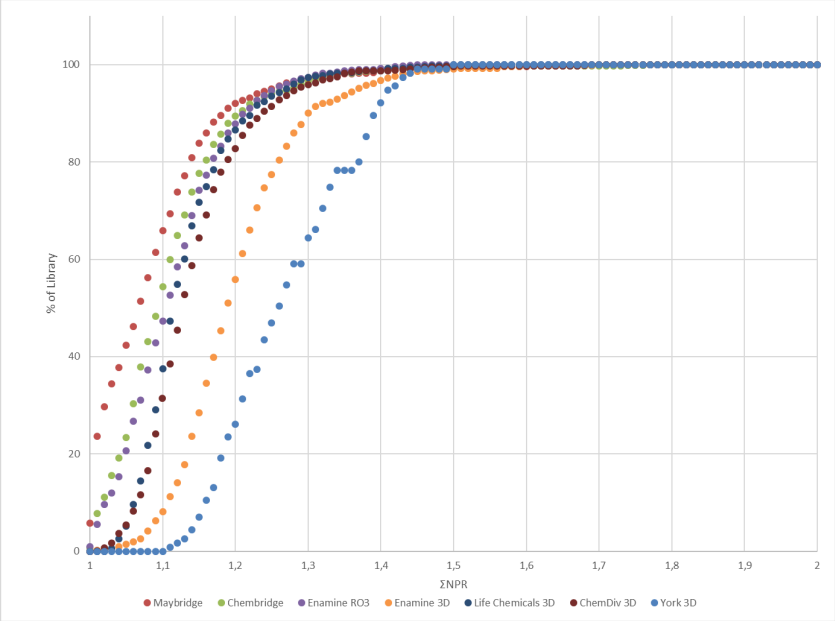

Figure 3.12: Cumulative PMI Plot Comparing the York 3-D Fragment Library (light blue) with Six Fragment Libraries

Overall, the York 3-D fragment library (115 compounds) was designed to be Ro3 compliant and analysis of physicochemical properties (MW, HAC, ClogP, RBN, HBD, HBA) shows that the collection also adheres to the updated Ro3 guidelines. The 115 3-D fragments compared favourably in terms of 3-D shape and targeting different areas of chemical space against six commercial fragment libraries including three 3-D focused collections. The favourable physicochemical properties and 3-D shape (with conformational and shape diversity) of the collection suggest that York 3-D fragments could provide high quality starting points in drug development with the potential to generate hits against a wide range of protein targets.

3.4 Fragment Screening of York 3-D Fragments

During the project, the York 3-D fragment library and subsets of the collection have been screened against various protein targets. The first fragment screen was carried out during a placement at Vernalis against three proteins: heat shock protein90α (Hsp90α), protein tyrosine phosphatase 1B (PTP1B) and serine/threonine-protein kinase (PAK4). Protein selection was based on availability at Vernalis and literature precedence for their crystallisation[140–142] which would be necessary for future X-ray crystallographic screening. At the time, 52 York 3-D fragments were available and the plan was to screen those using NMR spectroscopy, DSF/TSA and X-ray crystallography. The structures of the 52 3-D fragments are shown in Figure 3.13. They include 25 3-D fragments whose synthesis was described in Chapter 2.

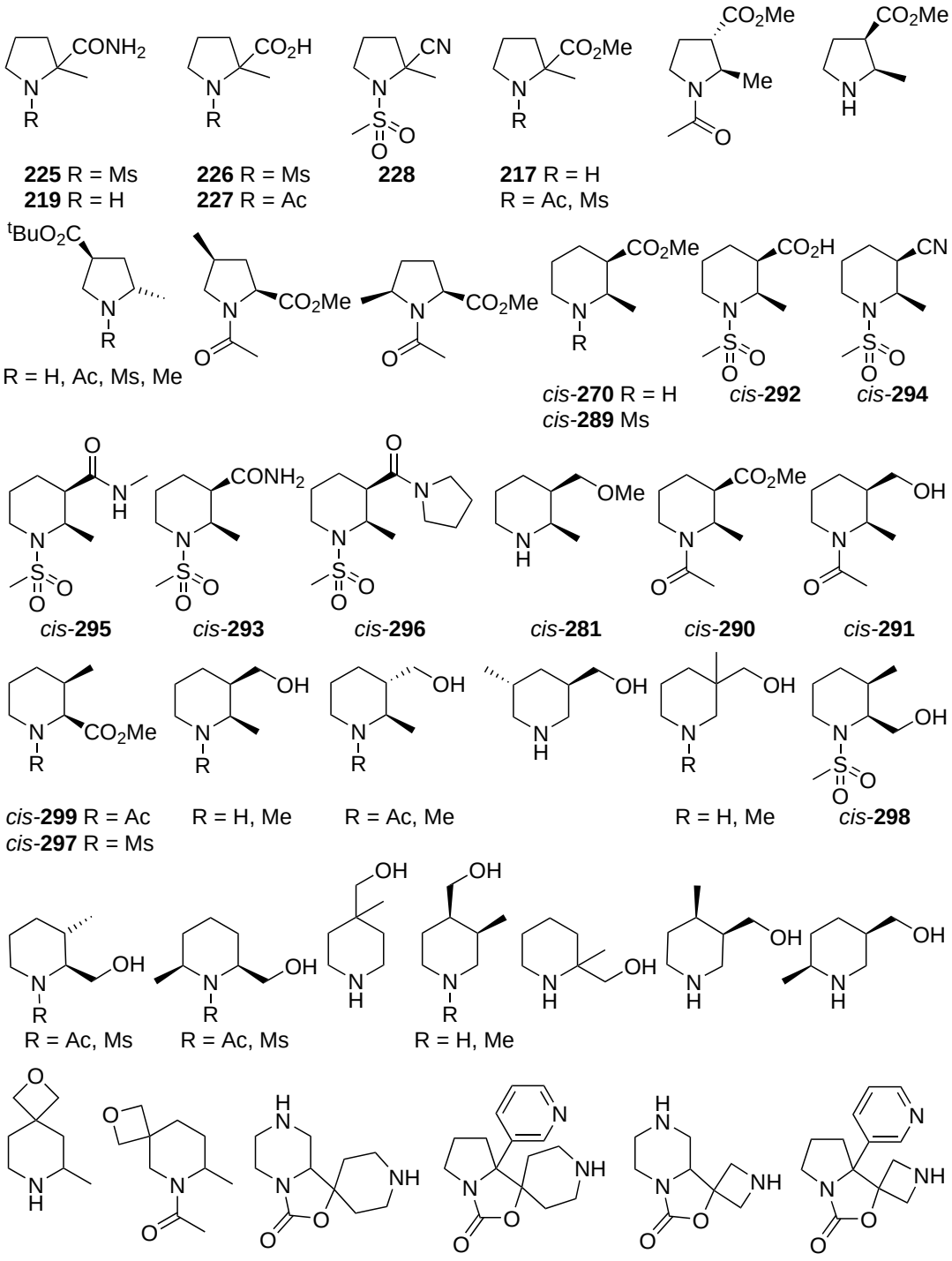

Figure 3.13: Structures of the 52 3-D Fragments

Heat shock protein90α (Hsp90α) forms the basis of a super-chaperone machine which assists in the folding, activation and stabilisation of key client proteins involved in signal transduction and transcriptional regulation.[140] The enzyme catalyses the hydroly-

sis of adenosine triphosphate (ATP) into adenosine diphosphate (ADP) and phosphate (P_i).[143] ATP binding induces a conformational change which allows the protein to exist in an *open* or *closed* state. Hsp90α is a well-established molecular target for cancer therapy. Therapeutic interest stems from its function in the maintenance and regulation of client proteins which in turn are involved in signal tranduction pathways leading to cell proliferation, cell cycle progression and apoptosis, as well as angiogenesis and metastasis in the diseased state. Inhibitors of Hsp90α are designed to target the ATP binding site although the exact mechanism behind the anticancer activity exhibited by Hsp90 inhibitors is unknown.

Protein tyrosine phosphatase 1B (PTP1B) forms part of a large group of enzymes which, together with protein tyrosine kinases, control and regulate signal transduction pathways implicated in a number of fundamental physiological processes including mitosis and insulin signaling.[144] More specifically, PTP1B is responsible for the dephosphorylation of tyrosine. The protein is of therapeutic interest as it has been reported to be involved in mammary tumourigenesis and metastasis where it is overexpressed together with protein tyrosine kinase HER2 (PTK HER2).[145] Currently, all drugs available on the market against PTP1B target its structured catalytic domain (1-321 aa). The majority of inhibitors were designed to mimic PTP1B's natural substrate, phosphotyrosine (pTyr). Inhibitors designed to bind to both the active site and adjacent regions display higher binding specificity.[146]

Serine/threonine-protein kinase (PAK 4) is one of a family of six p21-activated kinases which are involved in a number of cellular processes including regulation of cell motility, morphology, and cytoskeletal dynamics.[147] More recently, the PAK family have been implicated in oncogenic activity such as promoting cell proliferation, accelerating mitotic abnormalities and nuclear receptor-signaling.[148] In this sense they are an attractive target for cancer therapy. Most inhibitors of PAK4 are competitive with ATP and bind within the catalytic domain of the enzyme.

NMR spectroscopy is among the most commonly used methods for fragment screening. It can be used to detect fragment hits over a broad affinity range from covalent binding to binding in the millimolar range. Furthermore, it is a convenient fragment screening method as it requires neither preparation of the protein target in the way of crystallisation or immobilisation nor any assay development. Spectroscopic parameters such as chemical shift, diffusion, relaxation, and the tranfer of magnetisation between resonances of both the ligand and protein are influenced by changes between the bound and free state of a ligand. These differences allow for the design of NMR experiments to detect changes which occur on fragment binding. There are two types of NMR experiments used for fragment screening: protein-observed and ligand-observed NMR.

It was intended to use the ligand-observed NMR techniques of saturation transfer difference (STD), water-ligand observed *via* gradient spectroscopy (Water-LOGSY) and CPMG experiments to assess protein binding. NMR signals for the free (P_{free}) and bound (P_{bound}) fragment populations before and after the addition of a known protein inhibitor would be compared such that the intensity of the observed NMR signal (I_{obs}) can be defined as the $f(P_{bound})$, $f(P_{bound}–P_{free})$ or $f(P_{free})$ for STD, Water-LOGSY and CPMG experiments respectively. An example of a three compound screen (*a*, *b* and *c*) is shown in Figure 3.14. The structures of compounds *a*, *b* and *c* are unknown in this case and the raw data (provided by Vernalis) is provided to illustrate how a set of NMR data is analysed in a typical fragment screen.

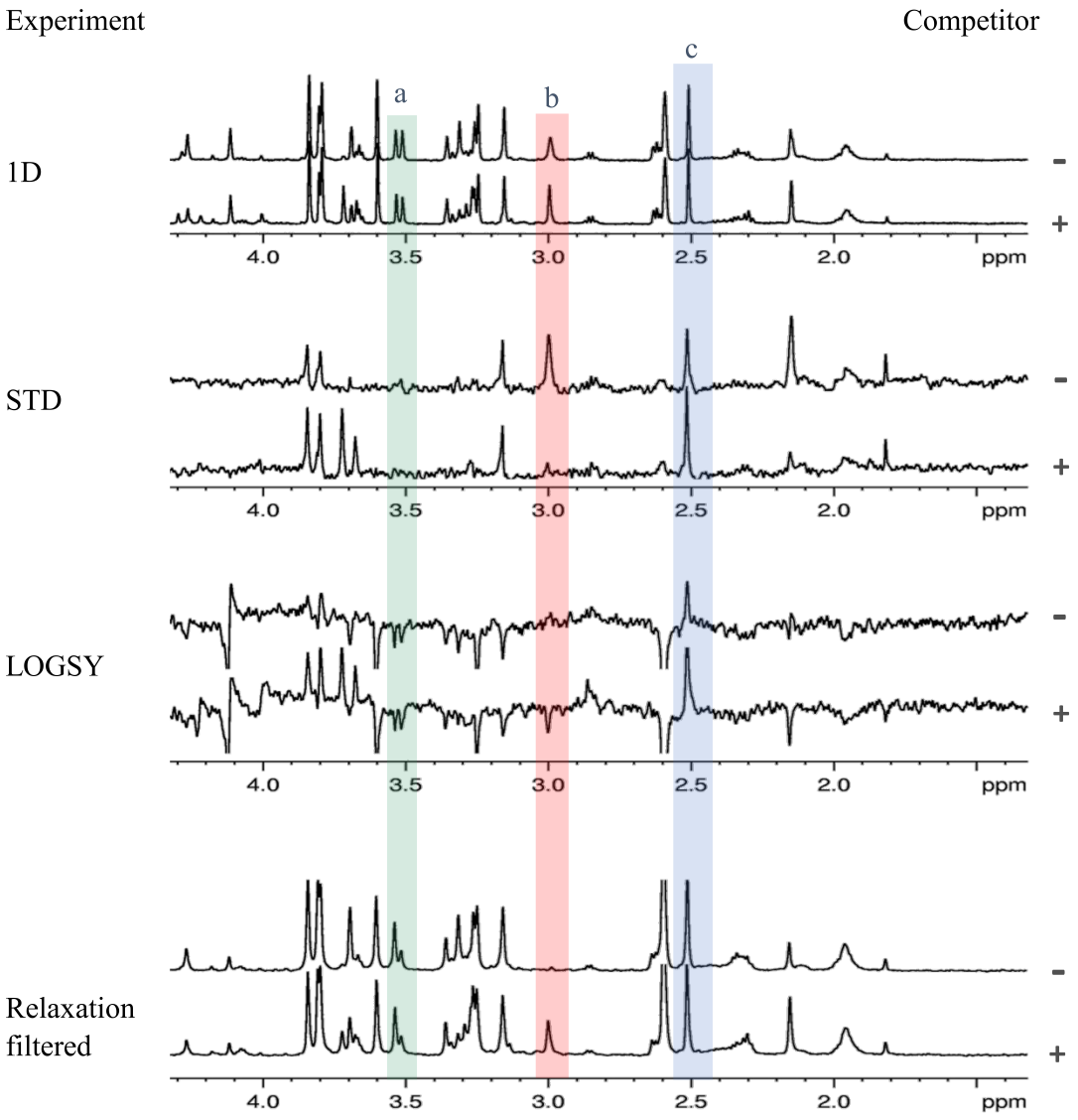

Figure 3.14: A Typical ^{1}H NMR Spectroscopic Screen with Vernalis Compounds *a*, *b* and *c*

Signals corresponding to compound *a* and *c* appear at chemical shifts of ∼3.5 ppm and ∼2.5 ppm, as highlighted. The signals at ∼3.5 ppm and ∼2.5 ppm in both the top and bottom NMR spectra remain identical across all four experiments (1D, STD, LOGSY, relaxation filtered). This indicates that, on adding a competitor (+), the fragment population (P_{bound}+P_{free}) remains unchanged. In contrast, signals corresponding to compound *b* appearing at 3.0 ppm indicate binding across three experiments (STD, LOGSY, relaxation filtered). On adding a competitor (+), the STD and Water-LOGSY

NMR signals are diminished as the population of bound fragment is displaced by the competitor. NMR signals for compound *b* in the CPMG run in the presence of the competitor (+) are enhanced as the population of unbound/free fragment is increased on protein binding of the competitor (+). Compound *b* can thus be considered a hit as STD, Water-LOGSY and CPMG NMR spectra show that it binds and is displaced by the competitor (+) in all three experiments.

Screening against Hsp90 and PAK4 was carried out with ligand-observed NMR which records changes in the ligand NMR spectrum due to interaction with the protein receptor in the bound state. The addition of a potent competitor prevents binding and this results in changes in the STD, Water-LOGSY and CPMG NMR spectra. The experiments were carried out in the presence and absence of known competitors VER-00082160 and Staurosporin (Figure 3.15) for Hsp90 and PAK4 respectively.[149,150] High fragment concentrations of 0.5 mM with 10 μM protein in a 20 mM 4-(2-hydroxyethyl)-1-piperazineethanesulfonic acid (HEPES) pH 7.5 buffer with 100 mM NaCl and 0.5 mM tris(2-carboxyethyl)phosphine (TCEP) were used. The 52 York 3-D fragments were screened in groups of four in order to reduce the amount of protein used. In most cases, groups were composed of two commercially available 2-D fragments and two 3-D fragments in order to minimise overlapping signals. The majority of selected 2-D fragments contain an aromatic group which was easily discernible in the NMR screen.

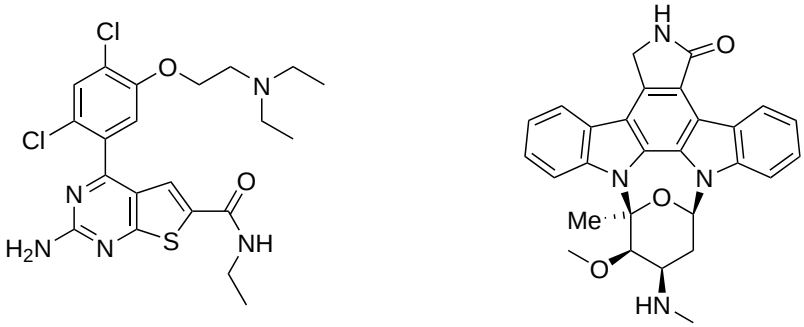

VER-00082160 *Staurosporin*

Figure 3.15: Structures of Competitors VER-00082160 and Staurosporin

An illustrative example of the ^{1}H NMR spectroscopic screening data obtained using fragments, **294**, **398**, **399** and **400** (Figure 3.16) is shown in Figure 3.17. The signals at 1.43 and 1.33 ppm, corresponding to the Me group of fragments **294** and **398** respectively, were used to assess protein binding. For 2-D fragments **399** and **400**, signals for the aromatic protons at 8.75 and 7.18 ppm were easily distinguished and helpful in identifying possible fragment hits. In this case, the highlighted signals for all four compounds exhibited no signs of protein binding with NMR signals in the STD, Water-LOGSY and CPMG NMR spectra remaining unchanged before (−) and after adding competitor (+). This assessment was carried out for all 52 3-D fragments. Disappointingly, no hits were recorded for any of the 3-D fragments.

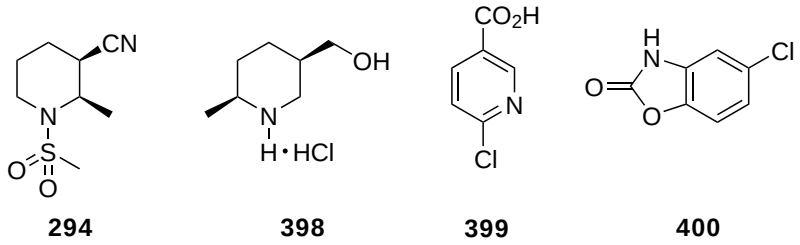

294 **398** **399** **400**

Figure 3.16: Structures of Fragments Used to Illustrate Analysis of ^{1}H NMR Spectroscopic Screening Data

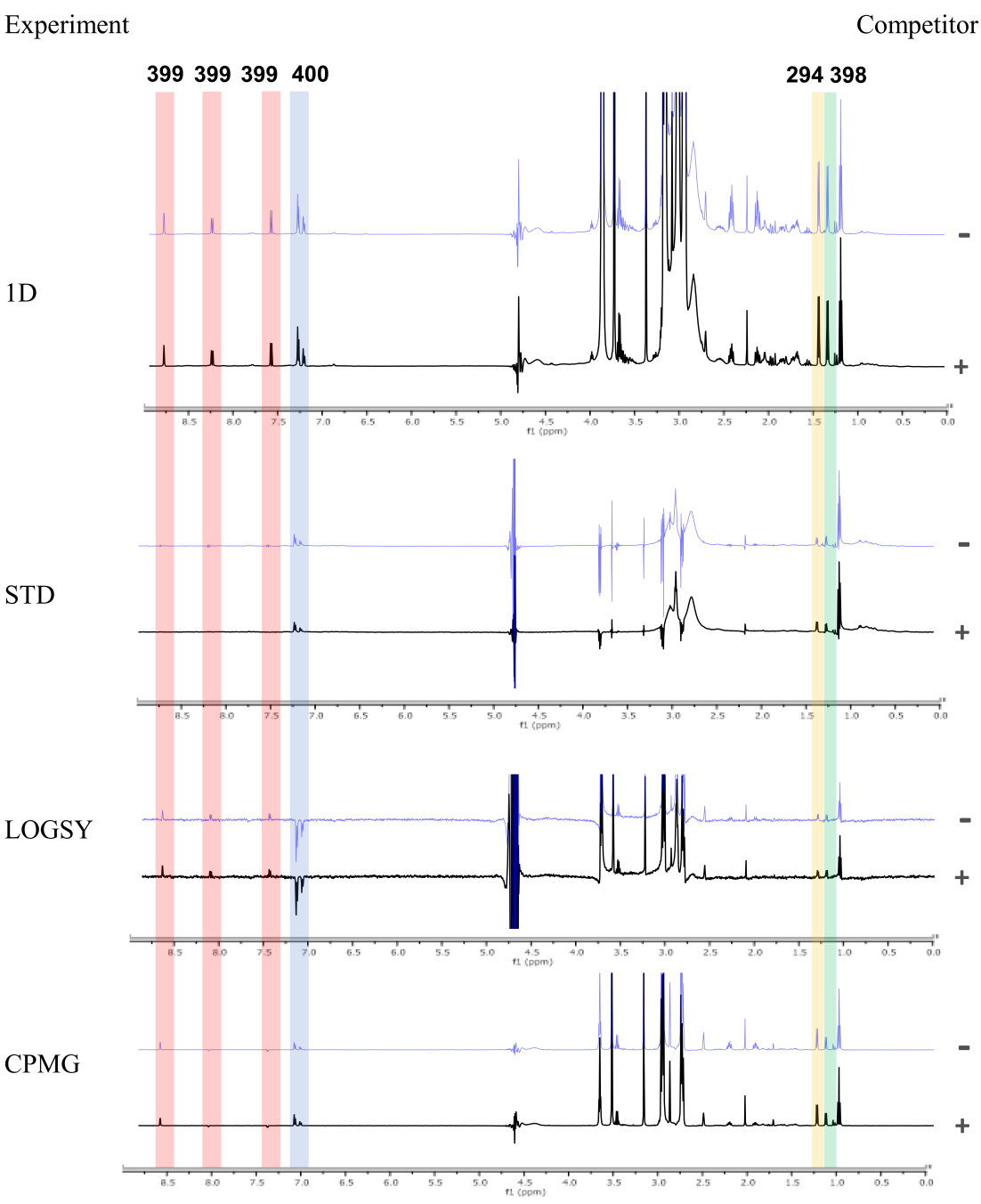

Figure 3.17: ^{1}H NMR Screening Data for Fragments **294**, **398 399** and **400**

Fragment screening against PTP1B was carried out using protein-observed NMR due to the absence of an appropriate PTP1B inhibitor. To this end, protein NMR spectra with (+) and without fragment (−) were compared. 3-D Fragments were screened on an individual basis with no comparative 2-D set. For example, slight broadening and changes in the chemical shift of protein NMR signals in the aliphatic region (< 0.8 ppm) after adding fragment **401** were taken to indicate potential binding to the protein (Figure 3.18).

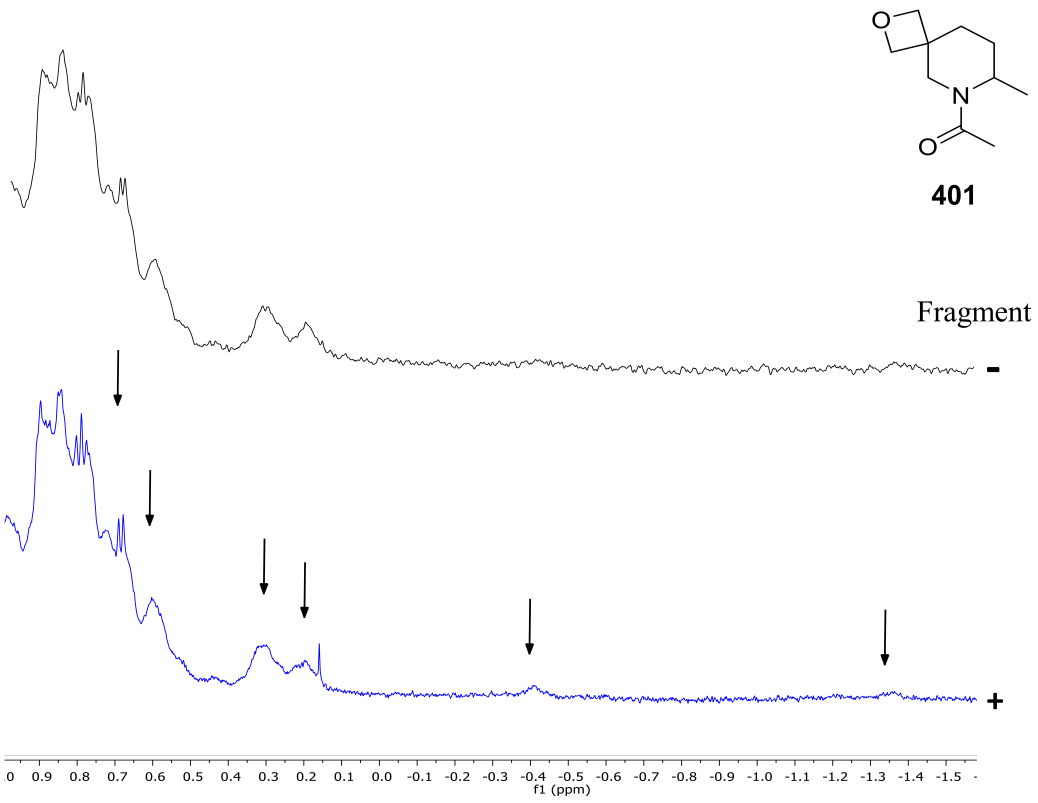

Figure 3.18: ^{1}H NMR Spectroscopic Data for PTP1B without (−) and with (+) Fragment **401**. Signals monitored for changes in chemical shift/shape on fragment addition are indicated with an arrow

Overall, slight perturbation of protein aliphatic signals on addition of the fragments shown in Figure 3.19 suggested possible binding. In order to validate this, the six potential hits were individually soaked with PTP1B crystals. The soaking conditions and results of the X-ray diffraction experiments are reported below in the X-ray crys-

tallographic screening section.

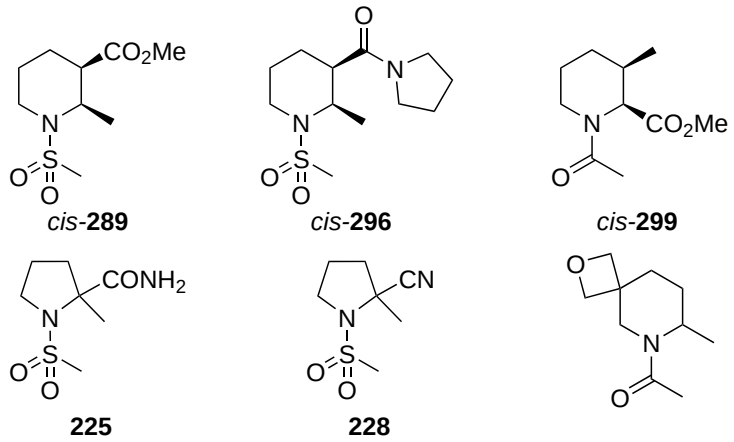

Figure 3.19: Structures of Potential York 3-D Fragment Hits by ^{1}H NMR Spectroscopy against PTP1B

The 52 York 3-D fragments were also screened using DSF/TSA by monitoring changes in the melting temperature (T_m) of the protein as previously described by Lo and co-workers.[151] Proteins were buffered in a 50 mM HEPES pH 7.5 buffer with 100 mM NaCl, 10 mM $MgCl_2$ and 1 mM dithiothreitol (DTT) at a concentration of 5 μM. Fragments were screened at a concentration of 1 mM and 5 mM. Compounds with a value of $\Delta\ T_m > 1$ °C were classified as hits. Using this threshold, 3-D fragment **270** registered as a hit against PAK4 (Figure 3.20). Piperidine **270** resulted in a $\Delta\ T_m$ shift of 1.07 °C and 1.77 °C at concentrations of 1 mM and 5 mM fragment respectively (Figure 3.21). Unfortunately, there were no other hits recorded by TSA.

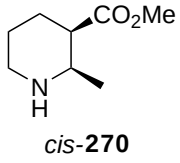

cis-**270**

Figure 3.20: Structure of York 3-D Fragment Hit by TSA against PAK4

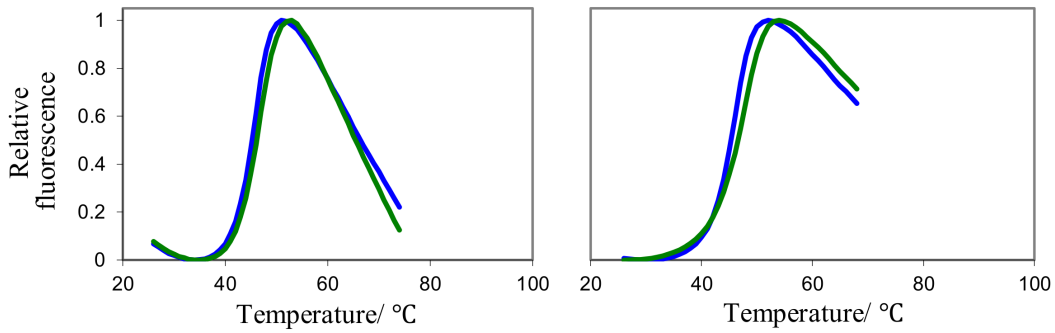

Figure 3.21: TSA results for fragment **270** at 1 mM and 5 mM of fragment

The 52 York 3-D fragments were also screened against Hsp90, PAK4 and PTP1B using X-ray crystallography. High concentrations of fragment are typically used in crystal soaking experiments to enable detection of weakly binding molecules. Fragment screening using X-ray crystallography is attractive as hits generated using this biophysical method result in a three-dimensional structure of the bound ligand-protein complex. Key information about the ligand binding mode including key protein-ligand interactions can be identified and applied to hit-to-lead optimisation campaigns. On the other hand, fragment screening by X-ray crystallography does pose many challenges. Firstly, experimental conditions for crystallisation of the target protein have to be established. This can take time and is not always possible. Secondly, the crystallised protein and crystal lattice must be stable and open enough to withstand soaking conditions and allow the fragment to access the binding site.

Conditions for protein crystallisation were trialled using the 24-well hanging-drop vapour diffusion technique. Hexa-histidine-tagged Hsp90 in a 20 mM tris(hydroxymethyl)aminomethane (tris) pH 7.5 buffer with 50 mM NaCl and 1 mM DTT was crystallised following literature conditions[140] with 24% polyethylene glycol (PEG) 3350 in a 0.1 M cacodylate buffer with 0.2 M $MgCl_2$. Under these conditions, Hsp90 crystals were observed to form within 18 h. Wells with varying percentages of PEG 3350 (22.5-32.5%) were also trialled but did not yield crystals. Data was collected at a resolution

of 1.95 Å. Molecular replacement was peformed with *Phaser*[152] using Protein Database (PDB) entry 1UYL as a starting model.[140] The space group for Hsp90 was determined to be I222. Refinement converged at a value of R_{free}/R factor of 23%/18% for the Hsp90 apo structure.

The PTP1B construct contains an *N*-terminal His tag, a TEV protease binding site and the PTP1B binding sequence. Protein purification was previously carried out in a 50 mM HEPES pH 6.8 buffer with 150 mM NaCl and 0.5 mM TCEP. The composition of the crystallant was tested by varying the percentage of PEG3350 and concentration of $MgCl_2$. Crystallization conditions containing 15-22.5% PEG 3350 in a 0.1 M HEPES pH 7.0 buffer with 0.15 M $MgCl_2$ afforded crystals after about 21 days. Wells with microseeds gave crystals in about 3 days. Interestingly, two crystal forms were observed as shown in Figure 3.22. Under these conditions, a higher number of block-shaped crystals (Figure 3.22a) were oberved with fewer examples of rod-shaped crystals (Figure 3.22b) occuring.

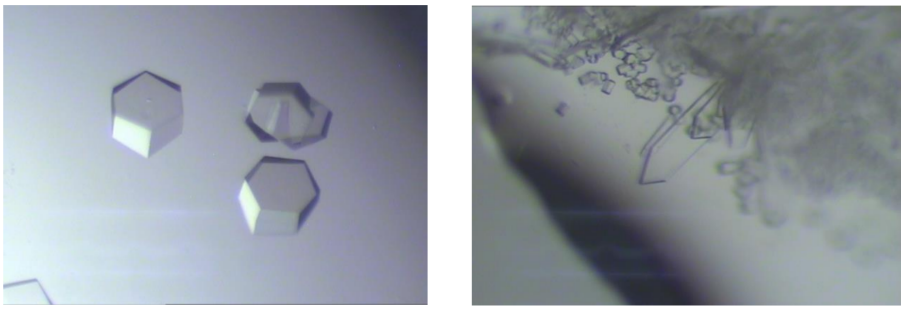

a b

Figure 3.22: Crystal Structures of PTP1B

Data were collected at a resolution of 2.10 Å. Molecular replacement was peformed with *Phaser*[152] using a single monomer of PDB entry 4BJO as a starting model.[153] The space group for PTP1B was determined to be P3121 for the block-shaped PTP1B crystals and P212121 for the rod-shaped PTP1B crystals. Refinement converged at R_{free}\R factor values of 21%/18% and 26%/22% for the block- and rod-shaped crys-

tals respectively of the PTP1B apo structure.

Crystallisation of histidine-tagged serine/threonine-protein kinase PAK4 was initially trialled following literature conditions[142] with 10-15% PEG400 in a 0.1 M tris pH 8.0 buffer with 1-2.1 M $(NH_4)_2SO_4$. No crystals were observed to form. Concern over the presence of imidazole in the original purification solution (a 50 mM HEPES pH 7.5 buffer with 500 mM NaCl, 250 mM imidazole and 10% glycerol) led us to dialyse the protein in a 50 mM HEPES pH 7.5 buffer with 150 mM NaCl, 1 mM DTT and 5 mM $MgCl_2$ over 18 h. The dialysed protein was concentrated to 10 $mg.ml^{-1}$ and crystallisation was attempted again. Unfortunately, no PAK4 crystals were observed to form.

Following crystallisation of Hsp90 and PTP1B, crystal soaks were set up with cocktails of 6-7 fragments (2.86-3.33 mM fragment in DMSO) per cocktail at 6 °C for 72 h−4 days. A further six individual fragment crystal soaks were set up for the six potential NMR hits against PTP1B (see Figure 3.19) at 6 °C for 4−11 days. Crystals were transferred to a cryoprotectant solution consisting of 20% glycerol and 80% of the crystallant and cryocooled in liquid nitrogen. Datasets for apo structures and crystal soaks were collected and processed at the Diamond Synchrotron using X-ray Detector Software (XDS) for processing single-crystal monochromatic diffraction data. Unfortunately, following analysis of all collected datasets, there were no hits by X-ray crystallography.

More recently, as part of a collaboration with the von Delft group, a crystallographic fragment screen of 1250 compounds (including 106 York 3-D fragments) against SARS-CoV-2 main protease (SARS-CoV-2 M^{pro}) at the Diamond-XChem facility revealed 74 hits including two York 3-D fragments (synthesised by Tom Downes and Paul Jones in the O'Brien group), shown in Figure 3.23.[154] The SARS-CoV-2 M^{pro} enzyme is one of two essential cysteine viral proteases of SARS-CoV-2, a zoonotic coronavirus responsible for COVID-19. Currently, there are no available drugs against the virus

with treatment limited to alleviating symptoms.

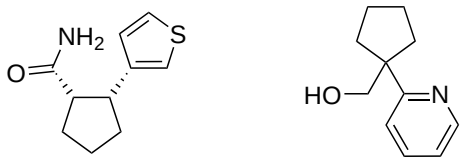

402 **403**

Figure 3.23: Structures of York 3-D Fragment Hits by X-ray Crystallography against SARS-CoV-2 M^{pro}

Significantly, fragment **403** bound at the dimer interface of the SARS-CoV-2 M^{pro} enzyme, providing opportunity for potential allosteric inhibition. A crystal structure of the M^{pro} dimer in complex with fragment **403** showed binding between seven amino acids with two key hydrogen bonds formed with the backbone of Phe3 (Figure 3.24). Overall, the 74 bound fragments were effectively used to probe both the active site (71 bound compounds) and the dimer interface (3 bound compounds) of the SARS-CoV-2 M^{pro} enzyme. The obtained structural data provides opportunities for the development of inhibitors against SARS-CoV-2 main protease with SAR studies.

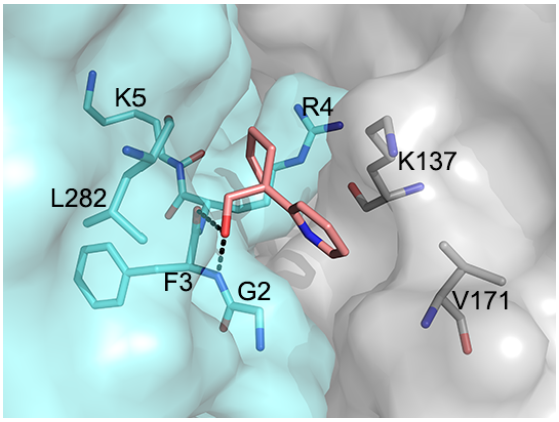

Figure 3.24: Surface of the SARS-CoV-2 M^{pro} Dimer (with protomers in grey and cyan) Bound with 3-D York Fragment **403**

The York 3-D fragment library (106 compounds) has also been screened (together with another six fragment libraries) against the SARS-CoV-2 Nsp^3 macrodomain as part of an X-ray crystallographic screen at the Diamond-XChem facility. The macrodomain dimer of SARS-CoV-2 Nsp^3 has four binding sites of biological relevance: the adenine

subsite, the proximal ribose subsite, the catalytic loop and the pyrophosphate loop. The adenine subsite and the pyrophosphate loop binding sites are of particular interest as they bind the natural ligand ADP-ribose and substrate respectively, providing opportunity for the development of potential competitive inhibitors against the enzyme. Overall, the screen revealed 57 fragment hits (with 68 binding events) including four York 3-D fragment hits (Figure 3.25). Notably, 3-D fragments **326** (see section 2.2 for synthesis), *cis*-**404** and *cis*-**406** bind to the adenine subsite of the active site. Fragments *cis*-**404** and *cis*-**405** also bind near the catalytic loop which interacts with other host proteins.

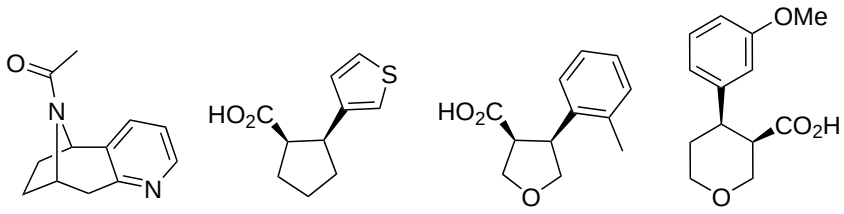

326 *cis*-**404** *cis*-**405** *cis*-**406**

Figure 3.25: Structures of York 3-D Fragment Hits by X-ray Crystallography against the SARS-CoV-2 Nsp^3 Macrodomain

A third screening campaign of the York 3-D fragment library (106 compounds) at the Diamond-XChem facility was recently carried out against an extracellular adenine receptor CD73. CD73 is a key molecule of interest and potential biomarker in cancer immunotherapy due to its involvment in the degradation of adenosine monophosphate (AMP) into adenosine which in turn acts on G-protein-coupled receptors to promote the progression of cancer.[155] Overall, the X-ray crystallographic screen revealed nine fragment hits shown in Figure 3.26. The synthesis of 2,3-disubstituted piperidine *cis*-**297** and 2,3-fused pyrroldines **336**, **341**, **351** and **345** was discussed in Chapter 2 (see sections 2.2 and 2.4).

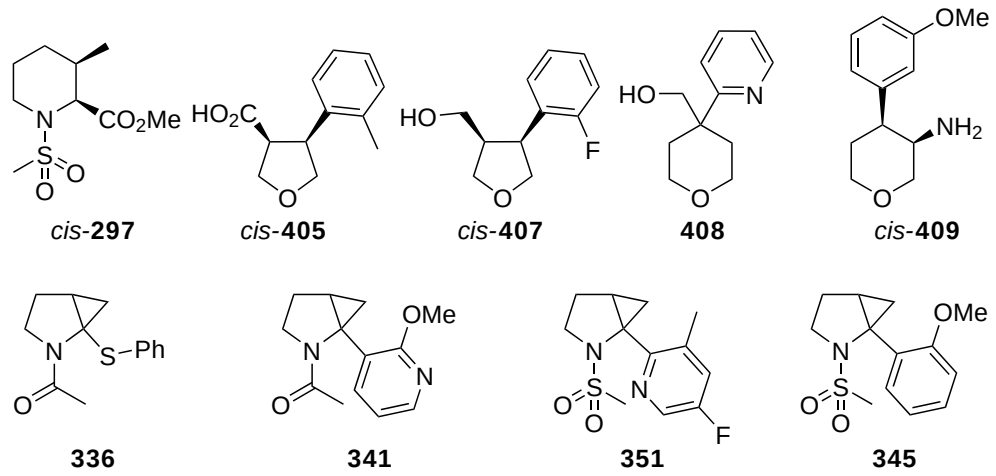

Figure 3.26: Structures of York 3-D Fragment Hits by X-ray Crystallography against CD73 Receptor

In summary, four fragment screening campaigns against six protein targets have been reported. Initial screening attempts of a 52 fragment subset of the York 3-D fragment library against three proteins (Hsp90α, PTP1B and PAK4) by NMR spectroscopy, TSA and X-ray crystallography at Vernalis did not reveal any hits. Although a single hit was recorded against PAK4 by TSA, this result could not be confirmed by NMR spectroscopy or X-ray crystallography screens. In general, screening was challenging due to the lack of aromatic groups and the lower than average HAC (and MW) of the 52-fragment collection which were designed to be structurally simple 3-D fragments with a limited number of binding groups (see Figure 3.13). These factors were postulated to affect both protein binding and detection as smaller fragments with no aromatic or heteroaromatic groups would bind weakly (with a low K_d) and therefore be difficult to detect. In addition, screening by ^{1}H NMR spectroscopy was problematic due to the abscence of aromatic signals. More recent screening campaigns of the York 3-D fragment library (106 fragments) against two proteases of SARS-CoV-2 (SARS-CoV-2 M^{pro} and the SARS-CoV-2 Nsp^3 macrodomain) and the adenine receptor CD73 at the Diamond-XChem facility have met with more success. Notably, 14 out of the 15 York 3-D fragment hits contain an aromatic or heteroaromatic group including tropane **326** and 2,3-fused pyrrolidines **336**, **341**, **351** and **345** (see Figures 3.25 and 3.26)

whose synthesis was described in Chapter 2 (see sections 2.3 and 2.4). Clearly, the incorporation of aromatic groups in 3-D fragment design is important for both protein binding and detection, evident by the higher hit-rate observed in the screening of second generation York 3-D fragments. Moreover, 3-D shape proved to be important as York 3-D fragment hits **403** (against SARS-CoV-2 M^{pro}) together with 3-D fragments **326**, *cis*-**404** and *cis*-**406** (against the SARS-CoV-2 Nsp^3 macrodomain) exhibited significant protein-binding interactions which could serve as starting points for the development of allosteric and competitive inhibitors against SARS-CoV-2 M^{pro} and the SARS-CoV-2 Nsp^3 macrodomain respectively.

4 Design and Synthesis of 3-D Building Blocks for Fragment Elaboration

Fragment elaboration is crucial in the field of FBDD for enabling optimisation of fragment hits with low binding affinity (μM or mM) into lead-like compounds with high binding affinity (nM) during drug development. Ideally, this process is guided by X-ray crystal structures of protein-ligand complexes, which provide information about key interactions and opportunities to link, grow or merge bound fragments into lead-like compounds (MW$\sim$400-500). Arguably, this poses one of the greatest obstacles in FBDD today as the synthetic chemistry needed for fragment elaboration is limited, creating a bottleneck and increasing the costs of the drug discovery process as a whole.

In this Chapter, a new approach to fragment elaboration, which attempts to address the fact that synthetic chemistry can be limiting in hit-to-lead development, is presented. Sections 4.1 and 4.2 discuss the design and synthesis of a set of 3-D building blocks with distinct synthetic vectors for elaboration. Attachment of 3-D building blocks to a, typically 2-D, fragment hit would enable the exploration of structure-activity relationships in lead-like compounds, ultimately allowing elaboration in 3-dimensions and the systematic exploration of chemical space (Figure 4.1). Section 4.3 covers the use of the 3-D building blocks in fragment elaboration via Suzuki-Miyaura cross-coupling.

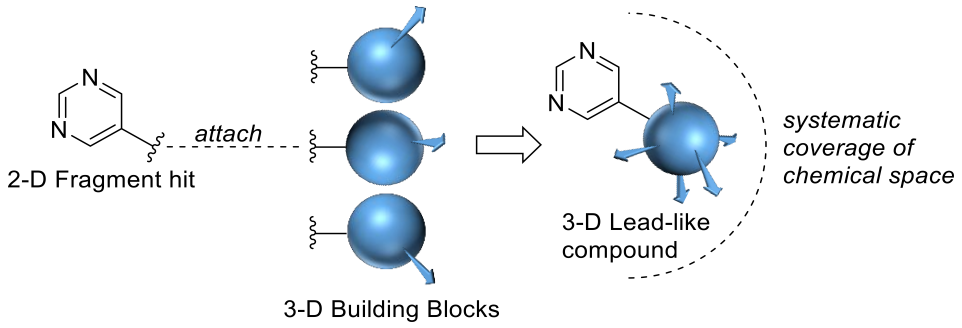

Figure 4.1: Use of 3-D Building Blocks for Elaboration of a 2-D Fragment Hit in 3-Dimensions

4.1 Modular Approach to Fragment Elaboration in 3-Dimensions

Researchers at Astex have highlighted the challenges with fragment elaboration by stating that 'synthetic organic chemistry is often the rate-limiting step in the fragment elaboration stage' and 'it should be possible to synthetically elaborate fragments in 3 dimensions from many different growth points/vectors using methodology that is experimentally worked out prior to fragment screening'. Indeed, these ideas encapsulate a potential limitation inherent in the work described in Chapter 2 of this thesis as the synthesis of the first and second generation 3-D fragments was rate-limiting, with many targeted fragments requiring bespoke multi-step synthetic routes. Moreover, synthetic elaboration of the York 3-D fragments, using two to three synthetic vectors, is potentially limiting. To illustrate this, if piperidine 3-D fragment **410** was a hit in a screening campaign and elaborated analogue **411** was designed to have potentially improved binding features, then the synthesis of 3-substituted piperidine **411** would be required. However, the direct modification of piperidine 3-D fragment **410** by incorporation of a pyridine group at the 3-position would pose a significant synthetic challenge (Scheme 4.1). With no synthetic vector at the 3-position, the synthesis of fragment **411** would require the development of an alternative, bespoke synthetic route, a timely and costly process in the lead-generation stage.

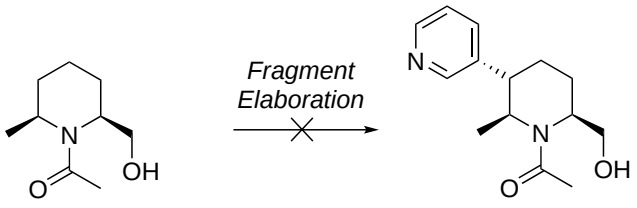

410 **411**

Scheme 4.1

Previous approaches to enable fragment elaboration, including those developed in our group, have focused on incorporation of synthetic vectors for fragment growth during the fragment design stage. For example, the amide and hydroxy groups of fragment

410 could easily be modified and/or different substituents attached. However, these are in fact the functionalities that are most likely to already be involved in protein binding events and so modifying them may not be the best approach for generation of a lead compound. Alternatively, functionalisation of different scaffold positions is possible using a scaffold diversity synthetic approach (see section 1.5.4) which allows the installation of different (polar and non-polar) groups by changing the substrates used. In this case, the number of positions of a given scaffold which can be functionalised or elaborated depends on, and is limited by, the methodology used. Overall, fragment elaboration along synthetic growth points or 3-D vectors in a controlled and potentially programmable manner remains unprecedented. Thus, as set out in the remainder of this section, it was our intention to develop a different approach to address the synthetic challenges with fragment elaboration. Notably, it was hoped that the new strategy would enable a controlled strategy for fragment growth along distinct 3-D vectors.

The long-term aim of the work described in this Chapter is to develop a modular synthetic platform, with potential for an automated workflow, to allow for fragment elaboration of, typically 2-D, fragment hits along distinct, X-ray structure-guided synthetic vectors into 3-D lead compounds. Figure 4.2 provides an overview of the proposed workflow. Initially, fragment hits would be identified following an X-ray crystallographic screening campaign (Figure 4.2A). Notably, aryl bromide fragment hits, recently termed 'FragLites' by Waring and co-workers,[156] and commercial aryl bromide analogues of 2-D fragment hits would each be chemically enabled for elaboration (Figure 4.2B). Then, elaboration of the X-ray fragment hit along multiple synthetic 3-D vectors would be possible by attachment, using the aryl bromide functionality as a synthetic handle, to a 3-D building block from a library of 3-D building blocks, each with a defined synthetic vector (Figure 4.2C). Overall, this process has the potential to be automated into a synthetic platform for fragment elaboration (Figure 4.2D) to allow the rapid generation of a library of 3-D lead compounds for screening (Figure 4.2E).

In this way, 2-D fragment hits could be effectively elaborated into 3-D lead compounds in a systematic, controllable and efficient manner.

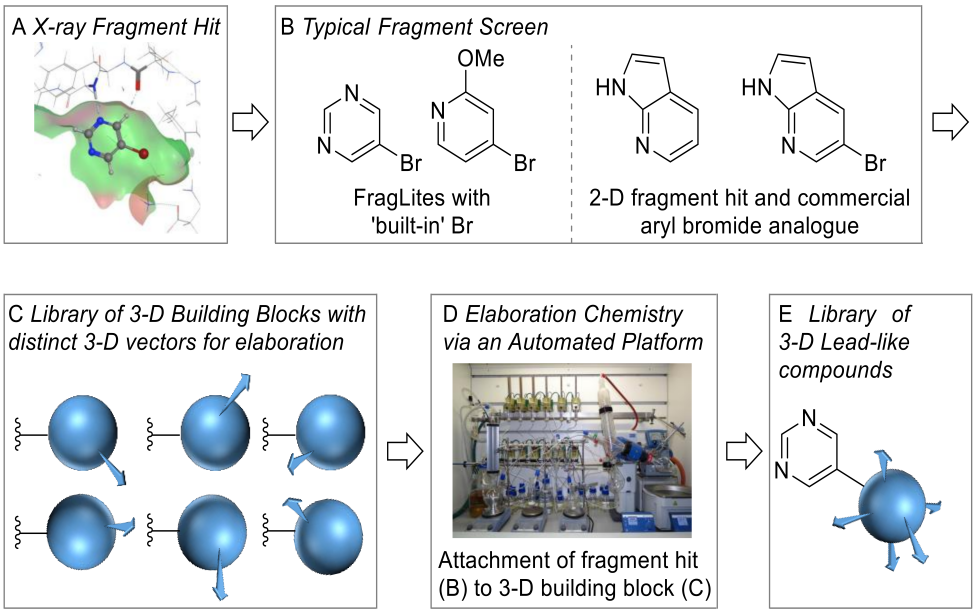

Figure 4.2: Modular Synthetic Platform for Fragment Elaboration in 3-Dimensions

It was anticipated that both FragLites and 2-D fragments could lead to fragment hits in screening campaigns. Fraglites are small fragments that contain pharmacophore doublets (either hydrogen bond donor/acceptor or hydrogen bond acceptor/acceptor) and a halogen (bromine or iodine). They have proved useful in assessing the drug-gability of protein targets, by taking advantage of the anomalous scattering of the halogen substituent, to effectively map interaction sites of the protein and elucidate ligand binding sites. Using this approach, efficient starting points for drug design have been identified which could effectively feed into our designed workflow. In addition, the potential of 2-D fragment collections could be explored as aryl bromide analogues of 2-D fragments are generally commercially available (or readily synthesised) and are thus suitable for the modular synthetic platform proposed. An illustrative example of how a 2-D fragment hit could be synthetically elaborated into a 3-D lead compound using the designed workflow in Figure 4.2 is outlined in Scheme 4.2. Attachment of a FragLite 2-D fragment hit, 3-bromopyrimidine, to bicyclic 3-D building block **208**

would enable elaboration in two directions along synthetic vectors (blue circle and *N*-Boc group). Notably, the structural rigidity of the bicycle in 3-D building block **208** ensures that the synthetic vectors are well-defined, enabling a controlled approach to hit-to-lead optimisation. Elaboration along the cyclopropyl-B(MIDA) vector (blue circle) would be possible using Suzuki-Miyaura cross-coupling between the aryl bromide and the cyclopropyl-B(MIDA) group (blue circle) of 3-D building block **208** to furnish α-aryl pyrrolidine **412**. Subsequent *N*-functionalisation would provide a second point for diversification to give elaborated lead compounds **413**. Clearly, a library of 3-D building blocks (including bicyclic building block **208**) with different synthetic vectors would enable the generation of a library of 3-D lead compounds and provide a novel approach to explore medicinally-relevant lead-like chemical space. The cyclopropyl-B(MIDA) functionality is crucial to the design of 3-D building blocks since it provides a rigid 3-D framework (and associated vector) and is suitably activated to facilitate Suzuki-Miyaura cross-coupling reactions.

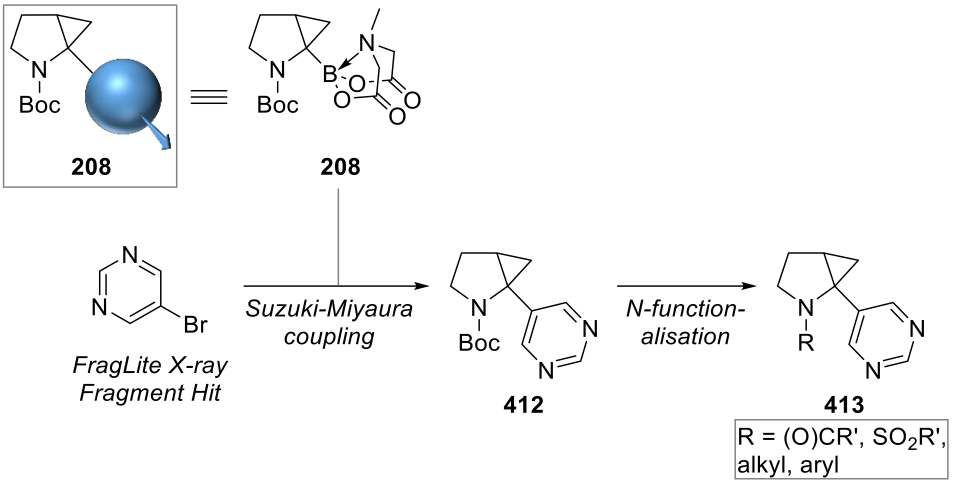

Scheme 4.2

As described in section 2.4.3, the synthesis and functionalisation of 3-D building block **208** has already been developed for the purposes of 3-D fragment generation in the synthesis of cyclopropyl pyrrolidine bicycles (see section 2.4.3). Importantly, the synthesis of cyclopropyl-B(MIDA) building block **208** was shown to be both viable (37%

yield over 3 steps) and scalable (5 g prepared). Furthemore, elaboration of both the cyclopropyl-B(MIDA) functionality (by Suzuki-Miyarua coupling) and the *N*-Boc group (by *N*-Boc removal followed by sulfonylation and reductive amination) has been shown (13 examples) demonstrating its suitability as a potential 3-D building block in medicinal chemistry (Scheme 4.3).

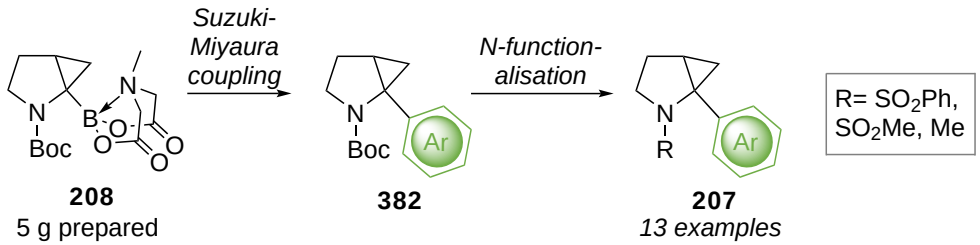

Scheme 4.3

Although not developed for the specific purpose of fragment elaboration in 3-dimensions, as we are proposing, Harris and co-workers at Pfizer have reported the synthesis and Suzuki-Miyaura cross-coupling of a set of fused cyclopropyl pyrrolidine and piperidine trilfluoroborate salts.[157] The 1-aryl-3-azabicyclo[3.1.0]hexane scaffold of cyclopropyl pinacol boronate **416** was constructed from vinyl pinacol boronate **414** using Simmons-Smith cyclopropanation (Scheme 4.4). The synthesis was complicated by the use of TFA which resulted in *N*-Boc removal, requiring an additional re-protection step. Furthermore, separation of starting material **414** from cyclopropyl pinacol boronate **415** by chromatography was not possible. Ultimately, a mixture of **414** and **415** was reacted with NBS and water, allowing for separation and isolation of cyclopropyl pinacol boronate **415** (since the alkene in **414** was converted into a bromohydrin which was readily separable by chromatography). Then, treatment of **415** with KHF_2 gave the trifluoroborate salt **416**. Overall, despite challenges, the synthetic route to building block **416** proved scalable with trifluoroborate salt **416** successfully synthesised on the gram-scale in a reasonable yield of 39% over 2 steps.

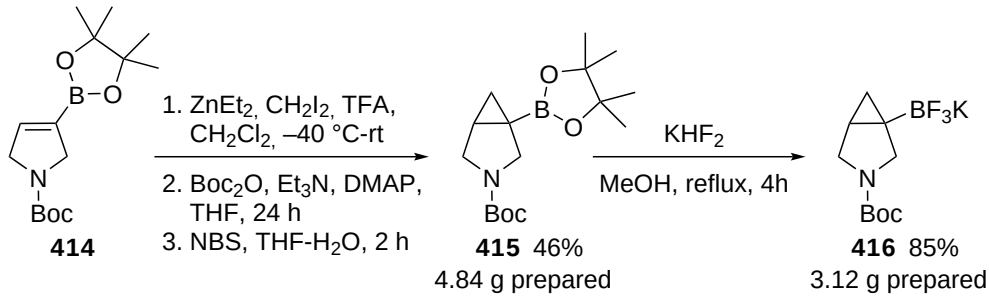

Scheme 4.4

With building block **416** in hand, a range of different Suzuki-Miyaura cross-coupling reactions were carried out by Harris *et al.* to generate a collection of arylated compounds based on the 1-aryl-3-azabicyclo[3.1.0]hexane scaffold (Scheme 4.5). Following optimisation of reaction conditions, various aryl bromides (and two aryl chlorides) were successfully coupled with the BF_3K group of building block **416** including a range of heterocyclic halides (pyridine, pyridones, *N*-oxides, pyrazoles and pyrazines), all in good yield. Interestingly, in their optimisation studies, coupling of the B(pin) equivalent **415** with 2-bromo-4-(trifluoromethyl)pyridine resulted in only a 24% yield of the cross-coupled product. Harris *et al.* attributed this to competing protodeboronation, which they noted is less likely to occur with trifluoroborates.[158]

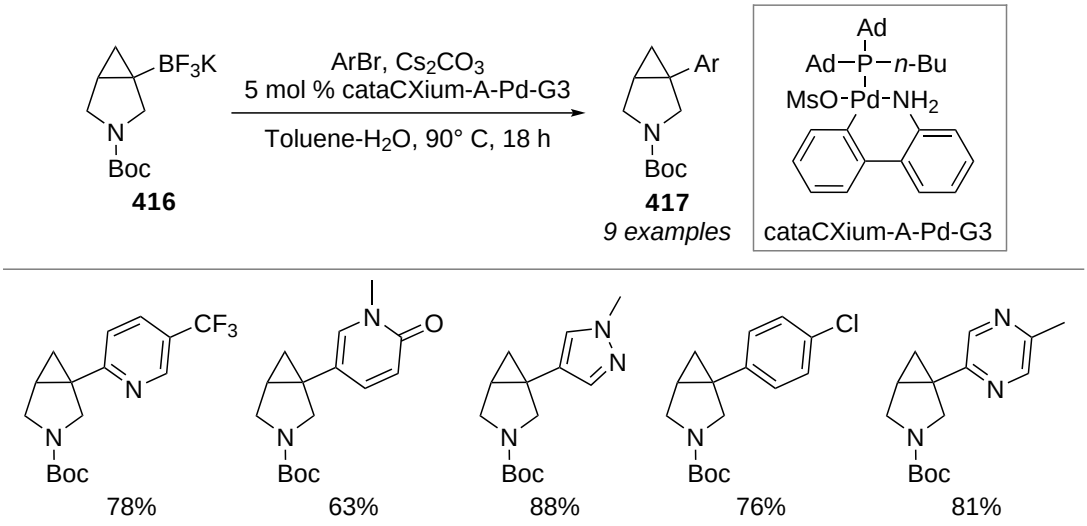

Scheme 4.5

The two-step synthetic procedure (Simmons-Smith and B(pin) to BF_3K conversion) to

generate **416** was extended to the synthesis of 6- and 1-aryl-3-azabicyclo[4.1.0]heptane scaffolds. Using established conditions for Suzuki-Miyaura cross-coupling of trifluoroborate salt **416**, elaboration of trifluoroborate salts **418** and **419** was possible with 3-substituted pyridine and 2-substituted pyrimidine bromides, giving the arylated piperidines in good yields (Scheme 4.6).

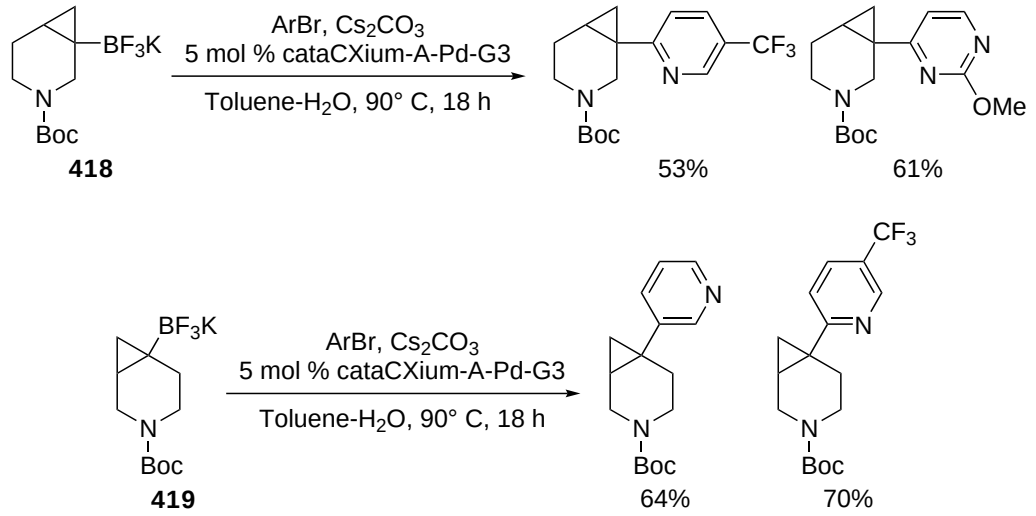

Scheme 4.6

Our previous work on the synthesis and elaboration of pyrrolidine cyclopropyl-B(MIDA) **208** and Pfizer's cyclopropyl-trifluoroborate building blocks **414**, **418** and **419** served as a basis for the design of a set of ten cyclopropyl-B(MIDA) 3-D building blocks in addition to the already developed building block **208** (Figure 4.3). At the outset, four key design criteria were applied. First, 3-D building blocks would be based on cyclopropyl azetidines, pyrrolidines and piperidines since these heterocycles are the most common four- five- and six-membered ring nitrogen heterocycles found in FDA-approved drugs.[64] In addition, the cyclopropyl group is present in eighteen FDA-approved drugs and, due to its structural rigidity and metabolic stability, is considered a privileged scaffold in medicinal chemistry.[116] Second, 3-D building blocks would be designed to possess properties which broadly fitted within the AstraZeneca 'rule of 2' guidelines[159] (MW $<$ 200, clogP $<$ 2, HBD $\leq$ 2 and HBA $\leq$ 4). Third, each 3-D building block would contain two common synthetic handles for elaboration, namely a cyclopropyl-

B(MIDA) group (for Suzuki-Miyaura cross-coupling) and a *N*-Boc protected amine (for functionalisation using amidation, sulfonamidation, S_NAr, Buchwald-Hartwig coupling and reductive amination). Fourth, each building block would provide a unique 3-D spatial relationship between the C–B bond and the group attached to the amine. With a wide range of 3-D building blocks with different exit vectors, 3-D chemical space could be effectively explored. Importantly, demonstration of Suzuki-Miyaura cross-couplings and amine functionalisation would provide proof-of-concept for the synthetic elaboration chemistry, indicating the potential of these 3-D building blocks for use in medicinal chemistry.

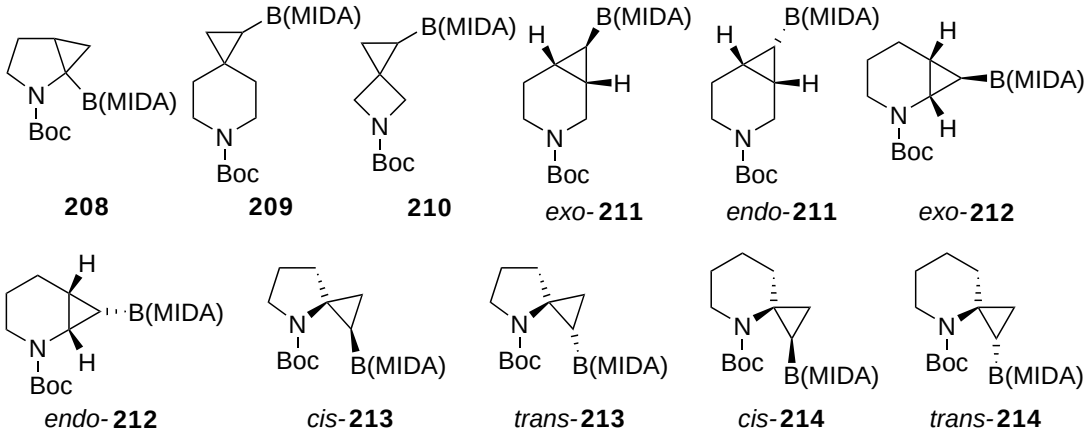

Figure 4.3: Structures of Targeted Cyclopropyl-B(MIDA) 3-D Building Blocks

The B(MIDA) group was selected as the synthetic handle for Suzuki-Miyaura cross-coupling for several reasons. To start with, B(MIDA) compounds are usually crystalline solids which are both silica- and bench-stable. Thus, they can be easily purified and stored for long periods of time. Moreover, as reported by Burke *et al.*,[124–127] B(MIDA) compounds are well-suited to act as building blocks in cross-coupling reactions as the less stable boronic acid group (required for Suzuki-Miyaura cross-coupling) can be conveniently released or unmasked *via* a slow-release mechanism under mildly basic conditions. Where necessary, other boron species such as BF_3K salts could also be utilised. It was envisaged that the cyclopropyl-B(MIDA) synthetic vector could be incorporated at all positions of a common nitrogen heterocyclic scaffold (pyrrolidine,

piperidine or azetidine). It was therefore anticipated that each 3-D building block would possess exit vectors that would enable the systematic exploration of lead-like chemical space. Using the four design criteria set out above, the design, synthesis and elaboration of a unique collection of cyclopropyl-B(MIDA) 3-D building blocks is presented in the rest of this Chapter.

4.2 Synthesis of Cyclopropyl-B(MIDA) 3-D Building Blocks

It was important that designed 3-D building blocks **208**-**214** (Figure 4.3) were synthetically tractable (ideally accessible in $\leq$ 5 steps) and that the reactions were scalable (allowing grams to be prepared) in order to be available for subsequent elaboration to libraries of lead-like compounds. A generalised synthetic plan that should be suitable for the synthesis of all of the building blocks is outlined in Scheme 4.7. First, the cyclopropyl group would be constructed using a well-established carbene-mediated cyclopropanation reaction. To this end, alkenes **420** would be converted into dibromocyclopropanes **421**. Then, debromination would give monobromides **422** as single diastereomers, hopefully with good diastereoselectivity where applicable. Importantly, reaction conditions for debromination would be tailored for each scaffold in order to control stereoselectivity (in the debromination of non-symmetrical scaffolds). The remaining halogen would then be used as a synthetic handle to form cyclopropyl-B(MIDA)s **425** over 2 steps: retentive Br-Li exchange and boronate trapping (to form either boronic acids **423** or pinacol boronates **424**) and subsequent reaction with MIDA to furnish 3-D building blocks **425**.

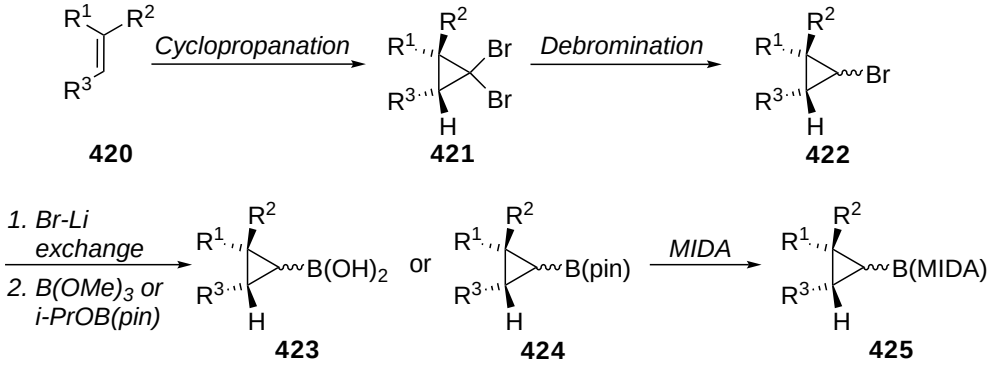

Scheme 4.7

4.2.1 Synthesis of Spirocyclic Cyclopropyl-B(MIDA) 3-D Building Blocks 209 and 210

It was anticipated that 4-spirocyclic cyclopropyl-B(MIDA) 3-D building block **209** could be accessed in 4 steps as outlined in Scheme 4.8. Dibromocyclopropanation of alkene **426** would give dibromocyclopropane **427**. Then, debromination would give monobromide **428**. Finally, Br-Li exchange and boronate trapping would, depending on the electrophile and work-up used, give boronic acid **430** or pinacol boronate **431** which, on reaction with MIDA, would give 3-D building block **209**.

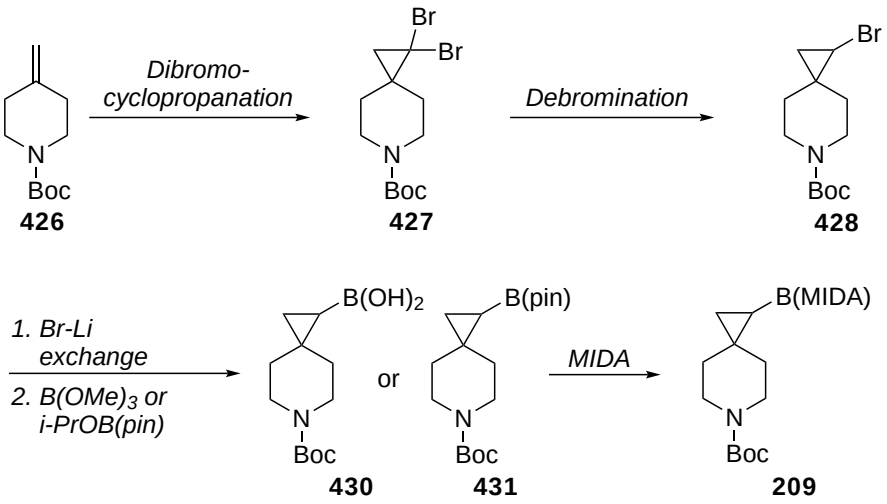

Scheme 4.8

Reaction of an alkene with $CHBr_3$ under basic conditions is a well-known approach for the construction of the dibromocyclopropane group.[160–162] Using typical conditions for the preparation of 1,1-dibromocyclopropanes,[162] reaction of commercially available alkene **426** with NaOH and $CHBr_3$ in a CH_2Cl_2/H_2O solution in the presence of $BnEt_3N^+Cl^-$ at 45 °C gave dibromocyclopropane **427** (Scheme 4.9). The work-up was challenging due to the formation of black sediment which made it difficult to see the aqueous/organic phase boundary in the separating funnel. Despite difficulties with filtration and separation of the organic from the aqueous layer, dibromocyclopropane **427** was isolated in reasonable yield (65%) following chromatography. Furthermore, the reaction proved scalable with 4.80 g of **427** prepared in one batch.

With dibromocyclopropane **427** in hand, methodology for debromination was considered. Various conditions for debromination of a dibromocyclopropane group have been reported.[163–168] Of these, a procedure that uses EtMgBr and a Ti(O*i*–Pr)$_4$ catalyst was selected.[169] Although debromination using a Grignard reagent on its own has been reported,[170,171] Baird *et al.* found that 2-10 mol% of Ti(O*i*–Pr)$_4$ promoted the debromination step by the formation of a highly reactive titanium intermediate **429** on loss of ethane (Scheme 4.9).[169] A radical mechanism (not shown) has also been proposed.[169] Using these conditions, reaction of dibromocyclopropane **427** (8.75 mmol scale) with EtMgBr and 10 mol% Ti(O*i*–Pr)$_4$ in THF at rt over 3 h gave, following work-up and chromatography, 1.86 g of monobromide **428** in 73% yield (Scheme 4.9). On half this scale, a 76% yield of monobromide **428** was obtained.

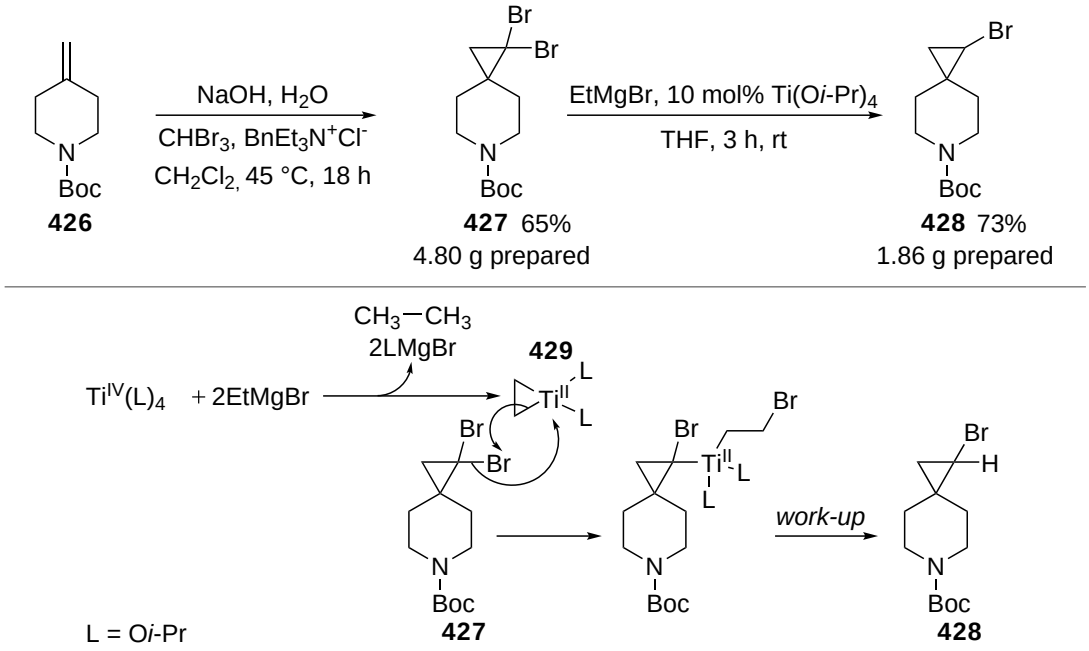

Scheme 4.9

Then, known Br-Li exchange[165] of monobromide **428** with *n*-BuLi in THF at −78 °C and boronate trapping with either B(OMe)$_3$ or *i*-PrOBpin using a procedure reported by Qui *et al.*[172] gave boronic acid **430** (following hydroloysis) or pinacol boronate **431** respectively (Scheme 4.10). For boronic acid **430**, the crude product was directly taken

on to B(MIDA) formation whereas in the case of cyclopropyl-B(pin) **431**, cyclopropyl-B(pin) **431** was isolated in 86% yield after chromatography. Conversion of boronic acids or pinacol boronates to MIDA boronates is well-established on vinyl and aryl boronic acids and boronates.[124,173] Following these conditions, boronic acid **430** was combined with MIDA in DMSO and toluene. The reaction flask was equipped with a Dean-Stark apparatus in order to remove the water formed and drive the equilibrium towards B(MIDA) building block **209**. Heating the reaction at 120 °C over 18 h furnished cyclopropyl-B(MIDA) building block **209** in 44% yield over 2 steps. Thus, **209** (1.48 g prepared) was obtained in 16% overall yield over 4 steps. Alternatively, reaction of pinacol boronate **431** with MIDA and $HC(OEt)_3$ in DMSO at 100 °C furnished cyclopropyl-B(MIDA) building block **209** in 40% yield. Under these conditions, the addition of $HC(OEt)_3$ acts as a trapping reagent for the pinacol generated, favouring the forward reaction. Thus, **209** was obtained in 21% overall yield over 4 steps.

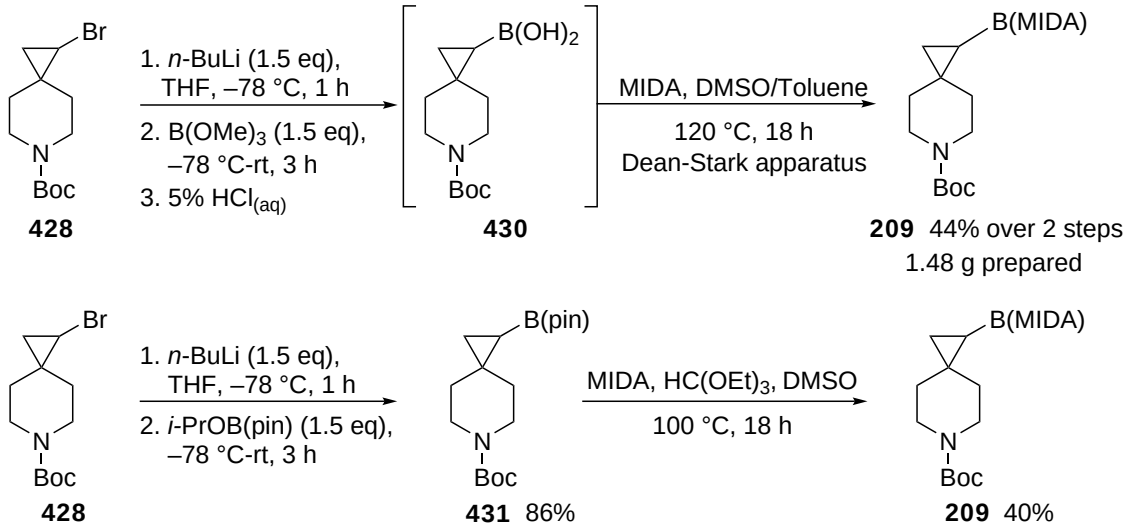

Scheme 4.10

Although both of the routes in Scheme 4.10 were successful, due to complications on work-up and purification of dibromocyclopropane **427**, an alternative synthesis of 3-D building block **209** was investigated. It was envisioned that dichlorocyclopropanation could provide another route to 3-D building block **209** (Scheme 4.11). To this end, using a similar procedure for dibromocyclopropanation,[162] dichlorocyclopropanation of

alkene **426** was carried out with NaOH and $CHCl_3$ in the presence of $BnEt_3N^+Cl^-$ at 45 °C over 18 h. Pleasingly, work-up proved to be facile and dichlorocyclopropane **432** was accessed in 89% yield. Then, using conditions reported for dechlorination of a *N*-Boc 2,3-fused dichlorocyclopropane piperidine,[162] dichlorocyclopropane **432** was treated with *s*-BuLi and TMEDA in Et_2O at −78 °C for 20 min. The plan was that Cl-Li exchange would occur on one of the chlorine atoms and the resulting organolithium would be protonated on work-up to give monochloride **433**. This worked reasonably well and monochloride **433** was isolated following quenching of the reaction (with H_2O), work-up and chromatography. In addition, a 24% yield of a mixture of alkenes (*E*)- and (*Z*)-**434** (unknown ratio) was isolated. The ^1H and ^{13}C NMR spectroscopic data were consistent with this mixture being due to alkene isomers rather than being due to *N*-Boc rotamers of one alkene: recording the ^1H NMR spectrum in d_6-DMSO at 25 °C and 100 °C gave the same spectra.

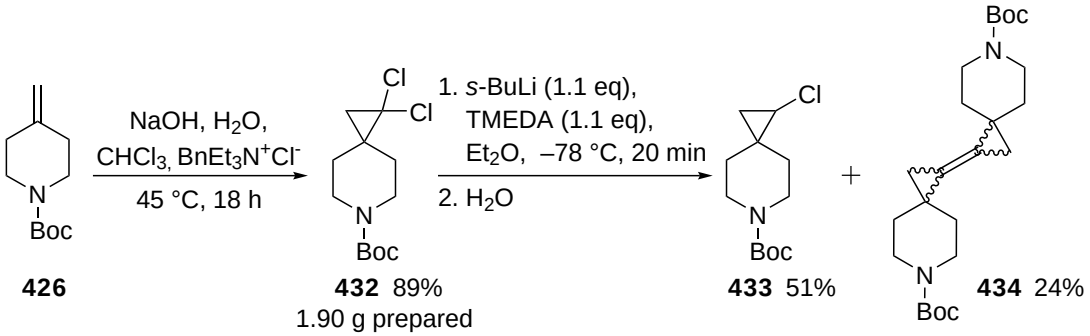

Scheme 4.11

Initially, lithiation conditions to form the boronic acid or pinacol boronate from monochloride **433** (*via* Cl-Li exchange and trapping with a boronate electrophile) were tested using diphenyl disulfide as an electrophile. To this end, reaction of monochloride **433** with *s*-BuLi and TMEDA in Et_2O at −78 °C for 20 min followed by the addition of diphenyl disulfide at −78 °C and warming to rt over 2 h failed to give cyclopropyl sulfide **435** (Scheme 4.12). However, trapping at the position α to the *N*-Boc group of monochloride **433** was observed and α-substituted piperidine **436** was isolated in 28% yield, probably as a mixture of diastereomers but it was not possible to establish

this for certain. As a result, a different route to 3-D building block **209** was therefore investigated.

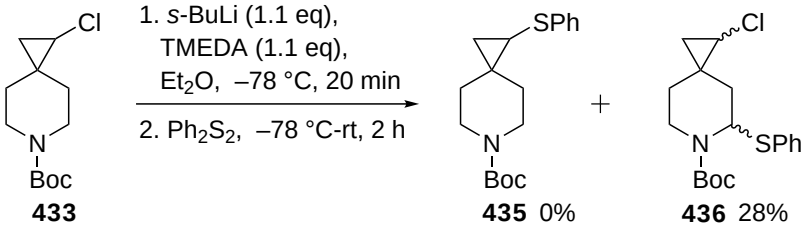

Scheme 4.12

In 2005, Renslo *et al.* reported the formation of a B(catechol) cyclopropane intermediate from dibromocyclopropane **437**, with subsequent conversion into alcohol *exo*-**438** (Scheme 4.13).[174] This was based on a method originally reported by Danheiser and Savoca.[175] Br-Li exchange of dibromocyclopropane **437** (with *n*-BuLi in THF at −95 °C for 10 min) gave lithiated species **439**. Subsequent trapping with HB(catechol) gave boronate **440**. Then, a hydride 1,2-migration with loss of the bromide anion *via* nucleophilic substitution with inversion gave pinacol boronate *exo*-**441**. Oxidation of pinacol boronate *exo*-**441** with aqueous $NaOH/H_2O_2$ gave alcohol *exo*-**438** in 15% yield. In this reaction, as well as in Danheiser's earlier work, the stereoselective formation of the *exo*-product was observed although reasons for this were not put forward by the authors.

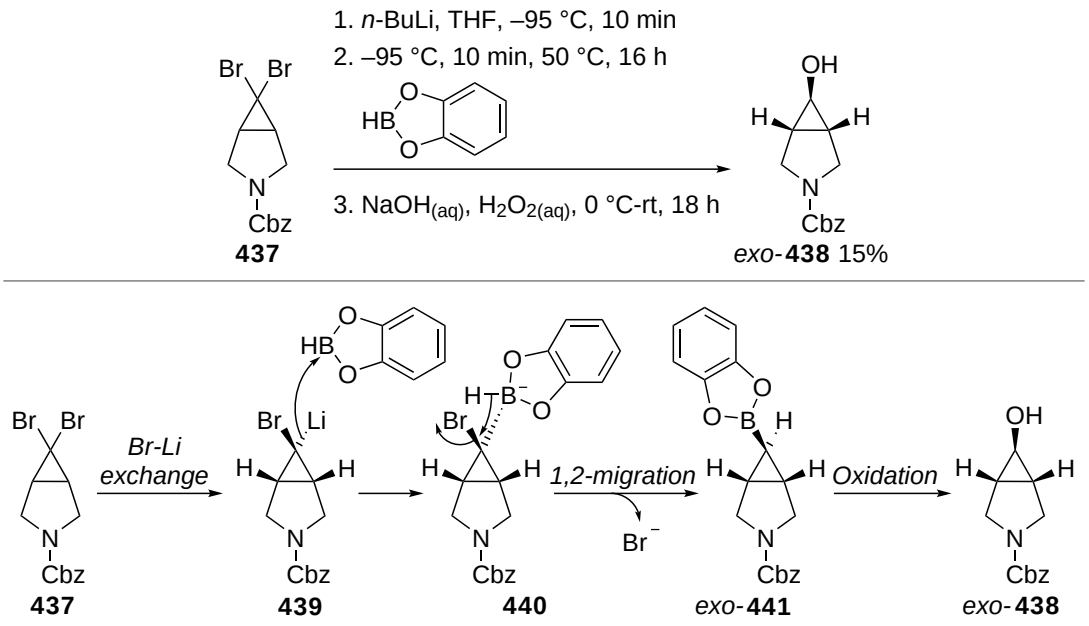

Scheme 4.13

It was thought that the Renslo and Danheiser approach could be applied to the direct conversion of dichlorocyclopropane **432** into pinacol boronate **431** in one step *via* Cl-Li exchange, trapping and 1,2-migration (Table 4.1). It was preferable to use dichlorocyclopropane **432** over dibromocyclopropane **427** due to the easier synthesis and isolation of **432**. Therefore, using previously established conditions for Cl-Li exchange, dichlorocyclopropane **432** was treated with *s*-BuLi and TMEDA in Et_2O at −78 °C for 20 min. Pleasingly, subsequent trapping with HBpin gave pinacol boronate **431** in 57% yield after chromatography (entry 1). A mixture of alkenes (*E*)- and (*Z*)-**434** were also isolated in 29% yield. It was thought that the formation of alkenes **434** by carbene dimerisation could be minimised at lower temperatures. Therefore, Cl-Li exchange and 1,2-migration on dichlorocyclopropane **432** was carried out at −100 °C. Under these conditions, the formation of pinacol boronate **431** was favoured (72% yield) with no alkenes **434** isolated (entry 2). Disappointingly, repeating the reaction on a larger scale (with 13.5 mmol of dichlorocyclopropane **432**) gave pinacol boronate **431** in a lower yield (36%) and resulted in the formation of diboronate **442** which was isolated in 5% yield after chromatography (entry 3). A 35:65 mixture (by ^{1}H NMR spectroscopy)

of alkenes **434** and HBpin (12% of **434**) was also isolated. Presumably, addition of *s*-BuLi on a large scale (at −100 °C) could create an exotherm, increasing the reaction temperature and favouring the formation of alkenes **434**.

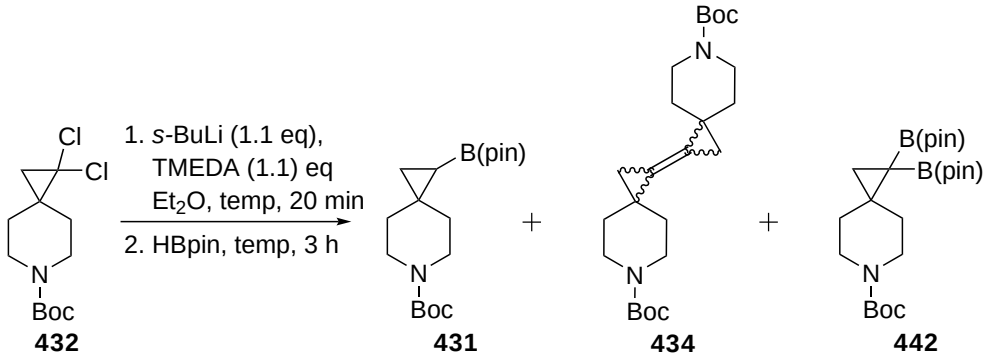

432 **431** **434** **442**

Table 4.1: Investigation of Conditions for Conversion of **432** into **431**

Entry	Conditions	Scale/ mmol	Yield %[a]
1	1. −78 °C 2. −78 °C-rt	1	57% **431**, 29% **434**, 0% **442**
2	1. −100 °C 2. −100 °C-rt	1	72% **431**, 0% **434**, 0% **442**
3	1. −100 °C 2. −100 °C-rt	13.5	36% **431**, 12% **434**[b]

[a] Yield after chromatography
[b] As a 35:65 mixture **434**:HBpin, 5% **442**

Conditions for the transformation of dichlorocyclopropanes to cyclopropyl-B(pin) derivatives were subsequently optimised by another group member, James Donald. It was found that milder lithiation conditions, using *s*-BuLi in THF at −78 °C, furnished pinacol boronate **431** in 58% yield on a large scale (Scheme 4.14). Pinacol boronate **444** was also successfully synthesised using these conditions. Interestingly, adding HB(pin) prior to treatment with *s*-BuLi prevented the formation of alkene **434** suggesting that Cl-Li exchange is faster than reaction of *s*-BuLi with HB(pin). Subsequent reaction of pinacol boronates **431** and **444** with MIDA and $HC(OEt)_3$ in DMSO at 100 °C over 24-48 h gave cyclopropyl-B(MIDA) 3-D building blocks **209** and **210** in multi-gram quantities.

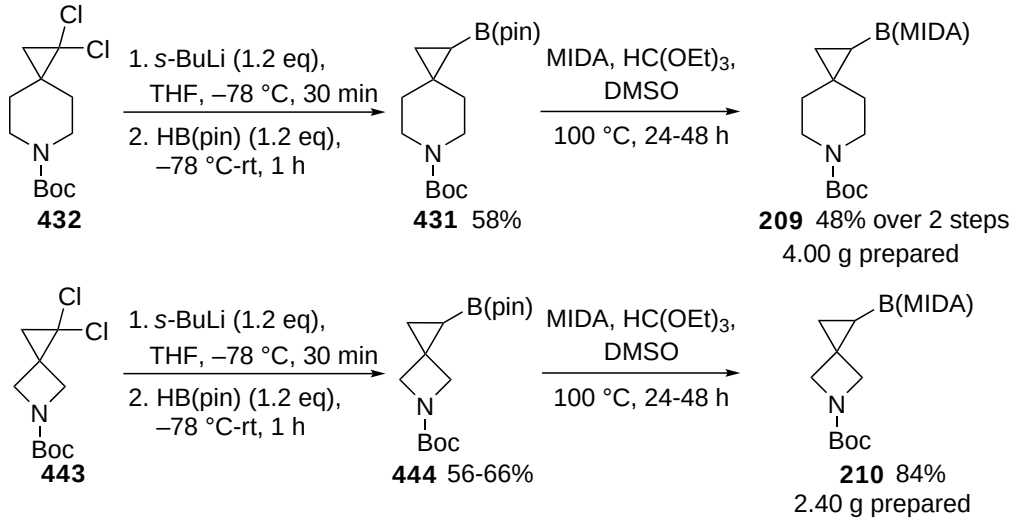

Scheme 4.14

4.2.2 Synthesis of a 3,4-Fused Cyclopropyl-B(MIDA) 3-D Building Block

Having successfully established a synthetic route to access spirocyclic 3-D building blocks **209** and **210**, we set out to apply the same synthetic strategy to the synthesis of 3,4-fused 3-D building blocks *exo*- and *endo*-**211** (Scheme 4.15). Since methodology for *exo*- and *endo*-selective debromination of dibromocyclopropanes is known,[163–171] it was anticipated that conditions could be adjusted to access both bromocyclopropanes *exo*- and *endo*-**446** diastereoselectively. Then, previously established chemistry (on the 4-spirocyclic bromocyclopropane **428**) would be used to access cyclopropyl-B(MIDA) 3-D building blocks *exo*- and *endo*-**211** over 2 steps.

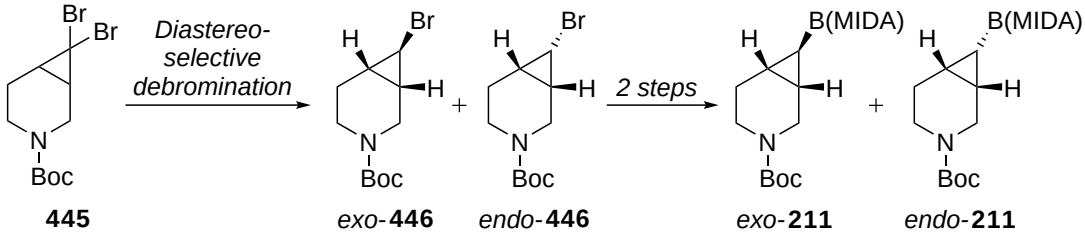

Scheme 4.15

Two selected examples using different conditions for debromination of dibromocyclopropane **447** are shown in Scheme 4.16. Baird and co-workers investigated the use of EtMgBr and 2 mol% $Ti(O\mathit{i}\text{–}Pr)_4$ in Et_2O as an approach to debrominate substituted

dibromo- and dichlorocyclopropanes.[170] Although diastereoselectivity was found to be poor (*exo*- and *endo*-**448** were isolated as a 20:80 mixture), these conditions have been useful for accessing cyclopropenes (generated from the bromocyclopropane) since the stereoselectivity of the debromination is unimportant in this case.[171] No explanation for the *endo*-selectivity in this reaction was proposed. In 1994, Harada, Oku *et al.* investigated the stereoselectivity of Br-Li exchange of *gem*-dibromocyclopropanes and dibromoalkenes using *n*-BuLi or lithium triorganozincates respectively.[168] For example, treatment of dibromocyclopropane **447** with *n*-BuLi in THF/hexane at −85 °C for 15 min favoured the formation of the *exo*-diastereomer giving a 98:2 mixture of *exo*- and *endo*-**448**.

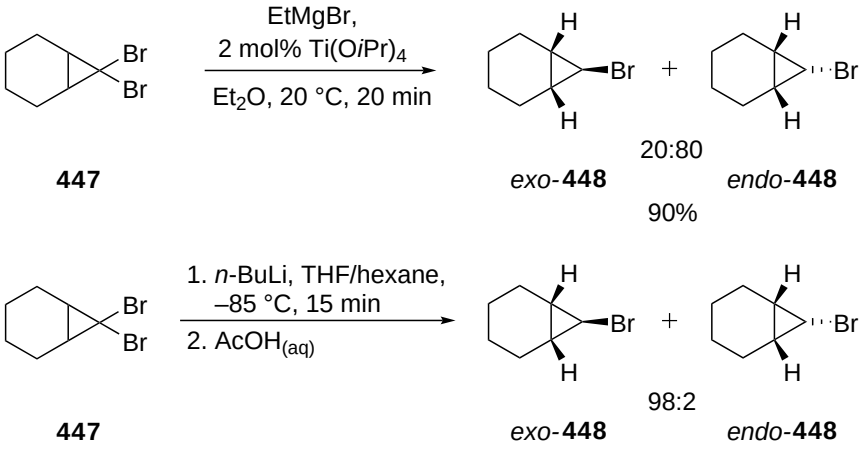

Scheme 4.16

The high diastereoselectivity observed in the BuLi-mediated debromination of dibromocyclopropane is not fully understood. Seyferth *et al.* reported a comparable result for debromination of dibromocyclopropane **447** under similar conditions.[163] They demonstrated that lithiated intermediate *exo*-**450** can react with dibromocyclopropane **449** *via* a Br-Li exchange process to form organolithium species *endo*-**450** (Scheme 4.17). Under thermodynamic conditions (using a slight excess of dibromocyclopropane **449**), the formation of lithiated species *exo*-**450** is favoured (> 99:1 dr), due to the increased stability of *exo*-**450** (with the Br group in the less hindered *exo*-position).

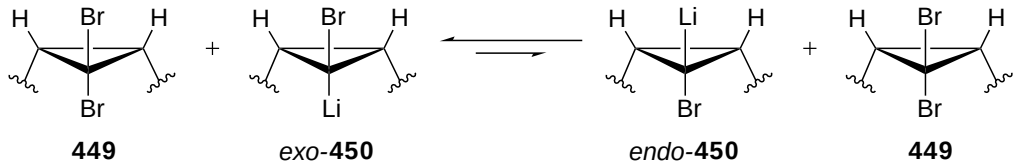

Scheme 4.17

Meijs and Doyle reported an alternative approach for debromination using dimethyl phosphite under basic conditions (KO*t*-Bu).[167] The reaction was found to proceed with high diastereoselectivity with bromocyclopropane *exo*-**448** isolated in 96% yield (Scheme 4.18). Zhao *et al.* used similar debromination conditions (dimethyl phosphite and K_2CO_3 in dioxane at 80 °C) and reported that *endo*-**448** was preferentially formed. However, our analysis of their spectroscopic data indicates that this is an erroneous result in the literature – in line with the KO*t*-Bu conditions, Zhao's reaction also generated *exo*-**448**.

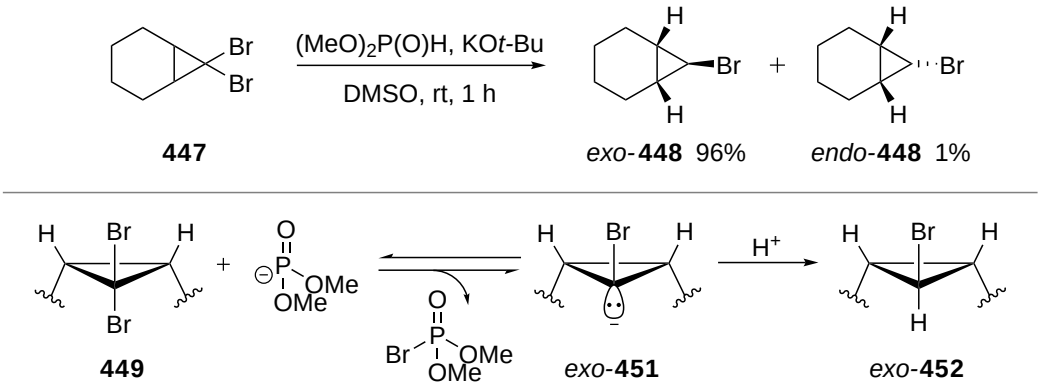

Scheme 4.18

Meijs and Doyle carried out studies to probe the mechanism of debromination by dimethyl phosphite.[167] It was found that the reaction worked even if carried out in the dark under an oxygen atmosphere or in the presence of a radical inhibitor. They therefore concluded that the reaction proceeded *via* an ionic pathway involving nucleophillic attack of the phosphite anion onto one of the bromine atoms (Scheme 4.18). Indeed, nucleophilic displacement of phosphanions on halogens is precedented.[176,177] The stereoselectivity of the reaction can be explained in terms of thermodynamics

since cyclopropyl carbanion *exo*-**451** (with the bromine atom in the less sterically hindered *exo*-position) would be thermodynamically preferred. Irreversible protonation of cyclopropyl carbanion *exo*-**451** would give *exo*-**452**.

In 1983, Shimizu *et al.* reported the use of $LiAlH_4$ and catalytic $AgClO_4$ for the debromination of a series of *gem*-dibromocyclopropanes.[164] It was found that reaction of dibromocyclopropane **447** with $LiAlH_4$ and 10 mol% $AgClO_4$ in THF at −20 °C for 15 min furnished bromocyclopropanes *endo*-**448** (77% yield) and *exo*-**448** (4% yield) (Scheme 4.19). Over-reduction to cyclopropane **453** was also observed, and was found to increase with longer reaction times. The authors noted that alternative Ag(I) salts such as AgCl were equally effective for debromination. A radical chain mechanism for debromination (following reduction of $AgClO_4$ to Ag(0) by $LiAlH_4$) was proposed although no explanation for the observed stereoselectivity was provided.

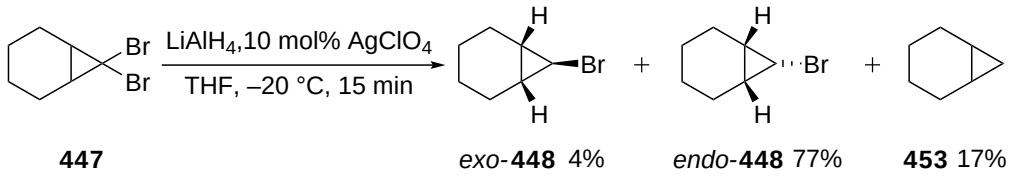

Scheme 4.19

Based on the literature background summarised above, it was anticipated that use of the different procedures for debromination would enable access to both *exo*- and *endo*-bromocyclopropanes *en route* to the targeted cyclopropyl-B(MIDA) 3-D building blocks. Initially, dibromocyclopropanation using the standard conditions (NaOH, $CHCl_3$, $BnEt_3N^+Cl^-$) gave dibromocyclopropane **445** in 75% yield (Scheme 4.20). The reaction proved to be readily scalable with 6.66 g of **445** prepared. To start, the EtMgBr/Ti(O*i*–Pr)$_4$ conditions for debromination were explored. Thus, dibromocyclopropane **445** was treated with EtMgBr and 10 mol% Ti(O*i*–Pr)$_4$ in THF at rt for 3 h. The reaction was not very high yielding but was moderately *endo*-selective with bromocyclopropane *endo*-**446** isolated in 24% yield, together with an 11% yield of bromocyclopropane *exo*-**446** (Scheme 4.20).

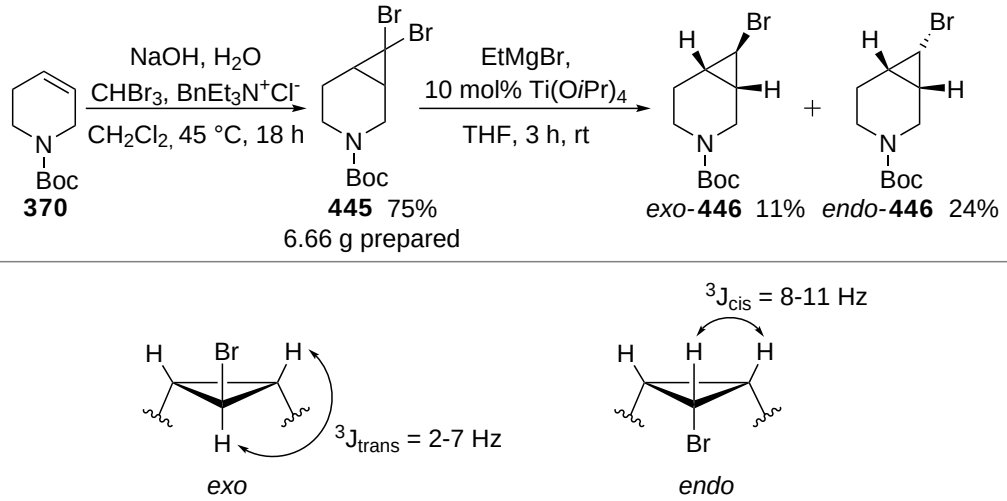

Scheme 4.20

The stereochemistry of bromocyclopropanes *exo*- and *endo*-**446** was assigned using ^{1}H NMR spectroscopy. Based on experimentally determined ^3J and ^2J values for a series of cyclopropanes, Hutton and Schaefer reported characteristic $^3J_{trans}$ and $^3J_{cis}$ coupling of 2-7 Hz and 8-11 Hz respectively (Scheme 4.20).[178] Using their analysis, the stereochemistry of *exo*-**446** was assigned based on the CHBr proton which appears as a dd at 2.58 ppm in the ^{1}H NMR spectrum with two $^3J_{trans}$ values of 3.5 Hz. In contrast, the CHBr proton of *endo*-**446** appears as a dd at 3.27 ppm with two $^3J_{cis}$ values of 7.5 Hz, consistent with $^3J_{cis}$ coupling across the cyclopropyl group.

Since the yield and diastereoselectivity were poor using the EtMgBr/Ti(Oi–Pr)$_4$ conditions, two other debromination methods were explored and the results of these, together with the initial result, are presented in Table 4.2. Treatment of dibromocyclopropane **445** with *n*-BuLi in THF at −78 °C for 25 min followed by an aqueous quench gave a 65:35 mixture of bromocyclopropanes *endo*- and *exo*-**446**. After chromatography, bromocyclopropanes *endo*-**446** and *exo*-**446** were obtained in 24% and 17% yield respectively (entry 2). This result is not consistent with the high *exo*-stereoselectivity observed by Harada, Oku *et al.* and Seyferth *et al.* on a structurally related di-

bromocyclopropane (see Scheme 4.16)[163,168] although the reaction temperatures were slightly different. In contrast, we had more success using Meijs and Doyle's dimethyl phosphite/KO*t*-Bu conditions for debromination (entry 3). Thus, reaction of dibromocyclopropane **445** with dimethyl phosphite and KO*t*-OBu at rt for 1 h gave bromocyclopropane *exo*-**446** exclusively (based on the ^{1}H NMR spectrum of the crude product). After chromatography, *exo*-**446** was isolated in 79% yield. The reaction was also scalable and gave *exo*-**446** (6.68 g prepared) in 70% yield from 33.0 mmol of dibromocyclopropane **445**. The KO*t*Bu should be added to a solution of the dibromocyclopropane and dimethyl phosphite in anhydrous DMSO. Addition of KO*t*Bu to the dibromocyclopropane in DMSO and subsequent addition of dimethyl phosphite led to decomposition with no bromocyclopropane *exo*-**446** isolated.

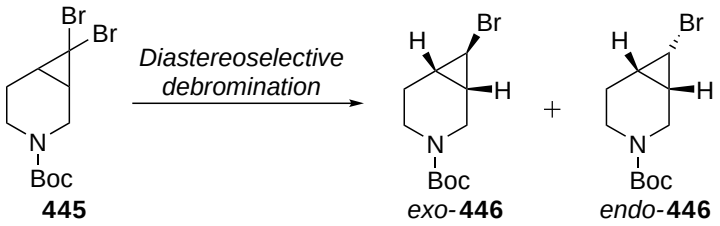

Table 4.2: Investigation of Conditions for Debromination of Dibromocyclopropane **445**

Entry	Conditions	*exo*-**446**:*endo*-**446**[a]	Yield %[b]
1	EtMgBr, 10 mol% Ti(O*i*–Pr)$_4$, THF, rt, 7 h	30:70	11% *exo*-**446**, 24% *endo*-**446**
2	(1) *n*-BuLi, THF, −78 °C, 24 min (2) H_2O	35:65	17% *exo*-**446**, 26% *endo*-**446**
3	$(MeO)_2P(O)H$, KO*t*-Bu, DMSO, rt, 1 h	100:0	79% *exo*-**446**

[a] Determined by ^{1}H NMR spectroscopy of the crude product
[b] Yield after chromatography

With a stereoselective route to bromocyclopropane *exo*-**446** in hand, we set out to try to improve on the two low yielding, poorly stereoselective routes to bromocyclopropane *endo*-**446**. To this end, attention turned to the $LiAlH_4/AgClO_4$ method reported by Shimizu *et al.* (see Scheme 4.19). The results of the attempts to access bromocyclopropane *endo*-**446** are summarised in Table 4.3. Initially, control experiments (in the absence of a Ag catalyst) were carried out (entries 1-3). Analysis of the crude re-

action mixtures (by ^{1}H NMR spectroscopy) for reaction of dibromocyclopropane **445** with $LiAlH_4$ in THF at −20 °C for 2, 4 and 18 h showed that a significant amount of starting material remained after 2 and 4 h with 70:30 and 45:55 mixtures of **445** to *endo*- and *exo*-**446** being formed. The formation of reduced cyclopropane **454** was also observed in the 4 and 18 h reactions. Interestingly, the reaction did appear to be *endo*-selective with 50-65:50-35 mixtures of *endo*- and *exo*-**446** being formed. Addition of AgCl (entries 4-6) improved conversion of **445** into *endo*-**446** (with 78-94:22-6 mixtures of *endo*- and *exo*-**446** being formed) but starting material **445** remained after 8 h at −20 °C (entry 5). Allowing the reaction to warm to rt over 18 h effected conversion (entry 6), with *endo*-**446** formed in a 94:6:0 ratio with *exo*-**446** and **445**, but (as noted by Shimizu *et al.*[164]) formation of cyclopropane **454** increased over this period. Reaction of dibromocyclopropane **445** with $LiAlH_4$ and 10 mol% $AgNO_3$ in Et_2O at −20 °C to rt over 18 h (entry 7) gave a 65:35 mixture of *endo*-**446** and *exo*-**446**. Finally, dibromocyclopropane **445** was reacted with $LiAlH_4$ and $AgClO_4$ in THF at −20 °C (entries 8-10). Unlike AgCl and $AgNO_3$, $AgClO_4$ resulted in 100% conversion of **445** with no starting material detected by ^{1}H NMR spectroscopy after 20 min (entry 8). Purification of the reaction mixture gave *endo*-**446** in 27% yield together with a 65:35 mixture of *exo*-**446** and cyclopropane **454**. Attempts to prevent over-reduction to cyclopropane **454** by shortening the reaction time failed to improve the yield of *endo*-**446** (entry 9) with bromocyclopropane *endo*-**446** isolated in 30% yield. Using less catalyst (2 mol% $AgClO_4$) over a longer time period (entry 10) gave a similar result with *endo*-**446** isolated in a 27% yield following chromatography. Ultimately, the use of Ag salts for the synthesis of bromocyclopropane *endo*-**446** was not very successful due to poor yields and problems with balancing effective conversion with over-reduction. The reaction of dibromocyclopropane **445** with $LiAlH_4$ and 10 mol% AgCl in THF at −20 °C-rt over 18 h (entry 6) provided a route to access *endo*-**446** in 31% yield but the low yield and formation of cyclopropane **454** precluded scale-up, which was not attempted.

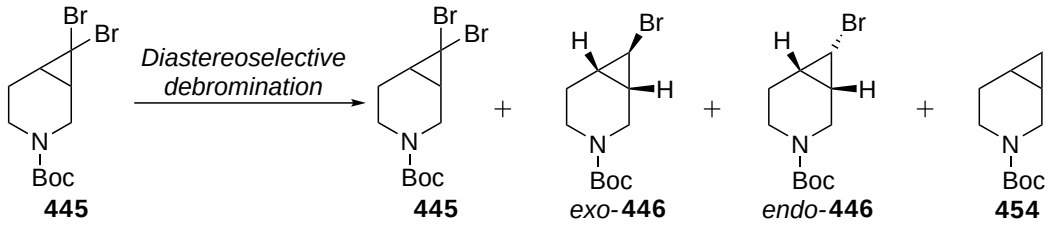

Table 4.3: Investigation of Conditions for Debromination of Dibromocyclopropane **445** using Ag Salts

Entry	Conditions	**445**:*exo*-**446**:*endo*-**446**:**454**[a]	Yield %[b]
1	$LiAlH_4$, THF, −20 °C, 2 h	70:15:**15**:0	-
2	$LiAlH_4$, THF, −20 °C, 4 h	42.5:10:**42.5**:5	-
3	$LiAlH_4$, THF, −20 °C-rt, 18 h	0:30:**60**:10	-
4	$LiAlH_4$, 10 mol% AgCl, THF, −20 °C, 2 h	50:10:**35**:5	-
5	$LiAlH_4$, 10 mol% AgCl, THF, −20 °C, 8 h	25:20:**45**:10	-
6	$LiAlH_4$, 10 mol% AgCl, THF, −20 °C–rt, 18 h	0:5:**80**:15	31% *endo*-**446**, 20:80 *exo*-**446**/**454**
7	$LiAlH_4$, 10 mol% $AgNO_3$, Et_2O, −20 °C–rt, 18 h	0:30:**60**:10	-
8	$LiAlH_4$, 10 mol% $AgClO_4$, THF, −20 °C–rt, 20 min	0:22.5:**55**:22.5	27% *endo*-**446**, 65:35 *exo*-**446**/**454**
9	$LiAlH_4$, 10 mol% $AgClO_4$, THF, −20 °C–rt, 12 min	0:35:**55**:10	30% *endo*-**446**, 5% **445**, 70:30 *exo*-**446**/**454**
10	$LiAlH_4$, 2 mol% $AgClO_4$, THF, −20 °C–rt, 3.5 h	25:15:**55**:5	27% *endo*-**446**, 5% **445**, 70:30 *exo*-**446**/**454**

[a] Determined by ^{1}H NMR spectroscopy of the crude product
[b] Yield after chromatography

To start with, 3-D cyclopropyl-B(MIDA) building block *exo*-**211** was synthesised using two general synthetic routes from bromocyclopropane *exo*-**446** (Scheme 4.21). Br-Li exchange with *n*-BuLi followed by trapping with either $B(OMe)_3$ or *i*-PrOBpin gave boronic acid *exo*-**455** or pinacol boronate *exo*-**456** respectively. Then, reaction with MIDA using the standard conditions gave 3-D cyclopropyl-B(MIDA) building block *exo*-**211**. Overall, synthesis of cyclopropyl-B(MIDA) *exo*-**211** *via* pinacol boronate

exo-**456** proceeded in a comparably higher yield to synthesis of the 3-D building block *via* boronic acid *exo*-**455**. Importantly, Br-Li exchange, trapping and reaction of the boronic acid/pinacol boronate with MIDA all proceeded with stereoretention, enabling synthesis of building block *exo*-**211** as a single diastereomer. In the ^{1}H NMR spectrum of *exo*-**211**, two $^3J_{cis}$ values of 6.0 Hz and 6.0 Hz for the CHB proton confirmed the assigned stereochemistry (Scheme 4.21). Using this approach, a gram-scale synthesis of 3-D cyclopropyl-B(MIDA) building block *exo*-**211** was accomplished (3.52 g prepared).

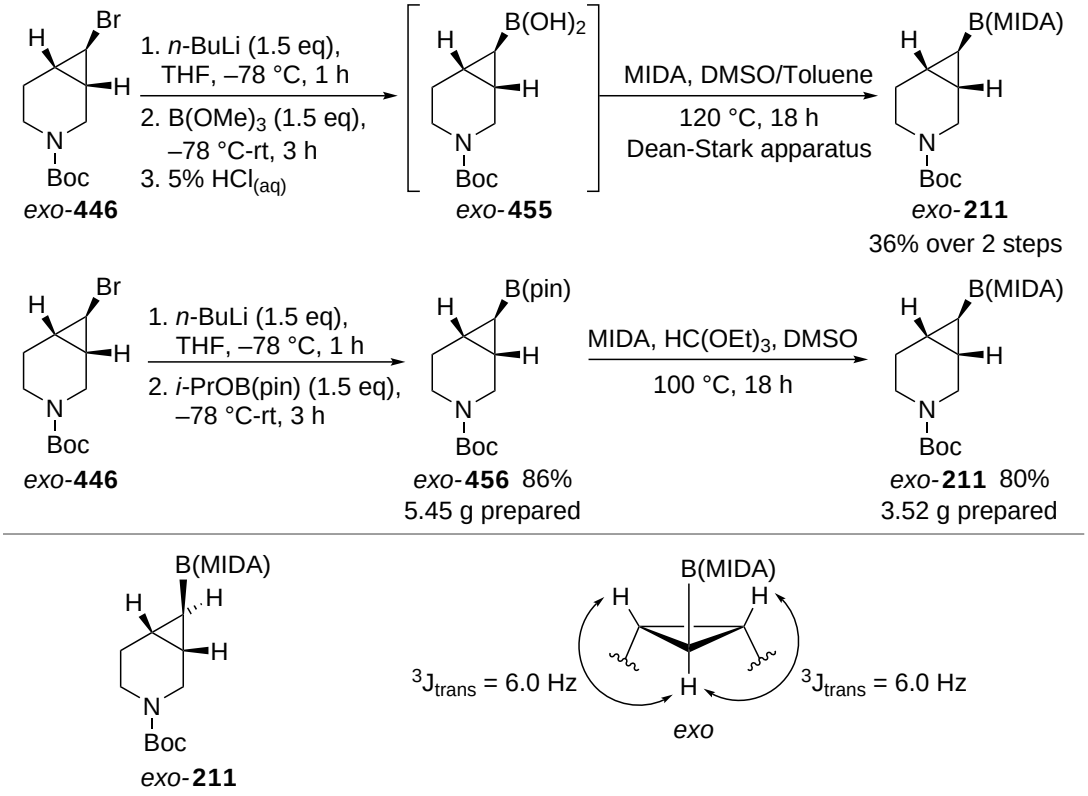

Scheme 4.21

It was anticipated that 3-D cyclopropyl-B(MIDA) building block *endo*-**211** could be generated using the same synthetic approach (Scheme 4.22). However, in this case, reaction of bromocyclopropane *endo*-**446** with with *n*-BuLi at −78 °C in THF for 1 h followed by trapping with either $B(OMe)_3$ or *i*-PrOBpin failed to give boronic acid *endo*-**455** or pinacol boronate *endo*-**456** respectively. The steric hindrance inherent in the *endo*-configuration of *endo*-**211** coupled with the relatively large size of $B(OMe)_3$

or *i*-PrOB(pin) could provide an explanation for the failure of the reaction.

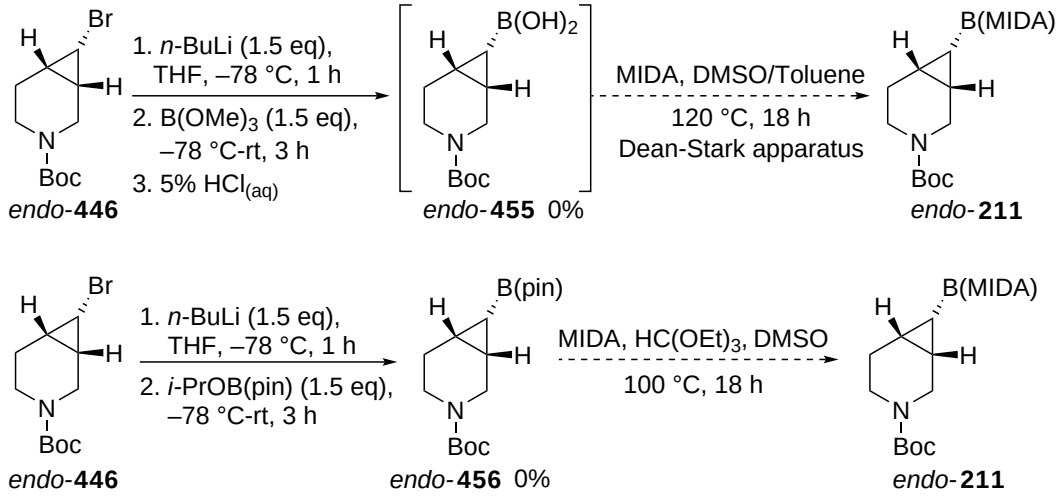

Scheme 4.22

In order to explore whether the issue was the steric hindrance of the boron species, an alternative approach (*via* borohydride *endo*-**457**) for the synthesis of *endo*-**456** was investigated. In particular, we anticipated that Br-Li exchange and trapping with a relatively small electrophile, borane·THF, could form borohydride *endo*-**457** *in situ* which, on reaction with pinacol, would give pinacol boronate *endo*-**456**. To this end, Br-Li exchange of bromocyclopropane *endo*-**446** using standard conditions (with *n*-BuLi at −78 °C in THF for 1 h) was followed by trapping with borane·THF at −78 °C for 1 h (Scheme 4.23). Using literature conditions for the hydroboration of a D-glucal derivative followed by reaction with pinacol,[179] the solution was warmed to 0 °C and stirred at 0 °C for 30 min. Then, pinacol was added (as a solution in THF) and left to react at rt for 18 h. Unfortunately, pinacol boronate *endo*-**456** was not isolated following work-up and purification by chromatography. The formation of borane *endo*-**457** could also not be confirmed.

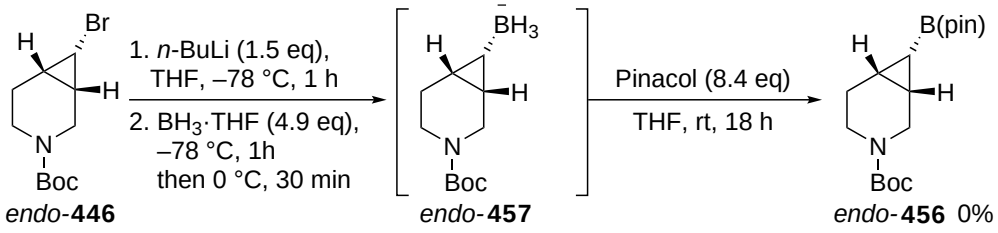

Scheme 4.23

An alternative synthetic route to B(MIDA) 3-D building block *exo*-**211** from dichlorocyclopropane **458** was also explored (Scheme 4.24). Using the Renslo and Danheiser approach,[174,175] Cl-Li exchange followed by trapping with HB(pin) and 1,2-migration could enable the synthesis of pinacol boronate *exo*-**456** directly in one step. Based on the literature precedent, it was expected that *exo*-**456** would be the major product.

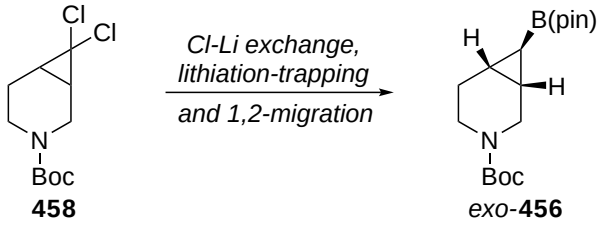

Scheme 4.24

Initially, dichlorocyclopropane **458** was synthesised using carbene-mediated cyclopropanation. To this end, dichlorocyclopropanation of alkene **370** gave dichlorocyclopropane **458** in 63% yield. Alkene **459**, presumably formed by allylic CH carbene insertion, and alkene **370** were also isolated (Scheme 4.25). In related work, allylic C-H activation and carbene insertion has been reported on cyclohexene.[180]

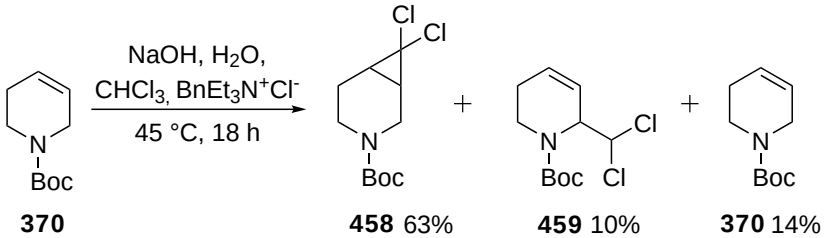

Scheme 4.25

Then, dichlorocyclopropane **458** was reacted with *s*-BuLi and TMEDA in Et_2O at −100

°C for 20 min. Addition of HBpin and subsequent quenching of the reaction gave an inseparable 75:25 mixture of pinacol boronates *exo*- and *endo*-**456** respectively in 41% yield following chromatography (Scheme 4.26). As expected, pinacol boronate *exo*-**456** was obtained as the major product. The *endo*- and *exo*- configurations of bicycles *endo*-**456** and *exo*-**460** were assigned by ^{1}H NMR spectroscopy. The CHBr proton of *endo*-**456** has $^{3}J_{cis}$ values of 9.0 Hz and 9.0 Hz whereas the CHBr proton of *exo*-**460** has $^{3}J_{trans}$ values of 3.5 Hz and 3.5 Hz consistent with $^{3}J_{cis}$ and $^{3}J_{trans}$ coupling across the cyclopropyl group respectively. Chlorocyclopropane *exo*-**460** (presumably formed by Cl-Li exchange and protonation) was also isolated in 5% yield. Two $^{3}J_{cis}$ values of 3.5 Hz and 3.5 Hz for the CHCl proton of *exo*-**460** enabled the assignment of the stereochemistry.

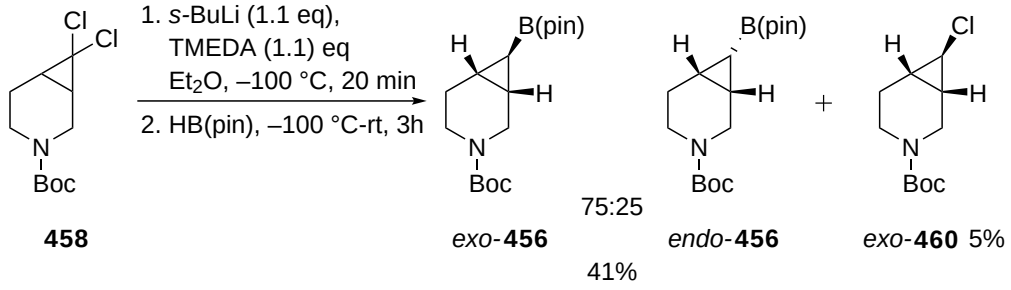

Scheme 4.26

Although conversion of pincaol boronates *exo*- and *endo*-**456** into the corresponding cyclopropyl-B(MIDA)s could provide a synthetic route towards 3-D building blocks *endo*- and *exo*-**211**, assuming *exo*- and *endo*-**211** are separable, work was halted due to the low yields observed. Ultimately, the previously established synthetic route to cyclopropyl-B(MIDA) building block *exo*-**211** from bromocyclpropane *exo*-**446** (see Scheme 4.21) proved more feasible, providing the cyclopropyl-B(MIDA) 3-D building block *exo*-**211** in 4 steps and an overall yield of 41%.

4.2.3 Synthesis of a 2,3-Fused Cyclopropyl-B(MIDA) 3-D Building Block

It was anticipated that 2,3-fused cyclopropyl-B(MIDA) 3-D building block *exo*-**212** could be synthesised in 3 steps from dibromocyclopropane **461** (Scheme 4.27). Debromination of **461**, using conditions previously established for the debromination of the 3,4-fused bromocyclopropane, would be expected to give bromocyclopropane *exo*-**462** exclusively. Then, Br-Li exchange and boronate trapping would give the boronic acid which, on reaction with MIDA, would give 3-D building block *exo*-**212** with stereoretention.

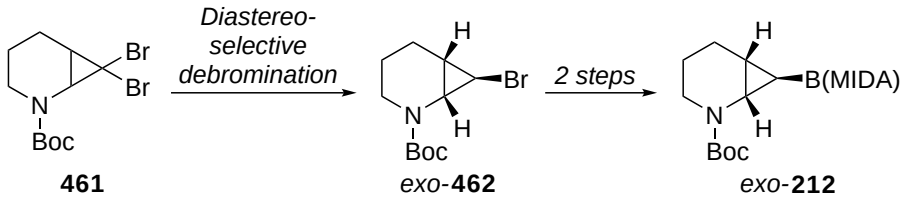

461 *exo*-**462** *exo*-**212**

Scheme 4.27

The synthesis of dibromo- and dichlorocyclopropanes for both 2,3-fused 5- and 6- membered nitrogen heterocycles has been reported.[162] Following reported conditions, reduction of *N*-Boc piperidone **463** (with DIBAL-H in THF at −78 °C for 2 h) and subsequent dehydration (with *p*-TsOH in toluene at reflux for 30 min) gave *N*-Boc enamide **465** (Scheme 4.28). *N*-Boc enamide **465** was found to be relatively unstable, initially resulting in a loss of material on chromatography. Therefore, on subsequent attempts, crude *N*-Boc enamide **465** was immediatedly subjected to dibromocyclopropanantion conditions (with $CHBr_3$, NaOH and $BnEt_3N^+Cl^-$ in CH_2Cl_2 at 45 °C for 18 h). Using this approach, dibromocyclopropane **461** was synthesised in an overall yield of 48% over 3 steps, slightly lower than that reported (62%).[162] Pleasingly, the synthetic route proved scalable with 3.59 g of dibromocyclopropane **461** prepared.

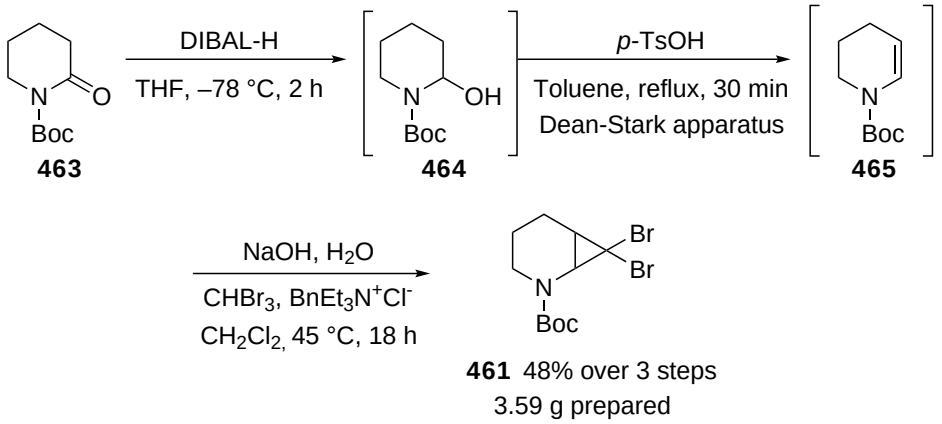

Scheme 4.28

With dibromocyclopropane **461** in hand, synthesis of 2,3-fused cyclopropyl-B(MIDA) 3-D building block *exo*-**212** was carried out over 3 steps. First, reaction with dimethyl phosphite and KO*t*-Bu in DMSO for 1 h gave bromocyclopropane *exo*-**462** as a single diastereomer in 80% yield (Scheme 4.29). The $^3J_{cis}$ and $^3J_{trans}$ values of 9.0 Hz and 2.0 Hz respectively for the cyclopropyl NCH proton of *exo*-**462** established the *exo*-stereochemistry. Then, Br-Li exchange and boronate trapping with $B(OMe)_3$ gave, following hydrolysis during work-up, boronic acid *exo*-**466**. Finally, reaction with MIDA gave 3-D building block *exo*-**212** in 23% yield over 2 steps. The three-step sequence was stereospecific, with the *exo*-stereochemistry of *exo*-**212** determined by ^{1}H NMR spectroscopy with $^3J_{cis}$ and $^3J_{trans}$ values of 8.0 Hz and 4.0 Hz respectively for the cyclopropyl NCH proton of *exo*-**212**.

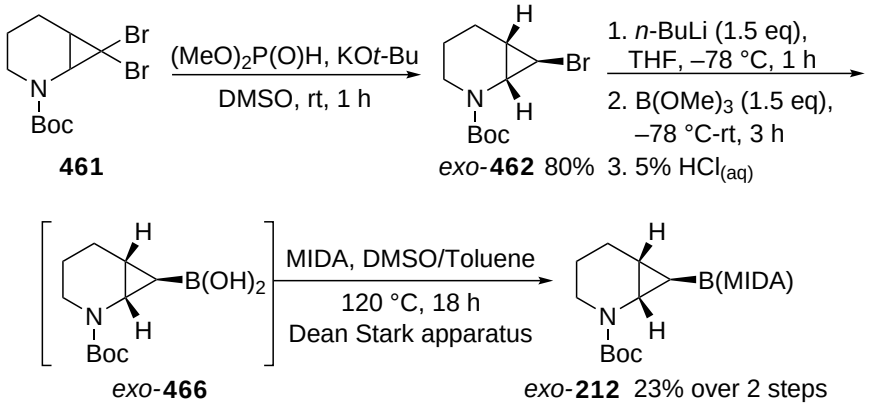

Scheme 4.29

Subsequently, a project student, Cameron Palmer, improved the synthetic route towards cyclopropyl-B(MIDA) building block *exo*-**212**. It was found that transformation of bromocyclopropane *exo*-**462** into the corresponding pinacol boronate (by Br-Li exchange and trapping with *i*-PrOB(pin)) proceeded in 70% yield. Then, B(pin) to B(MIDA) conversion (with MIDA and $H(OEt)_3$ in DMSO at 100 °C for 18 h) afforded 3-D building block *exo*-**212** in 47% yield (or 33% yield over 2 steps). Thus, using these improved conditions, 3-D building block *exo*-**212** was synthesised in 6 steps and an overall yield of 13%.

4.2.4 Synthesis of 2-Spirocyclic Cyclopropyl-B(MIDA) 3-D Building Blocks

We planned to synthesise 2-spirocyclic cyclopropyl-B(MIDA) 3-D building blocks *cis*- and *trans*-**213** from dibromocyclopropane **467** as outlined in Scheme 4.30. It was hoped that debromination of dibromocyclopropane **467** would proceed with high diastereoselectivity, due to the steric hindrance imposed by the spatial arrangement between the bulky *N*-Boc group and the two bromine atoms. Therefore, different conditions for debromination would be explored to attempt to access bromocyclopropanes *cis*-**468** and *trans*-**468**. Then, Br-Li exchange and boronate trapping followed by reaction with MIDA would give 2-spirocyclic cyclopropyl-B(MIDA) 3-D building blocks *cis*- and *trans*-**213**, hopefully as single diastereomers.

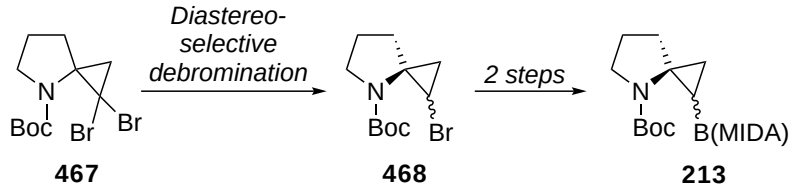

Scheme 4.30

The synthesis of dibromocyclopropane **467** from the corresponding *N*-Boc enamide has previously been reported by Laughlin *et al.*[181] Following their procedure, *N*-Boc enamide **471** was synthesised over 2 steps from alcohol **469** (Scheme 4.31). Tosylation of *N*-Boc prolinol **469** gave tosylate **470** in 85% yield. Then, elimination using DBU un-

der Finkelstein conditions gave *N*-Boc enamide **471** which, due to instability, was not purified following work-up. Immediate carbene-mediated dibromocyclopropanation of alkene **471** with $CHBr_3$ under basic conditions furnished dibromocyclopropane **467** in 59% over 2 steps (literature yield 27%[181]). Of note, dibromocyclopropane **467** was not stable at rt and storage at temperatures below 0 °C was necessary to prevent decomposition. Initial conditions used for the debromination of dibromocyclopropane **467** using dimethyl phosphite and KO*t*-Bu were unsuccessful in generating bromocyclopropanes *cis*- and *trans*-**468** and resulted in decomposition.

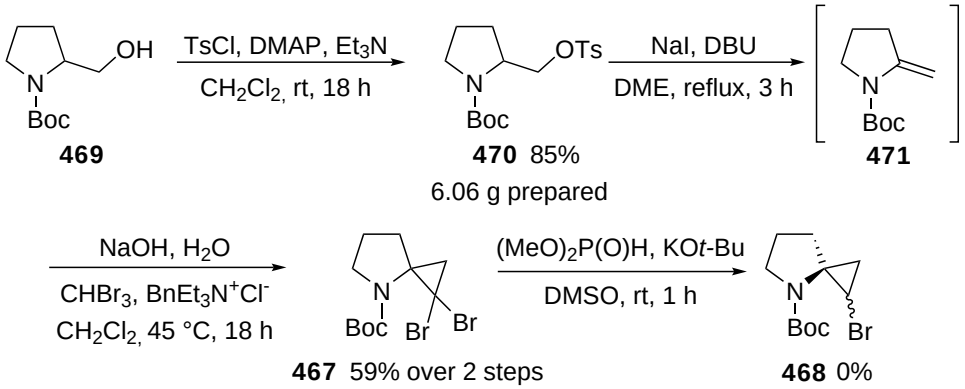

Scheme 4.31

A similar result was reported by Laughlin *et al.* for reaction of the analogous *N*-Ts bromocyclopropanes *cis*- and *trans*-**472** under basic conditions (Scheme 4.32).[181,182] In an effort to synthesise the 4-azaspiro[2,*n*]alkene **473**, a mixture of bromocyclopropanes *cis*- and *trans*-**472** was treated with KO*t*-Bu. These reaction conditions gave a complex mixture of unidentifiable products and alkene **473** was not isolated. However, debromination of a difluoro analogue **474** (with *i*-PrMgCl in CH_2Cl_2 at −78 °C for 15 min) followed by elimination (with KO*t*-Bu in THF at −78 °C) furnished 4-azaspiro[2,*n*]alkene **476** in 45% yield over 2 steps.

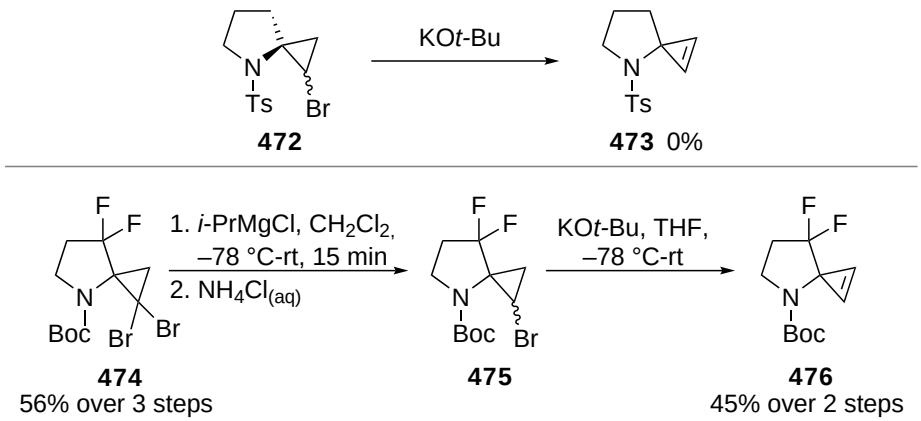

Scheme 4.32

It was hoped that the conditions reported by Laughlin *et al.* for debromination of difluoro-containing dibromocyclopropane **474** could be applied to the debromination of dibromocyclopropane **467**. Therefore, dimbromocyclopropane **467** was treated with *i*-PrMgCl in CH_2Cl_2 at −78 °C (Scheme 4.33). A reaction time of 2 h followed by quenching with saturated $NH_4Cl_{(aq)}$ was used to effect conversion to bromocyclopropane *cis*-**468** which was isolated as a single diastereomer in 55% yield following chromatography. In case bromocyclopropane *cis*-**468** was unstable at rt (as was the case with dibromocyclopropane **467**), *cis*-**468** was stored below 0 °C in the freezer. Proof of stereochemistry was provided by an X-ray crystal structure of the corresponding HCl salt, *cis*-**477**·HCl, generated on *N*-Boc removal of *cis*-**468**. The *cis*-configuration of *cis*-**477**·HCl can be explained in terms of steric hindrance. Br-Mg exchange should occur on the less sterically hindered bromide (situated *trans* to the *N*-Boc group). Then, subsequent quenching with saturated $NH_4Cl_{(aq)}$ would proceed with retention of configuration to give bromocyclopropane *cis*-**468**.

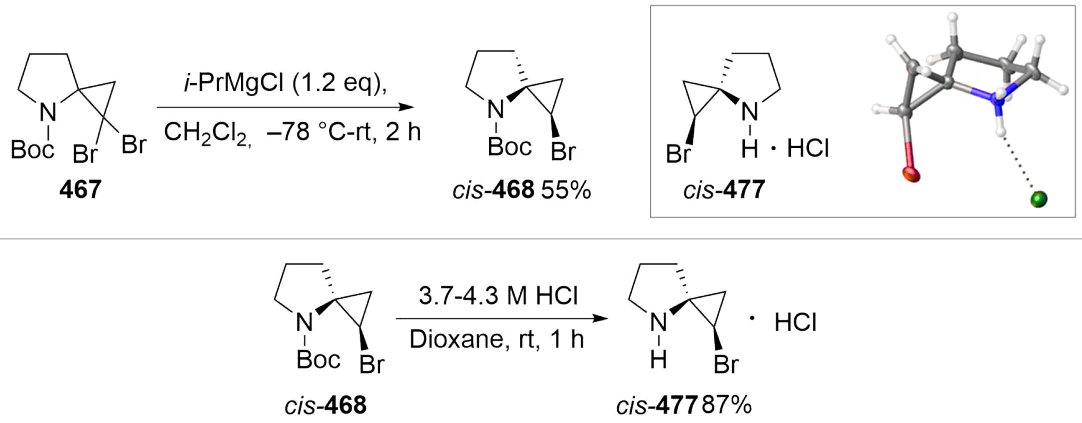

Scheme 4.33

With bromocyclopropane *cis*-**468** in hand, Br-Li exchange and boronate trapping gave the corresponding pinacol boronate *cis*-**478** in 73% yield (Scheme 4.34). Applying established conditions for B(pin) to B(MIDA) conversion (with MIDA and $HC(OEt)_3$ in DMSO at 100 °C for 18 h) gave a mixture of unidentifiable product and, unfortunately, none of 2-spirocyclic cyclopropyl-B(MIDA) building block *cis*-**542** could be isolated.

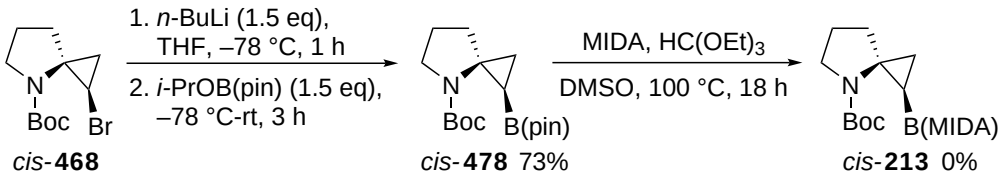

Scheme 4.34

An alternative synthesis towards *cis*- and/or *trans*-**213** from dichlorocyclopropane **479** was also considered. Cl-Li exchange followed by trapping (with a boron electrophile) and 1,2-migration could enable the synthesis of pinacol boronates *cis*- and *trans*-**478** in one step from dichlorocyclopropane **479** (Scheme 4.35). Initially, dehydration and dichlorocyclopropanation of pyrrolidine **470** gave dichlorocyclopropane **479** in 55% yield over 2 steps. Unfortunately, treatment of **479** with *s*-BuLi at −100 °C followed by trapping with HB(pin) did not give pinacol boronates *cis*- and/or *trans*-**478**.

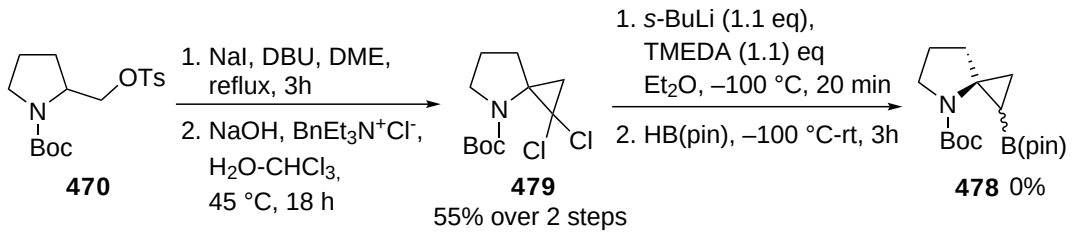

Scheme 4.35

Overall, the synthesis of 2-spirocyclic cyclopropyl-B(MIDA) 3-D building block *cis*-**213** was not possible. However, the synthesis of pinacol boronate *cis*-**478** was successful and gave *cis*-**478** in 5 steps and an overall yield of 20%. Future work could instead focus on the synthesis of the BF_3K analogue of *cis*-**542**.

4.2.5 Synthesis of a 2-Spirocyclic Cyclopropyl-B(MIDA) 3-D Building Block

A similar approach to that used in the previous section was also proposed for the synthesis of the analogous piperidine-based 2-spirocyclic cyclopropyl-B(MIDA) 3-D building blocks *cis*- and *trans*-**214** (Scheme 4.36). Debromination of dibromocyclopropane **481** could be used to access *cis*-**482** whereas alternative methods for debromination could be explored for the synthesis of bromocyclopropane *trans*-**482**. The C-Br bond could then be used as a synthetic handle to enable C-Br to B(pin) and B(pin) to B(MIDA) conversion over 2 steps in a stereospecific manner.

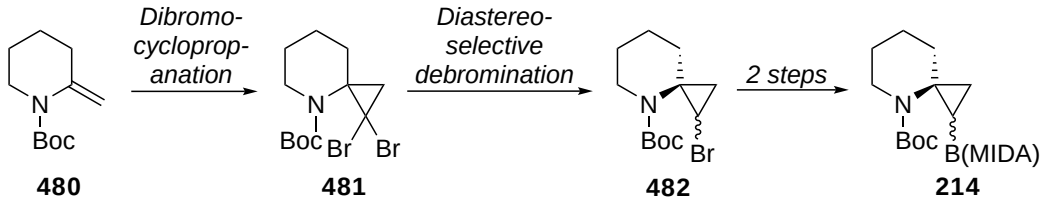

Scheme 4.36

Initially, the synthesis of *N*-Boc enamide **480** was attempted starting from alcohol **483** *via* tosylation and elimination. Tosylation of alcohol **483** is not known on the *N*-Boc protected piperidine scaffold. However, conditions for tosylation of *N*-Ts and *N*-Bn piperidines has been reported.[183,184] Using conditions which had proved successful

on the 5-membered nitrogen scaffold, alcohol **483** was reacted with *p*-TsCl, DMAP and Et_3N in CH_2Cl_2 at rt for 24 h (Scheme 4.37). Unfortunately, tosylation was unsuccessful and carbamate **485** was isolated in a 65% yield. Starting material **483** was also recovered in 20% yield. Presumably, the formation of carbamate **485** results from base-mediated cyclisation of the alcohol group onto the *N*-Boc group of **483**. There is clearly a stark difference in reaction outcomes between the 5- and 6-membered rings (see Scheme 4.31).

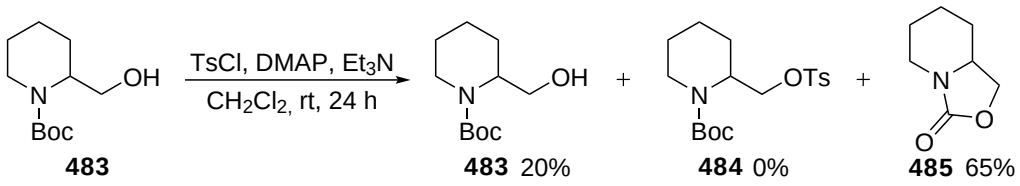

483 **483** 20% **484** 0% **485** 65%

Scheme 4.37

Without a feasible synthetic route to dibromocyclopropane **481** from alcohol **483**, the synthesis of 2-spirocyclic cyclopropyl-B(MIDA) 3-D building block *cis*- and *trans*-**214** was revised. In 1996, Beak *et al.* reported a synthetic route towards the 2-spirocyclic cyclopropyl scaffold using lithiation and cyclisation. In addition, subsequent cyclopropyl lithiation-trapping chemistry was also described.[118] Lithiation of **486** (with *s*-BuLi and TMEDA in Et_2O at −78 °C for 5 h) followed by cyclisation (at −78 °C-rt over 3 h) gave 2-spirocyclic cyclopropane **487** in 91% yield (Scheme 4.38). Interestingly, treatment of piperidine **487** with *s*-BuLi and TMEDA in Et_2O at −78 °C over 30 h resulted in regio- and diastereoselective lithiation at the β position on the cyclopropyl group to give, following trapping with dimethylcarbonate at −78 °C-rt over 3 h, piperidine *cis*-**488** as a single diastereomer in 64% yield.

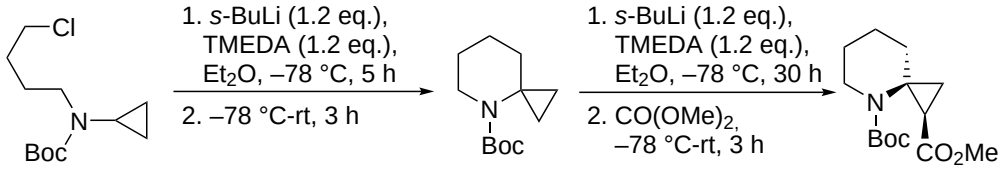

486 81% **487** 91% *cis*-**488** 64%

Scheme 4.38

We therefore planned to apply Beak's chemistry to the synthesis of 2-spirocyclic cyclopropyl-B(MIDA) 3-D building block *cis*-**214**. To this end, *N*-Boc protection of cyclopropylamine **490** with Boc_2O gave *N*-Boc cyclopropylamine **489** in 87% yield following chromatography (Scheme 4.39). Initial conditions reported by Beak *et al.* for the alkylation of cyclopropylamine **489** with NaH and 1-bromo-4-chlorobutane in THF at 0 °C over 10 h resulted in low yields with cyclopropylamine **486** isolated in < 20% yield and starting material **489** recovered. However, conditions for alkylation of 2-oxazolidinone[185] or an ethyl carbamate in the total synthesis of alkaloid(+)-(8*S*,13*R*)-cyclocelabenzine[186] using NaH in DMF with 1-bromo-4-chlorobutane (as the limiting reagent) worked much better. Using these conditions, alkylated cyclopropylamine **486** was isolated in 86% yield (Scheme 4.39).

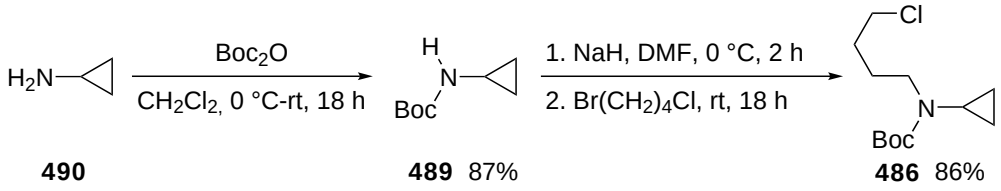

Scheme 4.39

With cyclopropylamine **486** in hand, conditions for lithiation and cyclisation based on Beak's work[118] were carried out as outlined in Scheme 4.40. Cyclopropylamine **486** was treated with *s*-BuLi and TMEDA in Et_2O at −78 °C over 2 h. Subsequent warming of the reaction to rt for 18 h furnished spirocyclic piperidine **487** in 42% yield following chromatography. Starting material **486** was also isolated in 7% yield. The yield of **487** was lower than that reported for lithiation/cyclisation of cyclopropylamine **486** (91%[118]). However, it was found that piperidine **487** was volatile, providing a possible explanation for the lower yield observed.

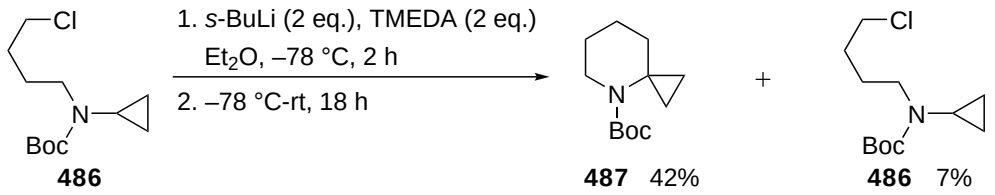

Scheme 4.40

Lithiation-trapping of piperidine **487** was then attempted. The reported conditions for lithiation of piperidine **487** with *s*-BuLi and TMEDA in Et_2O at −78 °C for 30 h[118] could not be replicated in our laboratory. We anticipated that the time for lithiation could be significantly reduced at higher temperatures. Therefore, piperidine **487** was treated with *s*-BuLi and TMEDA in Et_2O at −60 °C for 3 h. Subsequent trapping with diphenyl disulfide gave cyclopropyl sulfide *cis*-**491** as a single diastereomer in 52% yield (Scheme 4.41). In this and subsequent cases, the stereochemistry of *cis*-**491** was assumed based on the stereochemistry reported by Beak *et al.* in the synthesis of *cis*-**488**.[118] Interestingly, regioisomeric sulfide **492** was also isolated in 15% yield. Cyclopropyl piperidine **487** was also recovered in 21% yield. Lithiation-trapping of piperidine **487** using Beak's conditions with *s*-BuLi and TMEDA in Et_2O at −78 °C over a shorter time period of 7.5 h was also attempted. Suprisingly, subsequent trapping with dimethylcarbonate failed to give any of the trapped species *cis*-**488** with only starting material **487** isolated (51% yield) following chromatography.

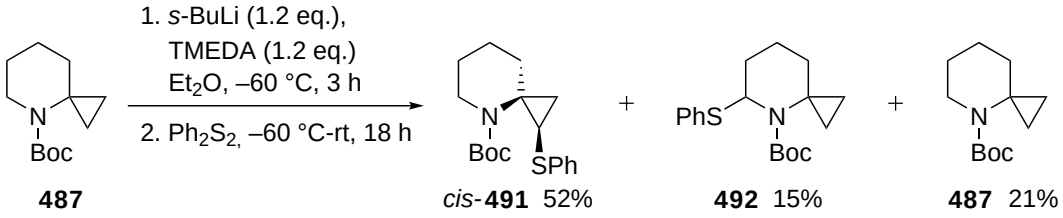

Scheme 4.41

Overall, identification of suitable conditions for the lithiation-trapping of piperidine **487** was challenging. First, the yields for lithiation-cyclisation of **486** to give piperidine **487** were low (17-42%). Second, the reaction proved unscalable with traces of **487** isolated on scales using > 4 mmol of cyclopropylamine **486**. Third, the volatility of

piperidine **487** created problems with removing moisture under vacuum, complicating the subsequent lithiation-trapping step which required anhydrous conditions. It was believed that the latter issue could be addressed by carrying out the second lithiation-trapping step of piperidine **487** *in situ*. To this end, piperidine **487** was generated using the established conditions for lithiation-cyclisation with *s*-BuLi and TMEDA in Et_2O at −78 °C. The reaction was then left to warm to rt over 18 h. Then, two sets of *in situ* lithiation-trapping conditions were trialled (conditions A and B). Using conditions A, the solution was cooled to −60 °C and piperidine **487** was treated *in situ* with *s*-BuLi for 5 h. Subsequent trapping with diphenyl disulfide at −60 °C-rt over 18 h gave cyclopropyl sulfide *cis*-**491** as a single diastereomer in 32% yield (Scheme 4.42). Regioisomeric sulfide **492** and cyclopropyl piperidine **487** were also isolated in yields of 8% and 13% respectively. In contrast, use of conditions B (with *s*-BuLi at −78 °for 8 h and trapping with diphenyl disulfide at −78 °C-rt over 18 h) gave cyclopropyl sulfide *cis*-**491** in a lower yield of 24%. Piperidine sulfide **492** and cyclopropyl piperidine **487** were also isolated in yields of 6% and 23% respectively (Scheme 4.42).

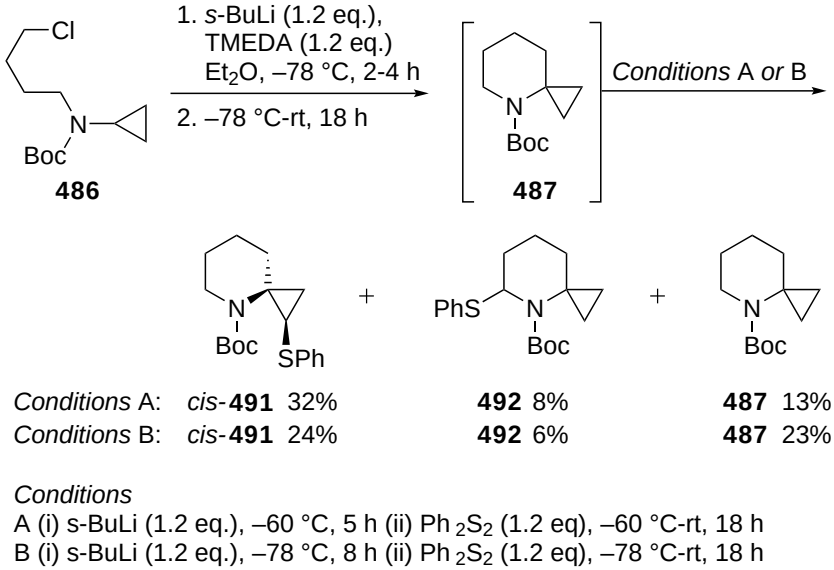

Scheme 4.42

The highest yielding synthetic route to cyclopropyl sulfide *cis*-**491** was then applied using similar conditions (based on conditions A) to the synthesis of pinacol boronate *cis*-**493** (Scheme 4.43). To this end, *in situ* generated piperidine **487** was treated with *s*-BuLi at −60 °C for 3 h. Subsequent trapping with *i*-PrOB(pin) at −60 °C-rt over 18 h gave cyclopropyl pinacol boronate *cis*-**493** in 11% yield. The *cis*-stereochemistry of *cis*-**493** has not been determined but is assumed based on results reported by Beak for the same 2-spirocyclic piperidine scaffold.[118] Piperidine pinacol boronate **494** and cyclopropyl piperidine **487** were also isolated in yields of 10% and 36% respectively.

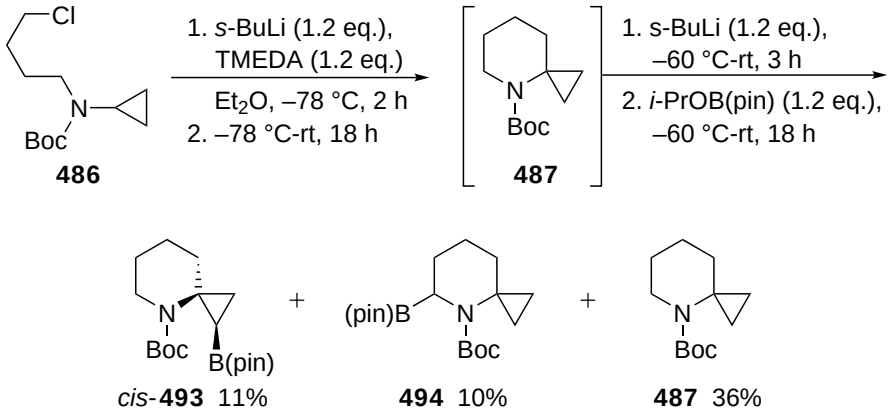

Scheme 4.43

Ultimately, the synthetic challenges posed by the synthesis of piperidine **487** and subsequent lithiation-trapping (resulting in low yields of trapped piperidines *cis*-**491** and *cis*-**493**) led us to discontinue with the proposed synthesis of 2-spirocyclic cyclopropyl-B(MIDA) 3-D building block *cis*-**214**.

4.3 Investigation of Methodology for the Functionalisation of Cyclopropyl-B(MIDA) 3-D Building Blocks

This section demonstrates the elaboration of cyclopropyl-B(MIDA) 3-D building blocks **208**, **209**, **210**, *exo*-**211** and *exo*-**212**. In particular, it was envisioned that functionalisation in two directions along synthetic vectors (cyclopropyl-B(MIDA) and *N*-Boc) would provide an illustrative example of how a 2-D fragment hit could be synthetically elaborated into a 3-D lead compound. To this end, efforts in the functionalisation of the cyclopropyl-B(MIDA) group (by Suzuki-Miyaura cross-coupling) and amine (by *N*-Boc removal and mesylation) are described. The use of FragLites in Suzuki-Miyaura coupling was of particular interest as they have been validated as 2-D fragment hits.[156] Therefore, the use of 3-D cyclopropyl-B(MIDA) buiding blocks for the elaboration of FragLites would provide 3-D lead compounds for hit-to-lead optimisation in drug development.

4.3.1 Overview of Cross-Coupling Reactions of Cyclopropyl-B(MIDA) and Potassium Trifluoroborate Derivatives

Suzuki-Miyaura cross-coupling involves the Pd-catalysed coupling of boronic acids and organohalides under basic conditions. Mild conditions, high functional group tolerance and facile set-up have led to its widespread use in both the pharmaceutical industry and academia alike. Examples of cross-coupling with secondary cyclopropyl boronates are well established[187–189] whereas the application of sp^2-sp^3 coupling with tertiary boronates is less well known,[190,191] presumably due to side-reactions (protodeborylation and β-hydride elimination) stemming from the more sterically hindered sp^3 hybridised carbon. In addition, cyclopropyl boronic acids can be inherently unstable. Thus, masking of the boronic acid with MIDA, pinacol or as a BF_3K salt is often used to prevent decomposition and/or side reactions.[192,193]

The use of the B(MIDA) group in cross-coupling was developed and popularised by

Burke *et al.* for cross-coupling of unstable boronic acids and as a reagent for applications in iterative, and automated, synthesis.[124–127] The long-term bench stability (to air and moisture) of vinyl and aryl B(MIDA) compounds and facile release of MIDA to give the boronic acid under mildy basic conditions has led to their widespread use in building block synthesis. Indeed, Suzuki-Miyaura cross-coupling of vinyl, ethynyl and aryl MIDA boronates is well-known.[124–127] There are far fewer examples which demonstrate Suzuki-Miyaura cross-coupling of the cyclopropyl-B(MIDA) group.[125,128,131] Typical reaction conditions for coupling are based on work carried out by Burke *et al.* who found that the choice of base, temperature and solvent were critical to favouring a 'slow-release' mechanism. Using this approach, a low concentration of boronic acid can be maintained which in turn can increase the rate of catalytic turnover relative to protodeborylation.

In 2009, Burke *et al.* carried out a study to compare the bench-top stability and cross-coupling efficiency of a series of boronic acids and the corresponding MIDA boronates.[125] Overall, the MIDA boronates were found to exhibit greater stability ($>$ 95% remaining after benchtop storage under air for 60 days) and give significantly higher yields following cross-coupling with a series of aryl and heteroaryl chlorides. As part of this study, some examples of the cross-coupling of cyclopropyl-B(MIDA) **495** were described. For example, cross-coupling of cyclopropyl-B(MIDA) **495** with aryl chlorides using 5 mol% $Pd(OAc)_2$, 10 mol% SPhos and K_3PO_4 in dioxane/H_2O at 60 °C for 6 h gave arylated compounds 79-97% yield (Scheme 4.44). Notably, deactivated (electron-rich and sterically hindered) aryl chlorides also cross-coupled successfully under these conditions to give **496** and **497** in good yields.

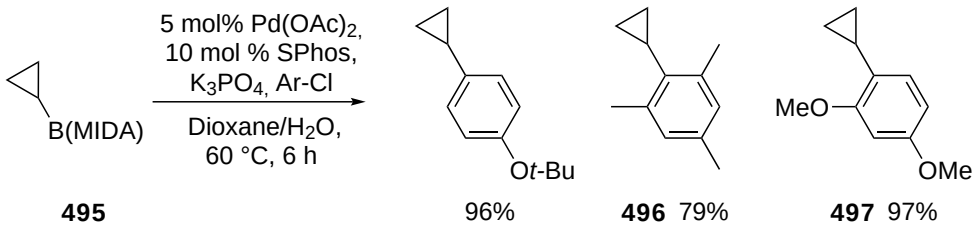

495 96% **496** 79% **497** 97%

Scheme 4.44

As part of a medicinal chemistry programme aimed at synthesising 3-hydroxyimidazolin-4-one derivatives, reported in a patent, de Man *et al.* carried out a Suzuki-Miyaura cross-coupling reaction with cyclopropyl-B(MIDA) **495** (Scheme 4.45).[131] Thus, cross-coupling of cyclopropyl-BMIDA **495** and an aryl bromide with 15 mol% $Pd(OAc)_2$, 30 mol% PCy_3 and Cs_2CO_3 in toluene/H_2O at 100 °C for 3 h gave functionalised imidazoldin-4-one **498** in 62% yield. Suzuki-Miyaura cross-coupling of the cyclopropyl-B(MIDA) group was also reported by Duncton *et al.* in the synthesis of *trans*-arylated trifluoromethylcyclopropanes (Scheme 4.45). Reaction of 2-(trifluoromethyl)cyclopropyl-B(MIDA) *trans*-**499** with a variety of aryl or heteroaryl bromides using 10 mol% $Pd(OAc)_2$, 20 mol% RuPhos and K_2CO_3 in toluene/H_2O at 100-115 °C for 18 h gave the arylated cyclopropanes in moderate yield. These examples demonstrate the stereospecificity of the Suzuki-Miyaura cross-coupling of cyclopropyl-B(MIDA) derivatives which is well established with cyclopropyl boronates and boronic acids.[194–196]

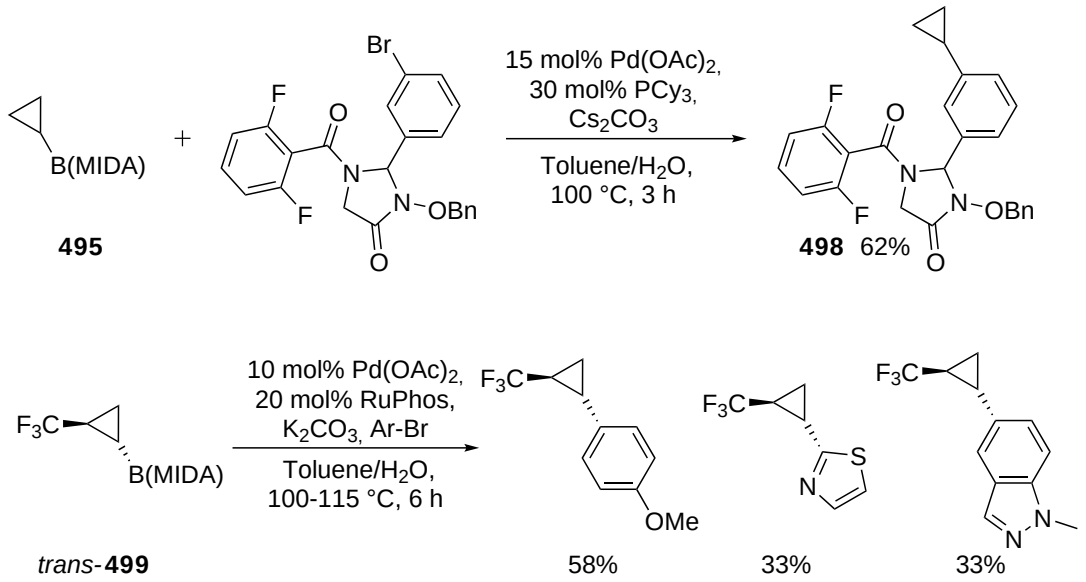

Scheme 4.45

Potassium trifluoroborate (BF_3K) salts, originally introduced by Molander,[197] have also been used in cross-coupling reactions as a means of introducing a cyclopropyl group. Trifluoroborates salts are typically white solids which are stable to air and moisture enabling facile handling and storage. The potassium trifluoroborate group can be hydrolysed or 'unmasked' *in situ* under aqueous conditions to generate the boronic acid which can then partake in Suzuki-Miyaura cross-coupling. Lennox and Lloyd-Jones have showed that the rate of potassium trifluoroborate hydrolysis is dependent on multiple variables including the R group in R-BF_3K, reaction vessel shape, material, size, and stirring rate.[198] As a result, extensive optimisation of cross-coupling conditions is often required.

In 2004, Deng *et al.* demonstrated the stereospecific Suzuki-Miyaura cross-coupling of cyclopropyl trifluoroborates with aryl bromides (Scheme 4.46).[199] During reaction optimisation, several conditions were found to give the arylated product in high yield. Overall, conditions using metal catalysts ($PdCl_2$(dppf), $Pd(OAc)_2$ with CyJohnPhos or $Pd(PPh_3)_4$) with bases (Cs_2CO_3 or $K_3PO_4{\cdot}3H_2O$) in solvent systems (THF/H_2O or toluene/H_2O) at reflux for 20 h were all successful in effecting conversion. Ultimately,

conditions were selected (based on affordability) and applied to the cross-coupling of various stereodefined cyclopropyl trifluoroborates with aryl bromides. To this end, cyclopropyl trifluoroborates *cis*- or *trans*-**500** were coupled with aryl bromides using 2 mol% $Pd(PPh_3)_4$ and 3 mol% $K_2CO_3{\cdot}H_2O$ in toluene/H_2O (3:1) at reflux for 20 h. Reactions proceeded with stereoretention to give the *cis*- or *trans*-arylated cyclopropanes in high yield.

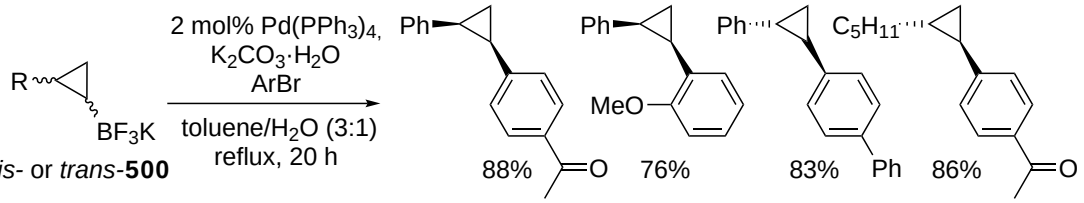

Scheme 4.46

Subsequently, Molander and Gormisky developed two sets of general conditions for cross-coupling of cyclopropyl trifluoroborate **501** with a series of aryl and heteroaryl chlorides (Scheme 4.47).[189] Following a screen using different Buchwald ligands, two bases (K_2CO_3 or $CsCO_3$) and three solvent systems, suitable cross-coupling conditions were identified. Reaction of cyclopropyl-trifluoroborate **501** with aryl chlorides using 3 mol% $Pd(OAc)_2$, 6 mol% XPhos and K_2CO_3 in CPME/H_2O (10:1) or THF/H_2O (10:1) at 100 °C for 24-48 h furnished the arylated cyclopropanes in high yield. Alternatively, cyclopropyl-trifluoroborate **501** could be cross-coupled with different heteroaryl chlorides using 2 mol% $Pd(OAc)_2$, 3 mol% *n*-BuPAd$_2$ and Cs_2CO_3 in toluene/H_2O (10:1) at 100 °C for 24 h to give the heteroaryl coupled cyclopropanes (eight examples) in good yield. Overall, the scope demonstrated successful coupling of the cyclopropyl-trifluoroborate group with electron-rich, electron-poor and sterically hindered aryl chlorides. Structural diversity was also evident with esters, ketones, aldehydes and nitriles represented.

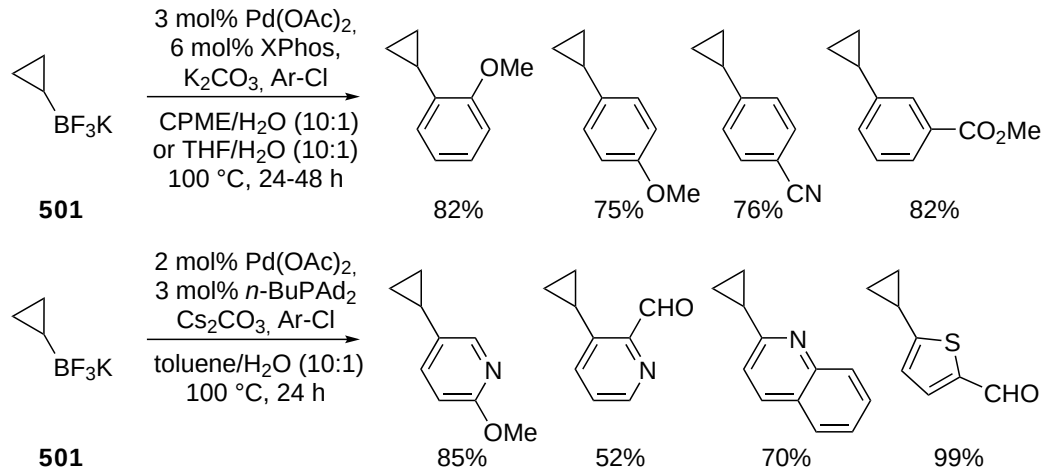

Scheme 4.47

More sterically hindered 1,1-disubstituted phenyl cyclopropyl trifluoroborates have also been sucessfully cross-coupled. For example, Harris *et al.* demonstrated that cross-coupling of cyclopropyl-trifluoroborate **502** with various aryl and heteroaryl bromides using 5 mol% cataCXium-A Pd G3, Cs_2CO_3 in 10:1 toluene/H_2O at 95 °C for 16 h afforded a series of *gem*-diarylcyclopropanes in moderate to good yield (Scheme 4.48). Previously, Harris *et al.* have also demonstrated cross-coupling of pyrrolidine **414** and piperidine trifluoroborates **418** and **419** (Figure 4.4) to give the arylated products in good yield (see Schemes 4.5 and 4.6).[157]

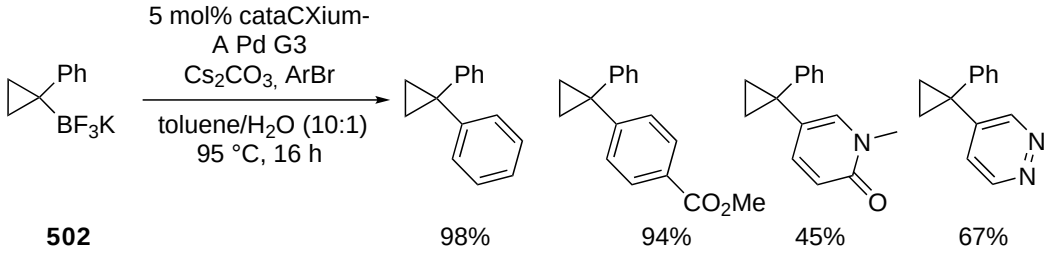

Scheme 4.48

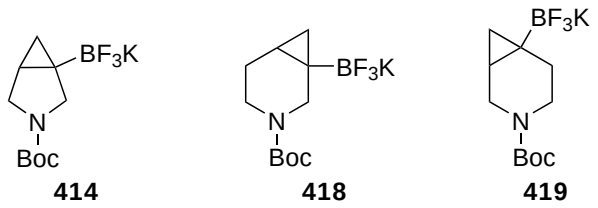

Figure 4.4: Pyrrolidine and Piperidine Trifluoroborates used in Suzuki-Miyaura Cross-Coupling

Overall, cross-coupling of cyclopropyl-B(MIDA) and potassium trifluoroborate derivatives works well using various, well-established conditions. In general, Pd catalysts such as $Pd(OAc)_2$ and $Pd(PPh_3)_4$ and ligands PCy_3, cataCXium A or Buchwald ligands (XPhos, RuPhos, SPhos) are popular for effecting conversion. In some cases, catalyst loading is high (10-15 mol%). The most commonly employed phosphine ligands are electron-rich and sterically bulky to increase the rate of oxidative addition and reductive elimination. Mildly basic conditions (using aqueous Cs_2CO_3 or K_2CO_3) allow for convenient unmasking of the B(MIDA) or potassium trifluoroborate to the corresponding boronic acid. Importantly, Suzuki-Miyaura cross-coupling of cyclopropyl-B(MIDA) and potassium trifluoroborate derivatives is stereospecific, proceeding with retention of stereochemistry.

4.3.2 Suzuki-Miyaura Cross-Coupling of Cyclopropyl-B(MIDA) 3-D Building Blocks

In order to demonstrate that 3-D building blocks **209**, **210**, *exo*-**211** and *exo*-**212** would be suitable for use in fragment elaboration, functionalisation of the B(MIDA) group of each respective 3-D building block using Suzuki-Miyaura cross-coupling was planned. In particular, it was decided that Waring's FragLites[156] would serve as the aryl bromide coupling partners since they contain aryl and heteroaryl bromides with hydrogen bond donor and acceptor groups. As such, they would represent some potentially challenging aryl bromides for Suzuki Miyaura cross-coupling which would allow for the exploration of the reaction scope. In addition, FragLites are a set of 2-D fragments that would be ideal for any planned elaboration in 3-D to a more potent compound, after the

initial FragLite hit was identified. The attachment of Fraglites to the 3-D building blocks would also provide proof-of-concept results for our proposed 3-D elaboration plans. Some examples of Fraglites are provided in Figure 4.5. As proposed by Waring *et al.*, the Fraglites fit into two distinct categories containing pharmacophore doublets, either hydrogen bond donor(red)/acceptor(blue) or hydrogen bond acceptor(blue)/acceptor(blue).

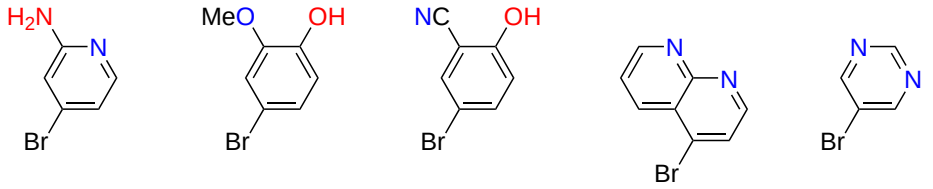

Figure 4.5: Examples of FragLites. Aryl bromides contain pharmacophore doublets with donors (red) and acceptors (blue)

Suzuki-Miyaura cross-coupling conditions, previously reported by de Man *et al.*[131] (see Scheme 4.45) and which had proved successful in the functionalisation of cyclopropyl-B(MIDA) building block **208** (see section 2.4.3), were selected. To this end, spirocyclic, 3,4- and 2,3-fused cyclopropyl-B(MIDA) 3-D building blocks **209**, *exo*-**211** and *exo*-**212** were cross-coupled with 3-bromopyrimidine as a representative FragLite in a pressure tube using 15 mol% $Pd(OAc)_2$, 30 mol% PCy_3 and Cs_2CO_3 in toluene/H_2O at 100 °C for 18 h to give cyclopropyl-pyrimidines **503**, *exo*-**505** and *exo*-**507** in 73%, 80% and 48% yield respectively, after chromatography (Scheme 4.49). Cross-coupling of cyclopropyl-BMIDA *exo*-**212** with 3-bromopyrimidine has since been repeated, using the same conditions, by a project student, Cameron Palmer, to give cyclopropyl-pyrimidine *exo*-**507** in an improved 64% yield.

The *exo*-stereochemistry of cyclopropyl-pyrimidines *exo*-**505** and *exo*-**507** was confirmed by ^3J values in the ^{1}H NMR spectra. Two $^3J_{trans}$ values of 5.0 and 5.0 Hz for the CHAr proton of *exo*-**505** confirmed the assigned *exo*-stereochemistry. Similarly, $^3J_{trans}$ and $^3J_{cis}$ values of 3.0 Hz and 8.5 Hz respectively for the cyclopropyl NCH proton (α to the nitrogen) of *exo*-**507** was consistent for the assigned *exo*-diastereomer.

For comparison, cross-coupling reactions of cyclopropyl-B(MIDA) 3-D building blocks **209** and *exo*-**211** with an electron-rich aryl bromide, 4-bromoanisole, were also carried out. These worked well and gave arylated cyclopropanes **504** and *exo*-**506**, each in 41% yield. Two $^{3}J_{trans}$ values of 5.0 and 5.0 Hz for the CHAr proton of *exo*-**506** confirmed the assigned *exo*-stereochemistry. Indeed, all other examples of cross-coupled aryl cyclopropanes on this scaffold exhibited similar features for the CHAr proton in their ^{1}H NMR spectra.

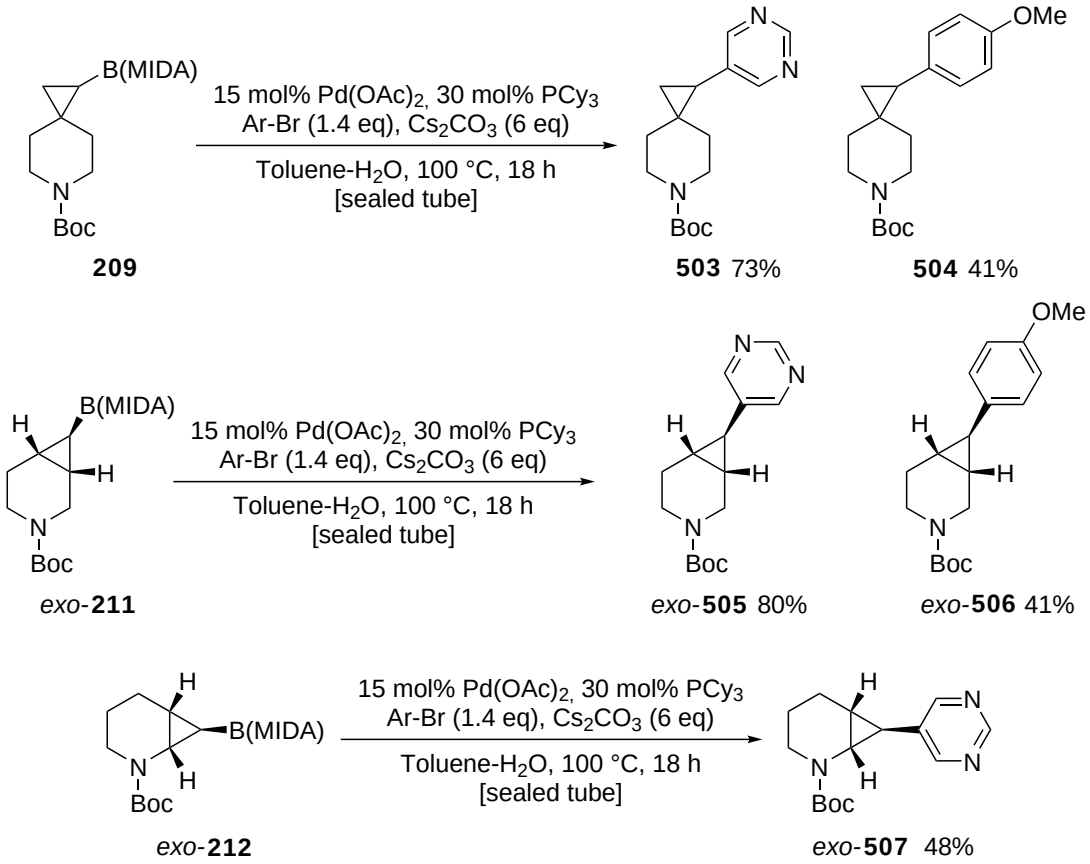

Scheme 4.49

Then, to explore the scope and limitations of the Suzuki-Miyaura cross-coupling reaction, reactions of 3,4-fused cyclopropyl-B(MIDA) 3-D building block **211** with a range of FragLites were explored. To this end, cyclopropyl-B(MIDA) *exo*-**211** was reacted with different Fraglites using the standard conditions for Suzuki-Miyaura cross-coupling. Pleasingly, aryl bromides containing both electron-rich (OMe, OH, NH_2)

and electron-deficient ($CONH_2$, SO_2Me, SO_2NH_2, CN) substitutents cross-coupled in moderate to excellent yield (Scheme 4.50). Some heteroaryl bromides were also tolerated and cyclopropyl pyrimidine *exo*-**505** (80% yield) and cyclopropyl pyridines *exo*-**512** (21% yield) and **513** (10% yield) were obtained. In general, yields were lower when coupling with aryl or heteroaryl bromides with an unprotected amine or alcohol, with arylated piperidines *exo*-**512**-**514** isolated in 10-52% yield. Cross-coupling with 4-bromo-2-methoxybenzonitrile, 4-bromopyridin-2-ol, 4-bromo-isooxazole and 4-bromopyrazole failed to give the arylated products *exo*-**518**-**521**.

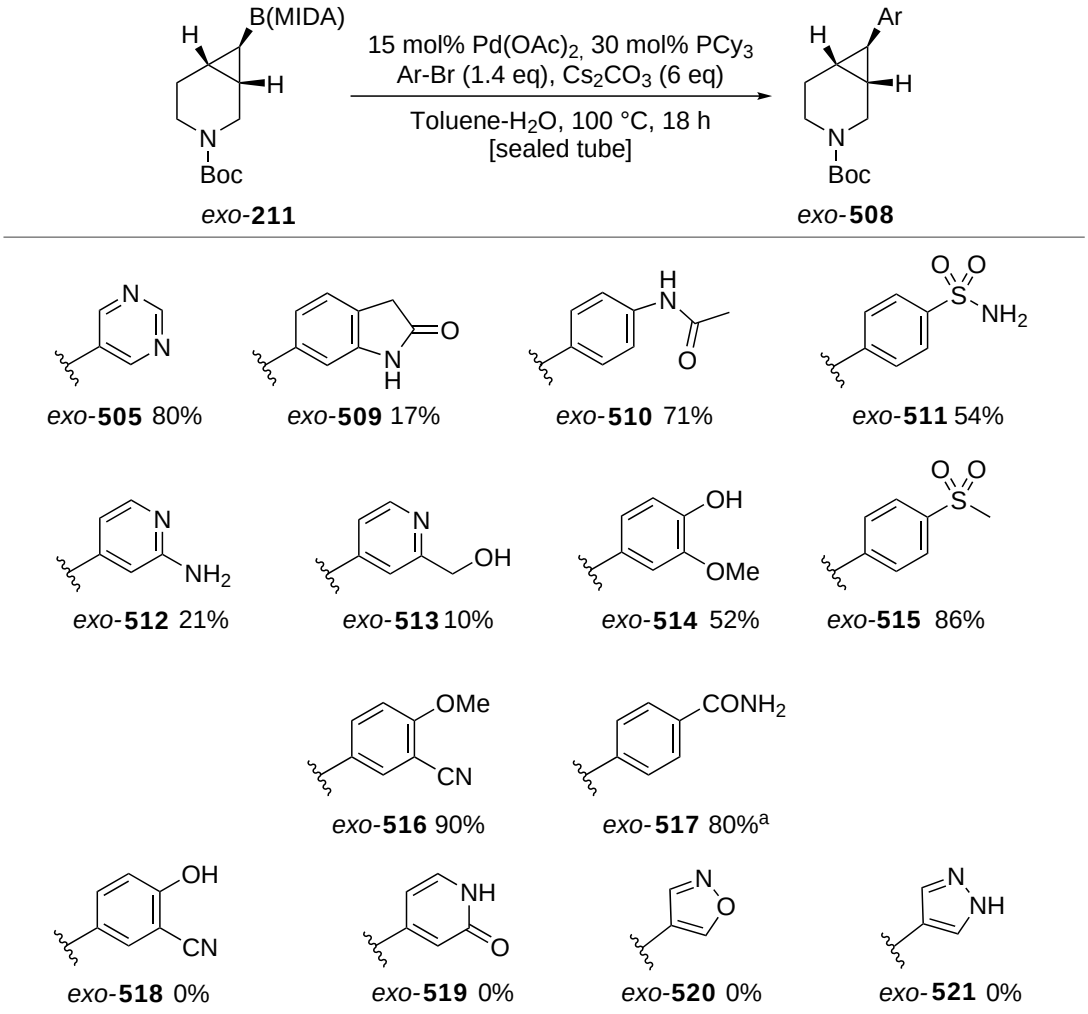

a Aryl bromide used but only the corresponding aryl iodide is a FragLite

Scheme 4.50

In some cases, low yields could be attributed to protodeborylation. For example,

Suzuki-Miyaura cross-coupling of cyclopropyl-B(MIDA) *exo*-**211** with 4-bromo-2-pyridi -nemethanol gave arylated piperidine *exo*-**513** in 10% yield with cyclopropyl piperidine **454** isolated as the major product in 36% yield (Scheme 4.51). Of note, cyclopropyl piperidine **454** is potentially volatile and have been formed in higher yield than reported.

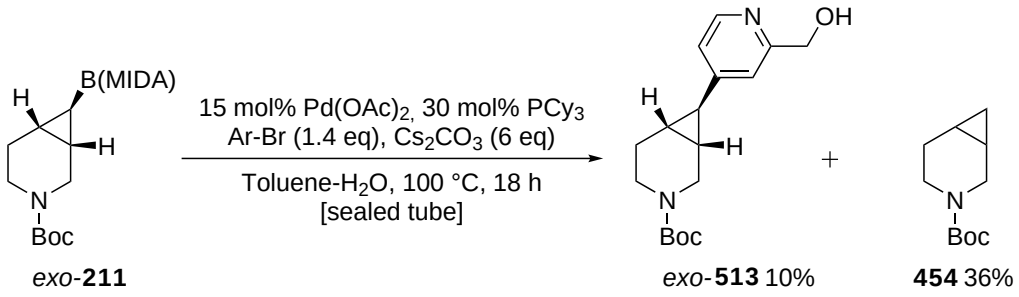

exo-**211** *exo*-**513** 10% **454** 36%

Scheme 4.51

Suzuki-Miyaura cross coupling of cyclopropyl-B(MIDA) *exo*-**211** with 4-bromo-2-methoxybenzyl alcohol was also problematic. In this case, oxidation of the activated benzylic alcohol to the corresponding aldehyde was observed and arylated piperidine *exo*-**523** was isolated in 16% yield (Scheme 4.52). Evidence for the formation of the aldehyde in *exo*-**523** was provided by a signal at 189.3 ppm in the ^{13}C NMR spectrum and a peak at 1680 cm^{-1} in the IR spectrum, both due to the C=O group. There was also a signal at 10.34 ppm in the ^{1}H NMR spectrum assigned to the aldehyde CH proton and no evidence of the benzylic CH_2OH protons.

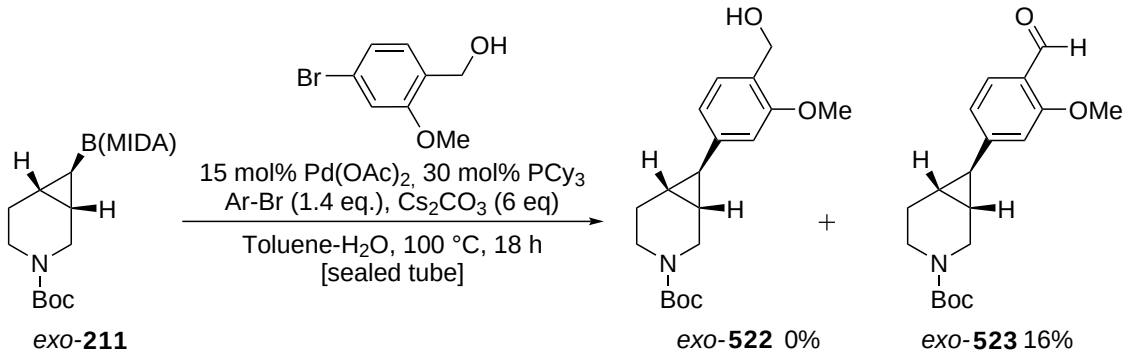

exo-**211** *exo*-**522** 0% *exo*-**523** 16%

Scheme 4.52

Overall, functionalisation of cyclopropyl-B(MIDA) 3-D building blocks **209**, *exo*-**211**

and *exo*-**212** using Suzuki-Miyaura coupling has been demonstrated. In addition, investigation of the scope of the reaction by cross-coupling of cyclopropyl-B(MIDA) *exo*-**211** with FragLites has been completed (14 examples) with ten of the 14 FragLites successfully giving the arylated products.

4.3.3 *N*-Functionalisation of Cyclopropyl-B(MIDA) 3-D Building Blocks

It was also important to demonstrate *N*-functionalisation of cyclopropyl-B(MIDA) 3-D building blocks in order to show that elaboration, along the *N*-Boc synthetic vector, is also possible. Previously, elaboration of cyclopropyl-B(MIDA) 3-D building block **208** by *N*-Boc removal and *N*-functionalisation (acylation, mesylation and reductive amination) was carried out with 13 examples (see section 2.4.3). Due to time constraints, I was not able to explore any *N*-functionalisation on the other 3-D building blocks. However, others in the group have carried out limited *N*-functionalisation studies and these results are included here for completeness. To date, mesylation of five pyrimidine-functionalised 3-D building blocks has been achieved (Scheme 4.53). Examples of *N*-functionalisation for both spirocyclic (**530** and **531**) and fused cyclopropylpyrimidines (*exo*-**532**, *exo*-**533** and **534**) has been carried out and, in four out of five cases, mesylated products were isolated in high yield (>80%). The X-ray structures of *exo*-**533** and **534** have been determined and clearly show the distinct 3-D vectors provided by the two different 3-D building blocks. Future work will focus on obtaining X-ray structures for the other generated 3-D lead compounds in order to analyse and compare the directional vectors formed between the C-Ar and N-S bond of each scaffold. This will also be expanded out to other building blocks which are currently being explored in the group.

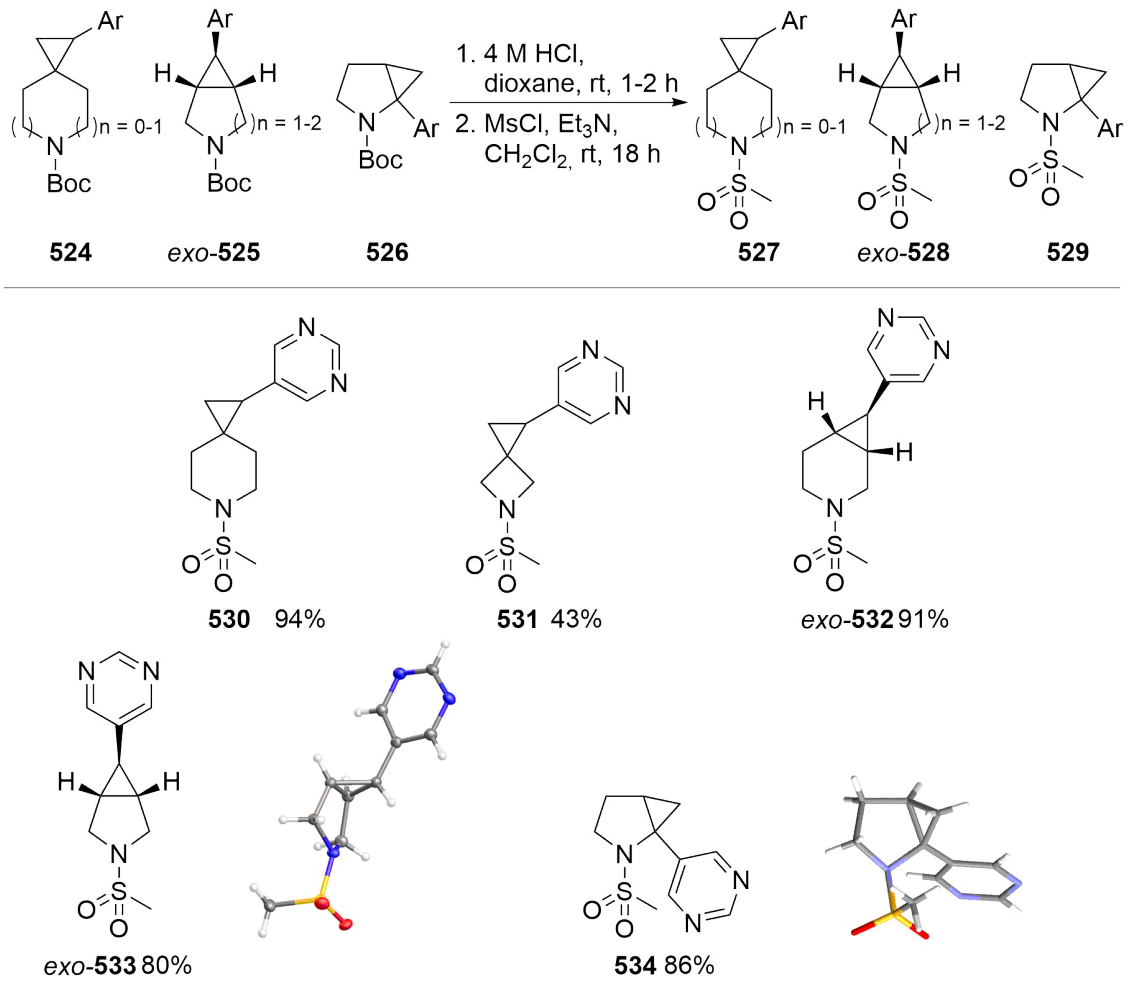

Scheme 4.53

In summary, a general synthetic route (using dibromocyclopropanation, debromination and Br-Li exchange/trapping) has been developed. This has enabled the synthesis of four novel cyclopropyl-B(MIDA) 3-D building blocks **209**, **210**, *exo*-**211** and *exo*-**212** in 4-7 steps. Notably, the use of dimethyl phosphite and KO*t*-Bu in DMSO at rt for 1 h for debromination provided access to the *exo*-diastereomers of 3,4-fused and 2,3-fused bromocyclopropanes exclusively. Subsequent Br-Li exchange, trapping and reaction with MIDA furnished 3,4-fused and 2,3-fused cyclopropyl-B(MIDA) 3-D building blocks *exo*-**211** and *exo*-**212** as single diastereomers. Access to the corresponding *endo*-diastereomer of the 3,4-fused bromocyclopropane *endo*-**446** is possible but yields for debromination were low (24-31%). Moreover, attempts to generate the pinacol

boronate or boronic acid from bromocyclopropane *endo*-**462** using Br-Li exchange and trapping were unsuccessful, presumably due to steric hindrance.

Suzuki-Miyaura cross-coupling of the cyclopropyl-B(MIDA) group of cyclopropyl pyrrolidine 3-D building block **208** (see section 2.4.3), spirocyclic 3-D building block **209**, 2,3- and 3,4-fused 3-D building blocks *exo*-**211** and *exo*-**212** has been demonstrated. In particular, successful coupling of 3,4-fused cyclopropyl-B(MIDA) 3-D building block *exo*-**211** with ten FragLites illustrates the scope of the reaction. Both aryl- and heteroaryl-bromides were tolerated with a range of functional groups (OMe, CN, OH, NHCOMe, $CONH_2$, SO_2Me, SO_2NH_2, NH_2, CH_2OH) represented.

5 Conclusions and Future Work

The work described in this thesis details the design and synthesis of 3-D fragments and 3-D building blocks for fragment elaboration. In Chapter 2, the successful design and synthesis of 41 3-D fragments based on 2,2-disubstituted pyrrolidine **203**, 2,3-disubstituted piperidines *cis*-**201** and *cis*-**202**, tropane **204**, 2,3-fused cyclopropyl pyrrolidine **206** and α-arylated 2,3-fused cyclopropyl pyrrolidine **207** scaffolds are described (Figure 5.1).

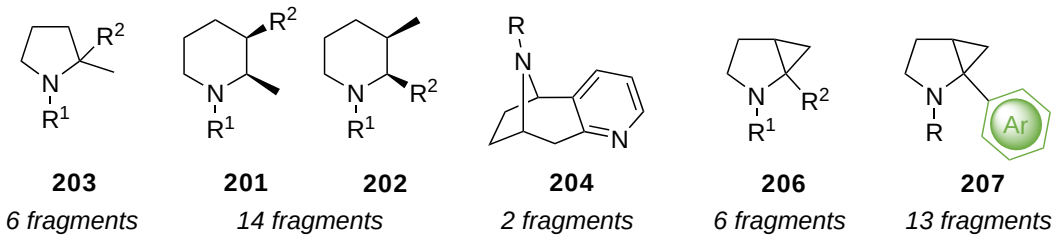

Figure 5.1: Structures of 2,2-Disubstituted Pyrrolidine, 2,3-Disubstituted Piperidine, Tropane and 2,3-Fused Cyclopropyl Pyrrolidine Scaffolds

Structural diversity and synthetic efficiency were key in the synthesis of the first iteration of 20 fragments based on the 2,2-disubstituted pyrrolidine and 2,3-disubstituted piperidine scaffolds, **203**, *cis*-**201** and *cis*-**202**. Molecular shape was also considered and, uniquely, targeted compounds for synthesis were selected based on 3-D shape and conformational diversity (by considering conformations up to 1.5 kcal mol^{-1} above the energy of the global minimum energy conformer) using PMI analysis. Following compound selection, fragment synthesis was carried out using established methodology towards previously synthesised ester and alcohol 3-D fragments. Then, *N*-functionalisation and functional group interconversion of the alcohol or ester groups furnished acid, amide, nitrile, primary alcohol and methyl ether groups in an expedient mannner. Notably, the use of four common intermediates, **216**, *cis*-**270**, *cis*-**271** and *cis*-**230**, gave targeted fragments in 1-4 steps (from the key intermediate). The design of a second iteration of 3-D fragments based on tropane **204** and 2,3-disubstituted fused pyrrolidine scaffolds **206** and **207** took into accout limitations in our initial design ideas and focused on synthetic tractability, scaffold diversity and the incorporation of

aromatic groups. To this end, tropane-based fragments **324** and **326** were successfully synthesised using a common piece of methodology in 3-4 steps from commercially available tropinone **320**. A second set of 19 3-D fragments based on 2,3-fused disubstituted pyrrolidine scaffolds **206** and **207** was generated using lithiation-trapping chemistry of key substrate **333**. In the first instance, trapping with different electrophiles and *N*-functionalisation (and/or modification of the acid and thio-ether groups) furnished six α-functionalised 3-D fragments **334**, **335**, **336**, **337**, *syn*-**338** and *anti*-**338** in 3-5 steps. A second synthetic route made use of a key cyclopropyl-B(MIDA) building block **208** which was synthesised on gram scale ($>$ 5 g prepared) in 2 steps from key substrate **333**. Suzuki-Miyaura cross-coupling to the B(MIDA) followed by *N*-functionalisation furnished 13 α-arylated fragments based on scaffold **207** in 4 steps. Synthesised 3-D fragments based on tropane scaffold **204** and 2,3-fused pyrrolidine scaffolds **206** and **207** are structurally diverse with both aromatic and heteroaromatic groups represented and, by design, exhibit good 3-D shape.

Chapter 3 covered the analysis of physicochemical properties of the 42 3-D fragments (Chapter 2) as well as the York 3-D fragment library (115 fragments). All synthesised 3-D fragments were designed to adhere to Ro3 guidelines with favourable physicochemical properties (MW, HAC, ClogP, HBA, HBD and RBC). Comparison of physicochemical properties and 3-D shape to six commercial fragment libraries showed that the York 3-D fragment collection was significantly more 3-D in shape with a lower mean lipophilicity (ClogP). Furthermore, the 3-D fragment collection is stable to prolonged storage in DMSO ($>$ 6 weeks) and in aqueous buffer ($>$ 24 h). Importantly, the majority of fragments (115 compounds) were shown to be soluble in aqueous buffer ($>$ 0.5 mM) suggesting that they were suitable for biophysical screening. To date, the York 3-D fragment library (52-106 compounds) has been screened against six protein targets. Initial screening attempts with a 52 compound subset against three protein targets (Hsp90α, PTP1B and PAK4) were unsuccessful due, in some cases, to problems with protein crystallisation. In addition, a lack of aromatic groups and the, on

average, low MW of compounds screened made screening by ^{1}H NMR challenging and the binding affinity low. More recent fragment screens (with 106 compounds) against SARS-CoV-2 proteins (SARS-CoV-2 M^{pro} and the SARS-CoV-2 Nsp^{3} macrodomain) and CD73 have revealed 15 3-D fragment hits. It is hoped that these fragment starting points could be further developed into active lead-like compounds.

Chapter 4 introduces and demonstrates a novel modular approach for fragment elaboration in order to address potential limitations in the design of 3-D fragments synthesised (Chapters 2 and 3) and to provide a strategy for overcoming challenges in FBDD hit-to-lead optimisation. To this end, five cyclopropyl-B(MIDA) 3-D building blocks **208** (previously synthesised in Chapter 2), **209**, **210**, *exo*-**211** and *exo*-**212** have been successfully synthesised (Figure 5.2). To date, 3-D building blocks **208**-*exo*-**211** were synthesised on gram-scale (2.40-5.00 g prepared) in 4-7 steps by applying a general synthetic route from the corresponding spiro-, *exo*- or *endo*-cyclic alkene. Elaboration of 3-D building blocks **208**, **209**, **210**, *exo*-**211** and *exo*-**212** *via* Suzuki-Miyaura cross-coupling of the B(MIDA) group has been successfully demonstrated in all cases. In particular, coupling of 2,3-fused pyrrolidine cyclopropyl-B(MIDA) **208** and 3,4-fused piperidine cyclopropyl-B(MIDA) *exo*-**211** with 14 aryl/heteroaryl bromides and ten FragLites respectively demonstrated that these 3-D building blocks are suitable for potential fragment elaboration and use in medicinal chemistry programmes.

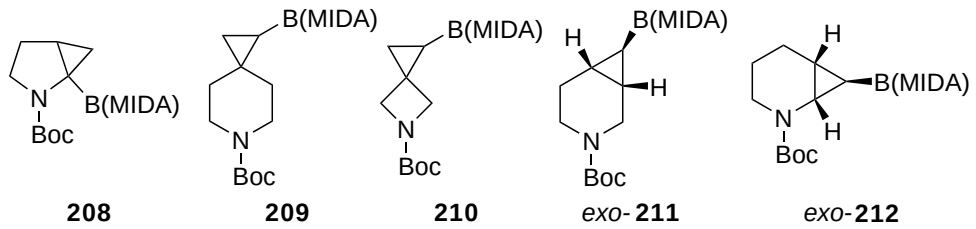

Figure 5.2: Structures of Synthesised Cyclopropyl-B(MIDA) 3-D Building Blocks

Future work will continue to focus on the generation of a library of 3-D building blocks for fragment elaboration. For example, cyclopropyl-B(MIDA) 3-D building block **540** could be synthesised in 5 steps from *N*-Boc tropinone **535** as outlined in Scheme

5.1. Ketone into alkene conversion using a Wittig reaction followed by an anticipated *exo*-selective dibromocyclopropanation would give the dibromocycloprane **537**. Li-Br exchange, trapping with *i*-PrOB(pin) and reaction with MIDA would then give spirocyclic tropane **540**. Other 3-D building blocks with different vectors are currently being designed and synthesised in the group.

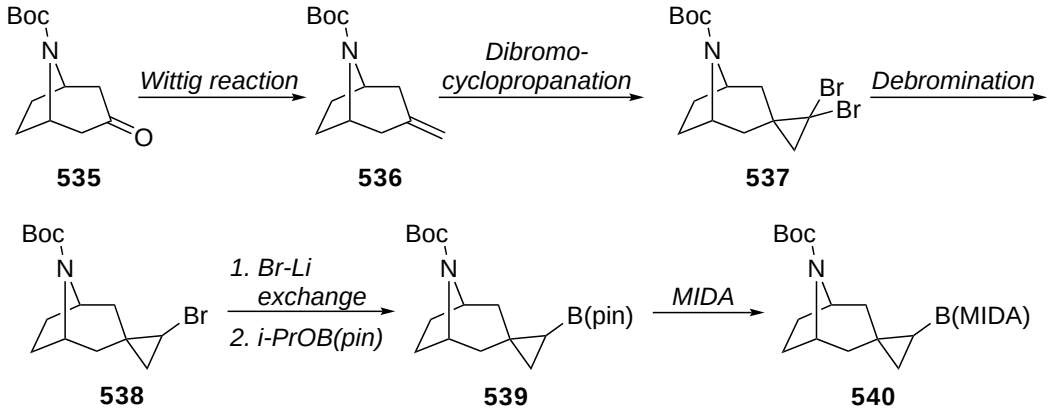

Scheme 5.1

Future collaboration with Waring's group in the application of the designed modular synthetic platform (described in section 4.1) to fragment elaboration is also planned. For example, 3-bromopyrimidine has been validated (by X-ray crystallography) as a 2-D fragment hit which binds in the ATP pocket of cyclin dependent kinase 2 (CDK2).[156] Using Suzuki-Miyaura cross-coupling and *N*-functionalisation, it should be possible to interrogate the CDK2 binding site by designing and synthesising a library of lead-like elaborated pyrimidine-containing compounds (Scheme 5.2). This would allow us to test the usefulness of the 3-D elaboration concept in a hit-to-lead optimisation setting.

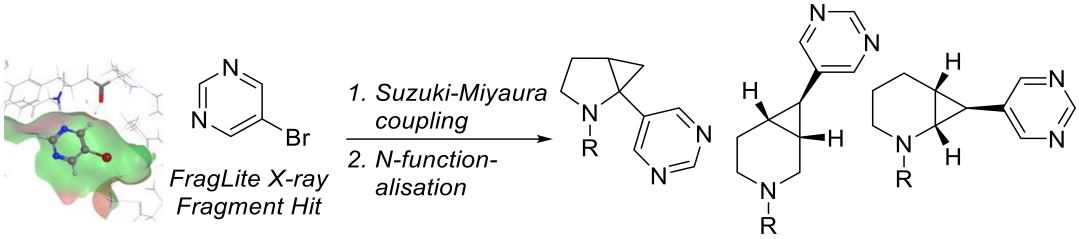

Scheme 5.2

6 Experimental

6.1 General methods

6.1.1 3-D Shape analysis protocol

A SMILES file containing the SMILES strings for all fragment compounds was generated using ChemDraw 18.0. 3-D structures were generated Pipeline Pilot 8.5.0.200, 2011, Accelrys Software Inc. Generated conformations were used to generate the three Principal Moments of Inertia (I1, I2 and I3) which were then normalised by dividing the two lower values by the largest (I1/I3 and I2/I3) using Pipeline Pilot built-in components. Prior to conformer generation a wash step was performed, which involved stripping salts and ionising the molecule at pH 7.4. Any stereocentre created here was left with undefined stereochemistry. SMILES strings were converted to their canonical representation. A list of allowed chirality at each centre is generated and a SMILES file with all possible stereoisomers was written. Conformers were generated using the BEST method in Catalyst using the rel option, run directly on the server and not through the built-in Conformation Generator component with a chosen maximum relative energy threshold of 20 kcal mol^{-1}, maximum of 255 conformers for each compound. Conformations were read, ones that cannot be represented by the canonical SMILES are discarded, with the remaining ones standardised to a single enantiomer. Duplicates were filtered with a RMSD threshold of 0.1. Minimisation with 200 steps of Conjugate Gradient minimisation with an RMS gradient tolerance of 0.1 was performed using the CHARMm forcefield with Momany-Rone partial charge estimation and a Generalised Born implicit solvent model. Duplicates were filtered again with a RMSD setting of 0.1.

6.1.2 ClogP calculations

ClogP Values were calculated at AstraZeneca using Daylight/Biobyte software (version 4.3.0).

6.1.3 General synthetic methods

All-non aqueous reactions were carried out under oxygen free Ar or N_2 using flame-dried glassware. Hexane was freshly distilled over CaH_2. Et_2O and THF were freshly distilled from sodium and benzophenone. Alkyllithiums were titrated against *N*-benzylbenzamide before use. TMEDA used in lithiation reactions was distilled over CaH_2 before use. Electrophiles *N*-methoxy-*N*-methylpyridine-3-carboxamide and *i*-PrOB(pin) were used without further purification. When CO_2 was used as an electrophile, dry ice was added to a flame-dried flask and the gas which evolved due to sublimation was transferred through a flask containing $CaCl_2$ by cannula and then added into the reaction flask by cannula. Brine refers to saturated aqueous sodium chloride solution and water is deionised water.

Flash column chromatography was carried out using Fluka Chemie GmbH silica (220440 mesh). Flash column chromatography was out carried according to standard techniques using silica gel (60 Å, 220-440 mesh particle size 40–63 μm) purchased from Sigma-Aldrich or Fluka silica gel, 35–70 μm, 60 Åand the solvent system as stated. Thin layer chromatography was carried out using Merck TLC Silica gel 60G F254 aluminium backed plates (100390 Supelco). Spots were visualised by UV and appropriate stains ($KMnO_4$, Vanillin, Ninhydrin). Melting points were carried out on a Gallenkamp melting point apparatus.

Proton (400 MHz) and carbon (100.6 MHz) NMR spectra were recorded on a Jeol ECX-400 or a JEOL ECS400 instrument using an internal deuterium lock. Chemical shifts (δ) are recorded in parts per million (ppm) and referenced to the residual solvent peak of the stated solvent, with tetramethylsilane defined as 0 ppm. NMR spectra were analysed, assigned and reported using recommended methods and DEPT as well as 2D NMR techniques such as HH-COSY, HMQC, HMBC and NOESY where required. Coupling constants (J) are quoted in Hertz. For samples recorded in $CDCl_3$,

chemical shifts are quoted in parts per million relative to $CHCl_3$ (δ_H 7.26 ppm) and $CDCl_3$ (δ_C 77.16 ppm, central line of triplet). For samples recorded in CD_3OD, chemical shifts are quoted in parts per million relative to CD_3OD (δH 3.31 ppm, central line of quintet) and CD_3OD (δ_C 49.0 ppm, central line of heptet). For samples recorded in d_6-DMSO, chemical shifts are quoted in parts per million relative to d_6-DMSO (δ_H 2.50 ppm, central line of quintet) and d_6-DMSO (δ_C 39.5 ppm, central line of quintet). For samples recorded in d_6-acetone, chemical shifts are quoted in parts per million relative to d_6-acetone (δ_H 2.05 ppm, central line of quintet) and d_6-acetone (δ_C 29.8 ppm, central line of heptet).

Infrared spectra were recorded on a PerkinElmer UATR 2 FT-IR spectrometer. Electrospray and Atmospheric Pressure Chemical ionisation techniques (ESI and APCI) have been applied and mass spectra were recorded at room temperature on a Bruker Daltronics microOTOF spectrometer. Optical rotations were recorded at room temperature on a Jasco DIP-370 polarimeter (using sodium D line, 589 nm) and $[\alpha]_D$ values are given in units of 10^{-1} deg cm^3 g^{-1}. Chiral stationary phase HPLC was performed on an Agilent 1200 series instrument and a multiple wavelength, UV/Vis diode array detector.

6.2 General synthetic procedures

General procedure A: *N*-Boc removal and amine acetylation

N-Boc protected amine (0.4 mmol, 1.0 eq.) was dissolved in HCl (4.0 mL of a 4 M solution in dioxane, 16 mmol, 40 eq.) and the resulting solution was stirred at rt for 1-2 h. Then, the solvent was evaporated under reduced pressure to give the crude HCl salt. Ac_2O (0.23 mL, 2.4 mmol, 6.0 eq.) was added dropwise to a stirred solution of the HCl salt in pyridine (2 mL) at rt under Ar and the resulting solution was stirred at rt for 1 h. Then, the solvent was evaporated under reduced pressure to give the crude product.

General Procedure B: Suzuki-Miyaura cross-coupling

N-Boc MIDA boronate or *N*-Boc IDA boronate (0.18 mmol, 1.0 eq.), Cs_2CO_3 (356 mg, 1.10 mmol, 6.0 eq.), PCy_3 (15 mg, 0.055 mmol, 0.3 eq.) and aryl bromide (0.26 mmol, 1.4 eq.) were dissolved in toluene (3.5 mL) and H_2O (0.3 mL) at rt. The resulting solution was degassed with Ar for 20 min and then $Pd(OAc)_2$ (6.1 mg, 0.027 mmol, 0.15 eq.) was added. The resulting mixture was stirred and heated in a sealed pressure tube at 100 °C for 20 h. The mixture was allowed to cool to rt and the solids were removed by filtration through Celite. EtOAc (10 mL) was added and the solution was washed with H_2O (10 mL) and brine (10 mL). The organic layer was dried (Na_2SO_4) and evaporated under reduced pressure to give the crude product.

6.3 Experimental for Chapter Two

1-*tert*-Butyl 2-methyl pyrrolidine-1,2-dicarboxylate 231

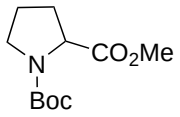

231

Thionyl chloride (3.47 mL, 47.8 mmol, 1.1 eq.) was added dropwise to a stirred solution of *rac*-proline (5.00 g, 43.4 mmol, 1.0 eq.) in MeOH (100 mL) at 0 °C under Ar. The resulting solution was stirred and heated at reflux for 1 h. After being allowed to warm to rt, the solvent was evaporated under reduced pressure to give the crude ester. Et_3N (6.10 mL, 43.4 mmol, 1.0 eq.) was added to a stirred solution of the crude methyl ester in CH_2Cl_2 (80 mL) at 0 °C under Ar. Then, a solution of Boc_2O (10.0 g, 43.4 mmol, 1.0 eq) in CH_2Cl_2 (20 mL) was added dropwise. The resulting solution was stirred at rt for 18 h. The solvent was evaporated under reduced pressure to give a wet solid. The wet solid was dissolved in Et_2O (50 mL) and the solution was washed with 1 M $HCl_{(aq)}$ (2 × 50 mL) and saturated $NaHCO_{3(aq)}$ (50 mL), dried ($MgSO_4$) and evaporated under reduced pressure to give the crude product as a pale yellow oil. Purification by flash column chromatography on silica with 80:20 to 70:30 hexane-EtOAc as eluent gave ester **231** (4.05 g, 74% over 2 steps) as a pale yellow oil, R_F (2:1 hexane-EtOAc) 0.45; IR (ATR) 2976, 2880, 1746 (C=O, CO_2Me), 1695 (C=O, Boc), 1391, 1157, 771 cm^{-1}; ^1H NMR (400 MHz, $CDCl_3$) (60:40 mixture of rotamers) δ 4.30 (dd, J = 8.5, 3.5 Hz, 0.4H, NCHCO), 4.20 (dd, J = 8.5, 4.0 Hz, 0.6H, NCHCO), 3.70 (m, 3H, OMe), 3.60-3.28 (m, 2H, NCH), 2.28-2.08 (m, 1H, CH), 2.01-1.75 (m, 3H, CH), 1.44 (s, 3.6H, CMe_3), 1.39 (s, 5.4H, CMe_3); ^{13}C NMR (100.6 MHz, $CDCl_3$) (rotamers) δ 173.9 (C=O, CO_2Me), 173.6 (C=O, CO_2Me), 154.5 (C=O, Boc), 153.9 (C=O, Boc), 79.97 (O*C*Me_3), 79.91 (O*C*Me_3), 59.2 (NCH), 58.8 (NCH), 52.2 (OMe), 52.0 (OMe), 46.7 (NCH_2), 46.4 (NCH_2), 31.0 (CH_2), 30.0 (CH_2), 28.5 (C*Me*$_3$), 28.4 (C*Me*$_3$), 24.4 (CH_2), 23.8 (CH_2). Spectroscopic data consistent with those reported in the literature.[71,73]

Lab Book Reference: HFK2-079

1-*tert*-Butyl 2-methyl 2-methylpyrrolidine-1,2-dicarboxylate 216

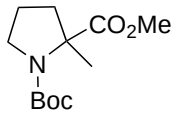

216

LHMDS (24.4 mL of a 1 M solution in THF, 24.40 mmol, 1.4 eq) was added dropwise to a stirred solution of **231** (4.02 g, 17.45 mmol, 1.0 eq) in THF (45 mL) at −20 °C under Ar. The resulting solution was stirred at −20 °C for 1.5 h. Then, methyl iodide (1.5 mL, 24.40 mmol, 1.4 eq) was added dropwise. After being allowed to warm to rt, the resulting solution was stirred at rt for 18 h. Saturated $NH_4Cl_{(aq)}$ (20 mL) and 35% $NH_{3(aq)}$ (20 mL) were added sequentially and the mixture was extracted with EtOAc (3 × 40 mL). The combined organic extracts were washed with brine (3 × 40 mL), dried ($MgSO_4$) and evaporated under reduced pressure to give the crude product as an orange oil. Purification by flash column chromatography on silica with 75:25 hexane-EtOAc as eluent gave methylated pyrrolidine **216** (3.97 g, 93%) as a pale yellow oil, R_F (3:2 hexane-EtOAc) 0.79; IR (ATR) 2976, 2877, 1741 (C=O, CO_2Me), 1694 (C=O, Boc), 1387, 1161, 773 cm^{-1}; ^1H NMR (400 MHz, $CDCl_3$) (70:30 mixture of rotamers) δ 3.67 (s, 3H, OMe), 3.57-3.42 (m, 2H, NCH), 2.18-2.08 (m, 1H, NCH), 1.94-1.78 (m, 3H, CH), 1.52 (s, 0.9H, NCMe), 1.47 (s, 2.1H, NCMe), 1.40 (s, 2.7H, CMe_3), 1.37 (s, 6.3H, CMe_3); ^{13}C NMR (100.6 MHz, $CDCl_3$) (rotamers) δ 175.4 (C=O, CO_2Me), 175.3 (C=O, CO_2Me), 154.0 (C=O, Boc), 153.6 (C=O, Boc), 79.9 (O*C*Me_3), 79.5 (O*C*Me_3), 65.2 (N*C*Me), 64.8 (N*C*Me), 52.2 (OMe), 47.9 (OMe), 40.2 (NCH_2), 39.2 (NCH_2), 28.5 (CH_2), 28.4 (CH_2), 23.4 (CH_2), 23.2 (CH_2), 22.9 (NC*Me*), 22.3 (NC*Me*); MS (EI) *m/z* 266 [(M + Na)$^+$, 100]; HRMS (ESI) *m/z* calcd for $C_{12}H_{21}NO_4$ [(M + Na)$^+$, 100] 266.1363, found 266.1370 (−2.2 ppm error). Spectroscopic data consistent with those reported in the literature.[72]

Lab Book Reference HFK 1-040

Methyl-1-methanesulfonyl-2-methylpyrrolidine-2-carboxylate 258

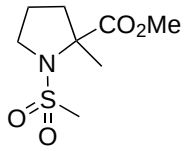

258

TFA (1 mL, 13 mmol, 16 eq) was added dropwise to a stirred solution of Boc protected ester **216** (200 mg, 0.822 mmol, 1.0 eq) in CH_2Cl_2 (5 mL) at rt under Ar. The resulting solution was stirred at rt for 1.5 h. Then, the solvent was evaporated under reduced pressure to give the crude TFA salt (385 mg). Et_3N (560 μL, 3.96 mmol, 4.8 eq) was added dropwise to a stirred solution of the TFA salt in CH_2Cl_2 (4 mL) at rt under Ar. The resulting solution was stirred at rt for 10 min and MsCl (140 μL, 1.80 mmol, 2.2 eq) was added dropwise. The resulting solution was stirred at rt for 18 h. The mixture was poured into water (10 mL) and extracted with CH_2Cl_2 (3 x 10 mL). The combined organics were dried ($MgSO_4$) and evaporated under reduced pressure to give the crude product as a yellow oil. Purification by flash column chromatography on silica with 70:30 to 50:50 hexane-EtOAc as eluent gave *N*-sulfonamide **258** (127 mg, 70%) as a white solid, mp 79-81 °C; R_F (1:1 hexane-EtOAc) 0.30; IR (ATR) 2955, 2882, 1735 (C=O), 1320, 1132, 518 cm^{-1}; ^1H NMR (400 MHz, $CDCl_3$) δ 3.73 (s, 3H, CO_2Me), 3.59-3.44 (m, 2H, NCH), 2.95 (s, 3H, SO_2Me), 2.29-2.12 (m, 1H, CH), 2.05-1.87 (m, 3H, CH), 1.65 (s, 3H, NCMe); ^{13}C NMR (100.6 MHz, $CDCl_3$) δ 174.8 (C=O), 68.9 (N*C*Me), 52.8 (OMe), 49.0 (NCH_2), 41.1 (CH_2), 39.7 (SO_2Me), 24.8 (CH_2), 23.5 (NC*Me*); MS (EI) *m/z* 244 [$(M + Na)^+$, 100]; HRMS (ESI) *m/z* calcd for $C_8H_{15}NO_4S$ [$(M + Na)^+$, 100] 244.0614, found 244.0614 (−0.2 ppm error).

Lab book reference HFK2-090

1-Methanesulfonyl-2-methylpyrrolidine-2-carboxylic acid 226

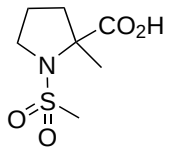

226

A solution of LiOH (110 mg, 4.59 mmol, 8.1 eq) in H_2O (4 mL) was added dropwise to a stirred solution of ester **258** (125 mg, 0.565 mmol, 1.0 eq) in MeOH (4 mL) at rt under Ar. The resulting solution was stirred at rt for 2.5 h. Then, the solvent was evaporated under reduced pressure. Then, H_2O (10 mL) was added and the mixture acidified to pH 2 with 12 M $HCl_{(aq)}$ (1 mL). EtOAc (10 mL) was added and the two layers were separated. The aqueous layer was extracted with EtOAc (3 × 10 mL) and the combined organics were dried ($MgSO_4$) and evaporated under reduced pressure to give acid **226** (100 mg, 85%) as a white solid, mp 127-129 °C; R_F (9:1 CH_2Cl_2-MeOH) 0.21; IR (ATR) 2893, 2676, 1701 (C=O), 1312, 1141, 767 cm^{-1}; ^1H NMR (400 MHz, d_4-MeOH) 4.90 (br s, 1H, OH), 3.68-3.42 (m, 2H, NCH), 2.99 (s, 3H, SO_2Me), 2.35-2.16 (m, 1H, CH), 2.12-1.87 (m, 3H, CH), 1.62 (s, 3H, NCMe); ^{13}C NMR (100.6 MHz, d_4-MeOH) 177.5 (C=O), 69.8 (N*C*Me), 50.0 (NCH_2),42.1 (CH_2), 39.7 (SO_2Me), 24.9 (NC*Me*), 24.4 (CH_2); MS (EI) *m/z* 230 [$(M + Na)^+$, 100]; HRMS (ESI) *m/z* calcd for $C_7H_{13}NO_4S$ [$(M + Na)^+$, 100] 230.0457, found 230.0452 (+2.4 ppm error).

Lab book reference HFK2-089

1-Acetyl-2-methyl-pyrrolidine-2-carboxylic ester 259

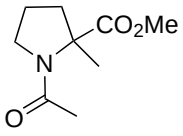

259

N-Boc protected ester **216** (300 mg, 1.23 mmol, 1.0 eq) was dissolved in HCl (6 mL of a 2 M solution in Et_2O, 12 mmol, 10.0 eq) and the resulting solution was stirred at

rt for 18 h. TLC indicated that starting material remained. Therefore, the solution was stirred and heated at 35 °C for 4 h. Then, the solvent was evaporated under reduced pressure to give the crude HCl salt (223 mg) as a white powder. Ac_2O (630 μL, 6.68 mmol, 6.0 eq) was added dropwise to a stirred solution of the crude HCl salt (223 mg) in pyridine (2 mL) at rt under Ar and the resulting solution was stirred at rt for 1 h. Then, the solvent was evaporated under reduced pressure to give the crude product. Purification by flash column chromatography on silica with 95:5 to 90:10 CH_2Cl_2-MeOH as eluent gave *N*-acetamide **259** (220 mg, 96%) as a yellow oil, R_F (9:1 CH_2Cl_2-MeOH) 0.73; IR (ATR) 2953, 1737 (C=O, CO_2Me), 1635 (C=O, amide), 1611, 1415, 728 cm^{-1}; ^1H NMR (400 MHz, $CDCl_3$) δ 3.61 (s, 3H, OMe), 3.59-3.47 (m, 2H, NCH), 2.14-2.02 (m, 1H, CH), 1.96 (s, 3H, C(O)Me), 1.98-1.89 (m, 2H, CH), 1.87-1.75 (m, 1H, CH), 1.52 (s, 0.15H, NCMe), 1.46 (s, 2.85H, NCMe); ^{13}C NMR (100.6 MHz, $CDCl_3$) δ 174.5 (C=O), 169.3 (C=O), 65.7 (N*C*Me), 52.4 (NCH_2), 49.0 (OMe), 38.7 (C(O)*Me*), 24.0 (NC*Me*), 22.9 (CH_2), 21.5 (CH_2); MS (EI) *m/z* 208 [$(M + Na)^+$, 100]; HRMS (ESI) *m/z* calcd for $C_9H_{15}NO_3$ [$(M + Na)^+$, 100] 208.0944, found 208.0945 (−1.1 ppm error).

Lab book reference HFK1-068

(*S*)-1-Acetyl-2-methyl-pyrrolidine-2-carboxylic acid 227

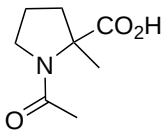

227

A solution of LiOH (90 mg, 0.486 mmol, 3.0 eq) in H_2O (3 mL) was added dropwise to a stirred solution of ester **259** (100 mg, 0.540 mmol, 1.0 eq) in MeOH (3 mL) at rt under Ar. The resulting solution was stirred and heated at 40 °C for 18 h. Then, the solution was allowed to cool to rt and the solvent was evaporated under reduced pressure. Then, H_2O (10 mL) was added and the mixture was acidified to pH 2 with 12 M $HCl_{(aq)}$ (0.5 mL). EtOAc (10 mL) was added and the two layers were separated.

The aqueous layer was extracted with EtOAc (3 × 10 mL) and the combined organics were dried ($MgSO_4$) and evaporated under reduced pressure to give acid **227** (74 mg, 80%) as a white solid, mp 119-121 °C; R_F (9:1 CH_2Cl_2-MeOH) 0.58; IR (ATR) 2979, 1727 (C=O, CO_2H), 1598 (C=O, amide), 1419, 1180, 725 cm^{-1}; ^1H NMR (400 MHz, $CDCl_3$) δ 10.37 (s, 1H, OH), 3.72-3.47 (m, 2H, NCH), 2.39 (ddd, J = 12.0, 7.0, 7.0 Hz, 1H, CH), 2.09 (s, 3H, C(O)Me), 2.06-1.90 (m, 2H, CH), 1.82 (br dd, J = 12.0, 7.0 Hz, 1H, CH), 1.56 (s, 3H, NCMe); ^{13}C NMR (100.6 MHz, $CDCl_3$) δ 176.0 (C=O), 171.5 (C=O), 66.9 (N*C*Me), 49.7 (NCH_2), 38.3 (CH_2), 23.8 (CH_2), 23.2 (C(O)*Me*), 21.7 (NC*Me*); MS (EI) *m/z* 194 [$(M + Na)^+$, 100]; HRMS (ESI) *m/z* calcd for $C_8H_{13}NO_3$ [$(M + Na)^+$, 100] 194.0788, found 194.0788 (+0.1 ppm error).

Lab book reference HFK1-079

1-Methanesulfonyl-2-methylpyrrolidine-2-carboxamide 225

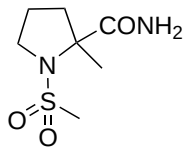

225

DIPEA (399 μL, 2.29 mmol, 3.0 eq) and T3P (339 μL of a 50% wt solution in EtOAc, 1.14 mmol, 1.5 eq) were added sequentially to a stirred solution of acid **226** (158 mg, 0.763 mmol, 1.0 eq) in CH_2Cl_2 (4 mL) at rt under Ar. Then, 35% $NH_{3(aq)}$ (1.12 mL, 3.81 mmol, 5 eq) was added and the solution was stirred and heated at 55 °C for 3 h. After being allowed to cool to rt, the solution was poured into water (10 mL) and 3 M $HCl_{(aq)}$ (1 mL) was added. The two layers were separated and the aqueous layer was extracted with EtOAc (3 × 10 mL). The combined organics were washed with 2 M $NaOH_{(aq)}$ (10 mL) and brine (10 mL), dried ($MgSO_4$) and evaporated under reduced pressure to give the crude product as a yellow oil. Purification by flash column chromatography on silica with 95:5 CH_2Cl_2-MeOH as eluent gave amide **225** (39 mg, 25%) as a cream solid, mp 117-119 °C; R_F (9:1 CH_2Cl_2-MeOH) 0.32; IR (ATR) 3457

(NH), 3356 (NH), 2983, 2879, 1668 (C=O), 1314, 1138, 728 cm^{-1}; ^1H NMR (400 MHz, $CDCl_3$) δ 6.58 (br s, 1H, NH), 5.87 (br s, 1H, NH), 3.70-3.55 (m, 1H, NCH), 3.49-3.29 (m, 1H, NCH), 2.95 (s, 3H, SO_2Me), 2.59-2.42 (m, 1H, CH), 2.07-1.77 (m, 3H, CH), 1.68 (s, 3H, NCMe); ^{13}C NMR (100.6 MHz, $CDCl_3$) δ 176.8 (C=O), 69.5 (N*C*Me), 50.1 (NCH_2), 41.3 (CH_2), 39.1 (SO_2Me), 23.2 (CH_2), 22.9 (NC*Me*); MS (EI) *m/z* 229 [(M + Na)$^+$, 100]; HRMS (ESI) *m/z* calcd for $C_7H_{14}N_2O_3S$ [(M + Na)$^+$, 100] 229.0617, found 229.0618 (−0.4 ppm error).

Lab book reference HFK2-092

1-Methanesulfonyl-2-methylpyrrolidine-2-carbonitrile 228

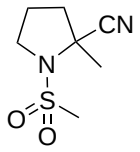

228

Et_3N (656 μL, 4.70 mmol, 2.4 eq) and trifluoroacetic anhydride (332 μL, 2.35 mmol, 1.2 eq) were sequentially added dropwise to a stirred solution of amide **225** (404 mg, 1.96 mmol, 1.0 eq) in THF (35 mL) at 0 °C under Ar. The resulting solution was stirred at 0 °C for 1 h and rt for 6 h. Then, the solvent was evaporated under reduced pressure. CH_2Cl_2 (25 mL) was added and the solution was washed with $NaHCO_{3(aq)}$ (25 mL). The aqueous layer was extracted with CH_2Cl_2 (2 × 20 mL). The combined organics were dried (Na_2SO_4) and evaporated under reduced pressure to give the crude product as an orange solid. Purification by flash column chromatography on silica with 50:50 hexane-EtOAc as eluent gave nitrile **228** (312 mg, 85%) as a white solid, mp 99-101 °C; R_F (1:1 hexane-EtOAc) 0.30; IR (ATR) 2987, 2938, 1330, 1146, 757, 517 cm^{-1} No 2260-2222 (C≡N) cm^{-1} band observed; ^1H NMR (400 MHz, $CDCl_3$) δ 3.65-3.54 (m, 1H, NCH), 3.48-3.43 (m, 1H, NCH), 3.03 (s, 3H, SO_2Me), 2.55-2.48 (m, 1H, CH), 2.21-1.94 (m, 3H, CH), 1.82 (s, 3H, NCMe); ^{13}C NMR (100.6 MHz, $CDCl_3$) δ 120.3 (CN), 58.2 (N*C*Me), 49.5 (NCH_2), 42.2 (CH_2), 37.0 (SO_2Me), 27.1 (NC*Me*), 22.9

(CH_2); MS (EI) *m/z* 211 [(M + Na)$^+$, 100]; HRMS (ESI) *m/z* calcd for $C_7H_{12}N_2O_2S$ [(M + Na)$^+$, 100] 211.0512, found 211.0514 (−1.3 ppm error).

Lab book reference HFK2-099

1-Acetyl-2-methyl-N-(prop-2-en-1-yl)pyrrolidine-2-carboxamide 260

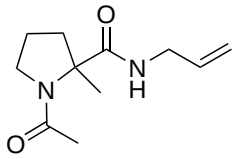

260

DIPEA (243 μL, 1.39 mmol, 1.9 eq) and allylamine (62 μL, 0.83 mmol, 1.1 eq) were added sequentially to a stirred solution of acid **227** (129 mg, 0.753 mmol, 1.0 eq) in CH_2Cl_2 (6 mL) at rt under Ar. Then, T3P (719 μL of a 50% wt solution in EtOAc, 1.13 mmol, 1.5 eq) was added and the solution was stirred at rt for 18 h. Then, the solution was poured into water (10 mL). The two layers were separated and the aqueous layer was extracted with EtOAc (3 × 10 mL). The combined organics were dried ($MgSO_4$) and evaporated under reduced pressure to give the crude product as a white solid. Purification by flash column chromatography on silica with 95:5 CH_2Cl_2-MeOH as eluent gave amide **260** (60 mg, 38%) as a colourless oil, R_F (9:1 CH_2Cl_2-MeOH) 0.56; IR (ATR) 3330 (NH), 2977, 1634 (C=O), 1522, 1407, 731 cm^{-1}; ^{1}H NMR (400 MHz, $CDCl_3$) δ 7.60 (br s, 1H, NH), 5.80 (dddd, J = 17.0, 10.5, 5.5, 5.5 Hz, 1H, =CH), 5.14 (dddd, J = 17.0, 3.0, 1.5, 1.5 Hz, 1H, =CH), 5.06 (dddd, J = 10.5, 3.0, 1.5, 1.5 Hz, 1H, =CH), 3.97-3.68 (m, 2H, NCH), 3.63-3.40 (m, 2H, NCH), 2.70 (ddd, J = 17.5, 5.1, 5.1 Hz, 1H, CH), 2.08 (s, 3H, C(O)Me), 1.90-1.79 (m, 2H, CH), 1.66 (s, 3H, NCMe) 1.64-1.59 (m, 1H, CH); ^{13}C NMR (100.6 MHz, $CDCl_3$) δ 174.0 (C=O), 171.0 (C=O), 134.4 (=CH), 115.7 (=CH_2), 68.8 (N*C*Me), 50.45 (NCH_2), 42.0 (NCH_2), 38.5 (CH_2), 24.2 (C(O)*Me*), 23.3 (CH_2), 23.1 (NC*Me*); MS (EI) *m/z* 233 [(M + Na)$^+$, 100]; HRMS (ESI) *m/z* calcd for $C_{11}H_{18}N_2O_2$ [(M + Na)$^+$, 100] 233.1260, found 233.1262 (−0.8 ppm error).

Lab book reference HFK3-055

1-Acetyl-*N*-[(3,4-dimethoxyphenyl)methyl]-2-methylpyrrolidine-2-carboxamide 261

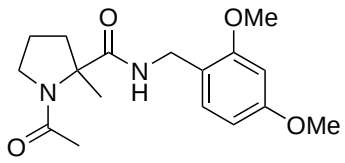

261

DIPEA (381 μL, 2.39 mmol, 1.9 eq) and 2,4-dimethoxybenzylamine (213 μL, 1.42 mmol, 1.1 eq) were added sequentially to a stirred solution of acid **227** (221 mg, 1.29 mmol, 1.0 eq) in CH_2Cl_2 (8 mL) at rt under Ar. Then, T3P (1.13 g of a 50% wt solution in EtOAc, 1.94 mmol, 1.5 eq) was added and the solution was stirred at rt for 18 h. Then, the solution was poured into water (10 mL). The two layers were separated and the aqueous layer was extracted with EtOAc (3 × 15 mL). The combined organics were dried ($MgSO_4$) and evaporated under reduced pressure to give the crude product. Purification by flash column chromatography on silica with 95:5 CH_2Cl_2-MeOH as eluent gave amide **261** (342 mg, 83%) as a cream solid, IR (ATR) 3344 (NH), 2939, 1633 (C=O), 1615, 1506, 1411, 1206 cm^{-1}; R_F (9:1 CH_2Cl_2-MeOH) 0.53; ^{1}H NMR (400 MHz, $CDCl_3$) δ (85:15 mixture of rotamers) 7.64-7.61 (m, 1H, NH), 7.15-7.13 (m, 1H, Ar), 6.42-6.38 (m, 2H, Ar), 4.37 (dd, J = 14.5, 6.0 Hz, 1H, NCHAr), 4.29 (dd, J = 14.5, 5.5 Hz, 1H, NCHAr), 3.81 (s, 3H, OMe), 3.77 (s, 3H, OMe), 3.58-3.43 (m, 2H, NCH), 2.64 (ddd, J = 12.5, 5.5, 5.5 Hz, 1H, CH), 2.16 (s, 0.5, C(O)Me), 2.07 (s, 2.5H, C(O)Me), 1.89-1.80 (m, 2H, CH), 1.64 (s, 3.5H, NCMe and CH), 1.56 (s, 0.5, NCMe); ^{13}C NMR (100.6 MHz, $CDCl_3$) (rotamers) δ 174.0 (C=O), 173.8 (C=O), 170.6 (C=O), 170.4 (C=O), 160.8 (*ipso*-Ar), 160.3 (*ipso*-Ar), 158.6 (*ipso*-Ar), 158.6 (*ipso*-Ar), 130.9 (Ar), 129.9 (Ar), 119.3 (*ipso*-Ar), 118.1 (*ipso*-Ar), 104.1 (Ar), 103.9 (Ar), 98.7 (Ar), 98.6 (Ar), 68.6 (N*C*Me), 66.7 (N*C*Me), 55.5 (OMe), 55.4 (OMe), 50.3 (NCH_2), 48.6 (NCH_2), 42.9 (N*C*H_2Ar), 40.1 (N*C*H_2Ar), 39.1 (CH_2), 38.7 (CH_2), 24.1

(C(O)Me), 23.9 (C(O)Me), 23.3 (CH_2), 22.9 (NC*Me*), 22.7 (NC*Me*), 22.0 (CH_2); MS (EI) *m/z* 343 [(M + Na)$^+$, 100]; HRMS (ESI) *m/z* calcd for $C_{17}H_{24}N_2O_4$ [(M + Na)$^+$, 100] 343.1628, found 343.1628 (0.0 ppm error).

Lab book reference HFK3-100

1-Acetyl-2-methylpyrrolidine-2-carboxamide 224

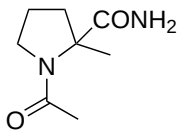

224

A solution of amide **261** (100 mg, 0.312 mmol, 1.0 eq.) in 1:6 H_2O-TFA (3.5 mL) was stirred and heated at 70 °C for 4 h. After being allowed to cool to rt, the solvent was evaporated under reduced pressure. Then, EtOAc (20 mL) and H_2O (20 mL) were added and the aqueous layer was extracted with EtOAc (3 × 30 mL). The combined organics were washed with brine (20 mL), dried ($MgSO_4$) and evaporated under reduced pressure to give the crude product. Purification by flash column chromatography on silica with 99:1 to 95:5 to 90:10 CH_2Cl_2-MeOH as eluent gave amide **224** (5 mg, 9%) as a cream solid, mp 74-76 °C; R_F (4:1 CH_2Cl_2-MeOH) 0.33; IR (ATR) 2926, 1727 (C=O), 1600, 1420, 1181, 725 cm^{-1}; ^{1}H NMR (400 MHz, $CDCl_3$) δ 3.59 (m, 2H, NCH), 2.66-2.59 (m, 1H, CH), 2.15 (s, 3H, C(O)*Me*), 2.02-1.91 (m, 2H, CH), 1.84-1.77 (m, 1H, CH), 1.64 (s, 3H, NCMe); ^{13}C NMR (100.6 MHz, $CDCl_3$) δ 172.6 (C=O), 50.3 (NCH_2), 38.1 (CH_2), 23.6 (CH_2), 23.5 (C(O)*Me*), 22.2 (NC*Me*), (C=O and and NCMe resonance not resolved); MS (EI) *m/z* 193 [(M + Na)$^+$, 100]; HRMS (ESI) *m/z* calcd for $C_8H_{14}N_2O_2$ [(M + Na)$^+$, 100] 193.1055, found 194.0790 (−0.1 ppm error).

Lab book reference HFK4-005

***tert*-Butyl 2-(hydroxymethyl)-2-methylpyrrolidine-1-carboxylate 263**

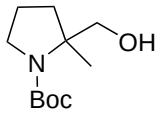

263

$LiBH_4$ (0.31 mL of a 4 M solution in THF, 1.23 mmol, 1.5 eq) was added dropwise to a stirred solution of ester **216** (200 mg, 0.82 mmol, 1.0 eq) in THF (5 mL) at 0 °C under Ar. The resulting solution was stirred at rt for 48 h. After cooling to −20 °C, water (5 mL) and 3 M $HCl_{(aq)}$ (5 mL) were added sequentially. The two layers were separated and the aqueous layer was extracted with EtOAc (3 x 20 mL). The combined organics were washed with brine (20 mL), dried ($MgSO_4$) and evaporated under reduced pressure to give alcohol **263** (157 mg, 89%) as a colourless oil, R_F (3:2 hexane-EtOAc) 0.50; IR (ATR) 3398 (OH), 2972, 2876, 1662 (C=O), 1391, 1170, 771 cm^{-1}; ^1H NMR (400 MHz, $CDCl_3$) δ 5.32 (d, J = 10.0 Hz, 1H, OH), 3.64 (dd, J = 10.0, 10.0 Hz, 1H, HOC*H*), 3.56 (br d, J = 10.0 Hz, 1H, HOC*H*), 3.52-3.45 (m, 1H, NCH), 3.31-3.24 (m, 1H, NCH), 1.88-1.69 (m, 2H, CH) 1.69-1.59 (m, 2H, CH), 1.42 (s, 9H, CMe_3), 1.33 (s, 3H, NCMe); ^{13}C NMR (100.6 MHz, $CDCl_3$) δ 156.1 (C=O, Boc), 80.1 (O*C*Me_3), 70.8 (OCH_2), 64.9 (N*C*Me), 48.6 (NCH_2), 37.7 (CH_2), 28.6 (C*Me*$_3$), 21.9 (CH_2), 20.4 (NC*Me*); MS (EI) *m/z* 238 [$(M + Na)^+$, 100]; HRMS (ESI) *m/z* calcd for $C_{11}H_{21}NO_3$ [$(M + Na)^+$, 100] 238.1414, found 238.1410 (+1.8 ppm error).

Lab Book Reference HFK1-015

***tert*-Butyl 2-(methoxymethyl)-2-methylpyrrolidine-1-carboxylate 264**

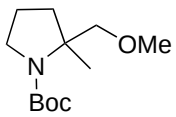

264

NaH (397 mg of a 60% dispersion in mineral oil, 9.90 mmol, 1.5 eq) was added portion-wise to a stirred solution of alcohol **263** (1.42 g, 6.60 mmol, 1.0 eq) in THF (24 mL)

at −78 °C under Ar. Then, methyl iodide (0.698 mL, 11.20 mmol, 1.7 eq) was added. After being allowed to warm to rt, the resulting mixture was stirred at rt for 18 h. Saturated $NH_4Cl_{(aq)}$ (20 mL) and 35% $NH_{3(aq)}$ (20 mL) were added sequentially and the mixture was extracted with EtOAc (3 × 40 mL). The combined organic extracts were dried (Na_2SO_4) and evaporated under reduced pressure to give the crude product as a yellow oil. Purification by flash column chromatography on silica with 80:20 hexane-EtOAc as eluent gave methyl ether **264** (561 mg, 37%) as a pale yellow oil, R_F (2:1 hexane-EtOAc) 0.38; IR (ATR) 2973, 2875, 1689 (C=O), 1364, 1174, 771 cm^{-1}; ^1H NMR (400 MHz, $CDCl_3$) (50:50 mixture of rotamers) δ 3.67 (d, J = 9.0 Hz, 0.5H, C*H*OMe), 3.49-3.45 (m, 1.5H), 3.38-3.35 (m, 1.5H),3.31 (s, 3H, OMe), 3.30-3.24 (m, 0.5H), 2.16-2.05 (m, 1H, CH), 1.78-1.56 (m, 3H, CH), 1.45 (s, 4.5H, C*Me*$_3$), 1.41 (s, 4.5H, C*Me*$_3$), 1.29 (s, 1.5H, NCMe), 1.24 (s, 1.5H, NCMe); ^{13}C NMR (100.6 MHz, $CDCl_3$) (rotamers) δ 154.4 (C=O), 153.8 (C=O), 79.4 (O*C*Me$_3$), 78.7 (O*C*Me$_3$), 77.3 (OCH_2), 76.3 (OCH_2), 62.8 (N*C*Me), 62.2 (N*C*Me), 59.3 (OMe), 48.7 (NCH_2), 38.3 (CH_2), 37.1 (CH_2), 28.7 (C*Me*$_3$), 23.2 (NC*Me*), 22.2 (CH_2), 22.1 (NC*Me*), 21.7 (CH_2); MS (EI) *m/z* 252 [(M + Na)$^+$, 100]; HRMS (ESI) *m/z* calcd for $C_{12}H_{23}NO_3$ [(M + Na)$^+$, 100] 252.1570, found 252.1566 (+1.7 ppm error).

Lab Book Reference HFK1-042

2-(Methoxymethyl)-2-methylpyrrolidine hydrochloride 222

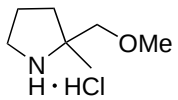

222

Methyl ether **264** (200 mg, 0.87 mmol, 1.0 eq) was dissolved in HCl (5 mL of a 2 M solution in Et_2O, 10 mmol, 11.0 eq) and the resulting solution was stirred at rt for 18 h. TLC indicated that starting material remained. HCl (3 mL of a 2 M solution in Et_2O, 6.0 mmol, 7.0 eq) was added and the resulting solution was stirred at rt for 6 h. Then, the solvent was evaporated under reduced pressure to give hydrochoride salt

222·HCl (123 mg, 85%) as a white solid, mp 100-104 °C; R_F (9:1 CH_2Cl_2-MeOH) 0.29; IR (ATR) 2895, 2653, 2504, 1394, 1107, 572 cm^{-1}; ^1H NMR (400 MHz, d_4-MeOH) δ 3.45 (s, 2H, CH_2OMe), 3.41 (s, 3H, OMe), 3.31-3.27 (m, 2H, NCH), 2.14-1.95 (m, 3H, CH), 1.83-1.78 (m, 1H, CH), 1.39 (s, 3H, NCMe); ^{13}C NMR (100.6 MHz, d_4-MeOH) δ 76.6 (*C*H_2OMe), 68.2 (N*C*Me), 59.6 (OMe), 46.3 (NCH_2), 34.7 (CH_2), 24.4 (CH_2), 21.7 (NC*Me*); MS (EI) *m/z* 130 [M^+, 100]; HRMS (ESI) *m/z* calcd for $C_7H_{16}NO$ [M^+, 100] 130.1226, found 130.1228 (−1.5 ppm error).

Lab Book Reference HFK1-062

2-Methyl-pyrrolidine-1,2-dicarboxylic acid 1-*tert*-butyl ester 238

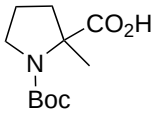

238

A solution of NaOH (1.88 g, 46.9 mmol, 3.0 eq) in H_2O (20 mL) was added dropwise to a stirred solution of ester **216** (3.80 g, 15.6 mmol, 1.0 eq) in MeOH (20 mL) at rt under Ar. The resulting solution was stirred and heated at 80 °C for 1 h. TLC indicated that starting material remained. NaOH (1.27 g, 32.8 mmol 2.1 eq) was added and the resulting solution was stirred and heated at 80 °C for 1 h. The mixture was allowed to cool to rt and the solvent was evaporated under reduced pressure. Then, H_2O (25 mL) was added and the mixture was acidified to pH 2 with 12 M $HCl_{(aq)}$ (3 mL). Et_2O (25 mL) was added and the two layers were separated. The aqueous layer was extracted with Et_2O (2 × 25 mL) and the combined organics were dried ($MgSO_4$) and evaporated under reduced pressure to give acid **238** (3.32 g, 93%) as a white solid, mp 90-93 °C (lit.,[72] 91-94 °C); R_F (3:2 hexane-EtOAc) 0.35; ^1H NMR (400 MHz, $CDCl_3$) (55:45 mixture of rotamers) δ 3.68-3.29 (m, 2H, NCH), 2.56-2.39 (m, 0.45H, CH), 2.28-2.21 (m, 0.55H, CH), 2.02-1.71 (m, 3H, CH), 1.58 (s, 1.35H, NCMe), 1.49 (s, 1.65H, NCMe), 1.44 (s, 4.05H, CMe_3), 1.40 (s, 4.95H, CMe_3); ^{13}C NMR (100.6 MHz, $CDCl_3$) (rotamers) δ 181.1 (C=O, CO_2H), 177.9 (C=O, CO_2H), 155.8 (C=O,

Boc), 153.7 (C=O, Boc), 81.2 (O*C*Me$_3$), 80.5 (O*C*Me$_3$), 66.2 (N*C*Me), 64.9 (N*C*Me), 48.6 (NCH$_2$), 47.9 (NCH$_2$), 40.5 (CH$_2$), 38.8 (CH$_2$), 28.6 (C*Me*$_3$), 28.4 (C*Me*$_3$), 23.1 (CH$_2$), 23.0 (NC*Me*), 22.9 (CH$_2$), 22.4 (NC*Me*). Spectroscopic data consistent with those reported in the literature.[72]

Lab book reference HFK1-034

N-(*t*-Butoxycarbonyl)-α-methylprolinamide 262

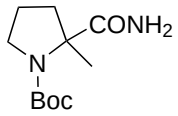

262

Et_3N (1.1 mL, 7.5 mmol, 1.0 eq) was added dropwise to a stirred solution of acid **238** (1.72 g, 7.51 mmol, 1.0 eq) in THF (80 mL) at rt under Ar. The resulting solution was cooled to −20 °C and isobutyl chloroformate (1.2 mL, 9.0 mmol, 1.2 eq) was added dropwise. After stirring at −20 °C for 40 min, 35% $NH_{3(aq)}$ (16 mL) was added and the mixture was allowed to warm to rt over 30 min. Then, the solvent was evaporated under reduced pressure and the residue was dissolved in EtOAc (50 mL). The solution was washed with $NaHCO_{3(aq)}$ (40 mL) and brine (40 mL), dried ($MgSO_4$) and evaporated under reduced pressure to give the crude product. Purification by flash column chromatography on silica with 60:40 hexane-EtOAc and then 90:10 CH_2Cl_2-MeOH as eluent gave amide **262** (608 mg, 36%) as a white solid, mp 106-108 °C; R_F (9:1 CH_2Cl_2-MeOH) 0.49; ^{1}H NMR (400 MHz, $CDCl_3$) (55:45 mixture of rotamers) δ 6.96 (br s, 0.45H, NH), 6.31 (br s, 0.55H, NH), 6.10 (br s, 1H, NH), 3.67-3.21 (m, 2H, NCH), 2.45 (br s, 0.55H, CH), 2.19 (br s, 0.55H, CH), 1.93-1.60 (m, 2.9H, CH), 1.53 (s, 1.35H, NCMe), 1.44 (s, 1.65H, NCMe), 1.34 (s, 9H, CMe_3); ^{13}C NMR (100.6 MHz, $CDCl_3$) (rotamers) δ 178.0 (C=O, $CONH_2$), 177.8 (C=O, $CONH_2$), 154.7 (C=O, Boc), 153.9 (C=O, Boc), 80.5 (O*C*Me$_3$), 80.3 (O*C*Me$_3$), 66.7 (N*C*Me), 65.9 (N*C*Me), 48.7 (NCH$_2$), 47.9 (NCH$_2$), 41.3 (CH$_2$), 39.0 (CH$_2$), 28.4 (C*Me*$_3$), 22.5 (NC*Me*). Spectroscopic data consistent with those reported in the literature.[200]

Lab book reference HFK1-070

α-Methylprolinamide hydrochloride 219·HCl

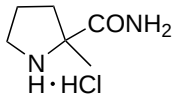

219

N-Boc protected amide **262** (200 mg, 0.93 mmol, 1.0 eq) was dissolved in HCl (3 mL of a 2 M solution in Et_2O, 5.6 mmol, 6.0 eq) and the resulting solution was stirred at rt for 18 h. TLC indicated that starting material remained. HCl (6 mL of a 2 M solution in Et_2O, 11.2 mmol, 12.0 eq) was added and the resulting solution was stirred at rt for 18 h. Then, the solvent was evaporated under reduced pressure to give hydrochoride salt **219**·HCl (67 mg, 47%) as a cream powder, mp 100-103 °C; IR (ATR) 3336 (NH), 3272 (NH), 3180 (NH), 1697 (C=O), 1629 (C=O), 609 cm^{-1}; ^1H NMR (400 MHz, d_4-MeOH) δ 3.40-3.30 (m, 2H, NCH), 2.39-2.28 (m, 1H, CH), 2.17-2.03 (m, 2H, CH), 2.00-1.88 (m, 1H, CH), 1.65 (s, 3H, NCMe); ^{13}C NMR (100.6 MHz, d_4-MeOH) δ 174.7 (C=O), 70.8 (N*C*Me), 46.6 (NCH_2), 37.3 (CH_2), 24.6 (CH_2), 22.4 (NC*Me*); MS (EI) *m/z* 129 [M^+, 100]; HRMS (ESI) *m/z* calcd for $C_6H_{13}N_2O$ [M^+, 100] 129.1022, found 129.1021 (−1.9 ppm error). Spectroscopic data consistent with those reported in the literature.[200]

Lab book reference HFK1-060

(*S*)-1-(*tert*-Butoxycarbonyl)-proline (*S*)-265

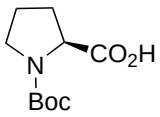

265

Boc_2O (1.04 g, 4.77 mmol, 1.5 eq) and Et_3N (0.61 mL, 4.3 mmol, 1.0 eq) were sequentially added to a stirred solution of (*S*)-proline (500 mg, 4.34 mmol, 1.0 eq) in

water-1,4-dioxane (1:1.5, 10 mL) at rt. The resulting solution was stirred at rt for 18 h. Then, the solvent was evaporated under reduced pressure and the residue was dissolved in EtOAc (30 mL). The solution was washed with 1 M $HCl_{(aq)}$ (30 mL) and brine (2 × 30 mL), dried ($MgSO_4$) and evaporated under reduced pressure to give *N*-Boc protected acid (*S*)-**265** (787 mg, 84%) as a white solid, mp 125-128 °C (lit.,[201] 137-139 °C); R_F (9:1 CH_2Cl_2-MeOH) 0.49; $[\alpha]_D$ −102.8 (*c* 1.0 in $CHCl_3$) [lit.[202], −92 (*c* 1.1 in $CHCl_3$)]; ^{1}H NMR (400 MHz, $CDCl_3$) (55:45 mixture of rotamers) δ 9.25 (s, 1H, OH), 4.35 (dd, J = 8.5, 3.0 Hz, 0.55H, NCH), 4.24 (dd, J = 8.5, 4.5 Hz, 0.45H, NCH), 3.61-3.50 (m, 0.45H, NCH), 3.51-3.40 (m, 1H, NCH), 3.40-3.29 (m, 0.55H, NCH), 2.36-2.17 (m, 1H, CH), 2.15-2.01 (m, 1H, CH), 2.00-1.81 (m, 2H, CH), 1.48 (s, 5H, CMe_3), 1.41 (s, 4H, CMe_3); ^{13}C NMR (100.6 MHz, $CDCl_3$) (rotamers) δ 179.1 (C=O, CO_2H), 175.2 (C=O, CO_2H), 156.6 (C=O, Boc), 154.0 (C=O, Boc), 81.6 (O*C*Me_3), 80.5 (O*C*Me_3), 59.3 (NCH), 59.0 (NCH), 47.1 (NCH_2), 46.5 (NCH_2), 31.0 (CH_2), 28.7 (CH_2), 28.5 (C*Me*$_3$), 28.4 (C*Me*$_3$), 24.5 (CH_2), 23.8 (CH_2). Spectroscopic data consistent with those reported in the literature.[201]

Lab Book Reference HFK1-012

1-*tert*-Butoxycarbonyl-2*S*-(2-benzimidazolyl)pyrrolidine (*S*)-266

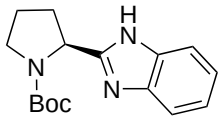

266

Et_3N (421 μL, 3.02 mmol, 1.3 eq) and isobutyl chloroformate (334 μL, 2.56 mmol, 1.1 eq) were sequentially added to a stirred solution of acid **265** (500 mg, 2.32 mmol, 1.0 eq) in THF (20 mL) at −20 °C under Ar. After stirring at −20 °C for 2 h, the resulting slurry was allowed to warm to rt and added to a stirred solution of *o*-phenylenediamine (276 mg, 2.56 mmol, 1.1 eq) in THF (10 mL) at −20 °C under Ar. The resulting solution was stirred at −20 °C for 1 h. After being allowed to warm to rt, the solution was stirred at rt for 18 h. Then, the solvent was evaporated under reduced pressure

and the residual solid was dissolved in EtOAc (20 mL). The solution was washed with 2 M $NaHCO_{3(aq)}$ (2 × 20 mL), dried ($MgSO_4$) and evaporated under reduced pressure to give the crude intermediate amide as a white solid. A solution of the crude amide in AcOH (15 mL) was stirred and heated at 75 °C for 18 h. After being allowed to cool to rt, the AcOH was evaporated under reduced pressure. Toluene (5 mL) was added and the solvent was evaporated under reduced pressure to give the crude product. Purification by flash column chromatography on silica with 80:20 to 70:30 hexane-EtOAc as eluent gave benzimidazole (*S*)-**266** (401 mg, 60%) as a white solid, mp 201-203 °C; R_F (3:2 hexane-EtOAc) 0.14; $[\alpha]_D$ −160.5 (*c* 1.0 in $CHCl_3$); IR (ATR) 2981, 1693 (C=O), 1678 (C=N), 1386, 1164, 747 cm^{-1}; ^1H NMR (400 MHz, $CDCl_3$) δ 10.69 (br s, 1H, NH), 7.79 (br s, 1H, Ar), 7.39 (br s, 1H, Ar), 7.23-7.14 (m, 2H, Ar), 5.11 (br d, J = 5.5 Hz, 1H, NCHAr), 3.40-3.38 (m, 2H, NCH), 3.06-2.99 (m, 1H, CH) 2.31-2.08 (m, 2H, CH), 2.06-1.86 (m, 1H, CH), 1.49 (s, 9H, CMe_3); ^{13}C NMR (100.6 MHz, $CDCl_3$) δ 156.7 (NCN or C=O), 155.0 (NCN or C=O), 142.3 (*ipso*-Ar), 134.2 (*ipso*-Ar), 122.9 (Ar), 122.0 (Ar), 119.6 (Ar), 111.0 (Ar), 80.8 (O*C*Me_3), 54.7 (NCH), 47.5 (NCH_2), 28.6 (C*Me*$_3$), 28.2 (CH_2), 25.0 (CH_2); MS (EI) *m/z* 288 [$(M + H)^+$, 100]; HRMS (ESI) *m/z* calcd for $C_{16}H_{21}N_3O_2$ [$(M + H)^+$, 100] 288.1707, found 288.1703 (−1.1 ppm error).
Lab book reference HFK1-050

2-Methylpropyl *N*-(2-[(2-methylpropoxy)carbonyl]aminophenyl)carbamate 268

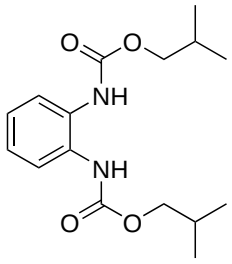

268

Et_3N (159 μL, 2.27 mmol, 1.3 eq) and isobutyl chloroformate (126 μL, 1.92 mmol, 1.1 eq) were sequentially added to a stirred solution of acid **238** (200 mg, 1.75 mmol, 1.0

eq) in THF (15 mL) at −20 °C under Ar. After stirring at −20 °C for 2 h, the resulting slurry was allowed to warm to rt and added to a stirred solution of *o*-phenylenediamine (104 mg, 1.92 mmol, 1.1 eq) in THF (5 mL) at −20 °C under Ar. The resulting solution was stirred at −20 °C for 1 h. After being allowed to warm to rt, the solution was stirred at rt for 18 h. Then, the solvent was evaporated under reduced pressure and the residual solid was dissolved in EtOAc (20 mL). The solution was washed with 2 M $NaHCO_{3(aq)}$ (2 × 20 mL), dried ($MgSO_4$) and evaporated under reduced pressure to give the crude intermediate as an oil. A solution of the crude intermediate in AcOH (5 mL) was stirred and heated at 75 °C for 18 h. After being allowed to cool to rt, the AcOH was evaporated under reduced pressure. Toluene (5 mL) was added and the solvent was evaporated under reduced pressure to give the crude product. Purification by flash column chromatography on silica with 90:10 to 80:20 to 60:40 hexane-EtOAc as eluent gave carbamate **268** (329 mg) as a white solid, mp 62-64 °C; IR (ATR) 3355 (NH), 2959, 2874, 1736 (C=O), 1679 (C=O), 1608, 1524, 1459, 1316 cm^{-1}; R_F (3:2 hexane-EtOAc) 0.83; ^1H NMR (400 MHz, $CDCl_3$) δ 7.46 (br s, 2H, Ar), 7.13-7.11 (m, 2H, Ar), 7.04 (br s, 2H, NH), 3.94 (d, J = 6.5 Hz, 4H, OCH_2), 2.01-1.91 (m, 2H, CH), 0.95 (d, J = 6.5 Hz, 12H, Me); ^{13}C NMR (100.6 MHz, $CDCl_3$) δ 155.1 (C=O), 130.2 (*ipso*-Ar), 125.8 (Ar), 124.5 (Ar), 71.9 (OCH_2), 28.1 (CH), 19.1 (Me); MS (EI) *m/z* 331 [$(M + Na)^+$, 100]; HRMS (ESI) *m/z* calcd for $C_{16}H_{24}N_2O_4$ [$(M + Na)^+$, 100] 331.1628, found 331.1630 (−0.9 ppm error).

Lab book reference HFK1-058

Methyl-2-methylpiperidine-3-carboxylate *cis*-270

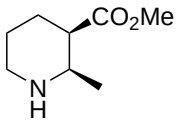

cis-**270**

Thionyl chloride (16 mL, 226 mmol, 12.0 eq) was added dropwise over 5 min to a stirred solution of acid **269** (2.58 g, 18.8 mmol, 1.0 eq) in MeOH (100 mL) at 0 °C under Ar.

The resulting solution was stirred and heated at reflux for 18 h. The mixture was then allowed to cool to rt and the solvent was evaporated under reduced pressure to give HCl salt **314**·HCl as a white powder. PtO_2 (427 mg, 1.88 mmol, 10 mol%, 0.1 eq) was added to a stirred solution of HCl salt **314**·HCl in AcOH (28 mL) at rt under Ar. The reaction flask was evacuated under reduced pressure and back-filled with Ar three times. After the final evacuation, H_2 was charged and the reaction mixture was stirred vigorously under a balloon of H_2 for 18 h. The solids were removed by filtration through Celite and washed with CH_2Cl_2 (60 mL). The solvent was evaporated under reduced pressure and CH_2Cl_2 (30 mL) was added. Then, 35% $NH_{3(aq)}$ (20 mL) was added and the two layers were separated. The organic layer was dried ($MgSO_4$) and evaporated under reduced pressure to give the crude product. Purification by flash column chromatography on silica with 93:5:2 CH_2Cl_2-MeOH-$NH_4OH_{(aq)}$ as eluent gave a 90:10 mixture (by ^{1}H NMR spectroscopy) of *cis*-**270** and *trans*-**270** (418 mg, 22%) as a pale yellow oil and amine *cis*-**270** (1.26 g, 67%) as a pale yellow oil, R_F (9:1 CH_2Cl_2-MeOH) 0.64; IR (ATR) 2937, 2858, 1723 (C=O), 1262, 1165 cm^{-1}; ^{1}H NMR (400 MHz, $CDCl_3$) δ 3.62 (s, OMe, 3H), 3.01 (ddd, J = 13.5, 4.0, 4.0 Hz, 1H, C*H*CO_2Me), 2.91-2.85 (m, 1H, NC*H*Me), 2.70 (br s, 1H, NH), 2.60 (ddd, J = 13.0, 13.0, 3.5 Hz, 1H, NCH), 2.49 (br dd, J = 13.0, 4.5 Hz, 1H, NCH), 2.01-1.88 (m, 1H, CH), 1.78-1.55 (m, 2H, CH), 1.40-1.24 (m, 1H, CH), 1.03 (d, J = 7.0 Hz, 3H, NCH*Me*); ^{13}C NMR (100.6 MHz, $CDCl_3$) δ 174.4 (C=O), 52.1 (N*C*HMe), 51.2 (OMe), 44.9 (NCH_2), 43.9 (*C*HCO_2Me), 26.0 (CH_2), 22.5 (CH_2), 18.8 (NCH*Me*); MS (EI) *m/z* 158 [M^+, 100]; HRMS (ESI) *m/z* calcd for $C_8H_{16}NO_2$ [M^+, 100] 158.1176, found 158.1175 (+0.3 ppm error). Diagnostic signal for *trans*-**270**: ^{1}H NMR (400 MHz, $CDCl_3$) 0.99 (d, J = 6.0 Hz, 3H, NCH*Me*). Spectroscopic data consistent with those reported in the literature for *cis*-**270**.[203]

Lab book reference HFK2-020

Methyl-1-methanesulfonyl-2-methylpiperidine-3-carboxylate *cis*-289

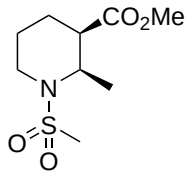

cis- **289**

Et_3N (1 mL, 7.5 mmol, 1.0 eq) was added dropwise to a stirred solution of amine **270** (1.18 g, 7.5 mmol, 1.0 eq) in CH_2Cl_2 (20 mL) at rt under Ar. The resulting solution was stirred at rt for 10 min and MsCl (1.8 mL, 23 mmol, 3.0 eq) was added dropwise. The resulting solution was stirred at rt for 18 h. The mixture was poured into water (20 mL) and extracted with CH_2Cl_2 (3 x 30 mL). The combined organics were dried ($MgSO_4$) and evaporated under reduced pressure to give the crude product as a white solid. Purification by flash column chromatography on silica with 85:15 to 50:50 hexane-EtOAc as eluent gave *N*-sulfonamide *cis*-**289** (1.6 g, 88%) as a white solid, mp 114-117 °C; R_F (1:1 hexane-EtOAc) 0.43; IR (ATR) 3005, 2961, 1731 (C=O), 1315, 1134, 784 cm^{-1}; ^1H NMR (400 MHz, $CDCl_3$) δ 4.55-4.49 (m, 1H, NC*H*Me), 3.66 (s, 3H, OMe), 3.63 (br dd, J = 13.0, 5.0 Hz, 1H, NCH), 2.93 (ddd, J = 13.0, 13.0, 2.5 Hz, 1H, NCH), 2.84 (s, 3H, SO_2Me), 2.71 (ddd, J = 12.5, 4.5, 4.5 Hz, 1H, C*H*CO_2Me), 1.95-1.83 (m, 1H, CH), 1.81-1.63 (m, 2H, CH), 1.60-1.41 (m, 1H, CH), 1.11 (d, J = 7.0 Hz, 3H, NCH*Me*); ^{13}C NMR (100.6 MHz, $CDCl_3$) δ 172.6 (C=O), 51.9 (OMe), 49.4 (N*C*HMe), 45.5 (*C*HCO_2Me), 40.2 (SO_2Me), 39.4 (NCH_2), 24.9 (CH_2), 20.1 (CH_2), 12.3 (NCH*Me*); MS (EI) *m/z* 258 [$(M + Na)^+$, 100]; HRMS (ESI) *m/z* calcd for $C_9H_{17}NO_4S$ [$(M + Na)^+$, 100] 258.0770, found 258.0766 (+1.3 ppm error).

Lab book reference HFK2-032

1-Methanesulfonyl-2-methylpiperidine-3-carboxylic acid *cis*-292

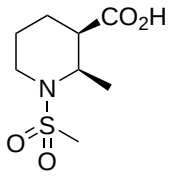

cis- **292**

A solution of LiOH (458 mg, 19.1 mmol, 5.0 eq) in H_2O (15 mL) was added dropwise to a stirred solution of ester *cis*-**289** (900 mg, 3.82 mmol, 1.0 eq) in MeOH (15 mL) at rt under Ar. The resulting solution was stirred and heated at 40 °C for 2 h. Then, the mixture was allowed to cool to rt and the solvent was evaporated under reduced pressure. Then, H_2O (10 mL) was added and the mixture acidified to pH 2 with 12 M $HCl_{(aq)}$ (1 mL). EtOAc (15 mL) was added and the two layers were separated. The aqueous layer was extracted with EtOAc (3 × 15 mL) and the combined organics were dried ($MgSO_4$) and evaporated under reduced pressure to give acid *cis*-**292** (789 mg, 93%) as a white solid, mp 116-119 °C; R_F (9:1 CH_2Cl_2-MeOH) 0.35; IR (ATR) 3212 (OH), 2978, 2956, 1732 (C=O), 1306, 1120 cm^{-1}; ^1H NMR (400 MHz, $CDCl_3$) δ 4.55-4.49 (m, 1H, NC*H*Me), 3.65 (br dd, J = 13.0, 4.0 Hz, 1H, NCH), 2.95 (ddd, J = 13.0, 13.0, 2.5 Hz, 1H, NCH), 2.86 (s, 3H, SO_2Me), 2.77 (ddd, J = 13.0, 4.0, 4.0 Hz, 1H, C*H*CO_2H), 1.99-1.87 (m, 1H, CH), 1.84-1.64 (m, 2H, CH), 1.62-1.43 (m, 1H, CH), 1.19 (d, J = 7.0 Hz, 3H, NCH*Me*); ^{13}C NMR (100.6 MHz, $CDCl_3$) δ 178.0 (C=O), 49.2 (N*C*HMe), 45.5 (SO_2Me), 40.3 (*C*HCO_2H), 39.3 (NCH_2), 24.9 (CH_2), 19.9 (CH_2), 12.3 (NCH*Me*); MS (EI) *m/z* 244 [$(M + Na)^+$, 100]; HRMS (ESI) *m/z* calcd for $C_8H_{15}NO_4S$ [$(M + Na)^+$, 100] 244.0614, found 244.0614 (−0.7 ppm error). Structure confirmed by X-ray crystallography (CCDC 1995344).

Lab book reference HFK2-037

1-Methanesulfonyl-2-methylpiperidine-3-carboxamide *cis*-293

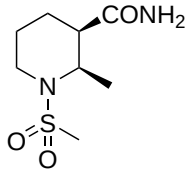

cis- **293**

DIPEA (132 μL, 0.759 mmol, 3.0 eq) and T3P (112 μL of a 50% wt solution in EtOAc, 0.380 mmol, 1.5 eq) were added sequentially to a stirred solution of acid *cis*-**292** (56 mg, 0.25 mmol, 1.0 eq) in CH_2Cl_2 (3 mL) at rt under Ar. The resulting solution was stirred at rt for 20 min. Then, 35% $NH_{3(aq)}$ (706 μL, 0.275 mmol, 1.1 eq) was added and the solution was stirred at rt for 1 h. The solution was poured into water (10 mL) and 3 M $HCl_{(aq)}$ (1 mL) was added. The two layers were separated and the aqueous layer was extracted with EtOAc (3 × 10 mL). The combined organics were washed with 2 M $NaOH_{(aq)}$ (10 mL) and brine (10 mL), dried ($MgSO_4$) and evaporated under reduced pressure to give amide *cis*-**293** (32 mg, 57%) as a white solid, mp 164-168 °C; R_F (9:1 CH_2Cl_2-MeOH) 0.39; IR (ATR) 3436 (NH), 3401 (NH), 2967, 2871, 1617 (C=O), 1134, 775 cm^{-1}; ^{1}H NMR (400 MHz, d_4-MeOH) δ 4.41-4.34 (m, 1H, NC*H*Me), 3.60 (br dd, J = 13.0, 4.0 Hz, 1H, NCH), 3.01 (ddd, J = 13.0, 13.0, 2.5 Hz, 1H, NCH), 2.92 (s, 3H, SO_2Me), 2.62 (ddd, J = 12.5, 4.5, 4.5 Hz, 1H, C*H*CONH$_2$), 1.89-1.67 (m, 3H, CH), 1.60-1.41 (m, 1H, CH), 1.16 (d, J = 7.0 Hz, 3H, NCH*Me*); ^{13}C NMR (100.6 MHz, d_4-MeOH) δ 177.6 (C=O), 51.6 (N*C*HMe), 47.4 (*C*HCONH$_2$), 40.4 (NCH_2), 40.3 (SO_2Me), 25.8 (CH_2), 21.2 (CH_2), 12.2 (NCH*Me*); MS (EI) m/z 243 [(M + Na)$^+$, 100]; HRMS (ESI) m/z calcd for $C_8H_{16}N_2O_3S$ [(M + Na)$^+$, 100] 243.0774, found 243.0771 (+3.5 ppm error).

Lab book reference HFK2-038

1-Methanesulfonyl-2-methylpiperidine-3-carbonitrile *cis*-294

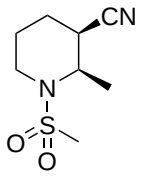

cis- **294**

Et_3N (88 μL, 0.63 mmol, 2.4 eq) and trifluoroacetic anhydride (45 μL, 0.32 mmol, 1.2 eq) were sequentially added dropwise to a stirred solution of amide *cis*-**293** (58 mg, 0.26 mmol, 1.0 eq) in THF (7 mL) at 0 °C under Ar. The resulting solution was stirred at 0 °C for 1 h. After being allowed to warm to rt, CH_2Cl_2 (10 mL) was added and the solution was washed with $NaHCO_{3(aq)}$ (10 mL). The aqueous layer was extracted with CH_2Cl_2 (2 × 10 mL). The combined organics were dried (Na_2SO_4) and evaporated under reduced pressure to give the crude product. Purification by flash column chromatography on silica with hexane and then 50:50 hexane-EtOAc as eluent gave nitrile *cis*-**294** (45 mg, 85%) as a cream solid, mp 108-111 °C; R_F (7:3 hexane-EtOAc) 0.48; IR (ATR) 2950, 2240 (C≡N), 1321, 1138, 769 (C=O), 1134, 775 cm^{-1}; ^1H NMR (400 MHz, $CDCl_3$) δ 4.44-4.38 (m, NC*H*Me), 3.63 (br dd, J = 13.0, 4.0 Hz, 1H, NCH), 2.97 (ddd, J = 13.0, 13.0, 3.0 Hz, 1H, NCH), 2.91 (ddd, J = 13.0, 4.5, 4.5 Hz, 1H, CHCN), 2.84 (s, 3H, SO_2Me), 2.11-1.97 (m, 1H, CH), 1.85 (dddd, J = 13.0, 13.0, 13.0, 4.0 Hz, 1H, CH), 1.79-1.71 (m, 1H, CH), 1.54 (ddddd, J = 13.0, 13.0, 13.0, 4.0, 4.0 Hz, 1H, CH), 1.38 (d, J = 7.0 Hz, 3H, NCH*Me*); ^{13}C NMR (100.6 MHz, $CDCl_3$) δ 119.8 (CN), 48.7 (N*C*HMe), 40.3 (SO_2Me), 38.8 (NCH_2), 32.2 (*C*HCN), 24.5 (CH_2), 22.5 (CH_2), 12.4 (NCH*Me*); MS (EI) *m/z* 225 [(M + Na)$^+$, 100]; HRMS (ESI) *m/z* calcd for $C_8H_{14}N_2O_2S$ [(M + Na)$^+$, 100] 225.0668, found 225.0657 (+4.5 ppm error). Structure confirmed by X-ray crystallography (CCDC 1995343).

Lab book reference HFK2-047

(1-Methanesulfonyl-*N*,2-dimethylpiperidine-3-carboxamide *cis*-295

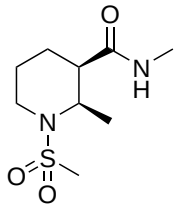

cis-**295**

DIPEA (347 μL, 2.0 mmol, 3.0 eq) and T3P (297 μL of a 50% wt solution in EtOAc, 0.996 mmol, 1.5 eq) were added sequentially to a stirred solution of acid *cis*-**292** (147 mg, 0.664 mmol, 1.0 eq) in CH_2Cl_2 (5 mL) at rt under Ar. The resulting solution was stirred at rt for 15 min. Then, methylamine (30 μL, 33% wt. in absolute EtOH, 0.731 mmol, 1.1 eq) was added and the solution was stirred at rt for 2 h. The solution was poured into water (10 mL) and 3 M $HCl_{(aq)}$ (1 mL) was added. The two layers were separated and the aqueous layer was extracted with EtOAc (3 $\times$ 10 mL). The combined organics were washed with 2 M $NaOH_{(aq)}$ (10 mL) and brine (10 mL), dried ($MgSO_4$) and evaporated under reduced pressure to give crude product. Purification by flash column chromatography on silica with EtOAc and then 90:10 CH_2Cl_2-MeOH as eluent gave amide *cis*-**295** (79 mg, 51%) as a colourless oil, R_F (9:1 CH_2Cl_2-MeOH) 0.52; IR (ATR) 3314 (NH), 2944, 1645 (C=O), 1317, 1133, 727 cm^{-1}; ^1H NMR (400 MHz, $CDCl_3$) δ 6.24 (br s, 1H, NH), 4.37-4.30 (m, 1H, NC*H*Me), 3.58 (br dd, J = 13.0, 4.5 Hz, 1H, NCH), 2.92 (ddd, J = 13.0, 13.0, 2.5 Hz, 1H, NCH), 2.82 (s, 3H, SO_2Me), 2.73 (d, J = 5.0 Hz, 3H, NH*Me*), 2.54 (ddd, J = 13.0, 4.0, 4.0 Hz, 1H, C*H*CONHMe), 1.81 (dddd, J = 13.0, 13.0, 13.0, 3.0 Hz, 1H, CH), 1.77-1.64 (m, 2H, CH), 1.49 (dddd, J = 13.0, 13.0, 13.0, 4.5, 4.5 Hz, 1H, CH), 1.11 (d, J = 7.0 Hz, 3H, NCH*Me*); ^{13}C NMR (100.6 MHz, $CDCl_3$) δ 172.6 (C=O), 50.6 (N*C*HMe), 46.8 (*C*HCONHMe), 40.1 (SO_2Me), 39.4 (NCH_2), 26.3 (NHMe), 24.9 (CH_2), 20.2 (CH_2), 11.9 (NCH*Me*); MS (EI) *m/z* 257 [$(M + Na)^+$, 100]; HRMS (ESI) *m/z* calcd for $C_9H_{18}N_2O_3S$ [$(M + Na)^+$, 100] 257.0930, found 257.0941 (−4.2 ppm error).

Lab book reference HFK2-048

1-Methanesulfonyl-2-methyl-3-(pyrrolidine-1-carbonyl)piperidine *cis*-296

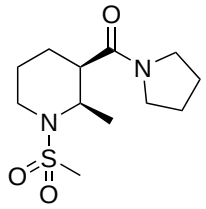

cis-**296**

DIPEA (246 μL, 1.41 mmol, 3.0 eq) and T3P (210 μL of a 50% wt solution in EtOAc, 0.705 mmol, 1.5 eq) were added sequentially to a stirred solution of acid *cis*-**292** (104 mg, 0.470 mmol, 1.0 eq) in CH_2Cl_2 (5 mL) at rt under Ar. The resulting solution was stirred at rt for 30 min. Then, pyrrolidine (43 μL, 0.517 mmol, 1.1 eq) was added and the solution was stirred at rt for 2 h. The solution was poured into water (10 mL) and 3 M $HCl_{(aq)}$ (1 mL) was added. The two layers were separated and the aqueous layer was extracted with EtOAc (3 $\times$ 10 mL). The combined organics were washed with 2 M $NaOH_{(aq)}$ (10 mL) and brine (10 mL), dried ($MgSO_4$) and evaporated under reduced pressure to give crude product. Purification by flash column chromatography on silica with EtOAc and then 95:5 CH_2Cl_2-MeOH as eluent gave amide *cis*-**296** (63 mg, 49%) as a colourless oil, R_F (19:1 CH_2Cl_2-MeOH) 0.42; IR (ATR) 2953, 1625 (C=O), 1320, 1139, 725 cm^{-1}; ^{1}H NMR (400 MHz, $CDCl_3$) δ 4.37-4.24 (m, 1H, NC*H*Me), 3.58 (br dd, J = 13.0, 4.5 Hz, 1H, NCH), 3.56-3.48 (m, 2H, NCH), 3.47-3.41 (m, 1H, NCH), 3.33-3.24 (m, 1H, NCH), 2.92 (ddd, J = 13.0, 13.0, 3.0 Hz, 1H, NCH), 2.79 (s, 3H, SO_2Me), 2.76 (ddd, J = 13.0, 4.0, 4.0 Hz, 1H, C*H*CON), 1.97 (dddd, J = 13.0, 13.0, 13.0, 4.0 Hz, 1H, CH), 1.94-1.86 (m, 2H, CH), 1.81-1.74 (m, 2H, CH), 1.73-1.69 (m, 1H, CH), 1.66-1.56 (m, 1H, CH), 1.51 (ddddd, J = 13.0, 13.0, 13.0, 4.0, 4.0 Hz, 1H, CH), 1.13 (d, J = 7.0 Hz, 3H, NCH*Me*); ^{13}C NMR (100.6 MHz, $CDCl_3$) δ 170.6 (C=O), 48.6 (N*C*HMe), 46.4 (NCH_2), 46.0 (NCH_2), 45.4 (CHCON), 40.2 (SO_2Me), 39.3 (NCH_2), 26.3 (CH_2), 25.0 (CH_2), 24.1 (CH_2), 20.4 (CH_2), 12.1 (NCH*Me*); MS (EI) *m/z* 297 [(M + Na)$^+$, 100]; HRMS (ESI) *m/z* calcd for $C_{12}H_{22}N_2O_3S$ [(M + Na)$^+$, 100] 297.1243, found 297.1250 (−2.5 ppm error).

Lab book reference HFK2-050

Methyl-1-acetyl-2-methylpiperidine-3-carboxylate *cis*-290

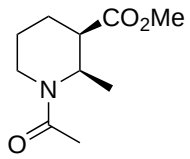

cis-**290**

Ac_2O (7.2 mL, 76 mmol, 6.0 eq) was added dropwise to a stirred 90:10 mixture of piperidines *cis*-**270** and *trans*-**270** (2.00 g, 12.73 mmol, 1.0 eq) in pyridine (12 mL) at rt under Ar. The resulting solution was stirred at rt for 18 h under Ar. Then, the solvent was evaporated under reduced pressure to give the crude product. Purification by flash column chromatography on silica with EtOAc as eluent gave *N*-acetamide *cis*-**290** (2.11 g, 83%) as a pale yellow oil, R_F (EtOAc) 0.24; IR (ATR) 2950, 1731 (C=O, CO_2Me), 1634 (C=O, amide), 1421, 1161, 1018; cm^{-1}; ^1H NMR (400 MHz, $CDCl_3$) (60:40 mixture of rotamers) δ 5.20 (dq, J = 7.0, 7.0 Hz, 0.6H, NC*H*Me), 4.42 (br dd, J = 13.5, 4.0 Hz, 0.4H, NCH), 4.33 (dq, J = 7.0, 7.0 Hz, 0.4H, NC*H*Me), 3.64 (s, 1.2H, OMe), 3.60 (s, 1.8, OMe), 3.52 (br dd, J = 13.5, 4.5 Hz, 0.6H, NCH), 3.04 (ddd, J = 13.5, 13.5, 3.0 Hz, 0.6H, NCH), 2.63-2.42 (m, 1.4H, CH), 2.07 (s, 1.2H, C(O)Me), 2.00 (s, 1.8H, C(O)Me), 1.91-1.60 (m, 3H, CH), 1.45-1.20 (m, 1H, CH), 1.06 (d, J = 7.0 Hz, 1.2H, NCH*Me*), 0.95 (d, J = 7.0 Hz, 1.8H, NCH*Me*); ^{13}C NMR (100.6 MHz, $CDCl_3$) (rotamers) δ 173.1 (C=O), 172.7 (C=O), 168.9 (C=O), 51.9 (OMe), 51.7 (OMe), 50.4 (CH), 45.7 (CH), 44.5 (CH), 44.5 (CH), 40.9 (NCH_2), 35.3 (NCH_2), 25.2 (CH_2), 24.3 (CH_2), 22.1 (C(O)*Me*), 21.5 (C(O)*Me*), 20.5 (CH_2), 20.4 (CH_2), 13.0 (NCH*Me*), 12.0 (NCH*Me*); MS (EI) *m/z* 222 [(M + Na)$^+$, 100]; HRMS (ESI) *m/z* calcd for $C_{10}H_{17}NO_3$ [(M + Na)$^+$, 100] 222.1101, found 222.1096 (+2.0 ppm error).

Lab book reference HFK2-034

1-[3-(Hydroxymethyl)-2-methylpiperidin-1-yl]ethan-1-one *cis*-291

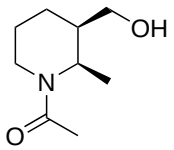

cis-**291**

$LiBH_4$ (0.58 mL of a 4 M solution in THF, 2.3 mmol, 2.3 eq) was added dropwise to a stirred solution of ester *cis*-**290** (200 mg, 1.00 mmol, 1.0 eq) in THF (6 mL) at 0 °C under Ar. The resulting solution was stirred at rt for 18 h. TLC indicated remaining starting material *cis*-**290**. The reaction was cooled to 0 °C and $LiBH_4$ (0.50 mL of a 4 M solution in THF, 2.0 mmol, 2.0 eq) was added. The resulting solution was stirred at rt for 6 h. Saturated $NH_4Cl_{(aq)}$ (10 mL) was added and the mixture was extracted with EtOAc (3 × 10 mL). The combined organic extracts were dried ($MgSO_4$) and evaporated under reduced pressure to give alcohol *cis*-**291** (110 mg, 64%) as a pale yellow oil, R_F (9:1 CH_2Cl_2-MeOH) 0.42; IR (ATR) 3377 (OH), 2931, 2863 (C=O), 1611, 1426, 727 cm^{-1}; ^1H NMR (400 MHz, $CDCl_3$) (50:50 mixture of rotamers) δ 4.83 (m, 0.5H, NC*H*Me), 4.39-4.29 (m, 0.5H, NCH), 4.16-4.02 (m, 1H, NC*H*Me and OH), 3.72 (s, 0.5H, OH), 3.52-3.44 (m, 0.5H, NCH), 3.43-3.36 (m, 0.5H, HOC*H*), 3.34-3.21 (m, 1.5H, C*H*CH_2OH and HOC*H*), 3.01 (ddd, J = 13.0, 13.0, 3.0 Hz, 0.5H, NCH), 2.49 (ddd, J = 13.0, 13.0, 3.0 Hz, 0.5H, NCH), 1.99 (s, 1.5H, C(O)Me), 1.95 (s, 1.5H, C(O)Me), 1.85-1.75 (m, 0.5H, CH), 1.73-1.50 (m, 1H, CH), 1.46-1.39 (m, 0.5H, CH), 1.34-1.09 (m, 2H, CH), 1.01 (d, J = 7.0 Hz, 1.5H, NCH*Me*), 0.89 (d, J = 7.0 Hz, 1.5H, NCH*Me*); ^{13}C NMR (100.6 MHz, $CDCl_3$) (rotamers) δ 169.3 (C=O), 169.0 (C=O), 64.3 (OCH_2), 63.9 (OCH_2), 50.2 (N*C*HMe), 44.8 (N*C*HMe), 42.1 (*C*HCH_2OH), 41.49 (NCH_2), 41.46 (*C*HCH_2OH), 36.1 (NCH_2), 25.7 (CH_2), 24.8 (CH_2), 21.9 (C(O)Me), 21.51 (CH_2), 21.47 (CH_2), 21.4 (C(O)Me), 11.2 (NCH*Me*), 10.6 (NCH*Me*); MS (EI) *m/z* 194 [(M + Na)$^+$, 100]; HRMS (ESI) *m/z* calcd for $C_9H_{17}NO_2$ [(M + Na)$^+$, 100] 194.1151, found 194.1142 (−5.0 ppm error).

Lab book reference HFK2-062

1-*tert*-Butyl 3-methyl-2-methylpiperidine-1,3-dicarboxylate *cis*-271 and methyl-2-methylpiperidine-3-carboxylate *trans*-271

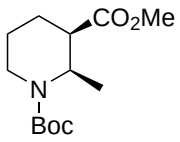

cis-**271**

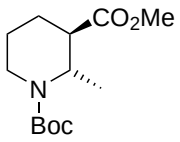

trans-**271**

Et_3N (432 μL, 7.00 mmol, 1.0 eq) and a solution of Boc_2O (1.58 g, 7.24 mmol, 1.1 eq) in CH_2Cl_2 (6 mL) were added sequentially to a stirred solution of a 90:10 mixture of piperidines *cis*-**270** and *trans*-**270** (1.10 g, 7.00 mmol, 1.0 eq) in CH_2Cl_2 (18 mL) at 0 °C under Ar. The resulting solution was stirred at rt for 18 h. The solvent was evaporated under reduced pressure. The residue was dissolved in Et_2O (25 mL) and the solution was washed with 1 M $HCl_{(aq)}$ (2 × 20 mL) and saturated $NaHCO_{3(aq)}$ (20 mL), dried ($MgSO_4$) and evaporated under reduced pressure to give the crude product as a colourless oil. Purification by flash column chromatography on silica with 95:5 to 90:10 hexane-EtOAc as eluent gave methyl ester *cis*-**271** (1.41 g, 78%) as a white solid, mp 49-51 °C (lit.,[101] 37 °C); R_F (4:1 hexane-EtOAc) 0.42; IR (ATR) 2974, 2950, 1736 (C=O, CO_2Me), 1687 (C=O, Boc), 1408, 1132, 856 cm^{-1}; ^1H NMR (400 MHz, $CDCl_3$) (50:50 mixture of rotamers) δ 4.78 (br s, 0.5H, NC*H*Me), 4.60 (br s, 0.5H, NC*H*Me), 3.95 (br d, J = 12.0 Hz, 0.5H, NCH), 3.82 (br d, J = 12.0 Hz, 0.5H, NCH), 3.65 (s, 1.5H, OMe), 3.63 (s, 1.5H, OMe), 2.84-2.64 (m, 1H, CH), 2.58 (ddd, J = 13.0, 4.0, 4.0 Hz, 1H, C*H*CO_2Me), 1.86-1.57 (m, 3H, CH), 1.47-1.36 (m, 10H, C*Me*$_3$ and CH), 0.98 (d, J = 7.0 Hz, 3H, NCH*Me*); ^{13}C NMR (100.6 MHz, $CDCl_3$) (rotamers) δ 173.4 (C=O, CO_2Me), 154.6 (C=O, Boc), 79.7 (O*C*Me_3), 51.8 (OMe), 51.7 (OMe), 48.0 (N*C*HMe), 46.8 (N*C*HMe), 45.2 (*C*HCO_2Me), 44.8 (*C*HCO_2Me), 38.6 (NCH_2), 37.5 (NCH_2), 28.5 (C*Me*$_3$), 24.9 (CH_2), 24.5 (CH_2), 20.5 (CH_2), 12.3 (NCH*Me*), 12.0 (NCH*Me*); MS (EI) *m/z* 280 [$(M + Na)^+$, 100]; HRMS (ESI) *m/z* calcd for $C_{13}H_{23}NO_4$ [$(M + Na)^+$, 100] 280.1519, found 280.1525 (+1.9 ppm error) and *trans*-**271** (83 mg, 4%) as a yellow

oil, R_F (4:1 hexane-EtOAc) 0.35; IR (ATR) 2973, 1735 (C=O, CO_2Me), 1686 (C=O, Boc), 1416, 1174, 862 cm^{-1}; ^1H NMR (400 MHz, $CDCl_3$) 4.81 (q, J = 7.0 Hz, 1H, NC*H*Me), 3.88 (br dd, J = 13.0, 4.0 Hz, 1H, NCH), 3.63 (s, 3H, OMe), 2.75 (ddd, J = 13.0, 13.0, 3.0 Hz, 1H, NCH), 2.39-2.29 (m, 1H, C*H*CO_2Me), 1.98 (br dd, J = 13.0, 3.0 Hz, 1H, CH), 1.77-1.65 (m, 1H, CH), 1.65-1.51 (m, 1H, CH), 1.45-1.37 (m, 10H, C*Me*$_3$ and CH), 1.16 (d, J = 7.0 Hz, 3H, NCH*Me*); ^{13}C NMR (100.6 MHz, $CDCl_3$) δ 173.9 (C=O, CO_2Me), 154.9 (C=O, Boc), 79.2 (O*C*Me_3), 51.8 (OMe), 47.3 (N*C*HMe), 44.0 (*C*HCO_2Me), 37.8 (NCH_2), 28.4 (C*Me*$_3$), 21.8 (CH_2), 20.5 (CH_2), 16.5 (NCH*Me*); MS (EI) *m/z* 280 [(M + Na)$^+$, 100]; HRMS (ESI) *m/z* calcd for $C_{13}H_{23}NO_4$ [(M + Na)$^+$, 100] 280.1519, found 280.1522 (−1.0 ppm error). Spectroscopic data consistent with those reported in the literature for *cis*-**271**.[101]

Lab book reference HFK1-096

1-[(2,2-Dimethylpropanoyl)oxy]-2-methylpiperidine-3-carboxylic acid *cis*-315

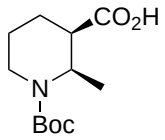

cis-**315**

A solution of LiOH (303 mg, 12.7 mmol, 5.0 eq) in H_2O (12 mL) was added dropwise to a stirred solution of ester *cis*-**271** (652 mg, 2.53 mmol, 1.0 eq) in MeOH (12 mL) at rt under Ar. The resulting solution was stirred at rt for 2 h. Then, the solvent was evaporated under reduced pressure. Then, H_2O (15 mL) was added and the mixture acidified to pH 2 with 12 M $HCl_{(aq)}$ (1 mL). EtOAc (20 mL) was added and the two layers were separated. The aqueous layer was extracted with EtOAc (3 × 15 mL) and the combined organics were dried ($MgSO_4$) and evaporated under reduced pressure to give acid *cis*-**315** (462 mg, 75%) as a white solid, mp 167-169 °C; R_F (1:1 hexane-EtOAC) 0.26; IR (ATR) 2975, 1733 (C=O, CO_2H), 1691 (C=O, Boc), 1413, 1134, 732 cm^{-1}; ^1H NMR (400 MHz, $CDCl_3$) δ 4.96-4.56 (m, 1H, NC*H*Me), 4.06-3.81 (m, 1H, NCH), 2.86-2.70 (m, 1H NCH), 2.65 (ddd, J = 13.0, 4.0, 4.0 Hz, 1H, C*H*CO_2H),

1.91-1.78 (m, 1H, CH), 1.78-1.56 (m, 2H, CH), 1.44 (s, 9H, CMe_3 and CH), 1.42-1.36 (m, 1H, CH), 1.08 (d, J = 7.0 Hz, 3H, NCH*Me*); ^{13}C NMR (100.6 MHz, $CDCl_3$) (rotamers) δ 178.4 (C=O, CO_2H), 154.8 (C=O, Boc), 80.0 (O*C*Me_3), 47.9 (N*C*HMe), 46.6 (N*C*HMe), 45.1 (*C*HCO_2H), 38.5 (NCH_2), 37.6 (NCH_2), 28.6 (C*Me*$_3$), 24.7 (CH_2), 20.4 (CH_2), 12.2 (NCH*Me*); MS (EI) *m/z* 266 [$(M + Na)^+$, 100]; HRMS (ESI) *m/z* calcd for $C_{12}H_{21}NO_4$ [$(M + Na)^+$, 100] 266.1363, found 266.1365 (−1.0 ppm error). Spectroscopic data consistent with those reported in the literature.[204]

Lab book reference HFK3-032

tert-Butyl-3-carbamoyl-2-methylpiperidine-1-carboxylate *cis*-316

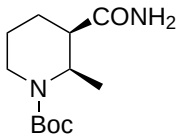

cis-**316**

DIPEA (917 μL, 5.26 mmol, 3.0 eq) and T3P (1.57 mL of a 50% wt solution in EtOAc, 5.27 mmol, 3.0 eq) were added sequentially to a stirred solution of acid *cis*-**315** (427 mg, 1.75 mmol, 1.0 eq) in CH_2Cl_2 (40 mL) at rt under Ar. The resulting solution was stirred at rt for 30 min. Then, 35% $NH_{3(aq)}$ (2.64 mL, 8.77 mmol, 5.0 eq) was added and the solution was stirred at rt for 18 h. The solution was poured into water (30 mL) and 3 M $HCl_{(aq)}$ (1 mL) was added. The two layers were separated and the aqueous layer was extracted with EtOAc (3 × 25 mL). The combined organics were washed with 2 M $NaOH_{(aq)}$ (25 mL) and brine (25 mL), dried ($MgSO_4$) and evaporated under reduced pressure to give crude product. Purification by flash column chromatography on silica with 95:5 hexane-CH_2Cl_2 as eluent gave amide *cis*-**316** (332 mg, 78%) as a white solid, mp 127-129 °C; R_F (9:1 CH_2Cl_2-MeOH) 0.36; IR (ATR) 3334 (NH), 2976, 1660 (C=O), 1404, 1157, 730 cm^{-1}; ^{1}H NMR (400 MHz, $CDCl_3$) δ 5.86 (br s, 2H, NH_2), 4.69-4.52 (m, 1H, NC*H*Me), 3.93-3.83 (m, 1H, NCH), 2.77 (ddd, J = 13.0, 3.0 Hz, 1H, NCH), 2.48 (ddd, J = 12.0, 4.0, 4.0 Hz, 1H, C*H*$CONH_2$), 1.88-1.61 (m, 3H, CH), 1.43 (s, 9H, CMe_3), 1.43-1.33 (m, 1H, CH), 1.07 (d, J = 7.0 Hz, 3H, NCH*Me*); ^{13}C NMR

(100.6 MHz, $CDCl_3$) δ 175.1 (C=O, $CONH_2$), 154.9 (C=O, Boc), 79.9 (O*C*Me_3), 48.3 (N*C*HMe), 45.9 (*C*H$CONH_2$), 38.3 (NCH_2), 28.6 (C*Me*$_3$), 24.8 (CH_2), 20.6 (CH_2), 11.9 (NCH*Me*); MS (EI) *m/z* 265 [$(M + Na)^+$, 100]; HRMS (ESI) *m/z* calcd for $C_{12}H_{22}N_2O_3$ [$(M + Na)^+$, 100] 265.1523, found 265.1526 (−1.2 ppm error).

Lab book reference HFK3-034

2-Methylpiperidine-3-carboxamide hydrochloride *cis*-276

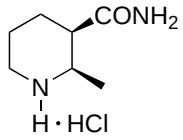

cis-**276**

N-Boc protected amide *cis*-**316** (56 mg, 0.23 mmol, 1.0 eq) was dissolved in HCl (10 mL of a 2 M solution in Et_2O, 20 mmol, 87 eq) and the resulting solution was stirred at rt for 18 h. Then, the solvent was evaporated under reduced pressure to give hydrochoride salt *cis*-**276**·HCl (46 mg) as a yellow oil, IR (ATR) 3162 (NH), 2952, 1634 (C=O), 748 cm^{-1}; ^1H NMR (400 MHz, D_2O) δ 4.43 (br s, 2H, NC*H*Me and NH) 2.92 (br s, 2H, NCH), 2.55 (br s, 1H, C*H*$CONH_2$), 2.35 (br s, 1H, NH), 1.50-1.29 (m, 4H, CH), 0.85 (br s, 3H, NCH*Me*); ^{13}C NMR (100.6 MHz, D_2O) δ 177.7 (C=O), 52.6 (N*C*HMe), 43.5 (NCH_2), 40.5 (*C*H$CONH_2$), 24.8 (CH_2), 17.8 (CH_2), 15.2 (NCH*Me*); MS (EI) *m/z* 143 [$(M)^+$, 100]; HRMS (ESI) *m/z* calcd for $C_7H_{15}N_2O$ [$(M)^+$, 100] 143.1179, found 143.1179 (+0.2 ppm error).

Lab book reference HFK3-038

.

***tert*-Butyl-3-cyano-2-methylpiperidine-1-carboxylate *cis*-317**

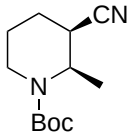

cis-**317**

Et_3N (249 μL, 1.78 mmol, 2.4 eq) and trifluoroacetic anhydride (126 μL, 0.892 mmol,

1.2 eq) were sequentially added dropwise to a stirred solution of amide *cis*-**316** (180 mg, 0.743 mmol, 1.0 eq) in THF (18 mL) at 0 °C under Ar. The resulting solution was stirred at 0 °C for 1 h. After being allowed to warm to rt, CH_2Cl_2 (25 mL) was added and the solution was washed with $NaHCO_{3(aq)}$ (20 mL). The aqueous layer was extracted with CH_2Cl_2 (2 × 20 mL). The combined organics were dried (Na_2SO_4) and evaporated under reduced pressure to give the crude product as a yellow liquid. Purification by flash column chromatography on silica with 85:15 hexane-EtOAc as eluent gave nitrile *cis*-**317** (134 mg, 80%) as a colourless oil, R_F (4:1 hexane-EtOAc) 0.37; IR (ATR) 2977, 2243 (C≡N), 1690 (C=O), 1409, 1160, 1139 cm^{-1}; ^1H NMR (400 MHz, $CDCl_3$) δ 4.72-4.51 (m, 1H, NC*H*Me), 3.94-3.90 (m, 1H, NCH), 2.84-2.69 (m, 2H, NCH and CHCN), 1.99-1.93 (m, 1H, CH), 1.82 (dddd, J = 13.0, 13.0, 13.0, 4.0 Hz, 1H, CH), 1.70-1.65 (m, 1H, CH), 1.43 (s, 9H, CMe_3), 1.41-1.31 (m, 1H, CH), 1.28 (d, J = 7.0 Hz, 3H, NCH*Me*); ^{13}C NMR (100.6 MHz, $CDCl_3$) δ 154.3 (C=O), 120.5 (CN), 80.4 (O*C*Me$_3$), 46.7 (N*C*HMe), 37.4 (NCH_2), 31.6 (*C*HCN), 28.5 (C*Me*$_3$), 24.4 (CH_2), 22.9 (CH_2), 12.3 (NCH*Me*); MS (EI) *m/z* 247 [(M + Na)$^+$, 100]; HRMS (ESI) *m/z* calcd for $C_{12}H_{20}N_2O_2$ [(M + Na)$^+$, 100] 247.1417, found 247.1421 (−1.4 ppm error).

Lab book reference HFK3-036

2-Methylpiperidine-3-carbonitrile hydrochloride *cis*-279

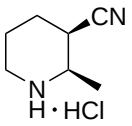

cis-**279**

N-Boc protected nitrile *cis*-**317** (78 mg, 0.35 mmol, 1.0 eq) was dissolved in HCl (5 mL of a 2 M solution in Et_2O, 10 mmol, 29 eq) and the resulting solution was stirred at rt for 36 h. Then, the solvent was evaporated under reduced pressure to give hydrochoride salt *cis*-**279**·HCl (48 mg) as a white solid, mp 188-190 °C; R_F (1:1 hexane-EtOAc) 0.75; IR (ATR) 2921, 2703, 2243 (C≡N), 1588, 1446, 1021 cm^{-1}; ^1H NMR (400 MHz, d_4-MeOH) 3.52 (m, 1H, NC*H*Me), 3.46 (m, 1H, NCH), 3.40-3.31 (m, 1H, NCH), 3.12-3.00

(m, 1H, CHCN), 2.12 (m, 1H, CH), 2.01-1.80 (m, 3H, CH), 1.47 (d, J = 7.0 Hz, 3H, NCH*Me*); ^{13}C NMR (100.6 MHz, d_4-MeOH) 118.7 (CN), 52.4 (N*C*HMe), 44.8 (NCH_2), 32.7 (*C*HCN), 26.0 (CH_2), 20.0 (CH_2), 17.5 (NCH*Me*); MS (EI) m/z 125 [M^+, 100]; HRMS (ESI) m/z calcd for $C_7H_{13}N_2$ [M^+, 100] 125.1073, found 125.1073 (+0.4 ppm error).

Lab book reference HFK3-042

tert-Butyl-3-(hydroxymethyl)-2-methylpiperidine-1-carboxylate *cis*-318

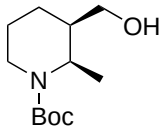

cis-**318**

A solution of methyl ester *cis*-**271** (89 mg, 0.35 mmol, 1.0 eq) in THF (2 mL) was added dropwise to a stirred suspension of lithium aluminium hydride (50 mg, 1.32 mmol, 3.8 eq) in THF (6 mL) at 0 °C under Ar. The resulting mixture was stirred at 0 °C for 1 h and then 2 M $NaOH_{(aq)}$ (50 μL), Et_2O (2 mL) and $MgSO_4$ (100 mg) were added dropwise slowly (care - exothermic quench). The mixture was allowed to warm to rt and the solids were removed by filtration through Celite and evaporated under reduced pressure to give alcohol *cis*-**318** (69 mg, 73%) as a colourless oil, R_F (7:3 hexane-EtOAc) 0.20; IR (ATR) 3434 (OH), 2974, 2930, 2862, 1687, 1661 (C=O), 1412, 1364, 1158 cm^{-1}; ^{1}H NMR (400 MHz, $CDCl_3$) δ 4.39 (br s, 1H, NC*H*Me), 3.82 (br s, 1H, NCH), 3.40-3.39 (m, 2H, HOC*H*), 2.76-2.70 (m, 1H, NCH), 2.49-2.30 (m, 1H, OH), 1.92-1.71 (m, 1H, C*H*CH_2OH), 1.70-1.49 (m, 2H, CH), 1.36-1.43 (m, 10H, C*Me*$_3$ and CH), 1.28-1.08 (m, 1H, CH), 0.96 (d, J = 7.0 Hz, 3H, NCH*Me*); ^{13}C NMR (100.6 MHz, $CDCl_3$) δ 155.1 (C=O, Boc), 79.4 (O*C*Me_3), 65.0 (OCH_2), 47.4 (N*C*HMe), 41.9 (*C*HCH_2OH), 38.6 (NCH_2), 28.6 (C*Me*$_3$), 25.4 (CH_2), 21.8 (CH_2), 10.9 (NCH*Me*); MS (EI) m/z 252 [(M + Na)$^+$, 100]; HRMS (ESI) m/z calcd for $C_{12}H_{23}NO_3$ [(M + Na)$^+$, 100] 252.1570, found 252.1574 (−1.6 ppm error).

Lab book reference HFK2-002

***tert*-Butyl-3-(methoxymethyl)-2-methylpiperidine-1-carboxylate *cis*-319**

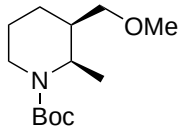

cis-**319**

NaH (79 mg of a 60% dispersion in mineral oil, 1.96 mmol, 1.6 eq) was added portionwise to a stirred solution of alcohol *cis*-**318** (282 mg, 1.23 mmol, 1.0 eq) in THF (6 mL) at −78 °C under Ar. Then, methyl iodide (139 μL, 2.22 mmol, 1.8 eq) was added. After being allowed to warm to rt, the resulting mixture was stirred at rt for 18 h. 35% $NH_{3(aq)}$ (20 mL) was added and the mixture was extracted with EtOAc (3 × 15 mL). The combined organic extracts were dried (Na_2SO_4) and evaporated under reduced pressure to give the crude product as a yellow oil. Purification by flash column chromatography on silica with 80:20 hexane-EtOAc as eluent gave methyl ether *cis*-**319** (286 mg, 96%) as a pale yellow oil, R_F (3:2 hexane-EtOAc) 0.67; IR (ATR) 2975, 2929, 2860, 1686 (C=O), 1409, 1364, 1140 cm^{-1}; ^1H NMR (400 MHz, $CDCl_3$) δ 4.51-4.20 (m, 1H, NC*H*Me), 3.98-3.73 (m, 1H, NCH), 3.27 (s, 3H, OMe), 3.16-3.07 (m, 2H, OCH), 2.72 (br s, 1H, NCH), 1.95-1.83 (m, 1H, C*H*CH_2OMe), 1.64-1.45 (m, 2H, CH), 1.42-1.31 (m, 10H, C*Me*$_3$ and CH), 1.29-1.09 (m, 1H, CH), 0.92 (d, J = 7.0 Hz, 3H, NCH*Me*); ^{13}C NMR (100.6 MHz, $CDCl_3$) (rotamers) δ 155.0 (C=O, Boc), 79.0 (O*C*Me_3), 75.1 (*C*H_2OMe), 58.8 (CH_2O*Me*), 48.0 (N*C*HMe), 47.1 (N*C*HMe), 39.1 (*C*HCH$_2$OMe), 38.2 (NCH_2), 28.5 (C*Me*$_3$), 25.3 (CH_2), 22.0 (CH_2), 10.9 (NCH*Me*); MS (EI) *m/z* 266 [(M + Na)$^+$, 100]; HRMS (ESI) *m/z* calcd for $C_{13}H_{25}NO_3$ [(M + Na)$^+$, 100] 266.1727, found 266.1729 (+0.8 ppm error).

Lab book reference HFK2-007

3-Ethoxy-2-methylpiperidine hydrochloride *cis*-281

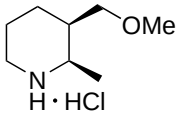

cis-**281**

N-Boc protected hydroxymethyl *cis*-**319** (90 mg, 0.37 mmol, 1.0 eq) was dissolved in HCl (2 mL of a 2 M solution in Et_2O, 4 mmol, 11.0 eq) and the resulting solution was stirred at rt for 18 h. TLC indicated that starting material remained. The solution was stirred and heated at 30 °C for 2 h. After being allowed to cool to rt, the solvent was evaporated under reduced pressure to give hydrochoride salt *cis*-**281**·HCl (69 mg) as a white solid, mp 71-73 °C; R_F (9:1 CH_2Cl_2-MeOH) 0.36; IR (ATR) 2952, 2810, 1456, 1135, 1097, 474 cm^{-1}; ^1H NMR (400 MHz, $CDCl_3$) δ 9.64 (br s, 1H, NH), 8.93 (br s, 1H, NH), 3.65 (br s, 1H, NC*H*Me), 3.37 (dd, J = 10.0, 6.0 Hz, 1H, C*H*OMe), 3.31-3.27 (m, 1H, C*H*OMe), 3.29 (s, 3H, OMe), 3.15-3.01 (m, 2H, NCH), 2.36-2.27 (m, 1H, CH), 1.90-1.80 (m, 2H, CH), 1.66-1.44 (m, 2H, CH), 1.36 (d, J = 7.0 Hz, 3H, NCH*Me*); ^{13}C NMR (100.6 MHz, $CDCl_3$) δ 73.0 (*C*H_2OMe), 59.1 (OMe), 51.0 (N*C*HMe), 40.2 (NCH_2), 36.2 (*C*HCH_2OMe), 22.4 (CH_2), 21.0 (CH_2), 12.0 (NCH*Me*); MS (EI) *m/z* 144 [M^+, 100]; HRMS (ESI) *m/z* calcd for $C_8H_{18}NO$ [M^+, 100] 144.1383, found 144.1385 (−1.6 ppm error).

Lab book reference HFK2-011

1-*tert*-Butyl 2-methyl-3-methylpiperidine-1,2-dicarboxylate *cis*-230 and 1-*tert*-Butyl 2-methyl-3-methylpiperidine-1,2-dicarboxylate *trans*-230

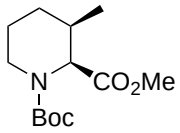

cis-**230**

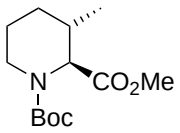

trans-**230**

PtO_2 (72 mg, 0.32 mmol, 5 mol%, 0.1 eq.) was added to a stirred solution of pyridine ester **272** (956 mg, 6.32 mmol, 1.0 eq.) in AcOH (7 mL) at rt under Ar. The reaction

flask was evacuated under reduced pressure and back-filled with Ar three times. After the final evacuation, H_2 was charged and the reaction mixture was stirred vigorously under a balloon of H_2 for 5 h. The solids were removed by filtration through Celite and washed with MeOH (30 mL). The filtrate was evaporated under reduced pressure to give the crude product which was dissolved in CH_2Cl_2 (10 mL) and $NH_4OH_{(aq)}$ (10 mL) was added. The two layers were separated and the aqueous layer was extracted with CH_2Cl_2 (3 × 20 mL). The combined organics were dried (Na_2SO_4) and evaporated under reduced pressure to give crude product which contained (by ^{1}H NMR spectroscopy) an 85:15 mixture of piperidines *cis*- and *trans*-**273**. Et_3N (2.27 mL, 16.3 mmol, 3.0 eq) and a solution of Boc_2O (1.78 g, 8.15 mmol, 1.5 eq) in CH_2Cl_2 (10 mL) were added sequentially to a stirred solution of the 85:15 mixture of piperidines *cis*- and *trans*-**273** (854 mg, 5.44 mmol, 1.0 eq) in CH_2Cl_2 (8 mL) at 0 °C under Ar. The resulting solution was stirred at rt for 60 h. The solvent was evaporated under reduced pressure. The residue was dissolved in Et_2O (20 mL) and the solution was washed with 1 M $HCl_{(aq)}$ (2 × 20 mL) and saturated $NaHCO_{3(aq)}$ (20 mL), dried ($MgSO_4$) and evaporated under reduced pressure to give the crude product as an orange solid. Purification by flash column chromatography on silica with 95:5 to 90:10 to 80:20 hexane-EtOAc as eluent gave ester *cis*-**230** (997 mg, 70%) as a yellow oil, R_F (9.5:0.5 hexane-EtOAc) 0.24 IR (ATR) 2934, 1738 (C=O, CO_2Me), 1692 (C=O, Boc), 1364, 1152, 871 cm^{-1}; ^{1}H NMR (400 MHz, $CDCl_3$) (50:50 mixture of rotamers) δ 4.72 (br s, 0.5H, NC*H*CO_2Me), 4.52 (br s, 0.5H, NC*H*CO_2Me), 3.93-3.82 (m, 1H, NCH), 3.64 (s, 3H, OMe), 3.26-3.09 (m, 1H, NCH), 1.83-1.76 (m, 1H, C*H*Me), 1.67-1.63 (m, 1H, CH), 1.56-1.46 (m, 1H, CH), 1.39 (s, 9H, CMe_3), 1.36-1.18 (m, 2H, CH), 0.96 (d, J = 7.1 Hz, 3H, CH*Me*); ^{13}C NMR (100.6 MHz, $CDCl_3$) (rotamers) δ 172.2 (C=O, CO_2Me), 171.98 (C=O, CO_2Me), 155.8 (C=O, Boc), 155.4 (C=O, Boc), 80.1 (O*C*Me_3), 59.3 (*C*HCO_2Me), 57.8 (*C*HCO_2Me), 51.3 (OMe), 41.2 (NCH_2), 40.4 (NCH_2), 33.2 (*C*HMe), 33.0 (*C*HMe), 28.4 (C*Me*$_3$), 28.0 (CH_2), 25.3 (CH_2), 24.9 (CH_2), 18.6 (Me); MS (EI) *m/z* 280 [(M + Na)$^+$, 100]; HRMS (ESI) *m/z* calcd for $C_{13}H_{23}NO_4$ [(M + Na)$^+$, 100] 280.1519, found 280.1528 (−3.0 ppm error) and an 80:20 mixture of piperidines *trans*-**230** and *cis*-**230** (261 mg,

19%) as a yellow oil, R_F (9.5:0.5 hexane-EtOAc) 0.10. Diagnostic signals for *trans*-**230**: ^{1}H NMR (400 MHz, $CDCl_3$) δ 3.69 (s, 3H, OMe), 3.00-2.75 (m, 1H, CH), 2.49-2.37 (m, 1H, CH), 1.06 (d, J = 7.1 Hz, 3H, CH*Me*). Spectroscopic data consistent with those reported in the literature for *cis*-**230**.[102]

Lab book reference HFK3-019

Methyl-1-methanesulfonyl-3-methylpiperidine-2-carboxylate *cis*-297

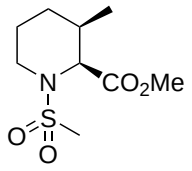

cis-**297**

TFA (1 mL, 13 mmol, 33 eq) was added dropwise to a stirred solution of *N*-Boc protected ester *cis*-**230** (100 mg, 0.389 mmol, 1.0 eq) in CH_2Cl_2 (5 mL) at rt under Ar. The resulting solution was stirred at rt for 1 h. Then, the solvent was evaporated under reduced pressure to give the crude TFA salt as a colourless oil. Et_3N (163 μL, 1.16 mmol, 3.0 eq) was added dropwise to a stirred solution the TFA salt in CH_2Cl_2 (5 mL) at rt under Ar. The resulting solution was stirred at rt for 10 min and MsCl (66 μL, 0.85 mmol, 2.2 eq) was added dropwise. The resulting solution was stirred at rt for 18 h. The mixture was poured into water (10 mL) and extracted with EtOAc (3 x 15 mL). The combined organics were dried ($MgSO_4$) and evaporated under reduced pressure to give the crude product as a yellow oil. Purification by flash column chromatography on silica with 95:5 hexane-EtOAc as eluent gave *N*-sulfonamide *cis*-**297** (66 mg, 73%) as a white solid, mp 50-52 °C; R_F (4:1 hexane-EtOAc) 0.32; IR (ATR) 2936, 1733 (C=O), 1326, 1146, 1000 cm^{-1}; ^{1}H NMR (400 MHz, $CDCl_3$) δ 4.50 (d, J = 6.0 Hz, 1H, NC*H*CO_2Me), 3.70 (s, 3H, OMe), 3.68-3.61 (m, 1H, NCH), 3.44 (ddd, J = 12.0, 12.0, 3.0 Hz, 1H, NCH), 2.76 (s, 3H, SO_2Me), 2.04-1.89 (m, 1H, C*H*Me), 1.82-1.71 (m, 1H, CH), 1.70-1.52 (m, 2H, CH), 1.35 (dddd, J = 13.0, 13.0, 13.0, 4.0 Hz, 1H, CH), 0.97 (d, J = 7.0 Hz, 3H, CH*Me*); ^{13}C NMR (100.6 MHz, $CDCl_3$) δ 171.4 (C=O), 59.2

(*C*HCO$_2$Me), 51.7 (OMe), 41.7 (NCH$_2$), 38.0 (SO$_2$Me), 34.1 (*C*HMe), 27.5 (CH$_2$), 25.3 (CH$_2$), 18.6 (Me); MS (EI) *m/z* 247 [(M + Na)$^+$, 100]; HRMS (ESI) *m/z* calcd for C$_9$H$_{17}$NO$_4$S [(M + Na)$^+$, 100] 258.0770, found 258.0773 (−0.6 ppm error).

Lab book reference HFK3-015

[1-Methanesulfonyl-3-methylpiperidin-2-yl]methanol *cis*-298

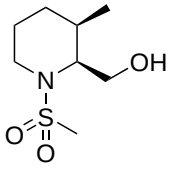

cis-**298**

A solution of ester *cis*-**297** (233 mg, 1.00 mmol, 1.0 eq) in THF (10 mL) was added dropwise to a stirred suspension of lithium aluminium hydride (83 mg, 2.19 mmol, 2.2 eq) in THF (20 mL) at 0 °C under Ar. The resulting mixture was stirred at 0 °C for 2 h and then H$_2$O (157 μL), 2 M NaOH$_{(aq)}$ (315 μL) and MgSO$_4$ (243 mg) were added dropwise slowly (care - exothermic quench). The mixture was allowed to warm to rt and the solids were removed by filtration through Celite. The filter cake was washed with MeOH (3 x 10 mL) and the solvent was evaporated under reduced pressure to give the crude product as a yellow oil. Purification by flash column chromatography on silica with 70:30 to 60:40 hexane-EtOAc as eluent gave alcohol *cis*-**298** (39 mg, 19%) as a colourless oil, R_F (1:1 hexane-EtOAc) 0.21; IR (ATR) 3502 (OH), 2930, 2876, 1313, 1140, 1059, 769 cm^{-1}; ^{1}H NMR (400 MHz, CDCl$_3$) δ 3.99-3.94 (m, 1H, NC*H*CH$_2$OH), 3.78 (dd, J = 12.0, 12.0 Hz, 1H, HOC*H*), 3.76-3.68 (m, 1H, NCH), 3.67 (dd, J = 12.0, 4.0 Hz, 1H, HOC*H*), 3.02-2.97 (m, 1H, NCH), 2.93 (s, 3H, SO$_2$Me), 2.07 (br s, 1H, OH), 1.94-1.86 (m, 1H, C*H*Me), 1.73-1.64 (m, 1H, CH), 1.64-1.47 (m, 2H, CH), 1.35-1.12 (m, 1H, CH), 0.92 (d, J = 7.0 Hz, 3H, CH*Me*); ^{13}C NMR (100.6 MHz, CDCl$_3$) δ 59.6 (N*C*HCH$_2$OH), 56.5 (OCH$_2$), 40.4 (SO$_2$Me), 39.9 (NCH$_2$), 33.5 (*C*HMe), 27.9 (CH$_2$), 25.8 (CH$_2$), 18.8 (Me); MS (EI) *m/z* 230 [(M + Na)$^+$, 100]; HRMS (ESI) *m/z* calcd for C$_{18}$H$_{17}$NO$_3$S [(M + Na)$^+$, 100] 230.0821, found 230.0820 (+0.5 ppm error).

Lab book reference HFK3-023

Methyl-1-acetyl-3-methylpiperidine-2-carboxylate *cis*-299

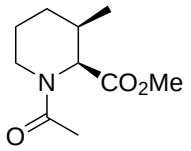

cis-**299**

TFA (1 mL, 13 mmol, 33 eq) was added dropwise to a stirred solution of *N*-Boc protected ester *cis*-**230** (100 mg, 0.389 mmol, 1.0 eq) in CH_2Cl_2 (5 mL) at rt under Ar. The resulting solution was stirred at rt for 1 h. Then, the solvent was evaporated under reduced pressure to give the crude TFA salt as a colourless oil. Ac_2O (220 μL, 2.30 mmol, 6.0 eq) was added dropwise to a stirred solution of the TFA salt in pyridine (5 mL) at rt under Ar and the resulting solution was stirred at rt for 18 h. Then, the solvent was evaporated under reduced pressure. The residue was dissolved in CH_2Cl_2 (10 mL). Then, H_2O (10 mL) was added and the two layers were separated. The aqueous layer was extracted with CH_2Cl_2 (3 $\times$ 10 mL) and the combined organics were dried ($MgSO_4$) and evaporated under reduced pressure to give the crude product as a yellow oil. Purification by flash column chromatography on silica with 80:20 hexane-EtOAc as eluent gave *N*-acetamide *cis*-**299** (72 mg, 94%) as a colourless oil, R_F (3:2 hexane-EtOAc) 0.13; IR (ATR) 2934, 1734 (C=O, CO_2Me), 1642 (C=O, amide), 1418, 1160, 1006 cm^{-1}; ^1H NMR (400 MHz, $CDCl_3$) (80:20 mixture of rotamers) δ 5.16 (d, J = 6.0 Hz, 0.8H, NC*H*CO_2Me), 4.50-4.40 (m, 0.2H, NCH), 4.32 (d, J = 6.0 Hz, 0.2H, NC*H*CO_2Me), 3.66-3.65 (m, 0.6H, OMe), 3.63-3.62 (m, 2.4H, OMe), 3.60-3.59 (m, 0.8H), 3.51 (ddd, J = 13.0, 13.0, 3.0 Hz, 0.8H, NCH), 2.84 (ddd, J = 13.0, 13.0, 3.0 Hz, 0.2H, NCH), 2.07-2.06 (m, 0.6H, C(O)Me), 2.06-2.05 (m, 2.4H, C(O)Me), 1.84-1.64 (m, 1H, C*H*Me), 1.61-1.50 (m, 1H, CH), 1.50-1.30 (m, 2.8H, CH), 1.30-1.15 (m, 0.2H, CH), 0.98 (d, J = 7.0 Hz, 2.4H, CH*Me*), 0.97 (d, J = 7.0 Hz, 0.6H, CH*Me*); ^{13}C NMR (100.6 MHz, $CDCl_3$) (rotamers) δ 171.5 (C=O), 170.5 (C=O), 170.1 (C=O), 170.1

(C=O), 61.1 (*C*HCO$_2$Me), 55.7 (*C*HCO$_2$Me), 51.8 (OMe), 51.4 (OMe), 43.3 (NCH$_2$), 38.0 (NCH$_2$), 33.7 (*C*HMe), 33.1 (*C*HMe), 27.9 (CH$_2$), 27.6 (CH$_2$), 25.6 (CH$_2$), 24.8 (CH$_2$), 22.1 (C(O)*Me*), 21.8 (C(O)*Me*), 18.6 (Me), 18.3 (Me); MS (EI) *m/z* 222 [(M + Na)$^+$, 100]; HRMS (ESI) *m/z* calcd for $C_{10}H_{17}NO_3$ [(M + Na)$^+$, 100] 222.1101, found 222.1108 (−3.9 ppm error).

Lab book reference HFK3-020

Benzyl 3-oxo-8-azabicyclo[3.2.1]octane-8-carboxylate 321

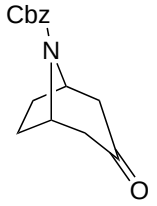

321

Benzylchloroformate (10.0 mL, 0.690 mol, 4.0 eq.) and K_2CO_3 (143 mg, 1.03 mmol, 0.06 eq.) were added to a stirred solution of tropinone **320** (2.40 g, 0.172 mmol, 1.0 eq.) in toluene (70 mL) at rt. The resulting solution was stirred and heated at reflux for 3 h. The mixture was allowed to cool to rt and the solvent was evaporated under reduced pressure. EtOAc (50 mL) and H_2O (50 mL) were added and the aqueous layer was extracted with EtOAc (3 × 40 mL). The combined organics were dried ($MgSO_4$) and evaporated under reduced pressure to give the crude product. Purification by flash column chromatography on silica with 70:30 EtOAc-hexane as eluent gave carbamate **321** (2.66 g, 60%) as a pale, yellow oil, R_F (1:1 hexane-EtOAc) 0.41; IR (ATR) 1702 (C=O), 1424, 1336, 1105, 1035 cm^{-1}; ^{1}H NMR (400 MHz, $CDCl_3$) δ 7.40-7.29 (m, 5H, Ph), 5.19 (s, 2H, OCH$_2$), 4.57 (br s, 2H, NCH), 2.87-2.50 (m, 2H, CHCO), 2.35 (br d, J = 16.0 Hz, 2H, CHCO), 2.16-2.02 (m, 2H, CH), 1.79-1.56 (m, 2H, CH); ^{13}C NMR (100.6 MHz, $CDCl_3$) (rotamers) δ 208.06 (C=O, ketone), 153.7 (C=O, Cbz), 136.5 (*ipso*-Ph), 128.7 (Ph), 128.4 (Ph), 128.2 (Ph), 67.4 (CH$_2$), 53.3 (NCH), 49.3 (*C*H$_2$CO), 48.8 (*C*H$_2$CO), 29.5 (CH$_2$), 28.7 (CH$_2$); MS (EI) *m/z* 282 [(M + Na)$^+$, 100]; HRMS (ESI) *m/z* calcd for $C_{15}H_{17}NO_3$ [(M + Na)$^+$, 100] 282.1101, found 282.1102 (−0.4 ppm

error). Spectroscopic data consistent with those reported in the literature.[205,206]

Lab book reference HFK3-046

Benzyl 6,12-diazatricyclo[7.2.1.0^{2,7}]dodeca-2(7),3,5-triene-12-carboxylate 331

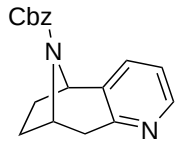

331

Propargylamine (82 μL, 1.3 mmol, 3.0 eq.) and $NaAuCl_4 \cdot 2H_2O$ (4.2 mg, 0.011 mmol, 0.025 eq.) were added to a stirred solution of ketone **321** (110 mg, 0.424 mmol, 1.0 eq.) in EtOH (4 mL) at rt under Ar. The resulting mixture was stirred at rt for 1 h and then stirred and heated at 100 °C for 20 h. The mixture was allowed to cool to rt and the solids were removed by filtration through Celite. The filter cake was washed with EtOH (3 × 10 mL) and the filtrate was evaporated under reduced pressure to give the crude product. Purification by flash column chromatography on silica with 50:50 to 20:80 hexane-EtOAc as eluent gave starting material **321** (16 mg, 15%) and *N*-Cbz pyridine **331** (30 mg, 24%) as a yellow oil, R_F (EtOAc) 0.25; IR (ATR) 1695 (C=O), 1409, 1306, 1097, 965 cm^{-1}; ^{1}H NMR (400 MHz, $CDCl_3$) δ 8.41 (d, J = 5.0 Hz, 1H, Ar), 7.47-7.18 (m, 6H, Ar), 7.06 (dd, J = 7.5, 5.0 Hz, 1H, Ar), 5.12-5.00 (m, 3H, NCH and OCH), 4.78-4.60 (m, 1H, CH, NCH), 3.61-3.36 (m, 1H, CH), 2.77 (d, J = 18.0 Hz, 1H, CH), 2.33-2.17 (m, 2H, CH), 1.91-1.84 (m, 1H, CH), 1.79-1.68 (m, 1H, CH); ^{13}C NMR (100.6 MHz, $CDCl_3$) (rotamers) δ 154.1 (C=O), 148.4 (Ar), 136.7 (*ipso*-Ar), 136.6 (*ipso*-Ar), 133.0 (Ar), 132.6 (Ar), 128.6 (Ar), 128.2 (Ar), 121.3 (Ar), 67.1 (OCH_2), 56.6 (NCH), 53.0 (NCH), 40.6 (CH_2), 40.0 (CH_2), 36.0 (CH_2), 35.3 (CH_2), 29.7 (CH_2), 28.8 (CH_2) (one *ipso*-Ar resonance not resolved); MS (EI) *m/z* 295 [(M + H)$^+$, 100]; HRMS (ESI) *m/z* calcd for $C_{18}H_{18}N_2O_2$ [(M + H)$^+$, 100] 295.1441, found 295.1444 (−1.0 ppm error).

Lab book reference HFK3-074

6,12-Diazatricyclo[7.2.1.0^{2,7}]dodeca-2(7),3,5-triene 324

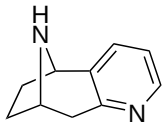

324

10% Pd/C (26 mg, 0.024 mmol, 0.027 eq., 10 wt% of **331**) was added to a stirred solution of **331** (257 mg, 0.873 mmol, 1.0 eq.) in MeOH (8 mL) at rt. Then, the reaction flask was evacuated under reduced pressure and back-filled with Ar three times. After a final evacuation, a balloon of H_2 was attached and the reaction mixture was stirred vigorously at rt under H_2 for 18 h. The solids were removed by filtration through Celite and washed with MeOH (15 mL). The filtrate was evaporated under reduced pressure to give the *N*-H pyridine **324** (134 mg, 96%) as an orange oil, R_F (4:1 CH_2Cl_2-MeOH) 0.57; IR (ATR) 2948, 2207, 1577, 1440, 906, 723, 642 cm^{-1}; ^{1}H NMR (400 MHz, $CDCl_3$) δ 8.44-8.42 (m, 1H, Ar), 7.34 (dd, J = 7.5, 1.5 Hz, 1H, Ar), 7.07 (br dd, J = 7.5, 5.0 Hz, 1H, Ar), 6.10 (s, 1H, NH), 4.49 (br d, J = 5.5 Hz, 1H, NCH), 4.18 (dd, J = 5.5, 5.5 Hz, 1H, NCH), 3.49 (dd, J = 18.0, 5.5 Hz, 1H, CHAr), 2.84 (br d, J = 18.0 Hz, 1H, CHAr), 2.43-2.17 (m, 2H, CH), 2.12-1.86 (m, 1H, CH), 1.79-1.71 (m, 1H, CH); ^{13}C NMR (100.6 MHz, $CDCl_3$) δ 152.9 (*ipso*-Ar), 149.1 (Ar), 135.3 (*ipso*-Ar), 133.2 (Ar), 121.6 (Ar), 57.4 (NCH), 53.8 (NCH), 40.5 (CH_2Ar), 35.6 (CH_2), 28.6 (CH_2); MS (EI) *m/z* 161 [(M + H)$^+$, 100]; HRMS (ESI) *m/z* calcd for $C_{10}H_{12}N_2$ [(M + H)$^+$, 100] 161.1073, found 161.1073 (−0.1 ppm error). The ^{1}H and ^{13}C NMR spectra were concentration dependent.

Lab book reference HFK3-082

1-6,12-Diazatricyclo[7.2.1.0^{2,7}]dodeca-2(7),3,5-trien-12-ylethan-1-one 326

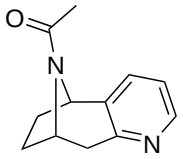

326

Ac_2O (276 μL, 2.92 mmol, 6.0 eq.) was added dropwise to a stirred solution of the amine **324** (78 mg, 0.49 mmol, 1.0 eq.) in pyridine (6 mL) at rt under Ar. The resulting solution was stirred at rt for 18 h. Then, the solvent was evaporated under reduced pressure. EtOAc (15 mL) and H_2O (15 mL) were added and the two layers were separated. The aqueous layer was extracted with EtOAc (3 × 15 mL). The combined organics were dried ($MgSO_4$) and evaporated under reduced pressure to give the crude product. Purification by flash column chromatography on silica with 95:5 CH_2Cl_2-MeOH as eluent gave *N*-Ac pyridine **326** (48 mg, 68%) as a white solid, mp 123-125 °C; R_F (9:1 CH_2Cl_2-MeOH) 0.41; IR (ATR) 1626 (C=O), 1438, 1421, 953, 922, 727 cm^{-1}; ^{1}H NMR (400 MHz, $CDCl_3$) (55:45 mixture of rotamers) δ 8.37 (dd, J = 5.0, 1.5, Hz, 0.45H, Ar), 8.33 (dd, J = 5.0, 1.5, Hz, 0.55H, Ar), 7.36 (dd, J = 7.5, 1.5 Hz, 0.55H, Ar), 7.30 (dd, J = 7.5, 1.5 Hz, 0.45H, Ar), 7.02 (dd, J = 7.5, 5.0 Hz, 1H, Ar), 5.37 (d, J = 6.5 Hz, 0.55H, NCH), 5.10-4.88 (m, 0.45H, NCH), 4.74 (d, J = 6.0 Hz, 0.45H, NCH), 4.57-4.32 (m, 0.55H, NCH), 3.46 (dd, J = 17.5, 5.0 Hz, 0.45H, CHAr), 3.32 (dd, J = 17.5, 6.5 Hz, 0.55H, CHAr), 2.85 (d, J = 18.0 Hz, 0.55H, CHAr), 2.72 (d, J = 18.0 Hz, 0.45H, CHAr), 2.36-2.25 (m, 1H, CH), 2.25-2.15 (m, 0.55H, CH), 2.15-2.08 (m, 0.45H, CH), 2.07 (s, 1.65H, Me), 1.99 (s, 1.35H, Me), 1.96-1.89 (m, 0.55H, CH), 1.88-1.80 (m, 0.45H, CH), 1.79-1.72 (m, 0.55H, CH), 1.71-1.62 (m, 0.45H, CH); ^{13}C NMR (100.6 MHz, $CDCl_3$) (rotamers) δ 167.2 (C=O), 166.8 (C=O), 154.6 (*ipso*-Ar), 153.2 (*ipso*-Ar), 148.6 (Ar), 148.1 (Ar), 136.5 (*ipso*-Ar), 135.6 (*ipso*-Ar), 133.3 (Ar), 132.2 (Ar), 121.5 (Ar), 121.1 (Ar), 58.3 (NCH), 54.1 (NCH), 53.9 (NCH), 50.6 (NCH), 41.3 (CH_2Ar), 39.8 (CH_2Ar), 36.3 (CH_2), 34.7 (CH_2), 30.0 (CH_2), 28.1 (CH_2), 21.8 (Me), 21.0 (Me); MS (EI) *m/z* 225 [(M + Na)$^+$, 100]; HRMS (ESI) *m/z* calcd for

$C_{12}H_{14}N_2O$ [$(M + Na)^+$, 100] 225.0998, found 225.1002 (−2.9 ppm error).

Lab book reference HFK3-076

Benzyl 2-bromo-3-oxo-8-azabicyclo[3.2.1]octane-8-carboxylate *exo*-**322**

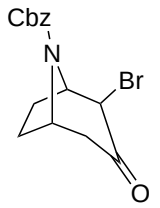

exo-**322**

A solution of ketone **321** (1.00 g, 3.86 mmol, 1.0 eq.) in THF (25 mL) was added dropwise over 10 min to a stirred solution of LHMDS (9.26 mL of a 1.0 M solution in THF, 9.26 mmol, 2.4 eq.) in THF (25 mL) at −78 °C under Ar. The resulting solution was stirred at −78 °C for 30 min. Then, TMSCl (2.45 mL, 19.3 mmol, 5.0 eq.) was added and the solution was stirred at −78 °C for 15 min. The reaction mixture was then allowed to warm to 0 °C and stirred for 15 min. Then, NBS (1.37 g, 7.71 mmol, 2.0 eq.) was added and the solution was stirred at 0 °C for 30 min. Saturated $NH_4Cl_{(aq)}$ (30 mL) was added and the two layers were separated. The aqueous layer was extracted with EtOAc (3 × 30 mL). The combined organics were washed with brine (30 mL), dried (Na_2SO_4) and evaporated under reduced pressure to give the crude product. Purification by flash column chromatography on silica with 60:40 to 50:50 hexane-Et_2O as eluent gave α-bromoketone *exo*-**322** (1.08 g, 83%) as a white solid, mp 94-96 °C; R_F (1:1 hexane-EtOAc) 0.74; IR (ATR) 1695 (C=O), 1421, 1331, 1101, 981 cm^{-1}; ^1H NMR (400 MHz, $CDCl_3$) δ 7.44-7.29 (m, 5H, Ph), 5.21-5.15 (m, 2H, OCH_2), 4.89-4.66 (m, 2H, NCH and CHBr), 4.16-4.01 (m, 1H, NCH), 3.33-3.22 (m, 1H, CHCO), 2.36-2.16 (m, 2H, CHCO and CH), 2.12-1.98 (m, 1H, CH), 1.78-1.71 (m, 1H, CH), 1.64 (ddd, J = 13.5, 9.5, 4.5 Hz, 1H, CH); ^{13}C NMR (100.6 MHz, $CDCl_3$) (rotamers) δ 201.2 (C=O, ketone), 153.7 (C=O, Cbz), 136.2 (*ipso*-Ar), 128.6 (Ar), 128.3 (br, Ar), 67.5 (OCH_2), 58.2 (CHBr), 53.1 (NCH), 52.4 (NCH), 44.5 (CH_2CO), 44.3 (CH_2CO), 28.7 (CH_2), 28.4 (CH_2), 27.9 (CH_2); 27.7 (CH_2) (one Ar resonance not resolved); MS

(EI) *m/z* 360 [(^{79}M + Na)$^+$, 100]; HRMS (ESI) *m/z* calcd for $C_{15}H_{16}{}^{79}BrNO_3$ [(^{79}M + Na)$^+$, 100] 360.0206, found 360.0199 (+2.0 ppm error).

Lab book reference HFK3-057

tert-Butyl 4-chloropiperidine-1-carboxylate 333

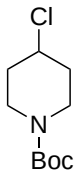

333

NCS (332 mg, 2.5 mmol, 1.0 eq) and PPh_3 (651 mg, 2.5 mmol, 1.0 eq) were added to a stirred solution of *N*-Boc-4-hydroxypiperidine (500 mg, 2.5 mmol, 1.0 eq) in CH_2Cl_2 (13 mL) at 0 °C under Ar. The resulting solution was stirred at rt for 16 h. The solvent was evaporated under reduced pressure. Et_2O was added (10 mL) and the solids were removed by filtration. The filtrate was evaporated under reduced pressure to give the crude product. Purification by flash column chromatography on silica with 95:5 hexane-Et_2O and then 90:10 hexane-Et_2O as eluent gave *N*-Boc-4-chloropiperidine **333** (247 mg, 40%) as a colourless oil, R_F (1:1 hexane-Et_2O) 0.50; IR (ATR) 1690 (C=O), 1417, 1248, 1163 cm^{-1}; ^{1}H NMR (400 MHz, $CDCl_3$) δ 4.17 (tt, J = 7.5, 3.5 Hz, 1H, CHCl), 3.68 (ddd, 2H, J = 13.5, 7.5, 7.0 Hz, NCH), 3.27 (ddd, 2H, J = 13.5, 7.5, 3.5 Hz, NCH), 1.99 (dddd, 2H, J = 14.0, 7.0, 3.5, 3.5 Hz, CH), 1.77 (m, 2H, CH), 1.49-1.37 (s, 9H, CMe_3); ^{13}C NMR (100.6 MHz, $CDCl_3$) δ 154.8 (C=O), 79.9 (O*C*Me_3), 57.1 (CHCl), 41.3 (NCH_2), 35.0 (CH_2), 28.5 (C*Me*$_3$); MS (EI) *m/z* 242 [(M + Na)$^+$, 100]; HRMS (ESI) *m/z* calcd for $C_{10}H_{18}{}^{35}ClNO_2$ [(M + Na)$^+$, 100] 242.0918, found 242.0920 (−0.7 ppm error) and an 80:20 mixture (by ^{1}H NMR spectroscopy) of **333** and alkene **543** (61 mg, i.e. 51 mg (9%) of **333** and 10 mg (2%) of alkene **543**) as a colourless oil. Diagnostic signals for alkene **543**: ^{1}H NMR (400 MHz, $CDCl_3$) δ 5.83-5.79 (m, 1H, =CH), 5.65-5.62 (m, 1H, =CH), 3.88-3.86 (m, 2H, NCH), 3.48 (dd, J = 11.5, 6.0 Hz, 2H, NCH).

Lab book reference HFK4-007

2-[(*tert*-Butoxy)carbonyl]-2-azabicyclo[3.1.0]hexane-1-carboxylic acid 371

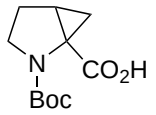

371

s-BuLi (1.02 mL of a 1.3 M solution in hexanes, 1.3 mmol, 2.6 eq.) was added dropwise to a stirred solution of *N*-Boc 4-chloropiperidine **333** (123 mg, 0.50 mmol, 1.0 eq.) and TMEDA (195 μL, 1.3 mmol, 2.6 eq.) in Et_2O (5 mL) at −78 °C under Ar. The resulting solution was stirred at −78 °C for 1 h. Then, CO_2 was added bubbled through the solution for 10 min. The solution was allowed to warm to rt over 2 h and stirred at rt for 30 min. Saturated $NH_4Cl_{(aq)}$ (10 mL) was added and the two layers were separated. The aqueous layer was acidified to pH 2 with 2 M $HCl_{(aq)}$ (10 mL) and extracted with Et_2O (3 × 10 mL). The combined organics were dried (Na_2SO_4) and evaporated under reduced pressure to give acid **371** as a white solid (994 mg, 72%), mp 80-85 °C; R_F (19:1 CH_2Cl_2-MeOH) 0.27; IR (ATR) 2978 (OH), 1692 (C=O), 1392, 1164, 728 cm^{-1}; ^1H NMR (400 MHz, $CDCl_3$) δ 10.92 (br s, 1H, OH), 3.80-3.73 (m, 1H, NCH), 3.51-3.46 (m, 1H, NCH), 2.34-2.12 (m, 2H, CH), 2.01-1.78 (m, 2H, CH), 1.43 (s, 9H, CMe_3), 1.09 (dd, J = 5.5, 5.5 Hz, 1H, CH); ^{13}C NMR (100.6 MHz, $CDCl_3$) δ 177.1 (C=O, CO_2H), 156.3 (C=O, Boc), 81.0 (O*C*Me_3), 50.5 (NCH_2), 47.7 (NC), 32.1 (CH), 28.3 (C*Me*$_3$), 26.2 (CH_2) (one CH_2 resonance not resolved); MS (EI) *m/z* 250 [(M + Na)$^+$, 100]; HRMS (ESI) *m/z* calcd for $C_{11}H_{17}NO_4$ [(M + Na)$^+$, 100] 250.1050, found 250.1049 (+0.5 ppm error). Spectroscopic data consistent with those reported in the literature.[207]

Lab book reference HFK4-047

***N*-Methoxy-*N*-methylpyridine-3-carboxamide 541**

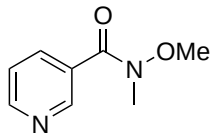

541

N,O-dimethylhydroxylamine·HCl (686 mg, 11.2 mmol, 1.0 eq.) and Et_3N (4.70 mL, 33.7 mmol, 3.0 eq.) were added to a stirred solution of nicotinoyl chloride (2.00 g, 11.2 mmol, 1.0 eq.) in CH_2Cl_2 (70 mL) at 0 °C under Ar. The resulting solution was allowed to warm rt and stirred at rt for 3 h. A 1:1 saturated solution of $NaHCO_{3(aq)}$ and $NH_4Cl_{(aq)}$ (100 mL) was added and the mixture was extracted with CH_2Cl_2 (3 × 50 mL). The combined organic extracts were dried ($MgSO_4$) and evaporated under reduced pressure to give the crude product. Purification by flash column chromatography on silica 95:5 CH_2Cl_2-MeOH as eluent gave the impure product. Purification by flash column chromatography on silica with EtOAc as eluent gave Weinreb amide **541** (1.17 g, 62%) as a yellow oil, IR (ATR) 1635 (C=O), 1413, 1382, 977 cm^{-1}; ^1H NMR (400 MHz, $CDCl_3$) δ 8.92 (br s, 1H, Ar), 8.65 (dd, J = 5.0, 1.5 Hz, 1H, Ar), 8.01-7.98 (m, 1H, Ar), 7.38-7.29 (m, 1H, Ar), 3.52 (s, 3H, OMe), 3.36 (s, 3H, NMe); ^{13}C NMR (100.6 MHz, $CDCl_3$) δ 167.5 (C=O), 151.4 (Ar), 149.3 (Ar), 136.3 (Ar), 129.9 (*ipso*-Ar), 123.1 (Ar), 61.4 (OMe), 33.2 (NMe); MS (EI) *m/z* 167 M^+; HRMS (ESI) *m/z* calcd for $C_7H_{12}N_2O_2$ M^+ 167.0815, found 167.0809 (+3.6 ppm error). Spectroscopic data consistent with those reported in the literature.[208]

Lab book reference HFK4-024

***tert*-Butyl 1-(pyridine-3-carbonyl)-2-azabicyclo[3.1.0]hexane-2-carboxylate 372**

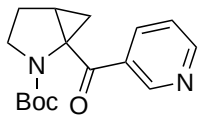

372

s-BuLi (1.57 mL of a 1.4 M solution in hexanes, 2.20 mmol, 2.2 eq.) was added drop-

wise to a stirred solution of *N*-Boc 4-chloropiperidine **333** (246 mg, 1.00 mmol, 1.0 eq.) in THF (15 mL) at −78 °C under Ar. The resulting solution was stirred at −78 °C for 1 h. Then, Weinreb amide **541** (366 mg, 2.20 mmol, 2.2 eq.) was added dropwise. The solution was allowed to warm to rt over 2 h and stirred at rt for 30 min. Saturated $NH_4Cl_{(aq)}$ (10 mL) was added and the two layers were separated. The aqueous layer was extracted with Et_2O (3 × 10 mL). The combined organics were dried (Na_2SO_4) and evaporated under reduced pressure to give the crude product. Purification by flash column chromatography on silica with 80:20 hexane-Et_2O to 98:2 CH_2Cl_2-MeOH as eluent gave the impure product **372**. Purification by flash column chromatography on silica with 50:50 hexane-EtOAc and 50:50 hexane-Et_2O gave *N*-Boc ketone **372** (124 mg, 43%) as a white solid, mp 85 °C; R_F (1:1 hexane-EtOAc) 0.22; IR (ATR) 1698 (C=O), 1389, 1367, 1093 cm^{-1}; ^1H NMR (400 MHz, $CDCl_3$) δ 9.05-8.99 (m, 1H, Ar), 8.73-8.67 (m, 1H, Ar), 8.10 (ddd, J = 8.0, 8.0, 2.0 Hz, 1H, Ar), 7.38 (dd, J = 8.0, 5.0 Hz, 1H, Ar), 4.10-3.85 (m, 1H, NCH), 3.46 (ddd, J = 9.5, 9.5, 9.5 Hz, 1H, NCH), 2.61-2.42 (m, 1H, CH), 2.24-2.06 (m, 3H, CH), 1.12 (s, 10H, CMe_3 and CH); ^{13}C NMR (100.6 MHz, $CDCl_3$) δ 196.5 (C=O, ketone), 155.3 (C=O, Boc), 152.7 (Ar), 149.5 (Ar), 135.5 (Ar), 132.3 (*ipso*-Ar), 123.3 (Ar), 81.2 (O*C*Me_3), 53.9 (NC), 47.9 (NCH_2), 33.5 (CH), 28.0 (C*Me*$_3$), 25.8 (CH_2), 20.1 (CH_2); MS (EI) *m/z* 311 [$(M + Na)^+$, 100]; HRMS (ESI) *m/z* calcd for $C_{16}H_{20}N_2O_3$ [$(M + Na)^+$, 100] 311.1366, found 311.1363 (+1.0 ppm error).

Lab book reference HFK4-026

tert-Butyl 1-(phenylsulfanyl)-2-azabicyclo[3.1.0]hexane-2-carboxylate 373

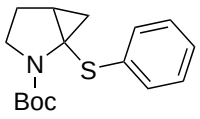

373

s-BuLi (9.80 mL of a 1.3 M solution in hexanes, 12.7 mmol, 2.6 eq.) was added dropwise to a stirred solution of *N*-Boc 4-chloropiperidine **333** (1.20 g, 4.88 mmol, 1.0 eq.)

in Et_2O (20 mL) at −78 °C under Ar. The resulting solution was stirred at −78 °C for 1 h. Then, a solution of diphenyl disulfide (2.77 g, 12.7 mmol, 2.6 eq.) in Et_2O (10 mL) was added dropwise. The solution was allowed to warm to rt over 2 h and stirred at rt for 30 min. Saturated $NH_4Cl_{(aq)}$ (10 mL) was added and the two layers were separated. The aqueous layer was extracted with Et_2O (3 × 10 mL). The combined organics were dried (Na_2SO_4) and evaporated under reduced pressure to give the crude product. Purification by flash column chromatography on silica with 95:5 to 90:10 to 85:15 to 80:20 hexane-Et_2O as eluent gave sulfide **373** (1.25 g, 88%) as a yellow oil, R_F (1:1 hexane-EtOAc) 0.61; IR (ATR) 1693 (C=O), 1363, 1165, 740 cm^{-1}; ^1H NMR (400 MHz, $CDCl_3$) δ 7.42-7.37 (m, 2H, Ph), 7.31-7.20 (m, 3H, Ph), 3.55 (ddd, J = 11.5, 9.0, 7.5 Hz, 1H, NCH), 3.49-3.44 (m, 1H, NCH), 2.16-2.05 (m, 1H, CH), 1.86-1.71 (m, 2H, CH), 1.65-1.56 (m, 1H, CH), 1.49 (s, CMe_3, 9H), 1.13 (dd, J = 5.5, 5.5 Hz, 1H, NCSPhC*H*); ^{13}C NMR (100.6 MHz, $CDCl_3$) δ 155.7 (C=O), 136.2 (*ipso*-Ph), 131.3 (Ph), 128.9 (Ph), 127.1 (Ph), 80.3 (O*C*Me_3), 53.3 (NC), 51.1 (NCH_2), 31.3 (CH_2), 29.4 (CH), 28.6 (C*Me*$_3$), 26.8 (CH_2); MS (EI) *m/z* 314 [(M + Na)$^+$, 100]; HRMS (ESI) *m/z* calcd for $C_{16}H_{21}NO_2S$ [(M + Na)$^+$, 100] 314.1185, found 314.1184 (+0.5 ppm error). Lab book reference HFK4-096

tert-Butyl 1-carbamoyl-2-azabicyclo[3.1.0]hexane-2-carboxylate 374

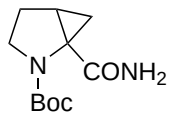

374

DIPEA (261 μL, 1.50 mmol, 1.7 eq.) and T3P (0.70 mL of a 50% wt solution in EtOAc, 1.32 mmol, 1.5 eq.) were added sequentially to a stirred solution of acid *cis*-**371** (200 mg, 0.880 mmol, 1.0 eq.) in CH_2Cl_2 (5 mL) at rt under Ar. The resulting solution was stirred at rt for 30 min. Then, 35% $NH_{3(aq)}$ (100 μL, 2.45 mmol, 2.8 eq.) was added and the solution was stirred at rt for 6 h. The solution was poured into water (10 mL) and 3 M $HCl_{(aq)}$ (1 mL) was added. The two layers were separated and the aqueous

layer was extracted with EtOAc (3 × 15 mL). The combined organics were washed with 2 M $NaOH_{(aq)}$ (15 mL) and brine (15 mL), dried ($MgSO_4$) and evaporated under reduced pressure to give crude product. Purification by flash column chromatography on silica with EtOAc gave amide **374** (127 mg, 64%) as a white solid, mp 85-90 °C; R_F (EtOAc) 0.22; IR (ATR) 3332 (NH), 1676 (C=O), 1366, 1169 cm^{-1}; ^1H NMR (400 MHz, $CDCl_3$) δ 6.44 (s, 1H, NH), 5.89 (s, 1H, NH), 3.79-3.60 (m, 2H, NCH), 2.26-2.17 (m, 1H, CH), 2.14-2.05 (m, 1H, CH), 2.01 (br dd, J = 5.5, 9.0 Hz, 1H, CH), 1.92-1.80 (m, 1H, CH), 1.45 (s, 9H, CMe_3), 0.92 (dd, J = 5.5, 5.5 Hz, 1H, CH); ^{13}C NMR (100.6 MHz, $CDCl_3$) δ 173.9 (C=O, $CONH_2$), 156.9 (C=O, Boc), 81.2 (O*C*Me_3), 51.9 (NCH_2), 49.9 (NC), 31.6 (CH), 28.4 (C*Me*$_3$), 26.8 (CH_2), 26.0 (CH_2); MS (EI) *m/z* 249 [(M + Na)$^+$, 100]; HRMS (ESI) *m/z* calcd for $C_{11}H_{18}N_2O_3$ [(M + Na)$^+$, 100] 249.1210, found 249.1207 (+1.1 ppm error).

Lab book reference HFK4-054

2-(Benzenesulfonyl)-2-azabicyclo[3.1.0]hexane-1-carboxamide 334

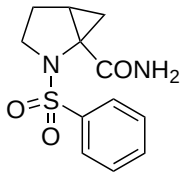

334

HCl (2.0 mL of a 4 M solution in dioxane, 8 mmol, 36 eq.) was added dropwise to a stirred solution of *N*-Boc protected amide **374** (50 mg, 0.22 mmol, 1.0 eq.) at rt under Ar. The resulting solution was stirred at rt for 1 h. Then, the solvent was evaporated under reduced pressure to give the crude HCl salt. Et_3N (154 μL, 1.10 mmol, 5.0 eq.) was added dropwise to a stirred solution the HCl salt in CH_2Cl_2 (5 mL) at rt under Ar. The resulting solution was stirred at rt for 10 min and $PhSO_2Cl$ (62 μL, 0.49 mmol, 2.2 eq.) was added dropwise. The resulting solution was stirred at rt for 18 h. The mixture was poured into water (10 mL) and extracted with CH_2Cl_2 (3 × 10 mL). The combined organics were dried ($MgSO_4$) and evaporated under reduced pressure to give

the crude product. Purification by flash column chromatography on silica with 90:10 to 70:30 hexane-EtOAc as eluent gave *N*-phenylsulfonyl pyrrolidine **334** (47 mg, 80%) as a white solid, mp 160-165 °C; R_F (7:3 CH_2Cl_2-acetone) 0.36; IR (ATR) 3348 (NH), 1668 (C=O), 1347, 1164, 599 cm^{-1}; ^1H NMR (400 MHz, d_4-MeOH) δ 7.90-7.87 (m, 2H, Ph), 7.80-7.71 (m, 1H, Ph), 7.69-7.61 (m, 2H, Ph), 3.76 (ddd, J = 10.5, 9.0, 3.0 Hz, 1H, NCH), 3.02-2.95 (m, 1H, NCH), 2.35-2.07 (m, 1H, CH), 1.91-1.67 (m, 2H, CH and CH), 1.53 (dd, J = 9.0, 6.0 Hz, 1H, CH), 0.28 (dd, J = 6.0, 6.0 Hz, 1H, CH); ^{13}C NMR (100.6 MHz, d_4-MeOH) δ 174.9 (C=O), 136.7 (*ipso*-Ph), 135.0 (Ph), 130.4 (Ph), 130.1 (Ph), 51.6 (NCH_2), 50.6 (NC), 31.8 (CH), 26.2 (CH_2), 16.3 (CH_2); MS (EI) *m/z* 289 [(M + Na)$^+$, 100]; HRMS (ESI) *m/z* calcd for $C_{12}H_{14}N_2O_3S$ [(M + Na)$^+$, 100] 289.0617, found 289.0616 (+0.4 ppm error).

Lab book reference HFK4-060

1-[1-(Pyridine-3-carbonyl)-2-azabicyclo[3.1.0]hexan-2-yl]ethan-1-one 335

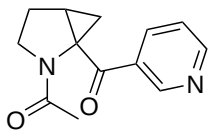

335

Using general procedure A, *N*-Boc protected amide **372** (100 mg, 0.347 mmol, 1.0 eq.) in HCl (4.0 mL of a 4 M solution in dioxane, 16 mmol, 40 eq.) and then Ac_2O (197 μL, 2.08 mmol, 6.0 eq.) in pyridine (2.50 mL) gave the crude product. Purification by flash column chromatography on silica with 95:5 CH_2Cl_2-MeOH as eluent gave *N*-Ac pyrrolidine **335** (60 mg, 77%) as a white solid, mp 90-95 °C; R_F (19:1 CH_2Cl_2-MeOH) 0.43; IR (ATR) 1676 (C=O, ketone), 1643 (C=O, amide), 1413, 916, 725 cm^{-1}; ^1H NMR (400 MHz, $CDCl_3$) (65:35 mixture of rotamers) δ 8.99 (br d, J = 1.5 Hz, 0.35H, Ar), 8.90 (br s, 0.65H, Ar), 8.76 (dd, J = 5.0, 1.5 Hz, 0.35H, Ar), 8.66 (br d, J = 5.0 Hz, 0.65H, Ar), 8.10 (ddd, J = 8.0, 2.0, 2.0 Hz, 0.65H, Ar), 8.05 (ddd, J = 8.0, 2.0, 2.0 Hz, 0.35H, Ar), 7.42-7.39 (m, 0.35H, Ar), 7.39-7.36 (m, 0.65H, Ar), 4.11-3.97 (m, 1.35H, NCH), 3.47-3.40 (m, 0.65H, NCH), 2.73-2.60 (m, 0.65H, CH), 2.57-2.53 (m,

0.35H, CH), 2.52-2.48 (m, 0.35H, CH), 2.42-2.36 (m, 0.35H, CH), 2.35-2.28 (m, 0.65H, CH), 2.22 (ddd, J = 9.0, 5.5, 1.0 Hz, 0.65H, CH), 2.17-2.10 (m, 0.35H, CH), 1.85 (s, 1.95H, C(O)Me), 1.83 (s, 1.05H, C(O)Me), 1.42-1.33 (m, 0.65H, CH), 1.14 (dd, J = 5.5, 5.5 Hz, 0.35H, CH),1.03 (dd, J = 5.5, 5.5 Hz, 0.65H, CH);^{13}C NMR (100.6 MHz, $CDCl_3$) (rotamers) δ 196.9 (C=O, ketone), 194.9 (C=O, ketone), 171.8 (C=O, amide), 170.8 (C=O, amide), 153.4 (Ar), 152.2 (Ar), 149.3 (Ar), 147.5 (Ar), 135.8 (Ar), 135.6 (Ar), 133.2 (*ipso*-Ar), 131.8 (*ipso*-Ar), 124.0 (Ar), 123.8 (Ar), 55.7 (NC), 53.6 (NC), 51.4 (NCH_2), 47.8 (NCH_2), 26.9 (CH_2), 26.6 (CH_2), 26.2 (CH_2), 22.9 (Me), 22.1 (Me), 18.3 (CH_2), 16.1 (CH), 15.4 (CH); MS (EI) m/z 253 [(M + Na)$^+$, 100]; HRMS (ESI) m/z calcd for $C_{13}H_{14}N_2O_2$ [(M + Na)$^+$, 100] 253.0947, found 253.0946 (+0.6 ppm error).

Lab book reference HFK4-064

1-[1-(Phenylsulfanyl)-2-azabicyclo[3.1.0]hexan-2-yl]ethan-1-one 336

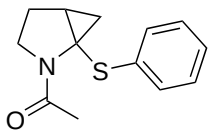

336

TFA (2 mL, 26 mmol, 38 eq) was added dropwise to a stirred solution of *N*-Boc protected amide **373** (200 mg 0.686 mmol, 1.0 eq.) in CH_2Cl_2 (9 mL) at rt under Ar. The resulting solution was stirred at rt for 1 h. Then, the solvent was evaporated under reduced pressure to give the crude TFA salt. Ac_2O (389 μL, 4.12 mmol, 6.0 eq.) was added dropwise to a stirred solution of the TFA salt in pyridine (5 mL) at rt under Ar and the resulting solution was stirred at rt for 18 h. Then, the solvent was evaporated under reduced pressure. The residue was dissolved in CH_2Cl_2 (10 mL). Then, H_2O (10 mL) was added and the two layers were separated. The aqueous layer was extracted with CH_2Cl_2 (3 × 10 mL) and the combined organics were dried ($MgSO_4$) and evaporated under reduced pressure to give the crude product. Purification by flash column chromatography on silica with 99:1 CH_2Cl_2-MeOH as eluent gave sulfide **336** (146 mg,

91%) as a yellow oil, R_F (9:1 CH_2Cl_2-MeOH) 0.18; IR (ATR) 1648 (C=O), 1393, 745, 692 cm^{-1}; ^1H NMR (400 MHz, $CDCl_3$) δ 7.47-7.41 (m, 2H, Ph), 7.34-7.28 (m, 3H, Ph), 3.91 (ddd, J = 12.0, 9.0, 2.5 Hz, 1H, NCH), 3.29-3.22 (m, 1H, NCH), 2.42 (s, 3H, Me), 2.13-1.93 (m, 2H, CH), 1.82 (dd, J = 9.0, 5.0 Hz, 1H, CH), 1.76-1.58 (m, 1H, CH), 1.19 (dd, J = 5.0, 5.0 Hz, 1H, CH); ^{13}C NMR (100.6 MHz, $CDCl_3$) δ 172.0 (C=O), 133.6 (*ipso*-Ph), 133.0 (Ph), 129.3 (Ph), 128.5 (Ph), 53.9 (NC), 52.6 (NCH_2), 33.9 (CH_2), 31.3 (CH), 26.7 (CH_2), 23.7 (Me); MS (EI) m/z 256 [$(M + Na)^+$, 100]; HRMS (ESI) m/z calcd for $C_{13}H_{15}NOS$ [$(M + Na)^+$, 100] 256.0767, found 256.0766 (+0.4 ppm error).

Lab book reference HFK4-056

tert-Butyl 1-(benzenesulfonyl)-2-azabicyclo[3.1.0]hexane-2-carboxylate 375

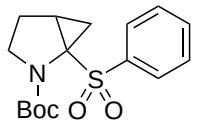

375

Urea hydrogen peroxide (141 mg, 1.50 mmol, 3.0 eq.) and pthalic anhydride (222 mg, 1.50 mmol, 3.0 eq.) were added to a stirred solution of sulfide **373** (146 mg, 0.500 mmol, 1.0 eq.) in EtOAc (2.5 mL) at rt under Ar. The resulting solution was stirred at rt for 18 h. Then, saturated $Na_2S_2O_{3(aq)}$ (10 mL) was added and the aqueous layer was extracted with EtOAc (3 × 10 mL). The combined organics were washed with 1 M $NaOH_{(aq)}$ (2 × 10 mL), H_2O (10 mL) and brine (10 mL), dried (Na_2SO_4) and evaporated under reduced pressure to give the crude product. Purification by flash column chromatography on silica with 4:1 hexane-EtOAc as eluent gave sulfone **375** (153 mg, 93%) as a colourless oil, R_F (1:1 hexane-EtOAc) 0.48; IR (ATR) 1702 (C=O), 1365, 1147, 1083 cm^{-1}; ^1H NMR (400 MHz, $CDCl_3$) δ 7.93-7.87 (m, 1H, Ph), 7.67-7.61 (m, 1H, Ph), 7.56-7.52 (m, 2H, Ph), 3.92 (dd, J = 11.5, 8.0 Hz, 1H, NCH), 3.50-3.43 (m, 1H, NCH), 2.65-2.59 (m, 1H, CH), 2.40 (dd, J = 9.5, 6.0 Hz, 1H, CH), 2.14-2.07 (m, 1H, CH), 1.71-1.58 (m, 1H, CH), 1.37 (dd, J = 6.0, 6.0 Hz, 1H, CH), 1.26 (s, 9H,

CMe_3); ^{13}C NMR (100.6 MHz, $CDCl_3$) δ 155.2 (C=O), 139.3 (*ipso*-Ph), 133.6 (Ph), 129.2 (Ph), 129.1 (Ph), 81.2 (O*C*Me_3), 64.8 (NC), 56.9 (NCH_2), 32.2 (CH_2), 31.0 (CH), 28.3 (CH_2), 28.1 (C*Me*$_3$); MS (EI) *m/z* 346 [(M + Na)$^+$, 100]; HRMS (ESI) *m/z* calcd for $C_{16}H_{21}NO_4S$ [(M + Na)$^+$, 100] 346.1083, found 346.1081 (+0.7 ppm error).

Lab book reference HFK4-061

1-[1-(Benzenesulfonyl)-2-azabicyclo[3.1.0]hexan-2-yl]ethan-1-one 337

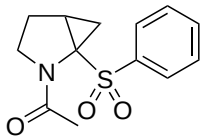

337

Using general procedure A, *N*-Boc protected sulfonamide **375** (118 mg 0.365 mmol, 1.0 eq.) in HCl (4.0 mL of a 4 M solution in dioxane, 16 mmol, 40 eq.) and then Ac_2O (207 μL, 2.19 mmol, 6.0 eq.) in pyridine (5 mL) gave the crude product. Purification by flash column chromatography on silica with 70:30 to 60:40 to 40:60 to 0:100 hexane-EtOAc as eluent gave sulfone **337** (79 mg, 82%) as a yellow solid, mp 116-118 °C; R_F (1:1 hexane-EtOAc) 0.23; IR (ATR) 1622 (C=O), 1145, 720, 554 cm^{-1}; ^1H NMR (400 MHz, $CDCl_3$) δ 7.85 (d, J = 8.0 Hz, 2H, Ar), 7.68-7.64 (m, 1H, Ph), 7.57-7.53 (m, 2H, Ph), 4.19-4.00 (m, 1H, NCH), 2.74-2.57 (m, 2H, NCH and CH), 2.51-2.38 (m, 1H, CH), 2.29 (s, 3H, Me), 2.04-1.82 (m, 2H, CH), 1.52-1.43 (m, 1H, CH); ^{13}C NMR (100.6 MHz, $CDCl_3$) δ 173.5 (C=O), 137.8 (*ipso*-Ph), 134.2 (Ph), 129.5 (Ph), 128.8 (Ph), 64.2 (NC), 55.4 (NCH_2), 33.2 (CH_2), 32.7 (CH), 27.2 (CH_2), 22.7 (Me).

Lab book reference HFK4-065

***tert*-Butyl-1-[(R)-benzenesulfinyl]-2-azabicyclo[3.1.0]hexane-2-carboxylate *syn*-376 and *anti*-376**

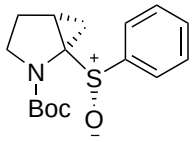

syn-**376**

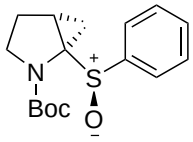

anti-**376**

Na_2CO_3 (157 mg, 1.48 mmol, 2.1 eq.) and *m*-CPBA (158 mg, 0.703 mmol, 1.0 eq.) were added to a stirred solution of sulfide **373** (205 mg, 0.703 mmol, 1.0 eq.) in CH_2Cl_2 (12 mL) at rt under Ar. The resulting solution was stirred for 18 h. The mixture was poured into ice-cold $NaHCO_{3(aq)}$ (20 mL) and extracted with CH_2Cl_2 (3 × 15 mL). The combined organics were dried (Na_2SO_4) and evaporated under reduced pressure to give the crude product which contained a 70:30 mixture (by ^{1}H NMR spectroscopy) of sulfoxides *syn*- and *anti*-**376**. Purification by flash column chromatography on silica with 80:20 to 65:35 to 60:40 hexane-EtOAc as eluent gave sulfoxide *syn*-**376** (142 mg, 66%) as a colourless oil, R_F (3:2 hexane-EtOAc) 0.29; IR (ATR) 1697 (C=O), 1365, 1164, 1046 cm^{-1}; ^{1}H NMR (400 MHz, $CDCl_3$) δ 7.63-7.61 (m, 2H, Ph), 7.52-7.38 (m, 3H, Ph), 3.63-3.22 (m, 1H, NCH), 2.98-2.68 (m, 1H, NCH), 2.35-2.20 (m, 1H, CH), 1.96-1.92 (m, 1H, CH), 1.73-1.70 (m, 2H, CH), 1.53 (br s, 9H, CMe_3), 1.17-1.14 (m, 1H, CH); ^{13}C NMR (100.6 MHz, $CDCl_3$) δ 155.1 (C=O), 142.8 (*ipso*-Ph), 131.5 (Ph), 129.0 (Ph), 124.8 (Ph), 81.4 (O*C*Me$_3$), 65.2 (NC), 52.3 (NCH_2), 29.4 (CH_2), 28.6 (C*Me$_3$*), 26.1 (CH_2), 21.1 (CH); MS (EI) *m/z* 330 [(M + Na)$^+$, 100]; HRMS (ESI) *m/z* calcd for $C_{16}H_{21}NO_3S$ [(M + Na)$^+$, 100] 330.1134, found 330.1139 (−1.4 ppm error) and sulfoxide *anti*-**376** (49 mg, 23%) as a white solid, mp 90-95 °C; R_F (3:2 hexane-EtOAc) 0.20; IR (ATR) 1693 (C=O), 1365, 1164, 748 cm^{-1}; ^{1}H NMR (400 MHz, $CDCl_3$) δ 7.63-7.61 (m, 2H, Ph), 7.49-7.44 (m, 3H, Ph), 3.85-3.71 (m, 1H, NCH), 3.67-3.56 (m, 1H, NCH), 2.30-2.19 (m, 1H, CH), 2.11-2.05 (m, 1H, CH), 1.86-1.74 (m, 1H, CH), 1.49 (s, 9H, CMe_3), 1.12 (dd, J = 6.0, 6.0 Hz, 1H, CH), 1.06-1.02 (m, 1H, CH); ^{13}C NMR (100.6 MHz, $CDCl_3$) δ 155.6 (C=O), 141.5 (*ipso*-Ph), 131.0 (Ph), 129.0 (Ph), 125.0 (Ph), 81.1 (O*C*Me$_3$), 70.1 (NC), 52.6 (NCH_2), 30.4 (CH_2), 28.5 (C*Me$_3$*), 27.0 (CH_2), 24.6 (CH);

MS (EI) *m/z* 330 [(M + Na)$^+$, 100]; HRMS (ESI) *m/z* calcd for $C_{16}H_{21}NO_3S$ [(M + Na)$^+$, 100] 330.1134, found 330.1133 (+0.3 ppm error).

Lab book reference HFK4-080

tert-Butyl-1-(phenylimino-λ^6-sulfanyl)-2-azabicyclo[3.1.0]hexane-2-carboxylate _syn_-377

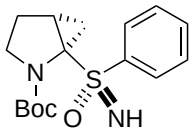

syn-**377**

$PhI(OAc)_2$ (629 mg, 1.95 mmol, 3.0 eq.) and ammonium carbamate (203 mg, 2.60 mmol, 4.0 eq.) were added to a stirred solution of sulfoxide *syn*-**376** (200 mg, 0.651 mmol, 1.0 eq.) in MeOH (4 mL) at rt under Ar. The resulting solution was stirred at rt for 18 h. Then, the solvent was evaporated under reduced pressure to give the crude product. Purification by flash column chromatography on silica with 70:30 hexane-EtOAc gave the impure product. Purification by flash column chromatography on silica with hexane to 70:30 to 50:50 hexane-EtOAc as eluent gave starting material *syn*-**376** (59 mg, 30%) and sulfoximine *syn*-**377** (139 mg, 66%) as a white solid, mp 112-115 °C; R_F (1:1 hexane-EtOAc) 0.20; IR (ATR) 3298 (NH), 1694 (C=O), 1365, 1234, 1130 cm^{-1}; ^{1}H NMR (400 MHz, $CDCl_3$) δ 8.01-7.93 (m, 2H, Ph), 7.63-7.55 (m, 1H, Ph), 7.54-7.46 (m, 2H, Ph), 3.73-3.68 (m, 1H, NCH), 2.93 (dddd, J = 10.5, 10.5, 10.5, 10.5 Hz, 1H, NCH), 2.50 (dd, J = 9.5, 6.0 Hz, 1H, CH), 2.27-2.21 (m, 1H, CH), 1.83 (dddd, J = 13.5, 7.5, 7.5, 1.5 Hz, 1H, CH), 1.55 (dddd, J = 13.5, 11.0, 8.0, 3.0 Hz, 1H, CH), 1.44 (s, 9H, CMe_3), 1.29 (dd, J = 6.0, 6.0 Hz, CH); ^{13}C NMR (100.6 MHz, $CDCl_3$) δ 155.6 (C=O), 139.4 (*ipso*-Ph), 133.1 (Ph), 129.4 (Ph), 129.0 (Ph), 81.6 (O*C*Me_3), 65.3 (NC), 55.7 (NCH_2), 31.7 (CH_2), 30.9 (CH), 28.4 (C*Me*$_3$), 28.0 (CH_2); MS (EI) *m/z* 345 [(M + Na)$^+$, 100]; HRMS (ESI) *m/z* calcd for $C_{16}H_{22}N_2NaO_3S$ [(M + Na)$^+$, 100] 345.1243, found 345.1243 (+0.3 ppm error).

Lab book reference HFK5-003

***N*-2-Acetyl-2-azabicyclo[3.1.0]hexan-1-yl(oxo)phenyl-λ^6-sulfanyl-ideneacetamide *syn*-378**

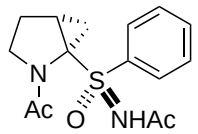

syn-**378**

Using general procedure A, *N*-Boc protected amide *syn*-**377** (90 mg 0.28 mmol, 1.0 eq.) in HCl (3.0 mL of a 4 M solution in dioxane, 12 mmol, 43 eq.) and then Ac_2O (106 μL, 1.12 mmol, 4.0 eq.) in pyridine (4 mL) gave the crude product. Purification by flash column chromatography on silica with 99:1 to 90:10 CH_2Cl_2-MeOH as eluent gave sulfoximine *syn*-**378** (74 mg, 74%) as a white solid, mp 100-105 °C; R_F (7:3 CH_2Cl_2-acetone) 0.36; IR (ATR) 1644 (C=O), 1378, 1359, 1246, 1217 cm^{-1}; ^1H NMR (400 MHz, $CDCl_3$) δ 7.88 (d, J = 8.0 Hz, 2H, Ph), 7.69-7.65 (m, 1H, Ph), 7.59-7.56 (m, 2H, Ph), 4.25-3.96 (m, 1H, NCH), 2.86-2.75 (m, 1H, NCH), 2.64-2.56 (m, 1H, CH), 2.55-2.46 (m, 1H, CH), 2.36 (s, 3H, Me), 2.14 (s, 3H, Me), 1.97-1.81 (m, 1H, CH), 1.72-1.58 (m, 1H, CH), 1.54-1.38 (m, 1H, CH); ^{13}C NMR (100.6 MHz, $CDCl_3$) δ 180.1 (C=O), 173.8 (C=O), 135.8 (*ipso*-Ph), 134.2 (Ph), 129.8 (Ph), 128.5 (Ph), 64.5 (NC), 56.5 (NCH_2), 34.3 (CH_2), 31.6 (CH), 27.2 (CH_2), 27.0 (Me), 22.8 (Me); MS (EI) *m/z* 329 [(M + Na)$^+$, 100]; HRMS (ESI) *m/z* calcd for $C_{15}H_{18}N_2O_3S$ [(M + Na)$^+$, 100] 329.0930, found 329.0940 (−2.9 ppm error).

Lab book reference HFK5-006

1-[-1-[(R)-Benzenesulfinyl]-2-azabicyclo[3.1.0]hexan-2-yl]ethan-1-one *syn*-379

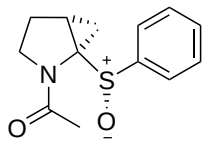

syn-**379**

Using general procedure A, *N*-Boc protected amide *syn*-**376** (632 mg 2.06 mmol, 1.0

eq.) in HCl (9.0 mL of a 4 M solution in dioxane, 36 mmol, 18 eq.) and then Ac_2O (1.17 mL, 12.3 mmol, 6.0 eq.) in pyridine (15 mL) gave the crude product. Purification by flash column chromatography on silica with 99:1 to 90:10 CH_2Cl_2-MeOH as eluent gave sulfoxide *syn*-**379** (334 mg, 65%) as a white solid, mp 58-60 °C; R_F (9:1 CH_2Cl_2-MeOH) 0.49; IR (ATR) 1651 (C=O), 1401, 1042, 751 cm^{-1}; ^1H NMR (400 MHz, $CDCl_3$) (60:40 mixture of rotamers) δ 7.65 (dd, J = 8.0, 2.0 Hz, 0.6H, Ph), 7.61-7.41 (m, 4.4H, Ph), 3.91 (ddd, J = 10.5, 8.5, 1.5 Hz, 0.6H, NCH), 3.32 (ddd, J = 10.5, 8.5, 5.0 Hz, 0.4H, NCH), 3.06 (ddd, J = 10.5, 9.0, 7.0 Hz, 0.4H, NCH), 2.48-2.42 (m, 0.8H, NCH and CH), 2.41 (s, 1.8H, Me), 2.39-2.33 (m, 0.6H, CH), 2.16 (dd, J = 10.0, 5.5 Hz, 0.6H, CH), 1.95 (dd, J = 9.5, 6.0 Hz, 0.4H, CH), 1.92-1.82 (m, 0.8H, CH), 1.86 (s, 1.2H, Me), 1.78-1.70 (m, 0.6H, CH), 1.60-1.52 (m, 0.6H, CH), 1.28 (dd, J = 5.5, 5.5 Hz, 0.6H, CH), 1.18 (dd, J = 6.0, 6.0 Hz, 0.4H, CH); ^{13}C NMR (100.6 MHz, $CDCl_3$) (rotamers) δ 171.5 (C=O), 170.5 (C=O), 142.9 (*ipso*-Ph), 141.7 (*ipso*-Ph), 132.1 (Ph), 131.6 (Ph), 129.4 (Ph), 128.9 (Ph), 125.2 (Ph), 124.5 (Ph), 65.4 (NC), 65.2 (NC), 54.1 (NCH_2), 52.7 (NCH_2), 29.6 (CH_2), 26.7 (CH_2), 26.2 (CH_2), 23.1 (Me), 22.7 (Me), 22.6 (CH_2), 22.3 (CH), 18.2 (CH);MS (EI) *m/z* 272 [(M + Na)$^+$, 100]; HRMS (ESI) *m/z* calcd for $C_{13}H_{15}NO_2S$ [(M + Na)$^+$, 100] 272.0716, found 272.0715 (+0.2 ppm error). Lab book reference HFK5-011

1-[-1-(Phenylimino-λ^6-sulfanyl)-2-azabicyclo[3.1.0]hexan-2-yl]ethan-1-one *syn*-338

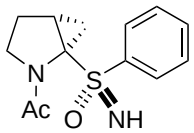

syn-**338**

$PhI(OAc)_2$ (1.18 g, 3.66 mmol, 3.0 eq.) and ammonium carbamate (381 mg, 4.88 mmol, 4.0 eq.) were added to a stirred solution of sulfoxide *syn*-**379** (304 mg, 1.22 mmol, 1.0 eq.) in MeOH (6 mL) at rt under Ar. The resulting solution was stirred at rt for 18 h. Then, the solvent was evaporated under reduced pressure to give the

crude product. Purification by flash column chromatography on silica with 99:1 to 98:2 CH_2Cl_2-MeOH as eluent gave starting material *syn*-**379** (74 mg, 24%) and sulfoximine *syn*-**338** (225 mg, 70%) as an oil, R_F (10:1 CH_2Cl_2-MeOH) 0.19; IR (ATR) 3264 (NH), 1651 (C=O), 1388, 1231, 991 cm^{-1}; ^1H NMR (400 MHz, $CDCl_3$) (50:50 mixture of rotamers) δ 7.90-7.94 (m, 2H, Ph), 7.67-7.60 (m, 1H, Ph), 7.58-7.49 (m, 2H, Ph), 4.18-4.08 (m, 0.5H, NCH), 3.54-3.50 (m, 0.5H, NCH), 3.3 -3.17 (m, 0.5H, NCH), 2.74-2.61 (m, 1.5H, NCH and CH), 2.57-2.44 (m, 1H, CH), 2.31 (s, 1.5H, Me), 2.02 (s, 1.5H, Me), 1.98-1.85 (m, 1H, CH), 1.74-1.59 (m, 0.5H, CH), 1.54-1.42 (m, 1H, CH), 1.39-1.33 (m, 0.5H, CH); ^{13}C NMR (100.6 MHz, $CDCl_3$) (rotamers) δ 173.7 (C=O), 171.6 (C=O), 140.1 (*ipso*-Ph), 133.7 (Ph), 133.2 (Ph), 130.3 (Ph), 129.4 (Ph), 129.1 (Ph), 65.1 (NC), 56.1 (NCH_2), 56.0 (NCH_2), 33.5 (CH_2), 32.3 (CH), 30.9 (CH_2), 28.8 (CH), 28.1 (CH_2), 27.5 (CH_2), 23.3 (Me); MS (EI) *m/z* 287 [$(M + Na)^+$, 100]; HRMS (ESI) *m/z* calcd for $C_{13}H_{16}N_2O_2S$ [$(M + Na)^+$, 100] 287.0825, found 287.0823 (+0.7 ppm error).

Lab book reference HFK5-016

1-[-1-[(R)-Benzenesulfinyl]-2-azabicyclo[3.1.0]hexan-2-yl]ethan-1-one *anti*-379

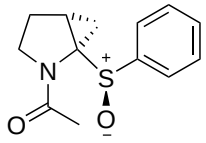

anti-**379**

Using general procedure A, *N*-Boc protected amide *anti*-**376** (244 mg 0.794 mmol, 1.0 eq.) in HCl (6.0 mL of a 4 M solution in dioxane, 24 mmol, 30 eq.) and then Ac_2O (450 μL, 4.76 mmol, 6.0 eq.) in pyridine (10 mL) gave the crude product. Purification by flash column chromatography on silica with 99:1 to 90:10 CH_2Cl_2-MeOH as eluent gave sulfoxide *anti*-**379** (162 mg, 82%) as a yellow oil, R_F (9:1 CH_2Cl_2-MeOH) 0.16; IR (ATR) 1652 (C=O), 1393, 1049 cm^{-1}; ^1H NMR (400 MHz, $CDCl_3$) (60:40 mixture of rotamers) δ 7.80 (br d, J = 7.0 Hz, 0.6H, Ph), 7.69-7.62 (m, 1.4H, Ph), 7.57-7.42 (m, 3H, Ph), 4.11-4.04 (m, 0.4H, NCH), 3.99 (br dd, J = 12.0, 8.0 Hz, 0.6H, NCH),

3.55 (ddd, J = 10.0, 9.5, 5.0 Hz, 0.4H, NCH), 2.58-2.50 (m, 0.6H, NCH), 2.44 (s, 1.8H, Me), 2.31-2.20 (m, 1H, CH), 2.20-2.14 (m, 0.6H, CH), 2.13 (s, 1.2H, Me), 2.03-1.89 (m, 1.2H, CH), 1.66-1.47 (m, 1.4H, CH and NCSOPhC*H*), 1.09 (dd, J = 6.5, 6.5 Hz, 0.4H, CH), 1.03 (dd, J = 9.5, 6.0 Hz, 0.4H, CH); ^{13}C NMR (100.6 MHz, $CDCl_3$) (rotamers) δ 173.4 (C=O), 171.3 (C=O), 142.2 (*ipso*-Ph), 140.8 (*ipso*-Ph), 131.9 (Ph), 130.9 (Ph), 129.4 (Ph), 128.9 (Ph), 125.3 (Ph), 124.9 (Ph), 71.2 (NC), 65.2 (NC), 55.1 (NCH_2), 52.5 (NCH_2), 34.2 (CH_2), 29.5 (CH_2), 28.3 (CH), 27.3 (CH_2), 26.5 (CH_2), 23.6 (Me), 23.0 (Me); MS (EI) m/z 272 [(M + Na)$^+$, 100]; HRMS (ESI) m/z calcd for $C_{13}H_{15}NO_2S$ [(M + Na)$^+$, 100] 272.0716, found 272.0715 (+0.2 ppm error).

Lab book reference HFK5-012

1-[-1-(phenylimino-λ^6-sulfanyl)-2-azabicyclo[3.1.0]hexan-2-yl]ethan-1-one *anti*-338

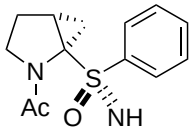

anti-**338**

$PhI(OAc)_2$ (628 mg, 1.95 mmol, 3.0 eq.) and ammonium carbamate (203 mg, 2.60 mmol, 4.0 eq.) were added to a stirred solution of sulfoxide *anti*-**379** (162 mg, 0.650 mmol, 1.0 eq.) in MeOH (6 mL) at rt under Ar. The resulting solution was stirred at rt for 18 h. Then, the solvent was evaporated under reduced pressure to give the crude product. Purification by flash column chromatography on silica with 99:1 to 98:2 CH_2Cl_2-MeOH as eluent gave sulfoximine *anti*-**338** (119 mg, 69%) as a cream solid, mp 110-112 °C; R_F (19:1 CH_2Cl_2-MeOH) 0.22; IR (ATR) 3251 (NH), 1650 (C=O), 1385, 1232, 726 cm^{-1}; ^{1}H NMR (400 MHz, $CDCl_3$) δ 7.99-7.91 (m, 2H, Ph), 7.65-7.62 (m, 1H, Ph), 7.56-7.53 (m, 2H, Ph), 4.14-4.09 (m, 1H, NCH) 2.82-2.78 (m, 1H, NCH), 2.72-2.64 (m, 1H, CH), 2.46-2.41 (m, 1H, CH), 2.25 (s, 3H, Me), 1.94-1.87 (m, 1H, CH), 1.55-1.46 (m, 1H, CH), 1.45-1.42 (m, 1H, CH); ^{13}C NMR (100.6 MHz, $CDCl_3$) δ 173.9 (C=O), 140.5 (*ipso*-Ph), 133.6 (Ph), 129.4 (Ph), 129.1 (Ph), 65.7 (NC), 55.6 (NCH_2),

33.5 (CH), 33.4 (CH_2), 27.6 (CH_2), 22.8 (Me); MS (EI) *m/z* 287 [$(M + Na)^+$, 100]; HRMS (ESI) *m/z* calcd for $C_{13}H_{16}N_2O_2S$ [$(M + Na)^+$, 100] 287.0825, found 287.0823 (+0.6 ppm error). Lab book reference HFK5-015

2-[(*tert*-Butoxy)carbonyl]-2-azabicyclo[3.1.0]hexan-1-ylboronic acid 380

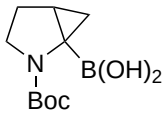

380

s-BuLi (16 mL of a 1.33 M solution in cyclohexane, 21 mmol, 2.6 eq.) was added dropwise to a stirred solution of *N*-Boc-4-chloropiperidine **333** (2.01 g, 8.13 mmol, 1.0 eq.) and TMEDA (3.2 mL, 21 mmol 2.6 eq.) in Et_2O (45 mL) at –78 °C under Ar. The resulting solution was stirred at –78 °C for 1 h. Then, $(i\text{–PrO})_3B$ (1.88 mL, 8.13 mmol, 1.0 eq) was added. After stirring at –78 °C for 10 min, the solution was allowed to warm to rt and stirred at rt for 18 h. 5% $HCl_{(aq)}$ (33 mL) was added and the mixture was extracted with Et_2O (3 × 50 mL). The combined organic extracts were dried ($MgSO_4$) and evaporated under reduced pressure gave the crude product. Purification by flash column chromatography on silica with 95:5 CH_2Cl_2-acetone to 90:10 CH_2Cl_2-MeOH as eluent gave boronic acid **380** (1.54 g, 83%) as a yellow oil, R_F (9:1 Et_2O-acetone) 0.13; IR (ATR) 3357 (OH), 1646 (C=O), 1392, 1365, 1166 cm^{-1}; ^1H NMR (400 MHz, $CDCl_3$) δ 7.78 (s, 2H, OH), 3.58-3.52 (m, 1H, NCH), 3.06-2.99 (m, 1H, NCH), 2.12-2.03 (m, 1H, CH), 1.97-1.92 (m, 1H, CH), 1.91-1.86 (m, 1H, CH), 1.44 (s, 9H, CMe_3), 1.00 (dd, J = 8.5, 5.5 Hz, 1H, CH), 0.76 (dd, J = 5.5, 5.5 Hz, 1H, CH); ^{13}C NMR (100.6 MHz, $CDCl_3$) (rotamers) δ 158.2 (C=O), 80.9 (O*C*Me_3), 80.7 (O*C*Me_3), 46.2 (NCH_2), 46.1 (NCH_2), 28.5 (C*Me*$_3$), 24.9 (br, CH_2), 24.2 (CH), 23.9 (CH), 18.2 (CH_2), 18.1 (CH_2); MS (EI) *m/z* 250 [$(M + Na)^+$, 100]; HRMS (ESI) *m/z* calcd for $C_{10}H_{18}BNO_4$ [$(M + Na)^+$, 100] 250.1221, found 250.1224 (−0.2 ppm error). In some bacthes, boronic acid **380** crystallised to a white solid.

Lab book reference HFK5-035

***tert*-Butyl 1-(6-methyl-4,8-dioxo-1,3,6,2-dioxazaborocan-2-yl)-2-azabicyclo [3.1.0]hexane-2-carboxylate 208**

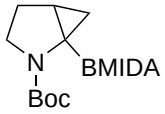

208

s-BuLi (16.0 mL of a 1.33 M solution in cyclohexane, 21.1 mmol, 2.6 eq.) was added dropwise to a stirred solution of *N*-Boc 4-chloropiperidine **333** (2.00 g, 8.13 mmol, 1.0 eq.) in Et_2O (30 mL) at –78 °C under Ar. The resulting solution was stirred at –78 °C for 1 h. Then, (i–PrO)$_3$B (1.88 mL, 8.14 mmol, 1.0 eq.) was added. After stirring at –78 °C for 10 min, the mixture was allowed to warm to rt and stirred at rt for 18 h. 5% $HCl_{(aq)}$ (30 mL) was added and the mixture was extracted with Et_2O (3 × 30 mL). The combined organic extracts were dried ($MgSO_4$) and evaporated under reduced pressure to give the crude boronic acid. Purification by flash column chromatography on silica with 95:5 CH_2Cl_2-acetone to 90:10 CH_2Cl_2-MeOH as eluent gave boronic acid **380** (1.54 g, 83%). MIDA (1.10 g, 7.46 mmol, 1.1 eq) was added to a stirred solution of boronic acid **380** (1.54 g, 6.78 mmol, 1.0 eq.) in toluene (4 mL) and anhydrous DMSO (4 mL) at rt under Ar. The resulting solution was connected to a Dean-Stark apparatus and stirred and heated at 120 °C for 18 h. The mixture was allowed to cool to rt and EtOAc (10 mL) was added. The mixture was washed with H_2O (3 × 10 mL) and the organic layer was dried ($MgSO_4$) and evaporated under reduced pressure to give MIDA boronate **208** (1.60 g, 59% over 2 steps) as a white solid, mp 240 °C (dec.); R_F (7:3 CH_2Cl_2-acetone) 0.39; IR (ATR) 1781 (C=O, ester), 1733 (C=O, ester), 1683 (C=O, Boc), 1410, 1304, 1044, 1013 cm^{-1}; ^{1}H NMR (400 MHz, d$_6$-acetone) δ 4.47 (d, J = 16.0 Hz, 1H, MeNCH), 4.27 (d, J = 17.5 Hz, 1H, MeNCH), 4.04 (d, J = 17.5 Hz, 1H, MeNCH), 4.01 (d, J = 16.0 Hz, 1H, MeNCH), 3.57 (ddd, J = 11.5, 10.0, 5.0 Hz, 1H, NCH), 3.45 (s, 3H, NMe), 3.25 (ddd, J = 11.5, 9.0, 7.0 Hz, 1H, NCH), 2.15-2.06 (m, 1H, CH), 1.88-1.81 (m, 1H, CH), 1.72-1.66 (m, 1H, CH), 1.39 (s, 9H, CMe$_3$), 1.00 (dd, J = 8.5, 5.0 Hz, 1H, CH), 0.73 (dd, J = 5.0, 5.0 Hz, 1H, CH); ^{13}C

NMR (100.6 MHz, d_6-acetone) δ 169.5 (C=O, ester), 169.1 (C=O, ester), 156.9 (C=O, Boc), 79.5 (O*C*Me$_3$), 65.4 (MeN*C*H$_2$), 64.6 (MeN*C*H$_2$), 49.9 (NCH$_2$), 47.4 (NMe), 28.6 (C*Me$_3$*), 26.4 (CH$_2$), 24.9 (CH), 19.4 (CH$_2$) (NCB resonance not resolved); MS (EI) *m/z* 361 [(M + Na)$^+$, 100]; HRMS (ESI) *m/z* calcd for $C_{15}H_{23}BN_2O_6$ [(M + Na)$^+$, 100] 361.1541, found 361.1544 (+0.1 ppm error).

Lab book reference HFK5-051

tert-Butyl 1-(4-methoxyphenyl)-2-azabicyclo[3.1.0]hexane-2-carboxylate 381 and _tert_-butyl 2-azabicyclo[3.1.0]hexane-2-carboxylate 356

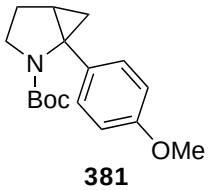

381

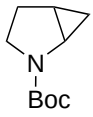

356

(Table 2.1, Entry 6)

Using general procedure B, *N*-Boc MIDA boronate **208** (400 mg, 1.18 mmol, 1.0 eq.), Cs_2CO_3 (2.31 g, 7.10 mmol, 6.0 eq.), PCy_3 (100 mg, 0.355 mmol, 0.3 eq.), $Pd(OAc)_2$, (40 mg, 0.18 mmol, 0.15 eq.) and 4-bromoanisole (208 μL, 1.66 mmol, 1.4 eq.) in toluene (13 mL) and H_2O (0.7 mL) gave the crude product. Purification by flash column chromatography on silica with 80:20 hexane-Et_2O as eluent gave arylated pyrrolidine **381** (264 mg, 77%) as a white solid, mp 69-71 °C; R_F (1:1 hexane-Et_2O) 0.48; IR (ATR) 1688 (C=O), 1516, 1363, 1244 cm^{-1}; ^{1}H NMR (400 MHz, $CDCl_3$) δ 7.19 (d, J = 9.0 Hz, 2H, Ar), 6.81 (d, J = 9.0 Hz, 2H, Ar), 3.86 (ddd, J = 11.5, 9.5, 6.0 Hz, 1H, NCH), 3.77 (s, 3H, OMe), 3.60-3.48 (m, 1H, NCH), 2.29 (dddd, J = 13.0, 9.5, 6.0, 6.0 Hz, 1H, CH), 1.93 (dddd, J = 13.0, 9.0, 6.0, 5.5 Hz, 1H, CH), 1.69 (dd, J = 9.0, 5.5 Hz, 1H, CH), 1.53-1.47 (m, 1H, CH), 1.23 (br s, 9H, CMe$_3$), 0.95 (dd, J = 5.5, 5.5 Hz, 1H, CH); ^{13}C NMR (100.6 MHz, $CDCl_3$) δ 158.1 (*ipso*-Ar), 156.1 (C=O), 133.6 (*ipso*-Ar), 127.7 (Ar), 113.4 (Ar), 79.4 (O*C*Me$_3$), 55.3 (OMe), 50.1 (NCH$_2$), 49.3 (N*C*Ar), 29.5 (CH), 28.3 (C*Me$_3$*), 26.7 (CH$_2$), 22.0 (CH$_2$); MS (EI) *m/z* 312 [(M +

Na)$^+$, 100]; HRMS (ESI) *m/z* calcd for $C_{17}H_{23}NO_3$ [(M + Na)$^+$, 100] 312.1570, found 312.1571 (−0.2 ppm error).

Lab book reference HFK5-041

(Table 2.1, Entry 1)

N-Boc MIDA boronate **208** (90 mg, 0.27 mmol, 1.0 eq.), $Pd(OAc)_2$ (3 mg, 0.013 mmol, 0.05 eq.), SPhos (10 mg, 0.027 mmol, 0.1 eq.) and aryl bromide (50 μL, 0.40 mmol, 1.5 eq.) were combined in dioxane (3 mL) at rt. The resulting mixture was stirred under Ar for 10 min (with active purging of the head-space with Ar). Then, $K_3PO_{4(aq)}$ (2.0 M, 1.0 mL, 2.00 mmol, 7.5 eq.) was degassed by sparging with Ar for 30 min and added. The resulting mixture was stirred and heated in a sealed tube at 60 °C for 18 h. The mixture was allowed to cool to rt. EtOAc (10 mL) was added and the solution was washed with $NaHCO_{3(aq)}$ (10 mL). The organic layer was dried (Na_2SO_4) and evaporated under reduced pressure to give the crude product which contained (by ^{1}H NMR spectroscopy) a 35:65 mixture of arylated pyrrolidine **381** and protobeboronation product **356**. Diagnostic signals for protobeboronation product **356**: ^{1}H NMR (400 MHz, $CDCl_3$) δ 2.91 (dd, J = 9.0, 19.5 Hz, 1H, NCH_2), 0.69-0.59 (m, 1H, CH), 0.52-0.49 (m, 1H, CH).

Lab book reference HFK5-029

(Table 2.1, Entry 2)

N-Boc MIDA boronate **208** (59 mg, 0.17 mmol, 1.0 eq.), $Pd(OAc)_2$ (2 mg, 0.0087 mmol, 0.05 eq.), SPhos (7 mg, 0.017 mmol, 0.1 eq.) and aryl bromide (33 μL, 0.26 mmol, 1.5 eq.) were combined in dioxane (2.2 mL) at rt. The resulting mixture was stirred under Ar for 10 min (with active purging of the head-space with Ar). Then, $K_3PO_{4(aq)}$ (2.0 M, 0.64 mL, 1.28 mmol, 7.5 eq.) was degassed by sparging with Ar for 30 min and added. The resulting mixture was stirred and heated in a sealed tube at 100 °C for 18 h. The mixture was allowed to cool to rt. EtOAc (10 mL) was added and the solution was washed with $NaHCO_{3(aq)}$ (10 mL). The organic layer was dried (Na_2SO_4)

and evaporated under reduced pressure to give the crude product which contained (by ^{1}H NMR spectroscopy) a 50:50 mixture of arylated pyrrolidine **381** and protobeboronation product **356**. Purification by flash column chromatography on silica with 95:5 to 90:10 to 80:20 hexane-Et_2O as eluent gave protobeboronation product **356** (4 mg, 13%) as a colourless oil, R_F (4:1 hexane-Et_2O) 0.30; IR (ATR) 1692 (C=O), 1406, 1168, 1105 cm^{-1}; ^{1}H NMR (400 MHz, $CDCl_3$) δ 3.69-3.55 (m, 1H, NCH), 3.47-3.18 (m, 1H, NCH), 2.94-2.86 (m, 1H, NCH), 2.12-1.97 (m, 1H, CH), 1.92-1.86 (m, 1H, CH), 1.51-1.39 (m, 1H, CH), 1.45 (s, 9H, CMe_3), 0.69-0.59 (m, 1H, CH), 0.52-0.49 (m, 1H, CH); ^{13}C NMR (100.6 MHz, $CDCl_3$) (rotamers) δ 155.4 (C=O, Boc), 79.4 (O*C*Me_3), 43.8 (NCH_2), 35.6 (NCH), 28.6 (C*Me*$_3$), 26.5 (CH_2), 25.7 (CH_2), 15.9 (CH), 15.1 (CH), 11.0 (CH_2); MS (EI) *m/z* 206 [(M + Na)$^+$, 100]; HRMS (ESI) *m/z* calcd for $C_{10}H_{17}NO_2$ [(M + Na)$^+$, 100] 206.1151, found 206.1157 (−2.9 ppm error) and arylated pyrrolidine **381** (9 mg, 18%).

Lab book reference HFK5-019

(Table 2.1, Entry 3)

N-Boc MIDA boronate **208** (90 mg, 0.27 mmol, 1.0 eq.), K_2CO_3 (99 mg, 0.71 mmol, 2.7 eq.), RuPhos (16 mg, 0.035 mmol, 0.13 eq.), $Pd(OAc)_2$ (4 mg, 0.017 mmol, 0.066 eq.) and aryl bromide (50 μL, 0.40 mmol, 1.5 eq.) were combined in toluene (1.7 mL) and H_2O (0.3 mL) at rt. The resulting mixture was degassed with Ar for 15 min and stirred and heated in a sealed tube at 100 °C for 18 h. The mixture was allowed to cool to rt and the solids were removed by filtration through Celite. EtOAc (10 mL) was added and the solution was washed with H_2O (10 mL). The organic layer was dried (Na_2SO_4) and evaporated under reduced pressure to give the crude product which contained (by ^{1}H NMR spectroscopy) a 50:50 mixture of arylated pyrrolidine **381** and protobeboronation product **356**. Purification by flash column chromatography on silica with 95:5 to 90:10 hexane-Et_2O as eluent gave protobeboronation product **356** (10 mg, 20%) and arylated pyrrolidine **381** (37 mg, 48%).

Lab book reference HFK5-030

(Table 2.1, Entry 4)

N-Boc MIDA boronate **208** (45 mg, 0.13 mmol, 1.0 eq.), K_2CO_3 (57 mg, 0.413 mmol, 3.1 eq.), RuPhos Pd G2 (4 mg, 0.013 mmol, 0.06 eq.) and aryl bromide (37 μL, 0.29 mmol, 1.1 eq.) were combined in dioxane (1.3 mL) and H_2O (0.3 mL) at rt. The resulting mixture was degassed with Ar for 15 min and stirred and heated in a sealed tube at 110 °C for 18 h. The mixture was allowed to cool to rt and the solids were removed by filtration through Celite. EtOAc (10 mL) was added and the solution was washed with H_2O (10 mL). The organic layer was dried (Na_2SO_4) and evaporated under reduced pressure to give the crude product which contained (by ^{1}H NMR spectroscopy) a 50:50 mixture of arylated pyrrolidine **381** and protobeboronation product **356**.

Lab book reference HFK5-036

(Table 2.1, Entry 5)

N-Boc MIDA boronate **208** (90 mg, 0.27 mmol, 1.0 eq.), $Pd(OAc)_2$ (6 mg, 0.027 mmol, 0.1 eq.), PCy_3 (15 mg, 0.053 mmol, 0.2 eq.) and aryl bromide (50 μL, 0.40 mmol, 1.5 eq.) were combined in toluene (4.4 mL) at rt. The resulting mixture was stirred under Ar for 10 min (with active purging of the head-space with Ar). Then, $K_3PO_{4(aq)}$ (2.0 M, 0.40 mL, 0.80 mmol, 3.0 eq.) was degassed by sparging with Ar for 30 min and added. The resulting mixture was stirred and heated in a sealed tube at 120 °C for 18 h. The mixture was allowed to cool to rt and the solids were removed by filtration through Celite. EtOAc (10 mL) was added and the solution was washed with H_2O (10 mL). The organic layer was dried (Na_2SO_4) and evaporated under reduced pressure to give the crude product which contained (by ^{1}H NMR spectroscopy) a 20:80 mixture of arylated pyrrolidine **381** and protobeboronation product **356**.

Lab book reference HFK5-034

***tert*-Butyl 1-(2-methoxyphenyl)-2-azabicyclo[3.1.0]hexane-2-carboxylate 367**

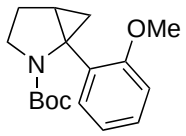

367

Using general procedure B, *N*-Boc MIDA boronate **208** (90 mg, 0.27 mmol, 1.0 eq.), Cs_2CO_3 (520 mg, 1.60 mmol, 6.0 eq.), PCy_3 (22 mg, 0.080 mmol, 0.3 eq.), $Pd(OAc)_2$, (9.0 mg, 0.040 mmol, 0.15 eq.) and 2-bromoanisole (46 μL, 0.37 mmol, 1.4 eq.) in toluene (3.0 mL) and H_2O (0.2 mL) gave the crude product. Purification by flash column chromatography on silica with 80:20 hexane-Et_2O as eluent gave arylated pyrrolidine **367** (56 mg, 73%) as a white solid, mp 78-80 °C; R_F (1:1 hexane-Et_2O 0.48); IR (ATR) 1685 (C=O), 1390, 1363, 751 cm^{-1}; ^1H NMR (400 MHz, $CDCl_3$) δ 7.32-7.26 (m, 1H, Ar), 7.21 (ddd, J = 8.0, 8.0, 2.0 Hz, 1H, Ar), 6.87 (dd, J = 8.0, 8.0 Hz, 1H, Ar), 6.82 (dd, J = 8.0, 1.0 Hz, 1H, Ar), 4.04-3.91 (m, 1H, NCH), 3.82 (s, 3H, OMe), 3.59-3.53 (m, 1H, NCH), 2.40-2.31 (m, 1H, CH), 1.96-1.88 (m, 1H, CH), 1.59-1.52 (m, 2H, CH), 1.21 (s, 9H, CMe_3), 0.90-0.88 (m, 1H, CH);^{13}C NMR (100.6 MHz, $CDCl_3$) δ 158.9 (*ipso*-Ar), 155.6 (C=O), 131.7 (Ar), 128.8 (*ipso*-Ar), 128.3 (Ar), 119.8 (Ar), 110.2 (Ar), 79.1 (O*C*Me_3), 55.6 (OMe), 50.6 (NCH_2), 46.9 (N*C*Ar), 28.4 (C*Me*$_3$), 27.4 (CH), 27.0 (CH_2), 22.9 (CH_2); MS (EI) *m/z* 312 [$(M + Na)^+$, 100]; HRMS (ESI) *m/z* calcd for $C_{17}H_{23}NO_3$ [$(M + Na)^+$, 100] 312.1570, found 312.1570 (−0.1 ppm error).
Lab book reference HFK5-039

***tert*-Butyl 1-1-[tris(propan-2-yl)silyl]-1H-pyrrolo[2,3-b]pyridin-6-yl-2-azabicyclo[3.1.0]hexane-2-carboxylate 383**

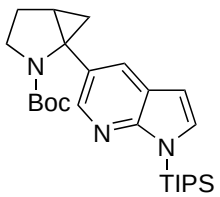

383

Using general procedure B, *N*-Boc MIDA boronate **208** (163 mg, 0.482 mmol, 1.0 eq.), Cs_2CO_3 (942 mg, 2.89 mmol, 6.0 eq.), PCy_3 (41 mg, 0.15 mmol, 0.3 eq.), $Pd(OAc)_2$, (16 mg, 0.072 mmol, 0.15 eq.) and 5-bromo-1-triisopropylsilanyl-1H-pyrrolo[2,3-b]pyridine (239 mg, 0.675 mmol, 1.4 eq.) in toluene (5 mL) and H_2O (0.3 mL) gave the crude product. Purification by flash column chromatography on silica with 90:10 hexane-Et_2O as eluent gave arylated pyrrolidine **383** (54 mg, 25%) as a yellow solid, mp 96-98 °C; R_F (4:1 hexane-EtOAc 0.38); IR (ATR) 1682 (C=O), 1386, 1167, 727 cm^{-1}; ^1H NMR (400 MHz, $CDCl_3$) δ 8.27 (d, J = 2.0 Hz, 1H, Ar), 7.78 (d, J = 2.0 Hz, 1H, Ar), 7.28 (d, J = 3.5 Hz, 1H, Ar), 6.49 (d, J = 3.5 Hz, 1H, Ar), 3.95 (ddd, J = 11.5, 9.5, 6.0 Hz, 1H, NCH), 3.57 (ddd, J = 11.5, 9.0, 6.0 Hz, 1H, NCH), 2.42-2.33 (m, 1H, CH), 2.04-1.97 (m, 1H, CH), 1.91-1.82 (m, 3H, SiC*H*Me), 1.78 (dd, J = 9.0, 5.5 Hz, 1H, CH), 1.68-1.56 (m, 1H, CH), 1.13 (d, J = 7.5 Hz, 18H, SiCH*Me*), 1.11 (s, 9H, CMe_3), 1.03 (dd, J = 5.5, 5.5 Hz, 1H, CH); ^{13}C NMR (100.6 MHz, $CDCl_3$) δ 156.1 (C=O), 152.9 (*ipso*-Ar), 142.6 (Ar), 131.5 (Ar), 128.9 (*ipso*-Ar), 126.6 (Ar), 121.7 (*ipso*-Ar), 102.7 (Ar), 79.5 (O*C*Me_3), 49.9 (NCH_2), 48.4 (N*C*Ar), 28.9 (CH), 28.3 (C*Me*$_3$), 26.6 (CH_2), 21.2 (CH_2), 18.3 (SiCH*Me*), 12.4 (Si*C*HMe); MS (EI) *m/z* 456 $(M + H)^+$; HRMS (ESI) *m/z* calcd for $C_{25}H_{41}N_3O_2Si$ $(M + H)^+$ 456.3046, found 456.3033 (−2.9 ppm error).

Lab book reference HFK5-063

2-(Benzenesulfonyl)-1-(4-methoxyphenyl)-2-azabicyclo[3.1.0]hexane 343

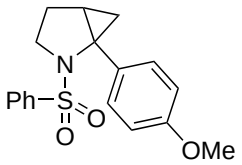

343

HCl (3.0 mL of a 4 M solution in dioxane, 12 mmol, 30 eq.) was added dropwise to a stirred solution of *N*-Boc protected amide **381** (115 mg, 0.398 mmol, 1.0 eq.) at rt under Ar. The resulting solution was stirred at rt for 1 h. Then, the solvent was

evaporated under reduced pressure to give the crude HCl salt. Et_3N (277 μL, 1.99 mmol, 5.0 eq.) was added dropwise to a stirred solution the HCl salt in CH_2Cl_2 (6 mL) at rt under Ar. The resulting solution was stirred at rt for 10 min and $PhSO_2Cl$ (112 μL, 0.876 mmol, 2.2 eq.) was added dropwise. The resulting solution was stirred at rt for 18 h. The mixture was poured into water (10 mL) and extracted with CH_2Cl_2 (3 $\times$ 10 mL). The combined organics were dried ($MgSO_4$) and evaporated under reduced pressure to give the crude product. Purification by flash column chromatography on silica with 80:20 hexane-EtOAc as eluent gave *N*-phenylsulfonyl pyrrolidine **343** (122 mg, 93%) as a yellow oil, R_F (1:1 hexane-EtOAc) 0.52; IR (ATR) 1516, 1349, 1245, 1165 cm^{-1}; ^1H NMR (400 MHz, $CDCl_3$) δ 7.75 (d, J = 8.0 Hz, 2H, Ar), 7.63-7.55 (m, 1H, Ar), 7.49 (dd, J = 8.0, 8.0 Hz, 2H, Ar), 7.36 (d, J = 9.0 Hz, 2H, Ar), 6.85 (d, J = 9.0 Hz, 2H, Ar), 3.80 (s, 4H, OMe and NCH), 2.87 (ddd, J = 10.5, 9.5, 8.0 Hz, 1H, NCH), 2.34-2.25 (m, 1H, CH), 1.92-1.87 (m, 1H, CH), 1.38-1.33 (m, 1H, CH), 1.21 (dd, J = 9.0, 6.0 Hz, 1H, CH), 0.40 (dd, J = 6.0 Hz, 1H, CH); ^{13}C NMR (100.6 MHz, $CDCl_3$) δ 158.8 (*ipso*-Ar), 136.7 (*ipso*-Ar), 132.8 (Ar), 131.4 (*ipso*-Ar), 129.5 (Ar), 128.7 (Ar), 128.5 (Ar), 113.6 (Ar), 55.4 (OMe), 49.7 (N*C*Ar), 47.9 (NCH_2), 27.5 (CH), 25.2 (CH_2), 11.7 (CH_2); MS (EI) *m/z* 352 [(M + Na)$^+$, 100]; HRMS (ESI) *m/z* calcd for $C_{18}H_{19}NO_3S$ [(M + Na)$^+$, 100] 352.0978, found 352.0980 (−0.7 ppm error). Lab book reference HFK5-043

2-Methanesulfonyl-1-(2-methoxyphenyl)-2-azabicyclo[3.1.0]hexane 345

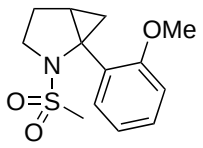

345

HCl (3.0 mL of a 4 M solution in dioxane, 12 mmol, 67 eq.) was added dropwise to a stirred solution of *N*-Boc protected amide **367** (53 mg, 0.18 mmol, 1.0 eq.) at rt under Ar. The resulting solution was stirred at rt for 1 h. Then, the solvent was evaporated under reduced pressure to give the crude HCl salt. Et_3N (128 μL, 0.916 mmol, 5.0 eq.)

was added dropwise to a stirred solution the HCl salt in CH_2Cl_2 (3 mL) at rt under Ar. The resulting solution was stirred at rt for 10 min and MsCl (31 μL, 0.40 mmol, 2.2 eq.) was added dropwise. The resulting solution was stirred at rt for 18 h. The mixture was poured into water (10 mL) and extracted with CH_2Cl_2 (3 × 10 mL). The combined organics were dried ($MgSO_4$) and evaporated under reduced pressure to give the crude product. Purification by flash column chromatography on silica with 70:30 hexane-EtOAc as eluent gave *N*-methanesulfonyl pyrrolidine **345** (39 mg, 80%) as a white solid, mp 86-88 °C; R_F (1:1 hexane-EtOAc 0.31); IR (ATR) 1331, 1149, 752, 517 cm^{-1}; ^1H NMR (400 MHz, $CDCl_3$) δ 7.42 (dd, J = 7.5, 2.0 Hz, 1H, Ar), 7.30 (ddd, J = 8.0, 7.5, 2.0 Hz, 1H, Ar), 6.93 (ddd, J = 7.5, 7.5, 1.0 Hz, 1H, Ar), 6.88 (dd, J = 8.0, 1.0 Hz, 1H, Ar), 3.88 (s, 3H, OMe), 3.75 (ddd, J = 9.0, 9.0, 3.0 Hz, 1H, NCH), 3.31-3.25 (m, 1H, NCH), 2.53 (s, 3H, SO_2Me), 2.46-2.37 (m, 1H, CH), 2.11-2.05 (m, 1H, CH), 1.66-1.61 (m, 1H, CH), 1.35-1.34 (m, 1H, CH), 1.33-1.32 (m, 1H, CH); ^{13}C NMR (100.6 MHz, $CDCl_3$) δ 159.3 (*ipso*-Ar), 132.6 (Ar), 129.7 (Ar), 126.2 (*ipso*-Ar), 120.4 (Ar), 110.7 (Ar), 55.7 (OMe), 48.5 (NCH_2), 47.0 (N*C*Ar), 38.8 (SO_2Me), 26.3 (CH), 26.2 (CH_2), 16.4 (CH_2); MS (EI) *m/z* 290 [$(M + Na)^+$, 100]; HRMS (ESI) *m/z* calcd for $C_{13}H_{17}NO_3S$ [$(M + Na)^+$, 100] 290.0821, found 290.0820 (+0.5 ppm error). Lab book reference HFK5-045

1-(1-1*H*-Pyrrolo[2,3-b]pyridin-6-yl-2-azabicyclo[3.1.0]hexan-2-yl)ethan-1-one 349

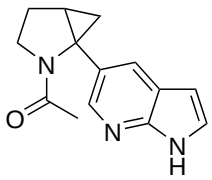

349

Using general procedure A, *N*-Boc protected amide **383** (49 mg, 0.11 mmol, 1.0 eq.) in HCl (5.0 mL of a 4 M solution in dioxane, 20 mmol, 185 eq.) and then Ac_2O (61 μL, 0.65 mmol, 6.0 eq.) in pyridine (3 mL) gave the crude product. Purification by

flash column chromatography on silica with 95:5 CH_2Cl_2-MeOH as eluent gave a 45:55 mixture (by ^{1}H NMR spectroscopy) of *N*-Ac pyrrolidine **349** and *N*-Ac pyrrolidine **384** (27 mg). 2 M $NaOH_{(aq)}$ (2 mL) was added to a 45:55 mixture of **349** and **384** (27 mg) in MeOH (3 mL) at rt under Ar. The resulting solution was stirred at rt for 2 h. Then, the solvent was evaporated under reduced pressure. H_2O (10 mL) was added and the mixture was extracted with CH_2Cl_2 (2 ×10 mL). The combined organics were dried ($MgSO_4$) and evaporated under reduced pressure to give *N*-Ac pyrrolidine **349** (5 mg, 19% over 2 steps) as a cream solid, mp 158-160 °C; R_F (9:1 CH_2Cl_2-MeOH) 0.33; IR (ATR) 3373 (NH), 1680 (C=O), 1392, 1159 cm^{-1}; ^{1}H NMR (400 MHz, $CDCl_3$) δ 10.93 (br s, 1H, NH), 8.29 (br s, 1H, Ar), 7.85-7.84 (m, 1H, Ar), 7.42-7.41 (m, 1H, Ar), 6.57-6.40 (m, 1H, Ar), 4.23-4.11 (m, 1H, NCH), 4.08-3.95 (m, 1H, NCH), 2.51-2.35 (m, 1H, CH), 2.15 (dd, J = 9.0, 5.5 Hz, 1H, CH), 2.07-1.91 (m, 2H, CH), 1.88 (s, 3H, C(O)Me), 1.83-1.70 (m, 1H, CH), 1.14 (dd, J = 5.5, 5.5 Hz, 1H, CH); ^{13}C NMR (100.6 MHz, $CDCl_3$) δ 172.3 (C=O), 148.1 (*ipso*-Ar), 141.4 (Ar), 128.2 (*ipso*-Ar), 126.6 (Ar), 126.5 (Ar), 120.3 (*ipso*-Ar), 100.7 (Ar), 52.2 (NCH_2), 49.2 (N*C*Ar), 32.4 (N*C*Ar), 27.3 (CH_2), 25.5 (CH_2), 23.8 (C(O)Me); MS (EI) *m/z* 264 [(M + Na)$^+$, 100]; HRMS (ESI) *m/z* calcd for $C_{14}H_{15}N_3O$ [(M + Na)$^+$, 100] 264.1107, found 264.1101 (+2.5 ppm error). Diagnostic signal for *N*-Ac pyrrolidine **384**: ^{1}H NMR (400 MHz, $CDCl_3$) δ 3.04 (s, 3.3H, C(O)Me).

Lab book reference HFK5-094

1-(4-Methoxyphenyl)-2-(pyridin-3-yl)-2-azabicyclo[3.1.0]hexane 385

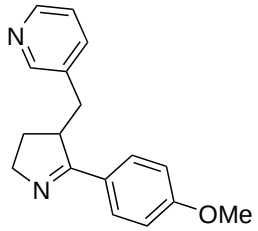

385

N-Boc protected amide **381** (100 mg, 0.346 mmol, 1.0 eq.) was dissolved in HCl (3.0

mL of a 4 M solution in dioxane, 12 mmol, 35 eq.) and the resulting solution was stirred at rt for 2 h. Then, the solvent was evaporated under reduced pressure to give the HCl salt. KO*t*-Bu (98 mg, 0.87 mmol, 2.5 eq.), *rac*-BINAP (13 mg, 0.020 mmol, 0.058 eq.), 3-bromopyridine (67 μL, 0.69 mmol, 2.0 eq.) and $Pd_2(dba)_3$ (9.5 mg, 0.010 mmol, 0.030 eq.) were added to the HCl salt in toluene (1.00 mL) at rt under Ar. The resulting solution was stirred and heated at 90 °C for 18 h. The mixture was allowed to cool to rt and the solvent was evaporated under reduced pressure. Saturated $NH_4Cl_{(aq)}$ (10 mL) was added and the two layers were separated. The aqueous layer was extracted with CH_2Cl_2 (4 × 10 mL). The combined organics were dried (Na_2SO_4) and evaporated under reduced pressure to give the crude product. Purification by flash column chromatography on silica with 80:20 to 50:50 CH_2Cl_2-acetone gave imine **385** (29 mg, 32%) as an orange solid, mp 72-74 °C; R_F (1:1 CH_2Cl_2-acetone) 0.1; IR (ATR) 1603, 1512, 1249, 1172 cm^{-1}; ^1H NMR (400 MHz, $CDCl_3$) δ 8.46 (br dd, J = 5.0, 2.0 Hz, 1H, Ar), 8.43 (br d, J = 2.0 Hz, 1H, Ar), 7.81 (d, J = 9.0 Hz, 2H, Ar), 7.42 (ddd, J = 8.0, 2.0, 2.0 Hz, 1H, Ar), 7.19 (ddd, J = 8.0, 5.0, 0.5 Hz, 1H, Ar), 6.96 (d, J = 9.0 Hz, 2H, Ar), 3.99 (ddd, J = 16.0, 9.0, 2.5 Hz, 1H, NCH), 3.85 (s, 3H, OMe), 3.69-3.62 (m, 1H, CH), 3.61-3.53 (m, 1H, NCH), 2.98 (dd, J = 14.0, 4.0 Hz, 1H, CH), 2.60 (dd, J = 14.0, 9.0 Hz, 1H, CH), 2.17-2.01 (m, 1H, CH), 1.86-1.79 (m, 1H, CH); ^{13}C NMR (100.6 MHz, $CDCl_3$) δ 174.6 (C=N), 161.5 (*ipso*-Ar), 150.4 (Ar), 148.0 (Ar), 136.5 (Ar), 135.1 (*ipso*-Ar), 129.6 (Ar), 126.3 (*ipso*-Ar), 123.4 (Ar), 114.2 (Ar), 59.3 (NCH_2), 55.5 (OMe), 48.0 (CH), 35.1 (CH_2), 28.7 (CH_2); MS (EI) *m/z* 267 $(M + H)^+$; HRMS (ESI) *m/z* calcd for $C_{17}H_{18}N_{20}$ $(M + H)^+$ 267.1492, found 267.1492 (−0.2 ppm error).

Lab book reference HFK5-057

***tert*-Butyl-1-4,8-dioxo-6-[(1R,2R,3R,5S)-2,6,6-trimethylbicyclo-[3.1.1]heptan-3-yl]-1,3,6,2-dioxazaborocan-2-yl-2-azabicyclo[3.1.0]hexane-2-carboxylates 397a and 397b**

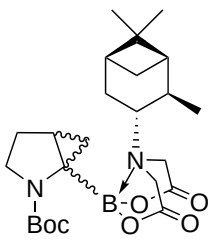

397a

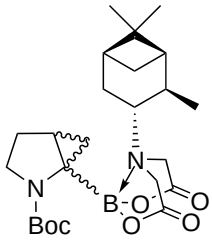

397b

Iminodiacetic acid **396** (296 mg, 1.10 mmol, 1.1 eq) was added to a stirred solution of boronic acid **380** (243 mg, 1.0 mmol, 1.0 eq) in toluene (2.5 mL) and anhydrous DMSO (2.5 mL) at rt under Ar. The resulting solution was connected to a Dean-Stark apparatus and stirred and heated at 112 °C for 2 h. The mixture was allowed to cool to rt and stirred at rt for 18 h. Then, H_2O (15 mL) was added and the mixture was extracted with Et_2O (3 x 15 mL). The combined organics were washed with brine (2 × 15 mL), dried ($MgSO_4$) and evaporated under reduced pressure to give the crude product. Purification by flash column chromatography on silica with 95:5 to 50:50 CH_2Cl_2-acetone as eluent gave MIDA boronate **397a** (57 mg, 12%) as a yellow oil, R_F (9:1 CH_2Cl_2-acetone) 0.53; $[\alpha]_D$ +4.4 (*c* 1.0 in $CHCl_3$); IR (ATR) 1750 (C=O, ester), 1683 (C=O, Boc), 1392, 1154, 1003 cm^{-1}; ^1H NMR (400 MHz, $CDCl_3$) diagnostic signals δ 4.74 (d, J = 15.0 Hz, 1H, NCHC(O)), 4.21 (d, J = 17.5 Hz, 1H, NCHC(O)), 3.99-3.79 (m, 1H, NCH) 3.70-3.50 (m, 2H, NCH), 3.47-3.33 (m, 2H, NCH), 1.39 (s, 9H, CMe_3) 1.34 (d, J = 7.0 Hz, 3H, Me), 1.24 (s, 3H, Me), 1.10 (dd, J = 9.0, 5.0 Hz, 1H, CH), 1.05 (s, 3H, Me), 0.88 (d, J = 11.0 Hz, 1H, CH), 0.84 (dd, J = 5.0, 5.0 Hz, 1H, CH); ^{13}C NMR (100.6 MHz, $CDCl_3$) diagnostic signals δ 169.8 (C=O, ester), 168.1 (C=O, ester), 156.7 (C=O, Boc), 80.9 (*C*Me_2), 79.6 (O*C*Me_3), 65.1 (NCH), 61.3 (N*C*H_2C(O)), 56.8 (N*C*H_2C(O)), 51.3 (NCH_2), 41.0 (*C*HMe), 39.1 (NCB), 28.5 (C*Me*$_3$), 27.5 (Me), 22.9 (Me), 22.8 (Me), 22.3 (CH_2); MS (EI) *m/z* 483 [$(M + Na)^+$, 100]; HRMS (ESI) *m/z* calcd for $C_{24}H_{37}BN_2O_6$ [$(M + Na)^+$, 100] 483.2637, found

483.2636 (+1.2 ppm error) and MIDA boronate **397b** (46 mg, 11%) as a white solid, R_F (9:1 CH_2Cl_2-acetone) 0.37; $[\alpha]_D$ −12.6 (*c* 1.0 in $CHCl_3$); IR (ATR) 1749 (C=O, ester), 1688 (C=O, Boc), 1391, 1366, 1150 cm^{-1}; ^1H NMR (400 MHz, $CDCl_3$) diagnostic signals δ 4.74 (d, J = 15.0 Hz, 1H, NCHC(O)), 4.34-4.17 (m, 2H, NCH), 3.68-3.42 (m, 3H, NCH), 3.20-3.13 (m, 1H, NCH), 1.42 (s, 9H, CMe_3), 1.27-1.18 (m, 6H, 2 × Me), 0.99-0.97 (m, 1H, CH), 0.96 (s, 3H, Me), 0.92 (d, 1H, J = 11.0 Hz, CH), 0.74 (dd, 1H J = 5.5 Hz, CH);^{13}C NMR (100.6 MHz, $CDCl_3$) diagnostic signals δ 169.0 (C=O, ester), 168.2 (C=O, ester), 157.2 (C=O, Boc), 81.0 (*C*Me_2), 80.0 (O*C*Me_3), 67.5 (NCH), 64.2 (N*C*H_2C(O)), 57.5 (N*C*H_2C(O)), 46.5 (NCH_2), 39.3 (NCB), 28.7 (Me), 28.5 (C*Me*$_3$), 25.1 (CH_2), 23.4 (Me), 22.9 (Me); MS (EI) *m/z* 483 [(M + Na)$^+$, 100]; HRMS (ESI) *m/z* calcd for $C_{24}H_{37}BN_2O_6$ [(M + Na)$^+$, 100] 483.2637, found 483.2644 (−0.5 ppm error). Isolated MIDA boronates **397a** and **397b** were slightly impure.

Lab book reference HFK5-071

tert-Butyl-1-(4-methoxyphenyl)-2-azabicyclo[3.1.0]hexane-2-carboxylate 381

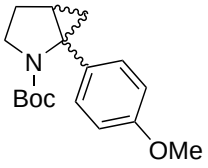

381

Using general procedure B, *N*-Boc boronate **397a** (57 mg, 0.12 mmol, 1.0 eq.), Cs_2CO_3 (242 mg, 0.744 mmol, 6.0 eq.), PCy_3 (10 mg, 0.037 mmol, 0.3 eq.), $Pd(OAc)_2$, (4.2 mg, 0.019 mmol, 0.15 eq.) and 4-bromoanisole (22 μL, 0.17 mmol, 1.4 eq.) in toluene (2.4 mL) and H_2O (75 μL) gave the crude product. Purification by flash column chromatography on silica with 90:10 to 80:20 hexane-Et_2O as eluent gave arylated pyrrolidine **381** (28 mg, 78%), $[\alpha]_D$ +29.5 (*c* 1.0 in $CHCl_3$); CSP-HPLC: Chiralcel OD-H (90:10 hexane-*i*-PrOH, 0.5 mL min[1]) 10.2 min (major), 6.92 min (minor).

Lab book reference HFK5-077

***tert*-Butyl-1-(4-methoxyphenyl)-2-azabicyclo[3.1.0]hexane-2-carboxylate *ent*-381**

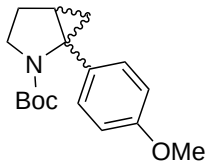

ent-**381**

Using general procedure B, *N*-Boc boronate **397b** (46 mg, 0.10 mmol, 1.0 eq.), Cs_2CO_3 (195 mg, 0.599 mmol, 6.0 eq.), PCy_3 (8.4 mg, 0.030 mmol, 0.3 eq.), $Pd(OAc)_2$, (3.4 mg, 0.015 mmol, 0.15 eq.) and 4-bromoanisole (18 μL, 0.14 mmol, 1.4 eq.) in toluene (2.1 mL) and H_2O (61 μL) gave the crude product. Purification by flash column chromatography on silica with 75:15 hexane-Et_2O as eluent gave arylated pyrrolidine *ent*-**381** (18 mg, 62%), $[\alpha]_D$ −29.7 (*c* 1.0 in $CHCl_3$); CSP-HPLC: Chiralcel OD-H (90:10 hexane-*i*-PrOH, 0.5 mL min[1]) 10.9 min (major), 10.0 min (minor).

Lab book reference HFK5-078

6.4 Experimental for Chapter Four

tert-Butyl 1,1-dibromo-6-azaspiro[2.5]octane-6-carboxylate 427

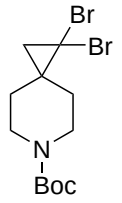

427

$CHBr_3$ (2.45 mL, 28.0 mmol, 1.4 eq.) and benzyltriethylammonium chloride (820 mg, 3.60 mmol, 0.2 eq.) were added to a stirred solution of *tert*-butyl 4-methylidenepiperidine-1-carboxylate **426** (3.94 g, 20.0 mmol, 1.0 eq.) in CH_2Cl_2 (45 mL) at rt. Then, a solution of NaOH (30.8 g, 770 mmol, 39 eq.) in H_2O (31 mL) was added. The resulting solution was stirred and heated at 45 °C for 18 h. The mixture was then allowed to cool to rt. Then, H_2O (40 mL) was added and the mixture was extracted with CH_2Cl_2 (3 × 40 mL). The combined organic extracts were dried (Na_2SO_4), decanted from the black sediment formed and evaporated under reduced pressure to give the crude product. Purification by flash chromatography on silica with 95:5 to 90:10 to 70:30 hexane-Et_2O as eluent gave dibromocyclopropane **427** (4.80 g, 65%) as a white solid, mp 102-105 °C; R_F (4:1 hexane-Et_2O) 0.39; IR (ATR) 1690 (C=O), 1419, 1239, 1168 cm^{-1}; ^1H NMR (400 MHz, $CDCl_3$) δ 3.61 (ddd, J = 13.5, 7.5, 4.0 Hz, 2H, NCH), 3.40 (ddd, J = 13.5, 7.5, 4.0 Hz, 2H, NCH), 1.83 (ddd, J = 13.5, 7.5, 4.0 Hz, 2H, CH), 1.68 (ddd, J = 13.5, 7.5, 4.0 Hz, 2H, CH), 1.48 (s, 2H, CH_2CBr_2), 1.46 (br s, 9H, CMe_3); ^{13}C NMR (100.6 MHz, $CDCl_3$) δ 154.9 (C=O), 79.9 (O*C*Me_3), 42.9 (NCH_2), 37.1 (CBr_2), 34.7 (CH_2), 33.1 (CH_2), 30.7(*C*CBr_2), 28.6 (C*Me*$_3$); MS (EI) *m/z* 390 [(^{79,79}M + Na)$^+$, 100]; HRMS (ESI) *m/z* calcd for $C_{12}H_{19}{}^{79}Br_2NO_2$ [(^{79,79}M + Na)$^+$, 100] 389.9675, found 389.9670 (+1.2 ppm error) and a 65:35 mixture (by ^1H NMR spectroscopy) of dibromocyclopropane **427** and *tert*-butyl 4-methylidenepiperidine-1-carboxylate **426** (1.70 g, i.e. 1.32 g (18%) of **427** and 380 mg (10%) of **426**).

Lab book reference HFK6-095

***tert*-Butyl 1-bromo-6-azaspiro[2.5]octane-6-carboxylate 428**

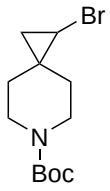

428

EtMgBr (2.5 mL of a 2 M solution in Et_2O, 5.0 mmol, 1.2 eq.) was added dropwise over 1 h (using a syringe pump) to a stirred solution of dibromocyclopropane **427** (1.51 g, 4.09 mmol, 1.0 eq.) and Ti(O*i*–Pr)$_4$ (122 μL, 0.410 mmol, 0.1 eq.) in THF (30 mL) at rt under Ar. The resulting solution was stirred at rt for 3 h. Then, H_2O (15 mL) and 20% $H_2SO_{4(aq)}$ (30 mL) were added dropwise slowly (care - exothermic quench) and the mixture was stirred at rt for 30 min. The mixture was extracted with Et_2O (3 × 20 mL). The combined organic extracts were washed with saturated $NaHCO_{3(aq)}$ (20 mL) and brine (20 mL), dried ($MgSO_4$) and evaporated under reduced pressure to give the crude product. Purification by flash column chromatography on silica with 85:15 hexane-EtOAc as eluent gave bromocyclopropane **428** (903 mg, 76%) as a white solid, mp 48-50 °C; R_F (4:1 hexane-Et_2O) 0.36; IR (ATR) 1683 (C=O), 1418, 1240, 1166, 1123 cm^{-1}; ^{1}H NMR (400 MHz, $CDCl_3$) δ 3.47-3.34 (m, 4H, NCH), 2.85 (dd, J = 7.5, 4.0 Hz, 1H, CHBr), 1.68-1.57 (m, 2H, CH), 1.43 (m, 10H, CMe_3 and CH), 1.31 (ddd, J = 13.5, 7.0, 4.0 Hz, 1H, CH), 1.03 (dd, J = 7.5, 6.5 Hz, 1H, CH), 0.71 (dd, J = 6.5, 4.0 Hz, 1H, CH); ^{13}C NMR (100.6 MHz, $CDCl_3$) δ 155.0 (C=O), 79.6 (O*C*Me$_3$), 43.1 (NCH_2), 34.8 (CH_2), 32.4 (CH_2), 28.5 (C*Me$_3$*), 27.8 (CHBr), 22.8 (*C*CHBr), 21.4 (CH_2) (NCH_2 resonance not resolved); MS (EI) *m/z* 312 [(^{79}M + Na)$^+$, 100]; HRMS (ESI) *m/z* calcd for $C_{12}H_{20}{}^{79}BrNO_2$ [(^{79}M + Na)$^+$, 100] 312.0570, found 312.0564 (+2.0 ppm error).

Lab book reference HFK6-099

In the same way, EtMgBr (5.3 mL of a 2 M solution in Et_2O, 10.5 mmol, 1.2 eq.),

dibromocyclopropane **427** (3.23 g, 8.75 mmol, 1.0 eq.) and Ti(O*i*–Pr)$_4$ (260 μL, 0.875 mmol, 0.1 eq.) in THF (50 mL) gave the crude product. Purification by flash column chromatography on silica with 90:10 to 80:20 hexane-EtOAc as eluent gave bromocyclopropane **428** (1.86 g, 73%) as a white solid.

Lab book reference HFK7-019

tert-Butyl 1-(4,4,5,5-tetramethyl-1,3,2-dioxaborolan-2-yl)-6-azaspiro[2.5]-octane-6-carboxylate 431

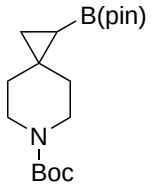

431

n-BuLi (520 μL of a 1.45 M solution in hexanes, 0.750 mmol, 1.5 eq.) was added dropwise to a stirred solution of bromocyclopropane **428** (145 mg, 0.500 mmol, 1.0 eq.) in THF (6 mL) at –78 °C under Ar. The resulting solution was stirred at –78 °C for 1 h. Then, *i*-PrOBpin (153 μL, 0.750 mmol, 1.5 eq.) was added and the solution was allowed to warm to rt. Saturated $NH_4Cl_{(aq)}$ (15 mL) was added and the mixture was extracted with Et_2O (3 × 20 mL). The combined organic extracts were washed with brine (20 mL), dried (Na_2SO_4) and evaporated under reduced pressure to give the crude product. Purification by flash column chromatography on silica with 90:10 to 80:20 hexane-Et_2O as eluent gave pinacol boronate **431** (146 mg, 86%) as a white solid, mp 58-60 °C; R_F (1:1 hexane-Et_2O) 0.44; IR (ATR) 1692 (C=O), 1412, 1143, 859 cm^{-1}; ^{1}H NMR (400 MHz, $CDCl_3$) δ 3.46-3.40 (m, 3H, NCH), 3.38-3.32 (m, 1H, NCH), 1.58-1.54 (m, 2H, CH), 1.45 (s, 9H, CMe_3), 1.36-1.33 (m, 2H, CH), 1.23 (s, 6H, Me), 1.20 (s, 6H, Me), 0.69-0.63 (m, 2H, CH), −0.19 (dd, J = 8.5, 7.0 Hz, 1H, CHB); ^{13}C NMR (100.6 MHz, $CDCl_3$) δ 155.2 (C=O), 83.2 (O*C*Me$_2$), 79.3 (O*C*Me$_3$), 44.1 (NCH_2), 37.4 (CH_2), 31.8 (CH_2), 28.6 (C*Me$_3$*), 25.3 (Me), 24.6 (Me), 17.7 (CH_2) (NCH_2, CHB and *C*CHB resonances not resolved); MS (EI) *m/z* 360 [(M + Na)$^+$, 100];

HRMS (ESI) *m/z* calcd for $C_{18}H_{32}BNO_4$ [$(M + Na)^+$, 100] 360.2317, found 360.2319 (+0.3 ppm error).

Lab book reference HFK7-005

tert-Butyl 1-(6-methyl-4,8-dioxo-1,3,6,2-dioxazaborocan-2-yl)-6-azaspiro-[2.5]-octane-6-carboxylate 209

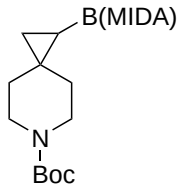

209

$HC(OEt)_3$ (374 μL, 2.25 mmol, 4.5 eq.) and MIDA (1.43 g, 9.75 mmol, 6.5 eq.) were added to a stirred solution of pinacol boronate **431** (506 mg, 1.50 mmol, 1.0 eq.) in anhydrous DMSO (7.5 mL) at rt. The resulting suspension was stirred and heated at 100 °C for 18 h. The mixture was then allowed to cool to rt and saturated $NH_4Cl_{(aq)}$ (20 mL) was added. The mixture was extracted with EtOAc (3 × 20 mL). The combined organic extracts were washed with brine (20 mL), dried ($MgSO_4$) and evaporated under reduced pressure to give the crude product. Purification by flash column chromatography on silica with 80:20 to 70:30 CH_2Cl_2-acetone as eluent gave recovered pincaol boronate **431** (194 mg, 38%) and MIDA boronate **209** (219 mg, 40%) as a white solid, mp 208-215 °C; R_F (7:3 CH_2Cl_2-acetone) 0.34; IR (ATR) 1746 (C=O, ester), 1676 (C=O, Boc), 1424, 1240, 1165 cm^{-1}; ^1H NMR (400 MHz, d_6-acetone) δ 4.19 (d, J = 17.0 Hz, 1H, MeNC*H*), 4.185 (d, J = 17.0 Hz, 1H, MeNC*H*), 4.07 (d, J = 17.0 Hz, 1H, MeNC*H*), 4.01 (d, J = 17.0 Hz, 1H, MeNC*H*), 3.59 (dddd, J = 13.0, 7.0, 4.0, 1 Hz, 1H, NCH), 3.52-3.46 (m, 1H, NCH), 3.40-3.24 (m, 2H, NCH), 3.18 (s, 3H, NMe), 1.68-1.62 (m, 1H, CH), 1.53-1.37 (m, 2H, CH), 1.43 (s, 9H, CMe_3), 1.30-1.21 (m, 1H, CH), 0.55 (dd, J = 9.5, 3.5 Hz, 1H, CH), 0.32 (dd, J = 3.5, 7.0 Hz, 1H, CHB), −0.24 (dd, J = 9.5, 7.0 Hz, 1H, CH); ^{13}C NMR (100.6 MHz, d_6-acetone) δ 169.13 (C=O, ester), 169.09 (C=O, ester), 155.2 (C=O, Boc), 79.1 (O*C*Me_3), 62.48 (MeN*C*H_2), 62.44 (MeN*C*H_2),

46.8 (NMe), 45.1 (NCH_2), 44.3 (NCH_2), 39.0 (CH_2), 31.9 (CH_2), 28.6 (CMe_3), 22.9 (CCHB), 15.1 (CH_2) (CHB resonance not resolved); MS (EI) *m/z* 389 $(M + H)^+$; HRMS (ESI) *m/z* calcd for $C_{17}H_{27}BN_2O_6$ $(M + Na)^+$ 389.1854, found 389.1867 (−2.4 ppm error).

Lab book reference HFK8-004

n-BuLi (9.57 mL of a 1.45 M solution in hexanes, 13.9 mmol, 1.5 eq.) was added dropwise to a stirred solution of bromocyclopropane **428** (2.69 g, 9.26 mmol, 1.0 eq.) in THF (96 mL) at –78 °C under Ar. The resulting solution was stirred at –78 °C for 1 h. Then, $B(OMe)_3$ (1.55 mL, 13.9 mmol, 1.5 eq.) was added. After stirring at –78 °C for 10 min, the solution was allowed to warm to rt and stirred at rt for 3 h. 5% $HCl_{(aq)}$ (37 mL) was added and the mixture was extracted with Et_2O (3 × 40 mL). The combined organic extracts were dried ($MgSO_4$) and evaporated under reduced pressure to give the crude boronic acid **430** (2.62 g). MIDA (1.26 g, 8.55 mmol, 1.1 eq.) was added to a stirred solution of boronic acid **430** in toluene (40 mL) and anhydrous DMSO (40 mL) at rt under Ar. The resulting solution was connected to a Dean-Stark apparatus and stirred and heated at 120 °C for 18 h. The mixture was allowed to cool to rt and EtOAc (40 mL) was added. The mixture was washed with H_2O (3 × 30 mL) and the organic layer was dried ($MgSO_4$) and evaporated under reduced pressure to give the crude product. Purification by flash column chromatography on silica with 90:10 to 80:20 to 50:50 CH_2Cl_2-acetone as eluent gave MIDA boronate **209** (1.48 g, 44% over 2 steps) as a white solid.

Lab book reference HFK7-027

***tert*-Butyl 1,1-dichloro-6-azaspiro[2.5]octane-6-carboxylate 432**

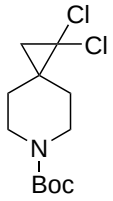

432

Benzyltriethylammonium chloride (170 mg, 0.760 mmol, 0.1 eq.) was added to a stirred solution of *tert*-butyl 4-methylidenepiperidine-1-carboxylate **426** (1.5 g, 7.6 mmol, 1.0 eq.) in $CHCl_3$ (20.0 mL, 249 mmol, 33 eq.) at rt. Then, a solution of NaOH (3.0 g, 75 mmol, 10 eq.) in H_2O (5 mL) was added. The resulting solution was stirred and heated at 50 °C for 3 h. The mixture was then allowed to cool to rt and stirred at rt for 18 h. Then, H_2O (20 mL) was added and the mixture was extracted with $CHCl_3$ (2 × 20 mL). The organic layer was washed with H_2O (20 mL) and brine (20 mL). The combined organic extracts were dried (Na_2SO_4) and evaporated under reduced pressure to give the crude product as a white solid. The crude product was washed with hexane (5 × 10 mL) to give dichlorocyclopropane **432** (1.90 g, 89%) as a white solid, mp 74-78 °C; R_F (7:3 hexane-Et_2O) 0.38; IR (ATR) 1692 (C=O), 1417, 1239, 1167 cm^{-1}; ^1H NMR (400 MHz, $CDCl_3$) δ 3.54 (ddd, J = 13.5, 7.5, 4.0 Hz, 2H, NCH), 3.45 (ddd, J = 13.5, 7.0, 4.0 Hz, 2H, NCH), 1.79 (ddd, J = 13.5, 7.0, 4.0 Hz, 2H, CH), 1.65 (ddd, J = 13.5, 7.5, 4.0 Hz, 2H, CH), 1.46 (br s, 9H, CMe_3), 1.29 (s, 2H, CH_2); ^{13}C NMR (100.6 MHz, $CDCl_3$) δ 154.9 (C=O), 79.8 (O*C*Me_3), 66.5 (CCl_2), 43.1 (NCH_2), 32.6 (CH_2), 31.6 (*C*CCl_2), 31.4 (CH_2), 28.6 (C*Me*$_3$); MS (EI) *m/z* 302 [(^{35,35}M + Na)$^+$, 100]; HRMS (ESI) *m/z* calcd for $C_{12}H_{19}{}^{35}Cl_2NO_2$ [(^{35,35}M + Na)$^+$, 100] 302.0685, found 302.0682 (+0.9 ppm error).

Lab book reference HFK6-086

***tert*-Butyl 1-chloro-6-azaspiro[2.5]octane-6-carboxylate 433 and *tert*-butyl 1-[-6-[(*tert*-butoxy)carbonyl]-6-azaspiro[2.5]octan-1-ylidene]-6-azaspiro-[2.5] octane-6-carboxylate 434**

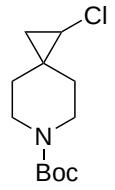

433

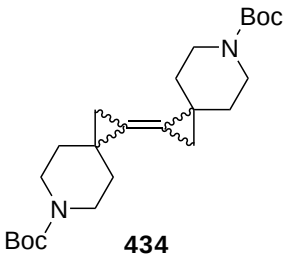

434

s-BuLi (866 μL of a 1.27 M solution in hexanes, 1.10 mmol, 1.1 eq.) was added dropwise to a stirred solution of dichlorocyclopropane **432** (280 mg, 1.00 mmol, 1.0 eq.) and TMEDA (165 μL, 1.10 mmol, 1.1 eq.) in Et_2O (11 mL) at –78 °C under Ar. The resulting solution was stirred at –78 °C for 20 min. Then, H_2O (20 mL) was added and the mixture was allowed to warm to rt. The mixture was extracted with Et_2O (3 × 20 mL) and the combined organic extracts were dried ($MgSO_4$) and evaporated under reduced pressure to give the crude product. Purification by flash column chromatography on silica with 90:10 to 70:30 hexane-Et_2O as eluent gave chlorocyclopropane **433** (124 mg, 51%) as a white solid, R_F (7:3 hexane-Et_2O) 0.44; IR (ATR) 1681 (C=O), 1421, 1237, 1167 cm^{-1}; ^1H NMR (400 MHz, $CDCl_3$) δ 3.54-3.41 (m, 3H, NCH), 3.40-3.34 (m, 1H, NCH), 2.93 (dd, J = 7.5, 4.0 Hz, 1H, CHCl), 1.70-1.58 (m, 2H, CH), 1.45 (s, 9H, CMe_3), 1.43-1.36 (m, 1H, CH), 1.31-1.24 (m, 1H, CH), 0.93 (dd, J = 7.5, 6.0 Hz, 1H, CH), 0.65 (dd, J = 6.0, 4.0 Hz, 1H, CH); ^{13}C NMR (100.6 MHz, $CDCl_3$) δ 155.0 (C=O), 79.6 (O*C*Me_3), 43.5 (NCH_2), 43.0 (NCH_2), 38.6 (CHCl), 34.8 (CH_2), 30.5 (CH_2), 28.6 (C*Me*$_3$), 23.5 (*C*CHCl), 21.2 (CH_2); MS (EI) *m/z* 268 [($^{35}M + Na)^+$, 100]; HRMS (ESI) *m/z* calcd for $C_{12}H_{20}{}^{35}ClNO_2$ [($^{35}M + Na)^+$, 100] 268.1075, found 268.1072 (+1.1 ppm error) and a 50:50 mixture of alkenes (*E*)- and (*Z*)-**434** (51 mg, 24%) as a white solid, mp 148-150 °C; IR (ATR) 1691 (C=O), 1418, 1236, 1167 cm^{-1}; ^1H NMR (400 MHz, $CDCl_3$) δ 3.75-3.72 (m, 2H, NCH), 3.55-3.49 (m, 2H, NCH), 3.46-3.40 (m, 2H, NCH), 3.25-3.19 (m, 2H, NCH), 1.66-1.60 (m, 3H, CH), 1.55-1.40 (m,

2H, CH), 1.475 (s, 9H, CMe_3), 1.465 (s, 9H, CMe_3), 1.36-1.30 (m, 3H, CH), 1.12 (br s, 2H, CH_2), 1.11 (br s, 2H, CH_2); ^{13}C NMR (100.6 MHz, $CDCl_3$) δ 155.1 (C=O), 155.0 (C=O), 119.7 (C=C), 119.1 (C=C), 79.6 (O*C*Me_3), 79.5 (O*C*Me_3), 44.2 (NCH_2), 34.5 (CH_2), 34.2 (CH_2), 28.6 (C*Me*$_3$), 22.5 (*C*C=C), 22.0 (*C*C=C), 16.2 (CH_2), 15.6 (CH_2); MS (EI) *m/z* 441 [[(M + Na)$^+$, 100], 100]; HRMS (ESI) *m/z* calcd for $C_{24}H_{38}N_2O_4$ [(M + Na)$^+$, 100] 441.2724, found 441.2725 (−0.3 ppm error).

Lab book reference HFK6-087

tert-Butyl 5-(phenylsulfanyl)-6-azaspiro[2.5]octane-6-carboxylate 436

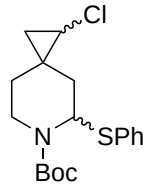

436

s-BuLi (1.27 M solution in hexanes, 0.25 mmol, 197 μL, 1.1 eq.) was added dropwise to a stirred solution of chlorocyclopropane **433** (56 mg, 0.23 mmol, 1.0 eq.) and TMEDA (38 μL, 0.25 mmol, 1.1 eq.) in Et_2O (6 mL) at –78 °C under Ar. The resulting solution was stirred at –78 °C for 20 min. Then, a solution of diphenyl disulfide (55 mg, 0.25 mmol, 1.1 eq.) in Et_2O (3 mL) was added and the solution was allowed to warm to rt and stirred at rt for 2 h. H_2O (10 mL) was added and the mixture was extracted with Et_2O (3 × 10 mL). The combined organic extracts were washed with brine (15 mL), dried ($MgSO_4$) and evaporated under reduced pressure to give the crude product. Purification by flash column chromatography on silica with 98:2 to 95:5 to 90:10 to 50:50 hexane-Et_2O as eluent gave chlorocyclopropyl sulfide **436** (23 mg, 28%) as a yellow oil, ^1H NMR (400 MHz, $CDCl_3$) δ 7.64-6.96 (m, 5H, Ph), 3.59-3.21 (m, 3H, NCH), 3.07-2.77 (m, 1H, CHCl), 1.70-1.61 (m, 3H, CH), 1.45 (s, 9H, CMe_3), 1.33-1.19 (m, 1H, CH), 0.93 (dd, J = 7.0, 7.0 Hz, 1H, CH), 0.71-0.59 (m, 1H, CH); MS (EI) *m/z* 376 [(^{35}M + Na)$^+$, 100]; HRMS (ESI) *m/z* calcd for $C_{18}H_{24}{}^{35}ClNO_2S$ [(^{35}M + Na)$^+$, 100] 376.1108, found 376.1106 (−0.2 ppm error). Chlorocyclopropyl sulfide **436**

is probably formed as a mixture of diastereomers but it was not possible to determine this from the ^{1}H NMR spectrum.

Lab book reference HFK6-090

tert-Butyl 1-(4,4,5,5-tetramethyl-1,3,2-dioxaborolan-2-yl)-6-azaspiro[2.5] -octane-6-carboxylate 431, _tert_-butyl 1-[-6-[(_tert_-butoxy)carbonyl]-6-aza-spiro[2.5]octan-1-ylidene]-6-azaspiro-[2.5]octane-6-carboxylate 434 and _tert_-butyl 1,1-bis(4,4,5,5-tetramethyl-1,3,2-dioxaborolan-2-yl)-6-azaspiro[2.5] octane-6-carboxylate 442

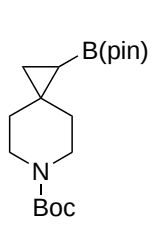

431

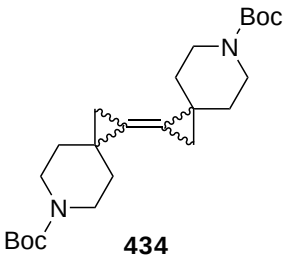

434

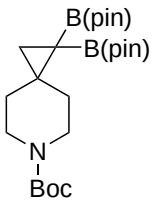

442

_s_-BuLi (814 μL of a 1.35 M solution in hexanes, 1.10 mmol, 1.1 eq.) was added dropwise to a stirred solution of dichlorocyclopropane **432** (280 mg, 1.00 mmol, 1.0 eq.) and TMEDA (165 μL, 1.10 mmol, 1.1 eq.) in Et_2O (11 mL) at –78 °C under Ar. The resulting solution was stirred at –78 °C for 20 min. Then, HB(pin) (218 μL, 1.50 mmol, 1.5 eq.) was added and the solution was allowed to warm to –50 °C over 1 h. The solution was then allowed to warm to rt and stirred at rt for 3 h. Then, H_2O (20 mL) was added and the mixture was extracted with Et_2O (3 × 20 mL). The combined organic extracts were dried (Na_2SO_4) and evaporated under reduced pressure to give the crude product. Purification by flash column chromatography on silica with 90:10 to 80:20 to 50:50 hexane-Et_2O as eluent gave pinacol boronate **431** (191 mg, 57%) as a colourless oil and a 50:50 mixture of alkenes (_E_)- and (_Z_)-**434** (61 mg, 29%) as a white solid.

Lab book reference HFK7-060

s-BuLi (814 μL of a 1.35 M solution in hexanes, 1.10 mmol, 1.1 eq.) was added dropwise to a stirred solution of dichlorocyclopropane **432** (266 mg, 1.00 mmol, 1.0 eq.) and TMEDA (165 μL, 1.10 mmol, 1.1 eq.) in Et_2O (11 mL) at –100 °C under Ar. The resulting solution was stirred at –100 °C for 20 min. Then, HB(pin) (218 μL, 1.50 mmol, 1.5 eq.) was added and the solution was allowed to warm to –50 °C over 1 h. The solution was then allowed to warm to rt and stirred at rt for 3 h. Then, H_2O (20 mL) was added and the mixture was extracted with Et_2O (3 × 20 mL). The combined organic extracts were dried (Na_2SO_4) and evaporated under reduced pressure to give the crude product. Purification by flash column chromatography on silica with 90:10 to 85:15 hexane-Et_2O as eluent gave pinacol boronate **431** (243 mg, 72%) as a colourless oil.

Lab book reference HFK7-061

s-BuLi (11.0 mL of a 1.35 M solution in hexanes, 14.9 mmol, 1.1 eq.) was added dropwise to a stirred solution of dichlorocyclopropane **432** (3.78 g, 13.5 mmol, 1.0 eq.) and TMEDA (2.20 mL, 14.9 mmol, 1.1 eq.) in Et_2O (148 mL) at –100 °C under Ar. The resulting solution was stirred at –100 °C for 20 min. Then, HB(pin) (6.43 mL, 20.3 mmol, 1.5 eq.) was added and the solution was allowed to warm to –50 °C over 1 h. The solution was then allowed to warm to rt and stirred at rt for 18 h. Then, H_2O (100 mL) was added and the mixture was extracted with Et_2O (3 × 75 mL). The combined organic extracts were dried (Na_2SO_4) and evaporated under reduced pressure to give the crude product. Purification by flash column chromatography on silica with 90:10 to 80:20 to 60:40 hexane-Et_2O as eluent gave pinacol boronate **431** (1.7 g, 36%) as a colourless oil and cyclopropyl diboronate **442** (316 mg, 5%) as a white solid, mp 140-142 °C; R_F (1:1 hexane-Et_2O) 0.46; IR (ATR) 1684 (C=O), 1409, 1238, 1121 cm^{-1}; ^1H NMR (400 MHz, $CDCl_3$) δ 3.70-3.54 (m, 2H, NCH), 3.28-3.22 (m, 2H, NCH), 1.67-1.60 (m, 2H, CH), 1.44 (s, 9H, CMe_3), 1.40-1.31 (m, 2H, CH), 1.21 (s, 12H, Me), 1.18 (s, 12H, Me), 0.88 (s, 2H, CH_2); MS (EI) *m/z* 486 [$(M + Na)^+$, 100]; HRMS (ESI) *m/z* calcd for $C_{24}H_{43}B_2NO_6$ [$(M + Na)^+$, 100] 486.3169, found 486.3161 (+3.4 ppm error)

and a 65:35 mixture (by ^{1}H NMR spectroscopy) of HB(pin) and a 50:50 mixture of alkenes (*E*)- and (*Z*)-**434** (1.02 g, i.e. 650 mg (12%) of alkenes **434**).

Lab book reference HFK7-085

tert-Butyl 7,7-dibromo-3-azabicyclo[4.1.0]heptane-3-carboxylate 445

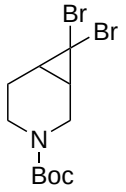

445

$CHBr_3$ (6.56 mL, 75.0 mmol, 3 eq.) and benzyltriethylammonium chloride (1.03 g, 4.50 mmol, 0.2 eq.) were added to a stirred solution of *tert*-butyl 1,2,3,6-tetrahydropyridine-1-carboxylate **370** (4.58 g, 25.0 mmol, 1.0 eq.) in CH_2Cl_2 (75 mL) at rt. Then, a solution of NaOH (39.0 g, 975 mmol, 39 eq.) in H_2O (39 mL) was added. The resulting solution was stirred and heated at 45 °C for 18 h. The mixture was then allowed to cool to rt. Then, H_2O (40 mL) was added and the mixture was extracted with CH_2Cl_2 (3 × 40 mL). The combined organic extracts were dried (Na_2SO_4), decanted from the black sediment formed and evaporated under reduced pressure to give the crude product. Purification by flash chromatography on silica with 95:5 to 90:10 to 70:30 hexane-Et_2O as eluent gave dibromocyclopropane **445** (6.66 g, 75%) as a yellow oil, R_F (1:1 hexane-Et_2O) 0.44; IR (ATR) 1689 (C=O), 1423, 1249, 1167 cm^{-1}; ^{1}H NMR (400 MHz, $CDCl_3$) (60:40 mixture of rotamers) δ 4.11-3.75 (m, 1.6H, NCH), 3.67-3.38 (m, 1.4H, NCH), 2.72 (m, 0.4H, NCH), 2.63-2.50 (m, 0.6H, NCH), 2.14-2.00 (m, 2H, CH), 1.91-1.74 (m, 1H, CH), 1.63 (m, 1H, CH), 1.42 (s, 9H, CMe_3); ^{13}C NMR (100.6 MHz, $CDCl_3$) (rotamers) δ 154.5 (C=O), 79.9 (O*C*Me_3), 40.3 (NCH_2), 39.8 (NCH_2), 39.5 (NCH_2), 38.6 (NCH_2), 36.6 (CBr_2), 36.5 (CBr_2), 28.6 (C*Me*$_3$), 26.7 (CH), 26.6 (CH), 25.9 (CH), 25.7 (CH), 20.9 (CH_2), 20.7 (CH_2); MS (EI) *m/z* 376 [(^{79,79}M + Na)$^+$, 100]; HRMS (ESI) *m/z* calcd for $C_{11}H_{17}{}^{79}Br_2NO_2$ [(^{79,79}M + Na)$^+$, 100] 375.9518, found 375.9507 (+3.0 ppm error).

Lab book reference HFK7-014

***tert*-Butyl-7-bromo-3-azabicyclo[4.1.0]heptane-3-carboxylate-*exo*-446, *endo*-446 and *tert*-butyl 3-azabicyclo[4.1.0]heptane-3-carboxylate 454**

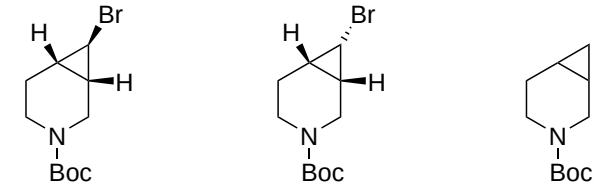

exo-**446** *endo*-**446** **454**

(Table 4.1, Entry 3)

Dimethyl phosphite (622 μL, 6.78 mmol, 6 eq.) was added to a stirred solution of dibromocyclopropane **445** (401 mg, 1.13 mmol, 1.0 eq.) in anhydrous DMSO (10 mL) at rt under Ar. Then, KO*t*-Bu (761 mg, 6.78 mmol, 6.0 eq.) was added portionwise and the resulting solution was stirred at rt for 1 h. Saturated $Na_2CO_{3(aq)}$ (15 mL) and Et_2O (20 mL) were added. The two layers were separated and the aqueous layer was extracted with Et_2O (3 × 20 mL). The combined organics were dried (Na_2SO_4) and evaporated under reduced pressure to give the crude product. Purification by flash column chromatography on silica with 95:5 hexane-EtOAc as eluent gave bromocyclopropane *exo*-**446** (259 mg, 79%) as a colourless oil, R_F (1:1 hexane-Et_2O) 0.52; IR (ATR) 1694 (C=O), 1366, 1168, 1129 cm^{-1}; ^1H NMR (400 MHz, $CDCl_3$) δ 3.97 (br d, J = 14.0 Hz, 1H, NCH), 3.37 (dd, J = 14.0, 5.0 Hz, 1H, NCH), 3.40-3.35 (m, 1H, CH), 2.87-2.75 (m, 1H, NCH), 2.58 (dd, J = 3.5, 3.5 Hz, 1H, CHBr), 1.97-1.89 (m, 1H, CH), 1.82-1.71 (m, 1H, CH), 1.56-1.50 (m, 1H, CH), 1.45-1.42 (m, 1H, CH), 1.43 (br s, 9H, CMe_3); ^{13}C NMR (100.6 MHz, $CDCl_3$) δ 154.9 (C=O), 79.9 (O*C*Me_3), 41.0 (br, NCH), 28.5 (C*Me*$_3$), 23.6 (CHBr), 22.1 (CH_2), 21.1 (CH), 19.9 (CH) (NCH_2 resonance not resolved); MS (EI) m/z 298 [(^{79}M + Na)$^+$, 100]; HRMS (ESI) m/z calcd for $C_{11}H_{18}{}^{79}BrNO_2$ [(^{79}M + Na)$^+$, 100] 298.0413, found 298.0407 (+1.9 ppm error). Lab book reference HFK7-095

In the same way, dimethyl phosphite (18.2 mL, 198 mmol, 6 eq.), dibromocyclopropane **445** (11.6 g, 33.0 mmol, 1.0 eq.) and KO*t*-Bu (14.8 g, 132 mmol, 4.0 eq.) in anhydrous DMSO (200 mL) gave the crude product. Purification by flash column chromatography on silica with 95:5 to 90:10 hexane-EtOAc as eluent gave bromocyclopropane *exo*-**446** (6.68 g, 70%) as a colourless oil.

Lab book reference HFK7-095

(Table 4.1, Entry 1)

EtMgBr (4.18 mL of a 3 M solution in Et_2O, 12.5 mmol, 1.2 eq.) was added dropwise over 1 h (using a syringe pump) to a stirred solution of dibromocyclopropane **445** (3.71 g, 10.5 mmol, 1.0 eq.) and Ti(O*i*–Pr)$_4$ (0.31 mL, 1.1 mmol, 0.1 eq.) in THF (60 mL) at rt under Ar. The resulting solution was stirred at rt for 7 h. Then, H_2O (30 mL) and 20% $H_2SO_{4(aq)}$ (75 mL) were added dropwise slowly (care - exothermic quench) and the mixture was stirred at rt for 30 min. The mixture was extracted with Et_2O (3 × 40 mL). The combined organic extracts were washed with saturated $NaHCO_{3(aq)}$ (40 mL) and brine (40 mL), dried ($MgSO_4$) and evaporated under reduced pressure to give the crude product which contained a 70:30 mixture (by ^{1}H NMR spectroscopy) of bromocyclopropanes *endo*-**446** and *exo*-**446**. Purification by flash column chromatography on silica with 95:5 to 50:50 hexane-EtOAc as eluent gave bromocyclopropane *exo*-**446** (345 mg, 11%) as a colourless oil, and bromocyclopropane *endo*-**446** (741 mg, 24%) as a pale yellow oil, R_F (1:1 hexane-Et_2O) 0.39; IR (ATR) 1687 (C=O), 1423, 1266, 1167 cm^{-1}; ^{1}H NMR (400 MHz, $CDCl_3$) δ 3.79-3.59 (m, 3H, NCH), 3.27 (dd, J = 7.5, 7.5 Hz, 1H, CHBr), 2.87-2.66 (br m, 1H, NCH), 2.01 (dddd, J = 14.5, 9.5, 4.5, 3.5 Hz, 1H, CH), 1.61 (dddd, J = 14.5, 10.5, 5.5, 3.5 Hz, 1H, CH), 1.44 (br s, 9H, CMe_3), 1.43-1.37 (m, 2H, CH); ^{13}C NMR (100.6 MHz, $CDCl_3$) δ 154.7 (C=O), 79.5 (O*C*Me$_3$), 39.6 (br NCH_2), 30.8 (CHBr), 28.7 (C*Me$_3$*), 19.5 (CH_2), 12.15 (CH), 12.0 (CH) (NCH_2 resonance not resolved); MS (EI) *m/z* 298 [(^{79}M + Na)$^+$, 100]; HRMS (ESI) *m/z* calcd for $C_{11}H_{18}{}^{79}BrNO_2$ [(^{79}M + Na)$^+$, 100] 298.0413, found 298.0409 (+1.5 ppm error).

Lab book reference HFK7-021

(Table 4.2, Entry 2)

n-BuLi (230 μL of a 2.44 M solution in hexanes, 0.550 mmol, 1.1 eq.) was added dropwise to a stirred solution of dibromocyclopropane **445** (178 mg, 0.500 mmol, 1.0 eq) in THF (8 mL) at –78 °C under Ar. The resulting solution was stirred at –78 °C for 25 min. Then, H_2O (4 mL) was added. The mixture was allowed to warm to rt and extracted with Et_2O (3 × 10 mL). The combined organic extracts were dried (Na_2SO_4) and evaporated under reduced pressure to give the crude product which contained a 65:35 mixture (by ^{1}H NMR spectroscopy) of bromocyclopropanes *endo*-**446** and *exo*-**446**. Purification by flash column chromatography on silica with 90:10 to 70:30 hexane-Et_2O as eluent gave bromocyclopropanes *exo*-**446** (37 mg, 26%) and *endo*-**446** (24 mg, 17%).

Lab book reference HFK8-011

(Table 4.2, Entry 4)

A solution of the dibromocyclopropane **445** (178 mg, 0.5 mmol, 1.0 eq.) in THF (2 mL) was added dropwise to a stirred suspension of lithium aluminium hydride (38 mg, 1.0 mmol, 1.0 eq.) and AgCl (7.2 mg, 0.050 mmol, 0.1 eq.) in THF (1 mL) at −20 °C under Ar. The resulting mixture was stirred at −20 °C for 2 h. Saturated potassium sodium tartrate$_{(aq)}$ (5 mL) was added dropwise slowly (care - exothermic quench) and the mixture was allowed to warm to rt. Et_{20} (10 mL) was added and the two layers were separated. The aqueous layer was extracted with Et_2O (3 × 10 mL) and the combined organics were dried ($MgSO_4$) and evaporated under reduced pressure to give crude product which contained a 50:10:35:5 mixture (by ^{1}H NMR spectroscopy) of **445**, *exo*-**446**, *endo*-**446** and **454**.

Lab book reference HFK7-064

(Table 4.2, Entry 5)

A solution of the dibromocyclopropane **445** (107 mg, 0.3 mmol, 1.0 eq.) in THF (1

mL) was added dropwise to a stirred suspension of lithium aluminium hydride (23 mg, 0.6 mmol, 2.0 eq.) and AgCl (4.3 mg, 0.030 mmol, 0.1 eq.) in THF (1 mL) at −20 °C under Ar. The resulting mixture was stirred at −20 °C for 8 h. Saturated potassium sodium tartrate$_{(aq)}$ (5 mL) was added dropwise slowly (care - exothermic quench) and the mixture was allowed to warm to rt. Et_{20} (10 mL) was added and the two layers were separated. The aqueous layer was extracted with Et_2O (3 × 10 mL) and the combined organics were dried ($MgSO_4$) and evaporated under reduced pressure to give crude product which contained a 25:20:45:10 mixture (by ^{1}H NMR spectroscopy) of **445**, *exo*-**446**, *endo*-**446** and **454**.

Lab book reference HFK7-068

(Table 4.2, Entry 6)

A solution of the dibromocyclopropane **445** (178 mg, 0.5 mmol, 1.0 eq.) in THF (2 mL) was added dropwise to a stirred suspension of lithium aluminium hydride (38 mg, 1.0 mmol, 1.0 eq.) and AgCl (7.2 mg, 0.050 mmol, 0.1 eq.) in THF (1 mL) at −20 °C under Ar. The resulting mixture was stirred at −20 °C for 2 h and then allowed to warm to rt and stirred at rt for 18 h. Saturated potassium sodium tartrate$_{(aq)}$ (5 mL) was added dropwise slowly (care - exothermic quench) and the mixture was allowed to warm to rt. Et_{20} (10 mL) was added and the two layers were separated. The aqueous layer was extracted with Et_2O (3 × 10 mL) and the combined organics were dried ($MgSO_4$) and evaporated under reduced pressure to give crude product which contained a 0:5:80:15 mixture (by ^{1}H NMR spectroscopy) of **445**, *exo*-**446**, *endo*-**446** and **454**. Purification by flash column chromatography on silica with 95:5 to 90:10 hexane-EtOAc as eluent gave bromocyclopropane *endo*-**446** (45 mg, 31%) and a 20:80 mixture (by ^{1}H NMR spectroscopy) of bromocyclopropane *exo*-**446** and cyclopropane **454** (11 mg, i.e. 3 mg (2%) of *exo*-**446** and 8 mg (8%) of **454**). Full characterisation data for **454** are described later.

Lab book reference HFK7-058

(Table 4.2, Entry 7)

A solution of the dibromocyclopropane **445** (71 mg, 0.2 mmol, 1.0 eq.) in Et_2O (0.5 mL) was added dropwise to a stirred suspension of lithium aluminium hydride (15 mg, 0.4 mmol, 2.0 eq.) and $AgNO_3$ (3.5 mg, 0.020 mmol, 0.1 eq.) in THF (1 mL) at −20 °C under Ar. The resulting mixture was stirred at −20 °C for 2 h and then allowed to warm to rt and stirred at rt for 18 h. Saturated potassium sodium tartrate$_{(aq)}$ (5 mL) was added dropwise slowly (care - exothermic quench) and the mixture was allowed to warm to rt. Et_{20} (10 mL) was added and the two layers were separated. The aqueous layer was extracted with Et_2O (3 × 10 mL) and the combined organics were dried ($MgSO_4$) and evaporated under reduced pressure to give crude product which contained a 0:30:60:10 (by ^{1}H NMR spectroscopy) of **445**, *exo*-**446**, *endo*-**446** and **454**.
Lab book reference HFK7-053

(Table 4.2, Entry 8)

A solution of the dibromocyclopropane **445** (178 mg, 0.5 mmol, 1.0 eq.) in THF (2 mL) was added dropwise to a stirred suspension of lithium aluminium hydride (38 mg, 1.0 mmol, 2 eq.) and $AgClO_4$ (10 mg, 0.05 mmol, 0.1 eq.) in THF (1 mL) at −20 °C under Ar. The resulting mixture was stirred at −20 °C for 20 min. Saturated potassium sodium tartrate$_{(aq)}$ (5 mL) was added dropwise slowly (care - exothermic quench) and the mixture was allowed to warm to rt. Et_{20} (10 mL) was added and the two layers were separated. The aqueous layer was extracted with Et_2O (3 × 10 mL) and the combined organics were dried ($MgSO_4$) and evaporated under reduced pressure to give crude product which contained a 0:22.5:55:22.5 mixture (by ^{1}H NMR spectroscopy) of **445**, *exo*-**446**, *endo*-**446** and **454**. Purification by flash column chromatography on silica with 90:10 to 70:30 hexane-Et_2O as eluent gave bromocyclopropane *endo*-**446** (39 mg, 27%) and a 65:35 mixture (by ^{1}H NMR spectroscopy) of bromocyclopropane *exo*-**446** and cyclopropane **454** (10 mg, i.e. 7 mg (5%) of *exo*-**446** and and 3 mg (3%) of **454**).
Lab book reference HFK7-082

(Table 4.2, Entry 9)

A solution of the dibromocyclopropane **445** (178 mg, 0.5 mmol, 1.0 eq.) in THF (2 mL) was added dropwise to a stirred suspension of lithium aluminium hydride (38 mg, 1.0 mmol, 2 eq.) and $AgClO_4$ (10 mg, 0.050 mmol, 0.1 eq.) in THF (1 mL) at -20 °C under Ar. The resulting mixture was stirred at −20 °C for 10 min. Saturated potassium sodium tartrate$_{(aq)}$ (5 mL) was added dropwise slowly (care - exothermic quench) and the mixture was allowed to warm to rt. Et_{20} (10 mL) was added and the two layers were separated. The aqueous layer was extracted with Et_2O (3 × 10 mL) and the combined organics were dried ($MgSO_4$) and evaporated under reduced pressure to give crude product which contained a 0:35:55:10 mixture (by ^{1}H NMR spectroscopy) of **445**, *exo*-**446**, *endo*-**446** and **454**. Purification by flash column chromatography on silica with 90:10 to 80:20 hexane-EtOAc as eluent gave bromocyclopropane *endo*-**446** (44 mg, 30%), starting material **445** (8 mg, 5%) and a 70:30 mixture (by ^{1}H NMR spectroscopy) of bromocyclopropane *exo*-**446** and cyclopropane **454** (27 mg, i.e. 21 mg (15%) of *exo*-**446** and 6 mg (6%) of **454**).

Lab book reference HFK7-094

(Table 4.2, Entry 10)

A solution of the dibromocyclopropane **445** (178 mg, 0.5 mmol, 1.0 eq.) in THF (2 mL) was added dropwise to a stirred suspension of lithium aluminium hydride (38 mg, 1.0 mmol, 2 eq.) and $AgClO_4$ (2 mg, 0.01 mmol, 0.02 eq.) in THF (1 mL) at −20 °C under Ar. The resulting mixture was stirred at −20 °C for 3.5 h. Saturated potassium sodium tartrate$_{(aq)}$ (5 mL) was added dropwise slowly (care - exothermic quench) and the mixture was allowed to warm to rt. Et_{20} (10 mL) was added and the two layers were separated. The aqueous layer was extracted with Et_2O (3 × 10 mL) and the combined organics were dried ($MgSO_4$) and evaporated under reduced pressure to give crude product which contained a 25:15:55:5 mixture (by ^{1}H NMR spectroscopy) of **445**, *exo*-**446**, *endo*-**446** and **454**. Purification by flash column chromatography on

silica with 90:10 to 70:30 hexane-EtOAc as eluent gave bromocyclopropane *endo*-**446** (39 mg, 27%), starting material **445** (9 mg, 5%) and a 70:30 mixture (by ^{1}H NMR spectroscopy) of bromocyclopropane *exo*-**446** and cyclopropane **454** (8 mg, i.e. 6 mg (4%) of *exo*-**446** and 2 mg (2%) of **454**).

Lab book reference HFK7-084

tert-Butyl 7,7-dichloro-3-azabicyclo[4.1.0]heptane-3-carboxylate 458 and *tert*-Butyl 4-(dichloromethyl)-1,2,3,4-tetrahydropyridine-1-carboxylate 459

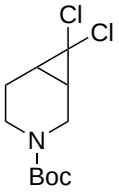

458

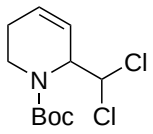

459

Benzyltriethylammonium chloride (228 mg, 1.00 mmol, 0.1 eq.) was added to a stirred solution of *tert*-butyl 1,2,3,6-tetrahydropyridine-1-carboxylate **370** (1.83 g, 10.0 mmol, 1.0 eq.) in $CHCl_3$ (26.5 mL, 330 mmol, 33 eq.) at rt. Then, a solution of NaOH (4.00 g, 100 mmol, 10 eq.) in H_2O (7 mL) was added. The resulting solution was stirred and heated at 50 °C for 3 h. The mixture was then allowed to cool to rt and stirred at rt for 18 h. Then, H_2O (25 mL) was added and the mixture was extracted with $CHCl_3$ (2 × 25 mL). The organic layer was washed with H_2O (25 mL) and brine (25 mL). The combined organic extracts were dried (Na_2SO_4) and evaporated under reduced pressure to give the crude product. Purification by flash column chromatography on silica with 95:5 to 60:40 hexane-EtOAc as eluent gave alkene **370** (257 mg, 14%) and, dichlorocyclopropane **458** (1.68 g, 63%) as a colourless oil, R_F (7:3 hexane-Et_2O) 0.13; IR (ATR) 1690 (C=O), 1421, 1167, 1133 cm^{-1}; ^{1}H NMR (400 MHz, $CDCl_3$) δ 4.03-3.84 (m, 1H, NCH), 3.79-3.27 (m, 2H, NCH), 2.82-2.51 (m, 1H, NCH), 2.09-1.85 (m, 2H, CH), 1.77-1.63 (m, 2H, CH), 1.39 (s, 9H, CMe_3); ^{13}C NMR (100.6 MHz, $CDCl_3$) δ 154.4 (C=O), 79.8 (O*C*Me_3), 64.8 (CCl_2), 38.7 (NCH_2), 37.8 (NCH_2), 28.5 (C*Me*$_3$), 25.5 (CH), 24.9 (CH), 18.6 (CH_2); MS (EI) *m/z* 288 [(^{35,35}M + Na)$^+$, 100]; HRMS (ESI) *m/z* calcd for

$C_{11}H_{17}{}^{35}Cl_2NO_2$ [(^{35,35}M + Na)$^+$, 100] 288.0529, found 288.0524 (+1.8 ppm error) and alkene **459** as a colourless oil (255 mg, 10%), R_F (7:3 hexane-Et_2O) 0.49; IR (ATR) 1692 (C=O), 1407, 1164, 1151 cm^{-1}; ^{1}H NMR (400 MHz, $CDCl_3$) (50:50 mixture of rotamers) δ 6.22-6.14 (m, 1H, =CH), 6.06-5.82 (m, 2H, =CH and $CHCl_2$), 4.77 (s, 0.5H, NCH), 4.67 (s, 0.5H, NCH), 4.19 (dd, J = 13.5, 5.5 Hz, 0.5H, NCH), 4.00 (dd, J = 13.5, 5.5 Hz, 0.5H, NCH), 3.22-3.15 (m, 0.5H, NCH), 3.07-3.00 (m, 0.5H, NCH), 2.33-1.94 (m, 2H, CH), 1.47 (s, 9H, CMe_3); ^{13}C NMR (100.6 MHz, $CDCl_3$) (rotamers) δ 154.8 (C=O), 154.2 (C=O), 130.5 (=CH), 130.1 (=CH), 120.7 (=CH), 120.4 (=CH), 81.1 (O*C*Me$_3$), 80.8 (O*C*Me$_3$), 73.9 ($CHCl_2$), 73.6 ($CHCl_2$), 58.8 (NCH), 57.9 (NCH), 38.6 (NCH_2), 36.9 (NCH_2), 28.5 (C*Me$_3$*), 24.7 (CH_2), 24.4 (CH_2); MS (EI) *m/z* 288 [(^{35}M + Na)$^+$, 100]; HRMS (ESI) *m/z* calcd for $C_{11}H_{17}{}^{35}ClNO_2$ [(^{35}M + Na)$^+$, 100] 288.0529, found 288.0533 (−1.5 ppm error).

Lab book reference HFK7-047

tert-Butyl-7-(4,4,5,5-tetramethyl-1,3,2-dioxaborolan-2-yl)-3-azabicyclo[4.1.0] heptane-3-carboxylate _exo_-456, _endo_-456 and _tert_-butyl-7-chloro-3-azabicyclo [4.1.0]heptane-3-carboxylate _exo_-460

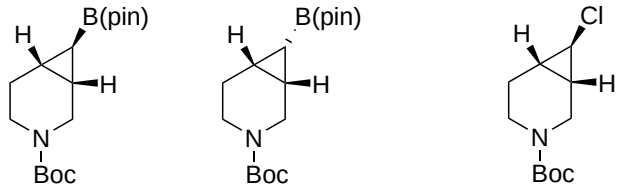

exo-**456** *endo*-**456** *exo*-**460**

s-BuLi (814 μL of a 1.35 M solution in hexanes, 1.10 mmol, 1.1 eq.) was added dropwise to a stirred solution of dichlorocyclopropane **458** (266 mg, 1.00 mmol, 1.0 eq.) and TMEDA (165 μL, 1.10 mmol, 1.1 eq.) in Et_2O (11 mL) at −100 °C under Ar. The resulting solution was stirred at −100 °C for 20 min. Then, HB(pin) (218 μL, 1.50 mmol, 1.5 eq.) was added and the solution was allowed to warm to −50 °C over 1 h. The solution was then allowed to warm to rt and stirred at rt for 3 h. Then, H_2O (20 mL) was added and the mixture was extracted with Et_2O (3 × 20 mL). The combined

organic extracts were dried (Na_2SO_4) and evaporated under reduced pressure to give the crude product. Purification by flash column chromatography on silica with 80:20 to 70:30 hexane-Et_2O as eluent gave a 75:25 mixture (by ^{1}H NMR spectroscopy) of pinacol boronates *exo*-**456** and *endo*-**456** (133 mg, 31%) as a colourless oil, R_F (3:2 hexane-EtOAc) 0.34; ^{1}H NMR (400 MHz, $CDCl_3$) diagnostic signals for *endo*-**456** δ 1.38 (s, 9H, CMe_3), 1.17 (s, 12H, Me), −0.02 (dd, J = 9.0, 9.0 Hz, 1H, CHB), ^{13}C NMR (100.6 MHz, $CDCl_3$) diagnostic signals for *endo*-**456** δ 155.5 (C=O), 79.3 (O*C*Me_2), 78.9 (O*C*Me_3), 40.5 (NCH_2), 39.4 (NCH_2), 28.5 (C*Me*$_3$), 24.7 (Me), 21.3 (CH_2), 14.7 (CH), 13.1 (CH), 12.1 (CHB) and chlorocyclopropane *exo*-**460** (16 mg, 5%) as a yellow oil, R_F (3:2 hexane-EtOAc) 0.44; IR (ATR) 1696 (C=O), 1422, 1367, 1167 cm^{-1}; ^{1}H NMR (400 MHz, $CDCl_3$) δ 3.97 (br d, J = 13.5 Hz, 1H, NCH), 3.40 (dd, J = 13.5, 5.0 Hz, 1H, NCH), 2.87-2.77 (m, 2H, NCH), 2.70 (dd, J = 3.5, 3.5 Hz, 1H, CHCl), 1.99-1.91 (m, 1H, CH), 1.83-1.71 (m, 1H, CH), 1.69-1.57 (m, 1H, CH), 1.51-1.45 (m, 1H, CH), 1.44 (s, 9H, CMe_3); ^{13}C NMR (100.6 MHz, $CDCl_3$) δ 154.9 (C=O), 80.0 (O*C*Me_3), 40.9 (NCH_2), 36.6 (CHCl), 28.6 (C*Me*$_3$), 21.8 (CH_2), 20.9 (CH), 19.7 (CH) (NCH_2 resonance not resolved); MS (EI) *m/z* 254 [(M + Na)$^+$, 100]; HRMS (ESI) *m/z* calcd for $C_{11}H_{18}ClNO_2$ [(M + Na)$^+$, 100] 254.0918, found 254.0923 (−1.5 ppm error). Full characeterisation for *exo*-**456** is provided below.

Lab book reference HFK7-062

tert-Butyl-7-(4,4,5,5-tetramethyl-1,3,2-dioxaborolan-2-yl)-3-azabicyclo [4.1.0]heptane-3-carboxylate *exo*-456

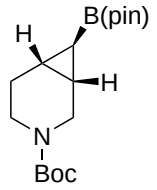

exo-**456**

n-BuLi (12.0 mL of a 2.44 M solution in hexanes, 29.5 mmol, 1.5 eq.) was added dropwise to a stirred solution of bromocyclopropane *exo*-**446** (5.71 g, 19.6 mmol, 1.0

eq.) in THF (200 mL) at −78 °C under Ar. The resulting solution was stirred at −78 °C for 1 h. Then, *i*-PrOBpin (6.00 mL, 29.5 mmol, 1.5 eq.) was added and the solution was allowed to warm to rt. Saturated $NH_4Cl_{(aq)}$ (200 mL) was added and the mixture was extracted with Et_2O (3 × 100 mL). The combined organic extracts were washed with brine (100 mL), dried (Na_2SO_4) and evaporated under reduced pressure to give the crude product. Purification by flash column chromatography on silica with 90:10 to 70:30 to 60:40 hexane-Et_2O as eluent gave pinacol boronate *exo*-**456** (5.45 g, 86%) as a pale yellow oil, R_F (7:3 hexane-Et_2O) 0.25; IR (ATR) 1692 (C=O), 1318, 1144, 1167 cm^{-1}; ^1H NMR (400 MHz, $CDCl_3$) δ 3.81-3.71 (m, 1H, NCH), 3.53 (dd, J = 13.5, 3.5 Hz, 1H, NCH), 3.38-3.20 (m, 1H, NCH), 3.10-2.90 (ddd, J = 13.5, 8.5, 5.5 Hz, 1H, NCH), 2.02-1.84 (m, 1H, CH), 1.76-1.65 (m, 1H, CH), 1.41 (s, 9H, CMe_3), 1.20 (s, 14H, Me and CH), −0.25 (dd, J = 5.5, 5.5 Hz, 1H, CHB); ^{13}C NMR (100.6 MHz, $CDCl_3$) (rotamers) δ 155.2 (C=O), 83.1 (O*C*Me_2), 79.3 (O*C*Me_3), 42.7 (NCH_2), 41.8 (NCH_2), 40.5 (NCH_2), 39.4 (NCH_2), 28.6 (C*Me*$_3$), 25.0 (Me) 24.9 (Me), 24.8 (Me), 23.1 (CH_2), 16.7 (CH), 15.1 (CH), 4.9 (CHB); MS (EI) *m/z* 346 [(M + Na)$^+$, 100]; HRMS (ESI) *m/z* calcd for $C_{17}H_{30}BNO_4$ [(M + Na)$^+$, 100] 346.2160, found 346.2162 (+0.3 ppm error).

Lab book reference HFK7-090

tert-Butyl-7-(6-methyl-4,8-dioxo-1,3,6,2-dioxazaborocan-2-yl)-3-azabicyclo [4.1.0]heptane-3-carboxylate *exo*-211

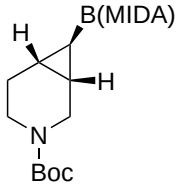

exo-**211**

$HC(OEt)_3$ (9.20 mL, 55.8 mmol, 4.5 eq.) and MIDA (11.9 mg, 80.6 mmol, 6.5 eq.) were added to a stirred solution of pinacol boronate *exo*-**456** (4.00 g, 12.4 mmol, 1.0 eq.) in anhydrous DMSO (60 mL) at rt. The resulting suspension was stirred and

heated at 100 °C for 24 h. The reaction was then allowed to cool to rt and saturated $NH_4Cl_{(aq)}$ (30 mL) was added. The mixture was extracted with EtOAc (3 × 30 mL). The combined organic extracts were washed with brine (30 mL), dried ($MgSO_4$) and evaporated under reduced pressure to give the crude product. Purification by recrystallisation from acetone gave MIDA boronate *exo*-**211** (3.52 g, 80%) as a beige solid, mp 189-192 °C; R_F (4:1 EtOAc-acetone) 0.23; IR (ATR) 1746 (C=O, ester), 1674 (C=O, Boc), 1243, 1283, 1004 cm^{-1}; ^1H NMR (400 MHz, d_6-acetone) δ 4.21 (d, 1H, J = 17.0 Hz, 1H, MeNC*H*), 4.17 (d, 1H, J = 17.0 Hz, 1H, MeNC*H*), 4.09 (d, J = 17.0 Hz, 1H, MeNC*H*), 4.04 (d, J = 17.0 Hz, 1H, MeNC*H*), 3.80 (br d, J = 13.3 Hz, 1H, NCH), 3.60-3.46 (m, 1H, NCH), 3.38 (ddd, J = 13.0, 11.5, 5.5 Hz, 1H, NCH), 3.20 (s, 3H, NMe), 3.08-2.86 (m, 1H, NCH), 2.00-1.84 (m, 1H, CH), 1.77-1.63 (m, 1H, CH), 1.41 (s, 9H, CMe_3), 1.03-0.80 (m, 2H, CH), −0.39 (dd, J = 6.0, 6.0 Hz, 1H, CHB); ^{13}C NMR (100.6 MHz, d_6-acetone) (rotamers) δ 169.0 (C=O, ester), 168.9 (C=O, ester), 155.4 (C=O, Boc), 79.1 (O*C*Me_3), 62.9 (MeN*C*H_2), 62.8 (MeN*C*H_2), 47.1 (NMe), 43.5 (NCH_2), 42.7 (NCH_2), 41.5 (NCH_2), 40.3 (NCH_2), 32.0 (CHB), 28.6 (C*Me*$_3$), 23.8 (CH_2), 23.3 (CH_2), 14.3 (CH), 12.3 (CH); MS (EI) *m/z* 375 [$(M + Na)^+$, 100]; HRMS (ESI) *m/z* calcd for $C_{16}H_{25}BN_2O_6$ [$(M + Na)^+$, 100] 375.1698, found 375.1703 (−0.5 ppm error).

Lab book reference HFK7-091

n-BuLi (688 μL of a 1.45 M solution in hexanes, 1.00 mmol, 1.5 eq.) was added dropwise to a stirred solution of bromocyclopropane *exo*-**446** (193 mg, 0.665 mmol, 1.0 eq.) in THF (8 mL) at −78 °C under Ar. The resulting solution was stirred at −78 °C for 1 h. Then, $B(OMe)_3$ (111 μL, 1.00 mmol, 1.5 eq.) was added. After stirring at −78 °C for 10 min, the solution was allowed to warm to rt and stirred at rt for 3 h. 5% $HCl_{(aq)}$ (2.60 mL) was added and the mixture was extracted with Et_2O (3 × 10 mL). The combined organic extracts were dried ($MgSO_4$) and evaporated under reduced pressure to give the crude boronic acid **455** (177 mg). MIDA (108 mg, 0.732 mmol, 1.1 eq.) was added to a stirred solution of boronic acid **455** in toluene (3 mL) and anhydrous

DMSO (3 mL) at rt under Ar. The resulting solution was connected to a Dean-Stark apparatus and stirred and heated at 120 °C for 18 h. The mixture was allowed to cool to rt and EtOAc (15 mL) was added. The mixture was washed with H_2O (3 × 10 mL) and the organic layer was dried ($MgSO_4$) and evaporated under reduced pressure to give the crude product. Purification by flash column chromatography on silica with 80:20 to 0:100 CH_2Cl_2-acetone as eluent gave MIDA boronate *exo*-**211** (85 mg, 36% over 2 steps) as a white solid.

Lab book reference HFK7-036

tert-Butyl 7,7-dibromo-2-azabicyclo[4.1.0]heptane-2-carboxylate 461

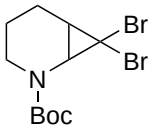

461

DIBAL-H (38.0 mL of a 1.0 M solution in hexane, 37.5 mmol, 1.5 eq.) was added dropwise to a stirred solution of **465** 1-*N*-Boc-2-piperidone (4.98 g, 25.0 mmol, 1.0 eq.) in THF (100 mL) at –78 °C under Ar. The resulting solution was stirred at –78 °C for 2 h. Then, saturated potassium sodium tartrate$_{(aq)}$ (50 mL) was added and the mixture was allowed to warm to rt and stirred at rt for 3 to give a mixture with two distinct layers. Then, H_2O (50 mL) was added and the mixture was extracted with EtOAc (3 × 100 mL). The combined organic extracts were dried ($MgSO_4$) and evaporated under reduced pressure to give the crude hydroxy piperidine **464** as a colourless oil. Then, *p*-TsOH·H_2O (13 mg, 65 μmol, 0.30 mol %) was added to a stirred solution of crude **464** in toluene (38 mL). The solutions was connected to a Dean-Stark apparatus and stirred and heated at reflux for 30 min. The reaction mixture was allowed to cool to rt and the solvent was evaporated under reduced pressure to give the crude *N*-Boc enamide **465**. Then, $CHBr_3$ (6.0 mL, 64 mmol, 3.0 eq.) and benzyltriethylammonium chloride (870 mg, 3.82 mmol, 0.2 eq.) were added to a stirred solution of *N*-Boc enamide **465** (3.89 g, 21.2 mmol, 1.0 eq.) at rt in CH_2Cl_2 (63 mL). Then, a solution of NaOH (33.1

g, 828 mmol, 39 eq.) in H_2O (33 mL) was added. The resulting solution was stirred and heated at 45 °C for 18 h. The mixture was then allowed to cool to rt. Then, H_2O (50 mL) was added and the mixture was extracted with CH_2Cl_2 (3 × 50 mL). The combined organic extracts were dried (Na_2SO_4), decanted from the black sediment formed and evaporated under reduced pressure to give the crude product. Purification by flash chromatography on silica with 95:5 to 90:10 to 60:40 hexane-Et_2O as eluent gave dibromocyclopropane **461** (2.57 g, 34%) as a yellow oil and 2.30 g of impure product. Further purification of the impure product by flash column chromatography on silica with 95:5 to 90:10 hexane-Et_2O as eluent gave dibromocyclopropane **461** (1.02 g, 14%) as a yellow oil. In total, this gave dibromocyclopropane **461** (3.59 g, 48%) as a yellow oil, R_F (4:1 hexane-Et_2O) 0.24; IR (ATR) 1702 (C=O), 1366, 1164, 758 cm^{-1}; ^1H NMR (400 MHz, $CDCl_3$) (80:20 mixture of rotamers) δ 3.41 (ddd, J = 12.0, 8.0, 4.0 Hz, 0.8H, NCH), 3.35 (d, J = 9.0 Hz, 0.2H, NCH), 3.27 (d, J = 9.0 Hz, 0.8H, NCH), 3.25-3.16 (m, 0.2H, NCH), 3.06 (ddd, J = 12.5, 6.5, 4.0 Hz, 0.2H, NCH), 2.88 (ddd, J = 12.0, 8.0, 4.0 Hz, 0.8H, NCH), 2.12-1.99 (m, 1.6H, CH), 1.77-1.65 (m, 1.2H, CH), 1.53 (s, 7.2H, CMe_3), 1.48 (s, 1.8H, CMe_3) 1.47-1.34 (m, 0.8H, CH); ^{13}C NMR (100.6 MHz, $CDCl_3$) (rotamers) δ 156.1 (C=O), 156.0 (C=O), 80.6 (O*C*Me_3), 80.5 (O*C*Me_3), 40.8 (NCH), 40.7 (NCH), 40.4 (NCH_2), 40.3 (NCH_2), 36.9 (CBr_2), 36.6 (CBr_2), 29.5 (CH), 29.1 (CH), 28.5 (C*Me*$_3$), 28.4 (C*Me*$_3$), 21.4 (CH_2), 21.3 (CH_2), 19.2 (CH_2), 18.9 (CH_2); MS (EI) *m/z* 376 [(^{79,79}M + Na)$^+$, 100]; HRMS (ESI) *m/z* calcd for $C_{11}H_{17}{}^{79}Br_2NO_2$ [(^{79,79}M + Na)$^+$, 100] 375.9518, found 375.9518 (−0.1 ppm error). Spectroscopic data consistent with those reported in the literature.[162]

Lab book reference HFK7-042

tert-Butyl-7-bromo-2-azabicyclo[4.1.0]heptane-2-carboxylate _exo_-462

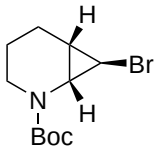

exo-**462**

Dimethyl phosphite (1.10 mL, 12.0 mmol, 6 eq.) was added to a stirred solution of dibromocyclopropane **461** (710 mg, 2.00 mmol, 1.0 eq.) in anhydrous DMSO (15 mL) under Ar. Then, KO*t*-Bu (1.35 g, 12.0 mmol, 6.0 eq.) was added portionwise and the resulting solution was stirred at rt for 1.5 h at rt. Saturated $Na_2CO_{3(aq)}$ (20 mL) and Et_2O (20 mL) were added. The two layers were separated and the aqueous layer was extracted with Et_2O (3 × 20 mL). The combined organic extracts were dried (Na_2SO_4) and evaporated under reduced pressure to give the crude product. Purification by flash column chromatography on silica with 95:5 to 90:10 hexane-EtOAc as eluent gave bromocyclopropane *exo*-**462** (440 mg, 80%) as a colourless oil, R_F (7:3 hexane-EtOAc) 0.55; IR (ATR) 1696 (C=O), 1365, 1160, 1130 cm^{-1}; ^1H NMR (400 MHz, $CDCl_3$) (80:20 mixture of rotamers) δ 3.76 (ddd, J = 13.0, 3.8, 3.8 Hz, 0.8H, NCH), 3.65-3.53 (m, 0.2H, NCH), 3.25-3.16 (m, 0.2H, NCH), 3.08 (dd, J = 9.0, 2.0 Hz, 0.8H, NCH), 2.61-2.57 (m, 0.2 Hz, CHBr), 2.54 (dd, J = 4.5, 2.0 Hz, 0.8H, CHBr), 2.47-2.40 (m, 1H, NCH), 2.03-1.93 (m, 1H, CH), 1.80-1.53 (m, 3H, CH), 1.50 (s, 7.2H, CMe_3), 1.46 (s, 1.8H, CMe_3), 1.22-1.04 (m, 1H, CH); ^{13}C NMR (100.6 MHz, $CDCl_3$) (rotamers) δ 156.2 (C=O), 155.7 (C=O), 80.1 (O*C*Me_3), 41.5 (NCH_2), 39.9 (NCH_2), 37.6 (NCH), 37.4 (NCH), 29.8 (C*Me*$_3$), 28.6 (C*Me*$_3$), 23.5 (CH), 23.1 (CH), 22.9 (CHBr), 22.3 (CH_2), 22.2 (CH_2), 22.1 (CH), 19.6 (CH_2); MS (EI) *m/z* 298 [($^{79}M + Na)^+$, 100]; HRMS (ESI) *m/z* calcd for $C_{11}H_{18}{}^{79}BrNO_2$ [($^{79}M + Na)^+$, 100] 298.0413, found 298.0413 (0.0 ppm error).

Lab book reference HFK7-067

tert-Butyl-7-(6-methyl-4,8-dioxo-1,3,6,2-dioxazaborocan-2-yl)-2-azabicyclo [4.1.0]heptane-2-carboxylate *exo*-212

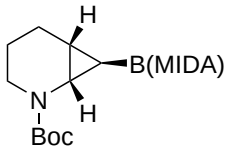

exo-**212**

n-BuLi (1.10 mL of a 1.45 M solution in hexanes, 1.56 mmol, 1.5 eq.) was added dropwise to a stirred solution of bromocyclopropane *exo*-**462** (301 mg, 1.04 mmol, 1.0 eq.) in THF (12 mL) at −78 °C under Ar. The resulting solution was stirred at −78 °C for 1 h. Then, $B(OMe)_3$ (174 μL, 1.56 mmol, 1.5 eq.) was added. After stirring at −78 °C for 10 min, the mixture was allowed to warm to rt and stirred at rt for 3 h. 5% $HCl_{(aq)}$ (4 mL) was added and the mixture was extracted with Et_2O (3 × 15 mL). The combined organic extracts were dried ($MgSO_4$) and evaporated under reduced pressure to give crude boronic acid **466** (293 mg). MIDA (168 mg, 1.14 mmol, 1.1 eq.) was added to a stirred solution of boronic acid **466** in toluene (6 mL) and anhydrous DMSO (6 mL) at rt under Ar. The resulting solution was connected to a Dean-Stark apparatus and stirred and heated at 120 °C for 18 h. The mixture was allowed to cool to rt and EtOAc (10 mL) was added. The mixture was washed with H_2O (3 × 10 mL) and the organic layer was dried ($MgSO_4$) and evaporated under reduced pressure to give the crude product. Purification by flash column chromatography on silica with 80:20 CH_2Cl_2-acetone as eluent gave MIDA boronate *exo*-**212** (80 mg, 23% over 2 steps) as a white solid, mp 180-184 °C; R_F (7:3 CH_2Cl_2-acetone) 0.47; IR (ATR) 1756 (C=O, ester), 1674 (C=O, Boc), 1396, 1278, 1166 cm^{-1}; ^1H NMR (400 MHz, d_6-acetone) (70:30 mixture of rotamers) δ 4.43 (d, J = 16.0 Hz, 0.7H, MeNC*H*), 4.22-4.11 (m, 2H, MeNC*H*) 4.06-4.01 (m, 0.6H, MeNC*H*), 3.97 (d, J = 16.0 Hz, 0.7H, MeNC*H*), 3.74 (ddd, J = 13.0, 4.0, 4.0 Hz, 0.3H, NCH), 3.65 (ddd, J = 13.0, 4.0, 4.0 Hz, 0.7H, NCH), 3.25 (s, 2.1H, NMe), 3.21 (s, 0.9H, NMe), 2.77 (dd, J = 8.0, 4.0 Hz, 0.3H, NCH), 2.67 (ddd, J = 12.5, 12.5, 2.5 Hz, 0.7H, NCH), 2.51 (ddd, J = 12.5, 12.5, 2.5 Hz, 0.3H, NCH), 2.45 (dd, J = 8.0, 4.0 Hz, 0.7H, NCH), 1.88-1.83 (m, 2H, CH), 1.60-1.54 (m, 1H, CH), 1.49 (s, 2.7H, CMe_3), 1.44 (s, 6.3H, CMe_3), 1.42-1.28 (m, 1H, CH), 1.26-1.19 (m, 0.7H, CH), 1.13-1.07 (m, 0.3H, CH), −0.19- −0.24 (m, 1H, CHB); ^{13}C NMR (100.6 MHz, d_6-acetone) (rotamers) δ 169.9 (C=O, ester), 169.1 (C=O, ester), 168.7 (C=O, ester), 168.6 (C=O, ester), 157.0 (C=O, Boc), 156.8 (C=O, Boc), 79.8 (O*C*Me_3), 79.5 (O*C*Me_3), 62.7 (MeN*C*H_2), 62.3 (MeN*C*H_2), 61.9 (MeN*C*H_2), 47.1 (NMe), 45.8 (NMe), 42.6 (NCH_2), 41.4 (NCH_2), 33.4 (NCH), 32.8 (NCH), 28.8 (C*Me*$_3$), 28.6 (C*Me*$_3$), 22.2

(CH_2), 22.1 (CH_2), 21.93 (CH_2), 21.85 (CH_2), 15.1 (CH), 14.7 (CH); MS (EI) *m/z* 375 [(M + Na)$^+$, 100]; HRMS (ESI) *m/z* calcd for $C_{16}H_{25}BN_2O_6$ [(M + Na)$^+$, 100] 375.1698, found 375.1705 (−1.0 ppm error).

Lab book reference HFK7-054

tert-Butyl 2-[(4-methylphenoxy)methyl]pyrrolidine-1-carboxylate 470

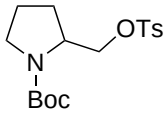

470

DMAP (25 mg, 0.20 mmol, 0.010 eq.) and Et_3N (3.6 mL, 26 mmol, 1.3 eq.) were added to a stirred solution of *N*-Boc-2-pyrrolidinemethanol **469** (4.03 g, 20.0 mmol, 1.0 eq) and *p*-TsCl (4.58 g, 24.0 mmol, 1.2 eq.) in CH_2Cl_2 (80 mL) at rt under Ar. The resulting solution was stirred at rt for 18 h. Then, the reaction mixture was acidified to pH 1 with 1 M $HCl_{(aq)}$ (80 mL). CH_2Cl_2 (150 mL) was added and the two layers were separated. The aqueous layer was extracted with CH_2Cl_2 (3 × 150 mL) and the combined organics were dried (Na_2SO_4) and evaporated under reduced pressure to give the crude product. Purification by flash column chromatography on silica with 90:10 to 80:20 to 70:30 hexane-EtOAc as eluent gave *N*-Boc pyrrolidine tosylate **470** (6.06 g, 85%) as a pale yellow oil, R_F (1:1 hexane-EtOAc) 0.50; IR (ATR) 1691 (C=O), 1394, 1363, 1174 cm^{-1}; ^{1}H NMR (400 MHz, $CDCl_3$) δ 7.77 (d, J = 8.0 Hz, 2H, Ar), 7.34 (d, J = 8.0 Hz, 2H, Ar), 4.16-4.02 (m, 1H, NCH), 3.99-3.83 (m, 2H, NCH), 3.29-3.26 (m, 2H, TsOCH), 2.44 (s, 3H, Me), 2.01-1.67 (m, 4H, CH), 1.37 (s, 9H, CMe_3); ^{13}C NMR (100.6 MHz, $CDCl_3$) δ 145.0 (C=O), 133.0 (*ipso*-Ar), 130.0 (Ar), 129.3 (*ipso*-Ar), 128.0 (Ar), 79.8 (O*C*Me$_3$), 70.1 ($TsOCH_2$), 55.6 (NCH), 46.6 (NCH_2), 28.5 (C*Me$_3$*), 23.9 (CH_2), 23.0 (CH_2), 21.8 (Me); MS (EI) *m/z* 378 [(M + Na)$^+$, 100]; HRMS (ESI) *m/z* calcd for $C_{17}H_{25}NO_5S$ [(M + Na)$^+$, 100] 378.1346, found 378.1350 (−1.2 ppm error). Spectroscopic data consistent with those reported in the literature.[209]

Lab book reference HFK7-037

***tert*-Butyl 1,1-dibromo-4-azaspiro[2.4]heptane-4-carboxylate 467**

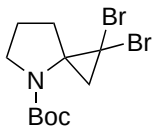

467

NaI (2.25 g, 15.0 mmol, 3 eq.) and DBU (1.49 mL, 10.0 mmol, 2 eq.) were added to a stirred solution of pyrrolidine tosylate **470** (1.78 g, 5.00 mmol, 1.0 eq.) in DME (18 mL) at rt under Ar. The resulting solution was stirred and heated at reflux for 3 h. The mixture was then allowed to cool to rt. Then, H_2O (20 mL) was added and the mixture was extracted with Et_2O (3 × 20 mL). The combined organic extracts were washed with saturated $NaHCO_{3(aq)}$ (20 mL) and brine (20 mL), dried (Na_2SO_4) and evaporated under reduced pressure to give *N*-Boc enamide **471**. $CHBr_3$ (0.63 mL, 7.2 mmol, 3.0 eq.) and benzyltriethylammonium chloride (109 mg, 0.48 mmol, 0.2 eq.) were added to a stirred solution of *N*-Boc enamide **471** (433 mg, 2.40 mmol, 1.0 eq.) in CH_2Cl_2 (8 mL) at rt. Then, a solution of NaOH (3.74 g, 93.6 mmol, 39 eq.) in H_2O (3.7 mL) was added. The resulting solution was stirred and heated at 45 °C for 18 h. The mixture was then allowed to cool to rt. Then, H_2O (30 mL) was added and the mixture was extracted with CH_2Cl_2 (3 × 20 mL). The combined organic extracts were dried (Na_2SO_4), decanted from the black sediment formed and evaporated under reduced pressure to give the crude product. Purification by flash chromatography on silica with 90:10 hexane-Et_2O as eluent gave dibromocyclopropane **467** (544 mg, 59% over 2 steps) as a yellow oil, R_F (4:1 hexane-Et_2O) 0.43; IR (ATR) 1697 (C=O), 1383, 1171, 1144 cm^{-1}; ^1H NMR (400 MHz, $CDCl_3$) δ 3.66-3.59 (m, 1H, NCH), 3.54-3.36 (m, 1H, NCH), 2.28-2.04 (m, 2H, CH), 1.98-1.88 (m, 3H, CH), 1.43 (s, 9H, CMe_3); ^{13}C NMR (100.6 MHz, $CDCl_3$) δ 154.0 (C=O), 80.0 (O*C*Me_3), 52.4 (CBr_2), 47.4 (NCH_2), 36.4 (NC), 34.0 (CH_2), 30.5 (CH_2), 28.5 (C*Me*$_3$), 21.3 (CH_2); MS (EI) *m/z* 376 [(^{79,79}M + Na)$^+$, 100]; HRMS (ESI) (ESI) *m/z* calcd for $C_{11}H_{17}{}^{79}Br_2NO_2$ [(^{79,79}M + Na)$^+$, 100] 375.9518, found 375.9519 (−0.1 ppm error). Spectroscopic data consistent with those

reported in the literature.[181]

Lab book reference HFK7-050

In the same way, NaI (4.50 g, 30.0 mmol, 3 eq.), DBU (3.0 mL, 20 mmol, 2 eq.), pyrrolidine tosylate **470** (3.96 g, 11.2 mmol, 1.0 eq.) in DME (36 mL) and then, $CHBr_3$ (2.9 mL, 34 mmol, 3.0 eq.), benzyltriethylammonium chloride (459 mg, 2.02 mmol, 0.2 eq.), CH_2Cl_2 (35 mL) and NaOH (17.5 g, 437 mmol, 39 eq.) in H_2O (17.5 mL) gave the crude product. Purification by flash chromatography on silica with 95:5 hexane-Et_2O as eluent gave dibromocyclopropane **467** (1.50 g, 38% over 2 steps) as a yellow oil.

Lab book reference HFK8-049

tert-Butyl-1-bromo-4-azaspiro[2.4]heptane-4-carboxylate *cis*-468

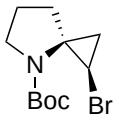

cis-**468**

i-PrMgCl (3.1 mL of a 2 M solution in THF, 6.2 mmol, 1.2 eq.) was added dropwise to a stirred solution of dibromocyclopropane **467** (1.83 g, 5.15 mmol, 1.0 eq.) in CH_2Cl_2 (45 mL) at −78 °C under Ar. The resulting solution was stirred at −78 °C for 2 h. Saturated $NH_4Cl_{(aq)}$ (20 mL) was added and the mixture was allowed to warm to rt. The mixture was extracted with CH_2Cl_2 (3 × 20 mL). The combined organic extracts were dried (Na_2SO_4) and evaporated under reduced pressure to give the crude product. Purification by flash column chromatography on silica with 95:5 to 70:30 hexane-EtOAc as eluent gave recovered dibromocyclopropane **467** (159 mg, 9%) and bromocyclopropane *cis*-**468** (771 mg, 55%) as a yellow oil, R_F (7:3 hexane-Et_2O) 0.32; IR (ATR) 1698 (C=O), 1389, 1365, 1145 cm^{-1}; ^1H NMR (400 MHz, $CDCl_3$) δ 3.68-3.61 (m, 1H, NCH), 3.52-3.37 (m, 1H, NCH), 2.74 (dd, J = 8.5, 4.5 Hz, 1H, CHBr), 2.27-2.19 (m, 1H, CH), 1.95-1.83 (m, 2H, CH), 1.46-1.42 (m, 2H, CH), 1.45 (s, 9H, CMe_3), 1.39-1.34 (m, 1H, CH); ^{13}C NMR (100.6 MHz, $CDCl_3$) 154.3 (C=O),

79.9 (O*C*Me$_3$), 47.6 (NCH$_2$), 46.5 (NC), 35.5 (CH$_2$), 28.5 (C*Me$_3$*), 26.6 (CHBr), 21.7 (CH$_2$), 17.3 (CH$_2$); MS (EI) *m/z* 298 [(^{79}M + Na)$^+$, 100]; HRMS (ESI) *m/z* calcd for $C_{11}H_{18}{}^{79}BrNO_2$ [(^{79}M + Na)$^+$, 100] 298.0413, found 298.0412 (+0.2 ppm error).
Lab book reference HFK8-008

1-Bromo-4-azaspiro[2.4]heptane hydrochloride *cis*-477·HCl

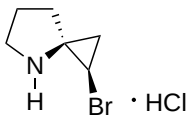

cis-**477**

N-Boc bromocyclopropane *cis*-**468** (94 mg, 0.34 mmol, 1.0 eq) was dissolved in HCl (2 mL of a 3.7-4.3 M solution in dioxane, 4.0-8.6 mmol, 12-25 eq.) and the resulting solution was stirred at rt for 1 h. Then, the solvent was evaporated under reduced pressure to give hydrochoride salt *cis*-**477**·HCl (63 mg, 87%) as a yellow solid, mp 138-140 °C; IR (ATR) 2670 (NH), 2051, 1455, 1051 cm^{-1}; ^{1}H NMR (400 MHz, d_4-MeOH) δ 3.55-3.49 (m, 2H, NCH), 3.46 (dd, J = 8.5, 5.5 Hz, 1H, CHBr), 2.35-2.17 (m, 3H, CH), 2.10-1.96 (m, 1H, CH), 1.69 (dd, J = 8.5, 8.5 Hz, 1H, CH), 1.57 (dd, J = 8.5, 5.5 Hz, 1H, CH); ^{13}C NMR (100.6 MHz, d_4-MeOH) 47.9 (NCH$_2$), 47.2 (NC), 31.7 (CH$_2$), 25.0 (CH$_2$), 21.8 (CH$_2$), 20.9 (CHBr); MS (EI) *m/z* 176 [^{79}M$^+$, 100]; HRMS (ESI) *m/z* calcd for $C_6H_{11}{}^{79}BrN$ [^{79}M$^+$, 100] 176.0069, found 176.0064 (+3.3 ppm error). Structure confirmed by X-ray crystallography (see Appendix A).
Lab book reference HFK8-052

***tert*-Butyl-1-(4,4,5,5-Tetramethyl-1,3,2-dioxaborolan-2-yl)-4-aza spiro[2.4]heptane-4-carboxylate *cis*-478**

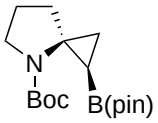

cis-**478**

n-BuLi (1.20 mL of a 2.44 M solution in hexanes, 2.10 mmol, 1.5 eq.) was added

dropwise to a stirred solution of bromocyclopropane *cis*-**468** (565 mg, 2.10 mmol, 1.0 eq.) in THF (20 mL) at −78 °C under Ar. The resulting solution was stirred at −78 °C for 1 h. Then, *i*-PrOBpin (612 μL, 3.00 mmol, 1.5 eq.) was added and the solution was allowed to warm to rt. Saturated $NH_4Cl_{(aq)}$ (15 mL) was added and the mixture was extracted with Et_2O (3 × 20 mL). The combined organic extracts were washed with brine (20 mL), dried (Na_2SO_4) and evaporated under reduced pressure to give the crude product. Purification by flash column chromatography on silica with 90:10 to 70:30 hexane-Et_2O as eluent gave pinacol boronate *cis*-**478** (497 mg, 73%) as a pale yellow oil, R_F (1:1 hexane-Et_2O) 0.38; IR (ATR) 1683 (C=O), 1388, 1142, 860 cm^{-1}; ^1H NMR (400 MHz, $CDCl_3$) δ 3.62-3.40 (br m, 1H, NCH), 3.30-3.14 (br m, 1H, NCH), 1.88-1.55 (br m, 5H, CH), 1.36 (s, 9H,CMe_3), 1.14 (s, 12H, Me), 0.91-0.72 (br m, 1H, CH), −0.01- −0.09 (br dd, 1H, CHB); ^{13}C NMR (100.6 MHz, $CDCl_3$) δ 153.9 (C=O), 82.2 (O*C*Me_2), 79.7 (O*C*Me_3), 47.4 (NC), 46.9 (NCH_2), 35.8 (CH_2), 28.5 (C*Me*$_3$), 25.3 (Me), 24.6 (Me), 22.3 (CH_2), 13.7 (CH_2), 7.7 (CHB); MS (EI) *m/z* 346 [(M + Na)$^+$, 100]; HRMS (ESI) *m/z* calcd for $C_{17}H_{30}BNO_4$ [(M + Na)$^+$, 100] 346.2160, found 346.2164 (−0.3 ppm error).

Lab book reference HFK8-021

tert-Butyl 1,1-dichloro-4-azaspiro[2.4]heptane-4-carboxylate 479

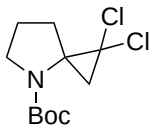

479

NaI (2.25 g, 15.0 mmol, 3 eq.) and DBU (1.49 mL, 10.0 mmol, 2 eq.) were added to a stirred solution of pyrrolidine tosylate **470** (1.78 g, 5.00 mmol, 1.0 eq.) in DME (18 mL) at rt under Ar. The resulting solution was stirred and heated at reflux for 3 h. The mixture was then allowed to cool to rt. Then, H_2O (20 mL) was added and the mixture was extracted with Et_2O (3 × 20 mL). The combined organic extracts were washed with saturated $NaHCO_{3(aq)}$ (20 mL) and brine (20 mL), dried (Na_2SO_4) and

evaporated under reduced pressure to give *N*-Boc enamide **471**. Benzyltriethylammonium chloride (114 mg, 0.500 mmol, 0.1 eq.) was added to a stirred solution of *N*-Boc enamide **471** in $CHCl_3$ (13.0 mL, 165 mmol, 33 eq.). Then, a solution of NaOH (2.00 g, 50.0 mmol, 10 eq.) in H_2O (3.3 mL) was added. The resulting solution was stirred and heated at 50 °C for 3 h. The mixture was then allowed to cool to rt and stirred at rt for 18 h. Then, H_2O (20 mL) was added and the mixture was extracted with $CHCl_3$ (2 × 20 mL). The organic layer was washed with H_2O (20 mL) and brine (20 mL). The combined organic extracts were dried (Na_2SO_4) and evaporated under reduced pressure to give the crude product. Purification by flash column chromatography on silica with 90:10 hexane-EtOAc as eluent gave dichlorocyclopropane **479** (731 mg, 55%) as a colourless oil, R_F (4:1 hexane-Et_2O) 0.44; IR (ATR) 1697 (C=O), 1384, 1147, 765 cm^{-1}; ^1H NMR (400 MHz, $CDCl_3$) δ 3.67-3.60 (m, 1H, NCH), 3.48 (ddd, J = 11.0, 9.0, 3.0 Hz, 2H, NCH), 2.19-2.03 (m, 2H, CH), 2.00-1.82 (m, 2H, CH), 1.66 (d, J = 9.0 Hz, 1H, CH), 1.43 (s, 9H, CMe_3); ^{13}C NMR (100.6 MHz, $CDCl_3$) δ 153.9 (C=O), 80.3 (O*C*Me_3), 63.8 (CCl_2), 53.1 (NC), 47.6 (NCH_2), 32.2 (CH_2), 28.5 (C*Me*$_3$), 28.1 (CH_2), 21.6 (CH_2); MS (EI) *m/z* 288 [(^{35,35}M + Na)$^+$, 100]; HRMS (ESI) *m/z* calcd for $C_{11}H_{17}{}^{35}Cl_2NO_2$ [(^{35,35}M + Na)$^+$, 100] 288.0529, found 288.0532 (−1.0 ppm error). Lab book reference HFK7-066

Hexahydro-1H-[1,3]oxazolo[3,4-a]pyridin-3-one 485

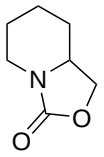

485

DMAP (5 mg, 0.04 mmol, 0.04 eq.) and Et_3N (181 μL, 1.30 mmol, 1.3 eq.) were added to a stirred solution of *N*-Boc-2-piperidinemethanol **483** (215 mg, 1.00 mmol, 1.0 eq) and *p*-TsCl (229 mg, 1.20 mmol, 1.2 eq.) in CH_2Cl_2 (5 mL) at rt under Ar. The resulting solution was stirred at rt for 18 h. Then, the reaction mixture was acidified

to pH 1 with 1 M $HCl_{(aq)}$ (5 mL). CH_2Cl_2 (10 mL) was added and the two layers were separated. The aqueous layer was extracted with CH_2Cl_2 (3 × 10 mL) and the combined organics were dried (Na_2SO_4) and evaporated under reduced pressure to give the crude product. Purification by flash column chromatography on silica with 95:5 to 90:10 to 80:20 to 50:50 hexane-EtOAc as eluent gave recoved alcohol **483** (42 mg, 20%) and cyclic carbamate **485** (92 mg, 65%) as a yellow oil, R_F (1:1 hexane-EtOAc) 0.18; IR (ATR) 1735 (C=O), 1420, 1242, 1040 cm^{-1}; ^1H NMR (400 MHz, $CDCl_3$) δ 4.36 (dd, J = 8.5, 8.5 Hz, 1H, OCH), 3.90-3.73 (m, 2H, OCH and NCH), 3.65-3.57 (m, 1H, NCH), 2.79 (ddd, J = 13.0, 13.0, 3.5 Hz, 1H, NCH), 1.88-1.85 (m, 1H, CH), 1.83-1.77 (m, 1H, CH), 1.65-1.62 (m, 1H, CH), 1.43-1.34 (m, 2H, CH), 1.33-1.25 (m, 1H, CH); ^{13}C NMR (100.6 MHz, $CDCl_3$) δ 157.1 (C=O), 68.2 (OCH_2), 54.5 (NCH), 41.4 (NCH_2), 30.5 (CH_2), 24.3 (CH_2), 22.6 (CH_2); MS (EI) *m/z* 164 [$(M + Na)^+$, 100]; HRMS (ESI) *m/z* calcd for $C_7H_{11}NO_2$ [$(M + Na)^+$, 100] 164.0682, found 164.0681 (+0.5 ppm error).

Lab book reference HFK7-100

tert-Butyl *N*-cyclopropylcarbamate 489

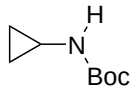

489

A solution of Boc_2O (8.1 g, 37 mmol, 1.1 eq) in CH_2Cl_2 (45 mL) was added to a stirred solution of cyclopropylamine **490** (2.3 mL, 34 mmol, 1.0 eq) in CH_2Cl_2 (67 mL) at 0 °C under Ar. The resulting solution was allowed to warm to rt and stirred at rt for 18 h. The solution was washed with H_2O (2 × 20 mL), dried (Na_2SO_4) and evaporated under reduced pressure to give the crude product. Purification by flash column chromatography on silica with 95:5 to 50:50 hexane-EtOAc as eluent gave N-Boc cyclopropylamine **489** (4.67 g, 87%) as a white solid, mp 50-54 °C (lit.,[210] 54-55 °C); R_F (9:1 hexane-EtOAc) 0.16; IR (ATR) 3359 (NH), 1685 (C=O), 1506, 1158, 619 cm^{-1};

^{1}H NMR (400 MHz, $CDCl_3$) δ 4.76 (br s, 1H, NH), 2.52-2.49 (m, 1H, NCH), 1.42 (s, 9H, CMe_3), 0.78-0.54 (m, 2H, CH), 0.53-0.29 (m, 2H, CH); ^{13}C NMR (100.6 MHz, $CDCl_3$) δ 156.8 (C=O), 79.5 (O*C*Me$_3$), 28.5 (C*Me$_3$*), 23.0 (NCH), 6.8 (CH_2); MS (EI) *m/z* 180 [(M + Na)$^+$, 100]; HRMS (ESI) *m/z* calcd for $C_8H_{15}NO_2$ [(M + Na)$^+$, 100] 180.0995, found 180.0997 (−0.9 ppm error). Spectroscopic data consistent with those reported in the literature.[211]

Lab book reference HFK5-061

tert-Butyl *N*-(4-chlorobutyl)-*N*-cyclopropylcarbamate 486

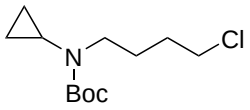

486

NaH (100 mg of 60% wt in mineral oil, 2.5 mmol, 2.5 eq.) was added to *N*-Boc cyclopropylamine **489** (236 mg, 1.50 mmol, 1.5 eq.) in DMF (6 mL) at 0 °C under Ar. The resulting solution was stirred at 0 °C for 2 h. Then, 1-bromo-4-chlorobutane (115 μL, 1.00 mmol, 1.0 eq.) was added and the solution was allowed to warm to rt. The resulting solution was stirred at rt for 18 h. Then, H_2O (10 mL) was added and the mixture was extracted with Et_2O (3 × 15 mL). The combined organic extracts were washed with brine (20 mL), dried ($MgSO_4$) and evaporated under reduced pressure to give the crude product. Purification by flash column chromatography on silica with 95:5 hexane-EtOAc as eluent gave alkyl chloride **486** (214 mg, 86% based on 1-bromo-4-chlorobutane) as a pale yellow oil, R_F (4:1 hexane-EtOAc) 0.48; IR (ATR) 1691 (C=O), 1396, 1365, 1156 cm^{-1}; ^{1}H NMR (400 MHz, $CDCl_3$) δ 3.55 (t, J = 6.5 Hz, 2H, CH_2Cl), 3.21 (t, J = 7.0 Hz, 2H, NCH_2), 2.50-2.44 (m, NCH, 1H), 1.85-1.61 (m, 2H, CH_2), 1.44 (s, 9H, CMe_3), 0.77-0.68 (m, 2H, CH), 0.63-0.51 (m, 2H, CH); ^{13}C NMR (100.6 MHz, $CDCl_3$) δ 156.8 (C=O), 79.6 (O*C*Me$_3$), 46.7 (NCH_2), 44.9 (CH_2Cl), 30.0 (CH_2), 28.7 (NCH), 28.6 (C*Me$_3$*), 25.9 (CH_2), 8.2 (CH_2); MS (EI) *m/z* 270 [(^{35}M + Na)$^+$, 100]; HRMS (ESI) *m/z* calcd for $C_{12}H_{22}{}^{35}ClNO_2$ [(^{35}M + Na)$^+$, 100] 270.1231,

found 270.1223 (+2.9 ppm error) and a 50:50 mixture (by ^{1}H NMR spectroscopy) of *N*-Boc cyclopropane **489** and alkyl chloride **486** (526 mg, i.e. 322 mg (quantitative) of alkyl chloride **486**). Spectroscopic data consistent with those reported in the literature.[118]

Lab book reference HFK6-010

In the same way, NaH (1.00 g of 60% wt in mineral oil, 25.0 mmol, 2.5 eq.), *N*-Boc cyclopropylamine **489** (2.36 g, 15.0 mmol, 1.5 eq.) and 1-bromo-4-chlorobutane (1.15 mL, 10.0 mmol, 1.0 eq.) in DMF (45 mL) gave the crude product. Purification by flash column chromatography on silica with 95:5 to 90:10 to 50:50 hexane-Et_2O as eluent gave alkyl chloride **486** (1.82 g, 73% based on 1-bromo-4-chlorobutane) as a pale yellow oil.

Lab book reference HFK6-024

***tert*-Butyl 4-azaspiro[2.5]octane-4-carboxylate 487**

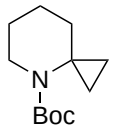

487

s-BuLi (7.3 mL, 1.1 M solution in hexanes, 8.0 mmol, 2.0 eq.) was added dropwise to a stirred solution of alkyl chloride **486** (992 mg, 4.0 mmol, 1.0 eq.) and TMEDA (1.2 mL, 8.0 mmol, 2.0 eq.) in Et_2O (60 mL) at –78 °C under Ar. The resulting solution was stirred at –78 °C for 2 h. Then, the reaction was allowed to warm slowly to rt over 3 h and stirred at rt for 15 h. Then, H_2O (10 mL) was added and the mixture was extracted with Et_2O (3 × 15 mL). The combined organic extracts were dried ($MgSO_4$) and evaporated under reduced pressure to give the crude product. Purification by flash column chromatography on silica with 97:3 to 85:15 hexane-Et_2O as eluent gave recovered alkyl chloride **486** (66 mg, 7%) and cyclopropyl piperidine **487** (351 mg, 42%) as a colourless oil, R_F (4:1 hexane-Et_2O) 0.37; IR (ATR) 1693 (C=O), 1379, 1284,

1152 cm^{-1}; ^1H NMR (400 MHz, $CDCl_3$) δ 3.39 (t, J = 5.5 Hz, 2H, NCH_2), 1.76-1.63 (m, 2H, CH_2), 1.54-1.46 (m, 2H, CH_2), 1.43 (s, 9H, CMe_3), 1.41-1.34 (m, 2H, CH_2), 0.86-0.77 (m, 2H, CH_2), 0.60-0.51 (m, 2H, CH_2); ^{13}C NMR (100.6 MHz, $CDCl_3$) δ 156.1 (C=O), 79.3 (O*C*Me_3), 46.8 (NCH_2), 38.8 (CN), 32.7 (CH_2), 28.6 (C*Me*$_3$), 25.5 (CH_2), 24.3 (CH_2), 14.5 (CH_2); MS (EI) m/z 234 [$(M + Na)^+$, 100]; HRMS (ESI) m/z calcd for $C_{12}H_{21}NO_2$ [$(M + Na)^+$, 100] 234.1464, found 234.1466 (−0.5 ppm error). Spectroscopic data consistent with those reported in the literature.[118]

Lab book reference HFK6-020

tert-Butyl 1-(phenylsulfanyl)-4-azaspiro[2.5]octane-4-carboxylate _cis_-491 and _tert_-Butyl 5-(phenylsulfanyl)-4-azaspiro[2.5]octane-4-carboxylate 492

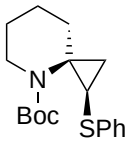

cis-**491**

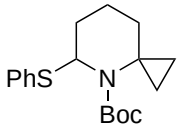

492

s-BuLi (563 μL, 1.1 M solution in hexanes, 0.619 mmol, 1.2 eq.) was added dropwise to a stirred solution of freshly distilled cyclopropyl piperidine **487** (109 mg, 0.516 mmol, 1.0 eq.) and TMEDA (93 μL, 0.62 mmol, 1.2 eq.) in Et_2O (3.4 mL) at –60 °C under Ar. The resulting solution was stirred at –60 °C for 3 h. Then, a solution of diphenyl disulfide (135 mg, 0.619 mmol, 1.2 eq.) in Et_2O (2 mL) was added and the reaction was allowed to warm slowly to rt over 3 h and stirred at rt for 15 h. Then, H_2O (5 mL) was added and the mixture was extracted with Et_2O (3 × 10 mL). The combined organic extracts were dried ($MgSO_4$) and evaporated under reduced pressure to give the crude product. Purification by flash column chromatography on silica with 97:3 to 80:20 hexane-Et_2O as eluent gave recovered cyclopropyl piperidine **487** (23 mg, 21%), cyclopropyl sulfide *cis*-**491** (86 mg, 52%) as a white solid, mp 95-98 °C; R_F (1:1 hexane-Et_2O) 0.57; IR (ATR) 1693 (C=O), 1382, 1364, 1153 cm^{-1}; ^1H NMR (400 MHz, $CDCl_3$) δ 7.40-7.32 (m, 2H, Ph), 7.31-7.24 (m, 2H, Ph), 7.18-7.10 (m, 1H, Ph), 4.19-3.96 (m, 1H, NCH), 2.75 (br dd, J = 13.0, 13.0 Hz, 1H, NCH), 2.29-

1.98 (m, 2H, CH), 1.85-1.81 (m, 1H, CH), 1.73-1.65 (m, 1H, CH), 1.61-1.50 (m, 4H, CH), 1.45 (s, 9H, CMe_3), 0.99-0.94 (m, 1H, C*H*SPh); ^{13}C NMR (100.6 MHz, $CDCl_3$) δ 156.1 (C=O), 138.5 (*ipso*-Ph), 128.9 (Ph), 127.3 (Ph), 125.3 (Ph), 79.8 (O*C*Me_3), 47.0 (NCH_2), 45.5 (NC), 33.7 (*C*HSPh), 28.5 (C*Me*$_3$), 25.1 (CH_2), 24.2 (CH_2) (two CH_2 resonances not resolved); MS (EI) *m/z* 342 [(M + Na)$^+$, 100]; HRMS (ESI) *m/z* calcd for $C_{18}H_{25}NO_2S$ [(M + Na)$^+$, 100] 342.1498, found 342.1496 (+0.7 ppm error) and piperidine sulfide **492** (24 mg, 15%) as an oil, R_F (1:1 hexane-Et_2O) 0.67; IR (ATR) 1686 (C=O), 1366, 1296, 1165 cm^{-1}; ^{1}H NMR (400 MHz, $CDCl_3$) δ 7.45-7.36 (m, 2H, Ar), 7.30-7.19 (m, 2H, Ar), 7.22-7.12 (m, 1H, Ar), 6.01-5.97 (m, 1H, NC*H*SPh) 2.17-1.83 (m, 4H, CH), 1.69-1.63 (m, 1H, CH), 1.41 (s, 9H, CMe_3), 1.20-1.15 (m, 1H, CH), 1.12-1.02 (m, 1H, CH), 0.94-0.84 (m, 1H, CH), 0.71-0.65 (m, 1H, CH), 0.61-0.56 (m, 1H, CH); ^{13}C NMR (100.6 MHz, $CDCl_3$) δ 155.0 (C=O), 136.1 (*ipso*-Ph), 130.8 (Ar), 129.0 (Ar), 126.6 (Ar), 80.4 (O*C*Me_3), 65.0 (N*C*HSPh), 35.0 (NC), 33.5 (CH_2), 31.3 (CH_2), 28.5 (C*Me*$_3$), 20.3 (CH_2), 15.5 (CH_2), 13.5 (CH_2); MS (EI) *m/z* 342 [(M + Na)$^+$, 100]; HRMS (ESI) *m/z* calcd for $C_{18}H_{25}NO_2S$ [(M + Na)$^+$, 100] 342.1498, found 342.1496 (+0.7 ppm error).

Lab book reference HFK6-043

s-BuLi (654 μL, 1.1 M solution in hexanes, 0.72 mmol, 1.2 eq.) was added dropwise to a stirred solution of starting material **486** (148 mg, 0.6 mmol, 1.0 eq.) and TMEDA (108 μL, 0.72 mmol, 1.2 eq.) in Et_2O (10 mL) at –78 °C under Ar. The resulting solution was stirred at –78 °C for 2 h. Then, the solution was allowed to warm slowly to rt over 3 h and stirred at rt for 15 h. Then, the solution was cooled to –60 °C and *s*-BuLi (654 μL, 1.1 M solution in hexanes, 0.72 mmol, 1.2 eq.) was added dropwise. The resulting solution was stirred at –60 °C for 5 h. Then, a solution of diphenyl disulfide (157 mg, 0.720 mmol, 1.2 eq.) in Et_2O (0.7 mL) was added and the solution was allowed to warm slowly to rt over 3 h and stirred at rt for 15 h. Then, H_2O (5 mL) was added and the mixture was extracted with Et_2O (3 × 15 mL). The combined organic extracts were dried ($MgSO_4$) and evaporated under reduced pressure to give the crude product.

Purification by flash column chromatography on silica with 97:3 to 80:20 hexane-Et_2O as eluent gave cyclopropyl piperidine **487** (20 mg, 13%), cyclopropyl sulfide *cis*-**491** (61 mg, 32%) and piperidine sulfide **492** (15 mg, 8%).

Lab book reference HFK6-050

s-BuLi (654 μL, 1.1 M solution in hexanes, 0.72 mmol, 1.2 eq.) was added dropwise to a stirred solution of alkyl chloride **486** (124 mg, 0.5 mmol, 1.0 eq.) and TMEDA (90 μL, 0.60 mmol, 1.2 eq.) in Et_2O (10 mL) at –78 °C under Ar. The resulting solution was stirred at –78 °C for 4 h. Then, the solution was allowed to warm slowly to rt over 3 h and stirred at rt for 15 h. Then, the solution was cooled to –78 °C and *s*-BuLi (654 μL, 1.1 M solution in hexanes, 0.72 mmol, 1.2 eq.) was added dropwise. The resulting solution was stirred at –78 °C for 8 h. Then, a solution of diphenyl disulfide (131 mg, 0.600 mmol, 1.2 eq.) in Et_2O (2 mL) was added and the solution was allowed to warm slowly to rt over 3 h and stirred at rt for 15 h. Then, H_2O (5 mL) was added and the mixture was extracted with Et_2O (3 × 15 mL). The combined organic extracts were dried ($MgSO_4$) and evaporated under reduced pressure to give the crude product. Purification by flash column chromatography on silica with 98:2 to 90:10 hexane-Et_2O as eluent gave cyclopropyl piperidine **487** (28 mg, 23%), cyclopropyl sulfide *cis*-**491** (38 mg, 24%) and piperidine sulfide **492** (9 mg, 6%).

Lab book reference HFK6-062

tert-Butyl 1-(4,4,5,5-tetramethyl-1,3,2-dioxaborolan-2-yl)-4-azaspiro[2.5] octane-4-carboxylate _cis_-493 and _tert_-butyl 5-(4,4,5,5-tetramethyl-1,3,2-dioxaborolan-2-yl)-4-azaspiro[2.5]octane-4-carboxylate 494

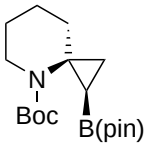

cis-**493**

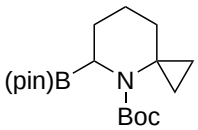

494

s-BuLi (654 μL, 1.1 M solution in hexanes, 0.72 mmol, 1.2 eq.) was added dropwise to a

stirred solution of alkyl chloride **486** (124 mg, 0.5 mmol, 1.0 eq.) and TMEDA (90 μL, 0.60 mmol, 1.2 eq.) in Et_2O (10 mL) at –78 °C under Ar. The resulting solution was stirred at –78 °C for 2 h. Then, the solution was allowed to warm slowly to rt over 3 h and stirred at rt for 15 h. Then, the reaction was cooled to –60 °C and *s*-BuLi (654 μL, 1.1 M solution in hexanes, 0.72 mmol, 1.2 eq.) was added dropwise. The resulting solution was stirred at –60 °C for 3 h. Then, *i*-PrOBpin (122 μL, 0.600 mmol, 1.2 eq.) was added and the solution was allowed to warm slowly to rt over 3 h and stirred at rt for 15 h. Then, H_2O (5 mL) was added and the mixture was extracted with Et_2O (3 × 15 mL). The combined organic extracts were washed with brine (20 mL), dried ($MgSO_4$) and evaporated under reduced pressure to give the crude product. Purification by flash column chromatography on silica with 90:10 to 80:20 hexane-Et_2O as eluent gave cyclopropyl piperidine **487** (45 mg, 36%), cyclopropyl pinacol boronate *cis*-**493** (18 mg, 11%) as a yellow oil, R_F (7:3 hexane-Et_2O) 0.26; IR (ATR) 1694 (C=O), 1388, 1364, 1144 cm^{-1}; ^1H NMR (400 MHz, $CDCl_3$) (50:50 mixture of rotamers) δ 4.19-3.92 (br m, 0.5H, NCH), 3.54-3.22 (br m, 1H, NCH), 2.84-2.63 (br m, 0.5H, NCH), 2.10-1.89 (br m, 0.5H, CH), 1.78-1.64 (br m, 3.5H, CH), 1.55-1.48 (br m, 1.5H, CH), 1.44 (s, 9H, CMe_3) 1.23 (s, 6H, Me), 1.18 (s, 6H, Me), 1.09-0.97 (br m, 0.5H, CH) 0.92-0.80 (br m, 2H, CH), 0.31- −0.15 (m, 1H, CHB); ^{13}C NMR (100.6 MHz, $CDCl_3$) δ 155.6 (C=O), 83.1 (O*C*Me_2), 79.1 (O*C*Me_3), 48.1 (NCH_2), 30.5 (CH_2), 29.8 (CH_2), 28.7 (C*Me*$_3$), 25.7 (Me), 25.2 (Me) (CHB, NC and CH_2 resonances not resolved); MS (EI) *m/z* 360 [(M + Na)$^+$, 100]; HRMS (ESI) *m/z* calcd for $C_{18}H_{32}BNO_4$ [(M + Na)$^+$, 100] 360.2317, found 360.2321 (−0.1 ppm error) and piperdine pinacol boronate **494** (16 mg, 10%) as a white solid, R_F (7:3 hexane-Et_2O) 0.16; IR (ATR) 1672 (C=O), 1369, 1152, 1108 cm^{-1}; ^1H NMR (400 MHz, $CDCl_3$) δ 2.50 (dd, J = 12.5, 3.5 Hz, 1H, CHB), 1.88-1.73 (m, 2H, CH), 1.70-1.64 (m, 1H, CH), 1.61 (ddd, J = 12.5, 3.0, 3.0 Hz, 1H, CH), 1.49 (s, 9H, CMe_3), 1.37 (ddd, J = 10.0, 6.5, 6.5 Hz, 1H, CH), 1.25-1.23 (m, 1H, CH), 1.18 (s, 6H, Me), 1.16 (s, 6H, Me), 0.89-0.80 (m, 1H, CH), 0.75-0.69 (m, 1H, CH), 0.60-0.54 (m, 1H, CH), 0.42-0.37 (m, 1H, CH); ^{13}C NMR (100.6 MHz, $CDCl_3$) δ 160.0 (C=O), 85.9 (O*C*Me_2), 80.1 (O*C*Me_3), 37.4 (NC), 34.5 (CH_2), 28.6 (C*Me*$_3$), 27.5 (CH_2), 25.3 (Me),

24.8 (CHB), 24.7 (CH_2), 14.0 (CH_2), 12.2 (CH_2); MS (EI) *m/z* 360 [(M + Na)$^+$, 100]; HRMS (ESI) *m/z* calcd for $C_{18}H_{32}BNO_4$ [(M + Na)$^+$, 100] 360.2317, found 360.2320 (0.0 ppm error).

Lab book reference HFK6-063

tert-Butyl 1-(pyrimidin-5-yl)-6-azaspiro[2.5]octane-6-carboxylate 503

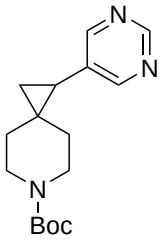

503

Using general procedure B, *N*-Boc MIDA boronate **209** (93 mg, 0.25 mmol, 1.0 eq.), Cs_2CO_3 (497 mg, 1.52 mmol, 6.0 eq.), PCy_3 (21 mg, 0.076 mmol, 0.3 eq.), $Pd(OAc)_2$, (8.6 mg, 0.038 mmol, 0.15 eq.) and 5-bromopyrimidine (57 mg, 0.36 mmol, 1.4 eq.) in toluene (3.5 mL) and H_2O (0.3 mL) gave the crude product. Purification by flash column chromatography on silica with EtOAc as eluent gave arylated piperidine **503** (54 mg, 73%) as a cream solid, mp 88-92 °C; R_F (EtOAc) 0.24; IR (ATR) 1685 (C=O), 1415, 1238, 1166 cm^{-1}; ^{1}H NMR (400 MHz, $CDCl_3$) δ 1H NMR (400 MHz, $CDCl_3$) 9.00 (s, 1H, Ar), 8.53 (s, 2H, Ar), 3.62-3.56 (m, 1H, NCH), 3.34 (ddd, J = 13.0, 8.5, 3.5 Hz, 1H, NCH), 3.30-3.25 (m, 1H, NCH), 3.14 (ddd, J = 13.0, 8.0, 3.5 Hz 1H, NCH), 1.87 (dd, J = 8.0, 6.0 Hz, 1H, CHAr), 1.61 (ddd, J = 12.5, 8.5, 4.0 Hz 1H, CH), 1.43-1.36 (m, 1H, CH); 1.39 (s, 9H, CMe_3), 1.23-1.13 (m, 1H, CH), 1.08-1.02 (m, 1H, CH), 1.01-0.94 (m, 2H, CH); ^{13}C NMR (100.6 MHz, $CDCl_3$) δ 157.1 (Ar), 156.5 (Ar), 154.9 (C=O, Boc), 132.5 (*ipso*-Ar), 79.6 (O*C*Me$_3$), 43.2 (br, NCH_2), 36.4 (CH_2), 30.0 (CH_2), 28.4 (C*Me*$_3$), 25.6 (*C*CHAr), 23.5 (CHAr), 15.8 (CH_2) (one NCH_2 resonance not resolved); MS (EI) *m/z* 312 [(M + Na)$^+$, 100]; HRMS (ESI) *m/z* calcd for $C_{16}H_{23}N_3O_2$ [(M + Na)$^+$, 100] 312.1682, found 312.1682 (+0.1 ppm error).

Lab book reference HFK8-036

***tert*-Butyl 1-(4-methoxyphenyl)-6-azaspiro[2.5]octane-6-carboxylate 504**

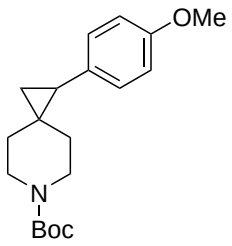

504

Using general procedure B, *N*-Boc MIDA boronate **209** (183 mg, 0.5 mmol, 1.0 eq.), Cs_2CO_3 (978 mg, 3.00 mmol, 6.0 eq.), PCy_3 (84 mg, 0.30 mmol, 0.3 eq.), $Pd(OAc)_2$, (17 mg, 0.076 mmol, 0.15 eq.) and 4-bromoanisole (88 μL, 0.70 mmol, 1.4 eq.) in toluene (11 mL) and H_2O (0.6 mL) gave the crude product. Purification by flash column chromatography on silica with 90:10 hexane-EtOAc as eluent gave arylated piperidine **504** (65 mg, 41%) as an amber oil, R_F (4:1 hexane-EtOAc) 0.30; IR (ATR) 1688 (C=O), 1514, 1238, 1168 cm^{-1}; ^1H NMR (400 MHz, $CDCl_3$) δ 7.09 (d, J = 8.5 Hz, 2H, Ar), 6.81 (d, J = 8.5 Hz, 2H, Ar), 3.78 (s, 3H, OMe), 3.56-3.44 (m, 2H, NCH), 3.23-3.20 (m, 2H, NCH), 1.93 (dd, J = 8.5, 5.5 Hz, 1H, CHAr), 1.51-1.46 (m, 2H, CH), 1.44 (s, 9H, CMe_3), 1.19-1.08 (m, 2H, CH), 0.85 (dd, J = 5.5, 5.5 Hz, 1H, CH), 0.79 (dd, J = 8.5, 5.5 Hz, 1H, CH); ^{13}C NMR (100.6 MHz, $CDCl_3$) δ 157.9 (*ipso*-Ar), 155.2 (C=O), 130.9 (*ipso*-Ar), 129.9 (Ar), 113.5 (Ar), 79.3 (O*C*Me_3), 55.4 (OMe), 43.6 (br, NCH_2), 36.8 (CH_2), 30.0 (CH_2), 28.6 (C*Me*$_3$), 27.9 (CHAr), 24.5 (*C*CHAr), 15.9 (CH_2) (one NCH_2 resonance not resolved); MS (EI) m/z 340 [$(M + Na)^+$, 100]; HRMS (ESI) m/z calcd for $C_{19}H_{27}NO_3$ [$(M + Na)^+$, 100] 340.1883, found 340.1882 (+0.2 ppm error).
Lab book reference HFK7-032

***tert*-Butyl-7-(pyrimidin-5-yl)-2-azabicyclo[4.1.0]heptane-2-carboxylate *exo*-507**

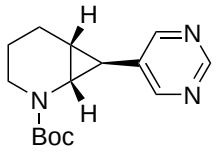

exo-**507**

Using general procedure B, *N*-Boc MIDA boronate *exo*-**212** (64 mg, 0.18 mmol, 1.0 eq.), Cs_2CO_3 (356 mg, 1.10 mmol, 6.0 eq.), PCy_3 (15 mg, 0.055 mmol, 0.3 eq.), $Pd(OAc)_2$, (6 mg, 0.03 mmol, 0.15 eq.) and 5-bromopyrimidine (41 mg, 0.26 mmol, 1.4 eq.) in toluene (3.5 mL) and H_2O (0.3 mL) gave the crude product. Purification by flash column chromatography on silica with Et_2O as eluent gave arylated piperidine *exo*-**507** (24 mg, 48%) as a cream solid, mp 78-80 °C; R_F (Et_2O) 0.24; IR (ATR) 1693 (C=O), 1557, 1388, 1163 cm^{-1}; ^1H NMR (400 MHz, $CDCl_3$) (75:25 mixture of rotamers) δ 9.01 (s, 0.75H, Ar), 8.99 (s, 0.25H, Ar), 8.48 (s, 2H, Ar), 3.86 (ddd, J = 13.0, 4.0, 4.0 Hz, 0.75H, NCH), 3.70 (ddd, J = 13.0, 4.0, 4.0 Hz, 0.25H, NCH), 3.17 (dd, J = 8.5, 3.0 Hz, 0.25H, NCH), 3.07-2.91 (m, 0.75H, NCH), 2.71 (ddd, J = 13.0, 13.0, 2.5 Hz, 0.25H, NCH), 2.60 (ddd, J = 13.0, 13.0, 2.5 Hz, 0.75H, NCH), 2.06-1.97 (m, 1H, CH), 1.96-1.86 (m, 1H, CH), 1.77-1.63 (m, 3H, CH), 1.45 (s, 2.5H, CMe_3 and CH), 1.40 (s, 0.75H, CH), 1.35 (s, 6.75H, CMe_3); ^{13}C NMR (100.6 MHz, $CDCl_3$) (rotamers) δ 156.4 (Ar), 156.3 (Ar), 156.1 (C=O), 155.9 (C=O), 154.8 (Ar), 154.5 (Ar), 135.9 (*ipso*-Ar), 134.7 (*ipso*-Ar), 80.1 (O*C*Me_3), 41.9 (NCH_2), 40.4 (NCH_2), 38.9 (NCH), 38.3 (NCH), 29.8 (CH_2), 28.6 (C*Me*$_3$), 28.5 (C*Me*$_3$), 24.8 (CH), 24.1 (CH), 22.2 (CH), 22.0 (CH_2), 21.8 (CH), 20.5 (CH_2), 20.4 (CH_2); MS (EI) *m/z* 298 [(M + Na)$^+$, 100]; HRMS (ESI) *m/z* calcd for $C_{15}H_{21}N_3O_2$ [(M + Na)$^+$, 100] 298.1526, found 298.1526 (0.0 ppm error). Lab book reference HFK8-037

***tert*-Butyl-7-(pyrimidin-5-yl)-3-azabicyclo[4.1.0]heptane-3-carboxylate *exo*-505**

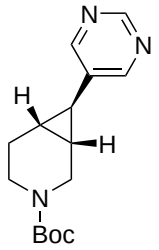

exo-**505**

Using general procedure B, *N*-Boc MIDA boronate *exo*-**211** (176 mg, 0.500 mmol, 1.0 eq.), Cs_2CO_3 (978 mg, 3.00 mmol, 6.0 eq.), PCy_3 (84 mg, 0.15 mmol, 0.3 eq.), $Pd(OAc)_2$, (17 mg, 0.076 mmol, 0.15 eq.) and 5-bromopyrimidine (111 mg, 0.700 mmol, 1.4 eq.) in toluene (7 mL) and H_2O (0.6 mL) gave the crude product. Purification by flash column chromatography on silica with EtOAc as eluent gave arylated piperidine *exo*-**505** (110 mg, 80%) as a colorless oil, R_F (EtOAc) 0.17; IR (ATR) 1683 (C=O), 1419, 1166, 725 cm^{-1}; ^1H NMR (400 MHz, $CDCl_3$) δ 8.93 (s, 1H, Ar), 8.34 (s, 2H, Ar), 4.04-3.89 (m, 1H, NCH), 3.55-3.43 (m, 2H, NCH), 2.94 (ddd, J = 13.5, 9.5, 5.5 Hz, 1H, NCH), 2.05-1.97 (m, 1H, CH), 1.90-1.76 (m, 1H, CH), 1.55 (dd, J = 5.0, 5.0 Hz, 1H, CHAr), 1.48-1.43 (m, 2H, CH), 1.41 (s, 9H, CMe_3); ^{13}C NMR (100.6 MHz, $CDCl_3$) (rotamers) δ 156.1 (Ar), 155.0 (C=O), 154.1 (Ar), 136.1 (*ipso*-Ar), 79.8 ($OCMe_3$), 42.1 (NCH_2), 41.4 (NCH_2), 40.8 (NCH_2), 39.8 (NCH_2), 28.5 (CMe_3), 22.4 (CHAr), 21.9 (CH), 20.4 (CH) (CH_2 resonance not resolved); MS (EI) *m/z* 298 [$(M + Na)^+$, 100]; HRMS (ESI) *m/z* calcd for $C_{15}H_{21}N_3O_2$ [$(M + Na)^+$, 100] 298.1526, found 298.1526 (0.0 ppm error).

Lab book reference HFK8-033

***tert*-Butyl-7-(4-methoxyphenyl)-3-azabicyclo[4.1.0]heptane-3-carboxylate *exo*-506**

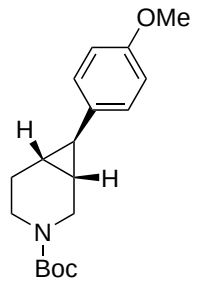

exo-**506**

Using general procedure B, *N*-Boc MIDA boronate *exo*-**211** (183 mg, 0.5 mmol, 1.0 eq.), Cs_2CO_3 (978 mg, 3.00 mmol, 6.0 eq.), PCy_3 (84 mg, 0.30 mmol, 0.3 eq.), $Pd(OAc)_2$, (17 mg, 0.076 mmol, 0.15 eq.) and 4-bromoanisole (88 μL, 0.70 mmol, 1.4 eq.) in toluene (11 mL) and H_2O (0.6 mL) gave the crude product. Purification by flash column chromatography on silica with 90:10 hexane-EtOAc as eluent gave arylated piperidine *exo*-**506** (65 mg, 41%) as an amber oil, R_F (1:1 hexane-Et_2O) 0.43; IR (ATR) 1687 (C=O), 1515, 1243, 1166 cm^{-1}; ^1H NMR (400 MHz, $CDCl_3$) δ 6.94 (d, J = 8.5 Hz, 2H, Ar), 6.80 (d, J = 8.5 Hz, 2H, Ar), 3.92 (br d, J = 13.5 Hz, 1H, NCH), 3.77 (s, 3H, OMe), 3.64-3.36 (m, 2H, NCH), 3.09-2.94 (m, 1H, NCH), 2.06-1.98 (m, 1H, CH), 1.92-1.77 (m, 1H, CH), 1.61 (dd, J = 5.0, 5.0 Hz, 1H, CHAr), 1.48 (s, 9H, CMe_3), 1.38-1.22 (m, 2H, CH); ^{13}C NMR (100.6 MHz, $CDCl_3$) (rotamers) δ 157.7 (*ipso*-Ar), 155.3 (C=O), 134.9 (*ipso*-Ar), 126.5 (Ar), 113.9 (Ar), 79.5 (O*C*Me_3), 55.4 (OMe), 42.6 (NCH_2), 41.8 (NCH_2), 41.0 (NCH_2), 40.1 (NCH_2), 28.6 (C*Me*$_3$), 26.7 (CHAr), 23.0 (CH_2), 22.6 (CH_2), 21.2 (CH), 19.7 (CH); MS (EI) *m/z* 326 [(M + Na)$^+$, 100]; HRMS (ESI) *m/z* calcd for $C_{18}H_{25}NO_3$ [(M + Na)$^+$, 100] 326.1727, found 326.1713 (+4.2 ppm error).

Lab book reference HFK8-010

***tert*-Butyl-7-(2-oxo-2,3-dihydro-1H-indol-6-yl)-3-azabicyclo[4.1.0]heptane-3-carboxylate *exo*-509**

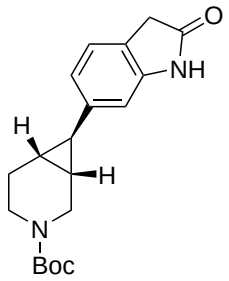

exo-**509**

Using general procedure B, *N*-Boc MIDA boronate *exo*-**211** (176 mg, 0.500 mmol, 1.0 eq.), Cs_2CO_3 (978 mg, 3.00 mmol, 6.0 eq.), PCy_3 (84 mg, 0.15 mmol, 0.3 eq.), $Pd(OAc)_2$, (17 mg, 0.076 mmol, 0.15 eq.) and 6-bromooxindole (148 mg, 0.700 mmol, 1.4 eq.) in toluene (7 mL) and H_2O (0.6 mL) gave the crude product. Purification by flash column chromatography on silica with 98:2 to 95:5 to 80:20 CH_2Cl_2-acetone as eluent gave the impure product. Further purification by flash column chromatography on silica with 60:40 hexane-EtOAc as eluent gave arylated piperidine *exo*-**509** (28 mg, 17%) as a yellow oil, R_F (7:3 hexane-EtOAc) 0.27; IR (ATR) 3240 (NH), 1688 (C=O), 1681 (C=O), 1246, 1167, 730 cm^{-1}; ^1H NMR (400 MHz, $CDCl_3$) δ 9.03 (s, 1H, NH), 7.07 (br d, J = 7.5 Hz, 1H, Ar), 6.68 (dd, J = 7.5, 1.5 Hz, 1H, Ar), 6.53 (br d, J = 1.5 Hz, 1H, Ar), 3.93 (br d, J = 13.5 Hz, 1H, NCH), 3.59-3.52 (m, 2H, NCH), 3.48 (s, 2H, C(O)CH), 3.06-2.94 (m, 1H, NCH), 2.05-1.97 (m, 1H, CH), 1.94-1.77 (m, 1H, CH), 1.62 (dd, J = 4.5, 4.5 Hz, 1H, CHAr), 1.47 (s, 9H, CMe_3), 1.41-1.28 (m, 2H, CH); ^{13}C NMR (100.6 MHz, $CDCl_3$) (rotamers) δ 178.5 (C=O, lactam), 155.3 (C=O, Boc), 143.4 (*ipso*-Ar), 143.0 (*ipso*-Ar), 124.4 (Ar), 122.4 (*ipso*-Ar), 119.8 (Ar), 107.0 (Ar), 79.7 (O*C*Me_3), 42.5 (NCH_2), 41.7 (NCH_2), 41.1 (NCH_2), 40.0 (NCH_2), 36.2 ($CH_2C(O)$), 28.6 (C*Me*$_3$), 27.6 (CHAr), 23.0 (CH), 22.6 (CH), 22.0 (CH_2), 20.4 (CH_2); MS (EI) *m/z* 351 [(M + Na)$^+$, 100]; HRMS (ESI) *m/z* calcd for $C_{19}H_{24}N_2O_3$ [(M + Na)$^+$, 100] 351.1679, found 351.1679 (+0.1 ppm error).

Lab book reference HFK8-019

***tert*-Butyl-7-(4-acetamidophenyl)-3-azabicyclo[4.1.0]heptane-3-carboxylate *exo*-510**

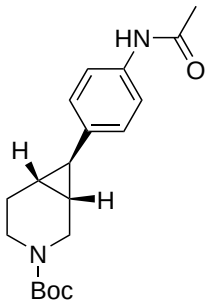

exo-**510**

Using general procedure B, *N*-Boc MIDA boronate *exo*-**211** (176 mg, 0.500 mmol, 1.0 eq.), Cs_2CO_3 (978 mg, 3.00 mmol, 6.0 eq.), PCy_3 (84 mg, 0.15 mmol, 0.3 eq.), $Pd(OAc)_2$, (17 mg, 0.076 mmol, 0.15 eq.) and 6-bromoacetanilide (150 mg, 0.700 mmol, 1.4 eq.) in toluene (7 mL) and H_2O (0.6 mL) gave the crude product. Purification by flash column chromatography on silica with 95:5 to 80:20 CH_2Cl_2-acetone as eluent gave arylated piperidine *exo*-**510** (117 mg, 71%) as a cream solid, mp 132-134 °C; R_F (4:1 CH_2Cl_2-acetone) 0.47; IR (ATR) 3306 (NH), 1662 (C=O), 1516, 1655, 730 cm^{-1}; ^1H NMR (400 MHz, $CDCl_3$) δ 7.61 (s, 1H, NH), 7.37 (d, J = 8.5 Hz, 2H, Ar), 6.93 (d, J = 8.5 Hz, 2H, Ar), 3.91 (br d, J = 13.5 Hz, 1H, NCH), 3.56 (dd, J = 13.5, 4.5 Hz, 1H, NCH), 3.52-3.38 (m, 1H, NCH), 3.05-2.95 (m, 1H, NCH), 2.14 (s, 3H, C(O)*Me*), 2.05-1.97 (m, 1H, CH), 1.89-1.74 (m, 1H, CH), 1.60 (dd, J = 4.5, 4.5 Hz, 1H, CHAr), 1.47 (s, 9H, CMe_3), 1.37-1.27 (m, 2H, CH); ^{13}C NMR (100.6 MHz, $CDCl_3$) (rotamers) δ 168.5 (C=O, C(O)Me), 155.3 (C=O, Boc), 138.9 (*ipso*-Ar), 135.7 (*ipso*-Ar), 126.0 (Ar), 120.2 (Ar), 79.7 (O*C*Me_3), 42.6 (NCH_2), 41.8 (NCH_2), 41.1 (NCH_2), 40.1 (NCH_2), 28.6 (C*Me*$_3$), 27.0 (CHAr), 24.6 (C(O)*Me*), 23.1 (CH_2), 22.6 (CH_2), 21.6 (CH), 20.1 (CH); MS (EI) *m/z* 353 [$(M + Na)^+$, 100]; HRMS (ESI) *m/z* calcd for $C_{19}H_{26}N_2O_3$ [$(M + Na)^+$, 100] 353.1836, found 353.1831 (+1.2 ppm error).

Lab book reference HFK8-020

***tert*-Butyl-7-(4-sulfamoylphenyl)-3-azabicyclo[4.1.0]heptane-3-carboxylate *exo*-511**

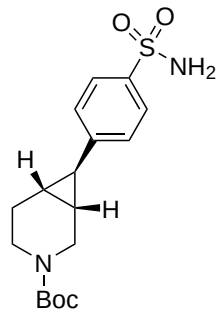

exo-**511**

Using general procedure B, *N*-Boc MIDA boronate *exo*-**211** (176 mg, 0.500 mmol, 1.0 eq.), Cs_2CO_3 (978 mg, 3.00 mmol, 6.0 eq.), PCy_3 (84 mg, 0.15 mmol, 0.3 eq.), $Pd(OAc)_2$, (17 mg, 0.076 mmol, 0.15 eq.) and 4-bromobenzenesulfonamide (165 mg, 0.700 mmol, 1.4 eq.) in toluene (7 mL) and H_2O (0.6 mL) gave the crude product. Purification by flash column chromatography on silica with 95:5 to 90:10 CH_2Cl_2-acetone as eluent gave arylated piperidine *exo*-**511** (47 mg, 54%) as a yellow oil, R_F (9:1 CH_2Cl_2-acetone) 0.44; IR (ATR) 3254 (NH), 1669 (C=O), 1426, 1161, 731 cm^{-1}; ^1H NMR (400 MHz, $CDCl_3$) δ 7.78 (d, J = 8.5 Hz, 2H, Ar), 7.08 (d, J = 8.5 Hz, 2H, Ar), 5.17 (s, 2H, NH_2), 3.95 (br d, J = 13.5 Hz, 1H, NCH), 3.55 (dd, J = 13.5, 4.5 Hz, 1H, NCH), 3.52-3.44 (m, 1H, NCH), 3.03-2.95 (m, 1H, NCH), 2.07-1.99 (m, 1H, CH), 1.94-1.78 (m, 1H, CH), 1.69 (dd, J = 4.5, 4.5 Hz, 1H, CHAr), 1.50-1.38 (m, 2H, CH), 1.46 (s, 9H, CMe_3); ^{13}C NMR (100.6 MHz, $CDCl_3$) (rotamers) δ 155.2 (C=O), 148.9 (*ipso*-Ar), 139.0 (*ipso*-Ar), 126.6 (Ar), 125.9 (Ar), 79.9 (O*C*Me_3), 42.3 (NCH_2), 41.7 (NCH_2), 41.0 (NCH_2), 39.9 (NCH_2), 28.6 (C*Me*$_3$), 27.5 (CHAr), 23.3 (CH), 22.8 (CH_2), 21.7 (CH); MS (EI) *m/z* 375 [(M + Na)$^+$, 100]; HRMS (ESI) *m/z* calcd for $C_{17}H_{24}N_2O_4S$ [(M + Na)$^+$, 100] 375.1349, found 375.1352 (−0.8 ppm error).

Lab book reference HFK8-022

***tert*-Butyl-7-(2-aminopyridin-4-yl)-3-azabicyclo[4.1.0]heptane-3-carboxylate *exo*-512**

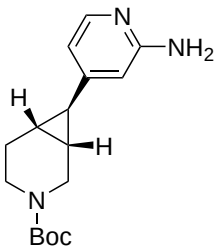

exo-**512**

Using general procedure B, *N*-Boc MIDA boronate *exo*-**211** (176 mg, 0.500 mmol, 1.0 eq.), Cs_2CO_3 (978 mg, 3.00 mmol, 6.0 eq.), PCy_3 (84 mg, 0.15 mmol, 0.3 eq.), $Pd(OAc)_2$, (17 mg, 0.076 mmol, 0.15 eq.) and 2-amino-4-bromopyridine (121 mg, 0.700 mmol, 1.4 eq.) in toluene (7 mL) and H_2O (0.6 mL) gave the crude product. Purification by flash column chromatography on silica with 99:1 to 97:3 to 90:10 CH_2Cl_2-methanol gave impure product. Further purification by flash column chromatography on silica with hexane to 99:1 EtOAc-Et_3N gave arylated piperidine *exo*-**512** (31 mg, 21%) as a yellow oil, R_F (99:1 EtOAc-Et_3N) 0.12; IR (ATR) 3320 (NH), 3306 (NH), 1678 (C=O), 1616, 1366, 1131, 728 cm^{-1}; ^1H NMR (400 MHz, $CDCl_3$) δ 7.86 (br d, J = 5.5 Hz, 1H, Ar), 6.22 (dd, J = 5.5, 1.5 Hz, 1H, Ar), 6.13 (br s, 1H, Ar), 4.53-4.23 (s, 2H, NH_2), 3.91 (br d, J = 13.5 Hz, 1H, NCH), 3.52 (dd, J = 13.5, 4.5 Hz, 1H, NCH), 3.49-3.37 (m, 1H, NCH), 3.02-2.90 (m, 1H, NCH), 2.03-1.95 (m, 1H, CH), 1.89-1.72 (m, 1H, CH), 1.49-1.35 (m, 3H, CH), 1.45 (s, 9H, CMe_3); ^{13}C NMR (100.6 MHz, $CDCl_3$) (rotamers) δ 158.5 (*ipso*-Ar), 155.1 (C=O), 154.3 (*ipso*-Ar), 147.9 (Ar), 111.3 (Ar), 105.2 (Ar), 79.7 (O*C*Me_3), 42.3 (NCH_2), 41.6 (NCH_2), 40.9 (NCH_2), 39.9 (NCH_2), 28.5 (C*Me*$_3$), 27.0 (CHAr), 22.8 (CH_2), 22.6 (CH), 21.0 (CH); MS (EI) *m/z* 290 (M + H)$^+$; HRMS (ESI) *m/z* calcd for $C_{15}H_{24}N_3O_2$ (M + H)$^+$ 290.1863, found 290.1864 (−0.4 ppm error).

Lab book reference HFK8-023

***tert*-Butyl 3-azabicyclo[4.1.0]heptane-3-carboxylate 454 and *tert*-butyl-7-[2-(hydroxymethyl)pyridin-4-yl]-3-azabicyclo[4.1.0]heptane-3-carboxylate *exo*-513**

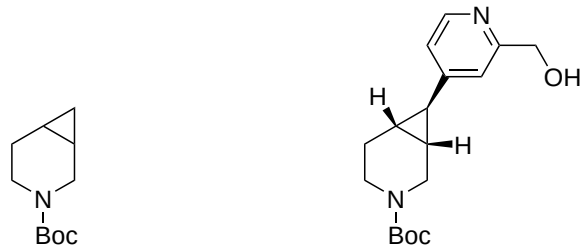

454 *exo*-**513**

Using general procedure B, *N*-Boc MIDA boronate *exo*-**211** (176 mg, 0.500 mmol, 1.0 eq.), Cs_2CO_3 (978 mg, 3.00 mmol, 6.0 eq.), PCy_3 (84 mg, 0.15 mmol, 0.3 eq.), $Pd(OAc)_2$, (17 mg, 0.076 mmol, 0.15 eq.) and 4-bromo-2-pyridinemethanol (132 mg, 0.700 mmol, 1.4 eq.) in toluene (7 mL) and H_2O (0.6 mL) gave the crude product. Purification by flash column chromatography on silica with 80:20 to 70:30 to 60:40 hexane-Et_2O gave cyclopropane **454** (36 mg, 36%) as a colourless oil, R_F (1:1 hexane-Et_2O) 0.35; IR (ATR) 1690 (C=O), 1420, 1247, 1169 cm^{-1}; ^1H NMR (400 MHz, $CDCl_3$) δ 3.72 (dd, J = 13.5, 1.0 Hz, 1H, NCH), 3.52 (dd, J = 13.5, 4.0 Hz, 1H, NCH), 3.35-3.23 (m, 1H, NCH), 2.98 (ddd, J = 13.5, 8.5, 5.5 Hz, 1H, NCH), 1.94-1.86 (m, 1H, CH), 1.71-1.60 (m, 1H, CH), 1.42 (s, 9H, CMe_3), 1.06-0.91 (m, 2H, CH), 0.60 (ddd, J = 8.5, 8.5, 5.0 Hz, 1H, CH), 0.12 (ddd, J = 8.5, 5.0, 5.0 Hz, 1H, CH); ^{13}C NMR (100.6 MHz, $CDCl_3$) (rotamers) δ 155.3 (C=O), 79.3 (O*C*Me_3), 42.3 (NCH_2), 40.8 (NCH_2), 40.1 (NCH_2), 28.6 (C*Me*$_3$), 22.8 (CH_2), 9.7 (CH), 9.1 (CH_2), 8.0 (CH); MS (EI) *m/z* 220 [(M + Na)$^+$, 100]; HRMS (ESI) *m/z* calcd for $C_{11}H_{19}NO_2$ [(M + Na)$^+$, 100] 220.1308, found 220.1306 (+0.8 ppm error) and impure product. Further purification by flash column chromatography on silica with 70:30 to 50:50 CH_2Cl_2-acetone as eluent gave impure product. Purification by flash column chromatography on silica with EtOAc to 80:20 to 70:30 to 60:40 CH_2Cl_2-acetone as eluent gave arylated piperidine *exo*-**513** (15 mg, 10%) as a yellow oil, R_F (1:1 CH_2Cl_2-acetone) 0.18; IR (ATR) 2927 (OH), 1684 (C=O), 1605, 1420, 1365, 1247 cm^{-1}; ^1H NMR (400 MHz,

$CDCl_3$) δ 8.35 (br s, 1H, Ar), 6.88 (br s, 1H, Ar), 6.81 (br s, 1H, Ar), 4.70 (br s, 2H, OCH), 3.98 (br d, J = 13.5 Hz, 1H, NCH), 3.54 (dd, J = 13.5, 4.5 Hz, 2H, NCH), 3.02-2.95 (m, 1H, NCH), 2.08-2.00 (m, 1H, CH), 1.92-1.79 (m, 1H, CH), 1.63 (dd, J = 4.5, 4.5 Hz, 1H, CHAr), 1.55-1.48 (m, 2H, CH), 1.47 (s, 9H, CMe_3); ^{13}C NMR (100.6 MHz, $CDCl_3$) (rotamers) δ 158.8 (*ipso*-Ar), 155.2 (C=O), 153.9 (*ipso*-Ar), 148.1 (Ar), 119.6 (Ar), 117.4 (Ar), 79.9 (O*C*Me_3), 64.2 ($HOCH_2$), 42.3 (NCH_2), 41.5 (NCH_2), 40.9 (NCH_2), 39.9 (NCH_2), 28.6 (C*Me*$_3$), 27.2 (CHAr), 23.6 (CH_2), 22.8 (CH), 22.0 (CH); MS (EI) *m/z* 327 [(M + Na)$^+$, 100]; HRMS (ESI) *m/z* calcd for $C_{17}H_{24}N_2O_3$ [(M + Na)$^+$, 100] 327.1679, found 327.1682 (−1.0 ppm error).

Lab book reference HFK8-028

tert-Butyl-7-(4-hydroxy-3-methoxyphenyl)-3-azabicyclo[4.1.0]heptane-3-carboxylate _exo_-514

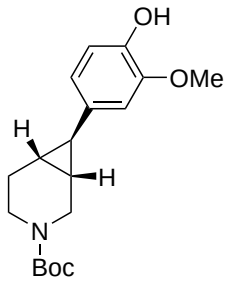

exo-**514**

Using general procedure B, *N*-Boc MIDA boronate *exo*-**211** (176 mg, 0.500 mmol, 1.0 eq.), Cs_2CO_3 (978 mg, 3.00 mmol, 6.0 eq.), PCy_3 (84 mg, 0.15 mmol, 0.3 eq.), $Pd(OAc)_2$, (17 mg, 0.076 mmol, 0.15 eq.) and 4-bromo-2-methoxyphenol (142 mg, 0.700 mmol, 1.4 eq.) in toluene (7 mL) and H_2O (0.6 mL) gave the crude product. Purification by flash column chromatography on silica with 95:5 to 90:10 to 80:20 hexane-EtOAc gave arylated piperidine *exo*-**514** (83 mg, 52%) as a colourless oil, R_F (7:3 hexane-EtOAc) 0.17; IR (ATR) 3306 (OH), 1674 (C=O), 1516, 1162, 728 cm^{-1}; ^{1}H NMR (400 MHz, $CDCl_3$) δ 6.80 (d, J = 8.0 Hz, 1H, Ar), 6.57-6.54 (m, 1H, Ar), 6.49 (dd, J = 8.0, 2.0 Hz, 1H, Ar), 5.65 (s, 1H, OH), 3.92 (br d, J = 13.5 Hz, 1H,

NCH), 3.86 (s, 3H, OMe), 3.58 (dd, J = 13.5, 5.0 Hz, 1H, NCH), 3.52-3.40 (m, 1H, NCH), 3.01 (ddd, J = 13.5, 9.0, 5.5 Hz, 1H, NCH), 2.06-1.98 (m, 1H, CH), 1.91-1.77 (m, 1H, CH), 1.60 (dd, J = 5.0, 5.0 Hz, 1H, CHAr), 1.47 (s, 9H, CMe_3), 1.39-1.20 (m, 2H, CH); ^{13}C NMR (100.6 MHz, $CDCl_3$) (rotamers) δ 155.3 (C=O), 146.6 (*ipso*-Ar), 143.7 (*ipso*-Ar), 134.7 (*ipso*-Ar), 117.8 (Ar), 114.4 (Ar), 108.9 (Ar), 79.6 ($OCMe_3$), 55.9 (OMe), 42.5 (NCH_2), 42.0 (NCH_2), 41.1 (NCH_2), 40.2 (NCH_2), 28.6 (CMe_3), 27.2 (CHAr), 22.8 (CH_2), 21.2 (CH), 19.6 (CH); MS (EI) m/z 342 [$(M + Na)^+$, 100]; HRMS (ESI) m/z calcd for $C_{18}H_{25}NO_4$ [$(M + Na)^+$, 100] 342.1676, found 342.1676 (−0.1 ppm error).

Lab book reference HFK8-024

tert-Butyl-7-(4-methanesulfonylphenyl)-3-azabicyclo[4.1.0]heptane-3-carboxylate *exo*-515

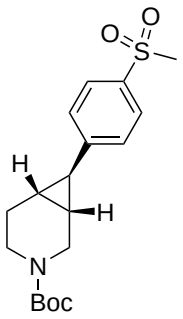

exo-**515**

Using general procedure B, *N*-Boc MIDA boronate *exo*-**211** (176 mg, 0.500 mmol, 1.0 eq.), Cs_2CO_3 (978 mg, 3.00 mmol, 6.0 eq.), PCy_3 (84 mg, 0.15 mmol, 0.3 eq.), $Pd(OAc)_2$, (17 mg, 0.076 mmol, 0.15 eq.) and 4-bromophenyl methyl sulfone (165 mg, 0.700 mmol, 1.4 eq.) in toluene (7 mL) and H_2O (0.6 mL) gave the crude product. Purification by flash column chromatography on silica with 60:40 hexane-EtOAc gave arylated piperidine *exo*-**515** (151 mg, 86%) as a yellow oil, R_F (7:3 hexane-EtOAc) 0.21; IR (ATR) 1680 (C=O), 1304, 1147, 726 cm^{-1}; ^{1}H NMR (400 MHz, $CDCl_3$) δ 7.74 (d, J = 8.0 Hz, 2H, Ar), 7.11 (d, J = 8.0 Hz, 2H, Ar), 3.94 (br d, J = 14.0 Hz, 1H, NCH), 3.52 (dd, J = 14.0, 4.5 Hz, 1H, NCH), 2.98-2.92 (m, 1H, NCH), 2.97 (s,

3H, SO_2Me), 2.04-1.96 (m, 1H, CH), 1.90-1.75 (m, 1H, CH), 1.68 (dd, J = 4.5, 4.5 Hz, CHAr), 1.50-1.45 (m, 1H, CH), 1.44-1.38 (m, 1H, CH), 1.43 (s, 9H, CMe_3); ^{13}C NMR (100.6 MHz, $CDCl_3$) (rotamers) δ 155.0 (C=O), 150.0 (*ipso*-Ar), 137.2 (*ipso*-Ar), 127.4 (Ar), 126.0 (Ar), 79.7 ($OCMe_3$), 44.6 (SO_2Me), 42.2 (NCH_2), 41.5 (NCH_2), 40.8 (NCH_2), 39.8 (NCH_2), 28.5 (CMe_3), 27.5 (CHAr), 23.5 (CH), 22.6 (CH_2), 21.9 (CH); MS (EI) *m/z* 374 [$(M + Na)^+$, 100]; HRMS (ESI) *m/z* calcd for $C_{18}H_{25}NO_4S$ [$(M + Na)^+$, 100] 374.1397, found 374.1397 (−0.3 ppm error).

Lab book reference HFK8-025

tert-Butyl-7-[4-(hydroxymethyl)-3-methoxyphenyl]-3-azabicyclo[4.1.0] heptane-3-carboxylate _exo_-523

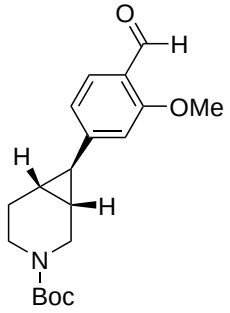

exo-**523**

Using general procedure B, *N*-Boc MIDA boronate *exo*-**211** (176 mg, 0.500 mmol, 1.0 eq.), Cs_2CO_3 (978 mg, 3.00 mmol, 6.0 eq.), PCy_3 (84 mg, 0.15 mmol, 0.3 eq.), $Pd(OAc)_2$, (17 mg, 0.076 mmol, 0.15 eq.) and 4-bromo-2-methoxybenzyl alcohol (152 mg, 0.700 mmol, 1.4 eq.) in toluene (7 mL) and H_2O (0.6 mL) gave the crude product. Purification by flash column chromatography on silica with 80:20 to 70:30 hexane-Et_2O gave impure product. Further purification by flash column chromatography on silica with hexane to 95:5 to 90:10 to 80:20 hexane-EtOAc gave arylated piperidine *exo*-**523** (27 mg, 16%) as a colourless oil, R_F (7:3 hexane-EtOAc) 0.38; IR (ATR) 2976, 1680 (C=O), 1604, 1395, 1244, 1163 cm^{-1}; ^1H NMR (400 MHz, $CDCl_3$) δ 10.34 (br d, J = 0.5 Hz, 1H, CHO), 7.69 (br d, J = 8.0 Hz, 1H, Ar), 6.62 (s, 1H, Ar), 6.57 (d, J = 8.0 Hz, 1H, Ar), 4.11-3.92 (m, 1H, NCH), 3.90 (s, 3H, OMe), 3.56 (dd, J = 13.5, 4.5 Hz, 1H,

NCH), 3.54-3.47 (m, 1H, NCH), 3.00 (ddd, J = 13.5, 9.5, 5.5 Hz, 1H, NCH), 2.09-2.01 (m, 1H, CH), 1.97-1.75 (m, 1H, CH), 1.68 (dd, J = 4.5, 4.5 Hz, 1H, CHAr), 1.59-1.49 (m, 2H, CH), 1.47 (s, 9H, CMe_3); ^{13}C NMR (100.6 MHz, $CDCl_3$) (rotamers) δ 189.3 (C=O, CHO), 162.0 (*ipso*-Ar), 155.2 (C=O), 152.9 (*ipso*-Ar), 128.9 (Ar), 122.7 (*ipso*-Ar), 117.1 (Ar), 109.0 (Ar), 79.8 ($OCMe_3$), 55.7 (OMe), 42.4 (NCH_2), 41.7 (NCH_2), 41.0 (NCH_2), 40.0 (NCH_2), 28.6 (CMe_3), 23.4 (CH), 23.1 (CH), 22.8 (CH_2), 21.7 (CH); MS (EI) m/z 354 [$(M + Na)^+$, 100]; HRMS (ESI) m/z calcd for $C_{19}H_{25}NO_4$ [$(M + Na)^+$, 100] 354.1676, found 354.1683 (−2.1 ppm error).

Lab book reference HFK8-027

tert-Butyl-7-(3-cyano-4-methoxyphenyl)-3-azabicyclo[4.1.0]heptane-3-carboxylate *exo*-516

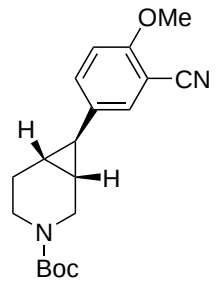

exo-**516**

Using general procedure B, *N*-Boc MIDA boronate *exo*-**211** (176 mg, 0.500 mmol, 1.0 eq.), Cs_2CO_3 (978 mg, 3.00 mmol, 6.0 eq.), PCy_3 (84 mg, 0.15 mmol, 0.3 eq.), $Pd(OAc)_2$, (17 mg, 0.076 mmol, 0.15 eq.) and 4-bromo-2-methoxybenzonitrile (149 mg, 0.700 mmol, 1.4 eq.) in toluene (7 mL) and H_2O (0.6 mL) gave the crude product. Purification by flash column chromatography on silica with 80:20 to 70:30 hexane-EtOAc gave arylated piperidine *exo*-**516** (148 mg, 90%) as a yellow oil, R_F (7:3 hexane-EtOAc) 0.25; IR (ATR) 2975, 2226 (C≡N), 1683 (C=O), 1504, 1246, 1165 cm^{-1}; ^{1}H NMR (400 MHz, $CDCl_3$) δ 7.18 (dd, J = 8.5, 2.5 Hz, 1H, Ar), 7.15 (d, J = 2.5 Hz, 1H, Ar), 6.84 (d, J = 8.5 Hz, 1H, Ar), 3.98-3.90 (m, 1H, NCH), 3.87 (s, 3H, OMe), 3.53 (dd, J = 13.5, 4.5 Hz, 1H, NCH), 3.50-3.40 (m, 1H, NCH), 2.97 (ddd, J = 13.5, 9.5, 5.5 Hz, 1H,

NCH), 2.05-1.97 (m, 1H, CH), 1.89-1.74 (m, 1H, CH), 1.58 (dd, J = 4.5, 4.5 Hz, 1H, CHAr), 1.45 (s, 9H, CMe_3), 1.34-1.23 (m, 2H, CH); ^{13}C NMR (100.6 MHz, $CDCl_3$) (rotamers) δ 159.4 (*ipso*-Ar), 155.2 (C=O), 135.6 (*ipso*-Ar), 131.9 (Ar), 130.4 (Ar), 116.7 (*ipso*-Ar), 111.4 (Ar), 101.6 (CN), 79.7 ($OCMe_3$), 56.2 (OMe), 42.3 (NCH_2), 41.5 (NCH_2), 41.0 (NCH_2), 39.9 (NCH_2), 28.5 (CMe_3), 26.1 (CH), 22.6 (CH_2), 21.5 (CH), 19.9 (CH); MS (EI) *m/z* 351 [$(M + Na)^+$, 100]; HRMS (ESI) *m/z* calcd for $C_{19}H_{24}N_2O_3$ [$(M + Na)^+$, 100] 351.1679, found 351.1686 (−1.8 ppm error).

Lab book reference HFK8-029

tert-Butyl-7-(4-carbamoylphenyl)-3-azabicyclo[4.1.0]heptane-3-carboxylate *exo*-517

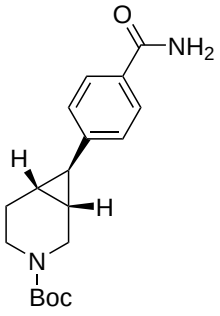

exo-**517**

Using general procedure B, *N*-Boc MIDA boronate *exo*-**211** (176 mg, 0.500 mmol, 1.0 eq.), Cs_2CO_3 (978 mg, 3.00 mmol, 6.0 eq.), PCy_3 (84 mg, 0.15 mmol, 0.3 eq.), $Pd(OAc)_2$, (17 mg, 0.076 mmol, 0.15 eq.) and 4-bromobenzamide (140 mg, 0.700 mmol, 1.4 eq.) in toluene (7 mL) and H_2O (0.6 mL) gave the crude product. Purification by flash column chromatography on silica with 90:10 to 75:15 to 80:20 to 60:40 CH_2Cl_2-acetone as eluent gave arylated piperidine *exo*-**517** (126 mg, 80%) as a yellow solid, mp 166-168 °C; R_F (3:2 CH_2Cl_2-acetone) 0.38; IR (ATR) 3191 (NH), 1664 (C=O), 1611, 1390, 1168, 730 cm^{-1}; ^{1}H NMR (400 MHz, $CDCl_3$) δ 7.70 (d, J = 8.0 Hz, 2H, Ar), 7.02 (d, J = 8.0 Hz, 2H, Ar), 6.40-6.19 (m, 2H, NH_2), 3.94 (br d, J = 13.5 Hz, 1H, NCH), 3.55 (dd, J = 13.5, 4.5 Hz, 1H, NCH), 3.52-3.41 (m, 1H, NCH), 3.05-2.94 (m, 1H, NCH), 2.06-1.98 (m, 1H, CH), 1.91-1.77 (m, 1H, CH), 1.67 (dd, J =

4.5, 4.5 Hz, 1H, CHAr), 1.48-1.37 (m, 2H, CH), 1.46 (s, 9H, CMe_3); ^{13}C NMR (100.6 MHz, $CDCl_3$) (rotamers) δ 169.6 (C=O, $CONH_2$), 155.2 (C=O, Boc), 147.7 (*ipso*-Ar), 130.4 (*ipso*-Ar), 127.6 (Ar), 125.4 (Ar), 79.7 ($OCMe_3$), 42.4 (NCH_2), 41.7 (NCH_2), 41.0 (NCH_2), 40.0 (NCH_2), 28.6 (CMe_3), 27.6 (CH), 22.9 (CH), 21.3 (CH) (one CH_2 resonance not resolved); MS (EI) *m/z* 339 [$(M + Na)^+$, 100]; HRMS (ESI) *m/z* calcd for $C_{18}H_{24}N_2O_3$ [$(M + Na)^+$, 100] 339.1679, found 339.1683 (−0.4 ppm error).

Lab book reference HFK8-032

A Crystallographic Data and Refinement Statistics

cis-**477**

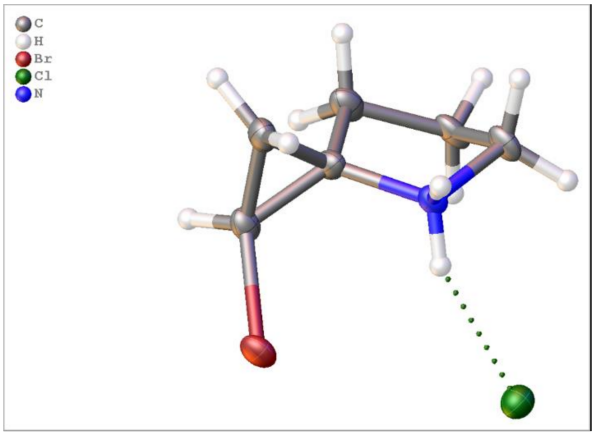

Table 1 Crystal data and structure refinement for *cis*-477

Identification code	*cis*-**477**
Empirical formula	$C_6H_{11}Br_{1.27}Cl_{0.73}N$
Formula weight	224.41
Temperature/K	110.00(10)
Crystal system	orthorhombic
Space group	Pnma
a/Å	8.3980(5)
b/Å	7.7280(3)
c/Å	12.7499(5)
α/°	90
β/°	90
γ/°	90
Volume/Å^3	827.46(7)
Z	4
ρ_{calc}g/cm^3	1.801
μ/mm^{-1}	6.413
F(000)	443.2
Crystal size/mm^3	0.219 × 0.132 × 0.087
Radiation	Mo Kα (λ = 0.71073)
2Θ range for data collection/°	7.848 to 61.01
Index ranges	$-11 \leq h \leq 10$, $-11 \leq k \leq 8$, $-18 \leq l \leq 17$
Reflections collected	4156
Independent reflections	1338 [R_{int} = 0.0419, R_{sigma} = 0.0425]
Data/restraints/parameters	1338/0/74
Goodness-of-fit on F^2	1.041
Final R indexes [I>=2σ (I)]	R_1 = 0.0313, wR_2 = 0.0553
Final R indexes [all data]	R_1 = 0.0437, wR_2 = 0.0593
Largest diff. peak/hole / e Å^{-3}	0.44/-0.38

Data collected by Theo Tanner, solved and refined by Adrian C Whitwood

Table 2 Fractional Atomic Coordinates ($\times 10^4$) and Equivalent Isotropic Displacement Parameters ($Å^2 \times 10^3$) for *cis*-477. U_{eq} is defined as 1/3 of of the trace of the orthogonalised U_{IJ} tensor

Atom	*x*	*y*	*z*	U(eq)
Br1	6148.3(4)	7500	6956.9(2)	23.65(11)
C1	7901(5)	7998(5)	6054(3)	20.5(9)
C2	9029(6)	6610(6)	5758(3)	23.1(9)
C3	7917(4)	7500	4946(2)	21.7(6)
C4	8473(6)	8448(6)	4032(3)	24.1(10)
C5	7134(8)	8209(8)	3216(5)	23.7(13)
C6	6625(8)	6363(8)	3408(5)	21.7(12)
N1	6580(4)	6249(4)	4572(2)	16.5(7)
Br2	3008.7(7)	7500	4632.8(4)	23.36(19)
Cl1	3008.7(7)	7500	4632.8(4)	23.36(19)

Table 3 Anisotropic Displacement Parameters ($Å^2 \times 10^3$) for *cis*-477. The Anisotropic displacement factor exponent takes the form: $-2\pi^2[h^2a^{*2}U_{11}+2hka^*b^*U_{12}+\ldots]$

Atom	U_{11}	U_{22}	U_{33}	U_{23}	U_{13}	U_{12}
Br1	30.25(19)	26.25(18)	14.46(16)	0	5.71(13)	0
C1	26(2)	18(2)	17.3(19)	-1.2(13)	2.0(17)	-4.8(15)
C2	25(2)	29(2)	16(2)	-3.1(17)	-1.4(19)	-2.5(19)
C3	19.6(15)	32.2(17)	13.4(14)	0	1.0(12)	0
C4	30(2)	23(2)	19(2)	-0.6(17)	7(2)	-7.0(18)
C5	37(4)	23(3)	11(3)	-1.7(19)	6(2)	0(2)
C6	35(3)	21(3)	9(2)	1(2)	2(2)	1(2)
N1	20.6(18)	14.8(17)	14.1(16)	1.2(13)	1.5(14)	0.0(14)
Br2	21.0(3)	23.8(3)	25.3(3)	0	-1.1(2)	0
Cl1	21.0(3)	23.8(3)	25.3(3)	0	-1.1(2)	0

Table 4 Bond Lengths for *cis*-477

Atom	Atom	Length/Å	Atom	Atom	Length/Å
Br1	C1	1.908(4)	C3	N1	1.556(4)
C1	C2	1.480(6)	C4	C5	1.543(8)
C1	C3	1.463(5)	C5	C6	1.509(7)
C2	C3	1.555(5)	C6	N1	1.488(7)
C3	C4	1.454(5)			

Table 5 Bond Angles for *cis*-477

Atom	Atom	Atom	Angle/°	Atom	Atom	Atom	Angle/°
C2	C1	Br1	120.1(3)	C4	C3	C1	130.1(2)
C3	C1	Br1	122.4(3)	C4	C3	C2	124.3(3)
C3	C1	C2	63.8(3)	C4	C3	N1	107.4(3)
C1	C2	C3	57.6(2)	C3	C4	C5	104.2(4)
C1	C3	C2	58.6(2)	C6	C5	C4	102.1(6)
C1	C3	N1	116.9(3)	N1	C6	C5	103.0(6)
C2	C3	N1	111.2(2)	C6	N1	C3	104.5(3)

Table 6 Hydrogen Bonds for *cis*-477

D	H	A	d(D-H)/Å	d(H-A)/Å	d(D-A)/Å	D-H-A/°
N1	H1B	Cl1	0.91	2.31	3.152(4)	153.4

Table 7 Torsion Angles for *cis*-477

A	B	C	D	Angle/°	A	B	C	D	Angle/°
Br1	C1	C2	C3	113.9(3)	C2	C1	C3	N1	99.6(3)
Br1	C1	C3	C2	-110.4(3)	C2	C3	C4	C5	150.2(3)
Br1	C1	C3	C4	139.1(4)	C2	C3	N1	C6	-130.4(4)
Br1	C1	C3	N1	-10.8(4)	C3	C4	C5	C6	-37.8(5)
C1	C2	C3	C4	119.8(3)	C4	C3	N1	C6	8.7(4)
C1	C2	C3	N1	-109.4(3)	C4	C5	C6	N1	43.2(5)
C1	C3	C4	C5	-134.2(4)	C5	C6	N1	C3	-32.2(5)
C1	C3	N1	C6	165.0(4)	N1	C3	C4	C5	17.9(4)
C2	C1	C3	C4	-110.5(4)					

Table 8 Hydrogen Atom Coordinates (Å×10^4) and Isotropic Displacement Parameters (Å^2×10^3) for *cis*-477

Atom	*x*	*y*	*z*	U(eq)
H1	8422.44	9137.28	6197.42	25
H2A	8773.96	5410.75	5974.22	28
H2B	10177.73	6893.85	5737.58	28
H4A	9490.2	7964.61	3770.54	29
H4B	8627.8	9687.67	4199.18	29
H5A	6246.53	9026.4	3341.14	28
H5B	7537.38	8366.03	2492.82	28
H6A	5563.3	6132.18	3101.1	26
H6B	7403.81	5535.62	3110.68	26
H1A	6776.51	5148.96	4790.92	20
H1B	5614.76	6589.34	4822.9	20

Table 9 Atomic Occupancy for *cis*-477

Atom	*Occupancy*	Atom	*Occupancy*	Atom	*Occupancy*
C1	0.5	H1	0.5	C2	0.5
H2A	0.5	H2B	0.5	C4	0.5
H4A	0.5	H4B	0.5	C5	0.5
H5A	0.5	H5B	0.5	C6	0.5
H6A	0.5	H6B	0.5	N1	0.5
H1A	0.5	H1B	0.5	Br2	0.267(2)
Cl1	0.3663(12)				

Experimental

Single crystals of $C_6H_{11}Br_{1.27}Cl_{0.73}N$ **[*cis*-477]** were **[crystallisation from methanol]**. A suitable crystal was selected and **[oil on 200 micrometre micromount]** on a **SuperNova, Dual, Cu at home/near, Eos** diffractometer. The crystal was kept at 110.00(10) K during data collection. Using Olex2 [1], the structure was solved with the SHELXT [2] structure solution program using Intrinsic Phasing and refined with the SHELXL [3] refinement package using Least Squares minimisation.

1. Dolomanov, O.V., Bourhis, L.J., Gildea, R.J, Howard, J.A.K. & Puschmann, H. (2009), J. Appl. Cryst. 42, 339-341.
2. Sheldrick, G.M. (2015). Acta Cryst. A71, 3-8.
3. Sheldrick, G.M. (2015). Acta Cryst. C71, 3-8.

Crystal structure determination of [*cis*-477]

Crystal Data for $C_6H_{11}Br_{1.2675}Cl_{0.7325}N$ (M =224.41 g/mol): orthorhombic, space group Pnma (no. 62), a = 8.3980(5) Å, b = 7.7280(3) Å, c = 12.7499(5) Å, V = 827.46(7) Å^3, Z = 4, T = 110.00(10) K, μ(Mo Kα) = 6.413 mm^{-1}, *Dcalc* = 1.801 g/cm^3, 4156 reflections measured (7.848° ≤ 2Θ ≤ 61.01°), 1338 unique (R_{int} = 0.0419, R_{sigma} = 0.0425) which were used in all calculations. The final R_1 was 0.0313 (I > 2σ(I)) and wR_2 was 0.0593 (all data).

Refinement model description

Number of restraints - 0, number of constraints - unknown.

Details:

```
1. Fixed Uiso
 At 1.2 times of:
  All C(H) groups, All C(H,H) groups, All N(H,H) groups
2. Shared sites
{Cl1, Br2}
3. Uiso/Uaniso restraints and constraints
Uanis(Cl1) = Uanis(Br2)
4. Others
 Sof(Br2)=0.5*(1-FVAR(2))
 Sof(Cl1)=0.5*FVAR(2)
 Fixed Sof: C1(0.5) H1(0.5) C2(0.5) H2A(0.5) H2B(0.5) C4(0.5) H4A(0.5)
 H4B(0.5) C5(0.5) H5A(0.5) H5B(0.5) C6(0.5) H6A(0.5) H6B(0.5) N1(0.5)
H1A(0.5)
 H1B(0.5)
5.a Ternary CH refined with riding coordinates:
 C1(H1)
5.b Secondary CH2 refined with riding coordinates:
 C2(H2A,H2B), C4(H4A,H4B), C5(H5A,H5B), C6(H6A,H6B), N1(H1A,H1B)
```

Abbreviations and Conventions

AlogP - atomic logP

Aq - aqueous

AMP - adenosine monophosphate

Br - broad

Boc - *tert*-butoxycarbonyl

cal - calibrant

Cbz - carboxybenzyl

CDK2 - cyclin dependent kinase 2

ClogP - compound logP

CP HLPC - chiral stationary phase HPLC

cm^{-1} - wavenumber

COX - chiral auxillary Oppolzer's camphorsultam

CPMG - Carr, Purcell, Meiboom, Gill

CSP - chiral staionary phase

d - doublet

DCE - dichloro ethane

DIPEA - di isopropyl ethylamine

DMAP - dimethyl aminopyridine

DMSO - dimethyl sulfoxide

DOS - diversity oriented synthesis

DSF - differential scanning fluorimetry

DTT - dithiothreitol

ee - enantiomeric excess

Eq. - equivalents

ESI - electrospray ionisation

Et_2O - diethyl ether

EtOAc - ethyl acetate

FBDD - fragment based drug discovery

FGI - functional group interconversion

Fsp^3 - fraction of sp^3 centres

GC-TS - giant cell tumour of the tendon sheath

GSK3β - glycogen synthase kinase 3β

g - gram(s)

h - hour(s)

H bond - hydrogen bond

HAC - heavy atom count

HBA - hydrogen bond acceptor

HBD - hydrogen bond donor

HEPES - 4-(2-hydroxyethyl)-1-piperazineethanesulfonic acid

HRMS - high resolution mass spectrometry

Hsp90α - heat shock protein α

HTS - high throughput screening

Hz - Hertz

IR - infra red

ITC - isothermal titration calorimetry

J - coupling constant in Hz

kcal mol^{-1} - kilocalories per mole

LE - ligand efficiency

LOGSY - ligand observed via gradient spectroscopy

m - multiplet

M - molar

m/z - mass to charge ratio

M^+ - molecular ion

Me - methyl

mg - milligrams

μM - micromolar

MIDA - *N*-methyliminodiacetic acid

min - minute(s)

mL - millilitre(s)

mmol - millimole(s)

MS - mass spectrometry

MW - molecular weight

NCS - *N*-chlorosuccinimide

nM - nanomolar

NMR - nuclear magnetic resonance

NPR - normalised principal moments of inertia ratio

NROT - number of rotatable bonds

Oxyma - ethyl cyanohydroxyiminoacetate

PAINS - pan assay interference compounds

PAK4 - serine/threonine-protein kinase

PBF - plane of best fit

PBP3 - penicillin binding protein 3

PCA - principal component analysis

PDB - protein database

PMI - principal moment of inertia

ppm - parts per million

PSA - polar surface area

PTK HER2 - protein tyrosine kinase HER2

PTOC - *N*-hydroxypyridine-2-thione carbamates

PTP1B - protein tyrosine phosphatase 1B

pTyr - phosphotyrosine

q - quartet

QC - quality control

RBN - rotatable bond number

RCM - ring closing metathesis

R_F - retention factor

Ro3 - rule of 3

rt - room temperature

SAR - structure activity relationship

SARS-CoV-2 M^{pro} - SARS-CoV-2 main protease

s - singlet

SMILES - simplified molecular-input line-entry system

(+)-sp surr - (+)-sparteine surrogate

SPR - surface plasmon resonance

STD - saturation transfer difference

T - triplet

TAP - thesis advisory panel

TCEP - tris(2-carboxyethyl)phosphine

TGCT - tenosynovial giant cell tumour

TFA - tri fluoro acetic acid

THF - tetrahydrofuran

T3P - *n*-propanephosphonic acid anhydride

TMEDA -tetramethylethylenediamine

TPSA - total polar surface area

Tris - tris(hydroxymethyl)aminomethane

TSA - thermal shift assay

UHP - urea hydrogen peroxide

WAC - weak affinity chromatography

YSBL - York structural biology laboratory

References

(1) Murray, C.; Rees, D. *Nat. Chem.* **2009**, *1*, 187–192.

(2) Hubbard, R.; Murray, J. *Methods Enzymol.*; Vol. 493; Chapter 20, pp 509–531.

(3) Congreve, M.; Chessari, G.; Tisi, D.; Woodhead, A. J. *J. Med. Chem.* **2008**, *51*, 3661–3680.

(4) Keserü, G. M.; Erlanson, D. A.; Ferenczy, G. G.; Hann, M. M.; Murray, C. W.; Pickett, S. D. *J. Med. Chem.* **2016**, *59*, 8189–8206.

(5) van Montfort, R. L.; Workman, P.; Lamoree, B.; Hubbard, R. *Essays Biochem.* **2017**, *61*, 453–464.

(6) Baker, M. *Nat. Rev.* **2013**, *12*, 5–7.

(7) Erlanson, D.; Fesik, S.; Hubbard, R.; Jahnke, W.; Jhoti, H. *Nat. Rev. Drug Discov.* **2016**, *15*, 605–619.

(8) Bollag, G.; Tsai, J.; Zhang, J.; Zhang, C.; Ibrahim, P.; Nolop, K.; Hirth, P. *Nat. Rev. Drug Discov.* **2012**, *11*, 873–886.

(9) Souers, A.; Leverson, J.; Boghaert, E.; Ackler, S.; Catron, N.; Chen, J.; Dayton, B.; Ding, H.; Enschede, S.; Fairbrother, W.; Huang, D.; Hymowitz, S.; Jin, S.; Khaw, S.; Kovar, P.; Lam, L.; Lee, J.; Maecker, H.; Marsh, K.; Mason, K.; Mitten, M.; Nimmer, P.; Oleksijew, A.; Park, C.; Park, C.; Phillips, D.; Roberts, A.; Sampath, D.; Seymour, J.; Smith, M.; Sullivan, G.; Tahir, S.; Tse, C.; Wendt, M.; Xiao, Y.; Xue, J.; Zhang, H.; Humerickhouse, R.; Rosenberg, S.; Elmore, S. *Nat. Med.* **2013**, *19*, 202–208.

(10) Perera, T. P.; Jovcheva, E.; Mevellec, L.; Vialard, J.; De Lange, D.; Verhulst, T.; Paulussen, C.; Van De Ven, K.; King, P.; Freyne, E.; Rees, D. C.; Squires, M.; Saxty, G.; Page, M.; Murray, C. W.; Gilissen, R.; Ward, G.; Thompson, N. T.; Newell, D. R.; Cheng, N.; Xie, L.; Yang, J.; Platero, S. J.; Karkera, J. D.;

Moy, C.; Angibaud, P.; Laquerre, S.; Lorenzi, M. V. *Mol. Cancer Ther.* **2017**, *16*, 1010–1020.

(11) Tap, W. D.; Wainberg, Z. A.; Anthony, S. P.; Ibrahim, P. N.; Zhang, C.; Healey, J. H.; Chmielowski, B.; Staddon, A. P.; Cohn, A. L.; Shapiro, G. I.; Keedy, V. L.; Singh, A. S.; Puzanov, I.; Kwak, E. L.; Wagner, A. J.; Von Hoff, D. D.; Weiss, G. J.; Ramanathan, R. K.; Zhang, J.; Habets, G.; Zhang, Y.; Burton, E. A.; Visor, G.; Sanftner, L.; Severson, P.; Nguyen, H.; Kim, M. J.; Marimuthu, A.; Tsang, G.; Shellooe, R.; Gee, C.; West, B. L.; Hirth, P.; Nolop, K.; van de Rijn, M.; Hsu, H. H.; Peterfy, C.; Lin, P. S.; Tong-Starksen, S.; Bollag, G. *N. Engl. J. Med.* **2015**, *373*, 428–437.

(12) Erlanson, D. Practical Fragments. `http://practicalfragments.blogspot.co.uk`.

(13) Barker, A.; Kettle, J.; Thorsten, N.; Pease, J. *Drug Discov. Today* **2013**, *18*, 298–304.

(14) Hann, M.; Oprea, T. *Curr. Opin. Chem. Biol.* **2004**, *8*, 255–263.

(15) Jencks, W. P. *PNAS* **1981**, *78*, 4046–4050.

(16) Shuker, S.; Hajduk, P.; Meadows, R.; Fesik, S. *Science* **1996**, *274*, 1531–1534.

(17) Hann, M.; Leach, A.; Harper, G. *J. Chem. Inf. Comput. Sci.* **2001**, *41*, 856–864.

(18) Leach, A.; M.M., H. *Med. Chem. Commun.* **2011**, *15*, 489–496.

(19) Murray, C.; Erlanson, D.; Hopkins, A.; Keserü, G.; Leeson, P.; Rees, D.; Reynolds, C.; Richmond, N. *ACS Med. Chem. Lett.* **2014**, *5*, 616–618.

(20) Bembenek, S. D.; Tounge, B. A.; Reynolds, C. H. *Drug Discov. Today* **2009**, *14*, 278–283.

(21) Palmer, N.; Peakman, T. M.; Norton, D.; Rees, D. C. *Org. Biomol. Chem.* **2016**, *14*, 1599–1610.

(22) Lipinski, C.; Lombardo, F.; B.W., D.; Feeney, P. *Drug Deliv. Rev.* **1997**, *3*, 3–25.

(23) Congreve, M.; R., C.; C., M.; Jhoti, H. *Drug Discov. Today* **2003**, *8*, 876–877.

(24) Reymond, J.-L. *Acc. Chem. Res.* **2015**, *48*, 722–730.

(25) Nadin, A.; Hattotuwagama, C.; Churcher, I. *Angew. Chem. Int. Ed.* **2012**, *51*, 1114–1122.

(26) Zhang, C.; Ibrahim, P. N.; Zhang, J.; Burton, E. A.; Habets, G.; Zhang, Y.; Powell, B.; West, B. L.; Matusow, B.; Tsang, G.; Shellooe, R.; Carias, H.; Nguyen, H.; Marimuthu, A.; Zhang, K. Y. J.; Oh, A.; Bremer, R.; Hurt, C. R.; Artis, D. R.; Wu, G.; Nespi, M.; Spevak, W.; Lin, P.; Nolop, K.; Hirth, P.; Tesch, G. H.; Bollag, G. *PNAS* **2013**, *110*, 5689–5694.

(27) Lovering, F.; Bikker, J.; Humblet, C. *J. Med. Chem.* **2009**, *52*, 6752–6756.

(28) Morley, A. D.; Pugliese, A.; Birchall, K.; Bower, J.; Brennan, P.; Brown, N.; Chapman, T.; Drysdale, M.; Gilbert, I. H.; Hoelder, S.; Jordan, A.; Ley, S. V.; Merritt, A.; Miller, D.; Swarbrick, M. E.; Wyatt, P. G. *Drug Discov. Today* **2013**, *18*, 1221–1227.

(29) Meyers, J.; Carter, M.; Mok, N. Y.; Brown, N. *Future Med. Chem.* **2016**, *8*, 1753–1767.

(30) Hall, R. J.; Mortenson, P. N.; Murray, C. W. *Prog. Biophys. Mol. Biol.* **2014**, *116*, 82–91.

(31) Hung, A.; Ramek, A.; Wang, Y.; Kaya, T.; Wilson, J.; Clemons, P.; Young, D. *Proc. Natl. Acad. Sci.* **2011**, *108*, 6799–6804.

(32) Sauer, W.; Schwarz, M. *J. Chem. Inf. Comput. Sci.* **2003**, *43*, 987–1003.

(33) Firth, N.; Brown, N.; Blagg, J. *J. Chem. Inf. Model* **2012**, *52*, 2516–2525.

(34) Ritchie, T.; Macdonald, S. *Drug Discov. Today* **2009**, *14*, 1011–1020.

(35) Downes, T. D.; Jones, S. P.; Klein, H. F.; Wheldon, M. C.; Atobe, M.; Bond, P. S.; Firth, J. D.; Chan, N. S.; Waddelove, L.; Hubbard, R. E.; Blakemore, D. C.; De Fusco, C.; Roughley, S. D.; Vidler, L. R.; Whatton, M. A.; Woolford, A. J.-A.; Wrigley, G. L.; O'Brien, P. *Chem. Eur. J. 26*, 8969–8975.

(36) Cox, B.; Zdorichenko, V.; Cox, P. B.; Booker-Milburn, K. I.; Paumier, R.; Elliott, L. D.; Robertson-Ralph, M.; Bloomfield, G. *ACS Med. Chem. Lett.* **2020**, *11*, 1185–1190.

(37) Murray, C. W.; Rees, D. C. *Angew. Chem. Int. Ed.* **2016**, *55*, 488–492.

(38) Schreiber, S. L. *Science* **2000**, *287*, 1964–1969.

(39) Wang, Y.; Wach, J.; Sheehan, P.; Zhong, C.; Zhan, C.; Harris, R.; Almo, S.; Bishop, J.; Haggarty, S.; Ramek, A.; Berry, K.; O'Herin, C.; Koehler, A.; Hung, A.; Young, D. *ACS Med. Chem. Lett.* **2016**, *7*, 852–856.

(40) Foley, D.; Doveston, R.; Churcher, I.; Nelson, A.; Marsden, S. *Chem. Commun.* **2015**, *51*, 11174–11177.

(41) Kidd, S. L.; Fowler, E.; Reinhardt, T.; Compton, T.; Mateu, N.; Newman, H.; Bellini, D.; Talon, R.; McLoughlin, J.; Krojer, T.; Aimon, A.; Bradley, A.; Fairhead, M.; Brear, P.; Díaz-Sáez, L.; McAuley, K.; Sore, H. F.; Madin, A.; O'Donovan, D. H.; Huber, K. V. M.; Hyvönen, M.; von Delft, F.; Dowson, C. G.; Spring, D. R. *Chem. Sci.* **2020**, *11*, 10792–10801.

(42) Zhang, R.; McIntyre, P. J.; Collins, P. M.; Foley, D. J.; Arter, C.; von Delft, F.; Bayliss, R.; Warriner, S.; Nelson, A. *Chem. Eur. J.* **2019**, *25*, 6831–6839.

(43) Prescher, H.; Koch, G.; Schuhmann, T.; Ertl, P.; Bussenault, A.; Glick, M.; Dix, I.; Petersen, F.; Lizos, D. E. *Bioorg. Med. Chem.* **2017**, *25*, 921–925.

(44) Morgan, K. F.; Hollingsworth, I. A.; Bull, J. A. *Chem. Commun.* **2014**, *50*, 5203–5205.

(45) Morgan, K. F.; Hollingsworth, I. A.; Bull, J. A. *Org. Biomol. Chem.* **2015**, *13*, 5265–5272.

(46) Chawner, S. J.; Cases-Thomas, M. J.; Bull, J. A. *Eur. J. Org. Chem.* **2017**, 5015–5024.

(47) Reddy Guduru, S. K.; Chamakuri, S.; Raji, I. O.; MacKenzie, K. R.; Santini, C.; Young, D. W. *J. Org. Chem.* **2018**, *83*, 11777–11793.

(48) Jain, P.; Raji, I. O.; Chamakuri, S.; MacKenzie, K. R.; Ebright, B. T.; Santini, C.; Young, D. W. *J. Org. Chem.* **2019**, *84*, 6040–6064.

(49) Chamakuri, S.; Jain, P.; Reddy Guduru, S. K.; Arney, J. W.; MacKenzie, K. R.; Santini, C.; Young, D. W. *J. Org. Chem.* **2018**, *83*, 6541–6555.

(50) Twigg, D. G.; Kondo, N.; Mitchell, S. L.; Galloway, W. R. J. D.; Sore, H. F.; Madin, A.; Spring, D. R. *Angew. Chem. Int. Ed.* **2016**, *55*, 12479–12483.

(51) Sveiczer, A.; North, A. J. P.; Mateu, N.; Kidd, S. L.; Sore, H. F.; Spring, D. R. *Org. Lett.* **2019**, *21*, 4600–4604.

(52) Troelsen, N. S.; Shanina, E.; Gonzalez-Romero, D.; Danková, D.; Jensen, I. S. A.; Śniady, K. J.; Nami, F.; Zhang, H.; Rademacher, C.; Cuenda, A.; Gotfredsen, C. H.; Clausen, M. H. *Angew. Chem. Int. Ed.* **2020**, *59*, 2204–2210.

(53) Guimond, N.; Gorelsky, S. I.; Fagnou, K. *J. Am. Chem. Soc.* **2011**, *133*, 6449–6457.

(54) Tran, N. C.; Dhondt, H.; Flipo, M.; Deprez, B.; Willand, N. *Tetrahedron Lett.* **2015**, *56*, 4119–4123.

(55) Prevet, H.; Flipo, M.; Roussel, P.; Deprez, B.; Willand, N. *Tetrahedron Lett.* **2016**, *57*, 2888–2894.

(56) Wang, Y.; Patil, P.; Dömling, A. *Synthesis* **2016**, *48*, 3701–3712.

(57) Chalyk, B. A.; Isakov, A. A.; Butko, M. V.; Hrebeniuk, K. V.; Savych, O. V.; Kucher, O. V.; Gavrilenko, K. S.; Druzhenko, T. V.; Yarmolchuk, V. S.; Zozulya, S.; Mykhailiuk, P. K. *Eur. J. Org. Chem.* **2017**, 4530–4542.

(58) Hassan, H.; Marsden, S. P.; Nelson, A. *Bioorg. Med. Chem.* **2018**, *26*, 3030–3033.

(59) King, T. A.; Stewart, H. L.; Mortensen, K. T.; North, A. J. P.; Sore, H. F.; Spring, D. R. *Chem. Eur. J.* **2019**, 5219–5229.

(60) Garner, P.; Cox, P. B.; Rathnayake, U.; Holloran, N.; Erdman, P. *ACS Med. Chem. Lett.* **2019**, *10*, 811–815.

(61) Grainger, R.; Heightman, T. D.; Ley, S. V.; Lima, F.; Johnson, C. N. *Chem. Sci.* **2019**, *10*, 2264–2271.

(62) Dean, C.; Rajkumar, S.; Roesner, S.; Carson, N.; Clarkson, G. J.; Wills, M.; Jones, M.; Shipman, M. *Chem. Sci.* **2020**, *11*, 1636–1642.

(63) Mateu, N.; Kidd, S. L.; Kalash, L.; Sore, H. F.; Madin, A.; Bender, A.; Spring, D. R. *Chem. Eur. J.* **2018**, *24*, 13681–13687.

(64) Vitaku, E.; Smith, D. T.; Njardarson, J. T. *J. Med. Chem.* **2014**, *57*, 10257–10274.

(65) Stead, D.; Carbone, G.; O'Brien, P.; Campos, K. R.; Coldham, I.; Sanderson, A. *J. Am. Chem. Soc.* **2010**, *132*, 7260–7261.

(66) Barker, G.; McGrath, J. L.; Klapars, A.; Stead, D.; Zhou, G.; Campos, K. R.; O'Brien, P. *J. Org. Chem.* **2011**, *76*, 5936–5953.

(67) Sheikh, N. S.; Leonori, D.; Barker, G.; Firth, J. D.; Campos, K. R.; Meijer, A. J. H. M.; O'Brien, P.; Coldham, I. *J. Am. Chem. Soc.* **2012**, *134*, 5300–5308.

(68) Rayner, P. J.; O'Brien, P.; Horan, R. A. J. *J. Am. Chem. Soc.* **2013**, *135*, 8071–8077.

(69) Pilot, B. P. Scientific Workflow Authoring Application for Data Analysis. http://accelrys.com/products/collaborative-science/biovia-pipeline-pilot/, 2017.

(70) Wheldon, M. C. Thesis (PhD). 2017; University of York.

(71) Kelleher, F.; Kelly, S.; McKee, V. *Tetrahedron* **2007**, *63*, 9235.

(72) Kelleher, F.; Kelly, S.; Watts, J.; McKee, V. *Tetrahedron* **2010**, *66*, 3525.

(73) Confalone, P.; Huie, E.; Soo, S.; Cole, G. *J. Org. Chem.* **1988**, *53*, 482–487.

(74) Seebach, D.; Boes, M.; Naef, R.; Schweizer, W. B. *J. Am. Chem. Soc.* **1983**, *105*, 5390–5398.

(75) Su, B.; Deng, M.; Wang, Q. *Eur. J. Org. Chem.* **2013**, 1979–1985.

(76) Baran, P. S.; Hafensteiner, B. D.; Ambhaikar, N. B.; Guerrero, C. A.; Gallagher, J. D. *J. Am. Chem. Soc.* **2006**, *128*, 8678–8693.

(77) Bittermann, H.; Gmeiner, P. *J. Org. Chem.* **2006**, *71*, 97–102.

(78) Kawabata, T.; Moriyama, K.; Kawakami, S.; Tsubaki, K. *J. Am. Chem. Soc.* **2008**, *130*, 4153–4157.

(79) Sheikh, N. S.; Leonori, D.; Barker, G.; Firth, J. D.; Campos, K. R.; Meijer, A. J. H. M.; O'Brien, P.; Coldham, I. *J. Am. Chem. Soc.* **2012**, *134*, 5300–5308.

(80) Barker, G.; O'Brien, P.; Campos, K. R. *Org. Lett.* **2010**, *12*, 4176–4179.

(81) Campos, K. R.; Klapars, A.; Waldman, J. H.; Dormer, P. G.; Chen, C. *J. Am. Chem. Soc.* **2006**, *128*, 3538–3539.

(82) Boddy, A. J.; Affron, D. P.; Cordier, C. J.; Rivers, E. L.; Spivey, A. C.; Bull, J. A. *Angew. Chem. Int. Ed.* **2019**, *58*, 1458–1462.

(83) Dunetz, J. R.; Xiang, Y.; Baldwin, A.; Ringling, J. *Org. Lett.* **2011**, *13*, 5048–5051.

(84) Lawandi, J.; Toumieux, S.; Seyer, V.; Campbell, P.; Thielges, S.; Juillerat-Jeanneret, L.; Moitessier, N. *J. Med. Chem.* **2009**, *52*, 6672–6684.

(85) Tang, F.; Qu, L.; Xu, Y.; Ma, R.; Chen, S.; Li, G. *Synth. Commun.* **2007**, *37*, 3793–3799.

(86) Isaac, M.; Slassi, A.; Edwards, L.; Xin, T.; Stefanac, T. US 2007/0259926 A1. 2007; Astrazeneca AB and Eolas Therapeutics, Inc.

(87) Thorat, P. B.; Goswami, S. V.; Khade, B. C.; Bhusare, S. R. *Tetrahedron: Asymmetry* **2012**, *23*, 1320–1325.

(88) Bilke, J.; Moore, S.; O'Brien, P.; Gilday, J. *Org. Lett.* **2009**, *11*, 1935–1938.

(89) Klaus, R.; Wolfgang, E.; Wolfhard, E.; Gerhard, D., M.; Henri; Heike, W.; Klausdieter, W.; Jürgen, K.; Horst, D.; Franz, E.; Schnorrenberg, G.; Michael, E.; Wolfgang, W. US5616620. 1997.

(90) Fink, B.; Zhao, Y.; Han, W.; Tokarski, J.; Vite, G.; Chen, P.; Norris, D.; Mastalerz, H.; Gavai, A. V. WO2005/66176 A1. 2005.

(91) Jones, S. P. Thesis (PhD). 2019; University of York.

(92) Kurokawa, M.; Shindo, T.; Suzuki, M.; Nakajima, N.; Ishihara, K.; Sugai, T. *Tetrahedron: Asymmetry* **2003**, *14*, 1323–1333.

(93) El-Fehail Ali, F.; Bondinell, W.; Huffman, W.; Amparo Lago, M.; R., M. K.; Kwon, C.; Miller, W.; Nguyen, T.; Takata, D. US5977101 A1. 1999; SmithKline Beecham Corporation.

(94) Shuman, R. T.; Ornstein, P. L.; Paschal, J. W.; Gesellchen, P. D. *J. Org. Chem.* **1990**, *55*, 738–741.

(95) Kamenecka, T.; Jiang, R.; Song, X. WO/2013/119639. 2013.

(96) Subramanyam, C.; Chattarjee, S.; Mallamo, J. P. *Tetrahedron Lett.* **1996**, *37*, 459–462.

(97) Whitten, J. P.; Muench, D.; Cube, R. V.; Nyce, P. L.; Baron, B. M.; McDonald, I. A. *Bioorg. Med. Chem. Lett.* **1991**, *1*, 441–444.

(98) Lorthiois, E.; Marek, I.; Normant, J. F. *J. Org. Chem.* **1998**, *63*, 566–574.

(99) Cox, C.; Flores, B.; Schreier, J. WO2010048016 A1. 2010; Merck Sharp and Dohme Corp.

(100) Eliel, E.; Wilen, S. *Stereochemistry of Organic Compounds*.

(101) Noël, R.; Vanucci-Bacqué, C.; Fargeau-Bellassoued, M.-C.; Lhommet, G. *Eur. J. Org. Chem.* **2007**, 476–486.

(102) Kamenecka, T.; Holenz, J.; Wesolowski, S.; Yuanjun, H.; Burli, R. WO2017/139603 A1. 2017; Astrazeneca AB and Eolas Therapeutics, Inc.

(103) O'Hagan, D. *Nat. Prod. Rep.* **2000**, *17*, 435–446.

(104) Abbiati, A.; Arcadi, A.; Bianchi, G.; Di Giuseppe, S.; Marinelli, F.; Rossi, E. *J. Org. Chem.* **2003**, *68*, 6959–6966.

(105) Sujatha, K.; Vedula, R. R. *Synth. Commun.* **2018**, *48*, 302–308.

(106) Facchinetti, V.; Avellar, M. M.; Nery, A. C. S.; Gomes, C. R. B.; Vasconcelos, T. R. A.; de Souza, M. V. N. *Synthesis* **2016**, *48*, 437–440.

(107) Kabalka, G. W.; Mereddy, A. R. *Tetrahedron Lett.* **2006**, *47*, 5171–5172.

(108) Fei, Z.; Wu, Q.; Zhang, F.; Cao, Y.; Liu, C.; Shieh, W.-C.; Xue, S.; McKenna, J.; Prasad, K.; Prashad, M.; Baeschlin, D.; Namoto, K. *J. Org. Chem.* **2008**, *73*, 9016–9021.

(109) Vlahovic, S.; Schädel, N.; Tussetschläger, S.; Laschat, S. *Eur. J. Org. Chem.* **2013**, 1580–1590.

(110) Reddy, G. M.; Garcia, J. R.; Reddy, V. H.; de Andrade, A. M.; Camilo, A.; Pontes Ribeiro, R. A.; de Lazaro, S. R. *Eur. J. Med. Chem.* **2016**, *123*, 508–513.

(111) Murray, L. M.; O'Brien, P.; Taylor, R. J. K. *Org. Lett.* **2003**, *5*, 1943–1946.

(112) Majewski, M.; Lazny, R. *J. Org. Chem.* **1995**, *60*, 5825–5830.

(113) Li, R.; Farmer, P. S.; Xie, M.; Quilliam, M. A.; Pleasance, S.; Howlett, S. E.; Yeung, P. K. F. *J. Med. Chem.* **1992**, *35*, 3246–3253.

(114) Cooper, K.; Fray, M. J.; Parry, M. J.; Richardson, K.; Steele, J. *J. Med. Chem.* **1992**, *35*, 3115–3129.

(115) Rayner, P. J.; O'Brien, P.; Horan, R. A. J. *J. Am. Chem. Soc.* **2013**, *135*, 8071–8077.

(116) Reznikov, A.; Klimochkin, Y. *Synthesis* **2020**, *52*, 781–795.

(117) Beak, P.; Wu, S.; Yum, E. K.; Jun, Y. M. *J. Org. Chem.* **1994**, *59*, 276–277.

(118) Park, Y.; Beak, P. *Tetrahedron* **1996**, *52*, 12333–12350.

(119) Bailey, W. F.; Beak, P.; Kerrick, S. T.; Ma, S.; Wiberg, K. B. *J. Am. Chem. Soc.* **2002**, *124*, 1889–1896.

(120) D'Arcy, R.; Grob, C. A.; Kaffenberger, T.; Krasnobajew, V. *Helvetica Chimica Acta* **1966**, *49*, 185–203.

(121) Lutz, M.; Wenzler, M.; Likhotvorik, I. *Synthesis* **2018**, *50*, 2231–2234.

(122) Feldman, K. S.; Fodor, M. D. *J. Org. Chem.* **2009**, *74*, 3449–3461.

(123) Zenzola, M.; Doran, R.; Degennaro, L.; Luisi, R.; Bull, J. A. *Angew. Chem. Int. Ed.* **2016**, *55*, 7203–7207.

(124) Gillis, E. P.; Burke, M. D. *J. Am. Chem. Soc.* **2007**, *129*, 6716–6717.

(125) Knapp, D. M.; Gillis, E. P.; Burke, M. D. *J. Am. Chem. Soc.* **2009**, *131*, 6961–6963.

(126) Gonzalez, J.; Ogba, O.; Morehouse, G.; Rosson, N.; Houk, K.; Leach, A.; Cheong, P.-Y.; M.D., B.; G.C., L.-J. *Nature Chem.* **2016**, *8*, 1067–1075.

(127) Lehmann, J.; Crouch, I.; Blair, D.; Trobe, M.; Wang, P.; Li, J.; Burke, M. *Nat. Commun.* **2019**, *10*, 1263.

(128) Duncton, M. A. J.; Singh, R. *Org. Lett.* **2013**, *15*, 4284–4287.

(129) Aktoudianakis, E.; Canales, E.; Currie, K. S.; Kato, D.; Li, J.; Link, J. O.; Metobo, S. E.; Saito, R. D.; Schroeder, S. D.; Shapiro, N.; Tse, W. C.; Wu, Q.; Hu, Y. E. PCT/US2018/016243. 2018; Gilead Sciences, Inc.

(130) Bhamidipati, S.; Clough, J.; Argade, A.; Singh, R.; Markovtosov, V.; Ding, P.; Yu, J.; Atuegbu, A.; Hong, H.; Darwish, I.; Thota, S. PCT/US2009/034159. 2009; Rigel Pharmaceuticals Inc.

(131) de Man, A. P. A.; Uitdehaag, J. C. M.; Sterrenburg, J. G.; de Wit, J. J. P.; Seegers, N. W. C.; van Doornmalen, A. M.; Buijsman, R. C.; Zaman, G. J. PCT/EP2017/055419. 2017; Netherlands Translational Research Center.

(132) Walker, S. D.; Barder, T. E.; Martinelli, J. R.; Buchwald, S. L. *Angew. Chem. Int. Ed.* **2004**, *43*, 1871–1876.

(133) Milne, J. E.; Buchwald, S. L. *J. Am. Chem. Soc.* **2004**, *126*, 13028–13032.

(134) Maiti, D.; Fors, B. P.; Henderson, J. L.; Nakamura, Y.; Buchwald, S. L. *Chem. Sci.* **2011**, *2*, 57–68.

(135) Ladd, C. L.; Roman, D. S.; Charette, A. B. *Tetrahedron* **2013**, *69*, 4479–4487.

(136) Rousseaux, S.; Liégault, B.; Fagnou, K. *Chem. Sci.* **2012**, *3*, 244–248.

(137) Dos Santos, A.; El Kaïm, L.; Grimaud, L.; Ramozzi, R. *Synlett* **2012**, *3*, 438–442.

(138) Downes, T. D. Thesis (PhD). 2019; University of York.

(139) Li, J.; Burke, M. D. *J. Am. Chem. Soc.* **2011**, *133*, 13774–13777.

(140) Wright, L.; Barril, X.; Dymock, B.; Sheridan, L.; Surgenor, A.; Beswick, M.; Drysdale, M.; Collier, A.; Massey, A.; Davies, N.; Fink, A.; Fromont, C.; Aherne, W.; Boxall, K.; Sharp, S.; Workman, P.; Hubbard, R. *Chem. Biol.* **2004**, *11*, 775.

(141) Kenny, P.; Newman, J.; Peat, T. *Acta. Cryst.* **2014**, *D70*, 565.

(142) Eswaran, J.; Lee, W.; Debreczeni, J.; Filippakopoulos, P.; Turnbull, A.; Fedorov, O.; Deacon, S.; Peterson, J.; Knapp, S. *Structure* **2007**, *15*, 201.

(143) Isaacs, J.; Xu, W.; Neckers, L. *Cancer Cell* **2003**, *3*, 213–217.

(144) Tonks, N. *Nat Rev Mol Cell Biol* **2006**, *7*, 833–46.

(145) Julien, S.; Dube, N.; Read, M.; Penney, J.; Paquet, M.; Han, Y.; Kennedy, B.; Muller, W.; Tremblay, M. *Nat Genet.* **2007**, *39*, 338–346.

(146) Desmarais, S.; Friesen, R.; Zamboni, R.; Ramachandran, C. *Biochem. J.* **1999**, *337*, 219–23.

(147) Vadlamudi, R.; Kumar, R. *Cancer and Metastasis Rev.* **2003**, *22*, 385–393.

(148) Kumar, R.; Gururaj, A.; Barnes, C. *Nat. Rev. Cancer* **2006**, *6*, 459–471.

(149) Brough, P.; Barril, X.; Borgognoni, J.; Chene, P.; Davies, N.; Davis, B.; Drysdale, M.; Dymock, B.; Eccles, S.; Garcia-Echeverria, C.; Fromont, C.; Hayes, A.; Hubbard, R.; Jordan, A.; Jensen, M.; Massey, A.; Merrett, A.; Padfield, A.; Parsons, R.; Radimerski, T.; Raynaud, F.; Robertson, A.; Roughley, S.; Schoepfer, J.; Simmonite, H.; Sharp, S.; Surgenor, A.; Valenti, M.; Walls, S.; Webb, P.; Wood, M.; Workman, P.; Wright, L. *J. Med. Chem.* **2009**, *52*, 4794–4809.

(150) Karaman, M.; Herrgard, S.; Treiber, D.; Gallant, P.; Atteridge, C.; Campbell, B.; Chan, K.; Ciceri, P.; Davis, M.; Edeen, P.; Faraoni, R.; Floyd, M.; Hunt, J.; Lockhart, D.; Milanov, Z.; Morrison, M.; Pallares, G.; Patel, H.; Pritchard, S.; Wodicka, L.; Zarrinkar, P. *Nat. Biotechnol.* **2008**, *26*, 127–132.

(151) Lo, M.; Aulabaugh, A.; Jin, G.; Cowling, R.; Bard, J.; Malamas, M.; Ellestad, G. *Anal. Biochem.* **2004**, *332*, 153–9.

(152) McCoy, A.; Grosse-Kunstleve, R.; Adams, P.; Winn, M.; Storoni, L.; Read, R. *J. Appl. Cryst.* **2007**, *40*, 658–674.

(153) Kenny, P.; Newman, J.; Peat, T. *Acta Cryst.* **2014**, *D70*, 565–571.

(154) Douangamath, A.; Fearon, D.; Gehrtz, P.; Krojer, T.; Lukacik, P.; Owen, C. D.; Resnick, E.; Strain-Damerell, C.; Aimon, A.; Ábrányi-Balogh, P.; Brandaõ-Neto, J.; Carbery, A.; Davison, G.; Dias, A.; Downes, T. D.; Dunnett, L.; Fairhead, M.; Firth, J. D.; Jones, S. P.; Keely, A.; Keserü, G. M.; Klein, H. F.; Martin, M. P.; Noble, M. E. M.; O'Brien, P.; Powell, A.; Reddi, R.; Skyner, R.; Snee, M.; Waring, M. J.; Wild, C.; London, N.; von Delft, F.; Walsh, M. A. *Nat. Commun.* **2020**, *11*, 5047.

(155) Antonioli, L.; Yegutkin, G.; Pacher, P.; Blandizzi, C.; G., H. *Trends Cancer* **2016**, *2*, 95–109.

(156) Wood, D. J.; Lopez-Fernandez, J. D.; Knight, L. E.; Al-Khawaldeh, I.; Gai, C.; Lin, S.; Martin, M. P.; Miller, D. C.; Cano, C.; Endicott, J. A.; Hardcastle, I. R.; Noble, M. E. M.; Waring, M. J. *J. Med. Chem.* **2019**, *62*, 3741–3752.

(157) Harris, M. R.; Li, Q.; Lian, Y.; Xiao, J.; Londregan, A. T. *Org. Lett.* **2017**, *19*, 2450–2453.

(158) Molander, G. A.; Sandrock, D. L. *Curr. Opin. Drug Discov. Devel.* **2009**, *12*, 811—823.

(159) Goldberg, F. W.; Kettle, J. G.; Kogej, T.; Perry, M. W.; Tomkinson, N. P. *Drug Discov. Today* **2015**, *20*, 11–17.

(160) Dehmlow, E. V.; Lissel, M. *Tetrahedron* **1981**, *37*, 1653–1658.

(161) Yamazaki, S.; Yamamoto, Y.; Fukushima, Y.; Takebayashi, M.; Ukai, T.; Mikata, Y. *J. Org. Chem.* **2010**, *75*, 5216–5222.

(162) Chen, C.; Kattanguru, P.; Tomashenko, O.; Karpowicz, R.; Siemiaszko, G.; Bhattacharya, A.; Calasansa, V.; Six, Y. *Org. Biomol. Chem.* **2017**, *15*, 5364–5372.

(163) Seyferth, D.; Lambert, R. L.; Massol, M. *J. Organomet. Chem.* **1975**, *88*, 255–286.

(164) Shimizu, N.; Watanabe, K.; Tsuno, Y. *Chem. Lett.* **1983**, *12*, 1877–1878.

(165) Duddu, R.; Eckhardt, M.; Furlong, M.; Knoess, H.; Berger, S.; Knochel, P. *Tetrahedron* **1994**, *50*, 2415–2432.

(166) Hirao, T.; Masunaga, T.; Ohshiro, Y.; Agawa, T. *J. Org. Chem.* **1981**, *46*, 3745–3747.

(167) Meijs, G. F.; Doyle, I. R. *J. Org. Chem.* **1985**, *50*, 3713–3716.

(168) Harada, T.; Katsuhira, T.; Hattori, K.; Oku, A. *Tetrahedron* **1994**, *50*, 7987–8002.

(169) Al Dulayymi, J. R.; Baird, M. S.; Bolesov, I. G.; Nizovtsev, A. V.; Tverezovsky, V. V. *J. Chem. Soc., Perkin Trans. 2* **2000**, *7*, 1603–1618.

(170) Al Dulayymi, J. R.; Baird, M. S.; Bolesov, I. G.; Tveresovsky, V.; Rubin, M. *Tetrahedron Lett.* **1996**, *37*, 8933–8936.

(171) Baird, M. S.; Nizovtsev, A. V.; Bolesov, I. G. *Tetrahedron* **2002**, *58*, 1581–1593.

(172) Qi, Q.; Yang, X.; Fu, X.; Xu, S.; Negishi, E.-i. *Angew. Chem. Int. Ed.* **2018**, *57*, 15138–15142.

(173) Lv, W.-X.; Li, Q.; Li, J.-L.; Li, Z.; Lin, E.; Tan, D.-H.; Cai, Y.-H.; Fan, W.-X.; Wang, H. *Angew. Chem. Int. Ed.* **2018**, *57*, 16544–16548.

(174) Renslo, A. R.; Jaishankar, P.; Venkatachalam, R.; Hackbarth, C.; Lopez, S.; Patel, D. V.; Gordeev, M. F. *J. Med. Chem.* **2005**, *48*, 5009–5024.

(175) Danheiser, R. L.; Savoca, A. C. *J. Org. Chem.* **1985**, *50*, 2401–2403.

(176) Bard, R. R.; Bunnett, J. F.; Traber, R. P. *J. Org. Chem.* **1979**, *44*, 4918–4924.

(177) Gillespie, D. G.; Walker, B. J. *J. Chem. Soc., Perkin Trans. 1* **1983**, 1689–1695.

(178) Hutton, H. M.; Schaefer, T. *Can. J. Chem.* **1963**, *41*, 684–689.

(179) Itoh, T.; Tamura, K.; Ueda, H.; Tanaka, T.; Sato, K.; Kuroda, R.; Aoki, S. *Bioorg. Med. Chem.* **2018**, *26*, 5922–5933.

(180) Davies, H. M. L.; Ren, P.; Jin, Q. *Org. Lett.* **2001**, *3*, 3587–3590.

(181) Kumar, P.; Zainul, O.; Laughlin, S. T. *Org. Biomol. Chem.* **2018**, *16*, 652–656.

(182) Kumar, P.; Jiang, T.; Li, S.; Zainul, O.; Laughlin, S. T. *Org. Biomol. Chem.* **2018**, *16*, 4081–4085.

(183) Shen, Z.; Lu, X.; Lei, A. *Tetrahedron* **2006**, *62*, 9237–9246.

(184) Deng, H.; Kooijman, S.; van den Nieuwendijk, A. M. C. H.; Ogasawara, D.; van der Wel, T.; van Dalen, F.; Baggelaar, M. P.; Janssen, F. J.; van den Berg, R. J. B. H. N.; den Dulk, H.; Cravatt, B. F.; Overkleeft, H. S.; Rensen, P. C. N.; van der Stelt, M. *J. Med. Chem.* **2017**, *60*, 428–440.

(185) Piper, J. R.; Stringfellow Jr., C. R.; Johnston, T. P. *J. Heterocycl. Chem.* **1967**, *4*, 298–300.

(186) Schultz, K.; Hesse, M. *Helv. Chim. Acta* **1996**, *79*, 1295–1304.

(187) Luithle, J. E. A.; Pietruszka, J. *J. Org. Chem.* **1999**, *64*, 8287–8297.

(188) Rubin, M.; Rubina, M.; Gevorgyan, V. *Chem. Rev.* **2007**, *107*, 3117–3179.

(189) Molander, G. A.; Gormisky, P. E. *J. Org. Chem.* **2008**, *73*, 7481–7485.

(190) de Meijere, A.; Khlebnikov, A. F.; Sünnemann, H. W.; Frank, D.; Rauch, K.; Yufit, D. S. *Eur. J. Org. Chem.* **2010**, 3295–3301.

(191) Leonori, D.; Aggarwal, V. K. *Angew. Chem. Int. Ed.* **2015**, *54*, 1082–1096.

(192) Molander, G. A.; Ellis, N. *Acc. Chem. Res.* **2007**, *40*, 275–286.

(193) Lennox, A. J. J.; Lloyd-Jones, G. C. *Isr. J. Chem.* **2010**, *50*, 664–674.

(194) Ma, H.-R.; Wang, X.-H.; Deng, M.-Z. *Synth. Commun.* **1999**, *29*, 2477–2485.

(195) Harris, M. R.; Wisniewska, H. M.; Jiao, W.; Wang, X.; Bradow, J. N. *Org. Lett.* **2018**, *20*, 2867–2871.

(196) Gagnon, A.; Duplessis, M.; Fader, L. *Org. Prep. and Proced. Int.* **2010**, *42*, 1–69.

(197) Molander, G. A.; Ito, T. *Org. Lett.* **2001**, *3*, 393–396.

(198) Lennox, A. J. J.; Lloyd-Jones, G. C. *J. Am. Chem. Soc.* **2012**, *134*, 7431–7441.

(199) Fang, G.-H.; Yan, Z.-J.; Deng, M.-Z. *Org. Lett.* **2004**, *6*, 357–360.

(200) Uehara, H.; Miyake, R.; Bando, K.; Kawabata, H.; Maeda, T. EP2716629 A1. 2014; API Corporation.

(201) Al-Azemi, T.; Mohamod, A.; Vinodh, M. *Tetrahedron* **2015**, *71*, 1523–1528.

(202) Alugubelli, S.; Pabbaraja, S. *Tetrahedron Lett.* **2012**, *53*, 5926–5928.

(203) Cox, C.; Flores, B.; Schreier, J. WO2010048016 A1. 2009; Merck Sharp and Dohme Corp.

(204) Atallah, G.; Chen, W.; Jia, Z.; Pozzan, A.; Raveglia, L.; Zanaletti, R. WO2016/196776 A2. 2016; Pharmacyclics LLC.

(205) Vlahovic, S.; Schädel, N.; Tussetschläger, S.; Laschat, S. *Eur. J. Org. Chem.* **2013**, 1580–1590.

(206) Fei, Z.; Wu, Q.; Zhang, F.; Cao, Y.; Liu, C.; Shieh, W.-C.; Xue, S.; McKenna, J.; Prasad, K.; Prashad, M.; Baeschlin, D.; Namoto, K. *J. Org. Chem.* **2008**, *73*, 9016–9021.

(207) Misaki, H.; Toru, M.; Yuya, O.; Osamu, K. EP2540728. 2013; Netherlands Translational Research Center.

(208) Baburajan, P.; Elango, K. *Synth. Commun.* **2015**, *45*, 531–538.

(209) Kumar, P.; Zainul, O.; Laughlin, S. *Org. Biomol. Chem.* **2018**, *16*, 652–656.

(210) Horáková, E.; Drabina, P.; Brůčková, L.; Stěpánková, K., S. Vorčáková; Sedlák, M. *Monatsh. Chem.* **2017**, *148*, 2143–2153.

(211) Tars, K.; Leitans, J.; Kazaks, A.; Zelencova, D.; Liepinsh, E.; Kuka, J.; Makrecka, M.; Lola, D.; Andrianovs, V.; Gustina, D.; Solveiga, G.; Liepinsh, E.; Kalvinsh, I.; Dambrova, M.; Loza, E.; Pugovics, O. *J. Med. Chem.* **2014**, *57*, 2213–2236.